TABLE OF CONTENTS

LIST OF FIGURES

CHAPTER 3

LIST OF TABLES

CHAPTER 1

CHAPTER 3

TABLE OF CONTENTS

LIST OF FIGURES

CHAPTER 6

CHAPTER 7

LIST OF TABLES

CHAPTER 6

CHAPTER 7

CHAPTER 1

INTRODUCTION

1) Body iron content and distribution

The human body contains about 50 mg Fe/kg body weight in males and 40 mg Fe/kg body weight in females. This iron is distributed between various compartments in the human body (1). The erythroid marrow (developing red blood cells) and circulating red blood cells contain about 32 mg Fe/kg body weight in males and 28 mg Fe/kg body weight in females as functional iron in haemoglobin. The remainder of functional iron is found as myoglobin mainly in muscle, 5 mg Fe/kg body weight in males and 4 mg Fe/kg body weight in females, and as iron-containing and iron-dependent enzymes throughout cells in the body, 1-2 mg Fe/kg body weight. Storage iron is contained in hepatocytes and in macrophages of the monocyte-macrophage system found in the liver, bone marrow, spleen and muscle. This comprises about 10-12 mg Fe/kg body weight in males and 5-6 mg Fe/kg body weight in females.

About 1 mg of iron is absorbed daily in the gastrointestinal tract. Gastrointestinal iron absorption from the gut lumen into the circulation occurs in three phases: 1) uptake of iron across the apical membrane of enterocytes, 2) intracellular translocation of iron and 3) transfer of iron across the basolateral membrane into the circulation (2). Uptake across the apical membrane (membrane facing the lumen) involves binding of inorganic iron (non-haem iron) or haem-iron to specific proteins (transporters) on the membrane. The major transporter involved in cellular inorganic iron uptake is the divalent metal

transporter – DMT1. DMT1 exclusively transports divalent metals (Fe^{2+}) and when inorganic iron in the diet is present as the Fe^{3+}-form, it necessitates the luminal conversion of Fe^{3+} to Fe^{2+} (2, 3, 4). This conversion of Fe^{3+} to Fe^{2+} in the lumen is achieved by an intestinal iron reductase – duodenal cytochrome B – Dcytb. Fe^{2+} is taken up by DMT1 into the cytoplasm of the enterocyte. Absorption of haem-iron occurs by means of a different transporter, an enterocyte haem importer, haem carrier protein 1 – HCP1. Once haem-iron has entered the enterocyte, it is likely cleaved by intracellular haem oxygenase 1 to release iron. Before the beginning of the third phase of iron absorption the absorbed and liberated Fe^{2+} joins the intracellular labile iron pool. From this intracellular labile iron pool, Fe^{2+} can either be stored in the iron storage protein ferritin or translocated to the basolateral membrane for transport into the circulation (2, 3). For transport into the circulation, Fe^{2+} binds to the basolateral membrane iron exporter protein – ferroportin. Upon reaching the extracellular face of the basolateral membrane of the enterocyte, Fe^{2+} is oxidized to Fe^{3+} by a membrane-bound multi-copper oxidase – hephaestin (3). The oxidation of Fe^{2+} to Fe^{3+} facilitates its transfer to the plasma iron transport protein transferrin (2, 3).

Iron circulates between the iron-containing compartments (intercellular iron shuttling) bound to the plasma iron transport protein transferrin. About 3 mg of iron is found in association with transferrin at any one time and the daily exchange of iron by plasma transferrin is about 30 mg. This transport iron amounts to about 0.2 mg Fe/kg body weight. Transferrin has two high-affinity binding sites for iron. Diferric transferrin, i.e., transferrin containing Fe^{3+} bound to both the iron binding sites, binds to a highly specific transferrin receptor on the cell membranes of cells allowing cellular uptake by receptor-mediated endocytosis. Iron is chelated by transferrin at the cell membrane of the cell releasing iron (such as the enterocyte) and the transferrin is subsequently bound by a transferrin receptor on the membrane of the cell accepting the iron (such as a developing

red blood cell). The receptors collect in clathrin-coated pits and facilitate transferrin internalisation into endocytic vesicles. The endosomes then become acidified. When the endosome reaches pH 5.5 protein conformation changes take place and thus result in the dissociation of Fe^{3+} from transferrin. Fe^{3+} is reduced to Fe^{2+} most likely by the endosomal reductase – Steap3. The formed Fe^{2+} is then transported from the endosome to the cytoplasm by the transporter DMT1. The transferrin-uptake cycle is completed when the endosome returns to, and fuses with the plasma membrane, returning apotransferrin (transferrin containing no iron) to the circulation and transferrin receptor to the plasma membrane. This allows both molecules to participate in another transferrin-uptake cycle (2, 3).

Cells contain a pool of chelatable or transit iron (Fe^{2+}) known as the labile iron pool bound to low molecular weight intracellular iron transport compounds, and it is thought that the endosomal iron released from transferrin transits this pool of iron. From this labile iron pool, Fe^{2+} can enter functional compartments or can be stored in ferritin (3). Since the labile pool of iron contains the metabolically and catalytically reactive iron, the magnitude of the labile pool of iron is maintained by sophisticated control mechanisms that regulate cellular iron uptake and storage in a coordinated manner. Storage of iron in association with ferritin is important since this protects cells against the deleterious effects of iron. In the labile iron pool, iron exists in the highly toxic Fe^{2+}-form. In this form iron can catalyse the production of harmful oxygen radicals in the Haber-Weiss reaction resulting in peroxidative damage to cellular structures. Whereas, in association with ferritin, iron is present as a soluble, nontoxic ferrihydrite mineral within the confines of the ferritin molecule. In order to ensure that the labile iron pool is kept within physiological ranges, the expression of the proteins involved in iron homeostasis such as transferrin, transferrin receptor and ferritin, is coordinately regulated. An increase in the intracellular free iron will, for instance, result in up-regulation of ferritin (increase in

efficiency of iron storage) and down-regulation of transferrin and transferrin receptor expression (decrease in iron uptake), whereas a decrease in intracellular free iron will result in the opposite. This coordinated, but divergent regulation of the expression of these proteins is governed by a single protein namely the iron-responsive protein (IRP), which can bind to iron-responsive elements (IREs) on the mRNAs of the iron homeostasis proteins. This protein is sensitive to intracellular iron levels and responds to these levels by regulation, at a posttranscriptional level, of the expression of the mRNA of the proteins responsible for iron uptake and storage. The presence of IREs in DMT1 and ferroportin mRNA suggests that their expression may also be controlled, at least in part, by the cellular iron content (5).

Red blood cell production and destruction is fairly dominant in iron metabolism. About two thirds of the iron in the human body is contained as functional iron in the haemoglobin of the red blood cells. Haemoglobin is responsible for binding oxygen and delivering it to the tissues and consists of a haem molecule, i.e., a protoporphyrin ring containing Fe^{2+}, as well as four globin protein chains, i.e., two α-chains and two β-chains. Haemoglobin production in developing red blood cells is a complex process requiring meticulous coordination of iron acquisition, protoporphyrin biosynthesis, and globin protein production (1). Iron is acquired by developing red blood cells through binding of transferrin to the transferrin receptor. Two to three million red blood cells are produced every second, therefore sufficient amounts of iron are required to enable the developing red blood cells to synthesise haemoglobin. In order for the bone marrow to supply this amount of new red blood cells, 30-40 mg of iron is needed on a daily basis by the erythroid (red blood cell forming) marrow. Since only 1 mg of iron is absorbed daily from the intestinal tract, iron from dying red blood cells is recycled (6).

The life-span of a circulating red blood cell is about 120 days. At this time these dying red blood cells will be taken up by macrophages of the monocyte-macrophage system present in the spleen, bone marrow and liver for recovery of their iron. The recovery of iron from these dying red blood cells provides most of the iron utilized by developing red blood cells for haemoglobin synthesis. After the red blood cell has been internalized into an acidic phagosome and most of the cellular constituents broken down, an enzyme, haem oxygenase, liberates iron from haem. The iron is transferred out of the phagosome by DMT1 into the cytoplasm where it will join the intracellular labile iron pool. From this intracellular iron pool, the iron will be either incorporated into ferritin for cellular storage or returned to the plasma. The movement of iron from the cell into the plasma is mediated by the plasma membrane transport protein – ferroportin. Iron will traverse the plasma membrane as Fe^{2+}. Upon reaching the extracellular side of the plasma membrane Fe^{2+} is oxidized to Fe^{3+} by caeruloplasmin. Caeruloplasmin is a serum multicopper oxidase, which facilitates movement of iron out of tissue stores and into transferrin by this oxidation process, similar to the protein hephaestin at the basolateral membrane of the enterocyte (3).

Various changes in body iron needs can bring about the modulation of iron homeostatic mechanisms in order to change plasma iron concentrations. Factors that can result in an increase in plasma iron concentrations include an increase in red blood cell production, hypoxia and iron deficiency. In contrast with these factors, diminished red blood cell production, iron overload and inflammation can bring about a decrease in the concentration of plasma iron. The molecule most likely responsible for bringing about these changes in iron homeostatic processes, is the liver-produced hepcidin. Hepcidin levels are increased in response to increased plasma iron, iron overload and inflammation and diminished in response to increased red blood cell production, hypoxia and iron deficiency (7, 8). Hepcidin binds to ferroportin and brings about the internalization and

degradation of ferroportin. This will result in less ferroportin available at the basolateral membrane of the enterocyte and the plasma membrane of the hepatocyte and macrophage for iron export into the circulation. In the enterocyte, this hepcidin-dependent internalization and degradation of ferroportin will reduce the dietary iron absorption, whereas in the macrophage hepcidin activity will attenuate cellular iron release. A decrease in iron transport into the circulation from the enterocyte will result in the accumulation of iron as ferritin in the enterocyte. Since enterocytes are viable for only one to two days, iron that accumulates within them is lost from the body when these senescent enterocytes are shed into the gut lumen (2, 3).

Ferritin is the major protein responsible for the sequestration, storage and release of intracellular iron. Ferritin can exist as different isoferritins. Various factors seem to play a role in the precise composition of a ferritin molecule and thus in its functioning as an iron storage protein.

2) Ferritin and ferritin isoforms:

Structure-function relationships, synthesis, degradation and secretion

Ferritin is the major intracellular protein involved in the storage and release of intracellular iron and since iron is needed in various cellular functions it does not come as a surprise that ferritin is expressed in every cell type thus far studied (9). Iron is essential for cellular functions such as oxygen transport, electron transfer, nitrogen fixation, DNA synthesis and the production of haemoproteins like haemoglobin and myoglobin (10). However, not all cell types harness iron for the same purposes or to the same extent and therefore the role of ferritin in the management of intracellular iron differs between the various types of cells. Ferritin can play a role in specialized functions, e.g. recycling of iron in macrophages and short- and long-term storage of iron as in hepatocytes, as well as in intracellular housekeeping functions where it provides a reserve for cytochromes,

nitrogenases, ribonucleotide reductases, haemoglobin and myoglobin (11). Perhaps equally important to its function in the storage and release of iron is the role that ferritin plays in the protection of cells against the deleterious effects of iron. Iron exists in two readily interconvertible redox states and, at physiological pH and oxygen tension, Fe^{2+} is readily oxidized to Fe^{3+}, followed by the hydrolysis of the Fe^{3+}-containing compounds and the formation of insoluble ferric hydroxide and oxyhydroxide polymers (10, 12). In addition, Fe^{2+} can catalyse the production of harmful oxygen radicals in the Haber-Weiss reaction resulting in peroxidative damage to cellular structures (10, 13). Within cells, iron probably exists in a low molecular weight, redox-active form only for short periods – mainly within the lysosomes. Lysosomes are therefore particularly vulnerable to oxidative stress and may burst due to intralysosomal Fenton-type chemistry with ensuing peroxidative destabilization of lysosomal membranes. This could result in leaky lysosomes and the induction of cellular damage, or even apoptotic or necrotic death due to the release of a range of powerful hydrolytic enzymes into the cytosol (14). By sequestering large amounts of iron as a soluble, non-toxic ferrihydrite mineral within the confines of the ferritin molecule, ferritin protects the cell against insoluble ferric oxide and oxyhydroxide formation, as well as against the production of oxygen radicals (15, 16).

Ferritin is widely distributed in cells and is found in the cytosol, nucleus, mitochondria and lysosomes and appears in plasma as a result of cellular secretion. This specific distribution enables ferritin to supply the particular enzymes and other proteins with appropriate amounts of iron, and equally important, places ferritin in close proximity to sites where large amounts of iron are metabolized. Ferritin is actively transported into the nucleus to provide, amongst others, ribonucleotide reductase with iron and to protect DNA from oxidative damage as a result of inappropriate oxygen radical production due to surplus amounts of iron (17). A specific type of ferritin is also found in mitochondria.

Mitochondria are confronted with large amounts of metabolically active iron and although most cell types contain only very small amounts of a mitochondrial ferritin, in certain conditions, a specific ferrritin is translocated to the mitochondrium to sequester unwanted amounts of iron (18). The regulation of ferritin distribution in different parts of the cytosol and in cellular organelles is controlled, in part, by the various mechanisms involved in the uptake of ferritin by the cellular organelles. Furthermore, ferritin binds to microtubules and this interaction can not only contribute to transport of ferritin to specific sites and organelles within the cell, but also to secretion of ferritin from the cell. Depolymerization of microtubules increase ferritin secretion and support the probable role of microtubules in regulating the intracellular concentration, distribution and release of ferritin under different physiological circumstances (19).

2.1) Structure of ferritin

Ferritin, like some of the other proteins involved in the regulation of iron homeostasis in the body, including transferrin and lactoferrin, can serve either as an iron donor or iron acceptor (20). However, unlike transferrin and lactoferrin, ferritin is capable of accepting, storing and donating vast amounts of iron. These abilities of ferritin are all a function of the structure of ferritin – especially that of the ferritin protein shell. Ferritin is a protein with a molecular weight of 450 000 daltons (11) and consists of an outer three-dimensional protein shell enclosing an 80 Å diameter inner cavity (21). In this inner cavity ferritin is capable of sequestering variable amounts of Fe^{3+}-atoms as a ferrihydrite mineral. When fully saturated, ferritin can store up to 4500 Fe^{3+}-atoms, but the usual amount is closer to 2000 Fe^{3+}-atoms (15, 21).

2.1.1) Structure of the ferritin protein shell

The outer three-dimensional protein shell contains a total of 24 protein subunits arranged symmetrically (15, 21). Two types of protein subunits exist, the H-subunit and

the L-subunit. The H-subunit (21 kDa) contains 178 amino acids while the L-subunit (19 kDa) contains 174 amino acids (9, 10). Each subunit is folded into 4 long α-helices (A, B, C, D), with a long loop between C and D, and a fifth short helix (E) at the C-terminal (21). Each subunit is roughly cylindrical (5.5 nm long and 2.7 nm wide) (9). For the L-subunit the amino acid arrangement into the various α-helices is as follows: long α-helix A (amino acid residues 10-39), long α-helix B (amino acid residues 45-72), long α-helix C (amino acid residues 92-120), long α-helix D (amino acid residues 124-155) and short α-helix E (amino acid residues 160-169) (15). The 4 long α-helices are aligned parallel to one another and are tightly packed into a cylindrical subunit bundle (9, 15), thus forming the main subunit axis. Between the 4 long α-helices the inter-helical contact region extends over a length of 35 Å (15), while the longest helix, i.e., the α-helix D, protrudes beyond this main inter-helical contact region and folds sharply back so that the α-helix E lies at an angle roughly 60 degrees to the main axis of the subunit (15, 21). The other feature of the subunit, that is, the long loop L (amino acid residues 73-91), joins the C-terminus of α-helix B to the N-terminus of α-helix C (15). Due to the inter-helical contacts and the arrangement of the subunit in the protein shell, the α-helices B and D have one face towards the inside of the ferritin protein shell, the α-helices A and C have one face each towards the outside of the shell, and the loop L is displayed on the outermost surface of the ferritin protein shell (15). This arrangement determines the types of amino acids situated on the inner face and the outer face of the subunit and therefore the subsequent intra-subunit and inter-subunit interactions. The secondary structure of the H-subunit is very similar to that of the L-subunit, despite the fact that they share only 55% amino acid sequence homology (9).

2.1.1.1) Intra-subunit and inter-subunit amino acid side-chain interactions of the ferritin protein shell

Highly conserved amino acid residues are involved in intra-subunit and inter-subunit interactions (9, 11, 22). The different types of intra-subunit and inter-subunit amino acid side-chain interactions that are important for ferritin folding and stability include hydrogen bonds, salt-bridges and hydrophobic interactions (11). The contributions of these types of interactions to the folding and stability of the H- and L-subunits differ significantly between the two types of subunits. The intra-subunit hydrogen bonds are about 50% more abundant in the H-subunit than in the L-subunit, whereas the salt bridges are more important in the stabilization of the L-subunit and accounts for about 30% of the stabilization energy of the L-subunit (23). Due to the large number of intra- and inter-subunit salt bridges the ferritin molecule is highly stable to thermal and chemical denaturation (21). In addition, the differences in intra-subunit interactions between the H-subunit and L-subunit result in a linear increase in the resistance to denaturation, with L-subunit homopolymers and heteropolymers containing a high L-subunit proportion significantly more resistant than H-subunit homopolymers (23, 24). One important difference in intra-chain interactions that contribute to the L-subunits being more stable than the H-subunits is the salt-bridge lysine 62 – glutamic acid 107 in the L-subunit which replaces the ferroxidase center of the H-subunit (24). However, these differences in intra-chain interactions between the H-subunit and L-subunit appear to be largely masked by the presence of strong inter-subunit contacts in assembled molecules consisting of a combination of H- and L-subunits (23). The interactions between subunits responsible for ferritin assembly involve about 50% of the subunit surface and most of the inter-subunit contacts are conserved in H- and L-subunits. The first inter-subunit interaction to take place in the assemblage of the ferritin protein shell is the formation of interactions along the main subunit axis between two subunits creating a dimer pair (11). One face of the subunit contains hydrophobic residues from

α-helix A (valine 20, leucine 24, tyrosine 28, leucine 31) and loop L (phenylalanine 78, leucine 81, proline 84). By interaction with an equivalent region of a second subunit this hydrophobic patch of some 22 Å in length is buried from solvent (15). Another hydrophobic region on the subunit surface is that comprising one face of α-helix E (leucine 154, leucine 161, tyrosine 164, leucine 165, leucine 169) that will also be buried from solvent upon subunit interactions. There are a large number of inter-subunit interactions that form regions of marked hydrophobicity and other regions where polar interactions predominate (15). If these hydrophobic residues are to be partially buried from solvent then further assembly of dimers must occur. Since the assembly of ferritin consisting of 24 subunits results in the complete concealment of all hydrophobic patches (15), the formation of such a molecule is very favourable.

2.1.1.2) Channels present in the ferritin protein shell

For either mineralization or demineralization of the iron core to occur it is important that substances such as Fe^{2+}/Fe^{3+}, oxidants, reductants and chelators can gain access to the interior of the ferritin molecule. In order for these molecules to gain entrance to the interior of the protein shell the ferritin protein shell contains two main types of channels with strikingly different physical properties. The first type of channel comprises six hydrophobic channels with fourfold symmetry (12 Å long and 3-4 Å wide), which are lined by 12 leucine side-chains in the L-subunit and 8 leucine plus 4 histidine side-chains in the H-subunit belonging to the α-helix D. The second type of channel includes 8 hydrophilic channels with threefold symmetry (3-4 Å wide), each lined by 6 carboxyl groups, 3 aspartate residues (on the cavity side of the shell) and 3 glutamate residues (towards the outside of the molecule) belonging to the α-helix E (15, 21, 25, 26). The carboxylate groups of the hydrophilic threefold channels are essential for rapid iron transport across the protein shell (27). The hydrophobic character of the 6 hydrophobic channels argues against a possible role for these channels in the transport of Fe^{2+}/Fe^{3+}-

ions into the interior of the ferritin molecule. These fourfold hydrophobic channels are found to be impermeable to all cations with the possible exception of protons. It is suggested that these fourfold channels facilitate proton transfer in and out of ferritin in order to maintain electroneutrality during iron deposition (28). However, the substitution of leucine for histidine in the H-subunit may confer iron transfer properties to the hydrophobic channel of the H-subunit since histidine has a strong affinity for iron (22). The hydrophilic channels are the most likely routes of iron entry into the protein shell and are probably functional in both the H-subunit and the L-subunit. This is indicated by a high degree of conservation of the three glutamates and three aspartates in both subunits (29). Furthermore, alteration of residues of the hydrophobic channels has little effect on the rate and specificity of the reaction whereas modifications of the carboxyl groups lining the hydrophilic channels reduces the rate of iron uptake by about 2-fold (30). The hydrophilic channel is funnel-shaped, broadening out towards the outside surface to give a wide hydrophilic region (15, 30). The hydrophilic regions at the outside surface of the hydrophilic channels contain negative charges surrounded by patches of positive charges creating electrostatic fields in order to direct Fe^{2+}-ions toward the channel entrance (29). Once iron has been directed to the opening of the hydrophilic channel, it is bound to hydrophilic residues located at the outer and inner openings of the channels (31). These residues include cysteine 130 and histidine 118, both of which face the outer opening of the hydrophilic channel (31), and aspartic acid 131 and glutamic acid 134 in the narrowest part of the channel (11, 30). Aside from the hydrophobic and hydrophilic channels present in the ferritin protein shell, a H-subunit specific channel exists that connects the ferroxidase site in the center of the H-subunit to the outer protein surface (22). Although, transfer of iron through this channel is in general less efficient, the transfer of Fe^{3+}-ions to the outside of ferritin may become important in certain conditions.

2.1.1.3) The ferroxidase catalytic center of the H-subunit of the ferritin protein shell

The first step in the iron sequestration process by ferritin involves the oxidation of Fe^{2+} to Fe^{3+} by oxygen and is facilitated by the ferroxidase center contained in the H-subunit (31). This ferroxidase center comprises various amino acid side-chains as important iron ligands in the multi-step oxidation of Fe^{2+} to Fe^{3+} and includes a cluster of hydrophilic amino acid residues (glutamic acid 27, glutamic acid 61, glutamic acid 62, histidine 65 and glutamic acid 107) which are embedded within each of the 4 α-helix bundles comprising the subunit (24, 32, 33). This ferroxidase center is present in the H-subunit, but absent in the L-subunit (24). The L-subunit's potential ferroxidase activity is lost (32) due to amino acid changes including glutamic acid 62 to lysine and histidine 65 to glycine, formation of a salt-bridge between lysine 62 and glutamic acid 107 (34) and swinging of glutamic acid 61 into a position facing the cavity (31).

2.1.1.4) The nucleation site of the L-subunit on the inner iron/protein interface of the ferritin protein shell

The second step in the iron sequestration process by ferritin involves the formation of Fe^{3+}-nuclei and the subsequent growth of an iron-core. In order for ferritin to support Fe^{3+}-nuclei formation and the growth of the iron mineral, ferritin must contain the Fe^{3+}-atoms in the inner cavity of the protein shell and stabilize subsequently incoming Fe^{3+}-atoms on the growing iron-core. This is accomplished by amino acid side-chain ligands present on the inner surface of the ferritin protein shell. Binding of Fe^{3+} to these ligands supports Fe^{3+}-nuclei formation, as well as the subsequent growth of the iron-core. This results in the contact of the ferritin protein shell with the iron core at several points on the inner surface, forming an iron/protein interface. These iron/protein interfaces, which define the sites of core nucleation, probably excist where the protein subunit dimers interact (11). In contrast to the first step in iron sequestration, i.e., oxidation of

iron, which is accomplished mainly by the H-subunits, this second step, i.e., Fe^{3+}-nuclei formation and the growth of the iron-core is mainly a function of the L-subunits, which supply the appropriate amino acid side-chains. These amino acid side-chains act as ligands for the initially formed Fe^{3+} or as negatively charged domains that lower the activation energy of iron-core formation (24). The reason that the H-subunits are less efficient in nucleation and iron-core formation is that only 7 of the hydrophilic amino acid side-chains in L-subunits that line the inner surface, and which are not involved in the formation of salt bridges or hydrogen bonds, but thought to bind iron, are conserved in H-subunits. Amino acids important in nuclei formation and growth of the iron-core include histidine 49, arginine 52, glutamic acid 53, glutamic acid 56, glutamic acid 57, arginine 59, glutamic acid 60, glutamic acid 61, arginine 64 and lysine 67 on α-helix B, with glutamic acid 136, lysine 139 and lysine 142 on α-helix D, as well as 3 residues at the C-terminus, i.e., lysine 172, histidine 173 and aspartic acid 174. The differences in amino acid side-chains between H- and L-subunits result in the loss of negative charges in the H-subunit on the inner iron/protein interface so that H-subunits have a lower ability to nucleate iron (15, 22, 24). A cluster of three L-subunit glutamates has specifically been implicated in Fe^{3+}-nuclei formation. This cluster of glutamates, i.e., glutamic acid 57, glutamic acid 60, and glutamic acid 61, form a region of negativity for the binding of Fe^{3+}. In the H-subunit glutamic acid 57 and glutamic acid 60 are substituted for histidine and glutamic acid 61 is involved in the ferroxidase center of the H-subunit. It is suggested that glutamic acid 61 could also play a role in the nucleation of Fe^{3+} after oxidation of Fe^{2+}. However, this putative nucleation site, involving glutamic acid 61, glutamic acid 64 and glutamic acid 67, does not play a role in nucleation and growth of the iron-core (35). In the L-subunit glutamic acid 61 is swung into a position on the inner cavity surface in proximity to glutamic acid 57 and glutamic acid 60 to participate in this cluster of negative charges responsible for the greater efficiency of L-subunits in iron-core nucleation (32, 36).

2.1.2) The iron mineral

The iron mineral is enclosed in a cavity by a protein shell and contains different types of environments in which the Fe^{3+}-ion is located. These different types of environments include:

1) iron atoms located at nucleation sites – these Fe^{3+}-ions are coordinated by amino acid side chain ligands from the inner protein surface and inorganic bonds from the mineral surface (13).

2) iron atoms at the surface of the mineral – these Fe^{3+}-ions are connected to the bulk mineral, as well as to the Fe^{3+}-ions within the nucleation sites in the protein shell through inorganic oxide/hydroxide linkages and there may be additional linkages to the Fe^{3+}-ions of the shell through dinucleating amino acid side-chain ligands (13).

3) iron atoms which are in environments corresponding to those of the bulk mineral connected through inorganic oxide/hydroxide linkages, where the Fe^{3+}-ions are located in the interstices between two hexagonally closely packed layers of oxygen (37, 38). The Fe^{3+}-ions appear to be in predominantly octahedral environments but up to one-third of the Fe^{3+}-ions are in tetrahedral sites, with an average of six oxygen atoms at a distance of approximately 2 Å. This, more or less, corresponds to the structure for ferrihydrite (13, 15, 29).

The iron core may differ between ferritin molecules, as well as within the same ferritin molecule, and can contain single or multiple crystallites and amorphous regions (29). One or more of such electron-dense crystallites are anchored to the inner surface of the protein shell (37). The average diameter of the iron cores range from 2.5-9 nm (29). The formation of a single crystallite approaching the inner diameter of the protein shell or the formation of various smaller crystallites depends on the availability of Fe^{2+}-ions/Fe^{3+}-ions during the later phases of mineral growth after nucleation has occurred (11). Striking features of the iron cores are their variable phosphate contents (21, 29).

Phosphate ions are found on the surface of the iron cores where they replace some of the surface hydroxyl groups (15). However, recent observations indicate that phosphate can also be found throughout the iron core, that cores can have ordered and disordered regions, and that the disorder increases when phosphate increases (11). *In vivo* the phosphate contents of ferritin iron cores appear to be in dynamic equilibrium with cell phosphate (15) and it has long been suggested that phosphate plays a role in iron homeostasis (13). This assumption has recently been supported by the fact that phosphate can stimulate the rate of iron uptake by providing binding sites on the mineral surface for incoming iron atoms and as such may play a role in the oxidation of Fe^{2+} on the mineral surface (39).

2.2) Mechanism of iron sequestration and release: The role of the ferritin protein shell in iron mineralization and demineralization

Ferritin concentrates iron in cells by directing the formation of a ferrihydrite mineral in the hollow cavity enclosed by the ferritin protein shell. This results in effective cellular iron concentrations of more than 10^{11} times the solubility of the Fe^{3+}-ion (40). In times of iron need ferritin releases iron by demineralization of the iron core. The exact steps involved in iron release are not completely known, but iron release involves the reduction of Fe^{3+} to Fe^{2+}. The rates of the processes involved in iron mineralization and demineralization are controlled by the protein shell (11) – this by influencing the local pH and redox potentials (13). The formation of the ferrihydrite mineral by ferritin is a multi-step process governed by the protein shell. Iron enters the ferritin cavity by passage through the channels situated in the protein shell facilitated by the presence of local iron binding sites (21). Upon entering the protein shell the iron is oxidized followed by hydrolysis, nucleation and iron core growth (15). Each of these steps contributes to the formation of a ferrihydrite mineral core from soluble Fe^{2+}-ions.

2.2.1) Oxidation of iron

2.2.1.1) Oxidation of Fe^{2+} by the ferroxidase center of the H-subunit

Oxidation of Fe^{2+} is an obligatory first step in order for an iron atom to finally be deposited in the cavity of ferritin. The H-subunit's ferroxidase center, formed by various amino acid side-chains, enzymatically oxidizes Fe^{2+} to Fe^{3+}. Enzymatic oxidation of Fe^{2+} by the ferroxidase center results in rates of iron oxidation several-fold faster than that which would occur during auto-oxidation of iron. This faster rate of iron oxidation results from the proper placement of Fe^{2+} atoms by the ligands of the ferroxidase center of the H-subunit for subsequent oxidation by O_2 (41). X-ray analysis has revealed three iron-binding sites per H-subunit. Sites A and B (3.8 Å apart) form a di-iron site and include a common bridging carboxylic acid residue. Ligands of site A also include one equivalent histidine and one glutamate glutamic acid 27, whereas site B has two carboxylate ligands in addition to the bridging carboxylate. These are glutamic acid 107 and glutamic acid 61. The third site, i.e., site C lies in the inner surface of the protein shell at a distance of 7 Å from the di-iron site. The first step in Fe^{2+} oxidation involves the binding of incoming Fe^{2+} atoms with each of sites A and B, followed by the formation of a μ-oxo-bridge (42). The affinity of site A for Fe^{2+} is higher than the affinity of site B, resulting in the occupation of site A by Fe^{2+} before site B. Binding of Fe^{2+} to site B follows O_2 binding and/or oxidation of the first Fe^{2+} (27). After about an hour of intermediate μ-oxo-bridged dimer formation, this complex splits into highly mobile Fe^{3+}-monomers that can move to the cavity for hydrolysis of the Fe^{3+}-compounds, nucleation and growth of the iron-core (33, 41). An unusually short distance of 2.53 Å between the two Fe^{2+} ions suggests the presence of a unique triply bridged structure requiring a small Fe-O-O angle. This geometry should favour decay of the peroxodiferric complex by the release of μ-oxo or μ-hydroxo diferric mineral precursors (43, 44). This would result in freeing of the ferroxidase sites for binding of additional Fe^{2+} and the start of another round of Fe^{2+} oxidation (31). A by-product

produced during the ferroxidase center oxidation of Fe^{2+} is H_2O_2, which can result in the subsequent production of Fenton chemistry-derived radicals (31).

2.2.1.2) Oxidation of Fe^{2+} on the surface of the growing iron core

During the initial stages of ferritin iron core mineralization, oxidation of Fe^{2+} takes place in the ferroxidase centers of the H-subunits of the ferritin protein shell. Once the mineral attains a certain critical size, oxidation of Fe^{2+} can additionally, and perhaps preferentially, occur on the surface of the growing iron core (13, 15, 31). Therefore, the main function of the ferroxidase center may be oxidation of sufficient iron from Fe^{2+} to Fe^{3+} for the initial nucleation events, and once these nuclei attained a sufficient size for oxidation to take place on the mineral surface, the H-subunit's role as a ferroxidase is superseded by oxidation on the mineral surface (34, 42).

2.2.2) Hydrolysis and nucleation of the formed Fe^{3+}-compound

The subsequent hydrolysis and nucleation of the generated Fe^{3+}-compound is governed by the amino acid side-chains of the L-subunit (31). The highly mobile Fe^{3+}-monomers are directed to the inner cavity and properly placed on the protein shell/mineral interface by these ligands. The subsequent hydrolysis and nucleation involves the hydrolysis and aggregation of Fe^{3+}-ions to form nuclei containing perhaps as few as four or five constituent Fe^{3+}-ions resulting in the production of iron oxyhydroxides and oxides (13, 29). Hydrolysis and nucleation of the Fe^{3+}-compound is favoured since binding of Fe^{3+} to the ligands lowers the activation energy of nucleation (13, 21). Such nuclei can become the solid phase once some critical nucleus size has been reached and will sustain iron mineral growth from these sites (13). These initial sites of nuclei formation on the inner surface of the protein shell, involving specific amino acid side-chains, will maintain contact with the iron core (13). This interaction with the iron core seems to be a key factor in the stabilization of the crystal by providing a neutral container, or more likely,

the interactions with negatively charged and neutral amino acid side-chains such as carboxylates, alkoxides, phenolates and imidazoles provide the necessary charge compensation (13).

2.2.3) Different iron oxidation kinetics and the formation of different reaction products by the ferroxidase center oxidation of iron and oxidation of iron on the mineral surface

Oxidation of Fe^{2+} by the ferroxidase center and oxidation of Fe^{2+} on the mineral surface take place under different conditions. These processes have different iron oxidation kinetics and result in the formation of different reaction products (36). At low Fe^{2+} concentrations (<50 Fe^{2+}-atoms/ferritin molecule) oxidation of Fe^{2+} is catalysed by the ferroxidase center and the reaction stoichiometry is as follows:

For the oxidation reaction: $2Fe^{2+} + O_2 + 2H^+ \rightarrow 2Fe^{3+} + H_2O_2$

For the subsequent hydrolysis reaction: $2Fe^{3+} + 4H_2O \rightarrow 2FeOOHcore + 6H^+$

For the sum of the oxidation and hydrolysis reactions: $2Fe^{2+} + O_2 + 4H_2O \rightarrow 2FeOOHcore + H_2O_2 + 4H^+$

In the presence of higher Fe^{2+} concentrations (>250 Fe^{2+}-atoms/ferritin molecule) the H-subunit ferroxidase site becomes kinetically saturated and the size of the growing mineral reaches a size sufficient to sustain oxidation of Fe^{2+} on the mineral surface. This results in the changing of the dominant mechanism of iron oxidation from the ferroxidase center to the mineral surface catalysed mechanism (31). The reaction stoichiometry changes to the following:

For the oxidation reaction: $4Fe^{2+} + O_2 + 4H^+ \rightarrow 4Fe^{3+} + 2H_2O$

For the subsequent hydrolysis reaction: $4Fe^{3+} + 8H_2O \rightarrow 4FeOOHcore + 12H^+$

For the sum of the oxidation and hydrolysis reactions: $4Fe^{2+} + O_2 + 6H_2O \rightarrow 4FeOOHcore + 8H^+$ (31).

Such differences in iron oxidation kinetics by ferritin are displayed in cells under varying conditions. Under cellular conditions where low Fe^{2+} concentrations relative to the amount of apoferritin may be expected, the ferroxidase activity of H-subunits is probably essential to initiate the formation of iron-nuclei and for iron mineralization to proceed at a significant rate (34). Autocatalytic Fe^{2+} oxidation on the surface of the growing iron mineral can only be significant once an initial iron-core has been established (34). However, it has certain advantages above the process that occurs in the ferroxidase center of the H-subunit. The first biologic advantage is that the potentially toxic production of hydrogen peroxide by the oxidation reaction, that takes place in the ferroxidase center, is replaced by the harmless reduction of di-oxygen to water via the oxidation reaction on the mineral surface (31, 42). As ferritin lacks catalase activity, the H_2O_2 produced during the ferroxidase center catalysed oxidation of iron results in some degradation of the ferritin protein shell. In effect, the protein itself acts as an anti-oxidant (31). Another advantage of such a change in iron kinetics is that it enhances the ability of ferritin to increase the rate of iron oxidation when challenged with a large amount of Fe^{2+}-ions. The ferroxidase center can be reutilized for another round of Fe^{2+} oxidation only once the generated Fe^{3+}-ion moves from the ferroxidase center into the iron storage cavity for subsequent nucleation. However, this rate of regeneration may be too slow to process a large number of Fe^{2+}-ions added at once, and under such conditions, oxidation on the mineral surface may occur even during earlier stages. These different oxidation abilities of ferritin to mineralize iron result in the formation of crystallites of different sizes. Under conditions favouring fast iron accumulation the 'ferrihydrite' produced has a relatively large crystallite size and a nearly all-or-none distribution within ferritin molecules, since the mineralization process will be favoured by oxidation of Fe^{2+} on the mineral surface (15) and the rate of iron deposition will be governed by the surface area of the iron mineral (38). However, under conditions of low

Fe^{2+} concentrations oxidation of Fe^{2+} will take place on different ferroxidase centers resulting in the formation of many small crystallites (15).

2.2.4) Migration of iron between ferritin molecules

Iron can migrate between ferritin molecules (24), either as Fe^{2+} or as Fe^{3+}. Migration of iron between ferritin molecules occurs if the movement of Fe^{2+}/Fe^{3+} to the next ferritin molecule results in favouring of the oxidation or hydrolysis/nucleation processes. Oxidation of Fe^{2+} results in the generation of highly mobile Fe^{3+}-ions, which subsequently have to be incorporated into a growing mineral crystal by a hydrolysis/nucleation process. Since L-subunits promote hydrolysis and nucleation of Fe^{3+} by binding of Fe^{3+} to specific L-subunit ligands, insufficient quantities of the L-subunit present in the ferritin molecule can result in the migration of Fe^{3+} to a ferritin molecule with sufficient quantities of L-subunit (32). The generated Fe^{3+} would move to the outer surface of the ferritin protein shell via a H-subunit specific channel linking the ferroxidase centers with the outer surface of the protein shell (30). This results in competition between ferritin molecules for iron and a tendency towards all-or-none distribution (15, 21, 24).

2.2.5) Non-specific Fe^{3+}-compound hydrolysis on the outer surface of the ferritin protein shell

When insufficient quantities of L-subunits exist for the entrapment of Fe^{3+} in the inner cavity Fe^{3+} can move to the outer surface of the protein shell where non-specific hydrolysis of Fe^{3+}-compounds can take place (36). Non-specific iron hydrolysis on the outer surface of the ferritin molecule can result in protein aggregation and precipitation (36). Spontaneous aerobic iron hydrolysis such as that which occurs on the outer surface of the ferritin protein shell appears to be caused by the formation of transient mono-

nuclear hydrated Fe^{3+}-compounds which have a strong tendency to aggregate and coagulate (36).

2.2.6) The cooperative roles of the H-subunit and L-subunit of the ferritin protein shell in iron mineralization

Since the H-subunit and the L-subunit of the protein shell have separate roles in the mineralization process of iron by ferritin and the specific properties of the two subunits are complementary and act synergistically, cooperation between these subunits is paramount for the efficient mineralization of iron by ferritin. The ratio of H-subunits to L-subunits is therefore important. While oxidation of Fe^{2+} by the ferroxidase center of the H-subunit accelerates the supply of Fe^{3+}, the subsequent hydrolysis and nucleation processes are driven by the L-subunit (29, 32). If insufficient quantities of the L-subunit are assembled into the protein shell non-specific hydrolysis of Fe^{3+}-compounds can take place on the outside of the protein shell. This may lead to aggregation and precipitation of ferritin molecules (36). Although very few H-subunits are necessary to initiate the process of iron oxidation, a deficit in H-subunits can result in poor iron sequestration abilities. Furthermore, H- and L-subunits can act cooperatively when in separate molecules (32).

The cooperative roles of the subunits of ferritin in the mineralization process of iron have been demonstrated by the formation of recombinant H-subunit or L-subunit homopolymers and recombinant H-subunit/L-subunit heteropolymers. *In vitro* experiments involving recombinant ferritin molecules showed that:

a) Both the H-subunit and L-subunit homopolymers have the capacity to incorporate iron, however, since the recombinant L-subunit homopolymer relies on auto-oxidation of iron for the initial generation of Fe^{3+} the recombinant H-subunit

homopolymer exhibits iron uptake and ferroxidase kinetics several-fold faster than the recombinant L-subunit homopolymer (9, 24, 36).

b) The rate of iron uptake increases with an increase in the H-subunit proportion from 0-35% of the ferritin molecule. A plateau is however reached with further increase in the H-subunit content (24).

c) Ferritin H-subunit homopolymers have a low ability to nucleate the generated Fe^{3+}, and therefore takes up and release iron faster since the generated Fe^{3+} is not tightly bound in an iron mineral (22).

d) Ferritin L-subunit homopolymers, when supplied with Fe^{3+} are more efficient in promoting iron mineralization than the corresponding H-subunit homopolymers (36).

e) H-subunit/L-subunit heteropolymers are more efficient in taking up iron than the parent homopolymers (36). A high synergism between the two subunits occurs in ferritins with low H-subunit content (10-30%) and high L-subunit content (70-90%), a few ferroxidase centers are sufficient to promote fast iron oxidation, and many L-subunits are needed to reduce non-specific iron hydrolysis and facilitate iron mineralization (36).

f) L-subunit homopolymers can incorporate some of the iron oxidized by H-subunit homopolymers (36).

g) The amount of soluble ferritin molecules increases sharply in heteropolymers with an L-subunit content higher than 70-80%, thus preventing the non-specific iron hydrolysis on the outside of the protein shell and the subsequent protein aggregation/precipitation (36).

h) H-subunit/L-subunit heteropolymers with low H-subunit content (18-30%) incorporate 3-4 times more iron than H-subunit homopolymers (36).

i) The most efficient heteropolymers for *in vitro* iron incorporation are structurally similar to the ferritins found in the tissues which accumulate iron, such as liver and spleen, which typically contain 80-95% L-subunit and 5-20% H-subunit. Other tissues

with lower needs for iron storage may prefer ferritins with higher H-subunit content which, having a higher ferroxidase activity, are probably more efficient for iron detoxification (32, 36).

j) L-subunit homopolymers containing nuclei will develop at the expense of L-subunit homopolymers without nuclei by autocatalytic growth processes on the surface of the iron mineral (24).

The respective and synergistic roles of the H-subunit and L-subunit of ferritin are also indicated *in vivo*, since *in vivo* H-subunit homopolymers are much less efficient than the H-subunit/L-subunit heteropolymers in taking up iron (41).

2.2.7) The release of iron from ferritin

Two mechanisms have been proposed for the release of iron from ferritin. Iron can be either released from the intact ferritin molecule or released upon the degradation of the ferritin molecule (45, 46). However, the relative importance of iron release *in vivo* by the one or the other of these mechanisms is not known. Two processes are chemically feasible for removing iron from the intact ferritin molecule – the first process the reduction of Fe^{3+} to Fe^{2+} followed by chelation of Fe^{2+} and the second the direct chelation of Fe^{3+} (21, 47, 48). The release of iron from ferritin by these two processes is accomplished with the aid of reductants and iron chelators that can cross the protein shell. Reductants and chelators gain access to the interior of the ferritin molecule through the threefold channels of the protein shell. It is suggested that the channels of the ferritin protein shell are dynamic and control the access of reductants and chelators, since reductants and chelators too large to pass through the channels can under certain conditions gain access to the interior of the ferritin molecule (47). Chaotropes can increase the access of reductants and chelators to the interior of ferritin by influencing the gating of the channel (47, 48). Various reductants and chelators, including

physiological and toxicological substances, can release iron from ferritin (48, 49, 50, 51). With the first of the two processes that remove iron from intact ferritin, i.e., the process involving the reduction of Fe^{3+} to Fe^{2+}, followed by chelation of Fe^{2+}, the reductant has to gain access to the interior of the protein shell to reduce the Fe^{3+} to Fe^{2+}. However, the formed Fe^{2+} will only leave the ferritin protein shell in the presence of a chelator (52). With the second of the two processes, i.e., the direct chelation of Fe^{3+} where the Fe^{3+} is not reduced, Fe^{3+} leaves the ferritin protein shell as an Fe^{3+}-complex. The hydrous ferric oxide cores can be reduced by one electron per iron atom accompanied by an uptake of two protons per electron from the surrounding medium (53). This is then followed by the chelation of Fe^{2+} and the transport to sites where Fe^{2+} is needed (53, 54). Effective reducing agents for the release of iron from ferritin include flavins, cysteine, glutathione, ascorbic acid and superoxide (10).

The initial rate of iron release shows a dependence on iron content, with maximum rate of release for relatively iron-poor molecules, which are one-third to one-half saturated with iron. It also depends on the surface area of the crystallite. This dependence resembles that for iron uptake and suggests a direct interaction between the surface of the iron core and the reducing agent (9, 11, 25). Furthermore, as iron atoms at the surface of the iron core could be expected to be more accessible to reducing agents than those in the interior, a last-in-first-out principle is obeyed (9). It has also been suggested that the release of iron from the intact ferritin molecule is sensitive to changes in conserved amino acids near the outside of the ferritin channels which are likely to be involved in regulating the localised unfolding of the protein shell in order to open the channels and release the reduced iron (55).

2.3) Isoferritins

2.3.1) Different H-subunit/L-subunit compositions of the ferritin protein shell

The multiple forms of ferritin have their molecular basis in the ratio of the two subunit types present, i.e., the H-subunit and the L-subunit (25). The ferritin protein shell exists as heteropolymers of various combinations of these two types of subunits (56) – a phenomenon that gives rise to the existence of isoferritins. As the roles of the H-subunit and L-subunit differ in the mineralization process, the subunit composition of ferritin will influence the metabolic properties of the assembled ferritin molecules (21, 36). H-subunit rich ferritins have been shown to accumulate and release iron faster than do L-subunit rich ferritins (9, 25, 57, 58) and it is suggested that the H-subunit rich ferritins permit more dynamic intracellular traffic of iron (25, 59). L-subunit rich ferritins apparently contain more iron than those ferritins rich in H-subunits (25, 60) and there are indications that the L-subunit rich ferritins predominate in cell types that play a role in the storage of iron (22, 25, 61, 62). However, increases in ferritins rich in the H-subunit have been shown to provide cells with increased resistance to H_2O_2 toxicity (41). It would further appear that a specific subunit composition may cater for iron storage, and that iron loading would increase the expression of the L-subunit whereupon these L-subunit rich isoferritins will sequester the bulk of the surplus iron (60, 63). In general L-subunit rich ferritins contain 1500 iron atoms or more whereas H-subunit rich ferritins contain less than a 1000 iron atoms (21). In situations of iron overload it may be advantageous to the cell to synthesize L-subunit rich ferritins, since these ferritins are not only able to store more iron but can also retain iron more firmly and turn over iron more slowly than H-subunit rich ferritins (64). The assumed role that the L-subunit rich ferritins play in the sequestration of the surplus iron during iron overload is underlined by the fact that their concentration in liver, serum and cultured cells is related to iron levels, whereas the H-subunit rich ferritins appear either to be non-affected (in liver) or negatively affected (in serum) by increases in iron concentrations (65). Furthermore,

upon iron supplementation of patients with functional iron deficiency in the presence of tissue iron overload there would appear to be a proportionately greater change in L-subunit rich ferritins than in H-subunit rich ferritins (65). Due to the H-subunit rich ferritin's more dynamic ability of iron uptake and release it would appear to be largely found in cells having high iron requirements for metabolic activities and a non-existent role in iron storage (66). Cells with a high content of H-subunit rich ferritins include erythroid cells, heart cells, pancreatic cells, kidney cells, lymphocytes and monocytes (38, 67), whereas the L-subunit rich ferritins are found predominantly in liver and spleen – organs associated with long-term iron storage (38, 62). The H- to L-subunit ratio of a specific type of cell does, however, not remain constant and the proportion of the H- and L-subunits present in the ferritin shell changes during differentiation and in various pathological states (10, 11, 22, 68).

The variations in the type of isoferritins present in erythroid cells are well studied. The presence of different isoferritins with different metabolic properties reflects the changing iron needs of the erythroid cell. The erythroid cells contain mainly H-subunit rich ferritins, which play a major role in the intracellular transport and donation of iron for the active synthesis of haem (61), particularly in immature erythroid cell precursors such as proerythroblasts and basophilic erythroblasts (63). However, when iron accumulates in erythroid tissue due either to an increase in the cellular uptake of iron or a decrease in iron usage for haem synthesis, the L-subunit rich ferritins seem to increase and to be closely related to the iron status of the cells (63, 66). The H-subunit/L-subunit ferritin composition is reported to decrease with erythroblast maturation (66), with H-subunit rich ferritin content higher in the early erythroblast fractions and decreasing with maturation. The content of L-subunit rich ferritin, apparently does not show such consistent changes with maturation (69).

The ferritin present in reticuloendothelial cells (63, 70) and other macrophage-like cells are predominantly L-subunit rich (71, 72). An exception is the ferritin in human peripheral blood monocytes, which seems to be rich in H-subunits (67). However, *in vitro* macrophages, which originate from monocytes, would appear to develop a L-subunit predominance. This phenomenon is mainly associated with the loss of H-subunits (67). At present indications are that the addition of iron can cause an increase in both H- and L-subunits despite the persistence of a very low H-subunit/L-subunit ratio. The presence of mainly L-subunit rich ferritin is in keeping with the role of the reticuloendothelial cell/other macrophage-like cells in the scavenging of effete cells and the sequestration and storage of large amounts of iron. An interesting phenomenon is the fact that the same type of process may also occur in the brain. Microglia, a macrophage-like cell present in the brain (71, 72), is responsible for the phagocytosis of cellular debris during axon remodeling and naturally occurring cell death in the developing brain (71). These cells contain predominantly L-subunit rich ferritins consistent with its role in long-term iron storage (72).

2.4) The synthesis of ferritin

The apoferritin molecule, consisting of 24 H- and L-subunits, is assembled from a cytosolic pool of available H- and L-subunits. This cytosolic pool of free H- and L-subunits is maintained by the supply of H- and L-subunits upon translation of H- and L-subunit mRNA by free polyribosomes and the proper folding of the polypeptide chains. While the composition of H- and L-subunits in the ferritin molecule is determined by the H- and L-subunits available in this pool, the quantity and composition of the H- and L-subunits in this pool of available subunits is regulated at both the transcriptional and translational levels of expression of the ferritin H- and L-subunit genes.

2.4.1) Assembly of ferritin from the pool of available H- and L-subunits

The twenty four-subunit ferritin protein shell is assembled in the cytosol from a pool of free, unassembled, or only partly assembled H- and L-subunits (21). These H- and L-subunits are synthesized by free polyribosomes and a basal concentration of free H- and L-subunits is maintained in this cytosolic pool of subunits. When this concentration rises as a consequence of the synthesis of new H- and L-subunits by free polyribosomes, subunits will be assembled into apoferritin in the cytosol near the polyribosomes. Since H- and L-subunits have the same conformation and many identical or similar amino acids are involved in the inter-subunit contact regions between H-subunit/H-subunit, H-subunit/L-subunit or L-subunit/L-subunit interactions, a complete range of subunit compositions of homopolymers and heteropolymers is possible (11, 21). However, homopolymers of ferritin consisting of either only H-subunits or only L-subunits are poorly represented in cells, suggesting the existence of preferential interactions between H- and L-subunits. This is in agreement with cross-linking experiments showing a preferential formation of H-subunit/L-subunit dimers (73).

Iron is incorporated into apoferritin or iron-poor ferritin molecules only once the ferritin shell is completely assembled from the available H- and L-subunits (21). This fraction of H- and L-subunits synthesized by free polyribosomes is destined for the intracellular sequestration of iron while a much smaller fraction of H- and L-subunits are synthesized by membrane-bound polyribosomes and once assembled the ferritin is secreted by the cell to the extracellular fluid (38).

2.4.2) Regulation of the expression of the H-subunit and L-subunit genes of ferritin

The H- and L-subunit genes of ferritin are expressed in most cells but the concentration of the assembled ferritin can vary 1000-fold among different cell types (11).

Furthermore, the composition of the H- and L-subunits in the ferritin molecule differs between different cell types, resulting in the cellular-dependent variation of isoferritin populations (21). This is achieved by the regulation of the expression of the H- and L-subunit genes of ferritin. Different mechanisms of regulation exist including transcriptional, modulation of transcript stability, translational depending on the metabolically available iron concentration and translational irrespective of the metabolically available iron concentration. The regulation of the transcription of the H- and L-subunit genes occurs mainly irrespective of the metabolically available iron concentration. However, there are indications that the transcription of the H- and L-subunit genes can be influenced by the metabolically available iron concentration in specific conditions (11, 64). The transcriptional regulatory mechanisms and stability of the mRNA determine the mRNA concentrations of the H- and L-subunits, whereas the translational regulatory mechanisms determine the magnitude of mRNA translation and the subsequent formation of the H- and L-subunits of ferritin. Therefore, the relative proportion of H- and L-subunits in the final ferritin molecules depends mostly on multiple transcriptional regulations (transcription or stability) that affect the respective proportion of H- and L-subunit mRNA in the total pool of translatable ferritin mRNA, whereas the total amount of ferritin produced in the cells depends on the magnitude of translation of the H- and L-subunit mRNA (10). Ferritin synthesis is stimulated during development, during cell differentiation, by pro-inflammatory cytokines, as well as by some hormones (74). Furthermore, a preferential increase in a specific subunit is elicited by the differential transcriptional regulation of the H- and L-subunit genes. The differentiation of various cells is associated with a consistent increase of ferritin mRNA and ferritin levels, and a preferential accumulation of the H-subunit as a consequence of a selective transcriptional regulation of the H-subunit gene needed to produce ferritin with a structure appropriate to a differentiated cell type (11, 21, 74). During inflammation, stimulation by the cytokine tumor necrosis factor (TNF), results in

transcriptional up-regulation of the H-subunit without a change in L-subunit expression. This gives rise to an increase in the H-subunit to L-subunit ratio of the produced ferritins (74). Up-regulation of the transcription of the H-subunit gene has also been found in cell lines overexpressing c-myc, in the pregnant uterus, in denervated skeletal muscle, in the atherosclerotic aorta, in response to other cytokines and after exposure to exogenous heme (10). Somewhat surprising, iron itself does not seem to affect the amount of H-subunit mRNA, although it has a stimulatory effect on the accumulation of L-subunit mRNA (10). L-subunit gene transcription and total cellular L-subunit mRNA appears to be dramatically increased by iron, whereas H-subunit transcription rates and H-subunit mRNA levels are only slightly increased (64).

2.4.3) The gene sequences of the H-subunit and the L-subunit of ferritin

The genes for the H- and L-subunits are contained on different chromosomes – the gene for the H-subunit on chromosome 11 and the gene for the L-subunit on chromosome 19 (9). The genes for the H- and L-subunit contain 3 introns and 4 exons (16) and the gene sequences for these two subunits show extensive homology in their coding regions with several common stretches of 20-30 nucleotides. However, they differ markedly in their non-coding regions (22). These differences are extremely important for differential regulation of the expression of the genes for these two subunits. Functional analysis for the 5' non-coding region for the H-subunit gene but not for the L-subunit gene has been reported. The 5' non-coding region of the H-subunit gene contains three regulatory regions. The first of these regions, the B-box, –42 to –62 nucleotides upstream from the start codon and closest to the transcription initiation site is responsive to cAMP. This B-box regulatory region is sensitive to the initiation of transcription by hormones and second messengers and binds to a protein complex termed B-box binding factor (Bbf). The B-box binding factor comprises the transcription factor NFY, the co-activator p300 and the histone acetylase p300/CBP associated factor (PCAF) (16, 21). The second

regulatory region identified in the 5' non-coding region of the H-subunit gene includes a region called the A-box at position –109 to –132 upstream from the start codon (transcription initiation site), which contains a consensus sequence for binding the polymerase II transcription factor SP1 responsible for about 50% of the activation of gene expression in several cell lines (16, 21). The third regulatory region consists of a stretch of 10 G's which are termed "G-fer" between –272 and –291 upstream from the start codon. It is suggested that binding of inhibitory factor 1 to this sequence results in the inhibition of H-subunit gene transcription (16, 21).

2.4.4) Translational regulation of the H-subunit and L-subunit mRNA expression via metabolically available iron

Ferritin is the major intracellular protein involved in storage and detoxification of iron. It is therefore not surprising that the expression of ferritin is extremely sensitive to the amount of metabolically available iron. In order to accomplish a finely tuned system of ferritin expression as a function of the size of the metabolically available iron pool (the labile iron pool) it is important that the ferritin gene structure contains sequences that sense the size of the labile iron pool (75). The 5'-untranslated region (5'-UTR) of both the H- and L-subunit mRNA contains a highly conserved 28-base sequence known as the iron-responsive element (IRE) sensitive to the metabolically available active iron (9). The IREs are comprised of cis-acting nucleotide sequences. These nucleotide sequences form stem-loop structures that contain a six-membered loop with the sequence CAGUGN (10). These stem-loop structures are recognized by trans-acting cytosolic RNA-binding proteins required for the coordinated expression of the H- and L-subunits (11). These cytosolic RNA-binding proteins, IRP1 and IRP2, cause a decrease in H- and L-subunit mRNA translation by binding to the stem-loop structures of the 5'-UTR of the respective mRNAs. IRP1 and IRP2 mediate the translational efficiency by obscuring the subsequent binding of the 43S translation pre-initiation complex needed for the initiation

of translation (76). IRP1 and IRP2 both sense and homeostatically control the metabolically available iron. For IRP1 this is accomplished by the existence of two conformationally distinct forms. IRP1 is a 90 kD iron-sulfur cluster protein. When iron is abundant it exists as a cytosolic aconitase. When iron is scarce it assumes an open configuration associated with the loss of iron atoms from the iron-sulfur cluster and the subsequent binding to the IRE stem-loop structure, acting as a repressor of ferritin translation (16). In contrast, the 105 kD IRP2 protein is regulated by degradation: IRP2 protein is abundant in iron scarcity, but is degraded rapidly in iron excess through targeting of a unique 73 amino acid sequence and subsequent oxidation and ubiquitination (16, 77). This response of ferritin synthesis to the size of the metabolically available pool of iron endows the cell with an exceptionally rapid system for increasing ferritin synthesis upon iron influx. Iron influx increases the labile iron pool and, via binding to the IRP1 and IRP2, causes a rapid increase in ferritin translation. This rapid response is achieved by a shift of stored mRNA from the ribonucleoprotein (RNP) fraction to polysomes (translational shift) (64). The translation of existing ferritin mRNA is more rapid than additional ferritin gene transcription followed by translation. The ferritin response to iron influx can thus be viewed as a protective rapid response system, allowing immediate formation of additional ferritin in which to store the surplus iron (78). Both the H-subunit and L-subunit mRNA shift from the RNP fraction to polysomes to the same extent (64). Nevertheless, the transcription of the L-subunit gene is preferentially stimulated by an increase in metabolically available iron (9) and results in an increase in the ratio of L-subunit to H-subunit mRNA, which appears first in the RNP fraction and later in the polysomes (64). This increase in the L-subunit to H-subunit mRNA ratio in the polysomes accounts for the change in the ratio of L-subunit to H-subunit protein synthesis following iron administration (64). Therefore, coordinated translational control and differential transcriptional control exists between these two genes (64).

2.4.5) Translational regulation of H-subunit and L-subunit expression irrespective of metabolically available iron

Various factors other than iron may alter the translational efficiency of the H- and L-subunit mRNA. This may be accomplished by binding of regulatory factors to specific sequences in the 5'-UTR other than the IRE or by changing the efficiency of the interaction between the IREs and IRPs. One specific sequence responsible for translational control is the twenty-nucleotide sequence downstream from the IRE known as the acute box (79). This sequence responsible for the enhancement of translation operates after iron-dependent translational initiation and the formation of the 43S ferritin mRNA scanning complex (76). Factors that can influence the efficiency of the interaction between the IRE and IRP include cytokines (80), various hormones that changes the phosphorylation status of the iron-responsive proteins (16, 79), oxidative stress – reactive oxygen species (61), haemin (61), phosphatases, hypoxia and reoxygenation (79) and nitric oxide (NO) that causes the activation of both IRP1 and IRP2. Mechanisms hypothesized to underlie NO-mediated induction of IRP binding activity include cluster disassembly (IRP1), intracellular iron chelation (IRP1 and IRP2), or increased *de novo* synthesis (IRP2) (16).

2.5) The degradation of ferritin

Two different processes can result in the degradation of cytosolic ferritin. The first of these involves the 20S proteasome enzymatic system in the cytosol and the second degradation in the lysosome by proteolytic enzymes. Depending on the type of cell, the iron status and whether ferritin is degraded free in the cytosol or within a lysosome, different amounts of iron are made available for metabolic processes. Degradation of ferritin in the cytosol results in the complete release of iron from ferritin, whereas degradation of ferritin in the confinements of a lysosome can result in the entrapment of ferritin iron (37). Iron-containing ferritin can ultrastructurally be identified in the cytosol

as either randomly dispersed ferritin particles or as clusters of ferritin particles. The ferritin clusters in the cytosol are accumulations of ferritin in which ferritin particles can be individually resolved. The existence of ferritin either as randomly dispersed ferritin particles or as clusters of ferritin particles depends on the magnitude of iron handling of the different cell types. In cell types handling relatively low quantities of iron, iron-containing ferritin occur as rare, isolated particles whereas in cell types handling greater quantities of iron such as haemopoietic bone marrow cells and cells of the reticuloendothelial system, iron-containing ferritin occurs more frequently as clusters (81). In most clusters the particles are of the iron-rich variety and thus appear larger and more electron dense than the dispersed cytosolic ferritin (81). Cluster formation prevents access of the proteins involved in the cytosolic degradation of ferritin and in this way protects the ferritin molecule against degradation. This may be a regulatory step in the pathway of ferritin degradation and iron release. However, as long as the ferritin cluster is not enclosed by a membrane, degradation of these ferritin clusters can result in the release of iron in times of iron shortage. Various studies indicated that the formation of large iron-rich ferritin particles, as a result of an increase in intracellular iron, results in the protection of ferritin molecules against degradation (38, 78, 82) and that iron-depleted ferritin is easily degraded (37, 83). The 20S proteasome enzymatic system is responsible for the degradation of damaged intracellular proteins and can recognize specifically, and degrade, oxidized proteins (84, 85). The ferritin protein shell is confronted by a multitude of possible oxidative stressors. The oxidation of Fe^{2+} by the ferroxidase center of the H-subunit results in the production of H_2O_2 which could oxidize the protein shell, and the surrounding Fe^{2+} can promote oxygen radical production by Fenton type chemistry. Oxidation of ferritin results in the loss of ferritin function and targeting of ferritin to the proteasome degradation system of the cell (84, 85). Oxidation of ferritin can also result in aggregation of ferritin molecules. Sulfhydryl groups, particularly, are oxidized followed by aggregation of ferritin as a result of the

formation of disulfide bridges between ferritin molecules (86). The H-subunit contains a cysteine at position 90 located on the BC-loop facing the exterior which is extremely susceptible to oxidation (87).

Ferritin cluster formation, however, might also stimulate the uptake of ferritin into lysosomes whereupon less iron will be released during ferritin degradation. The reason for this is that the release of iron during the degradation process relies on the accessibility of the iron core to the reducing system of the cell since dissolution of the iron core is generally determined by the reduction of Fe^{3+} to Fe^{2+}. Therefore, degradation of the ferritin protein shell in the cytosol gives $FMNH_2$ (the reducing system of the cell) easy access to the Fe^{3+}-ions and results in the complete dissolution of the iron core. The generated Fe^{2+}-ions are reutilized in metabolic processes or incorporated into new ferritin molecules. If however, ferritin is degraded within a secondary lysosome (charged with proteolytic enzymes) the iron can no longer readily be made available because it has been cut off from the $FMNH_2$ reducing system (37). Instead, digestion by lysosomal enzymes would proceed and the resulting aggregates of iron oxyhydroxide (ferritin cores) would no longer be provided with a mechanism for mobilizing and recycling their iron. This will result in aggregation of the ferritin cores and the formation of haemosiderin (37). Cytosolic degradation may therefore be the major iron turnover mechanism providing the cell with easily accessible iron for shunting into metabolic pathways, while degradation within membrane-encapsulated secondary lysosomes, with subsequent haemosiderin formation, may prevent the uncontrolled release of iron and may become prominent when there is iron overload (21, 37). Nevertheless, degradation of ferritin in lysosomes can also produce soluble iron, although these larger masses of ferritin/haemosiderin may require more time for the release of their iron contents. The iron so released would then be translocated back to the cytosol for reutilization in metabolic processes or sequestration by ferritin (10, 46, 88). Thus it seems that the

release of iron from lysosomes depends on the magnitude of aggregate formation and the subsequent deposition of iron as haemosiderin.

2.5.1) The formation of haemosiderin from ferritin

The absolute and relative amounts of iron stored in the form of the two iron reserves, ferritin and haemosiderin, vary with iron loading and cell type (15). There is slightly more ferritin than haemosiderin in the liver and spleen when total tissue iron content is normal. As total iron content increases a progressively higher percentage of iron occurs as haemosiderin (9, 15, 37, 89, 90). With overloading syndromes such as primary and secondary haemochromatosis, the iron content of haemosiderin can increase up to a 100-fold, whereas that of ferritin only increases 5- to 10-fold (13).

There is enough evidence to believe that haemosiderin is derived from ferritin as a result of degradation of the ferritin protein shell in secondary lysosomes (12, 15, 91). For instance, haemosiderin contains various amounts of degraded ferritin, as well as aggregated dense particles of irregular shape with diameters ranging from 10-75 Å, which ultrastructurally resemble iron cores (37, 90) and haemosiderin granules are recognised by anti-ferritin antibodies (21). Ferritin is frequently situated in secondary lysosomes and autophagosomes of normal cells, such as hepatocytes and macrophages but its quantity in these organelles increases greatly after loading with iron (92) – demonstrating the protective function of haemosiderin formation against the toxicity of iron. Ferritin finds its way into lysosomes by autophagocytosis and/or fusion of ferritin clusters with the lysosomal membrane. Autophagocytosis is responsible for the turnover of cellular constituents including cellular proteins and involves the formation of autophagic vacuoles by invagination of intracytoplasmic membranes enclosing a relatively large volume of cytoplasm, together with various cellular constituents (37). The autophagic vacuole receives digestive enzymes by fusion with a primary or secondary lysosome and

becomes an autophagosome (37). It is within this lysosomal organelle that the ferritin protein shell is degraded by the action of lysosomal proteases (93). It is suggested that the polymerization of ferritin (formation of oligomers of ferritin), which results in a change in solubility, heat stability and surface charge, may predispose ferritin to incorporation within lysosomes and transformation into haemosiderin (25, 90). Only once the ferritin protein shell has been modified, most probably by denaturation, resulting in the formation of insoluble ferritin molecules, does proteolytic decomposition of the ferritin protein shell by lysosomal enzymes take place (93). However, not all ferritin molecules in these lysosomal organelles are susceptible to the action of lysosomal proteases. Degradation of the ferritin protein shell results in the exposure of the iron oxyhydroxide mineral cores followed by aggregation of these oxyhydroxide particles and the formation of insoluble masses of iron oxyhydroxide (haemosiderin) (91, 92, 94). Although the main purpose of the formation of haemosiderin would appear to be protection against iron overload, these larger masses of ferritin/haemosiderin can, at a much slower rate, also release iron. This iron is then translocated back to the cytosol for reutilization in metabolic processes or sequestration by ferritin (10, 46, 88). Haemosiderin is, however, not necessarily the end product as massive quantities of iron oxyhydroxide (haemosiderin) from these secondary lysosomes, can accumulate to form cytoplasmic organelles known as siderosomes (92). The haemosiderin-containing siderosomes can thus be regarded as the end-product of secondary lysosome action in which the wall of the original secondary lysosome now encapsulates the digested ferritin iron cores (21, 37) – although clusters of electron-dense material without membranes or only partially enclosed membranes can also occur (21, 46, 82). Within siderosomes, ferritin can be identified as individual particles, in clusters, in paracrystalline hexagonal arrays, or forming circular arrangements (81). Siderosomes not only contain ferritin and haemosiderin, but occasionally also contain electron-dense amorphous or spicular iron-containing compounds which have as yet not been identified biochemically or

ultrastructurally. In cells with marked iron overload, solitary siderosomes seem to fuse and form larger bodies described as "compound siderosomes" (81).

2.5.2) The increased susceptibility of H-subunit rich ferritins to degradation

It is suggested that H-subunit rich ferritins are turning over more rapidly than L-subunit rich ferritins (22, 38, 78). Haemosiderin, which contains the degraded ferritin molecules as a result of the lysosomal breakdown of ferritin, shows the predominance of denatured subunits to be of the H-subunit type (89). It was shown that ferritin is more abundant in the iron overloaded liver than in the normal liver, and that it is richer in L-subunits displaying a L-subunit:H-subunit ratio from 5:1 to 12:1. In contrast, haemosiderin displayed a predominance of denatured H-subunits over denatured L-subunits (89). A mechanism may therefore exist for preferentially directing ferritins rich in the H-subunit into lysosomes resulting in the formation of haemosiderin containing a high proportion of denatured H-subunits. It was shown, *in vitro*, that a too great proportion of H-subunits in the ferritin protein shell result in ferritin aggregation. This may be due to the inadequacy of the ferritin protein shell to retain the formed Fe^{3+} resulting in the loss of Fe^{3+} and hydrolysis of Fe^{3+} on the outside of the ferritin molecule (21). This may be the signal for ferritin to be incorporated into lysosomes. Once inside the lysosome the presence of a large number of H-subunits in the ferritin protein shell increases the chances of degradation (60), since H-subunit rich ferritins, in the presence of denaturing conditions, are less stable than L-subunit rich ferritins (89, 95). The salt-bridge present in the L-subunit appears to be important for the differences in stabilities between H-subunit rich ferritins and L-subunit rich ferritins (57). Futhermore, H-subunit rich ferritins are more susceptible to proteolysis due to less ordered secondary structures (60). In particular, the loop L becomes more exposed and/or less immobilized when the proportion of H-subunits increases and therefore more accessible to lysosomal enzymes (25).

2.5.3) The reticuloendothelial cell and haemosiderin formation

The reticuloendothelial cell responsible for taking up and digesting effete red blood cells is confronted by tremendous amounts of iron as a result of the breakdown of the heme contained by the red blood cells. These surplus amounts of iron could result in iron-induced damage to the reticuloendothelial cell. In order to prevent possible iron-induced damage, the reticuloendothelial cell is capable of storing vast amounts of iron as haemosiderin. The reticuloendothelial cell takes up red blood cells and incorporates these red blood cells into phagocytic vacuoles, where digestion of the red blood cell and degradation of heme take place. The heme contained by the red blood cell is degraded in 5 hours. However remnants of the red blood cells could still be detected in the phagocytic vacuoles 24 hours after uptake of red blood cells by the reticuloendothelial cell. At this time, moderate numbers of free ferritin molecules are present in the cytosol. Forty-eight hours after red blood cell uptake the number of ferritin molecules in the cytosol is increased and continue to accumulate in the cytoplasm up to 96 hours after red blood cell uptake. However, from 48 hours onward ferritin is translocated into aggregates situated in autophagic vacuoles by a process of invagination of intracytoplasmic membranes followed by the formation of haemosiderin (37). The formation of haemosiderin in reticuolendothelial cells and other macrophage-like cells are influenced by inflammatory and infectious conditions. Macrophages subjected to increased oxidative stress also degrade ferritin faster (84). It is therefore suggested that during inflammatory and infectious conditions the proportion of poorly accessible (non-chelatable) iron associated with ferritin similarly increases, suggesting a pathway from non-ferritin iron to loosely associated ferritin iron to a well-sequestered non-chelatable form existing as haemosiderin (96). Cytokines such as tumor necrosis factor-α (TNF-α) and interferon-γ (IFN-γ) may be responsible for these effects during inflammatory and infectious conditions. These cytokines may increase lysosomal activity resulting in increased degradation of intracellular ferritin, leading to the formation of haemosiderin,

from which iron would be less easily liberated for subsequent extracellular release (97). *In vitro* incubation of cells with either TNF-α or IFN-γ increases the expression of ferritin H-subunit mRNA but not L-subunit mRNA (96). Such a differential regulation of ferritin subunit expression might result in increased amounts of haemosiderin formation since H-subunit rich ferritins are more susceptible to lysosomal degradation.

2.6) Ferritin in cellular organelles

2.6.1) Nuclear ferritin

H-subunit rich ferritins are transiently present in the nucleus where the presence of these H-subunit rich ferritins can be controlled by various factors such as abnormal increases in cellular iron levels, developmental status, pro-inflammatory cytokines and oxidative stress (17). A specific pathway has been shown for the translocation of cytoplasmic H-subunit rich ferritins, but not cytoplasmic L-subunit rich ferritins, into the nucleus (98). This pathway for the transportation of cytoplasmic H-subunit rich ferritins into the nucleus involves the nucleur pore complex (NPC) (17) and the translocation is an active process that requires energy in the form of ATP (17, 98). Although many proteins are translocated into the nucleus by binding of a nuclear localization signal to the nuclear pore complex, no such nuclear localization signal could be identified for H-subunit rich ferritins. However, since H-subunit rich ferritins, as well as the H-subunit rich ferritin mutant containing no ferroxidase center, are translocated to the nucleus but L-subunit rich ferritins are not, specific amino acids on the outside of the H-subunit rich ferritin molecule are implicated in this process (17). O-glycosylation is predicted as the cue for the specific translocation of H-subunit rich ferritins. Once the H-subunit rich ferritins are inside the nucleus these ferritins can form stable complexes with the DNA (99). This places the H-subunit rich ferritins in a strategic position to ward off possible oxidative onslaughts to DNA or, alternatively, to donate iron for enzyme activity and possibly the nicking of double stranded DNA that could result in relaxation of superhelical stress

(99). It was shown that not only does H-subunit rich ferritin form a stable complex with DNA (99), but that DNA also contains specific iron-binding sites (17).

Although the precise functions of H-subunit rich ferritins in the nucleus are still somewhat unclear indications are that H-subunit rich ferritin protects DNA and other nuclear constituents against oxidative damage (17), that it donates iron for iron-dependent enzyme or transcription activities (99) and that it may play a role in the regulation of the transcription of specific genes (100).

2.6.2) Mitochondrial ferritin

Mitochondrial ferritin is found in the matrix of the mitochondria under specific physiological conditions, but is low in most cell types. Mitochondrial ferritin is, in general, structurally and functionally analogous to cytosolic ferritin and its main function, similar to that of cytosolic ferritin, is to sequester surplus iron. It does, however, differ from cytosolic ferritin in various aspects (101). Where the ferritin present in the cytosol exists mainly as heteropolymers consisting of different combinations of the H- and the L-subunit, mitochondrial ferritin consists of only homopolymers of a subunit similar to the H-subunit of cytosolic ferritins (101). The mitochondrial ferritin subunit is encoded from an intronless gene located on chromosome 5q23.1, which is different from the H-subunit gene for the cytosolic ferritin. Nevertheless, a high degree of sequence homology exists between the cytosolic H-subunit and the mitochondrial ferritin subunit (101, 102). The mitochondrial ferritin subunit has about 80% sequence identity to cytosolic ferritin H-subunit in its coding region and 55% to that of the cytosolic ferritin L-subunit (103), with a structure very similar to H-subunit ferritin (18). More important, the mitochondrial ferritin subunit has complete conservation of the amino acids constituting the ferroxidase center (18). The mitochondrial ferritin gene is expressed in the cytosol as a 30 kDa polypeptide containing a N-terminal mitochondrial targeting

sequence of 60 amino acids. Once the 30 kDa polypeptide enters the matrix space of the mitochondria the targeting sequence is removed and the polypeptide processed into a subunit of 22 kDa (101). Typical hollow spherical ferritin shells containing 24 subunits are then assembled from these subunits.

As mitochondrial ferritin contains ferroxidase activity it can take up large amounts of iron. However, the ferroxidase activity is significantly lower than that of H-subunit rich cytosolic ferritin (102). This is partially due to the fact that only 12 of the 24 ferroxidase centers of mitochondrial ferritin would appear to be actively oxidizing Fe^{2+} to Fe^{3+}, and this at a reduced rate, and although a μ-peroxodiferric intermediate is formed, mitochondrial ferritin does not regenerate its ferroxidase center. The underlying reason that only some of the ferroxidase centers are involved in the oxidation process is that the side-chain of serine, in place of alanine at position 144, protrudes toward a channel that connects to the ferroxidase center – a configuration that may create steric hindrance to the movement of iron accounting for only 12 active ferroxidase centers and a stoichiometry of 24 Fe^{2+} oxidized per ferritin molecule. The oxidized Fe^{3+} is stabilized followed by nucleation. The negative patch of glutamic acid residues near the ferroxidase center, similar to that for the L-subunit of cytosolic ferritin, might constitute the nucleation site. Once nucleation has taken place autocatalytic mineral surface oxidation of iron occurs, resulting in slower oxidation of iron, but less H_2O_2 production early in the process of core formation (102).

Iron present in the cytosol transverses the double membrane of the mitochondria and is therefore readily taken up by mitochondrial ferritin (104). Mitochondrial ferritin, *in vitro*, takes up iron in a similar fashion as cytosolic ferritin, where Fe^{2+} is initially oxidized to Fe^{3+} by a ferroxidase center. This is then soon followed by iron-nuclei formation and autocatalytic Fe^{2+} oxidation on the mineral surface – since mitochondrial ferritin does

not regenerate its ferroxidase centers. This process was shown to occur at a slower rate than for cytosolic H-subunit rich ferritin. Despite the slower uptake, *in vivo*, mitochondrial ferritin displays a higher avidity for iron than cytosolic H-subunit rich ferritin. Although excess iron, even when processed by mitochondria, is said not to be retained in mitochondrial ferritin, but is sequestered into cytosolic ferritin (104), it would appear that over-expression of mitochondrial ferritin can lead to the depletion of cytosolic iron. In situations where increased amounts of mitochondrial ferritin are available, cytosolic ferritin and mitochondrial ferritin competes for cytosolic iron and since mitochondrial ferritin has a higher avidity for iron this can lead to the accumulation of iron in mitochondrial ferritin (104). This depletion of cytosolic iron dramatically increases IRP binding to IREs, followed by a decrease in cytosol ferritin levels and an increase in transferrin receptor expression (104, 105). In short it would at present appear that the high avidity of mitochondrial ferritin for iron, together with a low availability of this iron for chelation, could lower iron bioavailability in the cytosol (105). The functional implication of this is as yet not clear.

Under normal conditions most cell types contain only low amounts of mitochondrial ferritin and the stimuli for the expression of mitochondrial ferritin is still somewhat unclear. As mitochondrial ferritin does not contain an iron responsive element in its 5' untranslated region, as is the case for the H-subunit and L-subunit of cytosolic ferritin (101), one would presume that the expression of mitochondrial ferritin is not regulated by the labile iron pool as for cytosolic ferritin. However, when haem synthesis fails in patients with sideroblastic anaemia an increase in mitochondrial ferritin occurs together with the occurrence of ring sideroblasts (106).

Although details of the regulation of mitochondrial ferritin expression are not known the purpose of the presence of ferritin in the mitochondria is self-evident. The

mitochondrium is confronted with a great amount of iron since most of the metabolically active iron of the cell is processed in the mitochondria due to the synthesis of heam and iron-sulphur complexes (102, 105). Not only are mitochondria surrounded by iron, but mitochondria also produce great amounts of reactive oxygen species during oxidative respiration. This combination of iron and reactive oxygen species in the mitochondrium calls for the protection provided by mitochondrial ferritin in times of iron dyshomeostasis that may result in the oxidative damage of mitochondrial constituents (105).

2.7) Extracellular ferritin

Most of the synthesized ferritin remains within the cell where it sequesters and releases iron in order to maintain intracellular iron homeostasis. However, the content of ferritin varies between different cell types and maturation stages. The content of ferritin in peripheral white blood cells, for instance, is about 10^3 times higher than that of peripheral red blood cells, with monocytes showing the highest values (63). Aside from the presence of ferritin in the cytosol of the cell, various quantities of ferritin are found in the plasma. It is suggested that ferritin may enter the circulation either *via* secretion of ferritin by cells or through the release of ferritin from damaged cells (9). Both mechanisms probably contribute to plasma levels. Ferritin destined for intracellular iron homeostasis is synthesized on free polyribosomes whereas a small amount of ferritin may be synthesized on the rough endoplasmic reticulum for secretion into the plasma (107, 108). The range of plasma ferritin in the normal adult varies between 15-300 µg/l (9, 107) and consists mainly of glycosylated L-subunit rich ferritins containing insignificant amounts of iron, even in conditions of iron overload (10, 107, 108, 109). While the iron content of ferritin in the liver and spleen could be more than 0.2 µg Fe/µg protein in conditions of iron overload, the iron content of plasma ferritin can be as low as 0.02-0.07 µg Fe/µg protein (110).

The regulation and functions of secreted ferritins in the plasma remain an enigma. However, a quantitative relationship exists between the level of plasma ferritin and the amount of storage iron (111). In conditions of iron overload there is generally an increase in the expression of intracellular L-subunit rich ferritins, paralleled by an increase in these ferritins in the plasma (83). Although the specific cellular origin of plasma ferritin is not known (112), various experiments indicated a large contribution made by the reticuloendothelial cell. An increase in plasma ferritin levels is known to occur in parallel with the increase in reticuloendothelial cell ferritin after an increase in reticuloendothelial cell iron during phagocytosis of non-viable red blood cells (12, 109). However, elevated plasma ferritin levels are also seen in patients with parenchymal iron overload whose reticuloendothelial cells are virtually devoid of iron (12). Therefore, it would appear that the plasma ferritin reflects storage iron anywhere in the body, regardless of the type of cell in which it was stored (12). However, plasma ferritin concentration is affected by a number of factors other than the amount of storage iron including tissue necrosis, damage to ferritin-rich tissue, inflammation, infections, neoplastic disease and increased red blood cell turnover (38, 111, 112, 113). When any of these conditions are present the relationship between plasma ferritin concentration and amount of storage iron no longer holds. With tissue necrosis, as in hepatocellular injury, the increase in plasma ferritin is for instance due to the release of ferritin from the damaged cells, since the increase in ferritin is dependent on both the magnitude of cellular damage and liver iron stores (83). Furthermore, an increase in non-glycosylated, iron-rich ferritin has been reported upon tissue damage, which is indicative of the release of tissue ferritin from the damaged tissue and not as a result of active secretion (108).

It is suggested that the increase in plasma ferritin is related to an increased production of ferritin by the malignant cells in various neoplastic diseases. In leukemia the normal concentration of ferritin in circulating leukocytes is increased up to six-fold in acute

myeloblastic leukemia, more than twenty-fold in acute myelomonocytic leukemia and two- to three-fold in chronic granulocytic leukemia (109). In the presence of various solid tumours, including tumours of the breast, pancreas and liver, an increase of H-subunit rich ferritins was shown in the cells of the tumour, as well as an increase in plasma ferritin. In addition, the plasma ferritins reflected this increase in H-subunit rich ferritins of the tumour, therefore the tumours seem to produce and secrete these H-subunit rich ferritins (114, 115).

The concentration of ferritin in plasma is a function of the rate of secretion or release on the one hand, and the clearance by other tissues on the other (113). The major cell type responsible for the clearance of plasma ferritins is the hepatocyte. A specific receptor for both glycosylated and non-glycosylated ferritin has been demonstrated on the hepatocyte membrane (113). These receptors bind both the H-subunit and the L-subunit of ferritin (116). However, a significant difference is indicated between the rates of clearance for the non-glycosylated ferritins of tissues and the glycosylated plasma ferritins (113). These differences in clearance may result in a significantly longer half-life for the glycosylated, secreted ferritins in the circulation compared to that of the non-glycosylated tissue ferritins (9, 113, 116, 117).

2.7.1) The internalization of ferritin by cells

Iron delivery to cells in general, and to developing erythroid cells in particular, is largely attributed to diferric transferrin (118). However, developing erythroid cells possess on their surface, in addition to transferrin receptors, receptors that bind specifically, and internalize, H-subunit rich ferritin (118). This binding and internalization of H-subunit rich ferritins is accomplished by means of a specific saturable process and is highly regulated by the iron status of the cell (77). Since, extracellular ferritin, once internalized by the cell, is indistinguishable from intracellular ferritin, extracellular ferritin could

possibly also function as an iron donor (77). It is, for instance, known that internalized ferritin can increase the cellular labile iron pool and decrease the levels of the iron responsive protein, whereas apoferritin (containing no iron) has an opposite effect. This supports the notion that internalized ferritin is an iron donor and suggests that apoferritin behaves like an iron chelator (77).

Developing erythroid cells in the bone marrow are often found in close proximity to a central "mother" reticuloendothelial cell which "feeds" ferritin to these developing red blood cell precursors (46, 119). This process, known as rhopheocytosis, is a highly regulated pathway for iron assimilation by erythroid progenitor cells while cytosolic ferritin serves as an intermediate pool for iron for haem synthesis (118, 120, 121). Erythroid progenitor cells contain receptors for ferritin and ferritin finds its way into the erythroid precursors by receptor-mediated endocytosis (45, 118). Ferritin first binds to coated invaginations or pits before appearing in coated intracellular vesicles followed by joining of the cytosolic pool of ferritin (45).

Not only developing eryhroid precursors can take up ferritin but ferritin is also rapidly internalized by hepatocytes. This presumably also occurs via a receptor-mediated pathway. Other cells, capable of pinocytosis or more generally endocytosis, have also been shown to take up ferritin from extracellular fluid. Therefore, ferritin present intracellulary could have either been synthesized by the cell or could have been taken up (92). Internalized ferritin can subsequently be degraded, similar to intracellularly produced ferritin, within the cell (122, 123) and its iron contents released into the labile iron pool of the cell (124).

2.7.2) Other functions of ferritin

Ferritin seems to have functions beyond the control of iron bioavailability – amongst others the down-regulation of myelopoiesis and the suppression of certain immune responses. H-subunit rich ferritins are present in most biological fluids, but not, or only in low concentrations, in plasma (125). The ferritin present in plasma is mostly L-subunit rich. However, during certain disease states the concentration of H-subunit rich ferritin is increased. At present it would appear that the H-subunit rich ferritins are derived mostly from monocytes and macrophages as indicated by the secretion of H-subunit rich ferritins from many monocyte-macrophage cell lines, as well as by monocytes from blood and bone marrow (126). The release of H-subunit rich ferritins from monocytes is controlled by T-cell subsets. T-helper cells enhance release and T-suppressor cells suppress the release (9).

A number of effects have been attributed to these H-subunit rich plasma ferritins including the down-regulation of myelopoiesis and the suppression of various immune functions (112, 126). It has specifically been shown that H-subunit rich ferritins, but not L-subunit rich ferritins, down-regulate myelopoiesis (127), i.e., the growth and development of granulocytes, macrophages, erythrocytes and platelets (54, 128), both *in vitro* and *in vivo*. It has been suggested that H-subunit rich ferritins constitute part of a normal inhibitory feed-back mechanism for the proliferation of granulocyte-macrophage colony forming units (CFU-GM), multipotential colony forming units (CFU-GEMM) and erythroid burst forming units (BFU-E) (119, 128). H-subunit rich ferritin decreases the proliferation of cells during myelopoiesis by directly affecting these progenitor cells (128). Surface receptors specific for H-subunit rich ferritins have been shown on these progenitor cells (129). These effects of H-subunit rich ferritins are mediated via the ferroxidase activity of the H-subunits – most probably by inducing intracellular iron starvation (41, 125), since addition of iron completely counteracts the inhibitory effects

of the H-subunit rich ferritins (130). Not only does H-subunit rich ferritins down-regulate the production of cells involved in the immune system, but H-subunit rich ferritins also suppress various functions of immune cells. H-subunit rich ferritins can for instance exert inhibitory effects on E-rosette formation of T lymphocytes (CD2 is the surface molecule on T-lymphocytes which facilitates binding to sheep erythrocytes and the formation of so-called E-rosettes), suppress the *in vitro* responses of lymphocytes to various mitogens including PHA and con A, inhibit the mixed-lymphocyte reaction, inhibit delayed-type hypersensitivity responses, block the access to T-lymphocytes by various regulatory factors by sitting on the surface of the cells (9, 131) and decrease leukocyte migration (9). Receptors for H-subunit rich ferritins have also been found on various T-cell lines, CD4 and CD8 T-lymphocytes and on CD19 B-lymphocytes, and the expression of H-subunit rich ferritin binding sites on these cells appears to be closely and positively linked to their activation and proliferation status (118, 125). It would therefore appear that H-subunit rich ferritins may perhaps act as feedback inhibitors of activation of peripheral blood cells in a way similar to that suggested for the cells involved in myelopoiesis. Quiescent circulating lymphocytes, reticulocytes, erythrocytes and monocytes show little expression of the H-subunit rich ferritin receptor, but PHA-stimulated lymphocytes, Epo-induced BFU cells and differentiated macrophages have all been shown to express above average levels of the receptor (132) which may result in these cells being more susceptible to inhibition by H-subunit rich ferritins. Increased binding of H-subunit rich ferritins to peripheral lymphocytes have also been shown to occur in patients with malignant disorders and the magnitude of H-subunit rich ferritin binding to lymphocytes was shown to be related to the stage of the malignant process (133). It is postulated that two receptor systems exist for the binding and execution of H-subunit rich ferritin's effects. The first receptor system internalizes the bound ferritin. This system is similar to the receptor system operating in erythroid precursors. However, a regulatory effect on cell proliferation and maturation occurs, whereas in

erythroid precursors such a regulatory effect has not been observed (77, 118). The second receptor system, with a Kd three orders of magnitude lower, does not result in the internalization of the bound ferritin (77, 118). This suggests a mechanism for the regulation of cellular proliferation and maturation by ferritin not involving iron or the sequestration of iron.

2.8) In conclusion

Although we are still far from understanding the exact role of ferritin and its isoforms in health and disease new information on the functions of ferritin and the movement of iron within the protein shell are surfacing. Information on the recently identified mitochondrial ferritin (101, 103), a ferritin molecule with biochemical properties very similar to H-ferritin provides, for instance, new insight into the movement of iron within the ferritin protein shell rich in H-subunits (134).

There can be no doubt that the primary function of ferritin is to regulate the bioavailability of iron and that both the H-subunit, which contains the ferroxidase center for oxidation of Fe^{2+} to Fe^{3+}, and the L-subunit, which plays a paramount role in the subsequent nucleation of Fe^{3+} and growth of the iron-core, are required for optimal control of this bioavailability. However, even in the context of the regulation of iron bioavailability and the effects thereof many questions about the exact mechanisms and about the interplay between the H- and L-subunits remain. It would in general appear that an increase in expression of the H-subunit especially, during times of cellular stress such as occurs during inflammation, brings about rapid sequestration of iron. The H-subunit with its active ferroxidase center reduces the labile iron pool, which would result in increased IRP activity, decreased cellular proliferation and increased resistance to H_2O_2-induced oxidative stress – effects that are apparently down-regulated by prolonged iron overload or inhibition of the ferroxidase center (135, 136). Information on the

influence of the degree to which L-ferritin is expressed is still somewhat contradictory. While it is generally accepted that the L-subunit assists the H-subunit in enhancing the incorporation of iron into ferritin by providing the major nucleation sites the increased expression of the L-subunit or in the L-subunit/H-subunit ratio of ferritin is important in cells responsible for iron storage of vast amounts of iron. Although the results of a number of studies point to a role for L-ferritin in limiting the bioavailability of iron (64, 137, 138, 139), dramatic increases in the levels of L-ferritin as seen in hereditary hyperferritenemia cataract syndrome, constitutive down-regulation of L-ferritin due to a mutation in the L-subunit start codon (136) or modification of the levels of L-ferritin by transfection with siRNA and cDNA (136) do, in general, not seem to have a significant influence on iron availability or compartmentalization (136).

While the primary function of ferritin is generally considered that of an iron storage protein that regulates the bioavailability of iron, other functions, some related to iron bioavailability and others not, are emerging such as its role in cellular proliferation where L-ferritin seems to increase (136, 140, 141, 142) and H-ferritin to decrease proliferation (136), in erythropoiesis where the H-subunit/L-subunit ratio is important in supporting iron supply for haemoglobin synthesis or storage of excess iron (69) and its regulatory role in the immune system where H-subunit rich ferritins suppress certain immune responses and down-regulate myelopoiesis (112, 126). Of interest is the fact that the suggested opposing effects of H- and L-ferritin would appear to be mediated through different mechanisms with the suppressive function of H-ferritin brought about by its effect on bioavailable iron with that of L-ferritin being independent of bioavailable iron (136). In addition, H-ferritin expression would appear to have antiapoptotic effects – not related to its iron-binding function (143).

2.9) Figure 1: Heuristic presentation of intracellular ferritin metabolism

Synthesis of ferritin: Transcription (I) of the H-subunit and L-subunit ferritin genes occurs in the nucleus of the cell. This is followed by (II) the translocation of the H-subunit and L-subunit mRNA to a pool of translatable ferritin mRNA. Translation of the H-subunit and L-subunit mRNA of ferritin from this pool of translatable ferritin mRNA is largely controlled by iron from the labile iron pool (III) that contains the metabolically and catalytically reactive iron. In this pool of translatable ferritin mRNA (II) translation of the H-subunit and L-subunit mRNA, respectively, is prevented by binding of the iron responsive protein (IRP) to the iron responsive element (IRE) on the 5' non-coding stretch of H-subunit and L-subunit mRNA (II.1). Displacement of the IRP takes place upon binding of iron to IRP followed by translation (II.2). Translation of the ferritin mRNA takes place on free polyribosomes in the cytosol (IV). This is followed by folding of the translated H-subunit and L-subunit polypeptides into the α-helix rich tertiary structures of the H-subunit and L-subunit. These subunits form a pool consisting of H-subunits and L-subunits (V). From this pool of H-subunits and L-subunits the protein shell of ferritin consisting of 24 subunits symmetrically arranged is assembled (VI). The completely assembled iron-free ferritin (apoferritin) forms a pool of apoferritin containing different combinations of H- and L-subunits (VII). Ferritin can also be secreted from the cell (VIII).

Sequestration of iron (IX): Sequestration of iron is shown to occur after the ferritin protein shell is fully assembled. (IX.1) Oxidation of Fe^{2+} is performed by the ferroxidase centre of the H-subunit. This is followed by nuclei formation and iron core growth facilitated by L-subunits. Once the iron core reaches a sufficient size oxidation of Fe^{2+} can take place on the surface of the iron core. (IX.2) Oxidation of Fe^{2+} is performed by the ferroxidase centre of the H-subunit. However, if ferritin contains insufficient quantities of L-subunit for nuclei formation the formed Fe^{3+} can leave the ferritin molecule and move to a ferritin molecule containing sufficient quantities of L-subunit or

an already developed iron core, or (IX.3) the formed Fe^{3+} can leave the ferritin molecule followed by hydrolysis of Fe^{3+}-compounds on the outer surface of the ferritin molecule and ferritin aggregation.

Release of iron from ferritin (X): The release of iron from ferritin is shown to occur either by (X.1) simultaneous entry of a reductant and a chelator to the interior of the ferritin protein shell whereupon Fe^{3+} is reduced to Fe^{2+} in the confinements of the ferritin protein shell by the reductant followed by the release of Fe^{2+} as a Fe^{2+}-chelator complex, or (X.2) entry of only a chelator to the interior of the ferritin protein shell in which case Fe^{3+} is not reduced and leaves as a Fe^{3+}-chelator complex.

Distribution of ferritin (XI): Ferritin occurs in the cytosol either as dispersed ferritin particles (XI.1) or as ferritin clusters (XI.2).

Degradation of ferritin (XII): Two different processes can result in the degradation of ferritin. (XII.1) Degradation by the 20S proteasome enzymatic system, which recognises and degrades oxidised ferritin. (XII.2) Degradation by lysosome enzymes in a secondary lysosome. Ferritin finds its way into the secondary lysosome by either autophagocytosis (XII.2.1) or by targeting of ferritin to the secondary lysosome (XII.2.2). The latter can lead to haemosiderin and eventually siderosome formation.

Nuclear ferritin (XIII): Ferritin is also found in the nucleus. The ferritin in the nucleus consists of cytosolic H-subunit rich ferritins that are translocated back to the nucleus from the pool of apoferritin (VII) where these ferritins can form stable complexes with the DNA.

Mitochondrial ferritin (XV): Mitochondrial ferritin contains 24 identical subunits transcribed from a different gene than that for the cytosolic H-subunit and L-subunit (XIV). Upon transcription and translation the mitochondrial ferritin subunit polypeptide is translocated into the matrix of the mitochondria (XV.1). This is followed by the cleavage of the signal sequence and folding of the mitochondrial ferritin subunit (XV.2). Typical hollow spherical ferritin shells containing 24 subunits are then assembled from

these subunits (XV.3). Cytosolic iron from the labile iron pool (III) transverses the double membrane of the mitochondria followed by sequestration by mitochondrial ferritin (XV.4).

Processes involved in cellular iron acquisition (XVI-XVIII): (XVI) The transferrin receptor binds transferrin and is endocytosed. Upon acidification of the endosome iron is released into the labile iron pool (III). (XVII) The ferritin receptor binds ferritin and is endocytosed. Ferritin is degraded in a secondary lysosome and the released iron joins the labile iron pool (III). (XVIII) Red blood cells are phagocytosed followed by degradation and the release of heme iron by heme oxygenase. The released iron joins the labile iron pool (III).

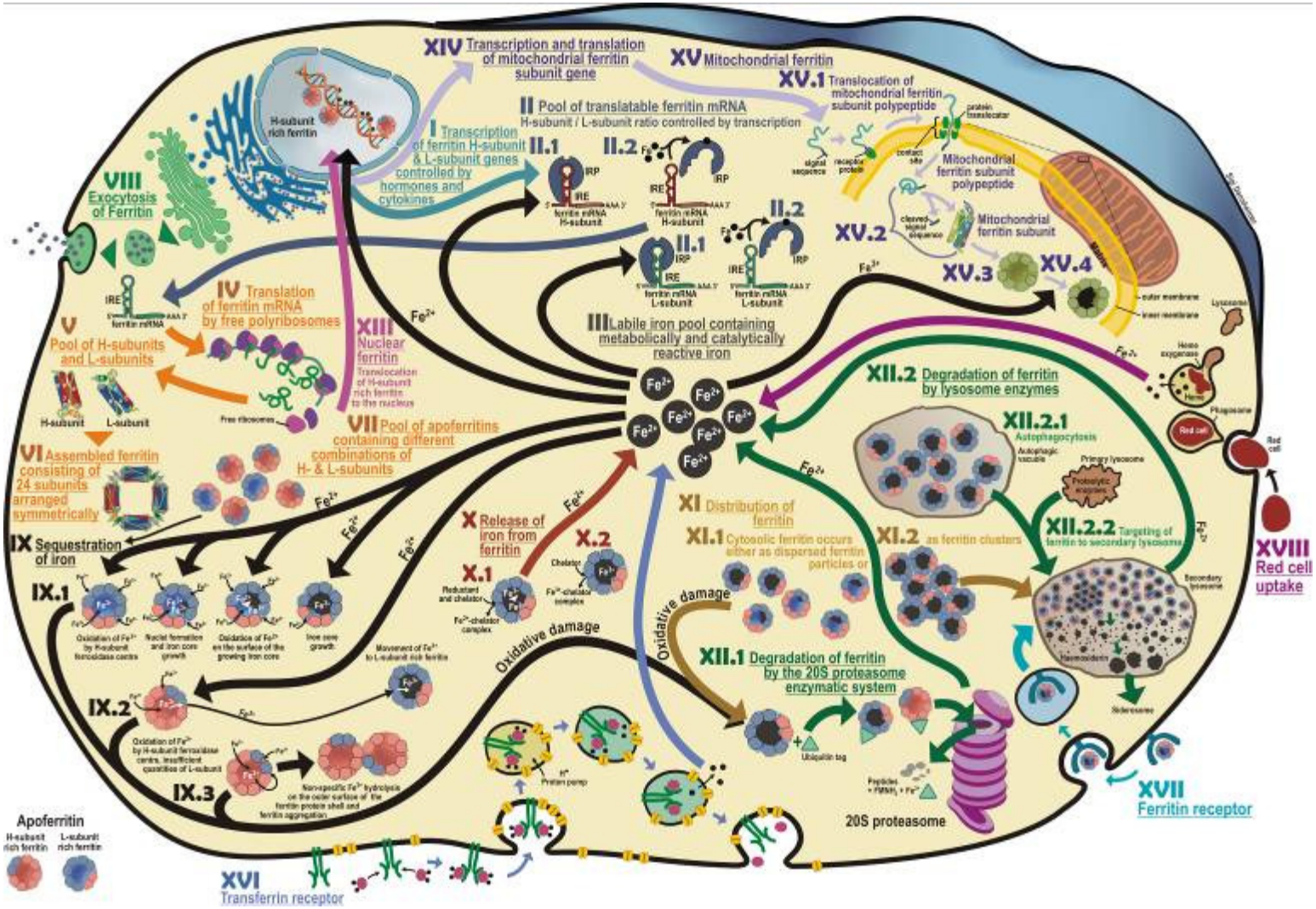
XIV Transcription and translation of mitochondrial ferritin subunit gene
XV Mitochondrial ferritin
XV.1 Translocation of mitochondrial ferritin subunit polypeptide
II Pool of translatable ferritin mRNA
H-subunit / L-subunit ratio controlled by transcription
I Transcription of ferritin H-subunit & L-subunit genes controlled by hormones and cytokines
VIII Exocytosis of Ferritin
IV Translation of ferritin mRNA by free polyribosomes
V Pool of H-subunits and L-subunits
XIII Nuclear ferritin
Translocation of H-subunit rich ferritin to the nucleus
III Labile iron pool containing metabolically and catalytically reactive iron
VII Pool of apoferritins containing different combinations of H- & L-subunits
VI Assembled ferritin consisting of 24 subunits arranged symmetrically
IX Sequestration of iron
X Release of iron from ferritin
XI Distribution of ferritin
XI.1 Cytosolic ferritin occurs either as dispersed ferritin particles or
XI.2 as ferritin clusters
XII.2 Degradation of ferritin by lysosome enzymes
XII.2.1 Autophagocytosis
XII.2.2 Targeting of ferritin to secondary lysosome
XII.1 Degradation of ferritin by the 20S proteasome enzymatic system
Oxidative damage
20S proteasome
XVIII Red cell uptake
XVII Ferritin receptor
XVI Transferrin receptor
Apoferritin

3) Ferritin and ferritin isoforms:

Protection against uncontrolled cellular proliferation, oxidative damage and inflammatory processes

The regulation of iron availability is of paramount importance for the viability of cells. Iron is, on the one hand essential for the functioning of various enzymes, while on the other, supports the formation of reactive oxygen species (ROS). Ferritin is a major iron storage protein that controls iron availability in the body. Ferritin consists of a protein shell enclosing an inner cavity where variable amounts of iron are stored as a ferrihydrite mineral. The ferritin protein shell consists of 24 subunits of two different types, the H-subunit and the L-subunit. The H- and L-subunits have different roles in the sequestration of iron. In view of the role of ferritin in iron homeostasis and the functional differences between the ferritin subunits, it does not come as a surprise that the H- and L-subunits of ferritin are differentially expressed in cells with different functions and in different disease states. Present indications are that, depending on the cell type, the developmental status, and the presence of pathological conditions, ferritins from different cells form characteristic populations of heteropolymers or isoferritins (57, 83). These heteropolymers or isoferritins are functionally distinct and, depending on the ratio of H- and L-subunits present in the ferritin protein shell, iron is differently metabolized.

Different combinations of the two subunits of ferritin give rise to the existence of isoferritins with different metabolic properties. H-subunit rich ferritins have been shown to accumulate and release iron faster than L-subunit rich ferritins (9, 25, 57, 58) and it is suggested that the H-subunit rich ferritins permit a more dynamic intracellular traffic of iron than L-subunit rich ferritins (25, 59). H-subunit rich ferritins are also responsible for the rapid sequestration of iron in situations where iron can contribute to damage to the cell. The expression of the H-subunit and the L-subunit of ferritin is controlled by

both transcriptional and translational mechanisms. However, there are indications that the level of H-subunits and H-subunit rich ferritins is strictly controlled by an additional mechanism. Cells limit the accumulation of H-subunits by differentially secreting H-subunits in variance with L-subunits. Such a mechanism could play a significant role in regulating the amount of cytosolic H-subunit rich ferritin and might protect the cell against unwarranted rapid sequestration of iron by H-subunit rich ferritins (144). L-subunit rich ferritins apparently contain more iron than those ferritins rich in H-subunits (25, 60) and there are indications that the L-subunit rich ferritins predominate in cell types that play a role in the storage of iron (22, 25, 62).

The differential expression of the H- and L-subunits of ferritin, i.e., the distribution of isoferritins are documented for various disease states. However, no clear-cut picture has emerged, either of the homeostatic changes that control the differential expression of these two subunits or the functional importance of different isoferritins. It is suggested that the optimum differential expression of these two subunits for a specific type of cell offers protection against uncontrolled cellular proliferation, increased oxidative stress and inflammatory conditions.

3.1) Ferritin and the differential expression of the H- and L-subunits of ferritin during uncontrolled cellular proliferation

Plasma ferritin is elevated in various types of cancers, irrespective of the amount of total body iron (145). It has been suggested that plasma ferritin levels can be used as tumour markers for prognostic purposes and in monitoring the activity of certain types of cancer (146, 147). In patients with solid tumors, such as pancreatic carcinoma, lung cancer and hepatoma, there is a particularly high prevalence of elevated plasma ferritin, and in patients with breast cancer, with metastasis, ferritin plasma concentrations are commonly elevated (38). Squamous cell carcinoma of the head and neck is marked by increased

plasma ferritin concentrations, which show a tendency to increase and to remain high in patients with a poor prognosis in contrast to patients with a favourable prognosis (148). The plasma ferritin concentrations of patients with haematologic malignancies are well documented. Extremely high plasma ferritin levels are seen in acute myeloblastic leukemia whereas in complete remission ferritin plasma concentrations could be returned back to normal (145). In Hodgkin's disease plasma ferritin concentrations are related to the stage of the disease, increasing from stage 1 to stage 4 (38). In non-Hodgkin's lymphoma a remarkable correlation exists between plasma ferritin concentrations and tumour histology. The highest plasma ferritin concentrations are found in patients with active histiocytic lymphoma and the lowest plasma ferritin concentrations in patients with lymphocytic lymphoma whereas intermediate plasma ferritin concentrations are found in patients with mixed histology (38). Many factors are suggested to contribute to the hyperferritinaemia associated with cancer, including inflammation, hepatic necrosis due to metastasis and chemotherapy, blood transfusions and a decrease in hepatic clearance of ferritin (149). In addition, a modified and increased synthesis and secretion of ferritin by tumour cells occur (146, 149, 150, 151). In many instances the increased ferritin is shown to be H-subunit rich (149, 152, 153, 154, 155, 156) and it has been suggested that the measurement of H-subunit rich ferritin may be of value in the diagnosis of malignancy (154).

3.1.1) Cellular proliferation, ferritin subunits and cancer

The most common feature of cancer is the abnormal proliferation of cells, either contained in a specific location, or following metastasis at different sites involving various organs. Iron is a necessary element for cellular proliferation and it is generally accepted that rapidly dividing cells require more iron for their growth and metabolism than resting cells. It is also known that cells normally display an increase in cellular proliferation upon an increase in the labile iron pool (138). The reason for the high need

for iron is that iron is necessary for the functioning of different enzymes involved in cellular proliferation, including ribonucleotide reductase, which controls a rate-limiting step in DNA synthesis, and for various mitochondrial enzymes involved in the metabolism of the cell (151, 157). Not only do malignant cells require more iron for growth and metabolism than normal cells, but the cellular labile iron pool can in turn modulate the magnitude of induced cellular proliferation by the oncogene H-ras (158). One way in which to bring about an increase in the cellular labile iron pool is by suppression of ferritin synthesis. The transcription factor encoded by the proto-oncogene c-MYC, which is responsible for proliferation of normal cells, can during uncontrolled expression, result in cellular transformation and excessive cellular proliferation. c-MYC can, where appropriate, activate or repress target genes in order to bring about cellular proliferation (159). The expression of the H-subunit gene is shown to be down-regulated by c-MYC and to be essential for the control of cellular proliferation and transformation by c-MYC (159). This is in agreement with the fact that the H-subunit is responsible for controlling the labile iron pool and that down-regulation of H-subunit expression would result in an increase in the labile iron pool.

3.1.2) Cellular differentiation

Ferritin is also implicated in the differentiation of cells. Cellular differentiation entails the expression of specific proteins in order for the cell to establish a differentiated phenotype and to perform specialized functions. Cellular differentiation is a controlled event and can be activated by a vast number of stimuli depending on the type of cell. Oligodendrocytes are for instance responsible for the synthesis and maintenance of central nervous system myelin and the differentiated phenotype of the oligodendrocyte will therefore express all proteins necessary for the assembly of large quantities of membranes (160). The stimuli responsible for inducing differentiation of oligodendrocytes involve the adhesion of the oligodendrocyte to a substrate. It was

shown that the expression of the H-subunit of ferritin is up-regulated upon substrate-adhesion and the induction of oligodendrocyte differentiation (160). In various other cell types, including pre-adipocytes, erythroid cells, neuronal cells and monocyte to macrophage differentiation, the expression of the H-subunit of ferritin is similarly up-regulated upon differentiation (74, 161, 162). In various cancers cellular differentiation can bring about the suppression of tumourigenicity since cellular differentiation results in cell cycle arrest and inhibition of cellular proliferation. Differentiation of, for instance colon carcinoma cells is, as for normal cells, accompanied by an increased expression of the H-subunit of ferritin (163). Metastasis is characteristic of the uncontrollable progression of cancer whereas tumour cells displaying a more differentiated phenotype generally show less metastatic activity. H-subunit rich ferritins may perhaps be involved in curtailing the spread of cancer as it was shown that the over-expression of the H-subunit of ferritin in a rat transitional cell carcinoma progression model is associated with less tumour cell metastasis (164). It would thus appear that the increased expression of the H-subunit of ferritin might be involved in the initiation of cellular differentiation and therefore the prevention of uncontrolled cellular proliferation and metastasis.

3.1.3) Programmed cell death (apoptosis)

Programmed cell death or apoptosis, in which cells actively participate in their own self-destruction, is an important process in eliminating abnormally proliferating cells. Once again ferritin is implicated. Many tumour-suppressor genes can induce apoptosis upon DNA damage or other cellular distress signals. One such tumour-suppressor gene, the transcription factor p53, is up-regulated in many types of malignant cells in an attempt to kill-off rapidly proliferating cells by activating the programmed cell death pathway. A shift in the H-subunit/L-subunit ratio would appear to occur in such conditions. H-subunit ferritin mRNA is for instance differentially up-regulated in an immortal human breast epithelial cell line treated with chemical carcinogens and in various breast cancer

cell lines, in contrast to mortal or primary human breast epithelial cell lines (153). Increased H-subunit ferritin mRNA was also detected in breast cancer tissue samples and tissue with ductal hyperplasia had higher expression of H-subunit than normal adjacent mammary tissue (153). This up-regulation of the H-subunit of ferritin may be an attempt of the cell to induce apoptosis since a significant correlation was shown between H-subunit and p53 expression in primary hepatic carcinoma tissue compared to non-malignant liver and healthy tissue (165).

From the above discussion one can perhaps speculate that an increase in the H-subunit of ferritin may play a role in curtailing excessive cellular proliferation and, although conclusive evidence does not exist, it would appear that a) hyperferritinemia with an increase in the H-subunit/L-subunit ratio occurs in many types of cancers, b) the H-subunit may perhaps stimulate differentiation in an attempt to curtail uncontrolled proliferation and c) that H-subunit expression is up-regulated together with p53 expression as part of the process of apoptosis. Whether H-subunit rich ferritins in this context act through the modulation of iron or as a growth factor is unclear.

3.2) The expression of the H- and L-subunits of ferritin in diseases and toxicities associated with an increase in reactive oxygen species (ROS) generation

Oxygen free radicals are implicated in the pathogenic processes of various diseases and toxicities and ROS are known to damage critical cellular components including DNA, proteins and lipids (166). The two reactive oxygen species, superoxide and hydrogen peroxide, are virtually always present in cells due to basal cellular processes and could also be formed upon activation of polymorphonuclear leucocytes and macrophages. However, it is only in the presence of iron that these two reactive oxygen species become highly toxic. Superoxide and hydrogen peroxide can interact to form the very toxic

hydroxyl radical in the Haber-Weiss reaction. However, the reaction rate for this reaction is very low, but when iron is present and once reduced by superoxide, it can rapidly form hydroxyl radicals in a reaction with hydrogen peroxide (167, 168).

Ferritin plays a prominent role in the protection of cellular constituents against such possible oxygen free radical onslaughts by sequestering iron in a non-toxic form. This is due to modulation of the expression of ferritin by a variety of factors associated with oxidative stress that act either directly on gene expression, or indirectly via the modification of the activity of the iron regulatory proteins (139, 169, 170). In disease states associated with an increase in reactive oxygen species the H-subunit of ferritin is preferentially up-regulated. Ferritin containing a high proportion of H-subunits increases the resistance against oxidative challenges since H-subunit rich ferritins are capable of rapidly sequestering redox-active iron, thus suppressing the formation of reactive oxygen species (138, 171, 172, 173).

3.2.1) Oxidative stress and neurodegenerative diseases

The brain contains high levels of iron and an uneven cerebral distribution of iron exists with high levels in the basal ganglia (substantia nigra, putamen, caudate nucleus and globus pallidus), red nucleus and dentate nucleus (174). The brain accumulates iron with age due to the slow turnover rate of iron and a continuous up-take of iron throughout life (175). The amount of iron accumulating in each brain region varies (176). Such an accumulation of iron could result in increased oxidative damage if increases in anti-oxidative mechanisms do not match that of iron.

The expression of ferritin has been shown to increase in different brain regions with normal aging and this, as a result of ferritin's iron-sequestering capabilities, would provide the brain with additional protection against age-related increases in oxidative

stress (176, 177, 178). The two subunits of ferritin are expressed to different extents in different brain regions and it changes with normal aging. In the young brain the H-subunit of ferritin is generally more abundant than the L-subunit – except in the globus pallidus where the ratio of H-subunit to L-subunit is 1:1. With normal aging both the H- and the L-subunit of ferritin increases. The H-subunits of ferritin increase in most brain regions in a remarkably consistent pattern, i.e., approximately two-fold. However, in the globus pallidus the increase is eight to ten-fold greater than the increase in the other regions. The increase in L-subunit expression is more region-specific than that of the H-subunit. In addition, the age-related expression of the H- and L-subunit of ferritin shows an increase in the H-subunit/L-subunit ratio for all brain regions, except for the substantia nigra where this ratio decreases with aging (176).

It has been suggested that the pathology of various neurodegenerative diseases, including Parkinson's disease and Alzheimer's disease, involves an excessive increase in iron in specific brain regions and that premature increases in iron may be an early risk factor for the onset of neurological disease (175). In both Parkinson's disease and Alzheimer's disease the normal age-associated increase in the expression of ferritin and the expected change in the H-subunit/L-subunit ratio fail to occur (176, 179, 180). An increase in iron content without the concomitant up-regulation of ferritin expression and the expected change in the H-subunit/L-subunit ratio would leave these brain regions vulnerable to oxidative stress. In Parkinson's disease, dopaminergic brainstem nuclei, particularly the substantia nigra pars compacta is destroyed. Clinical evidence that iron-induced oxidative damage may in fact be involved was provided by the observation of an increase in the total iron content without an increase in ferritin expression in the substantia nigra. Evidence of excessive oxidative damage was substantiated by the presence of increased basal levels of malondialdehyde and lipid hydroperoxides, markers of lipid peroxidation, as well as by a decrease in levels of reduced glutathione (179).

3.2.2) Oxidative stress and vascular disorders

The endothelium plays an important role in the regulation of vascular function and integrity. It produces many mediators responsible for the regulation of vasodilatation and vasoconstriction, blood-clotting including pro-thrombotic, anti-thrombotic and fibrinolytic substances, as well as molecules promoting the adhesion of platelets, monocytes and leukocytes (181). The endothelium is highly susceptible to damage caused by reactive oxygen species. Reactive oxygen species, for instance, cause changes in the ionic permeability of the endothelium (182), modulation of the fibrinolytic response of the endothelium (183), changes in the endothelium's contribution to platelet aggregation (184) and abnormal functioning of endothelium-derived relaxing factor (185, 186, 187, 188). Iron is responsible for generation of the very toxic hydroxyl radical via Fenton-type chemistry and these reactive oxygen species are implicated in the pathogenesis of numerous endothelium-associated vascular disorders including atherosclerosis, microangiopathic haemolytic anaemia, vasculitis and reperfusion injury (189). Oxidant-mediated injury potentiated by iron includes direct damage to the endothelial cells by reactive oxygen species, as well as promotion of the conversion of low-density lipoprotein to cytotoxic oxidized products. This iron-catalyzed oxidant injury to endothelial cells can be attenuated by the addition of exogenous iron chelators such as the lazaroids and desferoxamine (190).

One abundant source of redox-active iron in the vasculature is haem and exposure of endothelial cells to haem greatly enhances cellular susceptibility to oxidant-mediated injury (189). The most important source of haem within the vascular endothelium is haemoglobin. Upon oxidation of haemoglobin the released haem, a hydrophobic iron chelate, can be transferred to the endothelium and is rapidly incorporated into the endothelial cells (189). As a mechanism of defense against such free haem-induced toxicity cells, including endothelial cells, up-regulate haem oxygenase-1, as well as ferritin.

The expression of haem oxygenase-1 can be induced by a number of stressful stimuli including its own substrate haem, various haem proteins, heavy metals, UVA radiation, hypoxia, hyperoxia, ischaemia-reperfusion and many others (191). Haem oxygenase-1 is a haem-degrading enzyme that opens the porphyrin ring, producing biliverdin, carbon monoxide and free redox-active iron (192). Ferritin, which is simultaneously up-regulated, effectively sequesters the released iron and prevents the iron from taking part in oxidant-mediated cellular damage (189, 193). Aspirin has been shown to increase endothelial resistance to oxidative damage in bovine pulmonary artery endothelial cells by inducing the synthesis of ferritin, up to five-fold above basal levels, in a time and concentration-dependent fashion (194). In addition to the endothelial defense strategies against haem iron, local macrophages also play a role. Vascular associated macrophages can endocytose senescent erythrocytes or free haemoglobin as a haptoglobin-haemoglobin complex (195). After the breakdown of the haemoglobin by the macrophage the haem iron is released followed by sequestration of the iron by macrophage ferritin. Haem iron leads to increased synthesis and secretion of ferritin by macrophages (196). Erythrophagocytosis and haemoglobin catabolism by macrophages occur in microvessel-rich regions and contribute to the formation of iron deposits and ferritin induction in atheroma (195). However, the accumulation of iron in atherosclerotic lesions in the macrophage is known to exacerbate iron-induced damage to the vasculature by promoting, amongst others, LDL oxidation by reactive oxygen radical production (196).

The effect of haem on ferritin and ferritin subunit expression is experimentally confirmed. In haemin (ferriprotoporphyrin IX – the oxidized prosthetic group of haemoglobin) treated cells the iron uptake capacity of cells was seen to be greatly enhanced and to contain approximately three times more iron per ferritin molecule. The expression of the H-subunit of ferritin was elevated 12- to 15-fold whereas the L-subunit

was essentially unchanged. These results are consistent with the idea that H-subunit rich ferritins sequester redox active iron rapidly and copiously, thereby enhancing cellular resistance to oxidative damage (172). The same shift towards H-subunit rich ferritin can occur during post-ischaemic reoxygenation where iron could catalyse the production of reactive oxygen species. Over-expression of the H-subunit gene has been reported to provide protection against such ischaemia-reperfusion injury and to prevent cellular damage upon organ transplantation (197). In addition, the H-subunit may in these circumstances prevent cells from undergoing apoptosis induced by reactive oxygen species (193). The up-regulation of the H- to L-subunit ratio in similar conditions is, however, not uniformly supported. A significant induction of both the H- and L-subunit mRNA of ferritin was reported by Chi *et al* as a result of ischaemic events and it was shown that the H- and L-subunit mRNA can remain elevated for up to 336 hours after the onset of reperfusion. This increase in H- and L-subunit of ferritin was associated with iron deposits in areas where cell death and tissue necrosis was noted (198).

More evidence for the up-regulation of ferritin expression by ischaemic injury was seen in the myocardium, cerebral arteries and spinal cord. Ischaemia was seen to result in an enhanced ferritin content relative to the degree of ischaemia in the myocardium (199). Ferritin expression is also up-regulated during bleeding episodes, since haemolysis will substantially contribute to deleterious free redox active iron. In adventitial fibroblasts of cerebral arteries and cells in the subarachnoid space the increase in ferritin levels are known to persist for prolonged periods of time after subarachnoid haemorrhage (200). With traumatic spinal cord injury with haemorrhage, ferritin expression in microglia and astrocytes was seen to be significantly increased and to correlate with the severity of the injury (201).

3.2.3) UV-induced oxidative damage

Ultraviolet irradiation results in increased oxidative stress in various cell types exposed to sunlight, including the corneal epithelial cell and epidermal and dermal fibroblasts. Free iron, by supporting the Fenton reaction is known to exacerbate UV-induced oxidative damage to cellular constituents. As for other cell types challenged by increased reactive oxygen species generation, corneal epithelial cells and epidermal and dermal fibroblasts also display an increase in ferritin expression upon UV irradiation (202, 203). It has even been shown that corneal epithelial cells that contain increased amounts of nuclear ferritin show less DNA breakage (203). Although over-expression of the L-subunit of ferritin does not seem to have a major effect on cellular iron distribution or to protect lens epithelial cells against UV irradiation, over-expression of the H-subunit of ferritin appears to result in increased storage of iron in ferritin as well as protection of cells from UV (photo-oxidative stress) damage (204).

One can summarize by saying that ferritin synthesis in general would appear to be up-regulated in the presence of an oxidative onslaught. Indications are that, an increase in H-subunit rich ferritins could be the mediating factor in the protection against oxidative damage. The H-subunit rich ferritins accomplish this through the rapid sequestration of iron, thus preventing the generation of highly toxic oxygen radicals.

3.3) The expression of ferritin and the differential expression of the H- and L-subunits of ferritin in inflammatory conditions

The inflammatory response can be triggered by mechanical injury, chemical toxins, invasion by microorganisms and hypersensitivity reactions (205) and may be described as the body's attempt to invade the area of tissue damage, contain the response to an isolated area, destroy the initial injurious agent, break down damaged tissue and finally repair/regenerate the destroyed tissue. As part of the inflammatory response neutrophils

and macrophages are recruited to the inflammatory site. Neutrophils and macrophages are responsible for phagocytosis and degradation of microorganisms, immune complexes and necrotic tissue. These phagocytes engulf the substance and encapsulate it in a membrane-bound phagocytic vacuole (phagosome). Many different active substances including enzymes and oxygen radicals are delivered to the phagosome to destroy and degrade the phagocytosed material (206).

Oxygen radicals, i.e., molecules containing unpaired electrons are generated in large amounts during infectious conditions and inflammatory responses (207). They react with proteins, lipids and nucleic acids, resulting in degradation of the phagocytosed material in the confinements of the phagosome in the neutrophil and macrophage. However, large amounts of these toxic metabolites leak to the fluids and tissues in the area of the inflammatory reaction and by reacting with cellular constituents can result in substantial damage (206, 208). Iron, due to its role in Fenton-type chemistry, can result in exacerbation of oxygen radical production. Such an increase in unwanted oxygen radical production due to toxic amounts of iron can be seen in chronic inflammatory conditions such as rheumatoid arthritis. An increase in the iron content in the synovium is, for instance, present in rheumatoid arthritis (209) and a significant correlation exists between thiobarbituric acid-reactive material (lipid peroxidation product), the amount of iron in the synovial fluid and the inflammatory activity of the disease (210). Furthermore, when anaemic rheumatoid arthritis patients receive iron supplementation, lipid peroxidation is stimulated resulting in worsening of the synovial inflammation (211).

In general, a reduction in the bioavailability of iron will offer protection against cell injury by hydroxyl radicals that are generated from neutrophil- and macrophage-derived superoxides (212). Iron sequestration by cells in the zone of inflammation may therefore provide protection against the free radical assault (76). This role of host cell protection

against an increase in the free radical onslaught is consistent with observations that a reduction in ferritin sensitizes cells to pro-oxidant cytotoxicity, and that overexpression of ferritin reduces reactive oxidant species in cells challenged by oxidants and by implication reduces the oxidative toxicity (112). Macrophages, although contributing to the production of ROS, can also provide protection against it by reducing the available iron.

3.3.1) The macrophage, iron metabolism and ferritin in inflammatory conditions

The macrophage and other macrophage-like cells are responsible for handling large amounts of iron in the body. In inflammatory conditions the magnitude of iron released by the macrophage is strongly influenced. Inflammation produces a shift in iron handling by the macrophage in favour of iron storage, in time leading to haemosiderosis of the macrophage (9, 12, 213) and a corresponding hypoferraemia (9, 96, 97). It has been proposed that this abnormal retention of iron by the macrophage is caused by an increase in ferritin synthesis as a non-specific acute-phase reactant of inflammation (9, 214). This increase in ferritin synthesis occurs prior to the reduction of serum iron levels and is considered to result in a diversion of iron from the intracellular labile iron pool to ferritin and subsequently to haemosiderin (9, 215, 216, 217, 218). The increase in ferritin expression by the macrophage mostly influences the early phase of iron release. In normal conditions two-thirds of the iron entering the macrophage/reticuloendothelial system (RES) is released during this phase, but an increase in ferritin expression can result in a decrease in the release of iron during this phase to only 10% of the iron entering the macrophage/RES (218, 219). However, the slow release phase of iron from the macrophage is also influenced and can result in a situation where 33% of the iron is still present in storage form in the macrophage/RES after 60 days (220). Furthermore, once the macrophage and other macrophage-like cells have been activated, as occurs during inflammation, these cells express increased levels of transferrin receptors (96) and

are therefore able to acquire increased amounts of iron by endocytosis of the iron-transferrin-transferrin receptor complex. The increase in iron uptake via this route will contribute to the high magnitude of iron sequestration and to the ensuing haemosiderosis that develops in macrophages and other macrophage-like cells. These iron-withholding mechanisms are implemented as a defense strategy in order to deplete biologically active iron in the zone of inflammation or, once the inflammatory response cannot be contained, systemically (221). This is important because elevated levels of available iron can promote both the growth of infectious microorganisms and oxidative stress. It has also been shown that up-regulation of H-subunits results in the inhibition of pro-inflammatory cytokine induced apoptosis by suppressing reactive oxygen species generation (222). This probably occurs as a negative-feedback anti-inflammatory response.

3.3.2) Increased ferritin expression as a result of cytokine activation

Cell-to-cell communication molecules known as cytokines play an important role in mediating the process of inflammation (205). Inflammation progresses as a result of the action of pro-inflammatory cytokines, including Il-1, TNF, IFN-γ, Il-12, Il-18 and the granulocyte-macrophage colony-stimulating factor and is resolved by anti-inflammatory cytokines such as Il-4, Il-10, Il-13, IFN-α and TGF (223). Ferritin is considered to be one of the acute phase proteins and its expression has been shown to be increased by various cytokines (80, 214). Cytokine-induced increases in intracellular ferritin expression during the acute phase response can result in the sequestration of metabolically available iron in the macrophage/RES and the subsequent decrease in plasma iron. It has in fact been shown that activation of macrophages by cytokines such as TNF-α and Il-1 could result in the slower release of iron compared to non-stimulated macrophages, thus supporting the proposed role of cytokines in ferritin-mediated iron sequestration by macrophages (215, 224). The concept that an increase in intracellular

ferritin, as well as secretion of ferritin, can be induced by pro-inflammatory cytokines as part of the acute phase response is further supported by the fact that the secretion of ferritin was shown to be stimulated by cytokines in a primary human hepatocyte culture where IL-1α and Il-6 induced a transient secretion of ferritin at 24 hours, followed by a decline to baseline, and TNF treatment resulted in a sustained increase in ferritin secretion (16).

Cytokines reported to have the ability to induce ferritin expression include Il-1α, Il-1β, Il-2, Il-6, TNF-α, and IFN-γ – all pro-inflammatory cytokines (Table 1). These cytokines modulate ferritin expression by both transcriptional and translational mechanisms (80), but largely by an increase in the rate of transcription of the ferritin gene (16, 225). The expression of the ferritin subunits is differentially regulated by cytokines and it is mostly the H-subunit of ferritin that is increased by cytokine induction at variance with the L-subunit (225). *In vitro* experiments with various cell types showed an increase in H-subunit expression relative to L-subunit expression upon cytokine activation (Table 1).

The role of ferritin in inflammatory conditions can be summarized by saying that pro-inflammatory cytokines increase the production of ferritin early in the inflammatory response and that H-subunit rich ferritins are preferentially up-regulated at variance with L-subunit rich ferritins. This process does not only protect the body against reactive oxygen species generation, but in addition reduces the bioavailability of iron needed by pathogenic microorganisms.

3.4) Table 1: The effects of cytokines on the expression of H-subunits and L-subunits of ferritin

Cytokine	Cell type	Effect/H-subunit	Effect/L-subunit
Il-1β	Human Hepatoma Cells (212)	Not determined ↑ translation	↔ mRNA ↑ translation
Il-1β	Human Hepatoma Cells (226)	↔ mRNA ↑ translation 15-fold	↔ mRNA ↑ translation 6-fold
Il-6	Human Hepatoma Cells (226)	↔ mRNA ↑ translation 3-fold	↔ mRNA ↑ translation 4-fold
Il-1β	Primary Human Umbilical Vein Endothelial Cells (226)	↑ expression 4.8-fold ↔ mRNA	↑ expression 2.4-fold ↑ mRNA 30%
TNF-α	Mesenchymal, Myo-blasts, Myocytes, Adipocytes, Fibro-blasts (16)	↑ mRNA	↔ mRNA
Il-1α	Mesenchymal, Myo-blasts, Myocytes, Adipocytes, Fibro-blasts (16)	↑ mRNA	↔ mRNA

TNF-α	U937 Macrophage (16)	↑ mRNA	↔ mRNA
INF-γ	U937 Macrophage (16)	↑ mRNA	↔ mRNA
Il-1β	U937 Macrophage (16)	↔ mRNA	↔ mRNA
TNF-α	A549 Type-2 Alveolar Pneumocyte (16)	↑ mRNA	↔ mRNA
Il-1β	A549 Type-2 Alveolar Pneumocyte (16)	↑ mRNA	↔ mRNA
Il-1β	THP-1 Monocyte (227)	↔ mRNA	↔ mRNA
TNF-α	THP-1 Monocyte (227)	↑ mRNA	↑ mRNA
TGF	THP-1 Monocyte (227)	↔ mRNA	↔ mRNA
PDGF	THP-1 Monocyte (227)	↔ mRNA	↔ mRNA
Il-1	Aortic Smooth Muscle Cells (227)	↑ mRNA	↔ mRNA
TNF-α	Aortic Smooth Muscle Cells (227)	↑ mRNA	↔ mRNA

TGF	Aortic Smooth Muscle Cells (227)	↔ mRNA	↔ mRNA
PDGF	Aortic Smooth Muscle Cells (227)	↔ mRNA	↔ mRNA
TNF-α	Alveolar Epithelial Cells (228)	↑ subunit	↑ subunit but less
TNF-α	Primary Human Myoblasts (225)	↑ mRNA	↔ mRNA

3.5) In conclusion

Ferritin is a major iron storage protein that regulates the bioavailability of iron in the body. Although H- as well as L-subunits of ferritin are both necessary for sequestration and release of iron into and from ferritin, different isoferritins seem to have preferential functions. While, under basal conditions, the L-subunit rich isoferritins would appear to be the major storage depots and predominate in tissues with iron storage functions, H-subunit rich ferritins predominate in metabolically more active tissues and are up-regulated in conditions of stress. H-subunits seem to be the up-regulated subunits with, preferentially, regulatory functions. H-subunits are up-regulated when the need for rapid change of iron availability arises – very often to suppress unwarranted iron-stimulated events, such as the formation of toxic radicals, uncontrolled proliferation of cells or the growth of pathogenic microorganisms.

4) Aim of the study

The primary aim of the present study is to quantitatively measure the expression of the H-subunit and L-subunit of ferritin in the bone marrow macrophage and cells of the erythron in patients with chronic immune stimulation. A second aim is to investigate the possible role that the expression of the H-subunit and L-subunit of ferritin may have in the establishment and maintenance of an iron transfer block in patients with chronic immune stimulation.

Due to the amount of data it was necessary to divide the thesis into two volumes for binding purposes. Volume 1 contains the thesis proper. Volume 2 contains raw data, photographs and micrographs and experimental evaluation of the technique for ultrastructural immunolocalisation of the H-subunit and L-subunit of ferritin.

5) References

1) Brittenham GM. The red cell cycle. In: Brock JH, Halliday JW, Pippard MJ, Powell LW editors. Iron metabolism in health and disease. London: W.B. Saunders Company Ltd; 1994. p. 31-62.

2) Chung J, Wessling-Resnick M. Molecular mechanisms and regulation of iron transport. Critical Reviews in Clinical Laboratory Sciences 2003; 40(2): 151-182.

3) Donovan A, Roy CN, Andrews NC. The ins and outs of iron homeostasis. Physiology 2006; 21: 115-123.

4) Syed BA, Sargent PJ, Farnaud S, Evans RW. An overview of molecular aspects of iron metabolism. Hemoglobin 2006; 30(1): 69-80.

5) Pantopoulos K. Iron metabolism and the IRE/IRP regulatory system. Annals of the New York Academy of Sciences 2004; 1012: 1-13.

6) Cavill I. Erythropoiesis and iron. Best Practice & Research Clinical Haematology 2002; 15(2): 399-409.

7) Andrews NC, Schmidt PJ. Iron homeostasis. Annual Reviews in Physiology 2007; 69: 69-85.

8) Conrad ME, Barton JC. Factors affecting iron balance. American Journal of Hematology 1981; 10: 199-225.

9) Worwood M. Ferritin. Blood Reviews 1990; 4: 259-269.

10) Ponka P, Beaumont C, Richardson DR. Function and regulation of transferrin and ferritin. Seminars in Hematology 1998; 35(1): 35-54.

11) Theil EC. The ferritin family of iron storage proteins. Advances in Enzymology and Related Areas in Molecular Biology 1990; 63: 421-449.

12) Finch CA, Huebers HA, Cazzola M, Bergamaschi G, Bellotti V. Storage iron. In: Albertini A, Arosio P, Chiancone E, Drysdale J editors. Ferritins and isoferritins as biochemical markers. Amsterdam: Elsevier Science Publishers; 1984. p. 3-21.

13) Powell AK. Ferritin. Its mineralization. Metal Ions in Biological Systems 1998; 35: 515-561.

14) Persson HL, Nilsson KJ, Brunk UT. Novel cellular defences against iron and oxidation: ferritin and autophagocytosis preserve lysosomal stability in airway epithelium. Redox Report 2001; 6(1): 57-63.

15) Ford GC, Harrison PM, Rice DW, Smith JM, Treffry A, White JL *et al.* Ferritin: design and formation of an iron-storage molecule. Philosophical Transactions of the Royal Society of London 1984; 304: 551-565.

16) Torti FM, Torti SV. Regulation of ferritin genes and protein. Blood 2002; 99(10): 3505-3516.

17) Thompson KJ, Fried MG, Ye Z, Boyer P, Connor JR. Regulation, mechanisms and proposed function of ferritin translocation to cell nuclei. Journal of Cell Science 2002; 115: 2165-2177.

18) Levi S, Arosio P. Mitochondrial ferritin. International Journal of Biochemistry and Cell Biology 2004; 36: 1887-1889.

19) Hasan MR, Morishima D, Tomita K, Katsuki M, Kotani S. Identification of a 250 kDa putative microtubule-associated protein as a bovine ferritin; evidence for a ferritin-microtubule interaction. FEBS Journal 2005; 272: 822-831.

20) Levay PF, Viljoen M. Lactoferrin: a general review. Haematologica 1995; 80(3): 252-267.

21) Harrison PM, Arosio P. The ferritins: molecular properties, iron storage function and cellular regulation. Biochimica *et* Biophysica Acta 1996; 1275: 161-203.

22) Boyd D, Vecoli C, Belcher DM, Jain SK, Drysdale JW. Structural and functional relationships of human ferritin H and L chains deduced from cDNA clones. Journal of Biological Chemistry 1985; 260(21): 11755-11761.

23) Martsev SP, Vlasov AP, Arosio P. Distinct stability of recombinant L and H subunits of human ferritin: calorimetric and ANS binding studies. Protein Engineering 1998; 11(5): 377-381.

24) Wade VJ, Levi S, Arosio P, Treffry A, Harrison PM, Mann S. Influence of site-directed modifications on the formation of iron cores in ferritin. Journal of Molecular Biology 1991; 221: 1443-1452.

25) Chiancone E, Stefanini S. Heterogeneity of ferritin. I. Structural and functional aspects. In: Albertini A, Arosio P, Chiancone E, Drysdale J editors Ferritins and isoferritins as biochemical markers. Amsterdam: Elsevier Science Publishers; 1984. p. 23-32.

26) Levi S, Luzzago A, Franceschinelli F, Santambrogio P, Cesareni G, Arosio P. Mutational analysis of the channel and loop sequences of human ferritin H-chain. Biochemical Journal 1989; 264: 381-388.

27) Bou-Abdallah F, Arosio P, Santambrogio P, Yang X, Janus-Chandler C, Chasteen ND. Ferrous iron binding to recombinant human H-chain. An isothermal titration calorimetry study. Biochemistry 2002; 41: 11184-11191.

28) Takahashi T, Kuyucak S. Functional properties of threefold and fourfold channels in ferritin deduced from electrostatic calculations. Biophysical Journal 2003; 84: 2256-2263.

29) Chasteen ND, Harrison PM. Mineralization in ferritin: an efficient means of iron storage. Journal of Structural Biology 1999; 126: 182-194.

30) Levi S, Santambrogio P, Corsi B, Cozzi A, Arosio P. Evidence that residues exposed on the three-fold channels have active roles in the mechanism of ferritin iron incorporation. Biochemical Journal 1996; 317(Pt2): 467-473.

31) Chasteen ND. Ferritin. Uptake, storage, and release of iron. Metal Ions in Biological Systems 1998; 35: 479-514.

32) Levi S, Yewdall SJ, Harrison PM, Santambrogio P, Cozzi A, Rovida E *et al.* Evidence that H- and L-chains have co-operative roles in the iron-uptake mechanisms of human ferritin. Biochemical Journal 1992; 288: 591-596.

33) Santambrogio P, Levi S, Cozzi A, Corsi B, Arosio P. Evidence that the specificity of iron incorporation into homopolymers of human ferritin L- and H-chains is conferred by the nucleation and ferroxidase centres. Biochemical Journal 1996; 314: 139-144.

34) Lawson DM, Treffry A, Artymiuk PL, Harrison PM, Yewdall SJ, Luzzago A *et al.* Identification of the ferroxidase center in ferritin. FEBS Letters 1989; 254(1,2): 207-210.

35) Bou-Abdallah F, Biasiotto G, Arosio P, Chasteen ND. The putative "nucleation site" in human H-chain ferritin is not required for mineralization of the iron core. Biochemistry 2004; 43: 4332-4337.

36) Levi S, Santambrogio P, Cozzi A, Rovida E, Corsi B, Tamborini E *et al.* The role of the L-chain in ferritin iron incorporation; studies of homo and heteropolymers. Journal of Molecular Biology 1994; 238: 649-654.

37) Wixom RL, Prutkin L, Munro HN. Hemosiderin: Nature, Formation, and Significance. International Review of Experimental Pathology 1980; 22: 193-225.

38) Worwood M. Ferritin in human tissues and serum. Clinical Haematology 1982; 11(2): 275-307.

39) Polanams J, Ray AD, Watt RK. Nanophase iron phosphate, iron arsenate, iron vanadate and iron molybdate minerals synthesized within the protein cage of ferritin. Inorganic Chemistry 2005; 44(9): 3203-3209.

40) Takagi H, Shi D, Ha Y, Allewell NM, Theil EC. Localized unfolding at the junction of three ferritin subunits; a mechanism for iron release. Journal of Biological Chemistry 1998; 273(30): 18685-18688.

41) Cozzi A, Corsi B, Levi S, Santambrogio P, Albertini A, Arosio P. Overexpression of wild type and mutated human ferritin H-chain in HeLa cells. Journal of Biochemistry 2000; 275(33): 25122-25129.

42) Treffry A, Zhao Z, Quail MA, Guest JR, Harrison PM. Dinuclear center of ferritin: studies of iron binding and oxidation show differences in the two iron sites. Biochemistry 1997; 36: 432-441.

43) Hwang J, Krebs C, Huynh BH, Edmondson DE, Theil EC, Penner-Hahn JE. A short Fe-Fe distance in peroxodiferric ferritin: control of Fe substrate versus cofactor decay? Science 2000; 287(5450): 122-125.

44) Liu X, Theil EC. Ferritin reactions: direct identification of the site for the diferric peroxide reaction intermediate. Proceedings of the National Academy of Sciences of the United States of America 2004; 101(23): 8557-8562.

45) Aisen P. Ferritin receptors and the role of ferritin in iron transport. Targeted Diagnosis and Therapy 1991; 4: 339-354.

46) Deiss A. Iron metabolism in reticuloendothelial cells. Seminars in Hematology 1983; 20(2): 81-90.

47) Liu X, Jin W, Theil EC. Opening protein pores with chaotropes enhances Fe reduction and chelation of Fe from the ferritin biomineral. Proceedings of the National Academy of Sciences of the United States of America 2003; 100(7): 3653-3658.

48) Gálvez N, Ruiz B, Cuesta R, Colacio E, Dominguez-Vera JM. Release of iron from ferritin by aceto- and benzohydroxamic acids. Inorganic Chemistry 2005; 44(8): 2706-2709.

49) Agrawal R, Sharma PK, Rao GS. Release of iron from ferritin by metabolites of benzene and superoxide radical generating agents. Toxicology 2001; 168: 223-230.

50) Hynes MJ, Coinceanainn MO. Investigation of the release of iron from ferritin by naturally occurring antioxidants. Journal of Inorganic Biochemistry 2002; 90: 18-21.

51) Sánchez P, Gálvez N, Colacio E, Miñones E, Domínguez-Vera JM. Catechol releases iron(III) from ferritin by direct chelation without iron(II) production. Dalton Transactions 2005; 4: 811-813.

52) Jameson GNL, Jameson RF, Linert W. New insights into iron release from ferritin: direct observation of the neurotoxin 6-hydroxydopamine entering ferritin and reaching redox equilibrium with the iron core. Organic and Biomolecular Chemistry 2004; 2: 2346-2351.

53) Watt GD, Frankel RB, Papaefthymiou GC. Reduction of mammalian ferritin. Proceedings of the National Academy of Sciences of the United States of America 1985; 82: 3640-3643.

54) Joshi JG, Clauberg M. Ferritin: an iron storage protein with diverse functions. Biofactors 1988; 1(3): 207-212.

55) Jin W, Hidnori T, Pancorbo B, Theil EC. "Opening" the ferritin pore for iron release by mutation of conserved amino acids at interhelix and loop sites. Biochemistry 2001; 40: 7525-7532.

56) Arosio P, Adelman TG, Drysdale JW. On ferritin heterogeneity; further evidence for heteropolymers. Journal of Biological Chemistry 1978; 253(12): 4451-4458.

57) Arosio P, Levi S, Santambrogio P, Cozzi A, Luzzago A, Cesareni G *et al.* Structural and functional studies of human ferritin H and L chains. Current Studies in Hematology and Blood Transfusion 1991; 58: 127-131.

58) Wagstaff M, Worwood M, Jacobs A. Iron and isoferritins in iron overload. Clinical Science 1982; 62(5): 529-540.

59) Speyer BE, Fielding J. Ferritin as a cytosol iron transport intermediate in human reticulocytes. British Journal of Haematology 1979; 42: 255-267.

60) Bomford A, Conlon-Hollingshead C, Munro HN. Adaptive responses of rat tissue isoferritins to iron administration. Journal of Biological Chemistry 1981; 256(2): 948-955.

61) Coccia EM, Profita V, Fiorucci G, Romeo G, Affabris E, Testa U *et al.* Modulation of ferritin H-chain expression in Friend erythroleukemia cells: transcriptional and translational regulation by hemin. Molecular and Cellular Biology 1992; 12(7): 3015-3022.

62) Powell LW, Alpert E, Isselbacher KJ, Drysdale JW. Human isoferritins: organ specific iron and apoferritin distribution. British Journal of Haematology 1975; 30: 47-132.

63) Invernizzi R, Caccola M, De Fazio P, Rosti V, Ruggeri G, Arosio P. Immunocytochemical detection of ferritin in human bone marrow and peripheral blood cells using monoclonal antibodies specific for the H and L subunit. British Journal of Haematology 1990; 76: 427-432.

64) White K, Munro HN. Induction of ferritin subunit synthesis by iron is regulated at both the transcriptional and translational levels. Journal of Biological Chemistry 1988; 263(18): 8938-8942.

65) Ruggeri G, Iacobello C, Albertini A, Brocchi E, Levi S, Gabri E *et al.* Studies of human isoferritins in tissues and body fluids. In: Albertini A, Arosio P, Chiancone E, Drysdale J editors. Ferritins and isoferritins as biochemical markers. Amsterdam: Elsevier Science Publishers; 1984. p. 67-78.

66) Cazzola M, Dezza L, Bergamaschi G, Barosi G, Bellotti V, Caldera D *et al.* Biologic and clinical significance of red cell ferritin. Blood 1983; 62(5): 1078-1087.

67) Jones BM, Worwood M, Jacobs A. Isoferritins in normal leucocytes. British Journal of Haematology 1983; 55(1): 73-81.

68) Arosio P, Yokota M, Drysdale JW. Structural and immunological relationships of isoferritins in normal and malignant cells. Cancer Research 1976; 36: 1735-1739.

69) Hodgetts J, Peters SW, Hoy TG, Jacobs A. The ferritin content of normoblasts and megaloblasts from human bone marrow. Clinical Science 1986; 70: 47-51.

70) Ruggeri G, Santambrogio P, Bonfiglio, Levi S, Bugari G, Verardi R *et al.* Antibodies for denatured human H-ferritin stain only reticuloendothelial cells within the bone marrow. British Journal of Haematology 1992; 81: 118-124.

71) Cheepsunthorn P, Palmer C, Connor JR. Cellular distribution of ferritin subunits in postnatal rat brain. Journal of Comparative Neurology 1998; 400: 73-86.

72) Connor JR, Boeshore KL, Benkovic SA, Menzies SL. Isoforms of ferritin have a specific cellular distribution in the brain. Journal of Neuroscience Research 1994; 37(4): 461-465.

73) Santambrogio P, Levi S, Cozzi A, Rovida E, Albertini A, Arosio P. Production and characterization of recombinant heteropolymers of human ferritin H and L chains. Journal of Biological Chemistry 1993; 268(7): 12744-12748.

74) Festa M, Ricciardelli G, Mele G, Pietropaolo C, Ruffo A, Colonna A. Overexpression of H ferritin and up-regulation of iron regulatory protein genes during differentiation of 3T3-L1 pre-adipocytes. Journal of Biological Chemistry 2000; 275(47): 36708-36712.

75) Harford JB, Rouault TA, Klausner RD. The control of cellular iron homeostasis. In: Brock JH, Halliday JW, Pippard MJ, Powell LW editors. Iron metabolism in health and disease. London: W.B. Saunders Company Ltd; 1994. p. 123-149.

76) Rogers J, Lacroix L, Durmowitz G, Kasschau K, Andriotakis J, Bridges KR. The role of cytokines in the regulation of ferritin expression. Advances in Experimental Medicine and Biology 1994; 356: 127-132.

77) Meyron-Holtz EG, Vaisman B, Cabantchik ZI, Fibach E, Rouault TA, Hershko C *et al.* Regulation of intracellular iron metabolism in human erythroid precursors by internalized extracellular ferritin. Blood 1999; 94(9): 3205-3211.

78) Truty J, Malpe R, Linder MC. Iron prevents ferritin turnover in hepatic cells. Journal of Biological Chemistry 2001; 276(52): 48775-48780.

79) Thomson AM, Rogers JT, Leedman PJ. Iron-regulatory proteins, iron-responsive elements and ferritin mRNA translation. International Journal of Biochemistry and Cell Biology 1999; 31: 1139-1152.

80) Piñero DJ, Hu J, Cook BM, Scaduto Jr, RC, Connor JR. Interleukin-1β increases binding of the iron regulatory protein and the synthesis of ferritin by increasing the labile iron pool. Biochimica *et* Biophysica Acta 2000; 1497: 279-288.

81) Iancu TC. Ferritin and hemosiderin in pathological tissues. Electron Microscopy Reviews 192; 5: 209-229.

82) Iancu TC. Iron overload. Molecular Aspects of Medicine 1982; 6: 1-100.

83) Halliday JW, Powell LW. Serum ferritin and isoferritins in clinical medicine. Progress in Hematology 1979; 11: 229-266.

84) Mehlhase J, Sandig G, Pantopoulos K, Grune T. Oxidation-induced ferritin turnover in microglial cells: role of proteasome. Free Radical Biology and Medicine 2005; 38: 276-285.

85) Rudeck M, Volk T, Sitte N, Grune T. Ferritin oxidation in vitro: implication of iron release and degradation by the 20S proteasome. IUBMB Life 2000; 49: 451-456.

86) Welch KD, Van Eeden MC, Aust SD. Modification of ferritin during iron loading. Free Radical Biology and Medicine 2001; 31(8): 999-1006.

87) Welch KD, Reilly CA, Aust SD. The role of cysteine residues in the oxidation of ferritin. Free Radical Biology and Medicine 2002; 33(3): 399-408.

88) Radisky DC, Kaplan J. Iron in cytosolic ferritin can be recycled through lysosomal degradation in human fibroblasts. Biochemical Journal 1998; 336: 201-205.

89) Miyazaki E, Kato J, Kobune M, Okumura K, Sasaki K, Shintani N *et al.* Denatured H-ferritin subunit is a major constituent of haemosiderin in the liver of patients with iron overload. Gut 2002; 50: 413-419.

90) Ringeling PL, Cleton MI, Kroos MJ, Sorber LWJ, de Bruyn WC, Harrison PM *et al.* Lysosomal and cytosolic ferritins. A biochemical and electron-spectroscopic study. Biology of Metals 1989; 2: 114-121.

91) Fischbach FA, Gregory DW, Harrison PM, Hoy TJ, Williams JM. On the structure of hemosiderin and its relationship to ferritin. Journal of Ultrastructural Research 1971; 37: 495-503.

92) Richter GW. The iron-loaded cell – the cytopathology of iron storage. American Journal of Pathology 1978; 91(2): 363-404.

93) Richter GW. Studies of iron overload; rat liver siderosome ferritin. Laboratory Investigation 1984; 50(1): 26-35.

94) Weir MP, Sharp GA, Peters TJ. Electron microscopic studies of human haemosiderin and ferritin. Journal of Clinical Pathology 1985; 38: 915-918.

95) Kim S-W, Kim Y-H, Lee J. Thermal stability of human ferritin: concentration dependence and enhanced stability of an N-terminal fusion mutant. Biochemical and Biophysical Research Communications 2001; 289: 125-129.

96) Fahmy M, Young SP. Modulation of iron metabolism in monocyte cell line U937 by inflammatory cytokines: changes in transferrin uptake, iron handling and ferritin mRNA. Biochemical Journal 1993; 296: 175-181.

97) Alvarez-Hernández X, Licéaga J, McKay IC, Brock JH. Induction of hypoferremia and modulation of macrophage iron metabolism by tumor necrosis factor. Laboratory Investigation 1989; 61(3): 319-322.

98) Surguladze N, Patton S, Cozzi A, Fried MG, Connor JR. Characterization of nuclear ferritin and mechanism of translocation. Biochemical Journal 2005; 388: 731-740.

99) Surguladze N, Thompson KM, Beard JL, Connor JR, Fried MG. Interactions and reactions of ferritin with DNA. Journal of Biological Chemistry 2004; 279(15): 14694-14702.

100) Broyles RH, Belegu V, DeWitt CR, Shah SN, Stewart CA, Pye QN *et al.* Specific repression of β-globin promoter activity by nuclear ferritin. Proceedings of the National Academy of Sciences of the United States of America 2001; 98(16): 9145-9150.

101) Levi S, Corsi B, Bosisio M, Invernizzi R, Volz A, Sanford D *et al.* A human mitochondrial ferritin encoded by an intronless gene. Journal of Biological Chemistry 2001; 270(27): 24437-24440.

102) Bou-Abdallah F, Santambrogio P, Levi S, Arosio P, Chasteen ND. Unique iron binding and oxidation properties of human mitochondrial ferritin: a comparative analysis with human H-chain ferritin. Journal of Molecular Biology 2005; 347: 543-554.

103) Drysdale J, Arosio P, Invernizzi R, Cazzola M, Volz A, Corsi B *et al.* Mitochondrial ferritin: a new player in iron metabolism. Blood Cells, Molecules and Diseases 2002; 29(3): 376-383.

104) Corsi B, Cozzi A, Arosio P, Drysdale J, Santambrogio P, Campanella A *et al.* Human mitochondrial ferritin expressed in HeLa cells incorporates iron and affects cellular iron metabolism. Journal of Biological Chemistry 2002; 277(25): 22340-22347.

105) Nie G, Sheftel AD, Kim SF, Ponka P. Overexpression of mitochondrial ferritin causes cytosolic iron depletion and changes cellular iron homeostasis. Blood 2005; 105(5): 2161-2167.

106) Cazzola M, Invernizzi R, Bergamaschi G, Levi S, Corsi B, Travaglino E *et al.* Mitochondrial ferritin expression in erythroid cells from patients with sideroblastic anemia. Blood 2003; 101(5): 1996-2000.

107) Covell AM, Worwood M. Isoferritins in plasma. In: Albertini A, Arosio P, Chiancone E, Drysdale J editors. Ferritins and isoferritins as biochemical markers. Amsterdam: Elsevier Science Publishers; 1984. p. 49-65.

108) Cragg SJ, Wagstaff M, Worwood M. Detection of a glycosylated subunit in human serum ferritin. Biochemical Journal 1981; 199: 565-571.

109) Jacobs A, Worwood M. Ferritin in serum; clinical and biochemical implications. New England Journal of Medicine 1975; 292(18): 951-956.

110) Worwood M, Dawkins S, Wagstaff M, Jacobs A. The purification and properties of ferritin from human serum. Biochemical Journal 1976; 157: 97-103.

111) Cazzola M, Ascari A. Red cell ferritin as a diagnostic tool. British Journal of Haematology 1986; 62(2): 209-213.

112) Torti SV, Torti FM. Iron and ferritin in inflammation and cancer. Advances in Inorganic Biochemistry 1994; 10: 119-137.

113) Hershko C, Konijn AM. Serum ferritin in hematologic disorders. In: Albertini A, Arosio P, Chiancone E, Drysdale J editors. Ferritins and isoferritins as biochemical markers. Amsterdam: Elsevier Science Publishers; 1984. p. 143-158.

114) Kew MC, Torrance JD, Derman D, Simon M, Macnab M, Charlton RW *et al.* Serum and tumour ferritins in primary liver cancer. Gut 1978; 19(4): 294-299.

115) Niitsu Y, Onodera Y, Kohgo Y, Goto Y, Watanabe N, Urushizaki I. Isoferritins in malignant diseases. In: Albertini A, Arosio P, Chiancone E, Drysdale J editors. Ferritins and isoferritins as biochemical markers. Amsterdam: Elsevier Science Publishers; 1984. p. 113-127.

116) Halliday JW, Mack U, Powell LW. The kinetics of serum and tissue ferritins: relation to carbohydrate content. British Journal of Haematology 1979; 42: 535-546.

117) Bellotti V, Arosio P, Cazzola M, Cozzi A, Levi S, Meloni F *et al.* Characteristics of a ferritin-binding protein present in human serum. British Journal of Haematology 1987; 65(4): 489-493.

118) Meyron-Holtz EG, Fibach E, Gelvan D, Konijn AM. Binding and uptake of exogenous isoferritins by cultured human erythroid precursor cells. British Journal of Haematology 1994; 86: 635-641.

119) Jacobs A, Hodgetts J, Hoy TG. Functional aspects of isoferritins. In: Albertini A, Arosio P, Chiancone E, Drysdale J editors. Ferritins and isoferritins as biochemical markers. Amsterdam: Elsevier Science Publishers; 1984. p. 113-127.

120) Gelvan D, Fibach E, Meyron-Holtz EG, Konijn AM. Ferritin uptake by human erythroid precursors is a regulated iron uptake pathway. Blood 1996; 88(8): 3200-3207.

121) Konijn AM, Meyron-Holtz EG, Fibach E, Gelvan D. Cellular ferritin uptake: a highly regulated pathway for iron assimilation in human erythroid precursor cells. Advances in Experimental Medicine and Biology 1994; 356: 189-197.

122) Moss D, Hibbs AR, Stenzel D, Powell LW, Halliday JW. The endocytic pathway for H-ferritin established in live MOLT-4 cells by laser scanning confocal microscopy. British Journal of Haematology 1994; 88: 746-753.

123) Siegenberg D, Baynes RD, Bothwell TH, Macfarlane BJ, Lamparelli RD. Factors involved in the regulation of iron transport through reticuloendothelial cells. Proceedings of the Society of Experimental Biology and Medicine 1990; 193(1): 65-72.

124) Hulet SW, Heyliger SO, Powers S, Connor JR. Oligodendrocyte progenitor cells internalize ferritin via clathrin-dependent receptor mediated endocytosis. Journal of Neuroscience Research 2000; 61: 52-60.

125) Morikawa K, Oseko F, Morikawa S. A role for ferritin in hematopoiesis and the immune system. Leukemia and Lymphoma 1995; 18: 429-433.

126) Broxmeyer HE, Gentile P, Listowsky I, Cavanna F, Feickert HJ, Dorner MH *et al.* Acidic isoferritins in the regulation of hematopoiesis *in vitro* and *in vivo.* In: Albertini A, Arosio P, Chiancone E, Drysdale J editors. Ferritins and isoferritins as biochemical markers. Amsterdam: Elsevier Science Publishers; 1984. p. 97-111.

127) Broxmeyer HE, Lu L, Bicknell DC, Williams DE, Cooper S, Levi S *et al.* The influence of purified recombinant human heavy-subunit and light-subunit ferritins on colony formation *in vitro* by granulocyte-macrophage and erythroid progenitor cells. Blood 1986; 68(6): 1257-1263.

128) Broxmeyer HE. H-ferritin: a regulatory cytokine that down-modulates cell proliferation. Journal of Laboratory and Clinical Medicine 1991; 120(3): 367-370.

129) Fargion S, Arosio P, Fracanzani AL, Cislaghi V, Levi S, Cozzi A *et al.* Characteristics and expression of binding sites specific for ferritin H-chain on human cell lines. Blood 1988; 71: 753-757.

130) Broxmeyer HE, Cooper S, Levi S, Arosio P. Mutated recombinant human heavy-chain ferritins and myelosuppression in vitro and in vivo: a link between ferritin ferroxidase activity and biological function. Proceedings of the National Academy of Sciences of the United States of America 1991; 88: 770-774.

131) Hie-won L, Stahlhut MW, Evans AE. Isoferritins and prognosis of neuroblastoma: the immunological role of acidic isoferritins. In: Albertini A, Arosio P, Chiancone E, Drysdale J editors. Ferritins and isoferritins as biochemical markers. Amsterdam: Elsevier Science Publishers; 1984. p. 171-180.

132) Halliday JW, Ramm GA, Moss D, Powell LW. A new look at ferritin metabolism. Advances in Experimental Medicine and Biology 1994; 365: 149-156.

133) Ciriello MM, Cazzola M, Dezza L, Levi S, Arosio P. Measurement of ferritin-bearing lymphocytes in man. Preliminary studies on the use of monoclonal antibodies specific for the L and H subunits of ferritin. Tumori 1987; 73: 37-41.

134) Langlois d'Estaintot B, Santambrogio P, Granier T, Gallois B, Chevalier JM, Precigoux G *et al.* Crystal structure and biochemical properties of the human mitochondrial ferritin and its mutant Ser144Ala. Journal of Molecular Biology 2004; 340(2): 277-293.

135) Cozzi A, Corsi B, Levi S, Santambrogio P, Albertini A, Arosio P. Overexpression of wild type and mutated human ferritin H-chain in HeLa cells: in vivo role of ferroxidase activity. Journal of Biological Chemistry 2002; 275: 25122-25129.

136) Cozzi A, Corsi B, Levi S, Santambrogio P, Biasiotto G, Arosio P. Analysis of the biological functions of H- and L-ferritins in HeLa cells by transfection with siRNAs and cDNA: Evidence for a proliferative role of ferritin. Blood 2004; 103(6): 2377-2383.

137) Kakhlon O, Gruenbaum Y, Cabantchik ZI. Repression of the heavy chain increases the labile iron pool of human K562 cells. Biochemical Journal 2001; 356(pt2): 311-316.

138) Kakhlon O, Gruenbaum Y, Cabantchik ZI. Repression of ferritin expression increases the labile iron pool, oxidative stress, and short-term growth of human erythroleukemia cells. Blood 2001; 97: 2863-2871.

139) Orino K, Lehman L, Tsuji Y, Ayaki H, Torti SV, Torti FM. Ferrritin and the response to oxidative stress. Biochemical Journal 2001; 357: 241-247.

140) Blatt J, Wharton V. Stimulation of growth of neuroblastoma cells by ferritin in vitro. Journal of Laboratory and Clinical Medicine 1992; 119: 139-143.

141) Kakhlon O, Gruenbaum Y, Cabantchik ZI. Ferritin expression modulates cell cycle dynamics and cell responsiveness to H-ras-induced growth via expansion of the labile iron pool. Biochemical Journal 2002; 363(pt3): 431-436.

142) Kikyo N, Suda M, Kikyo N, Hagiwara K, Yasukawa K, Fujisawa M *et al.* Purification and characterization of a cell growth factor from a human leukaemia cell line: immunological identity with ferritin. Cancer Research 1994; 54: 268-271.

143) Cozzi A, Levi S, Corsi B, Santambrogio P, Campanella A, Gerardi G *et al.* The role of iron and ferritin in TNFα-induced apoptosis in HeLa cells. FEBS Letters 2003; 537: 187-192.

144) Goralska M, Holley BL, McGahan MC. Identification of a mechanism by which lens epithelial cells limit accumulation of overexpressed ferritin H-chain. Journal of Biological Chemistry 2003; 278(44): 42920-42926.

145) Aulbert E, Schmidt CG. Ferritin – a tumor marker in myeloid leukaemia. Cancer Detection and Prevention 1985; 8(1-2): 297-302.

146) Aulbert E, Steffens O. Serum ferritin – a tumor marker in malignant lymphomas? Onkologie 1990; 13(2): 102-108.

147) Silber JH, Evans AE, Fridman M. Models to predict outcome from childhood neuroblastoma: the role of serum ferritin and tumor histology. Cancer Research 1991; 51(5): 1426-1433.

148) Maxim PE, Veltri RW. Serum ferritin as a tumor marker in patients with squamous cell carcinoma of the head and neck. Cancer 1986; 57(2): 305-311.

149) Vernet M, Renversez JC, Lasne Y, Revenant MC, Charlier-de-Bressing C, Guillemin C *et al.* Comparison of six serum ferritin immunoassays and isoferritin spectrotypes in malignancies. Annales de Biologie Clinique 1995; 53: 419-427.

150) Kirkali Z, Guzelsoy M, Mungan MU, Kirkali G, Yorokoglu K. Serum ferritin as a clinical marker for renal cell carcinoma: influence of tumor size and volume. Urology International 1999; 62(1): 21-25.

151) Yang DC, Wang F, Elliott RL, Head JF. Expression of transferrin receptor and ferritin H-chain mRNA are associated with clinical and histopathological prognostic indicators in breast cancer. Anticancer Research 2001; 21(1B): 541-549.

152) Bevilacqua MA, Costanzo F, Buonaguro L, Cimino F. Ferritin H and L mRNAs in human neoplastic tissues. Italian Journal of Biochemistry 1988; 37(1): 1-7.

153) Higgy NA, Salicioni AM, Russo IH, Zhang PL, Russo J. Differential expression of human ferritin H chain gene in immortal human breast epithelial MCF-10F cells. Molecular Carcinogenesis 1997; 20(4): 332-339.

154) Jones BM, Worwood M, Jacobs A. Serum ferritin in patients with cancer: determination with antibodies to HeLa cell and spleen ferritin. Clinica Chimica Acta 1980; 106: 203-214.

155) Tripathi PK, Chatterjee SK. Elevated expression of ferritin H-chain mRNA in metastatic ovarian tumor. Cancer Investigation 1996; 14(6): 518-526.

156) Whittaker D, Torrance JD, Kew MC. Isolation of ferritin from human hepatocellular carcinoma. Scandinavian Journal of Haematology 1984; 33(5): 432-439.

157) Shterman N, Kupfer B, Moroz C. Comparison of transferrin receptors, iron content and isoferritn profile in normal and malignant human breast cell lines. Pathobiology 1991; 59(1): 19-25.

158) Kakhlon O, Gruenbaum Y, Cabantchik ZI. Repression of ferritin expression modulates cell responsiveness to H-ras-induced growth. Biochemical Society Transactions 2002; 30(4): 777-780.

159) Wu KJ, Polack A, Dalla-Favera R. Coordinated regulation of iron-controlling genes, H-ferritin and IRP-2, by c-MYC. Science 1999; 283(5402): 676-679.

160) Sanyal B, Polak PE, Szuchet S. Differential expression of the heavy-chain ferritin gene in non-adhered and adhered oligodendrocytes. Journal of Neuroscience Research 1996; 46(2): 187-197.

161) Marziali G, Perrotti E, Ilari R, Testa U, Coccia EM, Battistini A. Transcriptional regulation of the ferritin heavy-chain gene: the activity of the CCAAT binding factor NF-Y is modulated in heme-treated Friend leukemia cells and during monocyte-to-macrophage differentiation. Molecular and Cellular Biology 1997; 17(3): 1387-1395.

162) Vanlandingham JW, Levenson CW. Effect of retinoic acid on ferritin H expression during brain development and neuronal differentiation. Nutritional Neuroscience 2003; 6(1): 39-45.

163) Bevilacqua MA, Faniello MC, D'Agostino P. Transcriptional activation of the H-ferritin gene in differentiated Caco-2 cells parallels a change in the activity of the nuclear factor Bbf. Biochemical Journal 1995; 311 (Pt 3): 769-773.

164) Vet JA, van Moorselaar RJ, Debruyne FM, Schalken JA. Differential expression of ferritin heavy chain in a rat transitional cell carcinoma progression model. Biochimica *et* Biophysica Acta 1997; 1360(1): 39-44.

165) You SY, Zhang CY, Yi XP, Huang W. Evaluation of clinical significance of isoferritin by development of new monoclonal antibodies specific for acidic isoferritin. Hybridoma 2001; 20(4): 243-248.

166) Reif DW. Ferritin as a source of iron for oxidative damage. Free Radical Biology and Medicine 1992; 12: 417-427.

167) Biemond P, Swaak AJG, Van Eijk HG, Koster JF. Superoxide dependent iron release from ferritin in inflammatory diseases. Free Radical Biology and Medicine 1988; 4: 185-198.

168) Kehrer JP. The Haber-Weiss reaction and mechanisms of toxicity. Toxicology 2000; 149: 43-50.

169) Arosio P, Levi S. Ferritin, iron homeostasis, and oxidative damage. Free Radical Biology and Medicine 2002; 33(4): 457-463.

170) Tsuji Y, Ayaki H, Whitman SP, Morrow CS, Torti SV, Torti FM. Coordinate transcriptional and translational regulation of ferritin in response to oxidative stress. Molecular and Cellular Biology 2000; 20(16): 5818-5827.

171) Epsztejn S, Glickstein H, Picard V, Slotki IN, Breuer W, Beaumont C *et al.* H-ferritin subunit overexpression in erythroid cells reduces the oxidative stress response and induces multidrug resistance properties. Blood 1999; 4(1): 3593-3603.

172) Lin F, Girotti AW. Elevated ferritin production, iron containment, and oxidant resistance in hemin-treated leukaemia cells. Archives of Biochemistry and Biophysics 1997; 346(1): 131-141.

173) Picard V, Epsztejn S, Santambrogio P, Cabantchik ZI, Beaumont C. Role of ferritin in the control of the labile iron pool in murine erythroleukemia cells. Journal of Biological Chemistry 1998; 273(25): 15382-15386.

174) Gerlach M, Ben-shachar D, Riederer P, Youdim MB. Altered brain metabolism of iron as a cause of neurodegenerative diseases? Journal of Neurochemistry 1994; 63(3): 793-807.

175) Bartzokis G, Tishler TA, Shin IS, Lu PH, Cummings JL. Brain ferritin iron as a risk factor for age at onset in neurodegenerative diseases. Annals of the New York Academy of Sciences 2004; 1012: 224-236.

176) Connor JR, Snyder BS, Arosio P, Loeffler DA, LeWitt P. A quantitative analysis of isoferritins in select regions of aged, parkinsonian, and alzheimer's diseased brains. Journal of Neurochemistry 1995; 65: 717-724.

177) Dexter DT, Carayon A, Javoy-Agid F, Agid Y, Wells FR, Daniel SE *et al.* Alterations in the levels of iron, ferritin and other trace metals in Parkinson's disease and other neurodegenerative diseases affecting the basal ganglia. Brain 1991; 114(Pt 4): 1953-1975.

178) Hirose W, Ikematsu K, Tsuda R. Age-associated increases in heme oxygenase-1 and ferritin immunoreactivity in the autopsied brain. Legal Medicine 2003; 5: S360-S366.

179) Dexter DT, Jenner P, Schapira AHV, Marsden CD. Alterations in levels of iron, ferritin, and other trace metals in neurodegenerative diseases affecting basal ganglia. Annals of Neurology 1992; 32: S94-S100.

180) Faucheux BA, Martin ME, Beaumont C, Hunot S, Hauw JJ, Agid Y *et al.* Lack of up-regulation of ferritin is associated with sustained iron regulatory protein-1 binding activity in the substantia nigra of patients with Parkinson's disease. Journal of Neurochemistry 2002; 83(2): 320-330.

181) Hurairah H, Ferro A. The role of the endothelium in the control of vascular function. International Journal of Clinical Practice 2004; 58(2): 173-183.

182) Olesen SP. Free oxygen radicals decrease electrical resistance of microvascular endothelium in brain. Acta Physiologica Scandinavica 1987; 129(2): 181-187.

183) Shatos MA, Doherty JM, Orfeo T, Hoak JC, Collen D, Stump DC. Modulation of the fibrinolytic response of cultured human vascular endothelium by extracellularly generated oxygen free radicals. Journal of Biological Chemistry 1992; 267(1): 597-601.

184) Ikeda H, Koga Y, Oda T, Kuwano K, Nakayama H, Ueno T *et al.* Free oxygen radicals contribute to platelet aggregation and cyclic flow variations in stenosed and endothelium-injured canine coronary arteries. Journal of the American College of Cardiology 1994; 24(7): 1749-1756.

185) Annuk M, Zilmer M, Fellstrom B. Endothelium-dependent vasodilation and oxidative stress in chronic renal failure: impact on cardiovascular disease. Kidney International Supplement 2003; 84: S50-S53.

186) Keaney JF Jr, Vita JA. Atherosclerosis, oxidative stress, and antioxidant protection in endothelium-derived relaxing factor action. Proggress in Cardiovascular Diseases 1995; 38(2): 129-154.

187) Massy ZA, Ceballos I, Chadefaux-Vekemens B, Nguyen-Khoa T, Descamps-Latscha B, Drueke TB *et al.* Homocyst(e)ine, oxidative stress, and endothelium function in uremic patients. Kidney International Supplement 2001; 78: S243-S245.

188) Tribe RM, Poston L. Oxidative stress and lipids in diabetes: a role in endothelium vasodilator dysfunction? Vascular Medicine 1996; 1(3): 195-206.

189) Balla J, Vercellotti GM, Nath K, Yachie A, Nagy E, Eaton JW *et al.* Haem, haem oxygenase and ferritin in vascular endothelial cell injury. Nephrology Dialysis Transplantation 2003; 18(Suppl 5): v8-v12.

190) Juckett MB, Balla J, Balla G, Jessurun J, Jacob HS, Vercellotti GM. Ferritin protects endothelial cells from oxidized low density lipoprotein in vitro. American Journal of Pathology 1995; 147(3): 782-789.

191) Gonzales S, Erario MA, Tomaro ML. Heme oxygenase-1 induction and dependent increase in ferritin. A protective antioxidant stratagem in hemin-treated rat brain. Developments in Neuroscience 2002; 24: 161-168.

192) Motterlini R, Foresti R, Intaglietta M, Winslow RM. NO-mediated activation of heme oxygenase: endogenous cytoprotection against oxidative stress to endothelium. American Journal of Physiology 1996; 270(1 Pt 2): H107-H114.

193) Regan RF, Kumar N, Gao F, Guo Y. Ferritin induction protects cortical astrocytes from heme-mediated oxidative injury. Neuroscience 2002; 113(4): 985-994.

194) Oberle S, Polte T, Abate A, Podhaisky HP, Schroder H. Aspirin increases ferritin synthesis in endothelial cells: a novel antioxidant pathway. Circulation Research 1998; 82(9): 1016-1020.

195) Li W, Xu L-H, Yuan X-M. Macrophage haemoglobin scavenger receptor and ferritin accumulation in human atherosclerotic lesions. Annals of the New York Academy of Sciences 2004; 1030: 196-201.

196) Yuan X-M, Li W, Baird SK, Carlsson M, Melefors Ö. Secretion of ferritin by iron-laden macrophages and influence of lipoproteins. Free Radical Research 2004; 38(10): 1133-1142.

197) Berberat PO, Katori M, Kaczmarek E, Anselmo D, Lassman C, Ke B *et al.* Heavy chain ferritin acts as an antiapoptotic gene that protects livers from ischemia reperfusion injury. FASEB Journal 2003; 17(12): 1724-1726.

198) Chi SI, Wang CK, Chen JJ, Chau LY, Lin TN. Differential regulation of H- and L-ferritin messenger RNA subunits, ferritin protein and iron following focal cerebral ischemia-reperfusion. Neuroscience 2000; 100(3): 475-484.

199) Loncar R, Flesche CW, Deussen A. Myocardial ferritin content is closely related to the degree of ischaemia. Acta Physiologica Scandinavica 2004; 180: 21-28.

200) Ono S, Zhang Z-D, Marton LS, Yamini B, Windmeyer E, Johns L *et al.* Heme oxygenase-1 and ferritin are increased in cerebral arteries after subarachnoid hemorrhage in monkeys. Journal of Cerebral Blood Flow and Metabolism 2000; 20: 1066-1076.

201) Koszyca B, Manavis J, Cornish RJ, Blumbergs PC. Patterns of immunocytochemical staining for ferritin and transferrin in the human spinal cord following traumatic injury. Journal of Clinical Neuroscience 2002; 9(3): 298-301.

202) Applegate LA, Scaletta C, Panizzon R, Frenk E. Evidence that ferritin is UV inducible in human skin: part of a putative defense mechanism. Journal of Investigative Dermatology 1998; 111(1): 159-163.

203) Cai CZ, Birk DE, Linsenmayer TF. Nuclear ferritin protects DNA from UV damage in corneal epithelial cells. Molecular Biology of the Cell 1998; 9(5): 1037-1051.

204) Goralska M, Holley BL, McGahan MC. Overexpression of H- and L-ferritin subunits in lens epithelial cells: Fe metabolism and cellular response to UVB irradiation. Investigative Ophthalmology and Visual Science 2001; 42(8): 1721-1727.

205) Rankin JA. Biological mediators of acute inflammation. AACN Clinical Issues 2004; 15(1): 3-17.

206) Liu H, Pope RM. Phagocytes: mechanisms of inflammation and tissue destruction. Rheumatic Disease Clinics of North America 2004; 30(1): 19-39.

207) Di Virgilio F. New pathways for reactive oxygen species generation in inflammation and potential novel pharmacological targets. Current Pharmaceutical Design 2004; 10(14): 1647-1652.

208) Closa D, Folch-Puy E. Oxygen free radicals and the systemic inflammatory response. IUBMB Life 2004; 56(4): 185-191.

209) Giordano N, Vaccai D, Cintorino M, Minacci C, Magaro L, Battisti E *et al.* Histopathological study of iron deposit distribution in the rheumatoid synovium. Clinical Experiments in Rheumatology 1991; 9(5): 463-467.

210) Rowley D, Gutteridge JM, Blake D, Farr M, Halliwell B. Lipid peroxidation in rheumatoid arthritis: thiobarbituric acid-reactive material and catalytic iron salts in synovial fluid from rheumatoid patients. Clinical Science 1984; 66(6): 691-695.

211) Blake DR, Lunec J, Ahern M, Ring EF, Bradfield J, Gutteridge JM. Effect of intravenous iron dextran on rheumatoid synovitis. Annals of the Rheumatic Diseases 1985; 44(3): 183-188.

212) Rogers JT, Bridges KR, Durmowicz GP, Glass J, Auron PE, Munro HN. Translational control during the acute phase response; Ferritin synthesis in response to interleukin-1. Journal of Biological Chemistry 1990; 265(24): 14572-14578.

213) Lipschitz DA, Simon MO, Lynch SR, Dugard J, Bothwell TH, Charlton RW. Some factors affecting the release of iron from reticuloendothelial cells. British Journal of Haematology 1971; 21: 289-303.

214) Konijn AM, Hershko C. Ferritin synthesis in inflammation. I. Pathogenesis of impaired iron release. British Journal of Haematology 1977; 37(1): 7-16.

215) Alvarez-Hernández X, Felstein MV, Brock JH. The relationship between iron release, ferritin synthesis and intracellular iron distribution in mouse peritoneal macrophages. Evidence for a reduced level of metabolically available iron in elicited macrophages. Biochimica *et* Biophysica Acta 1986; 886: 214-222.

216) Fillet G, Beguin Y, Baldelli L. Model of reticuloendothelial iron metabolism in humans: abnormal behavior in idiopathic hemochromatosis and in inflammation. Blood 1989; 74(2): 844-851.

217) Jurado RL. Iron, infections, and anemia of inflammation. Clinical Infectious Diseases 1997; 25: 888-895.

218) Torrance JD, Charlton RW, Simon MO, Lynch SR, Bothwell TH. The mechanism of endotoxin-induced hypoferremia. Scandinavian Journal of Haematology 1978; 21: 403-410.

219) Fillet G, Cook JD, Finch CA. Storage iron kinetics. VII. A biologic model for reticuloendothelial iron transport. Journal of Clinical Investigation 1974; 53: 1527-1533.

220) Noyes WD, Bothwell TH, Finch CA. The role of the reticulo-endothelial cell in iron metabolism. British Journal of Haematology 1960; 6: 43-55.

221) Fuchs D, Zangerle R, Artner-Dworzak E, Weiss G, Fritsch P, Tilz GP *et al.* Association between immune activation, changes of iron metabolism and anaemia in patients with HIV infection. European Journal of Haematology 1993; 50: 90-94.

222) Pham CG, Bubici C, Zazzeroni F, Papa S, Jones J, Alvarez K *et al.* Ferritin heavy chain upregulation by NF-κB inhibits TNFα-induced apoptosis by suppressing reactive oxygen species. Cell 2004; 119: 529-542.

223) Hanada T, Yoshimura A. Regulation of cytokine signalling and inflammation. Cytokine Growth Factor Reviews 2002; 13(4-5): 413-421.

224) Savarino A, Pescarmona GP, Boelaert JR. Iron metabolism and HIV infection: reciprocal interactions with potentially harmful consequences. Cell Biochemistry and Function 1999; 17: 279-287.

225) Miller LL, Miller SC, Torti SV, Tsuji Y, Torti FM. Iron-independent induction of ferritin H chain by tumor necrosis factor. Proceedings of the National Academy of Sciences of the United States of America 1991; 88(11): 4946-4950.

226) Rogers JT. Ferritin translation by interleukin-1 and interleukin-6: The role of sequences upstream of the start codons of the heavy and light subunit genes. Blood 1996; 87(6): 2525-2537.

227) Pang J-HS, Jiang M-J, Chen Y-L, Wang F-W, Wang DL, Chu S-H *et al.* Increased ferritin gene expression in atherosclerotic lesions. Journal of Clinical Investigation 1996; 97(10): 2204-2212.

228) Stites SW, Plautz MW, Bailey K, O'Brien-Ladner AR, Wesselius LJ. Increased concentrations of iron and isoferritins in the lower respiratory tract of patients with stable cystic fibrosis. American Journal of Respiratory Critical Care Medicine 1999; 160(3): 796-801.

CHAPTER 2

MATERIALS AND METHODS

1) Funding

Funding for the study was obtained from various sources including;

1) Post-graduate Mentor Bursary Programme, University of Pretoria, South Africa
2) Skye Foundation, South Africa
3) HF Verwoerd Research Trust, South Africa
4) Durban 2000 HIV/AIDS Research Fund, University of Pretoria, South Africa
5) NAVKOM, University of Pretoria, South Africa

2) Investigators

All determinations were performed by the candidate except for standard diagnostic evaluations which were performed by the Chemical Pathology and Haematology laboratories, National Health Laboratory Services (NHLS), University of Pretoria, South Africa. Determinations performed by the student were conducted at the Department of Physiology, Faculty of Health Sciences and the Unit for Microscopy and Microanalysis, Faculty of Natural Sciences, University of Pretoria, South Africa.

3) Patients

Forty-eight patients attending the Department of Internal Medicine, Kalafong Hospital, University of Pretoria, for treatment of chronic diseases with a high prevalence of HIV infection were included in the study. Ethical clearance for the study for this group of patients was obtained from the Faculty of Health Sciences Research Ethics Committee, University of Pretoria (ethical clearance number 118/2003). Ten patients scheduled for hip replacement at the Department of Orthopaedics, Pretoria Academic Hospital, University of Pretoria were included in the study as a group of patients with less severe immune stimulation. These patients were all diagnosed with osteoarthritis and were HIV-negative. Ethical clearance for the study for this group of patients was obtained from the Faculty of Health Sciences Research Ethics Committee, University of Pretoria (ethical clearance number 285/2003).

4) Determinations of the study

1) The expression of the H-subunit and L-subunit of ferritin in bone marrow macrophages and cells of the erythron – ultrastructural immunolocalisation of the H-subunit and L-subunit of ferritin in bone marrow macrophages and cells of the erythron.
2) Serum iron markers including serum iron, transferrin, transferrin saturation, ferritin and soluble transferrin receptor.
3) Red blood cell characteristics including red blood cell count, haemoglobin, haematocrit, mean corpuscular volume, mean corpuscular haemoglobin, mean corpuscular haemoglobin concentration, red blood cell distribution width and reticulocyte production index.
4) Prussian blue iron stains of bone marrow aspirate and core bone marrow biopsy.

5) Cytokines including Il-1β, Il-2, Il-4, Il-5, Il-6, Il-8, Il-10, Il-12, TNF-α, TGF-β1, INF-γ and GM-CSF.

6) Neopterin.

7) C-reactive protein.

8) Pro-hepcidin and caeruloplasmin.

5) Samples obtained from patients

1) A bone marrow aspirate and core bone marrow biopsy from each of the 48 patients at Internal Medicine, Kalafong Hospital were obtained at the time they had their biopsies taken for diagnostic purposes. The core bone marrow biopsy was immediately processed according to the protocol for fixation of core bone marrow tissue. A bone marrow aspirate smear was made for a Prussian blue iron stain. The bone marrow aspirates and core bone marrow biopsies were taken from the posterior superior iliac crest with a Jamshidi needle. A core bone marrow sample from each of the 10 patients at Orthopaedics, Pretoria Academic Hospital was obtained during the hip replacement procedure. The core bone marrow sample was harvested from the femur (red marrow).

2) 25 ml of coagulated blood – processed within one hour. Blood was centrifuged at 2500 g at 12°C in order to separate the serum from the blood cells. Aliquots of the serum were frozen at -75°C.

3) 5 ml of coagulated blood for standard serum iron markers including iron, transferrin, transferrin saturation and ferritin.

4) 5 ml of EDTA blood for red blood cell characteristics.

6) Materials and methods

6.1) Ultrastructural immunolocalisation of the H-subunit and L-subunit of ferritin in bone marrow macrophages and cells of the erythron

The method for the ultrastructural immunolocalisation of the H-subunit and L-subunit of ferritin was not available and therefore had to be developed and evaluated by the candidate. The theoretical background, development and evaluation of the technique for the ultrastructural immunolocalisation of the H-subunit and L-subunit of ferritin are presented in Volume 2.

6.1.1) Fixation of core bone marrow tissue

Materials

1) Fixative consisting of 4% formaldehyde (FA), 0.05% glutaraldehyde (GA) in a 0.15 M sodium phosphate buffer. The fixative was prepared fresh immediately prior to the obtainment of bone marrow tissue. A 10% paraformaldehyde (Paraformaldehyde (Trioxymethylene), SPI Supplies, cat. no. 2615, Rick Loveland & Associates, Halfway House, South Africa) solution in deionised H_2O was prepared fresh in a fume hood. The solution was heated to 60-70°C with constant stirring. Once the solution had reached the proper temperature stirring was continued for 15 minutes. At this point the solution was milky. One to two drops of 1 N NaOH was added, with stirring, until the solution cleared (1). The 0.15 M sodium phosphate buffer was prepared from two stock solutions. A 0.3 M Na_2HPO_4 stock solution (di-Sodium hydrogen phosphate Dihydrate, Fluka, BioChemika, Ultra, cat. no. 71643, Sigma-Aldrich, Aston Manor, South Africa) and a 0.3 M NaH_2PO_4 stock solution (Sodium dihydrogen phosphate Dihydrate, Fluka, Biochemika, MicroSelect, cat. no. 71505, Sigma-Aldrich, Aston Manor, South Africa). The 0.3 M NaH_2PO_4 stock solution was added to the 0.3 M Na_2HPO_4 to pH 7.25 immediately prior to the obtainment of bone marrow

tissue. This 0.3 M sodium phosphate buffer was then diluted 1:1 with the 10% freshly prepared formaldehyde stock solution and deionised H_2O. This was then followed by the addition of the GA (Pure Glutaraldehyde 25% solution, E.M. grade, SPI Supplies, cat. no. 2607, Rick Loveland & Associates, Halfway House, South Africa).

2) Ethanol 99.9% Absolute A.R., Minema, Rick Loveland & Associates, Halfway House, South Africa.

3) LR White Resin, medium grade acrylic resin, London Resin Company LTD., Rick Loveland & Associates, Halfway House, South Africa.

4) Gelatine capsules, SPI Supplies, cat. no. 2302, Rick Loveland & Associates, Halfway House, South Africa.

5) Nickel grids, 200 MESH Hexagonal grids, SPI Supplies, cat. no. 2480N, Rick Loveland & Associates, Halfway House, South Africa.

Method

1) A piece of core bone marrow was obtained during the biopsy procedure at the bedside of the patient and placed immediately in the fixative on ice.

2) The bone marrow tissue was fixed for 24 hours at 6°C whilst being rotated (TAAB rotator, Wirsam Scientific, Richmond, South Africa).

3) The bone marrow tissue was washed 3 times for 20 minutes with the sodium phosphate buffer at 6°C whilst being rotated.

4) The bone marrow tissue was dehydrated as follows 50% EtOH, 70% EtOH, 30 minutes each at 6°C whilst rotating followed by 85% EtOH, 2 times 15 minutes at 6°C whilst being rotated.

5) The bone marrow tissue was infiltrated with 1:1 85% EtOH:LR White mixture for 30 minutes at 6°C whilst being rotated. LR White dissolved in 85% EtOH but not in 80% EtOH.

6) The bone marrow tissue was infiltrated with LR White, 2 times 30 minutes at 6°C whilst being rotated.

7) The bone marrow tissue was placed in gelatine capsules in fresh LR White and was then polymerised, without any air bubbles, for 24 hours at 50°C.

8) The block of bone marrow tissue was sectioned and the sections were placed on nickel grids since copper grids can be oxidised during the immunolabelling procedures.

6.1.2) Immunolabelling of the H-subunit and L-subunit of ferritin

Materials

1) 8% $NaJO_4$, Sodium (meta) periodate, Fluka, Biochemika, Ultra, cat. no. 71859, Sigma-Aldrich, Aston Manor, South Africa.

2) Phosphate buffered saline – 20 mmol/l sodium phosphate buffer, 0.15 mol/l sodium chloride. Two stock solutions were prepared – 20 mmol/l Na_2HPO_4, 0.15 mol/l NaCl and 20 mmol/l $NaH_2PO_4 \cdot H_2O$, 0.15 mol/l NaCl. The $NaH_2PO_4 \cdot H_2O$ stock solution was added to the Na_2HPO_4 stock solution to pH 7.4. Sodium chloride, SigmaUltra, cat. no. S7653, Sigma-Aldrich, Aston Manor, South Africa. di-Natriumhydrogenphosphate, cat. no. 6586, Merck Chemicals (Pty) LTD., Germiston, South Africa, Natriumdihydrogenphosphate-1-hydrate, cat. no. 6346, Merck Chemicals (Pty) LTD., Germiston, South Africa.

3) 0.5% Glycine, Pharmacia Biotech, cat. no. 17-1323-01, AEC Amersham (PTY) LTD, Sandton, South Africa.

4) BSA, Bovine Serum Albumin, Amersham Biosciences, cat. no. RPN 412 V, Separations Scientific, Randburg, South Africa.

5) FBS, Fetal Bovine Serum, filtered and gamma irradiated, cat. no. 306, Highveld Biologicals (Pty) Ltd, Halfway House, South Africa.

6) Tween-20, Polyoxyethylenesorbitan monolaurate, Sigma for Molecular Biology, cat. no. P-9416, Sigma-Aldrich, Aston Manor, South Africa.

7) Primary monoclonal antibodies, primary monoclonal antibody specific for the H-subunit of ferritin, RH02 and the monoclonal antibody specific for the L-subunit of ferritin, LF03 were obtained from Ramco Laboratories, Inc., Stafford, Texas, United States of America.

8) Secondary antibody, Anti-mouse IgG (whole molecule), gold conjugate, 10 nm, cat. no. G-7777, Sigma-Aldrich, Aston Manor, South Africa.

9) Glutaraldehyde, Pure Glutaraldehyde 25% solution, E.M. grade, SPI Supplies, cat. no. 2607, Rick Loveland & Associates, Halfway House, South Africa.

10) Uranyl acetate, SPI Supplies, cat. no. 2624, Rick Loveland & Associates, Halfway House, South Africa.

Method

1) The sections were incubated with 8% $NaJO_4$ in H_2O for 1 hour at room temperature. All procedures were performed by placing the section on a drop of the specific solution.

2) The sections were rinsed 3 times 5 minutes with phosphate buffered saline at room temperature.

3) The sections were blocked with 0.05% glycine in H_2O for 20 minutes at room temperature.

4) The sections were blocked with 1% BSA, 5% FBS, 0.05% Tween-20 in phosphate buffered saline for 1 hour at 30°C.

5) The sections were incubated with the primary monoclonal antibodies 1:10 diluted in 1% BSA, 5% FBS, 0.05% Tween-20, phosphate buffered saline for 4 hours at 30°C.

6) The sections were rinsed 3 times 5 minutes with 1% BSA, 5% FBS, 0.05% Tween-20 in phosphate buffered saline at room temperature.

7) The sections were incubated with the secondary antibody 1:50 in 1% BSA, 5% FBS, 0.05% Tween-20, phosphate buffered saline for 1 hour at 30°C.

8) The sections were rinsed for 3 times 5 minutes in 1% BSA, 5% FBS, 0.05% Tween-20 in phosphate buffered saline at room temperature.

9) The sections were rinsed 5 minutes with phosphate buffered saline at room temperature.

10) The sections were fixed with 2% GA in phosphate buffered saline at room temperature.

11) The sections were rinsed 3 times 5 minutes with deionised H_2O at room temperature.

12) To enhance the contrast of the sections, the sections were stained for 10 minutes with 0.3% uranyl acetate at room temperature.

13) The sections were dipped 15 times in 3 separate beakers with deionised H_2O.

14) The sections were then viewed with a Philips 301 transmission electron microscope.

6.1.3) Ultrastructural characteristics of bone marrow macrophages and cells of the erythron

Figures 1 a-e contain electron micrographs to show macrophages and cells of the erythron. Furthermore, these figures illustrate ferritin aggregates found in the cytoplasm of the cells and the possible mechanisms whereby iron is taken up by red blood cell precursors.

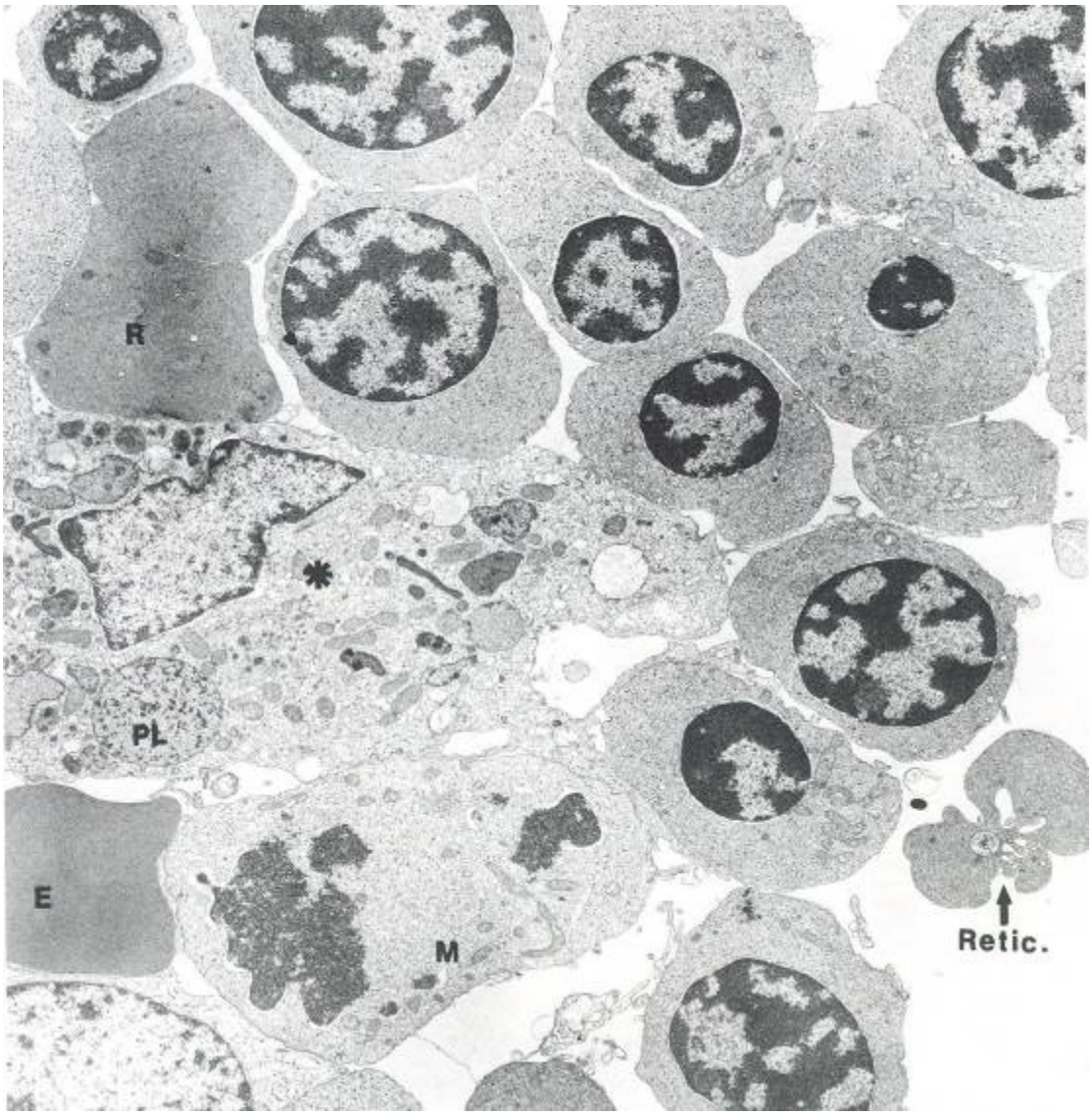

Figure 1a. Erythroblastic island. A macrophage (*) containing many inclusions probably reflecting phagolysosomes (PL) is surrounded by erythroid elements at all stages of differentiation and maturation. Note the erythroblast in mitosis (M), the young reticulocyte (Retic) shortly after nuclear extrusion, older reticulocytes (R) with a smoother contour, more electron dense cytoplasm but some residual organelles, and the mature erythrocyte (E) devoid of organelles and even more electron dense cytoplasm reflecting almost complete hemoglobinization (x 5500) (2).

Figure 1b. Two adjacent erythroblasts from the bone marrow of a patient with increased iron storage. Note ferritin particles located on the plasma membrane of both cells and invaginations of the surface membrane (arrows). Within the cell ferritin has accumulated in membrane-bound structures (Fe), golgi zone (G), centriole (C); asterisk indicates nuclear pore (x 57000) (2).

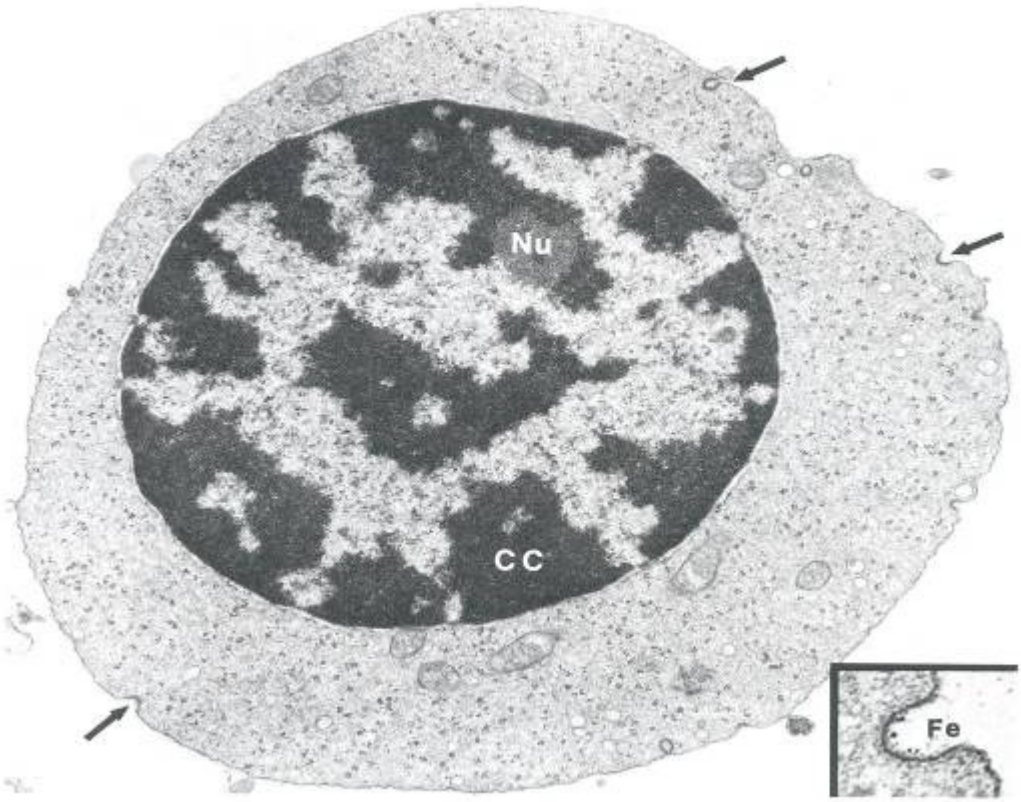

Figure 1c. Basophilic erythroblast with clumps of condensed chromatin (CC) and only a vestigial nucleolus (Nu). Although the cytoplasm is still replete with polyribosomes which would account for the degree of basophilia on light microscopy, the grey background indicates the presence of haemoglobin. Several pinocytotic vesicles of ferritin molecules (rhopheocytosis) (x 18000). Inset Fe = iron (x 40000) (2).

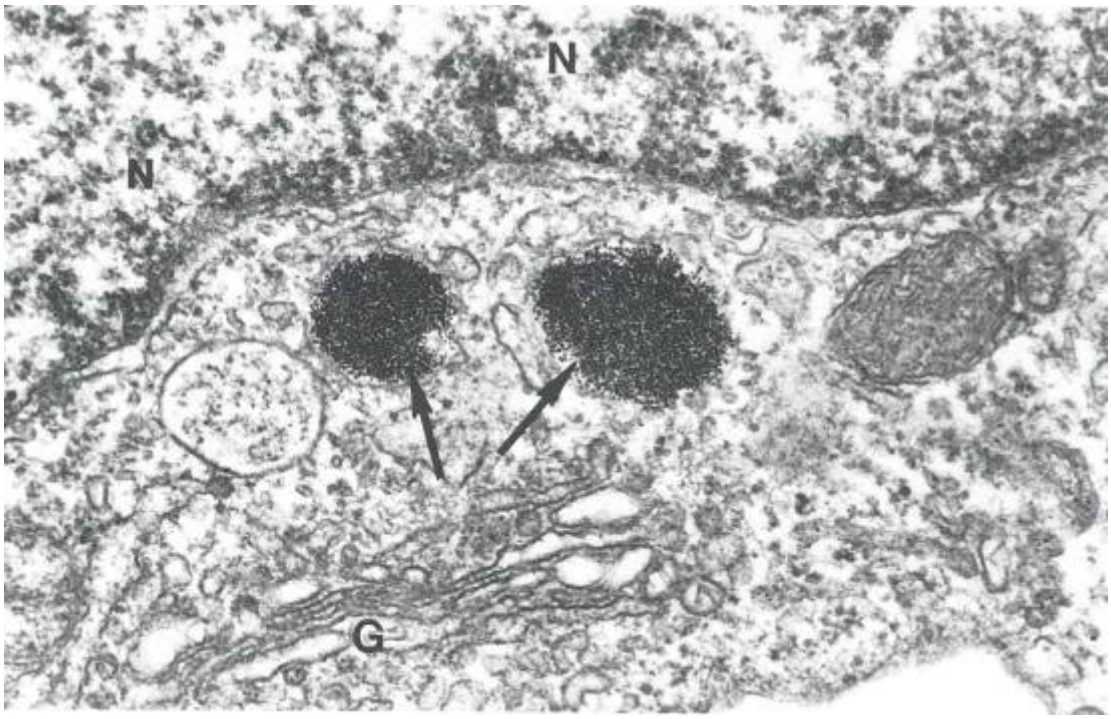

Figure 1d. Erythroblast from a patient with anaemia of chronic disease associated with "ineffective" erythropoiesis. Note the large membrane-inclusions containing ferritin (arrows), golgi apparatus (G), nucleus (N) (x 63000) (2).

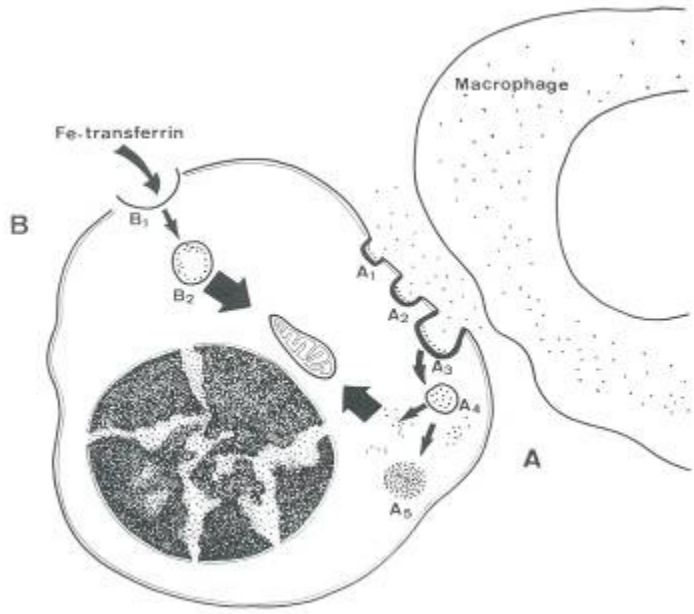

Figure 1e. Iron absorption in developing normoblasts. [The mechanisms by which iron is delivered to the mitochondria of the developing normoblasts for the incorporation into haem, are still controversial. Two principal patterns are illustrated in this schematic drawing, where the stipples represent

ferritin. According to pattern A, iron is transferred as preformed ferritin from a macrophage (the "nursing" cell) to the adjacent normoblast. The stages of this process correspond to the invagination of the cell membrane progressively enclosing ferritin molecules ($A_1 \rightarrow A_5$). According to pattern B, iron is selectively taken up by absorption to the erythroid cell surface of transferrin molecules, probably via specific cell receptors. Endocytosis of iron laden transferrin molecules or of transferrin-receptor complexes ($B_1 \rightarrow B_2$) leads to the internalization of iron for haem synthesis. Ferritin accumulates in the cytoplasm in the form of dispersed molecules or aggregates which may be either free or contained in membrane-bound vacuoles. Ferritin aggregates constitute a yellow-brown pigment known as haemosiderin and are responsible for positive staining of the erythroblasts with the Prussian blue reaction (2).]

6.1.4) Quantification of the immunolabelling of the H-subunit and L-subunit of ferritin

In order to quantify the immunolabelling of the H-subunit and L-subunit of ferritin the 10 nm gold particles were counted. The biggest area possible, consisting of only the cytosol of the cell, was demarcated. The amount of gold particles in this area was counted and expressed as count/μm^2. ImageTool was the software used to measure the area and facilitate the counting process. For each section the amount of gold particles was counted in three macrophages, not in close proximity, but on the same section. The mean was calculated and used in the statistical analysis of the data. For each patient the gold particles for three representative erythroblasts, three representative reticulocytes and three representative red blood cells were also counted. For not all patients these cells were easily distinguishable. These cells were all grouped together as cells of the erythron since no difference was shown for the expression of either the H-subunit or for the L-subunit of ferritin between these subsets of cells of the erythron. The mean for this population of cells were used as the count for the cells of the erythron and used in the statistical analysis of the data.

6.2) Serum iron markers

6.2.1) Serum iron

Serum iron measurements were determined on a BECKMAN COULTER™ SYNCHRON LX®20. Iron Reagent was used to measure the iron concentration by a timed-endpoint method. In the reaction, iron is released from transferrin by acetic acid and is reduced to the ferrous state by hydroxylamine and thioglycolate. The ferrous iron is immediately complexed with FerroZine® Iron Reagent. The system monitors the change in absorbance at 560 nm. This change in absorbance is directly proportional to the concentration of iron in the sample and is used by the SYNCHRON LX System to calculate and express the iron concentration.

Chemical reaction scheme;

Transferrin-$(Fe^{3+})_2$ → Transferrin + 2 Fe^{3+} (acetic acid pH 4.3)

Fe^{3+} + hydroxylamine + thioglycolate → Fe^{2+}

Fe^{2+} + 3FerroZine → Fe^{2+} + $(FerroZine)_3$

6.2.2) Serum transferrin

Serum transferrin measurements were determined on a BECKMAN COULTER™ SYNCHRON LX®20. Transferrin reagent was used to measure the transferrin concentration by a turbidometric method. In the reaction, transferrin combines with specific antibodies to form insoluble antigen-antibody complexes. The system monitors the change in absorbance at 340 nm. This change in absorbance is proportional to the concentration of transferrin in the sample and is used by the system to calculate and express the transferrin concentration based upon a single-point calibration.

Chemical reaction scheme;

Transferrin (antigen) + anti-transferrin antibody → antigen-antibody complex

6.2.3) Transferrin saturation

Transferrin saturation was calculated as follows;

Transferrin saturation (%) = (serum iron) / total iron binding capacity) x 100

= (serum iron) / serum transferrin x 25.1) x 100

= (serum iron) / serum transferrin) x 3.984

Where the total iron binding capacity = serum transferrin x 25.1

The total iron binding capacity (TIBC) indicates the maximum amount of iron needed to saturate serum transferrin (TRF), which is the primary iron transport protein. Theoretically, 1 mol of TRF (average molecular mass, 79 570 Da) can bind two mol of iron (55.8 Da) at two high affinity-binding sites for ferric iron. Therefore, TIBC correlates well with TRF concentration, and the theoretical ratio of TIBC (in µmol/l) to TRF (in g/l) is 25.1: TIBC (in µmol/l) = 25.1 X TRF (in g/l) (3).

6.2.4) Serum ferritin

Serum ferritin was determined by an immunometric assay, Immulite® 2000 Ferritin, for *in vitro* diagnostic use with the IMMULITE 2000 Analyzer, for the quantitative measurement of ferritin in serum.

6.2.5) Soluble transferrin receptor

The soluble transferrin receptor was determined by employing an ELISA from Ramco Laboratories, Inc., Texas, USA. The soluble transferrin receptor assay is an enzyme immunoassay based on the double antibody sandwich method. Plasma or serum samples are diluted in buffer and pipetted into microwells pre-coated with polyclonal antibody to transferrin receptor. Horseradish peroxidase (HRP) conjugated murine monoclonal antibody specific for transferrin receptor is added to the wells and the wells are incubated for two hours at room temperature. During this incubation, the transferrin receptor binds to the polyclonal antibodies adsorbed to the wells and the HRP-conjugated

secondary antibodies bind to the captured transferrin receptor. Any unbound transferrin receptor and excess HRP conjugate are removed from the wells by washing. Enzyme substrate (chromogen TMB) is added to the wells and through the action of HRP forms a blue product. Upon the addition of an acid stop solution, the blue product is converted to a yellow colour, the intensity of which is measured in a plate reader set at 450 nm. The optical density of the resulting solution is directly proportional to the concentration of transferrin receptor in the standard samples. A standard curve is generated by plotting the absorbance versus concentration of the transferrin receptor standards provided in the kit. The concentration of the transferrin receptor in the sample is then determined by comparing the sample's optical density reading with the standard curve graph.

6.3) Red blood cell characteristics

6.3.1) Red blood cell count

Red blood cell counts were determined by a Coulter Counter®. Red blood cells are suspended in a conductive liquid (diluent) and acts as an insulator. Each cell passes through an aperture and momentarily increases the resistance of the electrical path between the submerged electrodes on either side of the aperture. This causes a measurable electronic pulse. These pulses are counted and correlate to the amount of cells.

The red blood cell count is the number of erythrocytes measured directly, multiplied by the calibration constant and expressed as;

$RBC = n \times 10^6$ cells/µl

6.3.2) Haemoglobin concentration

Weight (mass) of haemoglobin determined from the degree of absorbance found through photocurrent transmittance is;

Hb (g/dl) = constant x $\log_{10}$ reference %T / sample %T

6.3.3) Haematocrit (Hct)

This is the relative volume of packed erythrocytes to whole blood, calculated as;

Hct (%) = RBC x MCV / 10

6.3.4) Mean corpuscular volume (MCV)

This is the average volume of individual erythrocytes derived from a RBS histogram. The system;

- Multiplies the number of RBCs in each channel by the size of the RBCs in that channel.
- Adds the products of each channel between 36 fl and 360 fl.
- Divides that sum by the total number of RBCs between 36 fl and 360 fl.
- Multiplies by a calibration constant and expresses MCV in femtoliters.

6.3.5) Mean corpuscular haemoglobin (MCH)

This is the weight of haemoglobin in the average erythrocyte count, calculated as;

MCH (pg) = Hb / RBC x 10

6.3.6) Mean corpuscular haemoglobin concentration (MCHC)

This is the average weight of haemoglobin in a measured dilution, calculated as;

MCHC (g/dl) = Hb / Hct x 100

6.3.7) Red blood cell distribution width (RDW)

RDW represents the size distribution spread of the erythrocyte population derived from the RBC histogram. It is the coefficient of variance (CV), expressed in percentage, of the RBC size distribution.

6.3.8) Reticulocyte production index (RPI)

Whole blood samples are incubated with a supravital dye, New Methylene Blue, in a special solution (reagent A). The dye precipitates the basophilic RNA network found in reticulocytes. This is followed by the addition of reagent B, a hypotonic clearing reagent, which clears haemoglobin and unbound stain from the cells. Stained reticulocytes differ from mature erythrocytes and other cell populations by light scatter, direct current measurements and opacity characteristics. Reticulocyte counts can then be measured in the Coulter Counter.

RPI = (Hct / 0.45 x reticulocyte %) / shift correction factor for haematocrit

- shift correction factors for hct; 45 = 1, 35 = 1.5, 25 = 2, 15 = 2.5
- reticulocyte % = the number of reticulocytes per 100 RBCs
- > 2.5 = blood loss with normal bone marrow response, < 2.5 = suppressed bone marrow

6.4) Prussian blue iron stain of bone marrow aspirate and core bone marrow biopsy

6.4.1) HCl-ferrocyanide iron stain of bone marrow aspirate smears

1) The smears were fixed in methanol for 10 minutes.

2) The smears were air-dried.

3) The smears were stained for 10 minutes in 2% potassium ferrocyanide/0.2 N HCl in a Coplin jar at 58°C.

4) The smears were rinsed in distilled water.

5) The smears were air-dried.

6) The smears were counter-stained with nuclear fast red for 10 minutes.

7) The smears were rinsed in distilled H_2O.

6.4.2) HCl-ferrocyanide iron stain of core bone marrow LR White plastic sections

Materials

1) Menzel-Glaser Superfrost® Plus Microscope Slides, Labotec, Halfway House, South Africa.

2) 10% ferrocyanide, Potassium hexacyanoferrate (II) Trihydrate, Fluka, Biochemika Ultra, cat. no. 60279, Sigma-Aldrich, Aston Manor, South Africa; 10% HCl, Hydrochloric acid 30%, Riedel-de-Haën, cat. no. 30053, Sigma-Aldrich, Aston Manor, South Africa.

3) 1% eosin, Eosin yellowish, Gurr®, Microscopy Material, cat. no. 45380, BDH Chemicals Ltd., England, in 70% ethanol (acidified with acetic acid).

Method

1) The 2 µm thick sections were placed on microscope slides.

2) The slides were rinsed in deionised H_2O.

3) The sections were stained for 1 hour in 10% ferrocyanide/10% HCl prepared just before use in Coplin jars at 25°C.

4) The slides were rinsed in deionised H_2O.

5) The sections were counter-stained with 1% eosin in 70% ethanol (acidified) for 10 minutes.

6) The slides were rinsed in deionised H_2O.

7) The slides were air-dried on a hot plate.

8) The sections were mounted with immersion oil and a cover slide.

6.5) Cytokines Il-1β, Il-2, Il-4, Il-5, Il-6, Il-8, Il-10, Il-12, TNF-α, TGF-β1, INF-γ and GM-CSF

6.5.1) Il-8, Il-1β, Il-6, Il-10, TNF-α and Il-12p70

Il-8, Il-1β, Il-6, Il-10, TNF-α and Il-12p70 were determined by employing the Human Inflammation Kit, BD™ Cytometric Bead Array (CBA) (The Scientific group, Midrand, South Africa). The BD™ Cytometric Bead Assay employs a series of particles with discrete fluorescence intensities to simultaneously detect multiple soluble analytes. The BD™ CBA is combined with flow cytometry to create a powerful multiplexed assay. The BD CBA system uses the sensitivity of amplified fluorescence to measure soluble analytes in a particle-based immunoassay. Each bead in a CBA provides a capture surface for a specific protein and is analogous to an individually coated well in an ELISA plate. The BD CBA capture bead mixture is in suspension to allow for the detection of multiple analytes in a small volume sample. Six bead populations with distinct fluorescence intensities have been coated with capture antibodies specific for Il-8, Il-1β, Il-6, Il-10, TNF-α and Il-12p70 proteins. The six bead populations are mixed together to form the BD™ CBA which is resolved in the FL3 channel of a flow cytometer such as the BD FACScan™ or BD FACSCalibur™ flow cytometer. The capture beads, PE-conjugated detection antibodies, and recombinant standards or test samples are mixed together to form sandwich complexes. Following acquisition of sample data using the flow cytometer, the sample results are generated in graphical and tabular form using the

BD™ CBA Analysis Software. The BD™ Cytometric Bead Assay Human Inflammation Kit can be used to quantitatively measure:

Interleukin-8 (Il-8)

Interleukin-1β (Il-1β)

Interleukin-6 (Il-6)

Interleukin-10 (Il-10)

Tumor Necrosis Factor-α (TNF-α)

Interleukin-12p70 (Il-12p70)

6.5.2) Il-2, Il-4, Il-5, Il-10, TNF-α and IFN-γ

Il-2, Il-4, Il-5, Il-10, TNF-α and IFN-γ were determined by employing the BD™ Cytometric Human Th1/Th2 Cytokine Kit (The Scientific group, Midrand, South Africa). The methodology is similar to that of the Inflammation Kit, BD™ Cytometric Bead Array (CBA). The BD™ Cytometric Bead Assay Human Th1/Th2 Cytokine Kit were used to quantitatively measure:

Interleukin-2 (Il-2)

Interleukin-4 (Il-4)

Interleukin-5 (Il-5)

Interleukin-10 (Il-10)

Tumor Necrosis Factor-α (TNF-α)

Interferon-γ (IFN-γ)

With the Th1/Th2 CBA cytokine kit the IFN-γ standards were lost and the measurement of IFN-γ was done by employing the human IFN-γ ELISA Kit, DRG Diagnostics, Germany.

IFN-γ determinations

The BD OptEIA™ test (The Scientific group, Midrand, South Africa) is a solid phase sandwich ELISA. It utilizes a monoclonal antibody specific for the IFN-γ coated on a 96-well plate. Standards and samples are added to the wells, and any IFN-γ present binds to the immobilised antibody. The wells are washed and streptavidin-horseradish peroxidase conjugate mixed with biotinylated anti-human IFN-γ antibody is added, producing an antibody-antigen-antibody "sandwich". The wells are again washed and TMB substrate solution is added, which produces a blue colour in direct proportion to the amount of IFN-γ present in the initial sample. The stop solution changes the colour from blue to yellow, and the microwell absorbances are read at 450 nm.

Il-10 and TNF-α

Il-10 and TNF-α were measured in both the Human Inflammation kit and the Human Th1/Th2 kit. The mean of these values were calculated and used for statistical analysis.

6.5.3) Transforming growth factor β1 (TGF-β1)

TGF-β1 measurements were performed by employing a TGF-β1 ELISA (DRG Diagnostics, Germany, Orb Diagnostics, Modderfontein, South Africa). The TGF-β1 ELISA kit is a solid-phase enzyme-linked immunosorbent assay which is based on the sandwich principle. Prior to testing, the standards and patient samples are diluted in assay buffer, acidified with HCl and then neutralised with NaOH. Afterwards, the neutralised standards and samples are added to the antibody-coated micotiter wells. After the first incubation the unbound sample material is removed by washing with diluted wash solution. Then a monoclonal mouse anti TGF-β1 antibody, a biotynilated anti mouse IgG andtibody and the Streptavidin-HRP enzyme complex are incubated in succession. An immuno-enzyme sandwich complex is formed. The unbound conjugate

is removed by washing. Subsequently substrate solution is added. After a definite time colour development is stopped by addition of stop solution and the absorbance at 450 nm is measured with a microtiterplate reader. The intensity of the colour development is proportional to the TGF-β1 concentration in the sample.

6.5.4) Granulocyte macrophage colony stimulating factor (GM-CSF)

GM-CSF measurements were performed by employing a GM-CSF ELISA (DRG Diagnostics, Germany, Orb Diagnostics, Modderfontein, South Africa). The DRG GM-CSF ELISA is a solid phase enzyme amplified sensitivity immunoassay (EASIA) performed on microtiter plate. The assay is based on an oligoclonal system in which a blend of monoclonal antibodies (MAbs) directed against different epitopes of GM-CSF is used. The use of a number of distinct MAbs avoids hyperspecificity and allows high sensitive assays with extended standard range and short incubation time. Standards or samples containing GM-CSF react with capture monoclonal antibodies (MAbs 1) coated on the micotiter well and with a monoclonal antibody (MAb 2) labelled with horseradish peroxidase (HRP). After an incubation period allowing the formation of a sandwich:coated MAbs 1 – GM-CSF – Mab 2 – HRP, the microtiter plate is washed to remove unbound enzyme labelled antibodies. Bound enzyme-labelled antibodies are measured through a chromogenic reaction. Chromogenic solution (TMB + H_2O_2) is added and incubated. The reaction is stopped with the addition of Stop solution (H_2SO_4) and the micotiter plate is then read at the appropriate wavelength. The amount of substrate turnover is determined colorimetrically by measuring the absorbance which is proportional to the GM-CSF concentration. A standard curve is plotted and the GM-CSF concentration in a sample is determined by interpolation from the standard curve.

6.6) Neopterin

Neopterin measurements were performed by employing a neopterin ELISA (DRG Diagnostics, Germany, Orb Diagnostics, Modderfontein, South Africa). The neopterin ELISA is a solid phase enzyme-linked immunosorbent assay (ELISA) based on the basic principle of a competitive ELISA. An unknown amount of antigen in the sample and a fixed amount of enzyme labelled antigen compete for the antibody-binding sites (rabbit-anti-neopterin). Both antigen-antibody complexes bind to the wells of the microtiter strips coated with a goat-anti-rabbit antibody. Unbound antibody is removed by washing. The intensity of the colour developed after the substrate incubation is inversely proportional to the amount of antigen in the sample. Results of samples can be determined directly using the standard curve.

6.7) C-reactive protein (CRP)

CRP measurements were performed by employing a CRP ELISA (DRG Diagnostics, Germany, Orb Diagnostics, Modderfontein, South Africa). The CRP ELISA is an enzyme immunoassay for the quantitative determination of CRP in human plasma and serum. Microtiterstrips coated with anti-CRP antibody are incubated with diluted standard sera and patient samples. During this incubation step CRP is bound specifically to the wells. After removal of the unbound serum proteins by a washing procedure, the antigen-antibody complex in each well is detected with specific peroxidase-conjugated antibodies. After removal of the unbound conjugate, the strips are incubated with a chromogen solution containing tetramethylbenzidin and hydrogen peroxide: a blue colour develops in proportion to the amount of immunocomplex bound to the wells of the strips. The enzymatic reaction is stopped by the addition of 2 N H_2SO_4 and the absorbance values at 450 nm are determined. A standard curve is obtained by plotting the standard absorbance values versus the corresponding standard values. The

concentration of CRP in patient samples is determined by interpolation from the standard curve.

6.8) Pro-hepcidin and caeruloplasmin

6.8.1) Pro-hepcidin

Pro-hepcidin measurements were performed by employing a hepcidin prohormone ELISA (DRG Diagnostics, Germany, Orb Diagnostics, Modderfontein, South Africa). The Hepcidin Prohormone ELISA Kit is a solid phase enzyme-linked immunosorbent assay (ELISA), based on the principle of competitive binding. The microtiter wells are coated with a polyclonal antibody directed towards an antigenic site on the Hepcidin Prohormone molecule (28-47 aa). Endogenous Hepcidin Prohormone of a patient sample competes with a Hepcidin Prohormone-biotin conjugate for binding to the coated antibody. After incubation the unbound conjugate is washed off. The amount of bound biotin conjugate is reverse proportional to the concentration of Hepcidin Prohormone in the sample. After addition of the substrate solution, the intensity of colour developed is reverse proportional to the concentration of Hepcidin Prohormone in the patient sample.

6.8.2) Caeruloplasmin

The caeruloplasmin assay is a measurement based on rate nephelometry. This measures the rate of increase in light scattered from particles suspended in solution as a result of complexes formed during an antigen-antibody reaction.

Chemical reaction scheme;

Caeruloplasmin(sample) + antibody → [caeruloplasmin(sample)-antibody (aggregates)]

7) Statistical analysis

Statistical analysis employed in this study included the Welch t-test and since groups were relatively small and variances could be large, use was also made of the ranksum (Mann-whitney) test. The p-values for both tests were reported and when interpreted, preference was given to the p-value of the ranksum test when the Welch t-test was not significant. Pearson's product-moment correlation coefficient (r) was employed to assess dependence between study parameters. Testing was done at the 0.05 level of significance.

8) Study design

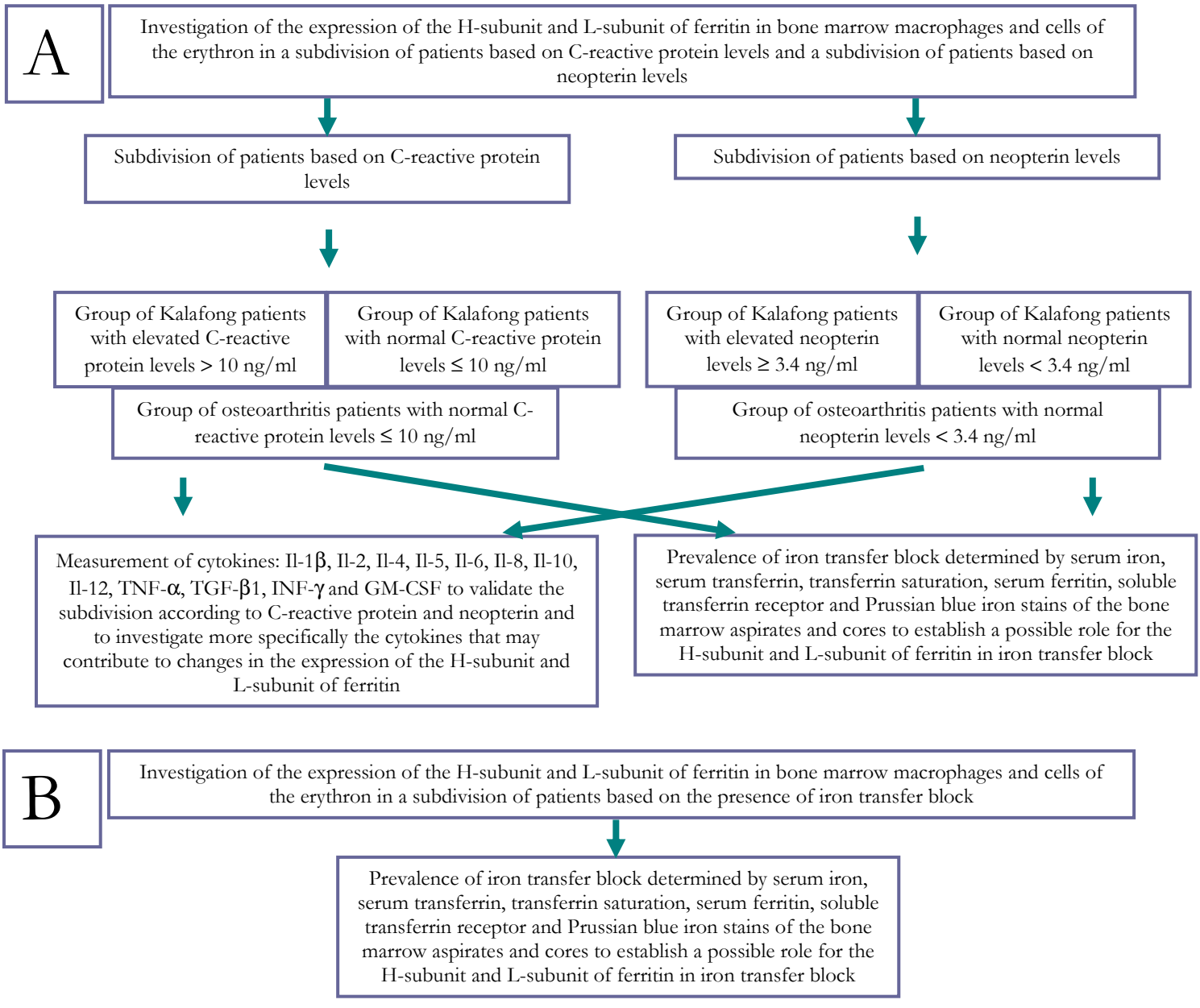

9) References

1) Oliver C. Fixation and embedding. In: Javois LC editor. Methods in Molecular Biology, vol. 34, Immunocytochemical Methods and Protocols. Totowa, New Jersey: Humana Press; 1994. p. 291-298.

2) Castoldi GL. Erythrocytes. In: Zucker-Franklin D, Greaves MF, Grossi CE, Marmont AM editors. Atlas of blood cells: function and pathology. Philadelphia: Lea & Febiger; 1981. p. 35-73.

3) Yamanishi H, Iyama S, Yamaguchi Y, Kanakura Y, Iwatani Y. Total iron-binding capacity calculated from serum transferrin concentration or serum iron concentration and unsaturated iron-binding capacity. Clinical Chemistry 2003; 49(1): 175-178.

CHAPTER 3

RESULTS

The primary purpose of this study was to investigate the expression of the H-subunit and L-subunit of ferritin in the bone marrow macrophage and cells of the erythron during chronic immune stimulation. In addition to this, various humoral factors were determined to assess the immune and iron status of the patients. In order to perform the H-subunit and L-subunit determinations blind, the diagnosis, immune and iron status of the patients were unknown to the investigator. The confounding factor for the inclusion of patients in this study was a bone marrow biopsy. Biopsies could, in line with the ethical clearance prescriptions for this study, only be obtained during a scheduled bone marrow biopsy for diagnostic purposes or during elective hip replacement surgery. Forty-eight patients attending the Department of Internal Medicine, Kalafong Hospital for treatment of chronic diseases, with a high prevalence of human immunodeficiency virus (HIV) infection were included in the study. Bone marrow tissue was obtained from the 48 patients during the scheduled bone marrow biopsy. All patients gave informed consent for the use of these samples including 25 ml of blood. Ethical clearance for the study was obtained from the Faculty of Health Sciences Research Ethics Committee, University of Pretoria (ethical clearance number 118/2003). Ten patients scheduled for hip replacement at the Department of Orthopaedics at the Pretoria Academic Hospital were included in the study as a group of patients with less severe immune stimulation. These patients were all diagnosed with osteoarthritis and were HIV-negative. Bone marrow tissue from the osteoarthritis patients was taken during hip replacement surgery.

All patients gave informed consent for the use of these samples including 25 ml of blood. Ethical clearance for the study was obtained from the Faculty of Health Sciences Research Ethics Committee, University of Pretoria (ethical clearance number 285/2003).

Table 1 shows the demographics of the patients from the Department of Internal Medicine and from the Department of Orthopaedics. Table 2 shows the diagnosis and HIV status of the patients from the Department of Internal Medicine. The diagnosis of the patients from the Department of Internal Medicine was diverse and included various types of infections (tuberculosis (TB), malaria, HIV), cancers (lung, breast), pancytopenias as a result of bone marrow suppression or peripheral destruction of blood cells, organ failures including renal failure, heart failure and liver failure, anaemias with different etiologies and various other pathologies that resulted in inflammatory reactions. This resulted in an extremely heterogenous group of patients. For the purpose of this study the immune status and iron status, respectively, were used to group these patients. The osteoarthritis patients were treated as a separate group.

Table 1. Demographics of the patients from the Department of Internal Medicine, Kalafong Hospital (patients 1-48) and the Department of Orthopaedics, Pretoria Academic Hospital (patients 1-10)

Patient	Age	Sex	Race
1	31	Female	Black
2	82	Female	Black
3	27	Female	Black
4	42	Female	Black
5	41	Female	Black
6	58	Female	White
7	46	Male	Black
8	72	Male	Black
9	29	Female	Black
10	22	Female	Black
11	42	Male	Black
12	54	Female	Black
13	33	Female	Black
14	44	Female	Black
15	40	Female	Black
16	25	Female	Black
17	33	Female	Black
18	36	Female	White
19	24	Female	Black
20	24	Female	Black
21	25	Female	Black
22	54	Female	White
23	31	Female	Black
24	33	Female	Black
25	47	Female	Black
26	50	Female	Black
27	18	Male	Black
28	45	Female	Black
29	62	Female	Black
30	45	Female	White
31	25	Female	Black
32	39	Female	Black
33	27	Female	Black
34	28	Female	Black
35	62	Female	Black
36	33	Female	Black
37	41	Female	Black
38	53	Female	Black
39	67	Male	Black
40	40	Male	Black
41	29	Male	Black
42	72	Male	Black
43	44	Male	Black
44	60	Female	Black
45	35	Male	Black
46	74	Female	Black
47	34	Female	Black
48	17	Female	Black

Patient	Age	Sex	Race
1	48	Female	Black
2	61	Female	White
3	63	Male	White
4	43	Female	White
5	62	Male	White
6	65	Female	White
7	77	Female	White
8	71	Male	White
9	65	Male	White
10	65	Female	White

Table 2. Diagnosis and HIV status of the patients from the Department of Internal Medicine, Kalafong Hospital

Patient	Diagnosis	HIV status
1	Pneumonia & sepsis, Escherichia coli & urinary tract infection & acute renal failure	positive
2	Heart failure & megaloblastic anaemia & pernicious	negative
3	Anaemia & idiopathic thrombocytic purpura & acute haemolytic anaemia vs disseminated intravascular coagulopathy, post mortem	positive
4	Carcinoid cancer & pneumonia & metastasis to the brain	negative
5	Idiopathic vasculitis & pancytopenia questioning antiphospholipid syndrome & uterine mass	negative
6	Malaria & idiopathic thrombocytic purpura	negative
7	Cruveilhier-Baumgarten disease & hypersplenism & TB	negative
8	Lung cancer & acute renal failure & pneumonia	negative
9	Pneumonia, Escherichia coli	positive
10	Idiopathic thrombocytic purpura & iron deficient anaemia & questioning systemic lupus erythematosus	negative
11	Retro viral disease & renal failure	positive
12	Metastatic breast cancer	negative
13	Pneumonia & confusion	positive
14	Pulmonary TB & effusion	positive
15	Megaloblastic anaemia	negative
16	Anaemia due to blood loss	negative
17	Retro viral disease & anaemia & kaposi's sarcoma & previous pulmonary TB	positive
18	Antiphospholipid syndrome & haemolytic anaemia	negative
19	Retro viral disease & bicytopenia & mycobacterium avium complex	positive
20	Retro viral disease & anaemia & dilated cardiomyopathy & antiphospholipid syndrome & TB & thrombosis	positive
21	Retro viral disease & TB & sepsis & anaemia & ascitis	positive
22	Chronic obstructive pulmonary disease & liver & kidney failure & pelagra & sepsis & ethanol abuse	negative
23	Retro viral disease & pneumonia & pancytopenia	positive
24	Idiopathic thrombocytic purpura	negative
25	Retro viral disease & diabetes mellitus & heart failure & obesity & splenomegaly & lymphadenopathy & TB, bone marrow	positive
26	Ethanol abuse & radial fracture & pulmonary TB & bradycardia & primary hypertension, increase calcium	negative
27	Massive splenomegaly & pancytopenia	negative
28	Megaloblastic anaemia & syphilis	negative
29	Delerium & TB & calcified nodes, post mortem = miliary TB	negative
30	OD & thrombocytopenia & macrocytosis & ethanol abuse	negative
31	Retro viral disease & pulmonary TB & pancytopenia	positive
32	Nephritis: hypertension, edema, proteinuria	negative
33	Pancytopenia & ascitis & TB & proteinuria & urinary tract infection & sepsis, ICU	negative
34	Retro viral disease & Hodgkin's disease & TB	positive
35	Hypertension & diabetes mellitus & leucocytosis, persistent	negative
36	Retro viral disease on HAART & pulmonary TB	positive
37	Retro viral disease & idiopathic thrombocytic purpura – immune, normal spleen	positive
38	Megaloblastic anaemia & hypothyroidism	negative
39	Anaemia	negative
40	Anaemia & pyrexia & miliary TB, bone marrow culture	positive
41	Pancytopenia & idiopathic thrombocytic purpura	positive
42	Iron deficient anaemia	negative
43	Iron deficient anaemia & peptic ulcer disease & pneumonia, Staphylococcus aureus	negative
44	Idiopathic 4-limb african gangrene	negative
45	Retro viral disease & pneumonia & pancytopenia	positive
46	Monoclonal gammopathy of undetermined significance & uterine mass	negative
47	Retro viral disease & pancytopenia & pneumonia	positive
48	Idiopathic thrombocytic purpura & bicytopenia	negative

1) Determinations of the study

1.1) The expression of the H-subunit and L-subunit in the macrophage of the bone marrow and cells of the erythron (Table 3). The electron micrographs and raw data of these determinations are contained in volume 2, chapter 6.

1.2) Serum iron markers including serum iron, transferrin, transferrin saturation, ferritin and soluble transferrin receptor (Table 4).

1.3) Red blood cell characteristics including red blood cell count, haemoglobin, haematocrit, mean corpuscular volume, mean corpuscular haemoglobin, mean corpuscular haemoglobin concentration, red blood cell distribution width and reticulocyte production index (Table 4).

1.4) Prussian blue iron stains of bone marrow aspirates and bone marrow core biopsies. Reports by Haematologists from the National Health and Laboratory Services and photographs are contained in volume 2, chapter 6.

1.5) Evaluations of the presence or absence of an iron transfer block are contained in volume 2, chapter 6.

1.6) Cytokines including Il-1, Il-2, Il-4, Il-5, Il-6, Il-8, Il-10, Il-12, TNF-α, TGF-β, INF-γ and GM-CSF (Table 5).

1.7) Neopterin (Table 5).

1.8) C-reactive protein (Table 5).

1.9) Pro-hepcidin and caeruloplasmin (Table 5).

2) Results of the study

2.1) Expression of the H-subunit and L-subunit of ferritin in bone marrow macrophages and cells of the erythron

The expression of the H-subunit and L-subunit of ferritin in the macrophage and cells of the erythron in the bone marrow were determined for both the patients from the Department of Internal Medicine, Kalafong Hospital (Kalafong patient group) and the Department of Orthopaedics, Pretoria Academic Hospital (osteoarthritis group). The results are expressed as count/μm^2. Table 3 contains the mean gold particle count/μm^2 for the macrophage, the cells of the erythron and the H-subunit/L-subunit ratios for the macrophages and cells of the erythron.

Table 3. Expression of the H-subunit and L-subunit of ferritin in the bone marrow macrophage and cells of the erythron for the Kalafong patient group (patients 1-48) and the osteoarthritis patient group (patients 1-10)

Patient	H-subunit macrophages count/µm²	L-subunit macrophages count/µm²	H-subunit/L-subunit macrophages	H-subunit erythron count/µm²	L-subunit erythron count/µm²	H-subunit/L-subunit erythron
1	127.8	68.3	1.9	244.8	109.8	2.2
2	107.7	68	1.6	198.2	132.2	1.5
3	82.3	62.7	1.3	104.7	119.2	0.88
4	119			174		
5	128	52.3	0.4	179.3	207.4	0.86
6	104.3	66	1.6	241.2	194.3	1.2
7	146.3	136.3	1.1	257.3	176.4	1.5
8	66.3	69.8	0.95	107.7	251.2	0.43
9	160.6	129.7	1.2	263.9	261.3	1
10	95.3	150.3	0.63	232.1	227.7	1
11						
12	29	75.3	0.38	70.3	145.7	0.48
13	61.5	148.7	0.41	142.8	190.6	0.75
14	61	118.3	0.52	182.3	135.1	1.3
15	41.8	126.5	0.33	86	190.1	0.45
16	65.7	124.3	0.53	112.6	199.8	0.56
17	126	119.3	1.1	164	181.2	0.9
18	64.3	103	0.62	90.3	190.2	0.47
19	140.8	148.7	0.95	119.5	273.7	0.44
20	37.5	107.7	0.35	68.3	126.9	0.54
21	96.7	85.5	1.1	94.5	144.6	0.65
22	110	94.5	1.2	117	160.5	0.73
23						
24	43.5	57.7	0.75	87.3	134.3	0.65
25	60.3	123.8	0.49	76.5	155.8	0.49
26	64.3	190	0.34	100.1	339.9	0.29
27	76.3	118	0.65	108.2	197.4	0.55
28	58.7	230.3	0.25	127	398.8	0.32
29	64.5	190	0.34	138.1	277.3	0.5
30	54.5	166.3	0.33	104.2	355.7	0.29
31						
32	61.3	100.7	0.61	107.5	261.4	0.41
33	91.9	152	0.6	101.5	269.7	0.38
34	45	163.7	0.27	64.5	223.2	0.29
35	54.3	137.3	0.4	133.3	335.7	0.4
36	58	59.3	0.98	117.7	259.4	0.45
37	59.7	106.7	0.56	140.4	173.7	0.81
38	70	92.8	0.75	154.6	213.5	0.72
39	66.8	79.7	0.84	59.2	220.8	0.27
40	161	115	1.4	149.8	152.6	0.98
41	93.7	113.5	0.83	141.1	225.7	0.63
42	133.5	151	0.88	128	203.8	0.63
43	66.7	92.7	0.72	107.4	321.6	0.33
44	146.7	95.7	1.5	133.1	158.6	0.84
45	130.3	122.7	1.1	160.9	289.3	0.56
46	132.7	95.7	1.4	231.1	191	1.2
47	153.7	91.5	1.7	173.4	241.3	0.72
48	75.5	87.7	0.86	123.6	224.9	0.55
1	54	107.7	0.5	87.1	124.9	0.7
2						
3	148.3	175.8	0.84	165.1	158	1
4						
5	113.3	120	0.94	195.4	146.5	1.3
6	88.7	131.3	0.68	130	284.3	0.46
7	138			120		
8	69.7	104.7	0.67	143.1	209.3	0.68
9						
10	219.3	177.7	1.2	201	269.7	0.75

2.2) Serum iron markers for the Kalafong patient group and osteoarthritis patient group

For the purpose of this study it is the iron status and derangements of iron metabolism that were investigated in relation to the expression of the H-subunit and L-subunit of ferritin in the bone marrow macrophage and cells of the erythron. In order to determine the iron status the concentrations of various relevant factors relating to iron metabolism were determined in the blood. These included serum iron, transferrin, transferrin saturation, ferritin and the soluble transferrin receptor (Table 4).

2.3) Red blood production for the Kalafong patient group and osteoarthritis patient group

Red blood cell charateristics are useful in evaluating the iron status since the production of red blood cells is directly influenced by the iron status and inflammatory conditions. Red blood cell production is influenced by inflammatory processes as a result of the derangement in iron metabolism but also due to suppression of the bone marrow. The following were measured in relation to red blood cell production, red blood cell count, haemoglobin, haematocrit, mean corpuscular volume, mean corpuscular haemoglobin, mean corpuscular haemoglobin concentration, red blood cell distribution width and reticulocyte production index (Table 4).

2.4) Cytokines, C-reactive protein, neopterin, pro-hepcidin and caeruloplasmin

The cytokines investigated included interferon-γ (INF-γ), tumor necrosis factor-α (TNF-α), interleukin-1β (Il-1β), interleukin-6 (Il-6), interleukin-12 (Il-12), interleukin-2 (Il-2), interleukin-8 (Il-8), granulocyte macrophage-colony stimulating factor (GM-CSF), interleukin-4 (Il-4), interleukin-5 (Il-5), transforming growth factor-β (TGF-β) and interleukin-10 (Il-10) (Table 5).

Table 4. Serum iron markers and red blood cell production for the Kalafong patient group (patients 1-48) and the osteoarthritis patient group (patients 1-10)

Patient	Iron µmol/l	Trans-ferrin g/l	Trans-ferrin saturation %	Ferritin µg/l	Soluble transferrin receptor µg/ml	Trans-ferrin/ log ferritin	Soluble transferrin R/ log ferritin	RCC x 10^{12}/l	Hb g/dl	Hct l/l	MCV fl	MCH pg	MCHC g/dl	RDW %	RPI
1	2.4	1.58	6.8	171	5	0.71	2.24	2.62	5.6	0.17	65.7	21.3	32.4	20.6	0.15
2	33.8	0.6	252.2	1139	15.5	0.2	5.07	1.55	6.3	0.18	116.2	40.9	35.1	22.7	0.19
3	19.8	1.8	45	224	13.8	0.77	5.87	1.17	3.5	0.11	93.7	29.8	31.8	43.8	1.72
4	5.6	0.99	25.2	7756	3.8	0.26	0.98	3.03	11.8	0.35	114	39.1	34.3	14.2	1.27
5	3.3	1.41	10.5	888	18.5	0.48	6.28	3.33	7.9	0.24	71.3	23.7	33.2	27.3	0.24
6	9.6	2.39	17.9	262	23	0.99	9.51	4.4	9.4	0.29	66	21.4	32.4	20.6	0.42
7	10	0.98	45.7	234	10	0.41	4.22	2.85	8.5	0.24	84.7	29.8	35.1	18.2	1.08
8	6	1.42	18.9	780	2.4	0.49	0.83	3.33	10.3	0.3	89.4	31	34.7	15.9	0.36
9	5.4	1.1	20	1657	6.5	0.34	2.02	3.14	9.4	0.27	86.2	29.8	34.6	16.5	
10	1.3	3.06	1.9	3	52	6.41	108.99	1.54	2.6	0.09	60.8	16.8	27.7	23	
11	5.4	1.53	15.8	334	2.4	0.61	0.95	1.23	4.2	0.12	99.1	34.1	34.4	21.8	0.88
12	13.2	2.77	21.3	58.6	6.5	1.57	3.68	5.77	14.9	0.48	82.4	25.9	31.3	15.7	
13	1.8	0.8	9	3975	4	0.22	1.11	1.91	4.7	0.15	76.8	24.6	32	15.8	
14	7.1	0.94	33.8	2096	5.8	0.28	1.75	3.38	9.5	0.29	85.8	28.2	32.9	15.8	
15	4.9	1.53	14.3	581	13.8	0.55	4.99	2.79	9	0.26	94.3	32.2	34.1	30.1	0.1
16	8.9	1.49	26.7	124	10.5	0.71	5.02	2.12	6.6	0.21	97.4	31.4	32.3	25	2.8
17	16.6	1.4	53	241	4.3	0.59	1.81	3.63	10.2	0.32	86.6	28.1	32.4	14.2	
18	13.4	1.64	36.5	304	32.5	0.66	13.09	0.87	3.2	0.1	113.1	37.1	32.8	20.1	2.04
19	1.7	1.17	6.5	669	9	0.41	3.19	1.96	4.9	0.16	83	25.2	30.4	20.3	0.26
20	2.3	2.15	4.8	83.1	20	1.12	10.42	3.84	9	0.31	79.8	23.5	29.5	18.4	
21	16.4	0.7		7316	8	0.18	2.07	2.7	6.9	0.22	82.3	25.7	31.3	19.8	
22	9.5	0.65		2855	4.5	0.19	1.3	3.78	13.3	0.4	106.5	35.3	33.1	14.2	
23	16.7	1.12	66.5	2016	5	0.34	1.51	2.67	6.9	0.23	84.5	25.7	30.4	19.1	
24	3.3	2.02	7.3	17.6	18	1.62	14.45	2.26	4	0.14	59.6	17.8	29.8	19.2	
25	2.9	3.23	4	3.7	23	5.69	40.48	3.77	5.8	0.21	54.4	15.4	28.4	22.8	0.24
26	10.2	2.3	19.8	116	4	1.11	1.94	4.16	13.7	0.42	100.1	32.9	32.9	14.2	
27	6	2.72	9.9	11	11	2.61	10.56	3.76	10	0.32	84.2	26.5	31.5	15.4	0.59
28	15.6	1.12	62.2	87.3	6	0.58	3.09	2.43	10.7	0.31	125.3	44.1	35.2	15.7	
29	11.4			5672	10.8		2.88	2.2	8.1	0.22	100.2	36.8	36.7	21.3	
30	14.4	2.3	25	50	5.3	1.35	3.12	4.23	13.7	0.435	102.8	32.4	31.5	15.7	
31	7.8	0.6	49	19644	3.5	0.14	0.82	2	4.6	0.142	71	23	32.4	18.7	
32	13.1	3.3	16	15	6.5	2.81	5.53	5.3	14.1	0.47	88.7	26.6	30	14.1	
33	7.4	1	29	45519	26.3	0.22	5.65	1.99	4.1	0.134	67.3	20.6	30.6	30.7	
34	4.8	1.1	18	913	10	0.37	3.38	1.29	3.5	0.129	100	27.1	27.1	18.9	
35	10.5	2.3	18	32	5.3	1.53	3.52	4.18	11.6	0.359	85.9	27.8	32.3	16.9	
36	8.7	0.9	39	2073	5.8	0.27	1.75	1.03	3.7	0.115	111.7	35.9	32.2	24.1	
37	16.9	1.9	35	29.1	11	1.3	7.51	1.66	4	0.132	79.5	24.1	30.3	29	0.08
38	39.6	1.8	88	63.1	14	1	7.78	0.99	2.7	0.087	87.9	27.3	31	33.6	0.06
39	36.6	1.6	91	782.8	4.5	0.55	1.56	0.95	3.3	0.101	106.3	34.7	32.7		0.01
40	8.9	1.4	25	5760	9.5	0.37	2.53	2.08	5.2	0.17	81.7	25	30.6	18	
41	3.9	4.3	4	4	33.5	7.14	55.64	1.57	2.8	0.107	68.2	17.8	26.2	27.1	0.15
42	4	2.9	6	37	36.3	1.85	23.15	2.71	5.9	0.23	84.9	21.8	25.7	33.9	0.63
43	3.3	3.2	4	23.4	25	2.34	18.26	2.99	5.9	0.207	69.2	19.7	28.5	18.5	
44	4.8	1.8	11	289.1	3	0.73	1.22	3.77	9.5	0.301	79.8	25.2	31.6	15.4	
45	13.5	1.5	36	859.8	6.3	0.51	2.15	2.99	9.6	0.305	102	32.1	31.5	14.9	
46	4.5	1.9	9	301.1	7	0.77	2.82	4.69	13.7	0.417	88.9	29.2	32.9	14.4	
47	1.7	1.4	5	266.9	17	0.58	7.01	1.16	3.2	0.101	87.1	27.6	31.7	33.6	0.73
48	6.9	3.4	8	21.6	25	2.55	18.73	2.47	4.5	0.168	68	18.2	26.8	26.7	0.11
1	7.3	2.41	13.5	30.8	4.8	1.62	3.23	4.06	13.5	0.41	101.2	33.3	32.9	12.9	
2	18.6	1.95	42.7	120	1.8	0.94	0.87	4.22	14	0.41	97.4	33.2	34	12.7	
3	14.7	1.68	39.1	219	1.5	0.72	0.64		14.9	0.44					
4	8.8	2.2	17.9	170	3.4	0.99	1.52	4.62	16.1	0.481	104.2	35	33.6	12.4	
5	15	2	33.5	59	3.8	1.13	2.15	5.17	16.1	0.46	88.8	31.2	35.1	12.8	
6	11	2.1	23.4	35	3.4	1.36	2.2	3.91	11.8	0.359	91.9	30.2	32.9	12.6	
7	5.2	0.9	25.9	54	2.5	0.52	1.44	5.2	15.1	0.49	94.3	29.2	30.9	14.1	
8	18.3	1.5	54.5	163	1.8	0.68	0.81	6	17.2	0.535	89.2	28.7	32.2	13.8	
9	7	3	10.4	16	5.8	2.49	4.82	5.04	14.7	0.444	88.1	29.1	33	13.1	
10	22.6	2.4	42.1	75	4	1.28	2.13	5.06	15.2	0.467	92.3	30.1	32.6	12.1	

Table 5. Humoral factors for the Kalafong patient group (patients 1-48) and the osteoarthritis patient group (patients 1-10)

Patient	Il-1	Il-2	Il-4	Il-5	Il-6	Il-8	Il-10	Il-12	TNF-alpha	TGF-beta	INF-gamma	GM-CSF	Neopterin	C-reactive protein	Pro-hepcidin	Caerulo-plasmin
	pg/ml								pg/ml	ng/ml	pg/ml	pg/ml	ng/ml	mg/l	ng/ml	g/l
1	7.4	7.7	3.1	1.7	37.4	115	8.3	13.6	4.8	15.5	0.1	16.5	46.8	137.6	88	0.6
2	2.2	16.3	0.5	1	13	21.2	3	5.8	3.1	3.4	0.1	0.5	15.4	16.7	123	0.3
3	23.8	10.5	2.8	2.6	9739	1020	117	15.2	7	24.5	6.5	33.5	50.1	67	98	0.7
4	0.2	17.5	3.2	7.2	151	37.6	8.3	0.5	2.5	9.4	9.5	0.5	21.3	330	198	0.5
5	30.9	21.4	3.8	2.4	141	68.9	10.1	8.4	15.6	11.8	16	32.1	23.9	118	255	0.4
6	3	8	6.5	1.3	0.5	0.5	10.1	0.5	1.4	4.4	0.1	0.5	1.6	0.33	275	0.4
7	0.2	16.4	2.6	2.4	26.1	19.3	4	8.4	3.3	6.8	1.5	0.5	6.7	28.9	158	0.4
8	12	15.8	5	2.9	8917	1135	11.1	4.1	2.9	3.6	1.5	2	3.4	100	115	0.5
9	3.4	8	5.4	1.6	26.4	77	1.2	0.5	1.3	15.4	0.1	4	6.2	47	108	0.4
10	4	28.3	3.1	2.9	16.3	17	8.7	13.3	5	3	0.1	0.5	4	2.2	140	0.5
11	1.9	13.9	0.5	4.1	44	51.7	4.3	0.5	1.8	3.6	0.1	0.5	66.3	71	250	0.4
12	0.2	7	3.1	1.9	1	11.5	4.3	0.5	3	8	0.1	0.5	2.2	2.5	173	0.7
13	2.6	2.1	5.1	2.6	149	36.7	46	6.2	3.2	5.4	0.5	0.5	37.7	92.4	78	0.4
14	0.2	11.5	2.3	3.1	63.4	39.9	2.4	0.5	3.1	8.3	71.5	8.5	23	138.1	112	0.3
15	0.2	17.6	0.5	2.7	2.4	16.5	3.3	3.5	3	5.4	9.5	240	1.9	0.28	173	0.4
16	0.2	10.1	5.3	3.7	4.7	12.8	11.7	0.5	1.4	17.9	0.1	39.2	10.8	6.3	114	0.4
17	0.2	15.5	2.4	15.5	8.2	39.4	8.2	0.5	2.8	9.1	7	28	52.6	2.5	133	0.4
18	18.6	8.8	0.5	1.8	12.8	18.6	8.7	7.9	8.3	8.3	2.5	25.2	19.4	20.7	149	0.8
19	0.9	21	0.5	2.8	25.5	123	53.9	2.5	4.4	13	7.5	0.5	41.2	28.2	105	
20	0.2	0.5	3.4	0.7	341	27.8	2.7	0.5	0.98	24.4	0.1	2	2.2	90	63	0.4
21	0.2	19.1	3.6	2.9	92	292	5.3	0.5	5.2	8	7.5	5	39	133.1	75	0.5
22	1.2	14.6	0.5	3.4	490	342	15.8	2.7	4.2	8.4	0.1	0.5	38.6	254	149	0.5
23	4.8	11.9	0.5	2.2	5.6	52.8	6.4	0.5	2.1	6.9	2.5	4	20	71	1525	0.4
24	0.2	12.9	4.3	3.6	56.9	26.3	10.7	0.5	1.4	5.5	0.1	47.2	3.9	8.2	154	0.4
25	0.2	4.1	0.5	2	3.6	18.5	4.5	0.5	0.96	13.3	0.1	0.5	4.3	0.65	123	0.4
26	0.2	2.4	0.5	1.2	5.8	19.2	3.5	8.3	3.5	24.7	8.5	7	2	10.1	158	0.3
27	0.96	5.3	0.5	3.7	2.8	15.1	4.4	2.3	3.1	3.9	0.1	15	4.2	1	145	0.3
28	5.4	13	1.8	0.1	46.2	30.4	3.4	3.1	2.3	14	1.5	7	2.7	21.7	122	0.4
29	4.7	4.3	2.2	2.5	155	196	66.7	9.3	4.1	9.3	156	1	80.2	134	102	0.7
30	1.6	15.9	0.5	4.5	2.8	12.9	3.7	7.3	3.2	16	0.1	0.5	1.4	19.6	212	0.5
31	41.2	8.9	5.1	4.1	1655	4466	17.5	3.7	3.8	7	17	1.2	83.5	200	118	0.7
32	0.2	10.2	0.5	2.5	1.5	11	2.1	5.5	2.3	10.5	0.1	0.5	2	3	212	0.4
33	0.2	6.8	3.7	2.1	125	688	316	0.5	6.2	11.5	366	5	55.7	19.7	115	0.6
34	0.2	0.5	4.3	3.6	585	20.9	4.9	0.5	2.8				8.9	45.5	149	
35	0.88	8.6	6.7	3.8	1.5	13.6	4.3	8.5	3.2	25.4	0.1	0.5	2	5.2	198	0.6
36	0.2	2.7	2.4	5	51.8	390	66.9	4.7	8.8	7.9	5.5	0.5	63	45.5	112	0.3
37	0.2	15.6	3.5	0.1	7	8.4	6.9	5.4	3	5.2	1.5	10.1	7.3	2	133	0.2
38	0.2	0.5	0.5	3.2	9.3	19.5	7.4	10.2	2.6	6.5	0.1	59	5.9	1	158	0.6
39	2	0.5	0.5	4.1	2.9	16.1	8.8	3.4	2	11.8	0.1	0.5	17.1	7.3	158	0.9
40	18.5	0.5	5.7	4.5	453	173	10.5	3.6	3.1	17.5	4.5	1.1	38	52.5	180	0.4
41	9.8	0.5	0.5	0.1	1.9	13.3	2.2	7.9	3.7	6.4	0.1	0.5	2.8	0.5	173	0.6
42	1.6	22	2.4	1	5.4	24.1	2.7	6.8	2.2	23.9	0.1	0.5	2.2	0.94	175	0.3
43	0.2	0.5	0.5	3.8	0.89	15.7	2.6	5	1.7	23	0.1	0.5	7.3	1.3	140	0.5
44	1.6	13.6	2	3.8	17.5	108	6.1	4.1	2.2	23.7	0.1	0.5	6.6	20.8	120	0.3
45	0.2	19.7	4.6	19.9	6.9	95.2	1.6	6.6	1.9	9.4	0.1	0.5	12.9	8.6	135	0.3
46	3.1	14.6	0.5	3.6	6.6	12.6	3.5	6.3	4	27.9	0.1	10.1	3.1	16.6	152	0.7
47	1.8	8.9	0.5	2.1	42.8	107	3	4.7	1.8	10.7	29.5	0.5	50.6	53	122	0.4
48	0.2	0.5	0.5	1.5	2.6	6.8	1.4	7.6	2.2	6.5	0.1	1.2	1.9	0.04	114	0.4
1	1.9	10.5	4.8	4.6	7.1	31.3	4.4	2.5	3.7	24.1	0.1	0.5	1.9	5.5	130	0.5
2	10.7	0.5	0.5	2.3	4.7	21.6	2.3	0.5	3.6	18.4	0.1	0.5	2.3	0.56	146	0.5
3	0.2	7.1	0.5	3.5	2.7	11.8	3.1	0.5	3.2	10.4	0.1	0.5	1.7	2.77	122	0.2
4	0.2	14	5.5	3.6	7.6	22.2	2.9	0.5	2.7	23.2	0.1	1.2	3.4	17.3	114	0.5
5	0.2	0.5	0.5	3.7	5.5	16	2	0.5	2.7	18.7	0.1	0.5	1.8	1.59	138	0.6
6	1.7	2	0.5	3.1	3.3	20.4	1.1	0.5	1.6	16.3	0.1	20.5	2.6	2.22	114	0.5
7	0.2	11	3	1.1	8.3	10.8	5.9	0.5	0.92	14.3	0.1	5.8	2	0.26	120	0.3
8	0.2	7.7	5.1	0.1	4.8	20.7	2.7	0.5	2	17.7	0.1	3	1.7	1.22	152	0.5
9	0.2	10.6	4.2	1.5	3.4	23.1	2.3	4.3	3.4	20.9	0.1	0.5	2.1	0.68	155	0.6
10	0.2	3	0.5	0.1	2.3	11.8	0.5	0.5	1.6	18.8	0.1	2.5	2.4	2.04	215	0.3

3) Statistical analysis of the study

For the Kalafong patient group three different subdivisions were investigated statistically. The osteoarthritis patients were treated as a separate group and included with each of the subdivisions of the Kalafong patients for statistical evaluation.

1) Kalafong patients were subdivided into two groups based on normal and elevated C-reactive protein levels. Refer to table 6, table 9 and bar diagram figures 1a-33a.

2) Kalafong patients were subdivided into two groups based on normal and elevated neopterin levels. Refer to table 7, table 10 and bar diagram figures 1b-33b.

3) Kalafong patients were subdivided into two groups based on the presence or absence of an iron transfer block. Refer to table 8, table 11 and bar diagram figures 1c-33c.

For the subdivision based on C-reactive protein and the osteoarthritis patients, the subdivision based on neopterin and the osteoarthritis patients and the subdivision based on the presence or absence of an iron transfer block and the osteoarthritis patients the groups were compared using the Welch t-test and since groups were relatively small and variances could be large, use was also made of the ranksum (Mann-whitney) test. The p-values for both tests were reported and when interpreted, preference was given to the p-value of the ranksum test when the Welch t-test was not significant. Testing was done at the 0.05 level of significance. A p-value of 0.05 and less was taken as statistically significant and a p-value of > 0.05 and < 0.1 was considered as marginally different.

Correlations for the study

Pearson's product-moment correlation coefficient (r) was employed to assess dependence between study parameters.

Table 6. Descriptive statistics and statistical evaluation of expression of the H-subunit and L-subunit of ferritin, serum iron markers, red blood cell production, pro-hepcidin and caeruloplasmin for the C-reactive protein subdivision of the Kalafong patients and the osteoarthritis patients

				CRP elevated vs CRP normal			CRP elevated vs osteoarthritis		CRP normal vs osteoarthritis	
Variable		CRP Elevated	CRP normal	t-test	Mann-Whitney	Osteo-arthritis	t-test	Mann-Whitney	t-test	Mann-Whitney
H-subunit macrophages count/µm²	Mean SD N	96.9 40.6 25	76.5 30 19	0.074	0.159	118.8 56.1 7	0.256	0.374	0.02	0.06
L-subunit macrophages count/µm²	Mean SD N	117.8 45.9 26	107.7 26.8 19	0.397	0.646	136.2 32.8 6	0.363	0.218	0.042	0.098
H-subunit/L-subunit macrophages	Mean SD N	0.99 0.58 25	0.73 0.29 19	0.086	0.205	0.81 0.26 6	0.474	0.549	0.564	0.408
H-subunit cells of erythron count/µm²	Mean SD N	144.4 57.6 25	128.1 48.7 19	0.326	0.456	148.8 41.2 7	0.853	0.538	0.329	0.193
L-subunit cells of erythron count/µm²	Mean SD N	212.3 76.6 26	215.6 54.4 19	0.873	0.581	198.8 66.8 6	0.693	0.809	0.537	0.525
H-subunit/L-subunit cells of erythron	Mean SD N	0.78 0.47 25	0.61 0.24 19	0.163	0.414	0.83 0.31 6	0.831	0.549	0.091	0.075
Serum iron µmol/l	Mean SD N	9 6.9 29	11.3 10.6 19	0.405	0.898	12.9 5.9 10	0.102	0.058	0.619	0.142
Transferrin g/l	Mean SD N	1.3 0.5 28	2.5 0.83 19	0	0.0002	2 0.57 10	0.003	0.002	0.098	0.261
Transferrin saturation %	Mean SD N	34.2 47.7 26	24.3 26.5 19	0.382	0.106	30.3 14.4 10	0.71	0.437	0.439	0.094
Ferritin µg/l	Mean SD N	3903.1 8942.6 29	166.8 270.3 19	0.033	0.002	94.2 69.6 10	0.03	0.0001	0.281	0.359
Soluble transferrin receptor µg/ml	Mean SD N	9.5 7.4 29	17.3 12.9 19	0.023	0.336	3.3 1.4 10	0.0001	0.0006	0.0002	0

Transferrin/ log ferritin	Mean SD N	0.51 0.31 28	2.2 2 19	0.002	0.0008	1.2 0.58 10	0.005	0.0003	0.044	0.183
Soluble transferrin receptor/ log ferritin	Mean SD N	3.4 2.9 29	18.1 26.1 19	0.025	0.065	2 1.3 10	0.04	0.131	0.015	0.0003
Red blood cell count x 10^{12}/l	Mean SD N	2.6 1.1 29	2.9 1.4 19	0.322	0.0008	4.8 0.67 9	0	0	0	0.002
Haemoglobin g/dl	Mean SD N	7.6 3.5 29	7.2 3.8 19	0.739	0.004	14.9 1.5 10	0	0	0	0.0001
Haematocrit l/l	Mean SD N	0.23 0.1 29	0.24 0.12 19	0.908	0.001	0.45 0.05 10	0	0	0	0.0002
Mean corpuscular volume fl	Mean SD N	91.3 15.6 29	80.3 14.9 19	0.018	0.926	94.2 5.7 9	0.416	0.3	0.002	0.006
Mean corpuscular haemoglobin pg	Mean SD N	29.8 6.1 29	24.5 5.9 19	0.004	0.71	31.1 2.2 9	0.344	0.287	0.0002	0.003
Mean corpuscular haemoglobin concentration g/dl	Mean SD N	32.5 2 29	30.3 2.4 19	0.002	0.353	33 1.2 9	0.373	0.39	0.0003	0.002
Red blood cell distribution width %	Mean SD N	20.2 6.6 29	21.1 8.2 19	0.689	0.479	12.9 0.64 9	0	0	0.0004	0.0002
RPI	Mean SD N	0.81 0.65 11	0.47 0.8 11	0.29	0.039					
Neopterin ng/ml	Mean SD N	29.5 24.8 29	7.7 11.7 19	0.0002	0	2.2 0.52 10	0	0.0001	0.053	0.017
Pro-hepcidin ng/ml	Mean SD N	135.2 48.2 28	159.3 38.6 19	0.065	0.039	140.6 30.2 10	0.686	0.479	0.164	0.118
Caeruloplasmin g/l	Mean SD N	0.47 0.15 27	0.46 0.16 19	0.733	0.643	0.45 0.14 10	0.644	0.986	0.891	0.76
CD4 x 10^{6}/l	Mean SD N	293 397.7 20	449.3 664.9 10	0.505	0.072					

Table 7. Descriptive statistics and statistical evaluation of expression of the H-subunit and L-subunit of ferritin, serum iron markers, red blood cell production, pro-hepcidin and caeruloplasmin for the neopterin subdivision of the Kalafong patients and the osteoarthritis patients

				Neopterin elevated vs neopterin normal			Neopterin elevated vs osteoarthritis		Neopterin normal vs osteoarthritis	
Variable		Neopterin elevated	Neopterin normal	t-test	Mann-Whitney	Osteo-arthritis	t-test	Mann-Whitney	t-test	Mann-Whitney
H-subunit macrophages count/µm²	Mean SD N	94.7 37.3 31	72.4 34 13	0.071	0.037	118.8 56.1 7	0.17	0.3	0.033	0.052
L-subunit macrophages count/µm²	Mean SD N	108.1 34.3 32	126.8 47.5 13	0.147	0.26	136.2 32.8 6	0.073	0.085	0.668	0.456
H-subunit/L-subunit macrophages	Mean SD N	0.97 0.49 31	0.66 0.43 13	0.051	0.023	0.81 0.26 6	0.445	0.564	0.43	0.188
H-subunit cells of erythron count/µm²	Mean SD N	141.4 54.6 31	127.8 53.3 13	0.452	0.322	148.8 41.2 7	0.739	0.463	0.378	0.191
L-subunit cells of erythron count/µm²	Mean SD N	200.7 54.9 31	245.7 85.7 13	0.41	0.115	198.8 66.8 6	0.938	0.873	0.255	0.335
H-subunit/L-subunit cells of erythron	Mean SD N	0.77 0.42 31	0.57 0.31 13	0.139	0.062	0.83 0.31 6	0.742	0.51	0.116	0.035
Serum iron µmol/l	Mean SD N	10.4 9.6 35	8.7 4.5 13	0.423	0.898	12.9 5.9 10	0.322	0.096	0.08	0.063
Transferrin g/l	Mean SD N	1.5 0.7 34	2.5 0.84 13	0.0008	0.0002	2 0.57 10	0.025	0.012	0.104	0.153
Transferrin saturation %	Mean SD N	35.2 45.8 32	17.4 15.1 13	0.058	0.106	30.3 14.4 10	0.604	0.497	0.049	0.028
Ferritin µg/l	Mean SD	3277.4 8236	126.8 164.5	0.03	0.002	94.2 69.6	0.029	0.003	0.528	0.804

	N	35	13			10				
Soluble transferrin receptor µg/ml	Mean SD N	11.8 10.2 35	14.8 11.5 13	0.416	0.336	3.3 1.4 10	0	0.0002	0.004	0.0002
Transferrin/ log ferritin	Mean SD N	0.96 1.4 34	1.8 1.7 13	0.118	0.0008	1.2 0.57 10	0.48	0.008	0.213	0.306
Soluble transferrin receptor/ log ferritin	Mean SD N	8.5 19 35	11.2 14.9 13	0.599	0.065	2 1.3 10	0.053	0.042	0.045	0.001
Red blood cell count x 10^{12}/l	Mean SD N	2.3 0.95 35	3.7 1.2 13	0.002	0.0008	4.8 0.67 9	0	0	0.161	0.057
Haemoglobin g/dl	Mean SD N	6.4 2.9 35	10.2 3.9 13	0.005	0.004	14.9 1.5 10	0	0	0.001	0.001
Haematocrit l/l	Mean SD N	0.2 0.08 35	0.33 0.12 13	0.002	0.001	0.45 0.05 10	0	0	0.003	0.01
Mean corpuscular volume fl	Mean SD N	86.8 16.2 35	87.3 16.3 13	0.925	0.926	94.2 5.7 9	0.034	0.081	0.182	0.082
Mean corpuscular haemoglobin pg	Mean SD N	27.9 6.3 35	27.2 7.2 13	0.767	0.71	31.1 2.2 9	0.018	0.074	0.087	0.053
Mean corpuscular haemoglobin concentration g/dl	Mean SD N	31.9 2.2 35	30.8 3 13	0.247	0.353	33 1.2 9	0.051	0.081	0.03	0.066
Red blood cell distribution width %	Mean SD N	20.6 7.5 35	20.3 6.8 13	0.872	0.479	12.9 0.64 9	0	0	0.002	0.0001
RPI	Mean SD N	0.75 0.8 17	0.28 0.23 5	0.047	0.272					
C-reactive protein mg/l	Mean SD N	64.7 77.2 35	13.1 24.4 13	0.001	0.002	3.4 5.1 10	0	0.0004	0.184	0.457
Pro-hepcidin ng/ml	Mean SD N	135.6 40 34	169.2 52.2 13	0.05	0.02	140.6 30.2 10	0.678	0.642	0.114	0.071
Caeruloplasmin g/l	Mean SD	0.47 0.16	0.47 0.14	0.957	0.889	0.45 0.14	0.748	0.848	0.741	0.975

	N	33	13			10				
CD4 x 10^6/l	Mean SD N	304.6 492.6 27	710 443.1 3	0.229	0.072					

Table 8. Descriptive statistics and statistical evaluation of expression of the H-subunit and L-subunit of ferritin, serum iron markers, red blood cell production, pro-hepcidin and caeruloplasmin for the iron transfer block subdivision of the Kalafong patients and the osteoarthritis patients

				Fe-block vs no Fe-block			Fe-block vs osteoarthritis		No Fe-block vs Osteoarthritis	
Variable		**Fe-block**	**No Fe-block**	**t-test**	**Mann-Whitney**	**Osteo-arthritis**	**t-test**	**Mann-Whitney**	**t-test**	**Mann-Whitney**
H-subunit macrophages count/µm²	Mean SD N	99.5 41 22	78.5 30.8 23	0.06	0.12	118.8 56.1 7	0.424	0.445	0.109	0.074
L-subunit macrophages count/µm²	Mean SD N	113.1 39.4 21	113.6 40.3 23	0.968	0.981	136.2 32.8 6	0.175	0.18	0.181	0.139
H-subunit/L-subunit macrophages	Mean SD N	1 0.57 21	0.76 0.39 23	0.116	0.178	0.81 0.26 6	0.251	0.448	0.732	0.451
H-subunit cells of erythron count/µm²	Mean SD N	141.5 50.9 22	135.1 57.1 23	0.691	0.364	148.8 41.2 7	0.706	0.508	0.493	0.292
L-subunit cells of erythron count/µm²	Mean SD N	211.5 59.6 21	217.5 76.1 23	0.774	0.972	198.8 66.8 6	0.684	0.641	0.567	0.706
H-subunit/L-subunit cells of erythron	Mean SD N	0.74 0.44 21	0.68 0.36 23	0.651	0.647	0.83 0.31 6	0.588	0.414	0.28	0.161
Serum iron µmol/l	Mean SD N	9.1 7.5 25	10.8 9.6 23	0.514	0.718	12.9 5.9 10	0.132	0.053	0.451	0.137
Transferrin g/l	Mean SD N	1.3 0.42 24	2.3 0.92 23	0	0.0001	2 0.57 10	0.003	0.001	0.328	0.457

Transferrin saturation %	Mean SD N	27.7 21.7 22	32.3 52.5 23	0.702	0.301	30.3 14.4 10	0.69	0.371	0.869	0.153
Ferritin µg/l	Mean SD N	2709.6 4210.9 25	2113.8 9465 23	0.783	0	94.2 69.6 10	0.005	0.0001	0.317	0.814
Soluble transferrin receptor µg/ml	Mean SD N	7.1 4.4 25	18.5 12.1 23	0.0002	0	3.3 1.4 10	0.0004	0.002	0	0
Transferrin/ log ferritin	Mean SD N	0.48 0.28 24	2 1.9 23	0.002	0	1.2 0.57 10	0.004	0.0002	0.088	0.457
Soluble transferrin receptor/ log ferritin	Mean SD N	2.6 1.9 25	16.5 23.9 23	0.011	0	2 1.3 10	0.313	0.454	0.008	0
Red blood cell count x 10^{12}/l	Mean SD N	2.5 0.95 25	2.9 1.4 23	0.237	0.348	4.8 0.67 9	0	0	0	0.002
Haemoglobin g/dl	Mean SD N	7.3 3.2 25	7.5 4.1 23	0.834	0.934	14.9 1.5 10	0	0	0	0
Haematocrit l/l	Mean SD N	0.22 0.09 25	0.24 0.13 23	0.558	0.796	0.45 0.05 10	0	0	0	0.0002
Mean corpuscular volume fl	Mean SD N	89.8 13 25	83.9 18.6 23	0.214	0.208	94.2 5.7 9	0.186	0.212	0.024	0.024
Mean corpuscular haemoglobin pg	Mean SD N	29.1 5 25	26.2 7.7 23	0.122	0.101	31.1 2.2 9	0.12	0.178	0.009	0.019
Mean corpuscular haemoglobin concentration g/dl	Mean SD N	32.4 1.9 25	30.8 2.7 23	0.024	0.027	33 1.2 9	0.263	0.274	0.003	0.013
Red blood cell distribution width %	Mean SD N	19.7 5.5 24	22.3 7.5 23	0.197	0.273	12.9 0.64 9	0	0	0	0
RPI	Mean SD N	0.41 0.41 10	0.84 0.89 12	0.158	0.291					

Neopterin ng/ml	Mean SD N	31.7 24.5 25	9.2 14.5 23	0.0004	0.0002	2.2 0.52 10	0	0	0.03	0.014
C-reactive protein mg/l	Mean SD N	84.1 83.2 25	14.5 22.3 23	0.0004	0.0001	3.4 5.1 10	0.0001	0.0001	0.03	0.147
Pro-hepcidin ng/ml	Mean SD N	194 281 25	151.6 44.7 23	0.463	0.256	140.6 30.2 10	0.357	0.688	0.418	0.367
Caeruloplasmin g/l	Mean SD N	0.44 0.16 23	0.49 0.14 23	0.291	0.214	0.45 0.14 10	0.905	0.507	0.439	0.674
CD4 x 10^6/l	Mean SD N									

Table 9. Descriptive statistics and statistical evaluation of all cytokines for the C-reactive protein subdivision of the Kalafong patients and the osteoarthritis patients

				CRP elevated vs CRP normal			CRP elevated vs osteoarthritis		CRP normal vs osteoarthritis	
Variable		**CRP elevated**	**CRP normal**	**t-test**	**Mann-Whitney**	**Osteo-arthritis**	**t-test**	**Mann-Whitney**	**t-test**	**Mann-Whitney**
GM-CSF pg/ml	Mean SD N	6.1 9.4 28	23.4 55.5 19	0.194	0.882	3.6 6.2 10	0.344	0.448	0.14	0.763
Interleukin-1beta pg/ml	Mean SD N	6.5 10.3 29	1.3 2.3 19	0.013	0.01	1.6 3.3 10	0.029	0.036	0.816	0.829
Interleukin-2 pg/ml	Mean SD N	10.7 6.3 29	9.9 8.2 19	0.72	0.499	6.7 4.9 10	0.051	0.067	0.203	0.488
Interleukin-4 pg/ml	Mean SD N	2.5 1.8 29	2.4 2.2 19	0.917	0.761	2.5 2.2 10	0.996	0.947	0.939	0.942
Interleukin-5 pg/ml	Mean SD N	2.8 1.5 29	4.1 5 19	0.313	0.924	2.4 1.6 10	0.418	0.552	0.189	0.462
Interleukin-6	Mean	807.6	7.2	0.081	0	5	0.081	0	0.468	0.313

pg/ml	SD N	2384.6 29	12.6 19			2.1 10				
Interleukin-8 pg/ml	Mean SD N	334.6 845.2 29	20.1 19.9 19	0.055	0	18.9 6.4 10	0.054	0.0009	0.823	0.359
Interleukin-10 pg/ml	Mean SD N	28.1 61.6 29	5.6 3.3 19	0.059	0.09	2.7 1.5 10	0.035	0.0005	0.004	0.028
Interleukin-12 pg/ml	Mean SD N	4.6 4 29	4.7 3.8 19	0.962	0.906	1.1 1.3 10	0.0001	0.005	0.001	0.007
TNF-alpha pg/ml	Mean SD N	4.1 2.9 29	2.5 0.97 19	0.007	0.007	2.5 0.96 10	0.014	0.067	0.843	0.714
TGF-beta ng/ml	Mean SD N	12.4 7.1 28	10.5 7.1 19	0.369	0.209	18.3 4.1 10	0.003	0.011	0.0007	0.005
INF-gamma pg/ml	Mean SD N	25.6 73.8 28	1 2.6 19	0.09	0.0008	0.1 0 10	0.079	0.0008	0.135	0.193

Table 10. Descriptive statistics and statistical evaluation of all cytokines for the neopterin subdivision of the Kalafong patients and the osteoarthritis patients

				Neopterin elevated vs neopterin normal			Neopterin elevated vs osteoarthritis		Neopterin normal vs osteoarthritis	
Variable		**Neopterin elevated**	**Neopterin normal**	**t-test**	**Mann-Whitney**	**Osteo-arthritis**	**t-test**	**Mann-Whitney**	**t-test**	**Mann-Whitney**
GM-CSF pg/ml	Mean SD N	10.2 15.6 34	20.8 65.9 13	0.574	0.482	3.6 6.2 10	0.054	0.427	0.366	0.947
Interleukin-1beta pg/ml	Mean SD N	5.4 9.7 35	2 2.8 13	0.075	0.537	1.6 3.3 10	0.057	0.117	0.721	0.373
Interleukin-2 pg/ml	Mean SD N	10.7 7.1 35	9.3 7.1 13	0.538	0.577	6.7 4.9 10	0.049	0.101	0.306	0.455
Interleukin-4 pg/ml	Mean SD N	2.6 1.8 35	2.1 2.3 13	0.472	0.271	2.5 2.2 10	0.888	0.866	0.673	0.713

Interleukin-5 pg/ml	Mean SD N	3.9 3.7 35	1.9 1.4 13	0.011	0.011	2.4 1.6 10	0.072	0.219	0.478	0.514
Interleukin-6 pg/ml	Mean SD N	661.1 2187.6 35	32.3 93.6 13	0.099	0.0003	5 2.1 10	0.085	0.0005	0.314	0.193
Interleukin-8 pg/ml	Mean SD N	282.4 775.9 35	15.4 8.3 13	0.05	0.0001	18.9 6.4 10	0.053	0.007	0.258	0.321
Interleukin-10 pg/ml	Mean SD N	24.9 56.3 35	3.6 2.1 13	0.032	0.0006	2.7 1.5 10	0.026	0.0002	0.238	0.193
Interleukin-12 pg/ml	Mean SD N	4.5 4.2 35	5.1 3.1 13	0.587	0.364	1.1 1.3 10	0.0001	0.007	0.0005	0.003
TNF-alpha pg/ml	Mean SD N	3.8 2.8 35	2.7 0.89 13	0.048	0.451	2.5 0.96 10	0.035	0.252	0.722	0.664
TGF-beta ng/ml	Mean SD N	10.2 5.8 34	15.2 8.9 13	0.082	0.119	18.3 4.1 10	0.0001	0.0004	0.281	0.457
INF-gamma pg/ml	Mean SD N	21 67.4 34	1.6 3.3 13	0.103	0.056	0.1 0 10	0.079	0.003	0.135	0.112

Table 11. Descriptive statistics and statistical evaluation of all cytokines for the iron transfer block subdivision of the Kalafong patients and the osteoarthritis patients

				Fe-block vs no Fe-block			Fe-block vs osteoarthritis		No Fe-block vs osteoarthritis	
Variable		**Fe-block**	**No Fe-block**	**t-test**	**Mann-Whitney**	**Osteo-arthritis**	**t-test**	**Mann-Whitney**	**t-test**	**Mann-Whitney**
GM-CSF pg/ml	Mean SD N	15.2 48.6 24	10.9 17.4 23	0.684	0.937	3.6 6.2 10	0.259	0.514	0.085	0.628
Interleukin-1beta pg/ml	Mean SD N	5.5 10.3 25	3.4 6.1 23	0.386	0.497	1.6 3.3 10	0.099	0.107	0.286	0.275
Interleukin-2 pg/ml	Mean SD	11 6.9	9.6 7.3	0.503	0.363	6.7 4.9	0.047	0.062	0.184	0.409

	N	25	23			10				
Interleukin-4 pg/ml	Mean SD N	2.7 1.9 25	2.2 2 23	0.39	0.306	2.5 2.2 10	0.8	0.764	0.734	0.755
Interleukin-5 pg/ml	Mean SD N	4.2 4.3 25	2.3 1.3 23	0.045	0.043	2.4 1.6 10	0.07	0.214	0.957	0.984
Interleukin-6 pg/ml	Mean SD N	525.4 1782.4 25	453.1 2025.5 23	0.896	0.002	5 2.1 10	0.157	0.0005	0.3	0.667
Interleukin-8 pg/ml	Mean SD N	321.1 893.6 25	89.4 246.5 23	0.223	0.0001	18.9 6.4 10	0.104	0.0007	0.185	0.695
Interleukin-10 pg/ml	Mean SD N	15.2 19.9 25	23.5 68 23	0.582	0.122	2.7 1.5 10	0.005	0.0007	0.158	0.014
Interleukin-12 pg/ml	Mean SD N	4 3.4 25	5.4 4.3 23	0.2	0.224	1.1 1.3 10	0.0009	0.008	0.0001	0.004
TNF-alpha pg/ml	Mean SD N	3.8 2.9 25	3.2 1.9 23	0.391	0.477	2.5 0.96 10	0.071	0.177	0.228	0.638
TGF-beta ng/ml	Mean SD N	10.4 5.6 24	12.8 8.3 23	0.258	0.64	18.3 4.1 10	0.0001	0.0007	0.016	0.06
INF-gamma pg/ml	Mean SD N	14.8 33.7 24	16.5 76.2 23	0.924	0.0007	0.1 0 10	0.043	0.0006	0.313	0.117

4) Bar diagrams for variables for the different subdivisions

Figures 1a-33a contain bar diagrams for all variables for the C-reactive protein subdivision. Figures 1b-33b contain bar diagrams for all variables for the neopterin subdivision. Figures 1c-33c contain bar diagrams for all variables for the iron transfer block subdivision. Error bars refer to the standard deviation.

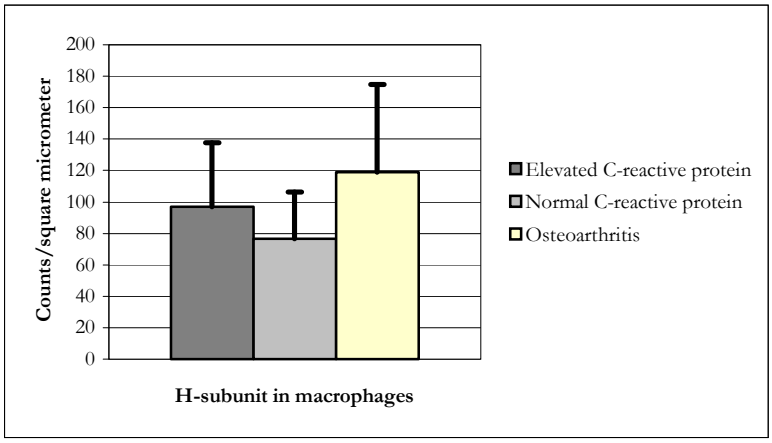

Figure 1a.
Marginally higher for elevated CRP group compared to normal CRP group.
No significant difference between elevated CRP group and osteoarthritis group.
Significantly higher for osteoarthritis group compared to normal CRP group.

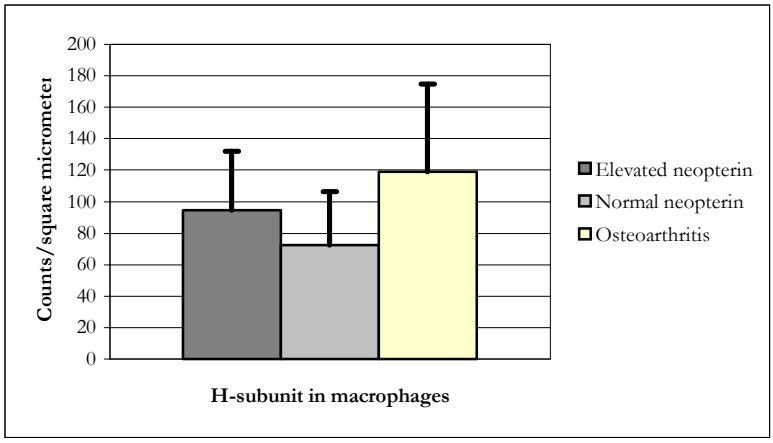

Figure 1b.
Significantly higher for elevated neopterin group compared to normal neopterin group.
No significant difference between elevated neopterin group and osteoarthritis group.
Significantly higher for osteoarthritis group compared to normal neopterin group.

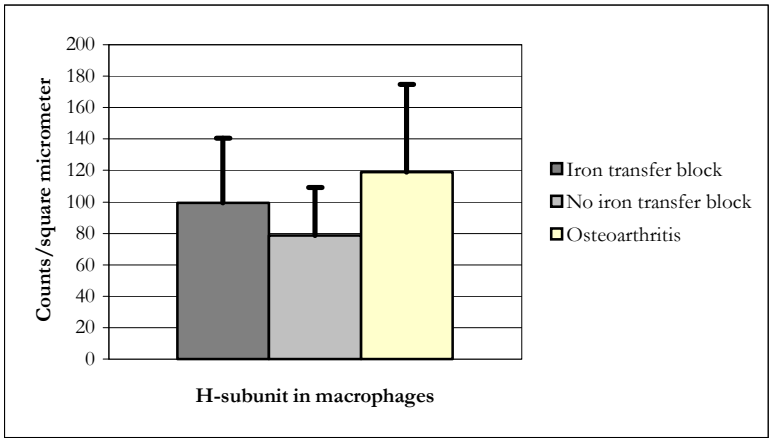

Figure 1c.
Marginally higher for iron transfer block group compared to no iron transfer block group.
No significant difference between iron transfer block group and osteoarthritis group.
Marginally higher for osteoarthritis group compared to no iron transfer block group.

Figure 1a – 1c. Differences in expression of the H-subunit of ferritin in the macrophage for the C-reactive protein subdivision, the neopterin subdivision and the iron transfer block subdivision.

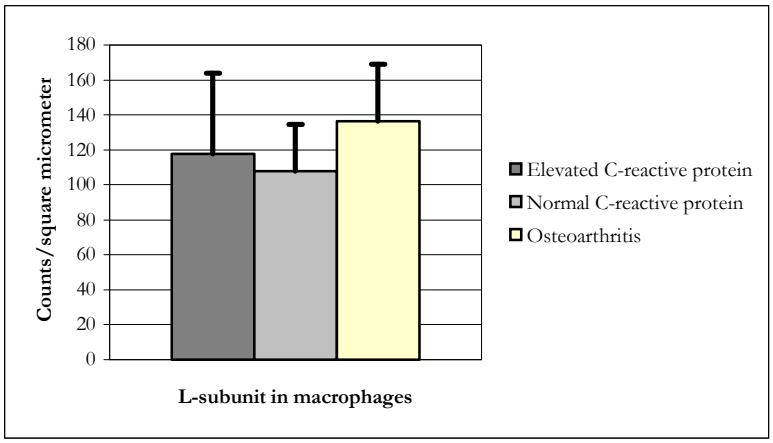

Figure 2a.
No significant difference between elevated CRP group and normal CRP group.
No significant difference between elevated CRP group and osteoarthritis group.
Significantly higher for osteoarthritis group compared to normal CRP group.

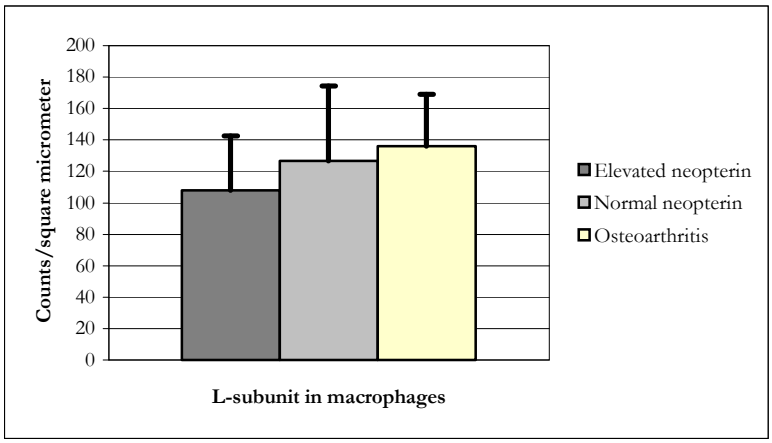

Figure 2b.
No significant difference between elevated neopterin group and normal neopterin group.
Marginally lower for elevated neopterin group compared to osteoarthritis group.
No significant difference between normal neopterin group and osteoarthritis group.

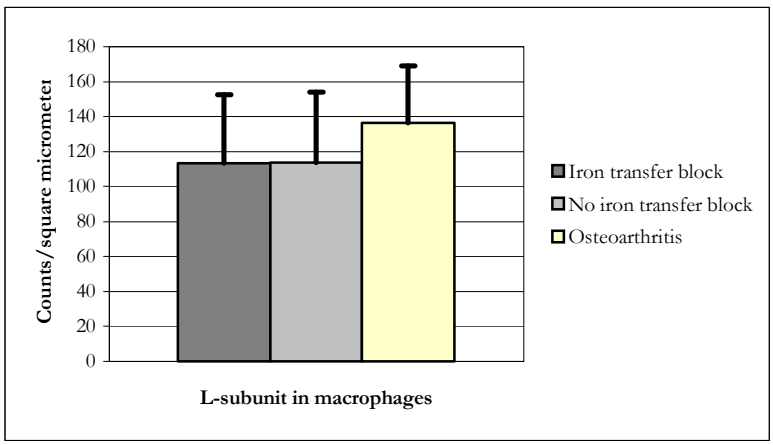

Figure 2c.
No significant difference between iron transfer block group and no iron transfer block group.
No significant difference between iron transfer block group and osteoarthritis group.
No significant difference between no iron transfer block group and osteoarthritis group.

Figure 2a – 2c. Differences in expression of the L-subunit of ferritin in the macrophage for the C-reactive protein subdivision, the neopterin subdivision and the iron transfer block subdivision.

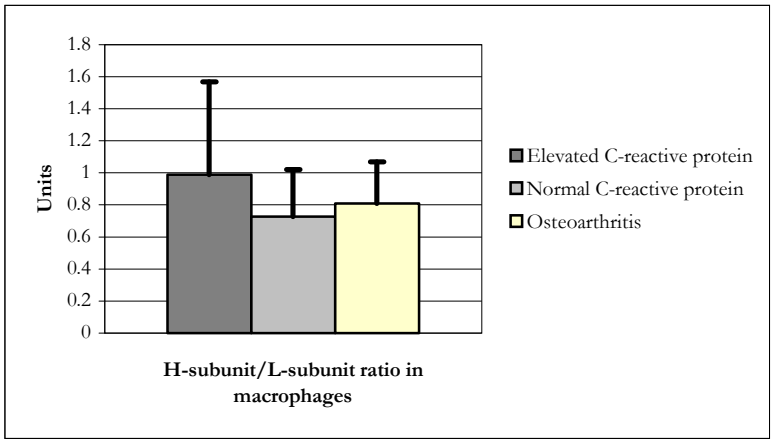

Figure 3a.
Marginally higher for elevated CRP group compared to normal CRP group.
No significant difference between elevated CRP group and osteoarthritis group.
No significant difference between normal CRP group and osteoarthritis group.

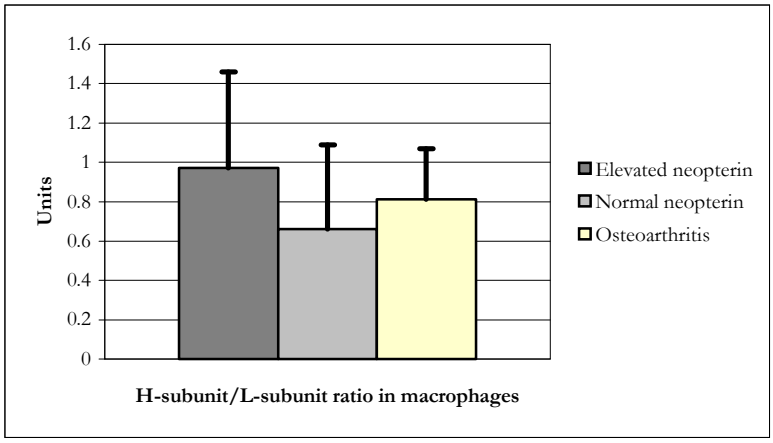

Figure 3b.
Significantly higher for elevated neopterin group compared to normal neopterin group.
No significant difference between elevated neopterin group and osteoarthritis group.
No significant difference between normal neopterin group and osteoarthritis group.

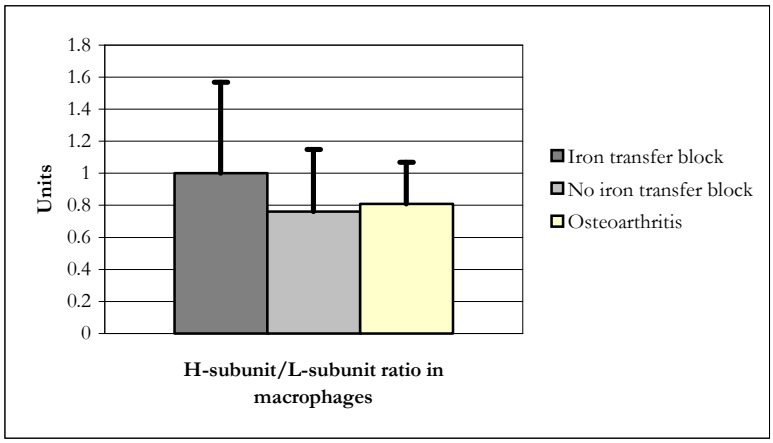

Figure 3c.
No significant difference between iron transfer block group and no iron transfer block group.
No significant difference between iron transfer block group and osteoarthritis group.
No significant difference between no iron transfer block group and osteoarthritis group.

Figure 3a – 3c. Differences in H-subunit/L-subunit ratio in the macrophage for the C-reactive protein subdivision, the neopterin subdivision and the iron transfer block subdivision.

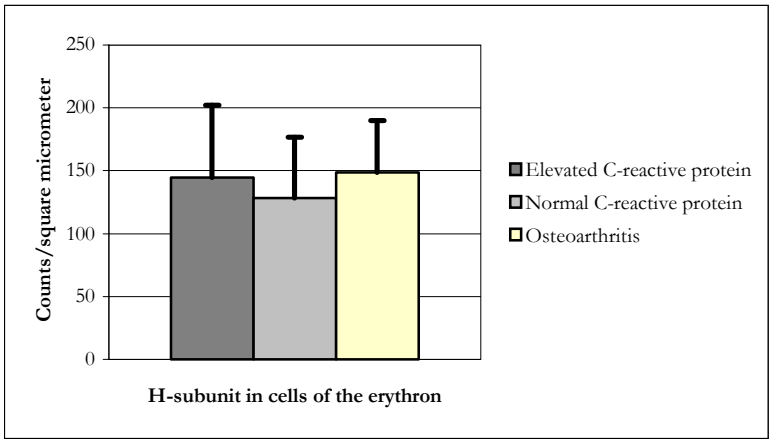

Figure 4a.
No significant difference between elevated CRP group and normal CRP group.
No significant difference between elevated CRP group and osteoarthritis group.
No significant difference between normal CRP group and osteoarthritis group.

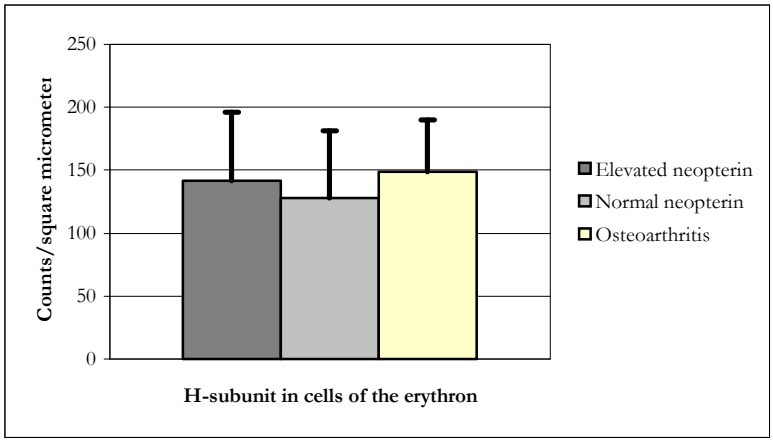

Figure 4b.
No significant difference between elevated neopterin group and normal neopterin group.
No significant difference between elevated neopterin group and osteoarthritis group.
No significant difference between normal neopterin group and osteoarthritis group.

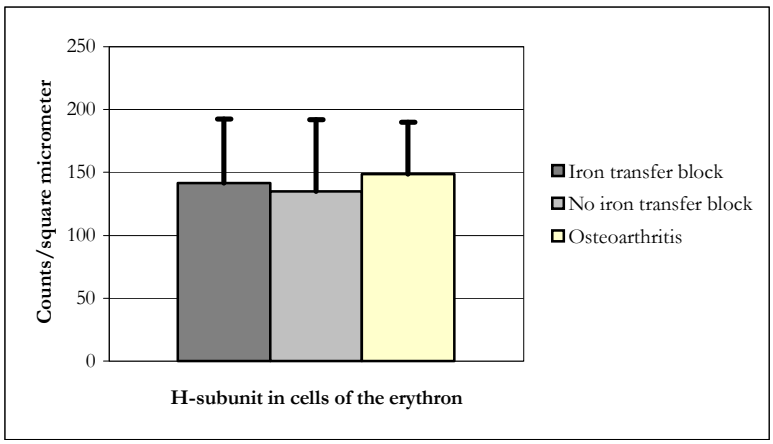

Figure 4c.
No significant difference between iron transfer block group and no iron transfer block group.
No significant difference between iron transfer block group and osteoarthritis group.
No significant difference between no iron transfer block group and osteoarthritis group.

Figure 4a – 4c. Differences in expression of the H-subunit of ferritin in cells of the erythron for the C-reactive protein subdivision, the neopterin subdivision and the iron transfer block subdivision.

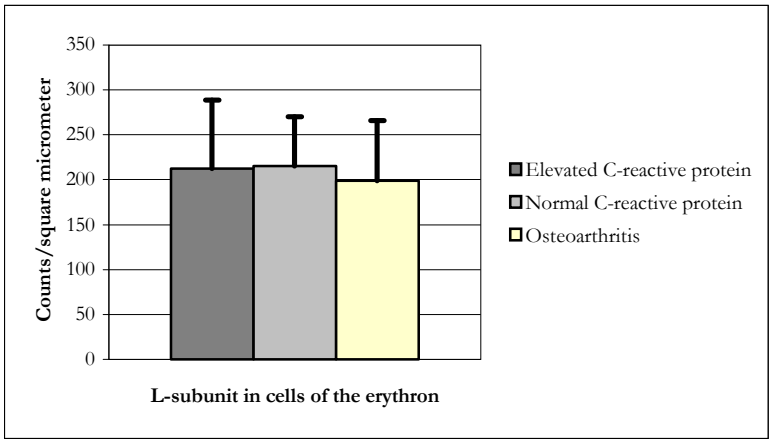

Figure 5a.
No significant difference between elevated CRP group and normal CRP group.
No significant difference between elevated CRP group and osteoarthritis group.
No significant difference between normal CRP group and osteoarthritis group.

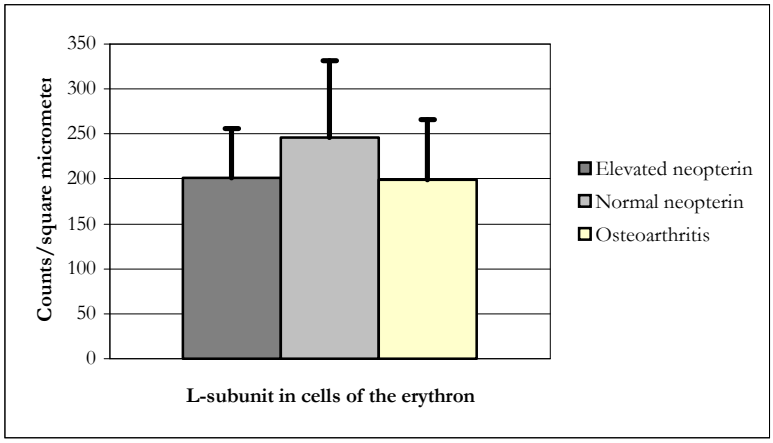

Figure 5b.
No significant difference between elevated neopterin group and normal neopterin group.
No significant difference between elevated neopterin group and osteoarthritis group.
No significant difference between normal neopterin group and osteoarthritis group.

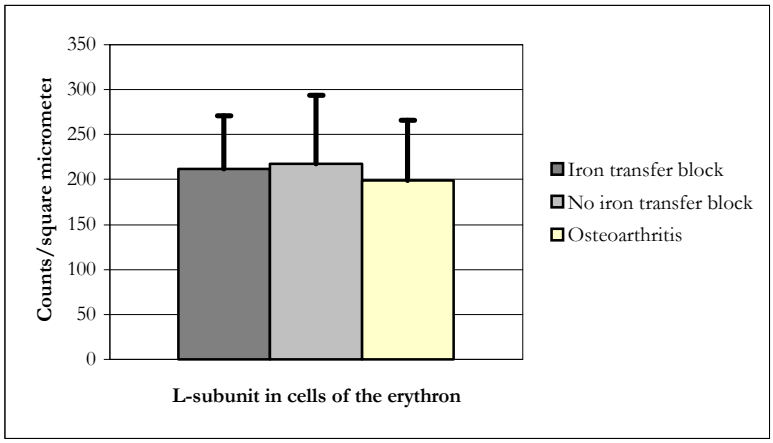

Figure 5c.
No significant difference between iron transfer block group and no iron transfer block group.
No significant difference between iron transfer block group and osteoarthritis group.
No significant difference between no iron transfer block group and osteoarthritis group.

Figure 5a – 5c. Differences in expression of the L-subunit of ferritin in cells of the erythron for the C-reactive protein subdivision, the neopterin subdivision and the iron transfer block subdivision.

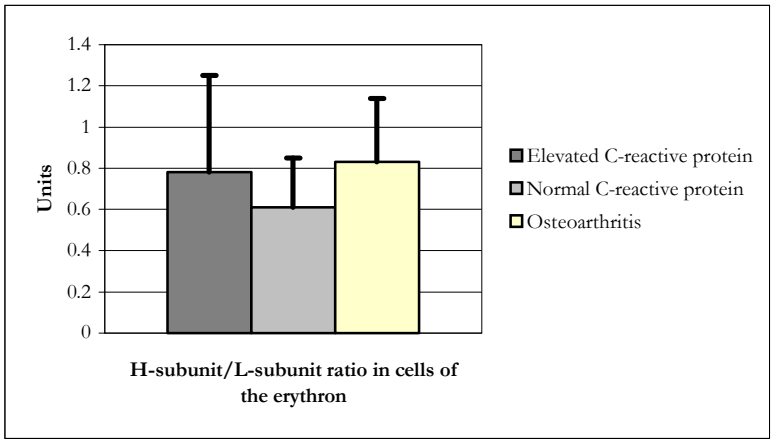

Figure 6a.
No significant difference between elevated CRP group and normal CRP group.
No significant difference between elevated CRP group and osteoarthritis group.
Marginally higher for osteoarthritis group compared to normal CRP group.

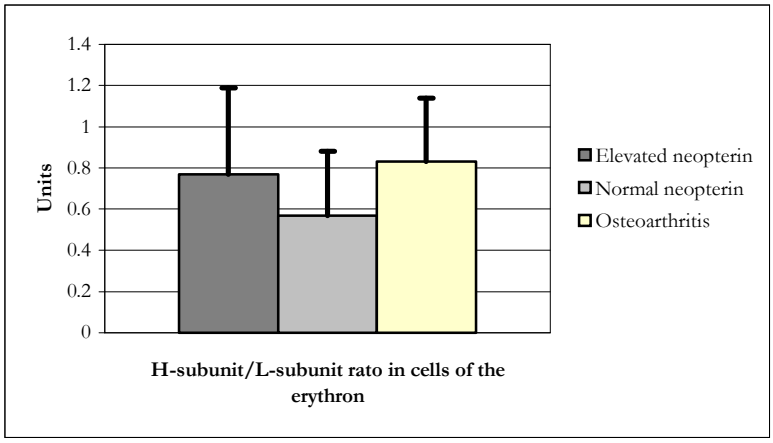

Figure 6b.
Marginally higher for elevated neopterin group compared to normal neopterin group.
No significant difference between elevated neopterin group and osteoarthritis group.
Significantly higher for osteoarthritis group compared to normal neopterin group.

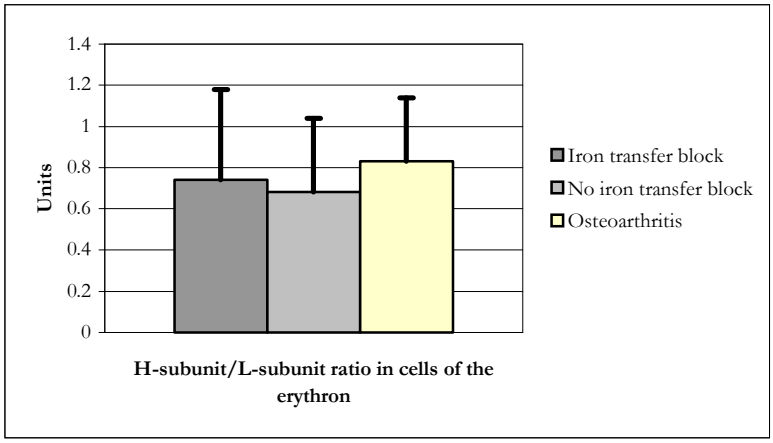

Figure 6c.
No significant difference between iron transfer block group and no iron transfer block group.
No significant difference between iron transfer block group and osteoarthritis group.
No significant difference between no iron transfer block group and osteoarthritis group.

Figure 6a – 6c. Differences in H-subunit/L-subunit ratio in cells of the erythron for the C-reactive protein subdivision, the neopterin subdivision and the iron transfer block subdivision.

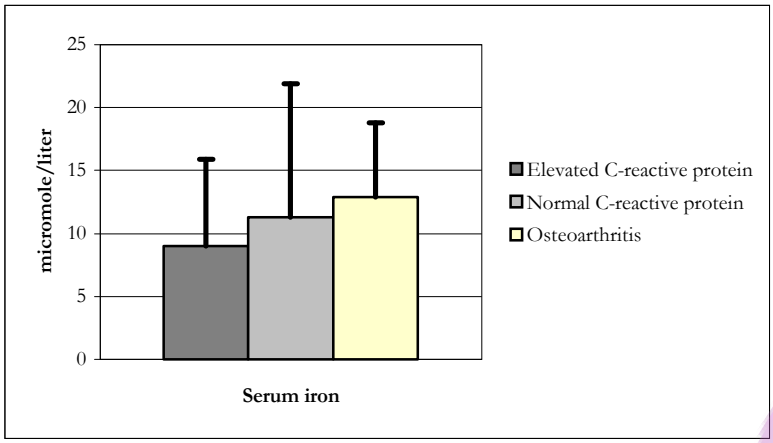

Figure 7a.
No significant difference between elevated CRP group and normal CRP group.
Marginally lower for elevated CRP group compared to osteoarthritis group.
No significant difference between normal CRP group and osteoarthritis group.

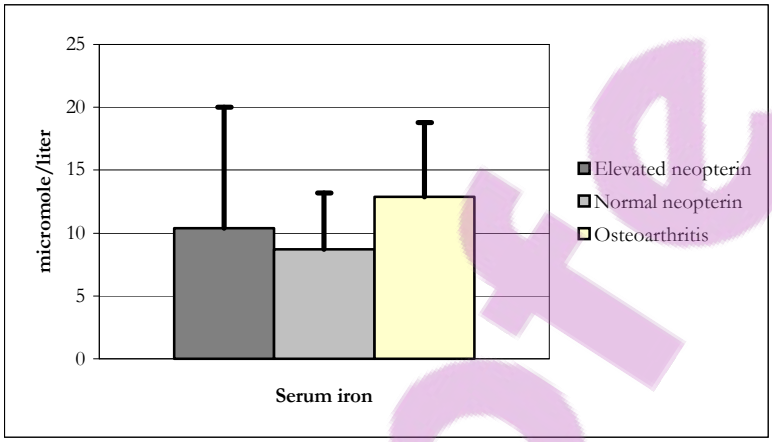

Figure 7b.
No significant difference between elevated neopterin group and normal neopterin group.
Marginally lower for elevated neopterin group compared to osteaoarthritis group.
Marginally lower for normal neopterin group compared to osteoarthritis group.

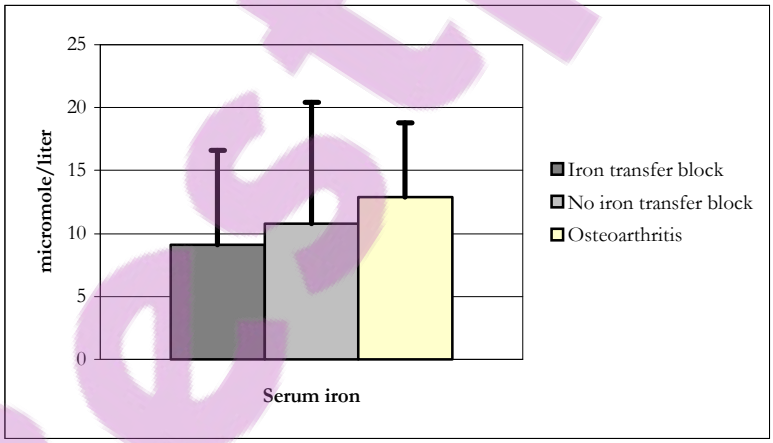

Figure 7c.
No significant difference between iron transfer block group and no iron transfer block group.
Marginally lower for iron transfer block group compared to osteoarthritis group.
No significant difference between no iron transfer block group and osteoarthritis group.

Figure 7a – 7c. Differences in serum iron for the C-reactive protein subdivision, the neopterin subdivision and the iron transfer block subdivision.

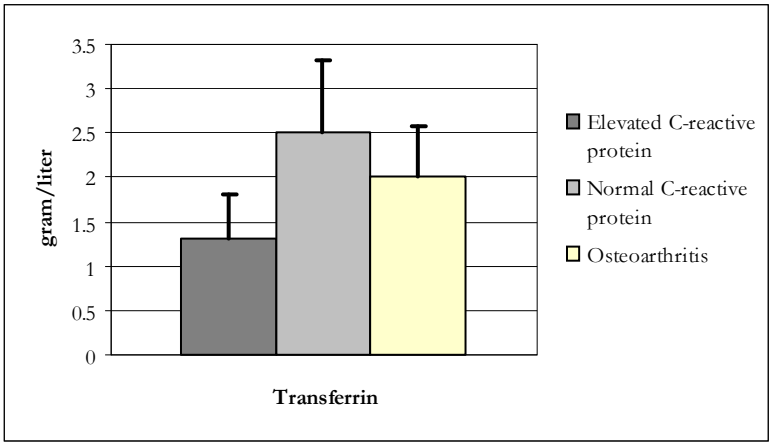

Figure 8a.
Significantly lower for elevated CRP group compared to normal CRP group.
Significantly lower for elevated CRP group compared to osteoarthritis group.
No significant difference between normal CRP group and osteoarthritis group.

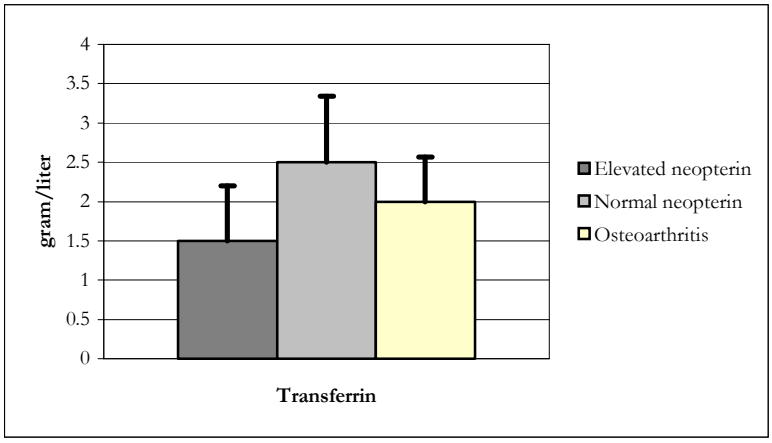

Figure 8b.
Significantly lower for elevated neopterin group compared to normal neopterin group.
Significantly lower for elevated neopterin group compared to osteoarthritis group.
No significant difference between normal neopterin group and osteoarthritis group.

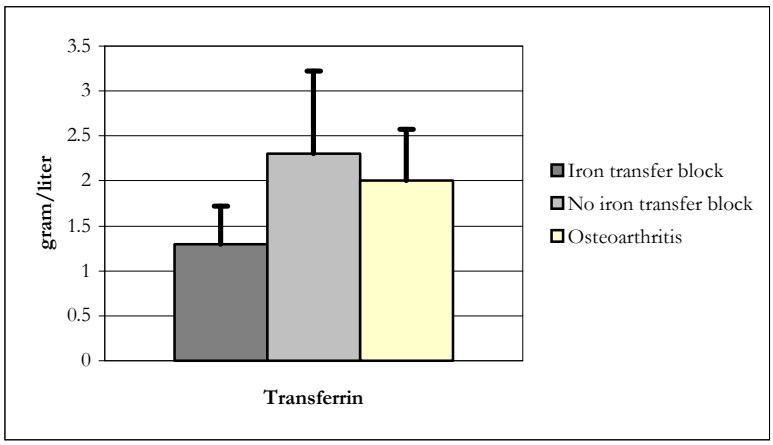

Figure 8c.
Significantly lower for iron transfer block group compared to no iron transfer block group.
Significantly lower for iron transfer block group compared to osteoarthritis group.
No significant difference between no iron transfer block group and osteoarthritis group.

Figure 8a – 8c. Differences in transferrin for the C-reactive protein subdivision, the neopterin subdivision and the iron transfer block subdivision.

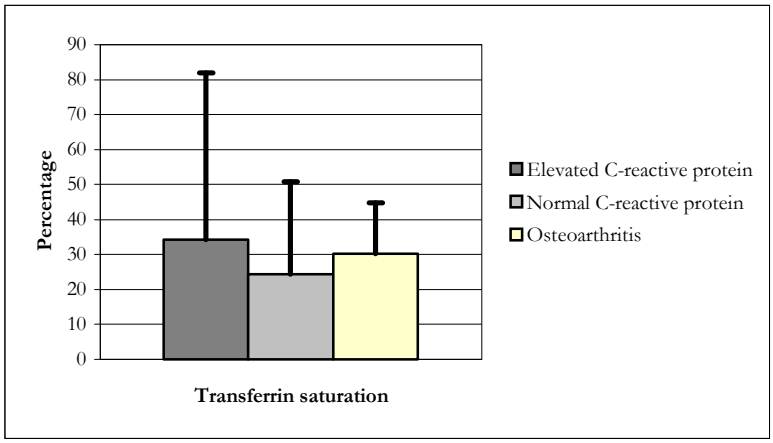

Figure 9a.
No significant difference between elevated CRP group and normal CRP group.
No significant difference between elevated CRP group and osteoarthritis group.
No significant difference between normal CRP group and osteoarthritis group.

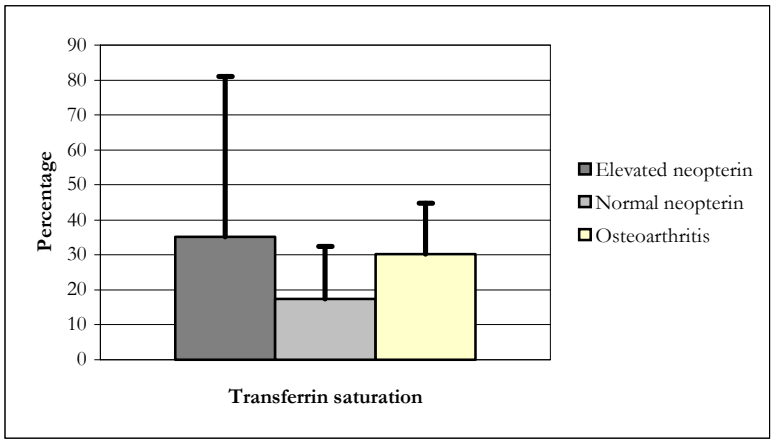

Figure 9b.
Marginally lower for normal neopterin group compared to elevated neopterin group.
No significant difference between elevated neopterin group and osteoarthritis group.
Significantly lower for normal neopterin group compared to osteoarthritis group.

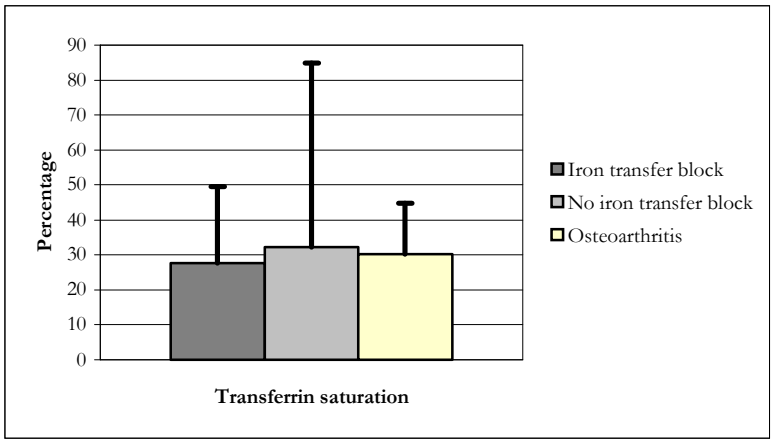

Figure 9c.
No significant difference between iron transfer block group and no iron transfer block group.
No significant difference between iron transfer block group and osteoarthritis group.
No significant difference between no iron transfer block group and osteoarthritis group.

Figure 9a – 9c. Differences in transferrin saturation for the C-reactive protein subdivision, the neopterin subdivision and the iron transfer block subdivision.

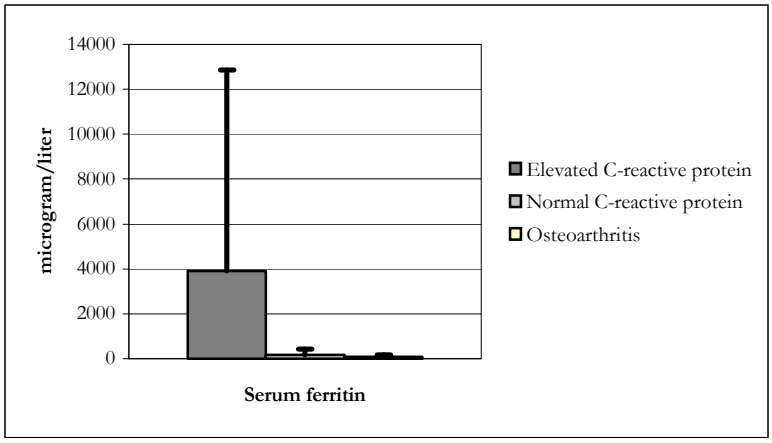

Figure 10a.
Significantly higher for elevated CRP group compared to normal CRP group.
Significantly higher for elevated CRP group compared to osteoarthritis group.
No significant difference between normal CRP group and osteoarthritis group.

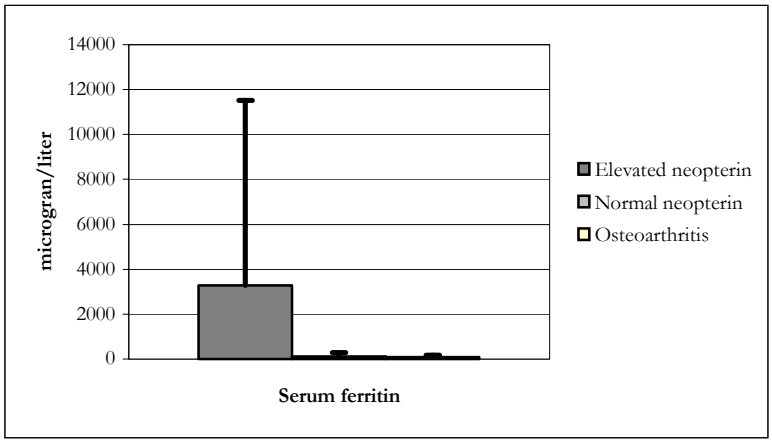

Figure 10b.
Significantly higher for elevated neopterin group compared to normal neopterin group.
Significantly higher for elevated neopterin group compared to osteoarthritis group.
No significant difference between normal neopterin group and osteoarthritis group.

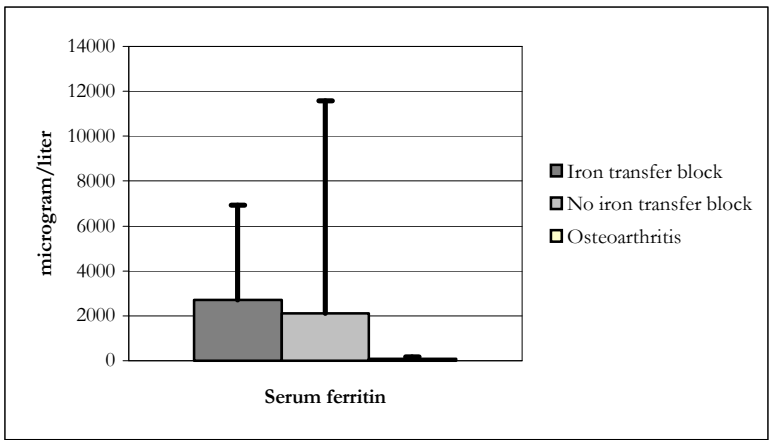

Figure 10c.
Significant higher for iron transfer block group compared to no iron transfer block group.
Significantly higher for iron transfer block group compared to osteoarthritis group.
No significant difference between no iron transfer block group and osteoarthritis group.

Figure 10a – 10c. Differences in serum ferritin for the C-reactive protein subdivision, the neopterin subdivision and the iron transfer block subdivision.

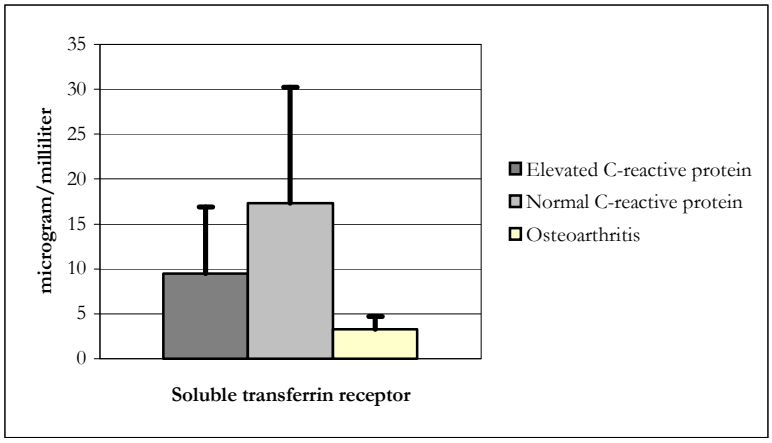

Figure 11a.
Significantly lower for elevated CRP group compared to normal CRP group.
Significantly higher for elevated CRP group compared to osteoarthritis group.
Significantly higher for normal CRP group compared to osteoarthritis group.

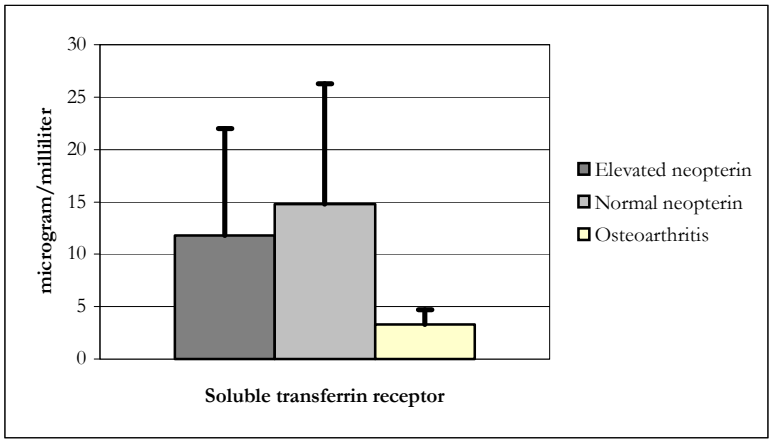

Figure 11b.
No significant difference between elevated neopterin group and normal neopterin group.
Significantly higher for elevated neopterin group compared to osteoarthritis group.
Significantly higher for normal neopterin group compared to osteoarthritis group.

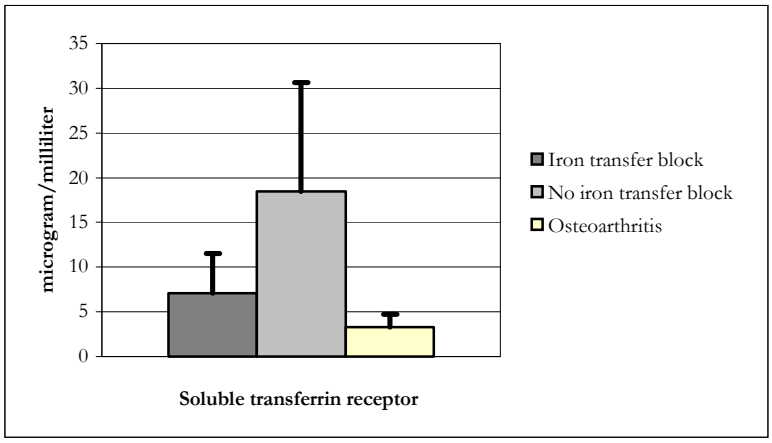

Figure 11c.
Significantly lower for iron transfer block group compared to no iron transfer block group.
Significantly higher for iron transfer block group compared to osteoarthritis group.
Significantly higher for no iron transfer block group compared to osteoarthritis group.

Figure 11a – 11c. Differences in soluble transferrin receptor for the C-reactive protein subdivision, the neopterin subdivision and the iron transfer block subdivision.

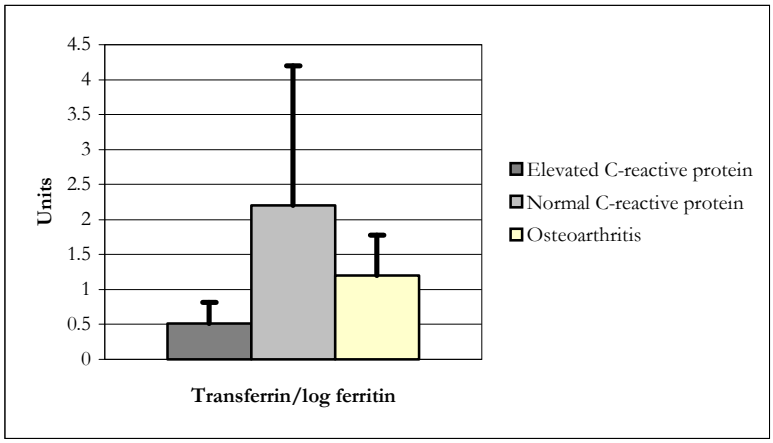

Figure 12a.
Significantly lower for elevated CRP group compared to normal CRP group.
Significantly lower for elevated CRP group compared to osteoarthritis group.
Significantly higher for normal CRP group compared to osteoarthritis group.

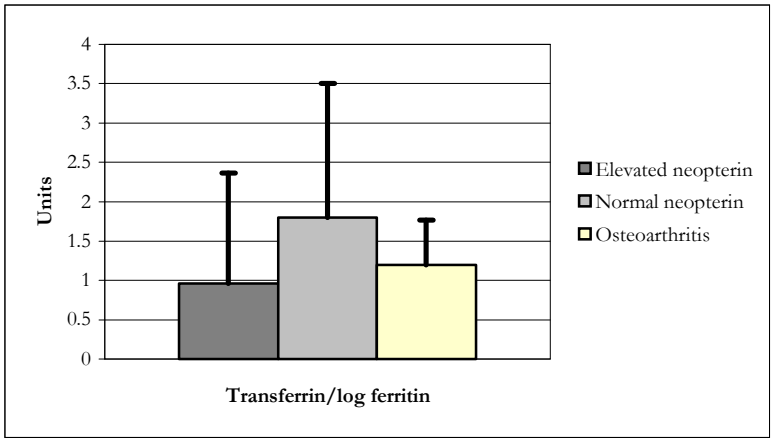

Figure 12b.
Significantly lower for elevated neopterin group compared to normal neopterin group.
Significantly lower for elevated neopterin group compared to osteoarthritis group.
No significant difference between normal neopterin group and osteoarthritis group.

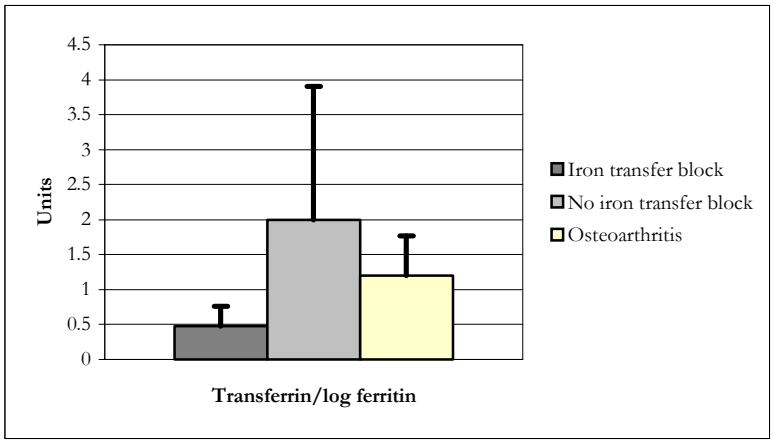

Figure 12c.
Significantly lower for iron transfer block group compared to no iron transfer block group.
Significantly lower for iron transfer block group compared to osteoarthritis group.
Marginally higher for no iron transfer block group compared to osteoarthritis group.

Figure 12a – 12c. Differences in transferrin/log ferritin ratio for the C-reactive protein subdivision, the neopterin subdivision and the iron transfer block subdivision.

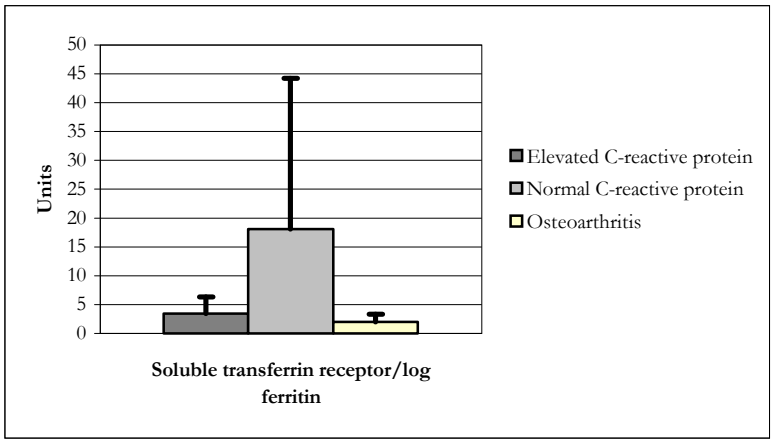

Figure 13a.
Significantly lower for elevated CRP group compared to normal CRP group.
Significantly higher for elevated CRP group compared to osteoarthritis group.
Significantly higher for normal CRP group compared to osteoarthritis group.

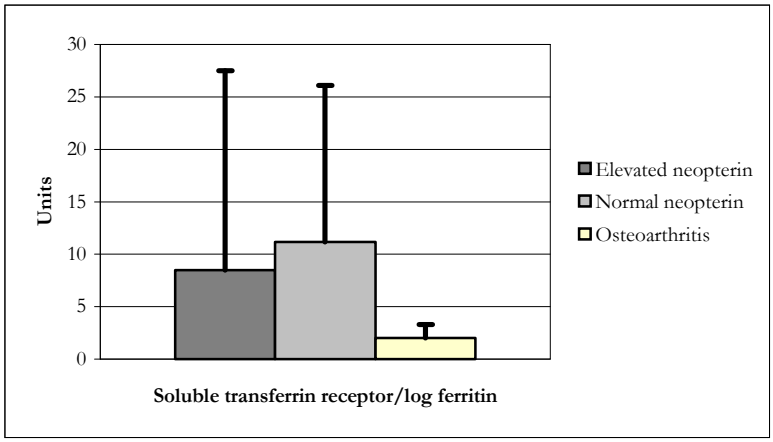

Figure 13b.
Marginally lower for elevated neopterin group compared to normal neopterin group.
Significantly higher for elevated neopterin group compared to osteoarthritis group.
Significantly higher for normal neopterin group compared to osteoarthritis group.

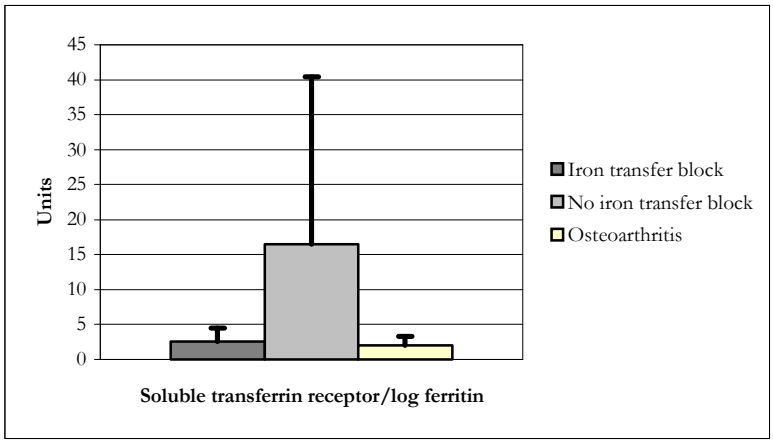

Figure 13c.
Significantly lower for iron transfer block group compared to no iron transfer block group.
No significant difference between iron transfer block group and osteoarthritis group.
Significantly higher for no iron transfer block group compared to osteoarthritis group.

Figure 13a – 13c. Differences in soluble transferrin receptor/log ferritin ratio for the C-reactive protein subdivision, the neopterin subdivision and the iron transfer block subdivision.

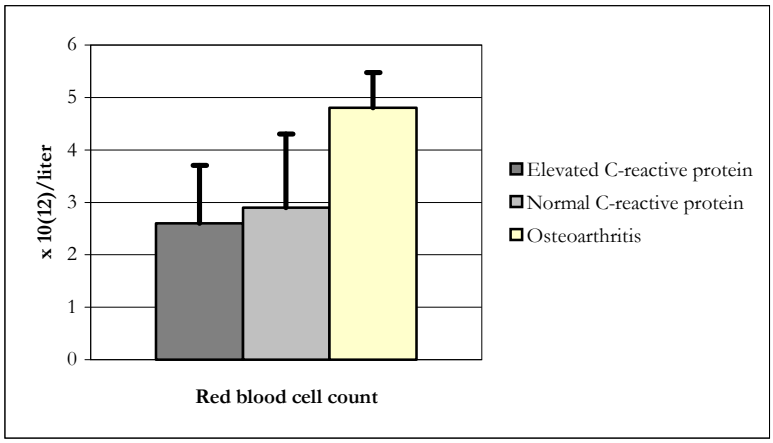

Figure 14a.
Significantly lower for elevated CRP group compared to normal CRP group.
Significantly lower for elevated CRP group compared to osteoarthritis group.
Significantly lower for normal CRP group compared to osteoarthritis group.

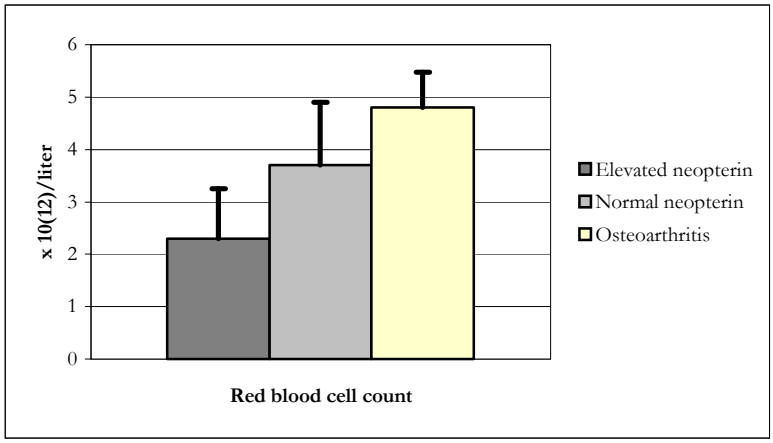

Figure 14b.
Significantly lower for elevated neopterin group compared to normal neopterin group.
Significantly lower for elevated neopterin group compared to osteoarthritis group.
Marginally lower for normal neopterin group compared to osteoarthritis group.

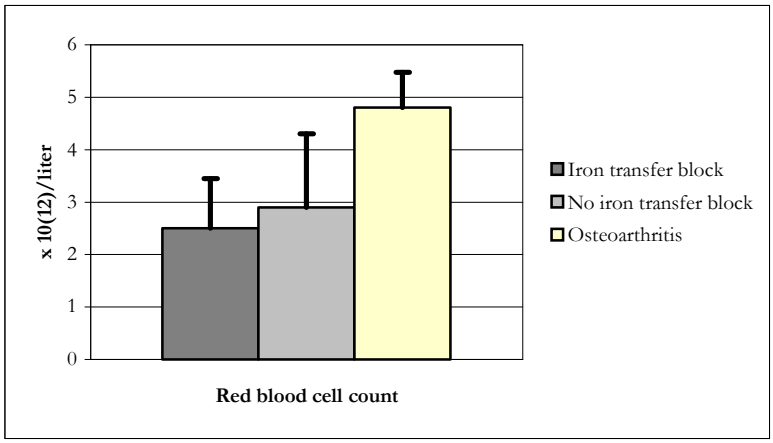

Figure 14c.
No significant difference between iron transfer block group and no iron transfer block group.
Significantly lower for iron transfer block group compared to osteoarthritis group.
Significantly lower for no iron transfer block group compared to osteoarthritis group.

Figure 14a – 14c. Differences in red blood cell count for the C-reactive protein subdivision, the neopterin subdivision and the iron transfer block subdivision.

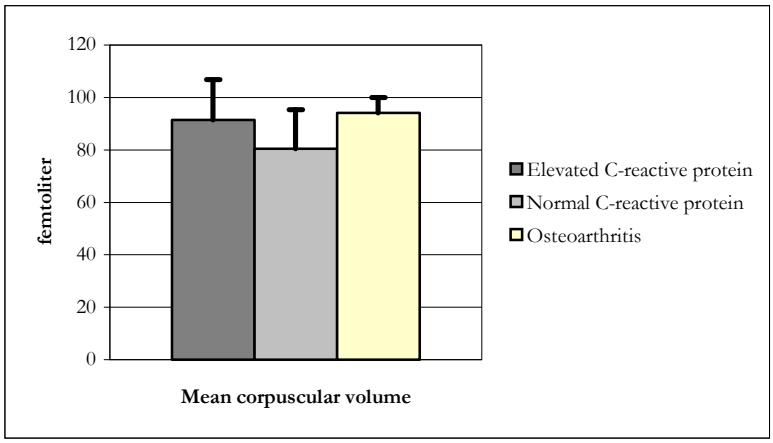

Figure 15a.
Significantly higher for elevated CRP group compared to normal CRP group.
No significant difference between elevated CRP group and osteoarthritis group.
Significantly lower for normal CRP group compared to osteoarthritis group.

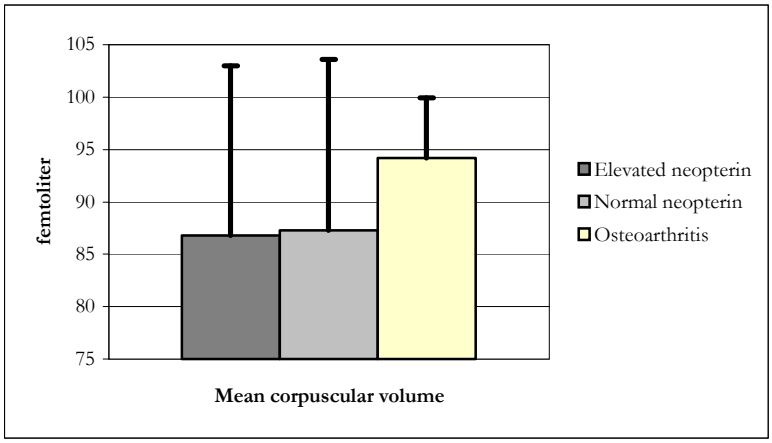

Figure 15b.
No significant difference between elevated neopterin group and normal neopterin group.
Significantly lower for elevated neopterin group compared to osteoarthritis group.
Marginally lower for normal neopterin group compared to osteoarthritis group.

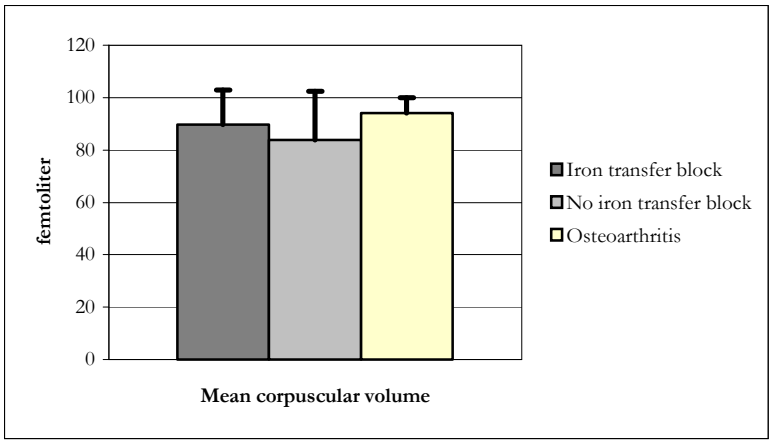

Figure 15c.
No significant difference between iron transfer block group and no iron transfer block group.
No significant difference between iron transfer block group and osteoarthritis group.
Significantly lower for no iron transfer block group compared to osteoarthritis group.

Figure 15a – 15c. Differences in mean corpuscular volume for the C-reactive protein subdivision, the neopterin subdivision and the iron transfer block subdivision.

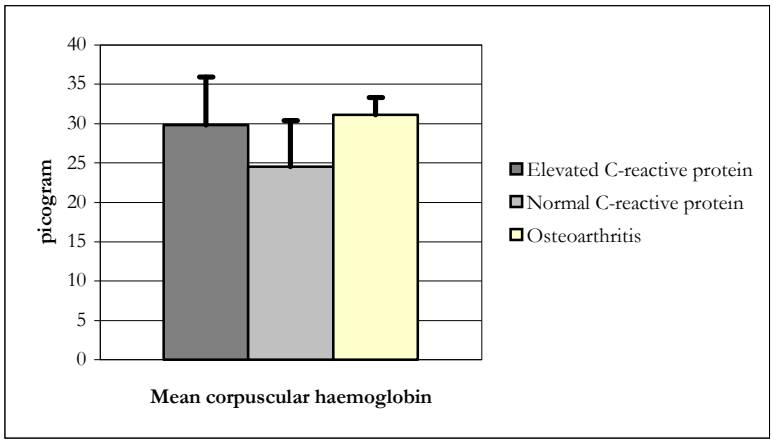

Figure 16a.
Significantly higher for elevated CRP group compared to normal CRP group.
No significant difference between elevated CRP group and osteoarthritis group.
Significantly lower for normal CRP group compared to osteoarthritis group.

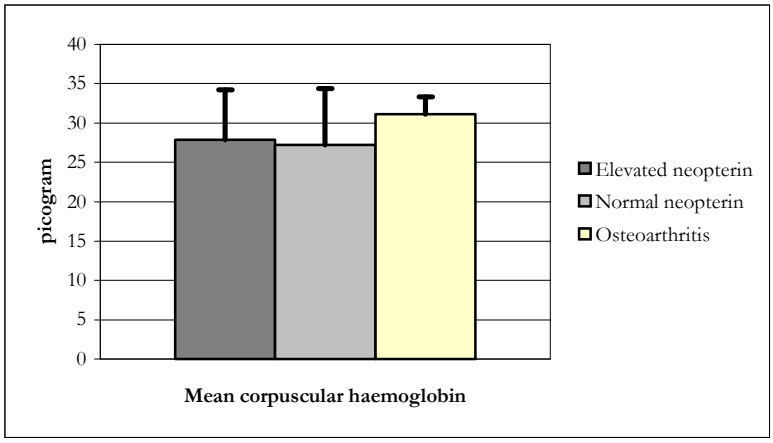

Figure 16b.
No significant difference between elevated neopterin group and normal neopterin group.
Significantly lower for elevated neopterin group compared to osteoarthritis group.
Marginally lower for normal neopterin group compared to osteoarthritis group.

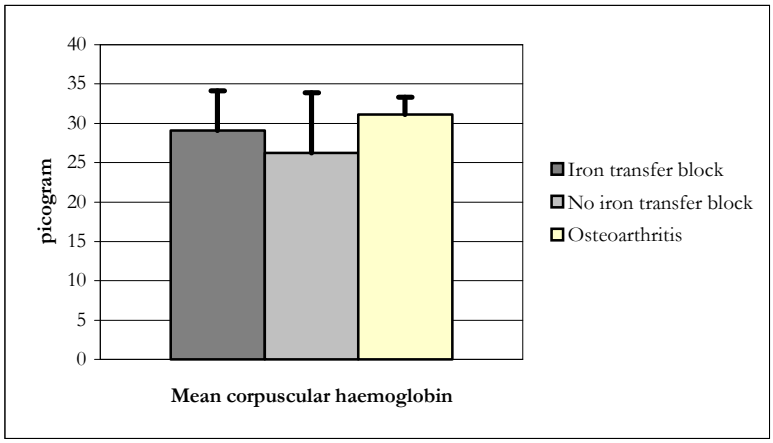

Figure 16c.
No significant difference between iron transfer block group and no iron transfer block group.
No significant difference between iron transfer block group and osteoarthritis group.
Significantly lower for no iron transfer block group compared to osteoarthritis group.

Figure 16a – 16c. Differences in mean corpuscular haemoglobin for the C-reactive protein subdivision, the neopterin subdivision and the iron transfer block subdivision.

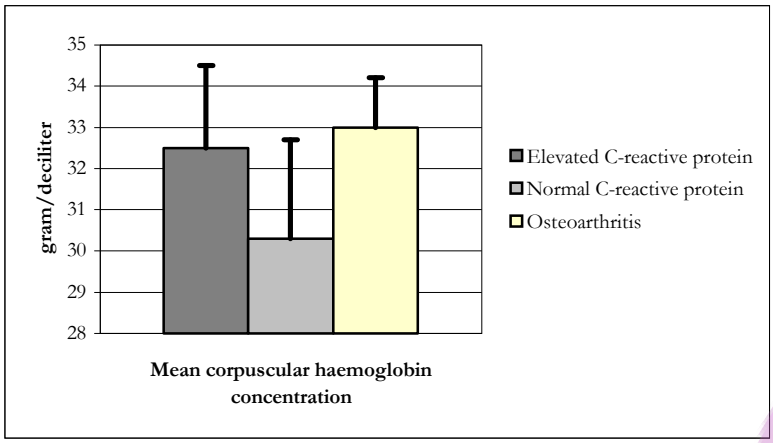

Figure 17a.
Significantly higher for elevated CRP group compared to normal CRP group.
No significant difference between elevated CRP group and osteoarthritis group.
Significantly lower for normal CRP group compared to osteoarthritis group.

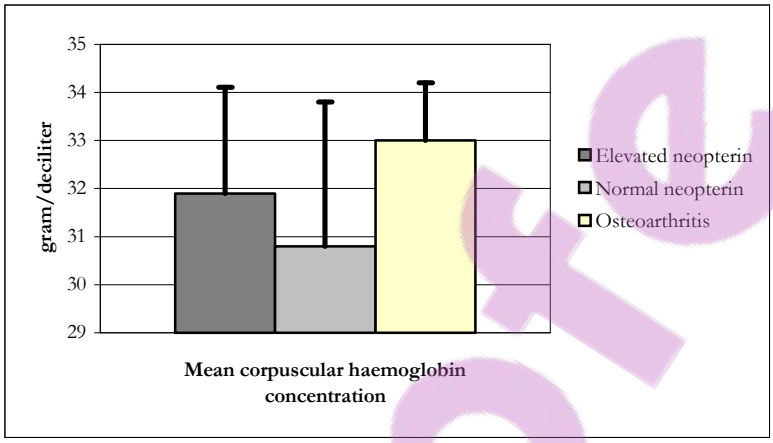

Figure 17b.
No significant difference between elevated neopterin group and normal neopterin group.
Marginally lower for elevated neopterin group compared to osteoarthritis group.
Significantly lower for normal neopterin group compared to osteoarthritis group.

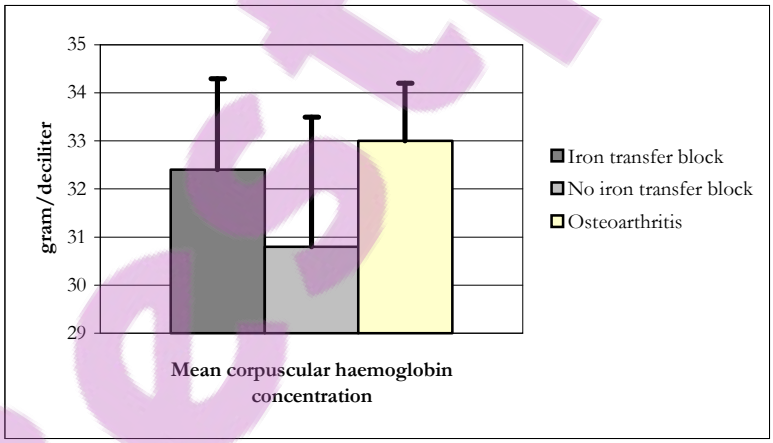

Figure 17c.
Significantly higher for iron transfer block group compared to no iron transfer block group.
No significant difference between iron transfer block group and osteoarthritis group.
Significantly lower for no iron transfer block group compared to osteoarthritis group.

Figure 17a – 17c. Differences in mean corpuscular haemoglobin concentration for the C-reactive protein subdivision, the neopterin subdivision and the iron transfer block subdivision.

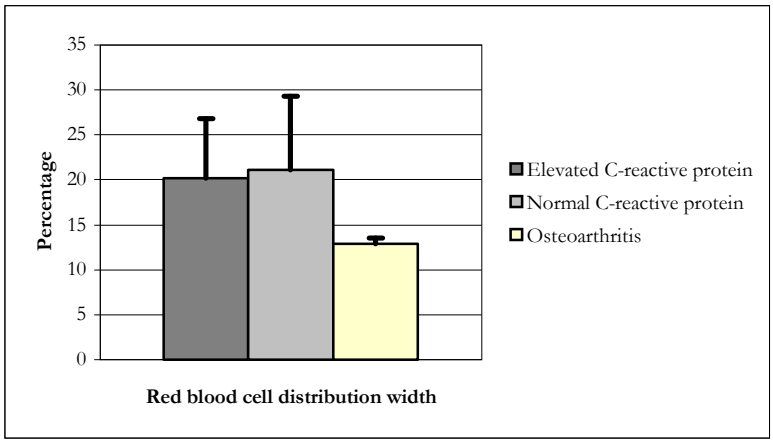

Figure 18a.
No significant difference between elevated CRP group and normal CRP group.
Significantly higher for elevated CRP group compared to osteoarthritis group.
Significantly higher for normal CRP group compared to osteoarthritis group.

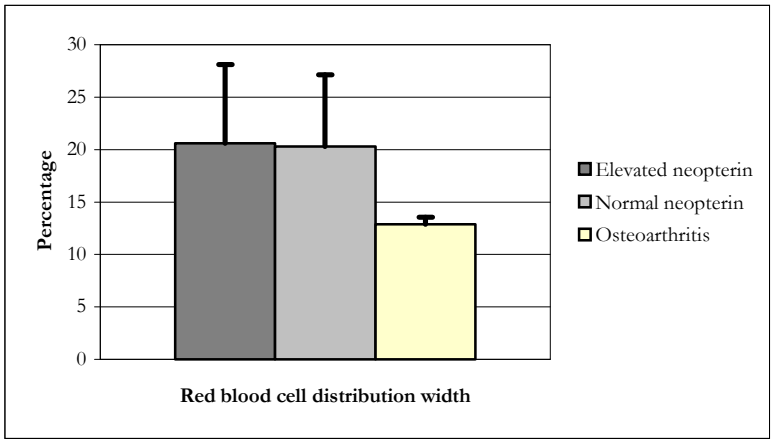

Figure 18b.
No significant difference between elevated neopterin group and normal neopterin group.
Significantly higher for elevated neopterin group compared to osteoarthritis group.
Significantly higher for normal neopterin group compared to osteoarthritis group.

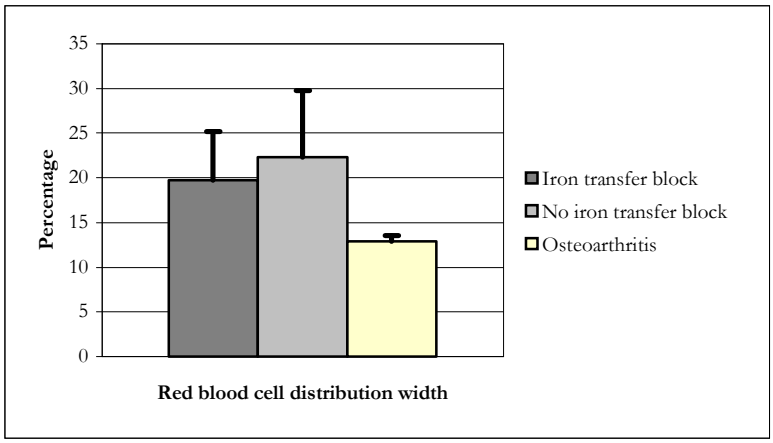

Figure 18c.
No significant difference between iron transfer block group and no iron transfer block group.
Significantly higher for iron transfer block group compared to osteoarthritis group.
Significantly higher for no iron transfer block group compared to osteoarthritis group.

Figure 18a – 18c. Differences in red blood cell distribution width for the C-reactive protein subdivision, the neopterin subdivision and the iron transfer block subdivision.

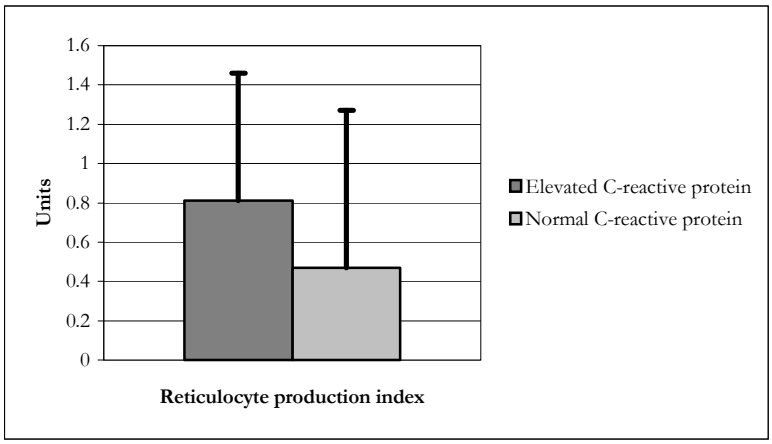

Figure 19a.
Significantly higher for elevated CRP group compared to normal CRP group.

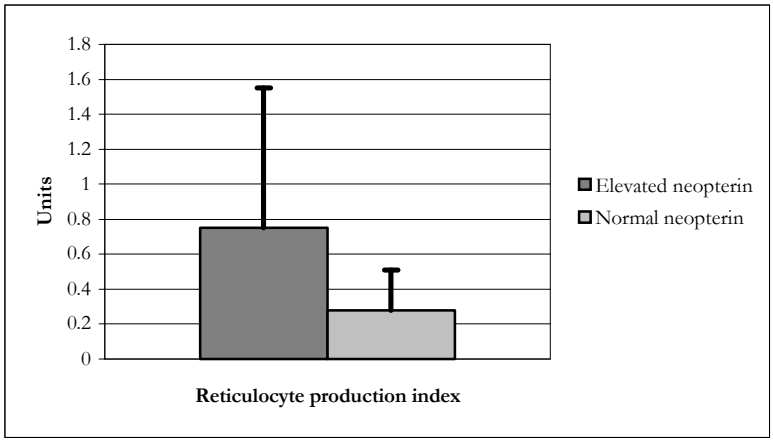

Figure 19b.
Significantly higher for elevated neopterin group compared to normal neopterin group.

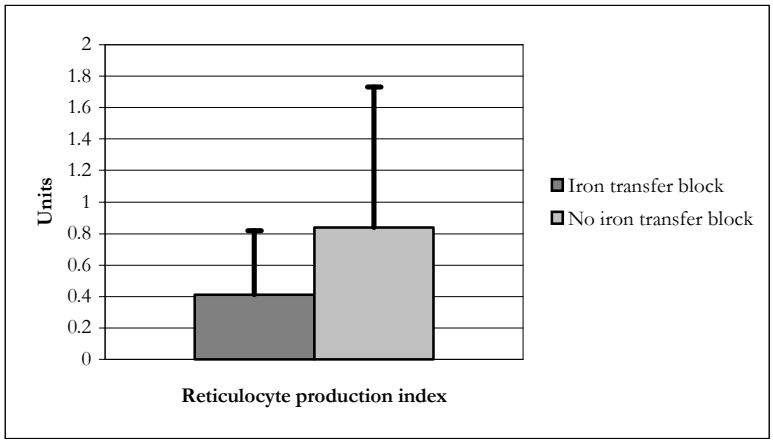

Figure 19c.
No significant difference between iron transfer block group and no iron transfer block group.

Figure 19a – 19c. Differences in reticulocyte production index for the C-reactive protein subdivision, the neopterin subdivision and the iron transfer block subdivision. The reticulocyte production index was not determined for the osteoarthritis patients.

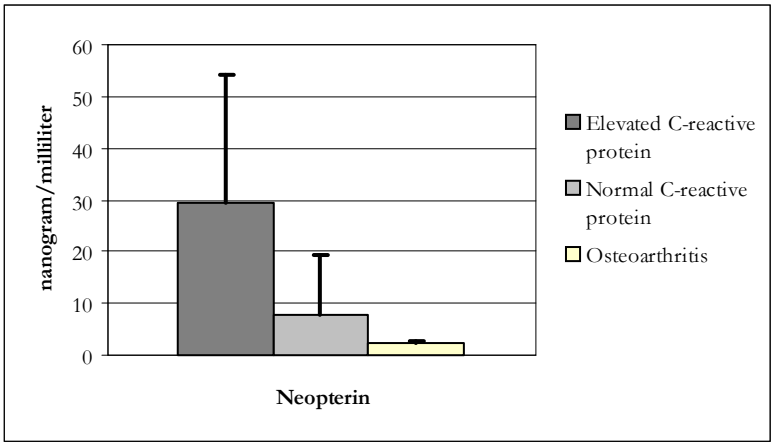

Figure 20a.
Significantly higher for elevated CRP group compared to normal CRP group.
Significantly higher for elevated CRP group compared to osteoarthritis group.
Significantly higher for normal CRP group compared to osteoarthritis group.

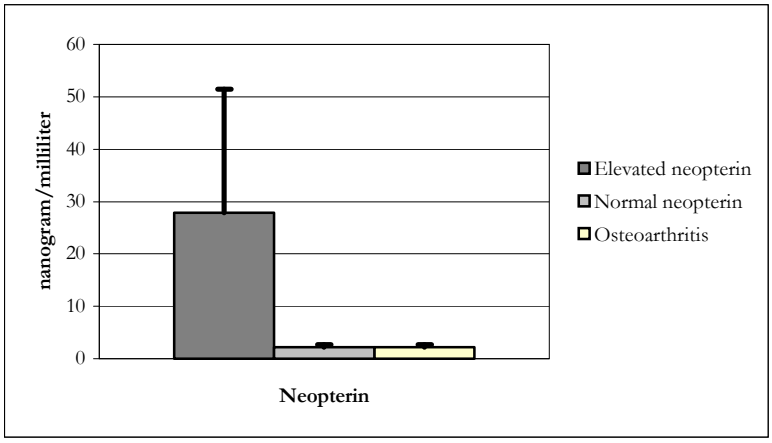

Figure 20b.
Significantly higher for elevated neopterin group compared to normal neopterin group.
Significantly higher for elevated neopterin group compared to osteoarthritis group.
No significant difference between normal neopterin group and osteoarthritis group.

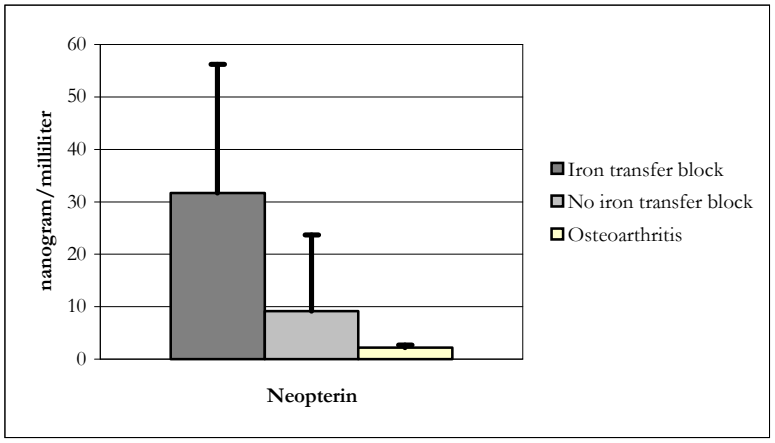

Figure 20c.
Significantly higher for iron transfer block group compared to no iron transfer block group.
Significantly higher for iron transfer block group compared to osteoarthritis group.
Significantly higher for no iron transfer block group compared to osteoarthritis group.

Figure 20a – 20c. Differences in neopterin for the C-reactive protein subdivision, the neopterin subdivision and the iron transfer block subdivision.

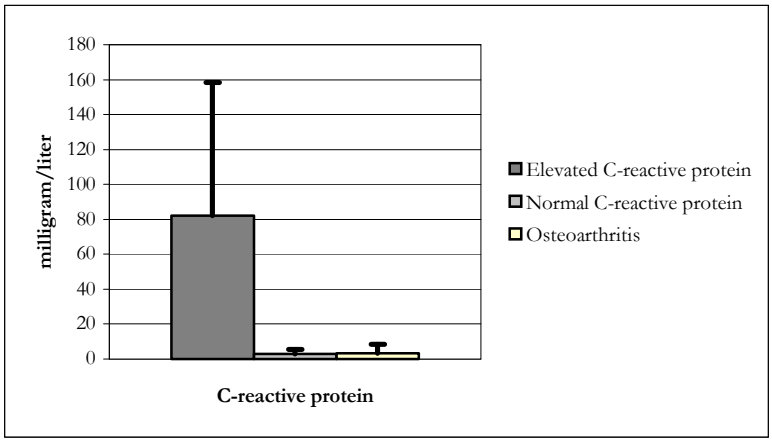

Figure 21a.
Significantly higher for elevated CRP group compared to normal CRP group.
Significantly higher for elevated CRP group compared to osteoarthritis group.
No significant difference between normal CRP group and osteoarthritis group.

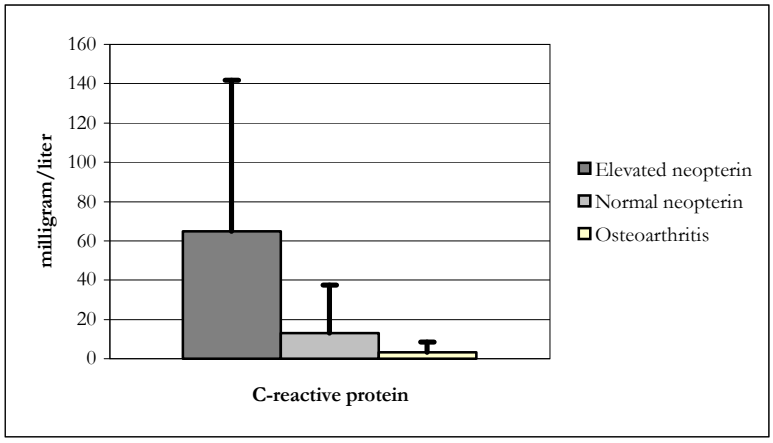

Figure 21b.
Significantly higher for elevated neopterin group compared to normal neopterin group.
Significantly higher for elevated neopterin group compared to osteoarthritis group.
No significant difference between normal neopterin group and osteoarthritis group.

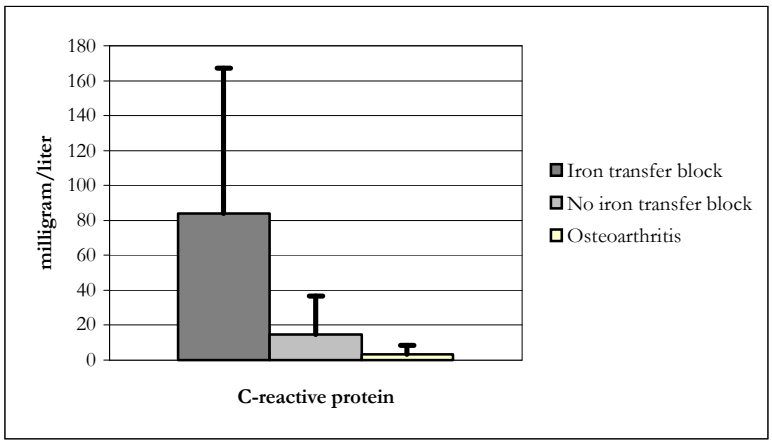

Figure 21c.
Significantly higher for iron transfer block group compared to no iron transfer block group.
Significantly higher for iron transfer block group compared to osteoarthritis group.
Significantly higher for no iron transfer block group compared to osteoarthritis group.

Figure 21a – 21c. Differences in C-reactive protein for the C-reactive protein subdivision, the neopterin subdivision and the iron transfer block subdivision.

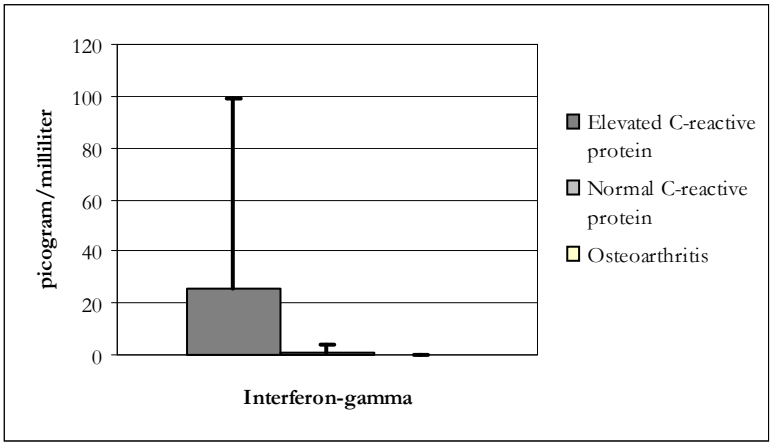

Figure 22a.
Significantly higher for elevated CRP group compared to normal CRP group.
Significantly higher for elevated CRP group compared to osteoarthritis group.
No significant difference between normal CRP group and osteoarthritis group.

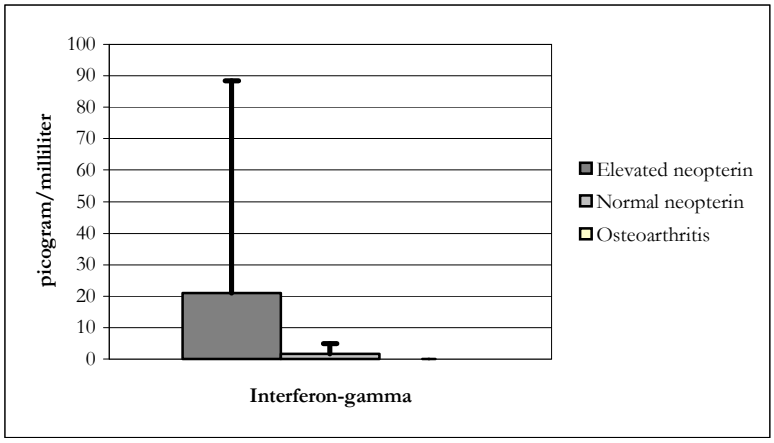

Figure 22b.
Marginally higher for elevated neopterin group compared to normal neopterin group.
Significantly higher for elevated neopterin group compared to osteoarthritis group.
No significant difference between normal neopterin group and osteoarthritis group.

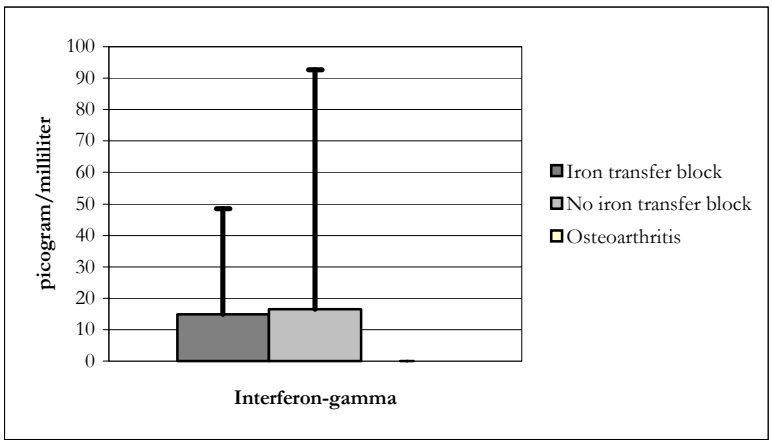

Figure 22c.
Significantly higher for iron transfer block group compared to no iron transfer block group.
Significantly higher for iron transfer block group compared to osteoarthritis group.
No significant difference between no iron transfer block group and osteoarthritis group.

Figure 22a – 22c. Differences in interferon-γ for the C-reactive protein subdivision, the neopterin subdivision and the iron transfer block subdivision.

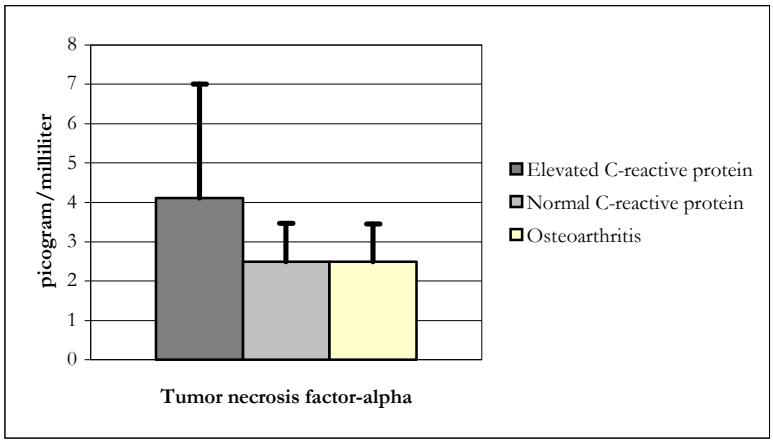

Figure 23a.
Significantly higher for elevated CRP group compared to normal CRP group.
Significantly higher for elevated CRP group compared to osteoarthritis group.
No significant difference between normal CRP group and osteoarthritis group.

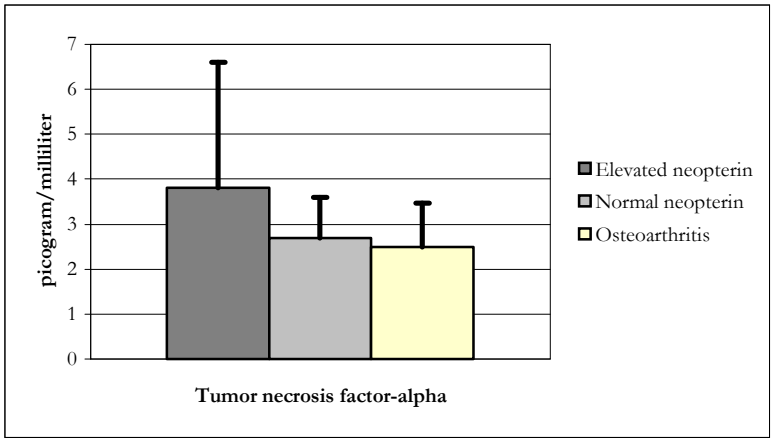

Figure 23b.
Significantly higher for elevated neopterin group compared to normal neopterin group.
Significantly higher for elevated neopterin group compared to osteoarthritis group.
No significant difference between normal neopterin group and osteoarthritis group.

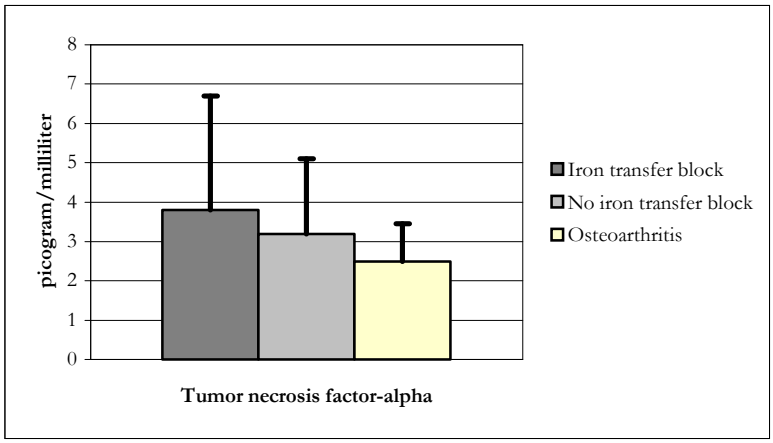

Figure 23c.
No significant difference between iron transfer block group and no iron transfer block group.
Marginally higher for iron transfer block group compared to osteoarthritis group.
No significant difference between no iron transfer block group and osteoarthritis group.

Figure 23a – 23c. Differences in tumor necrosis factor-α for the C-reactive protein subdivision, the neopterin subdivision and the iron transfer block subdivision.

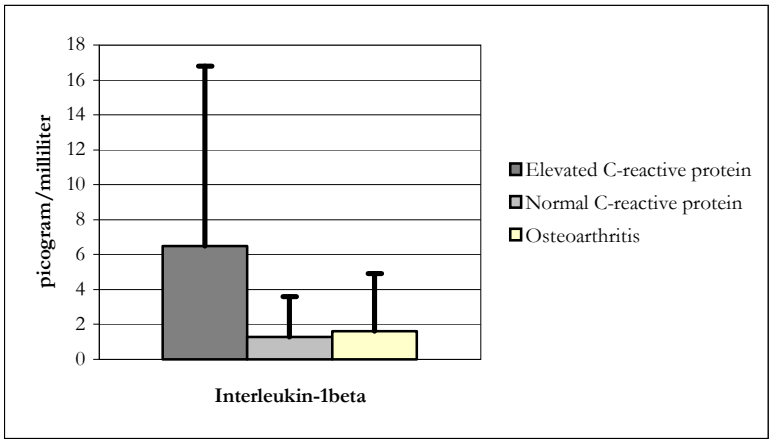

Figure 24a.
Significantly higher for elevated CRP group compared to normal CRP group.
Significantly higher for elevated CRP group compared to osteoarthritis group.
No significant difference between normal CRP group and osteoarthritis group.

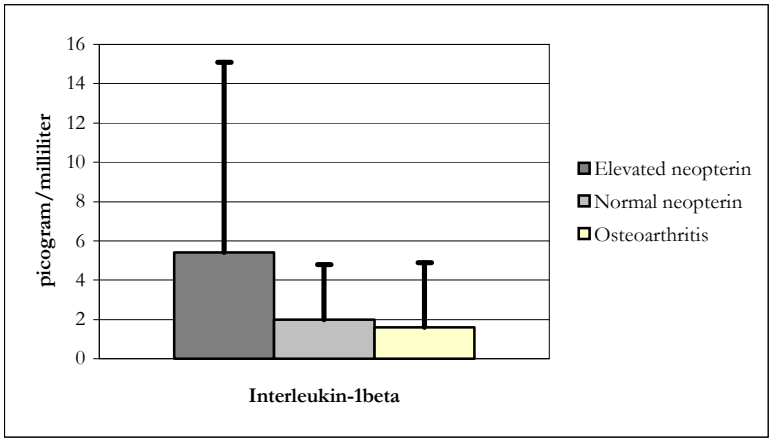

Figure 24b.
Marginally higher for elevated neopterin group compared to normal neopterin group.
Marginally higher for elevated neopterin group compared to osteoarthritis group.
No significant difference between normal neopterin group and osteoarthritis group.

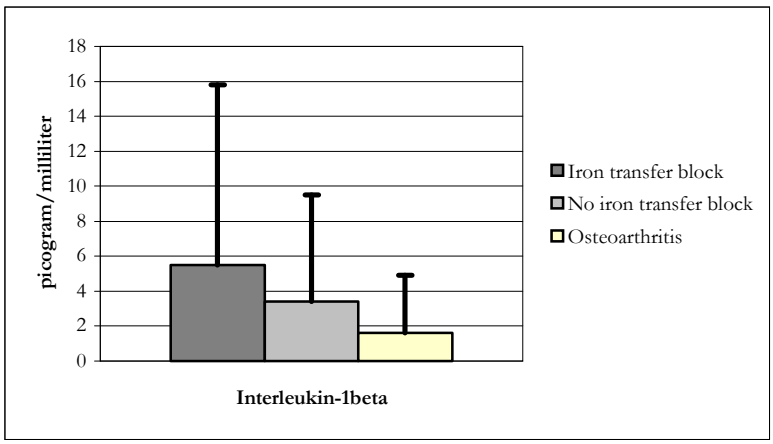

Figure 24c.
No significant difference between iron transfer block group and no iron transfer block group.
No significant difference between iron transfer block group and osteoarthritis group.
No significant difference between no iron transfer block group and osteoarthritis group.

Figure 24a – 24c. Differences in interleukin-1β for the C-reactive protein subdivision, the neopterin subdivision and the iron transfer block subdivision.

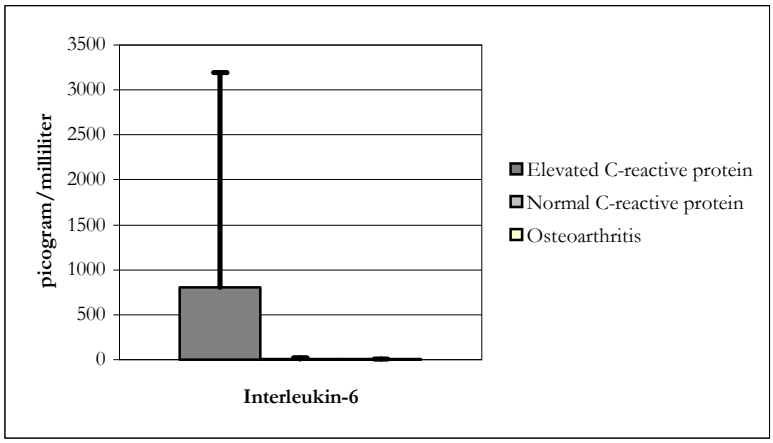

Figure 25a.
Significantly higher for elevated CRP group compared to normal CRP group.
Significantly higher for elevated CRP group compared to osteoarthritis group.
No significant difference between normal CRP group and osteoarthritis group.

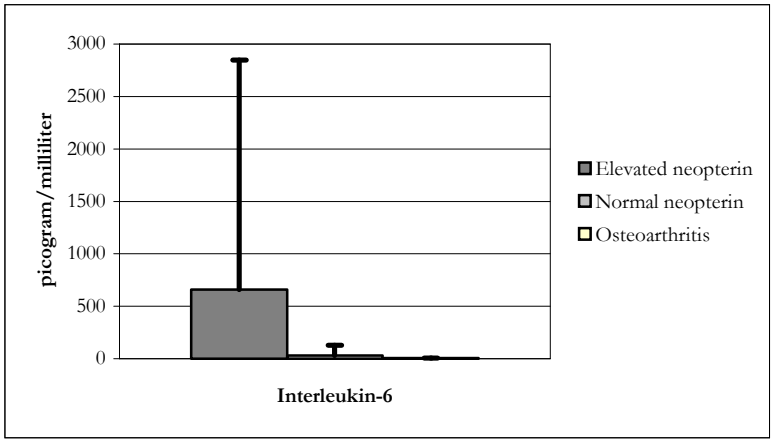

Figure 25b.
Significantly higher for elevated neopterin group compared to normal neopterin group.
Significantly higher for elevated neopterin group compared to osteoarthritis group.
No significant difference between normal neopterin group and osteoarthritis group.

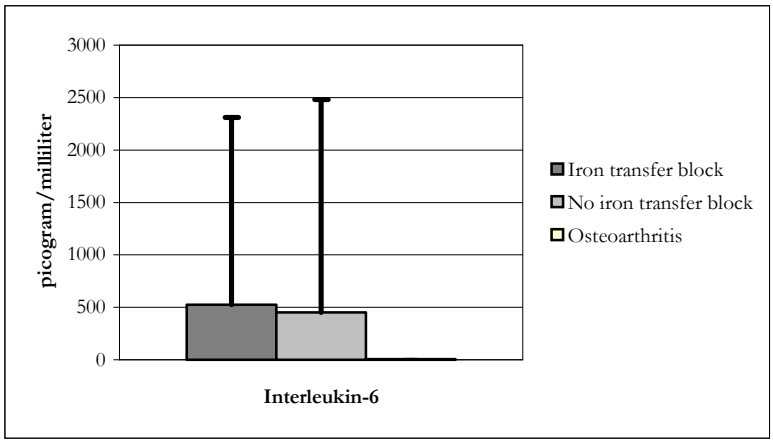

Figure 25c.
Significantly higher for iron transfer block group compared to no iron transfer block group.
Significantly higher for iron transfer block group compared to osteoarthritis group.
No significant difference between no iron transfer block group and osteoarthritis group.

Figure 25a – 25c. Differences in interleukin-6 for the C-reactive protein subdivision, the neopterin subdivision and the iron transfer block subdivision.

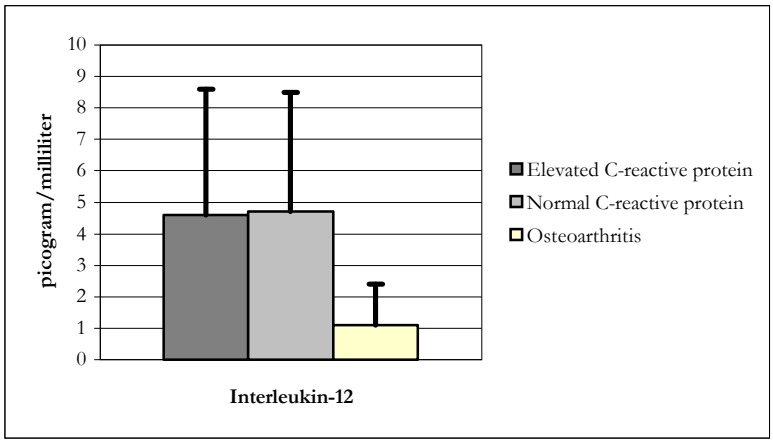

Figure 26a.
No significant difference between elevated CRP group and normal CRP group.
Significantly higher for elevated CRP group compared to osteoarthritis group.
Significantly higher for normal CRP group compared to osteoarthritis group.

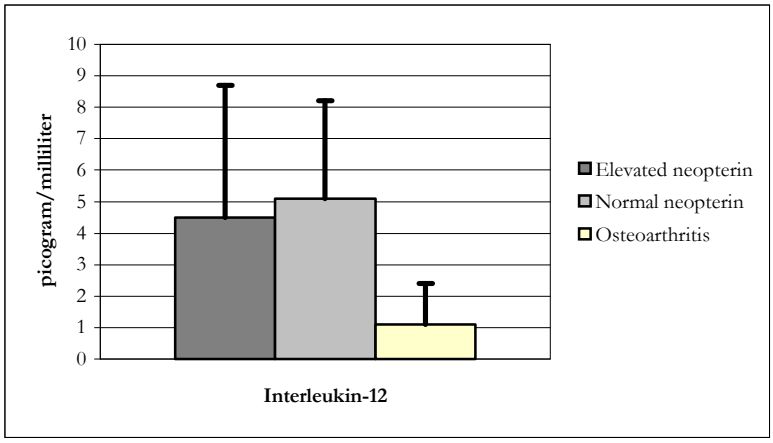

Figure 26b.
No significant difference between elevated neopterin group and normal neopterin group.
Significantly higher for elevated neopterin group compared to normal neopterin group.
Significantly higher for elevated neopterin group compared to osteoarthritis group.

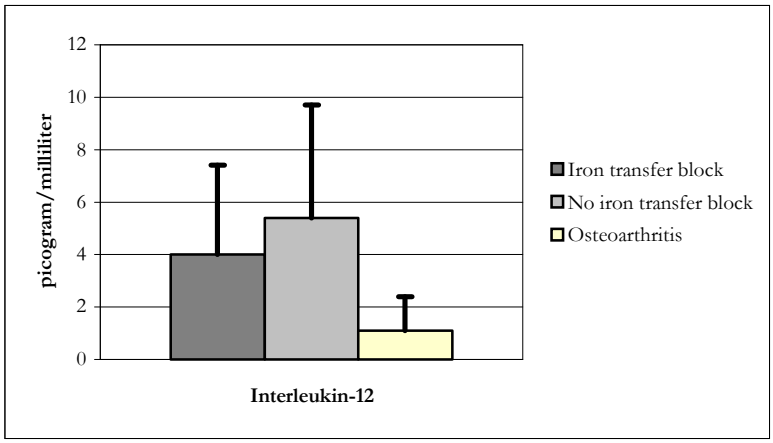

Figure 26c.
No significant difference between iron transfer block group and no iron transfer block group.
Significantly higher for iron transfer block group compared to osteoarthritis group.
Significantly higher for no iron transfer block group compared to osteoarthritis group.

Figure 26a – 26c. Differences in interleukin-12 for the C-reactive protein subdivision, the neopterin subdivision and the iron transfer block subdivision.

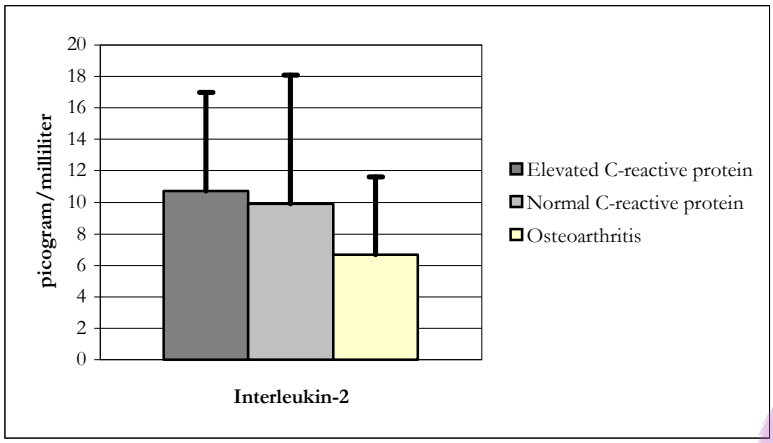

Figure 27a.
No significant difference between elevated CRP group and normal CRP group.
Marginally higher for elevated CRP group compared to osteoarthritis group.
No significant difference between normal CRP group and osteoarthritis group.

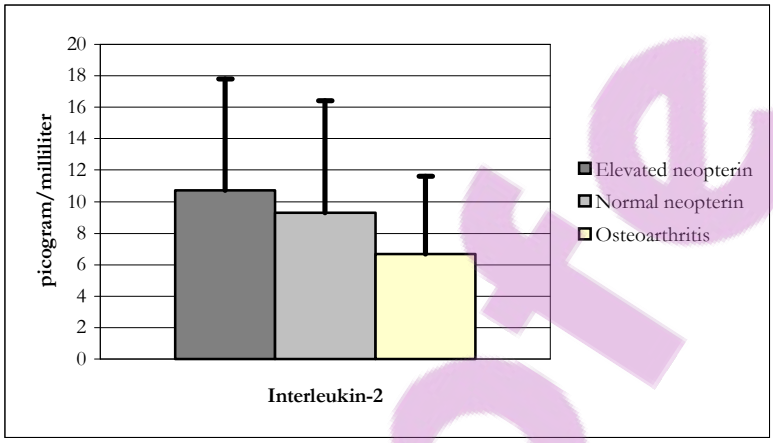

Figure 27b.
No significant difference between elevated neopterin group and normal neopterin group.
Significantly higher for elevated neopterin group compared to osteoarthritis group.
No significant difference between normal neopterin group and osteoarthritis group.

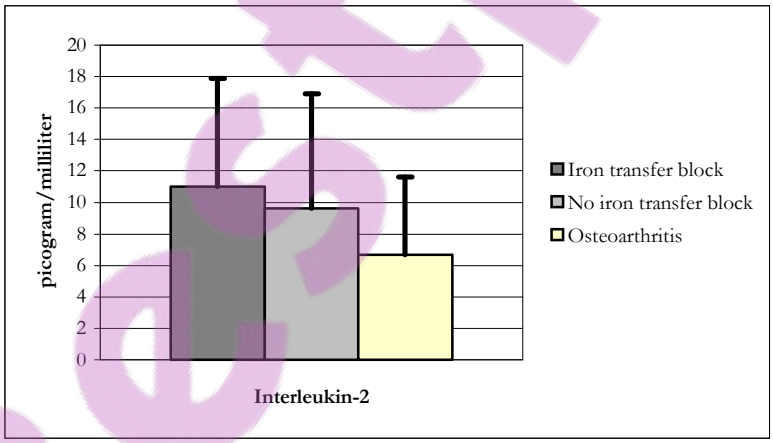

Figure 27c.
No significant difference between iron transfer block group and no iron transfer block group**.**
Significantly higher for iron transfer block group compared to osteoarthritis group.
No significant difference between no iron transfer block group and osteoarthritis group.

Figure 27a – 27c. Differences in interleukin-2 for the C-reactive protein subdivision, the neopterin subdivision and the iron transfer block subdivision.

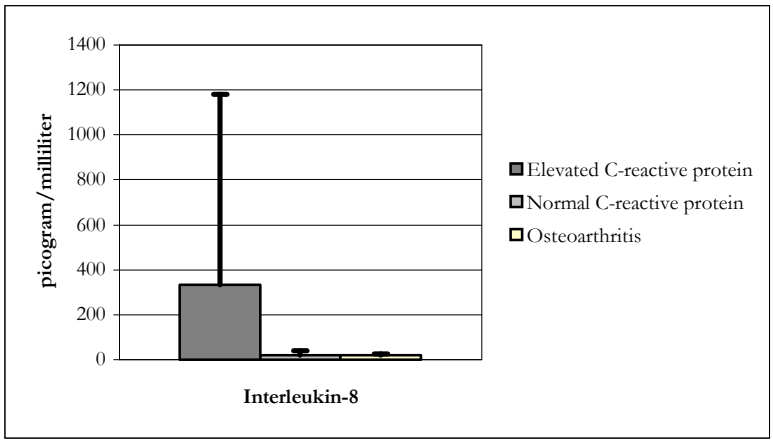

Figure 28a.
Significantly higher for elevated CRP group compared to normal CRP group.
Significantly higher for elevated CRP group compared to osteoarthritis group.
No significant difference between normal CRP group and osteoarthritis group.

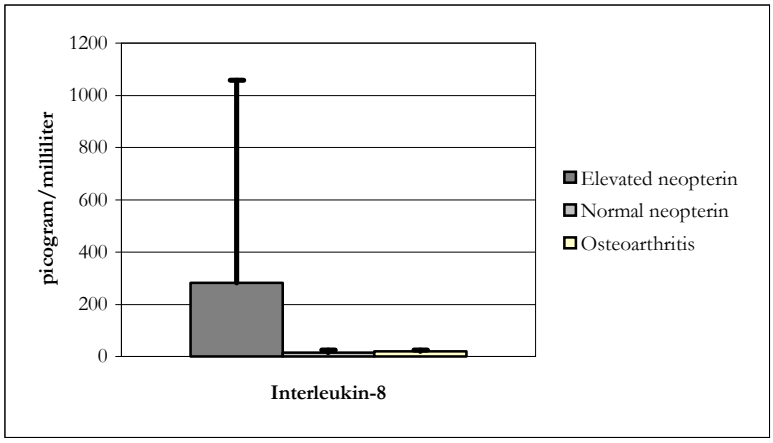

Figure 28b.
Significantly higher for elevated neopterin group compared to normal neopterin group.
Significantly higher for elevated neopterin group compared to osteoarthritis group.
No significant difference between normal neopterin group and osteoarthritis group.

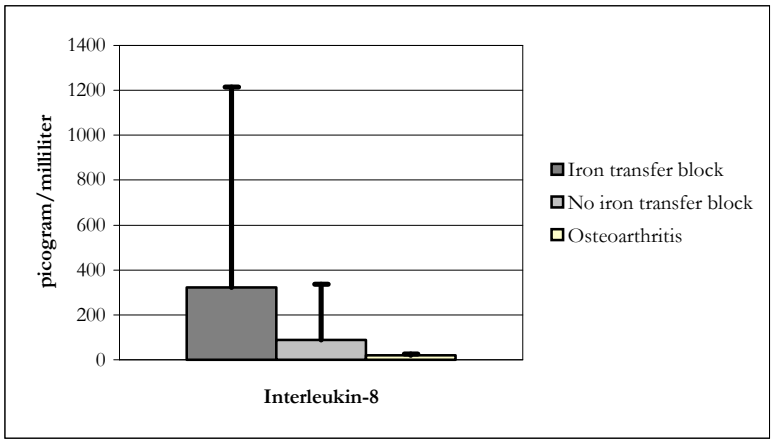

Figure 28c.
Significantly higher for iron transfer block group compared to no iron transfer block group.
Significantly higher for iron transfer block group compared to osteoarthritis group.
No significant difference between no iron transfer block group and osteoarthritis group.

Figure 28a – 28c. Differences in interleukin-8 for the C-reactive protein subdivision, the neopterin subdivision and the iron transfer block subdivision.

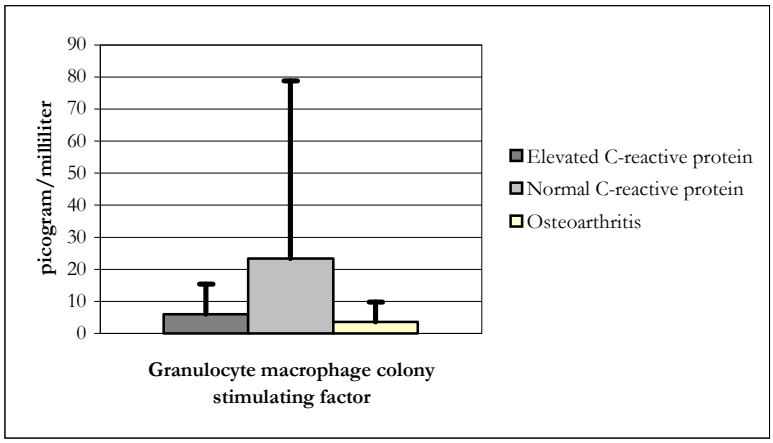

Figure 29a.
No significant difference between elevated CRP group and normal CRP group.
No significant difference between elevated CRP group and osteoarthritis group.
No significant difference between normal CRP group and osteoarthritis group.

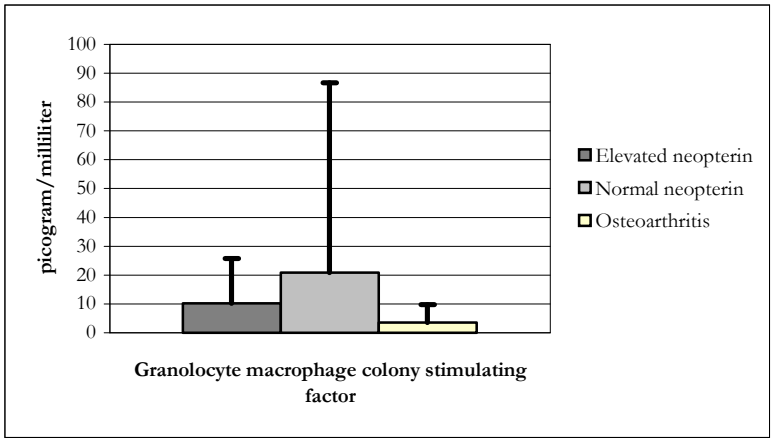

Figure 29b.
No significant difference between elevated neopterin group and normal neopterin group.
Marginally higher for elevated neopterin group compared to osteoarthritis group.
No significant difference between normal neopterin group and osteoarthritis group.

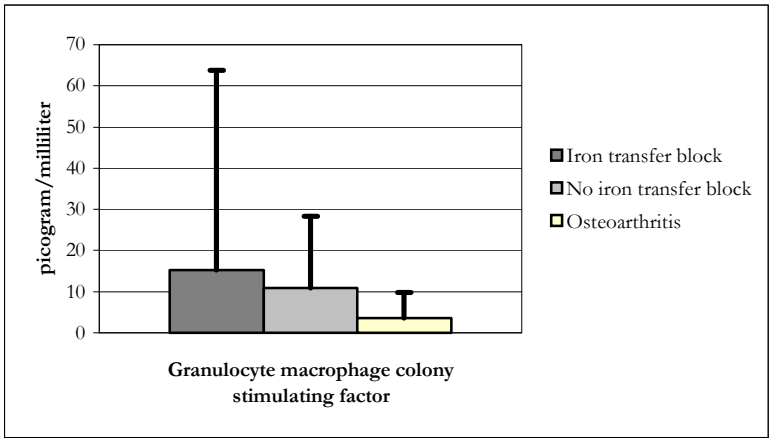

Figure 29c.
No significant difference between iron transfer block group and no iron transfer block group.
No significant difference between iron transfer block group and osteoarthritis group.
Marginally higher for no iron transfer block group compared to osteoarthritis group.

Figure 29a – 29c. Differences in granulocyte macrophage colony stimulating factor for the C-reactive protein subdivision, the neopterin subdivision and the iron transfer block subdivision.

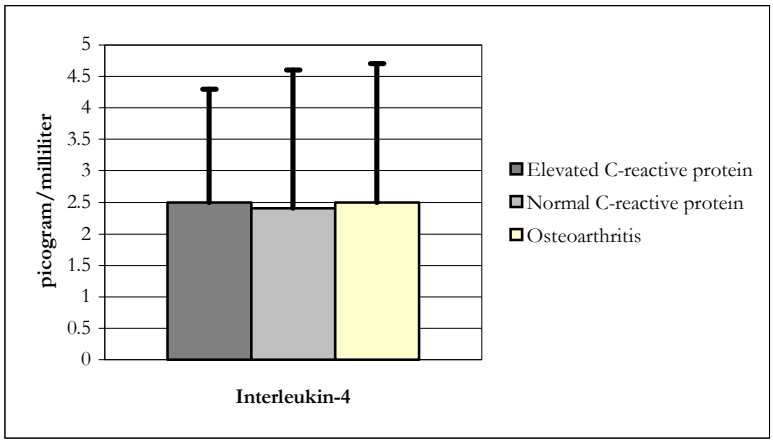

Figure 30a.
No significant difference between elevated CRP group and normal CRP group.
No significant difference between elevated CRP group and osteoarthritis group.
No significant difference between normal CRP group and osteoarthritis group.

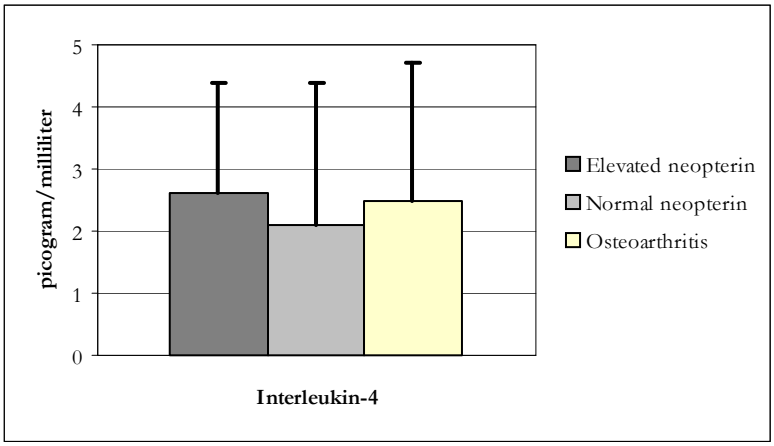

Figure 30b.
No significant difference between elevated neopterin group and normal neopterin group.
No significant difference between elevated neopterin group and osteoarthritis group.
No significant difference between normal neopterin group and osteoarthritis group.

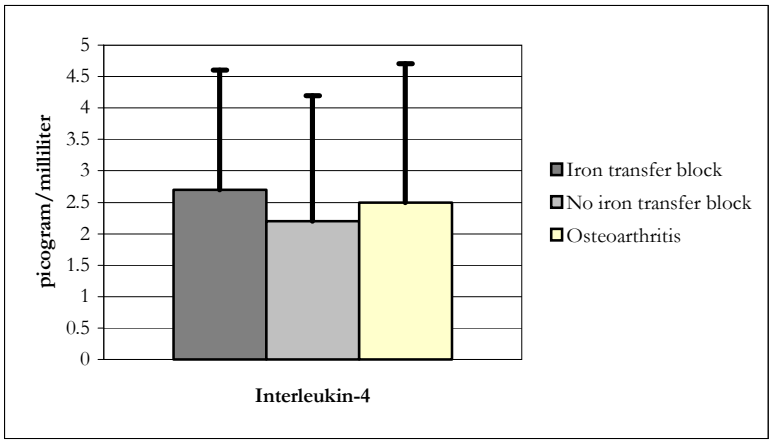

Figure 30c.
No significant difference between iron transfer block group and no iron transfer block group.
No significant difference between iron transfer block group and osteoarthritis group.
No significant difference between no iron transfer block group and osteoarthritis group.

Figure 30a – 30c. Differences in interleukin-4 for the C-reactive protein subdivision, the neopterin subdivision and the iron transfer block subdivision.

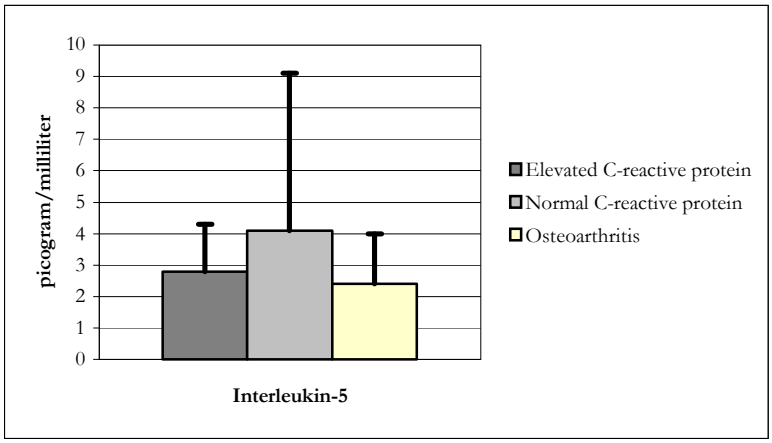

Figure 31a.
No significant difference between elevated CRP group and normal CRP group.
No significant difference between elevated CRP group and osteoarthritis group.
No significant difference between normal CRP group and osteoarthritis group.

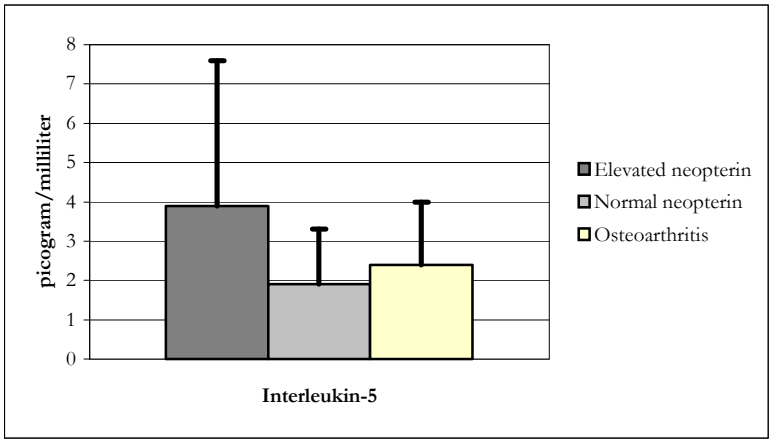

Figure 31b.
Significantly higher for elevated neopterin group compared to normal neopterin group.
Marginally higher for elevated neopterin group compared to osteoarthritis group.
No significant difference between normal neopterin group and osteoarthritis group.

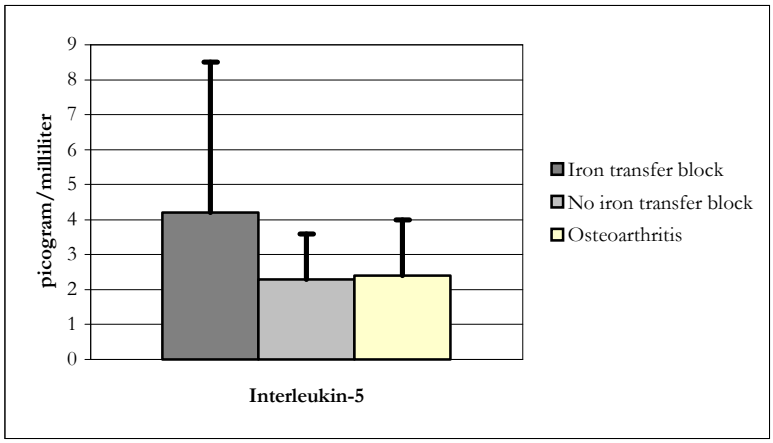

Figure 31c.
Significantly higher for iron transfer block group compared to no iron transfer block group.
Marginally higher for iron transfer block group compared to osteoarthritis group.
No significant difference between no iron transfer block group and osteoarthritis group.

Figure 31a – 31c. Differences in interleukin-5 for the C-reactive protein subdivision, the neopterin subdivision and the iron transfer block subdivision.

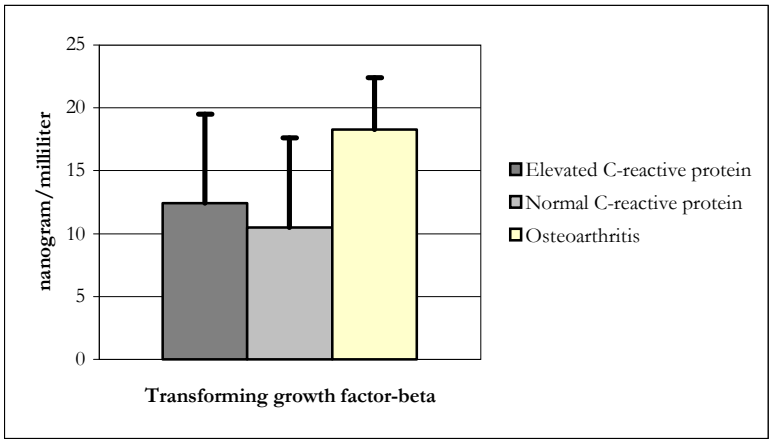

Figure 32a.
No significant difference between elevated CRP group and normal CRP group.
Significantly lower for elevated CRP group compared to osteoarthritis group.
Significantly lower for normal CRP group compared to osteoarthritis group.

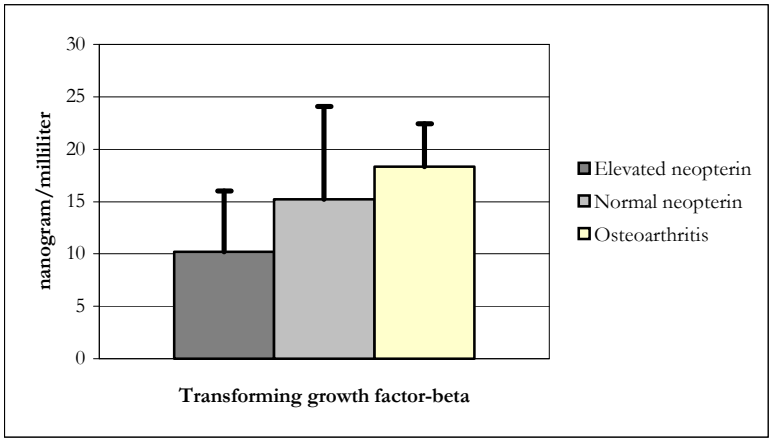

Figure 32b.
Marginally lower for elevated neopterin group compared to normal neopterin group.
Significantly lower for elevated neopterin group compared to osteoarthritis group.
No significant difference between normal neopterin group and osteoarthritis group.

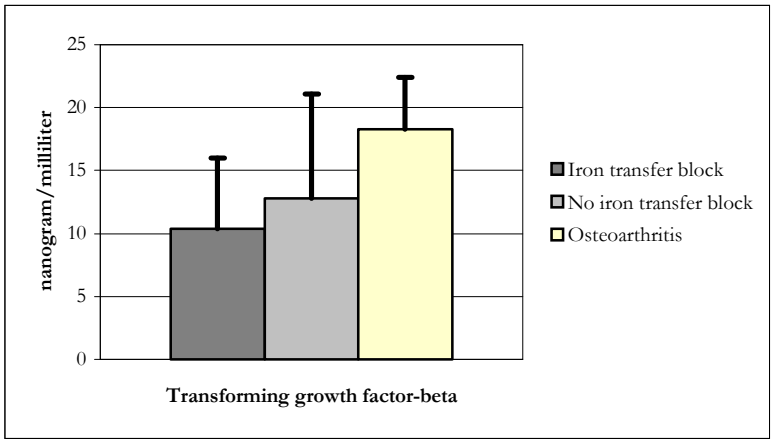

Figure 32c.
No significant difference between iron transfer block group and no iron transfer block group.
Significantly lower for iron transfer block group compared to osteoarthritis group.
Significantly lower for no iron transfer block group compared to osteoarthritis group.

Figure 32a – 32c. Differences in transforming growth factor-β for the C-reactive protein subdivision, the neopterin subdivision and the iron transfer block subdivision.

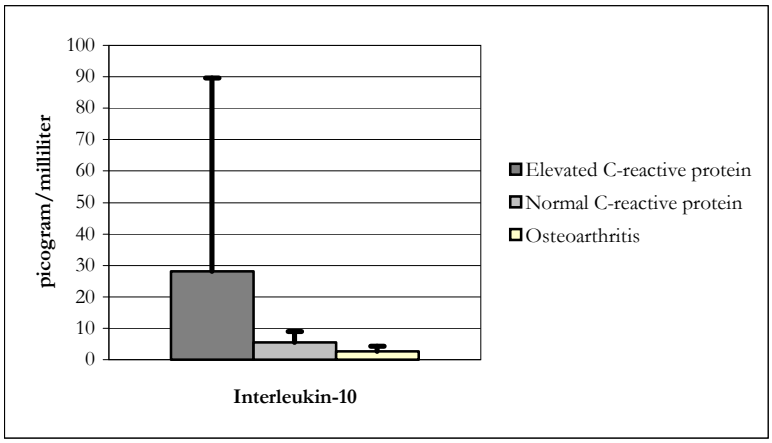

Figure 33a.
Marginally higher for elevated CRP group compared to normal CRP group.
Significantly higher for elevated CRP group compared to osteoarthritis group.
Significantly higher for normal CRP group compared to osteoarthritis group.

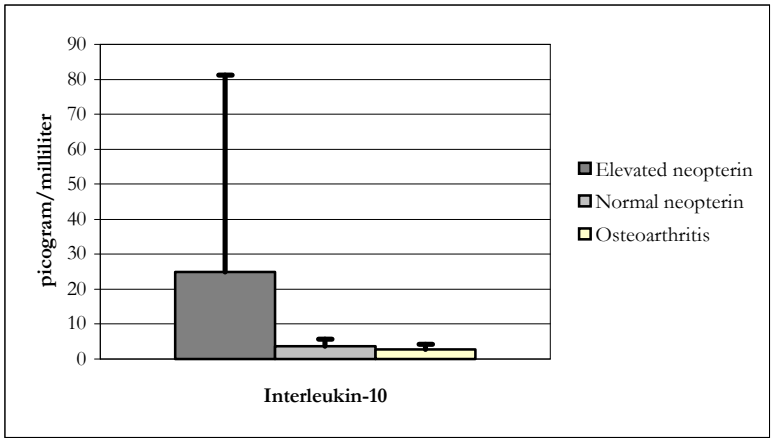

Figure 33b.
Significantly higher for elevated neopterin group compared to normal neopterin group.
Significantly higher for elevated neopterin group compared to osteoarthritis group.
No significant difference between normal neopterin group and osteoarthritis group.

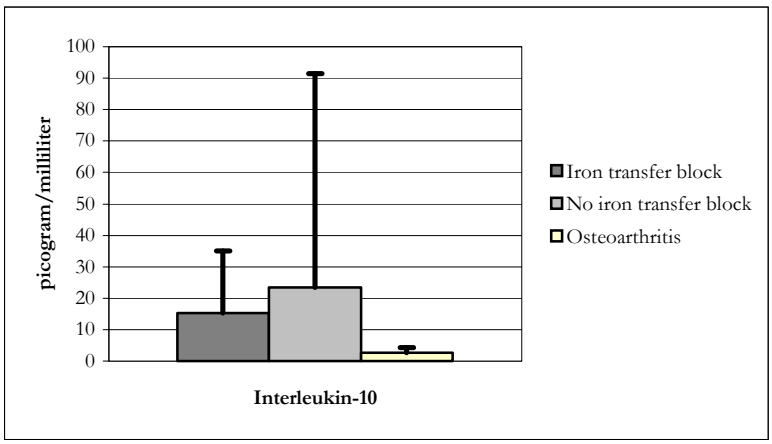

Figure 33c.
No significant difference between iron transfer block group and no iron transfer block group.
Significantly higher for iron transfer block group compared to osteoarthritis group.
Significantly higher for no iron transfer block group compared to osteoarthritis group.

Figure 33a – 33c. Differences in interleukin-10 for the C-reactive protein subdivision, the neopterin subdivision and the iron transfer block subdivision.

5) Correlations in the different subgroups of the Kalafong patients and the group of osteoarthritis patients

5.1) Correlations in the group of Kalafong patients with normal C-reactive protein

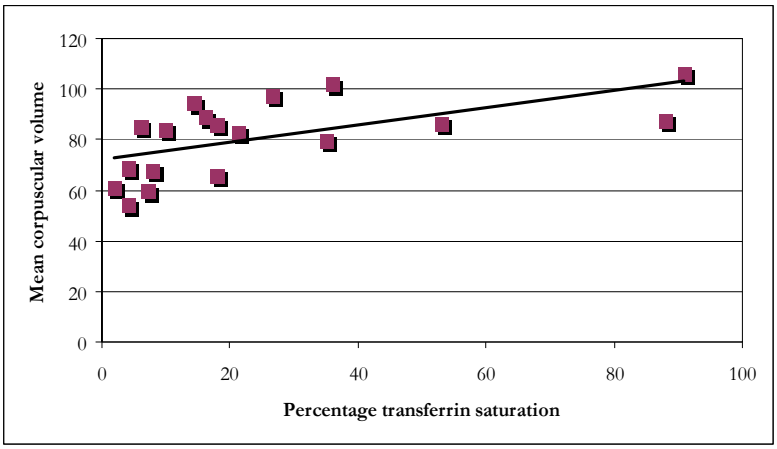

Figure 1.
Correlation between the percentage transferrin saturation and the mean corpuscular volume in the group of Kalafong patients with normal CRP (r-value = 0.62, p-value = 0.005).

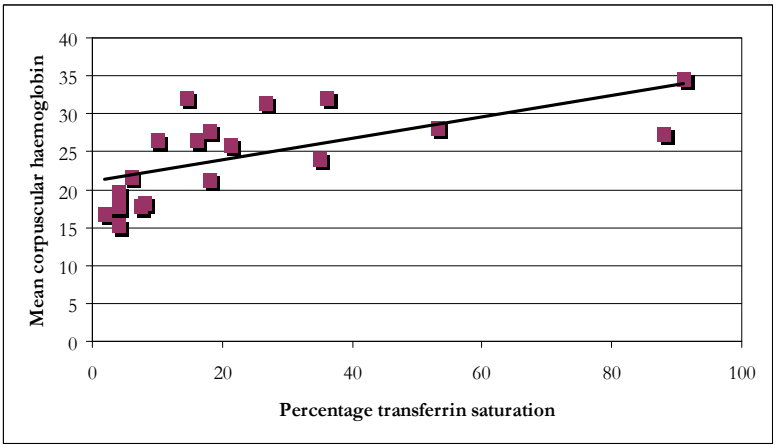

Figure 2.
Correlation between the percentage transferrin saturation and the mean corpuscular haemoglobin in the group of Kalafong patients with normal CRP (r-value = 0.64, p-value = 0.003).

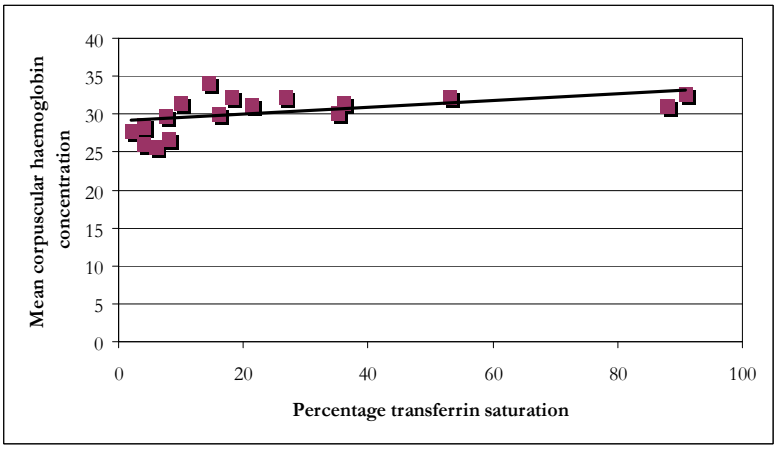

Figure 3.
Correlation between the percentage transferrin saturation and the mean corpuscular haemoglobin concentration in the group of Kalafong patients with normal CRP (r-value = 0.49, p-value = 0.033).

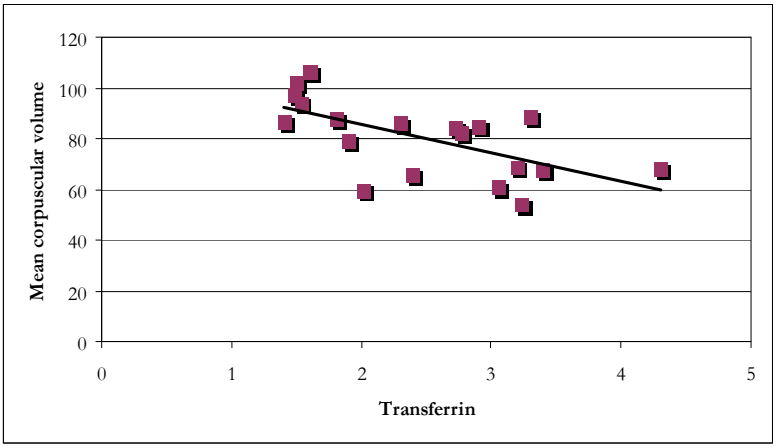

Figure 4.
Correlation between transferrin and the mean corpuscular volume in the group of Kalafong patients with normal CRP (r-value = 0.62, p-value = 0.005).

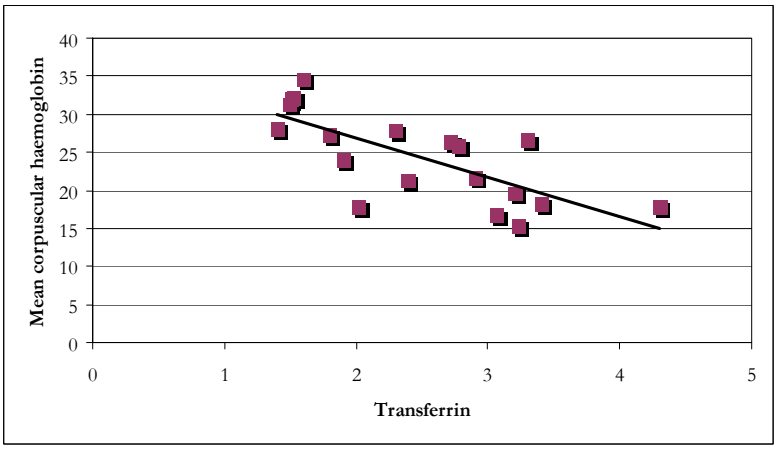

Figure 5.
Correlation between transferrin and the mean corpuscular haemoglobin in the group of Kalafong patients with normal CRP (r-value = 0.74, p-value = 0.0003).

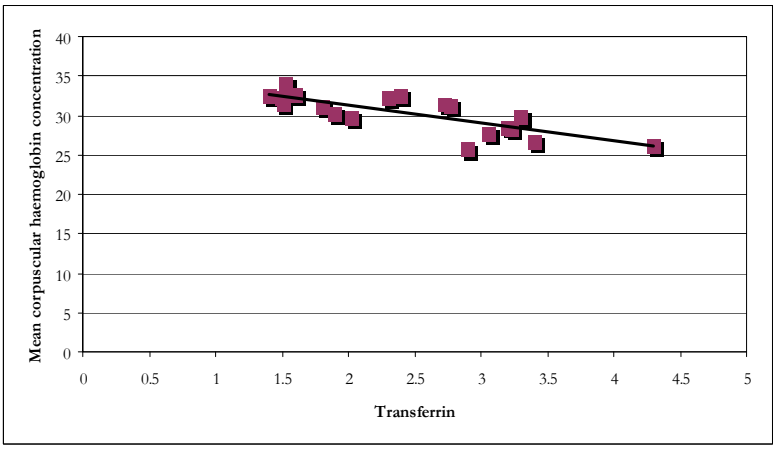

Figure 6.
Correlation between transferrin and the mean corpuscular haemoglobin concentration in the group of Kalafong patients with normal CRP (r-value = 0.79, p-value = 0.0001).

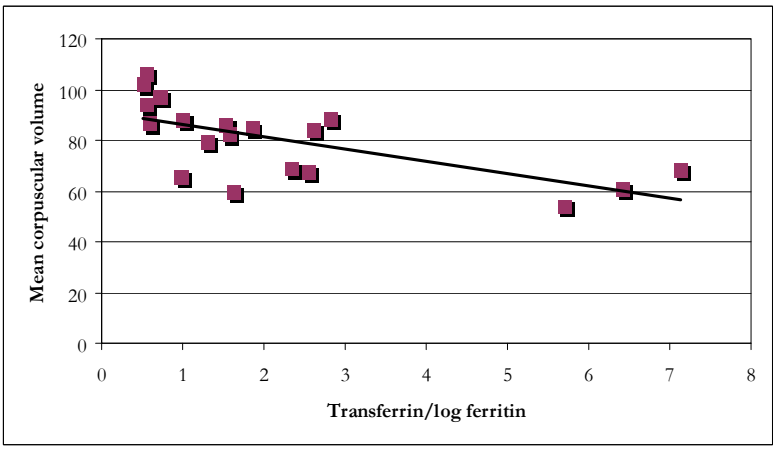

Figure 7.
Correlation between the transferrin/log ferritin ratio and the mean corpuscular volume in the group of Kalafong patients with normal CRP (r-value = 0.66, p-value = 0.002).

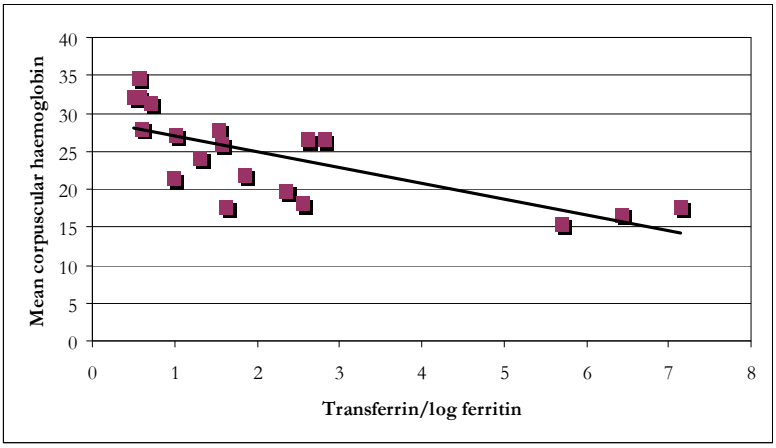

Figure 8.
Correlation between the transferrin/log ferritin ratio and the mean corpuscular haemoglobin in the group of Kalafong patients with normal CRP (r-value = 0.72, p-value = 0.0005).

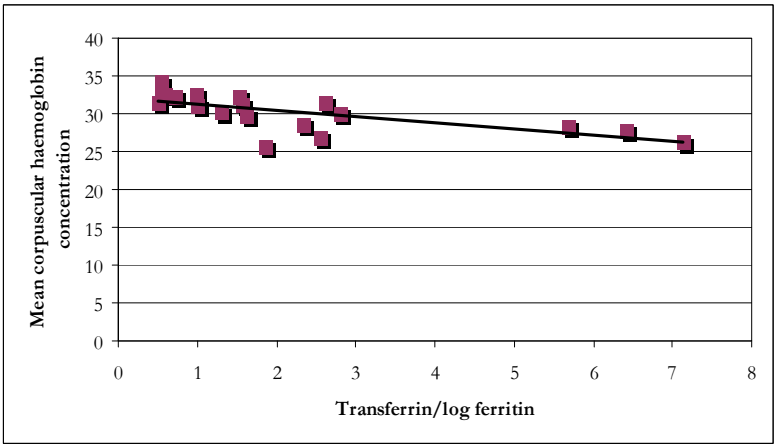

Figure 9.
Correlation between the transferrin/log ferritin ratio and the mean corpuscular haemoglobin concentration in the group of Kalafong patients with normal CRP (r-value = 0.70, p-value = 0.001).

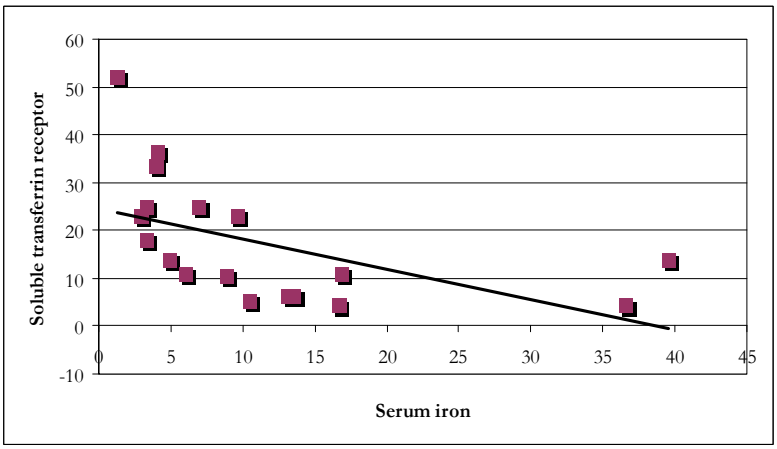

Figure 10.
Correlation between serum iron and the soluble transferrin receptor in the group of Kalafong patients with normal CRP (r-value = 0.52, p-value = 0.024).

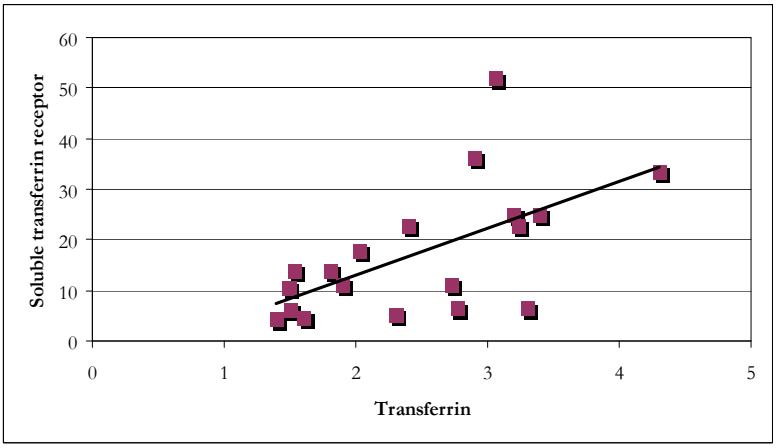

Figure 11.
Correlation between transferrin and the soluble transferrin receptor in the group of Kalafong patients with normal CRP (r-value = 0.59, p-value = 0.007).

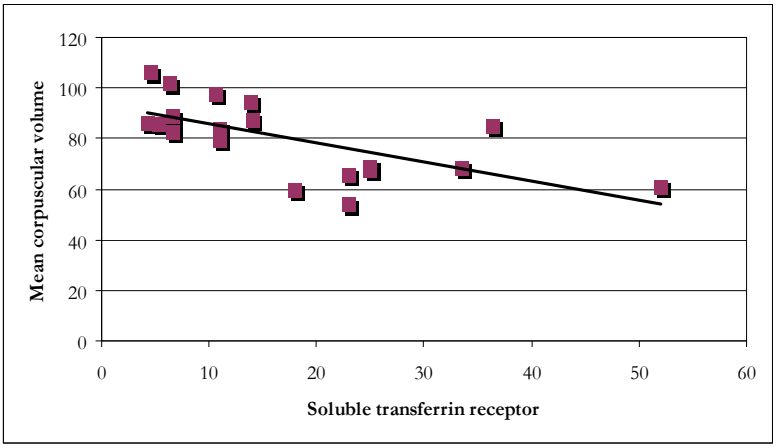

Figure 12.
Correlation between the soluble transferrin receptor and the mean corpuscular volume in the group of Kalafong patients with normal CRP (r-value = 0.65, p-value = 0.002).

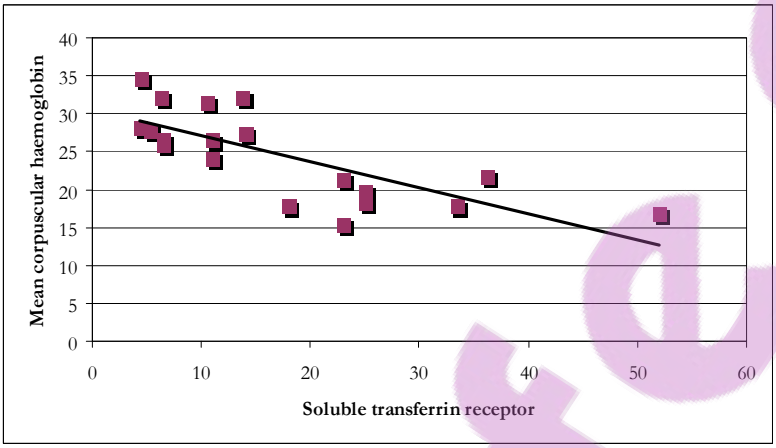

Figure 13.
Correlation between the soluble transferrin receptor and the mean corpuscular haemoglobin in the group of Kalafong patients with normal CRP (r-value = 0.75, p-value = 0.0002).

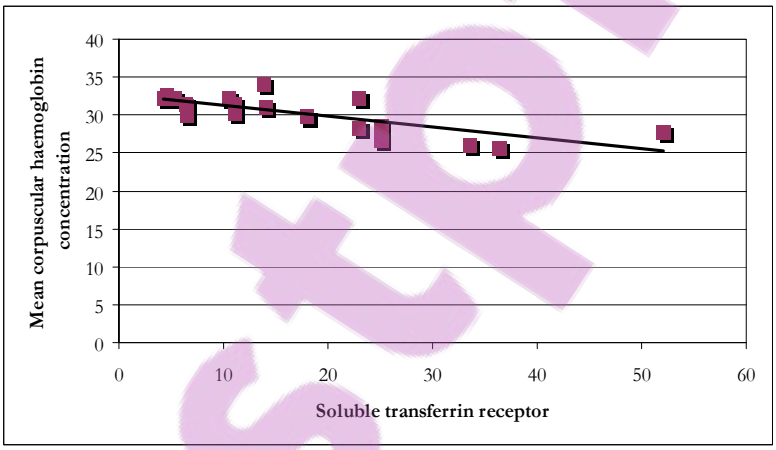

Figure 14.
Correlation between the soluble transferrin receptor and the mean corpuscular haemoglobin concentration in the group of Kalafong patients with normal CRP (r-value = 0.75, p-value = 0.0002).

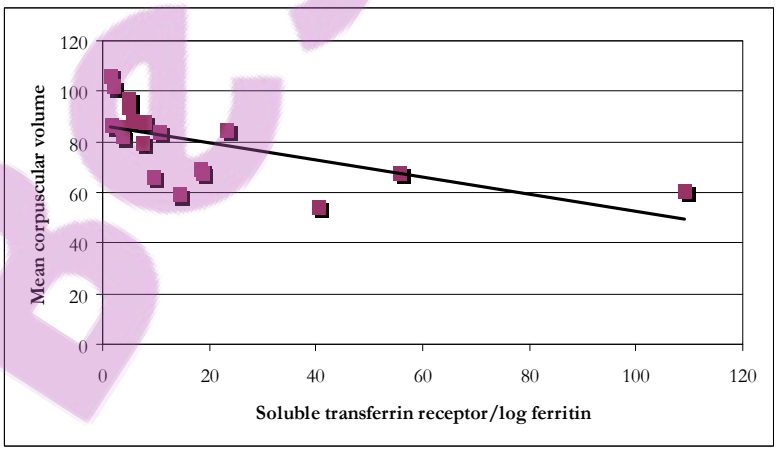

Figure 15.
Correlation between the soluble transferrin receptor/log ferritin ratio and the mean corpuscular volume in the group of Kalafong patients with normal CRP (r-value = 0.60, p-value = 0.007).

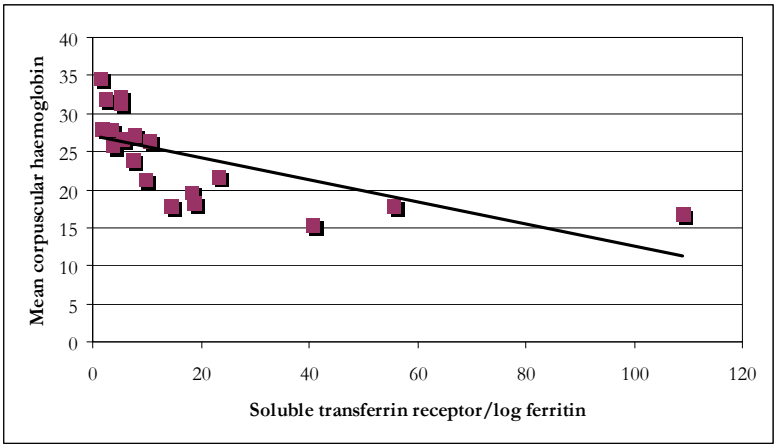

Figure 16.
Correlation between the soluble transferrin receptor/log ferritin ratio and the mean corpuscular haemoglobin in the group of Kalafong patients with normal CRP (r-value = 0.65, p-value = 0.003).

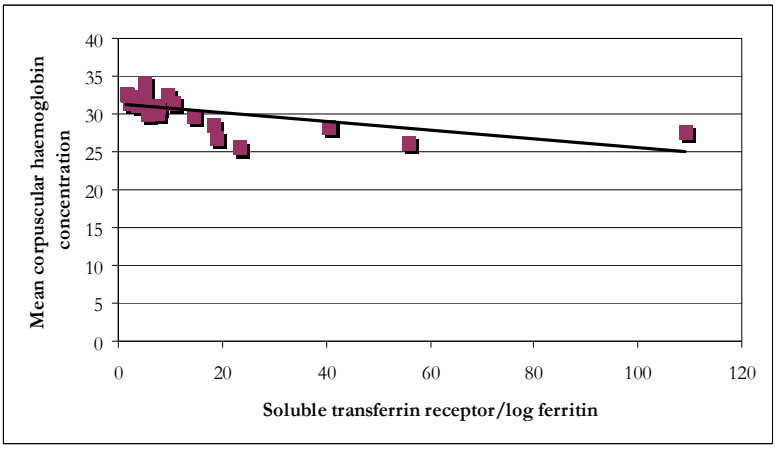

Figure 17.
Correlation between the soluble transferrin receptor/log ferritin ratio and the mean corpuscular haemoglobin concentration in the group of Kalafong patients with normal CRP (r-value = 0.61, p-value = 0.005).

5.2) Correlations in the group of Kalafong patients with normal neopterin

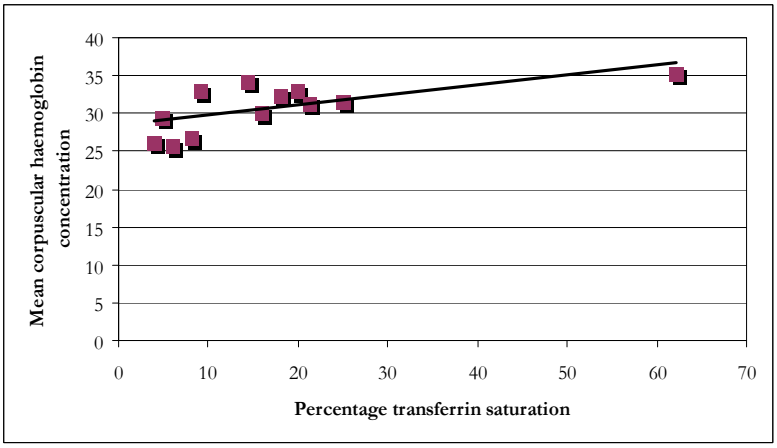

Figure 1.
Correlation between the percentage transferrin saturation and the mean corpuscular haemoglobin concentration in the group of Kalafong patients with normal neopterin (r-value = 0.65, p-value = 0.015).

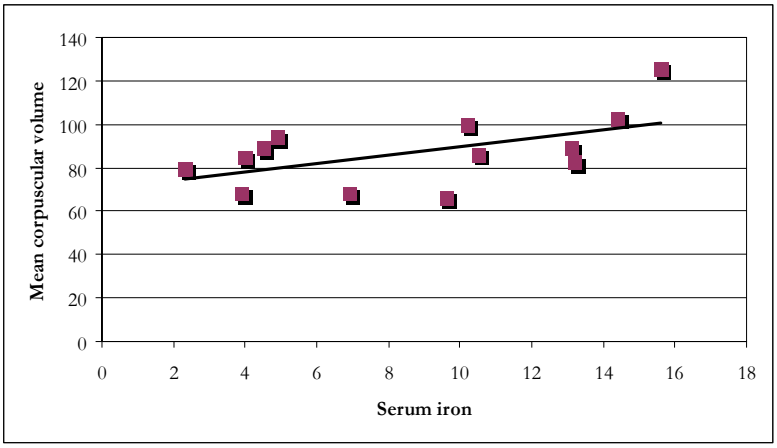

Figure 2.
Correlation between serum iron and the mean corpuscular volume in the group of Kalafong patients with normal neopterin (r-value = 0.55, p-value = 0.053).

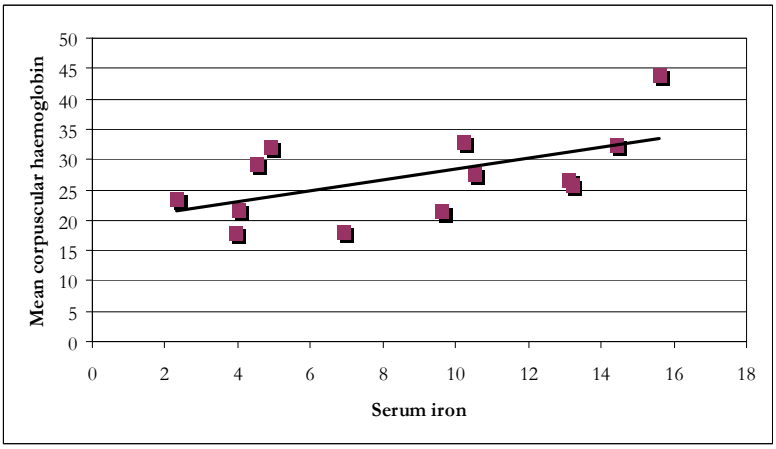

Figure 3.
Correlation between serum iron and the mean corpuscular haemoglobin in the group of Kalafong patients with normal neopterin (r-value = 0.57, p-value = 0.040).

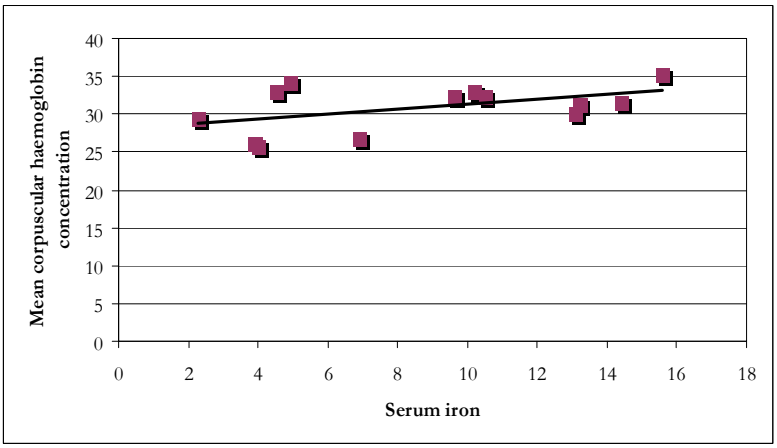

Figure 4.
Correlation between serum iron and the mean corpuscular haemoglobin concentration in the group of Kalafong patients with normal neopterin (r-value = 0.49, p-value = 0.091).

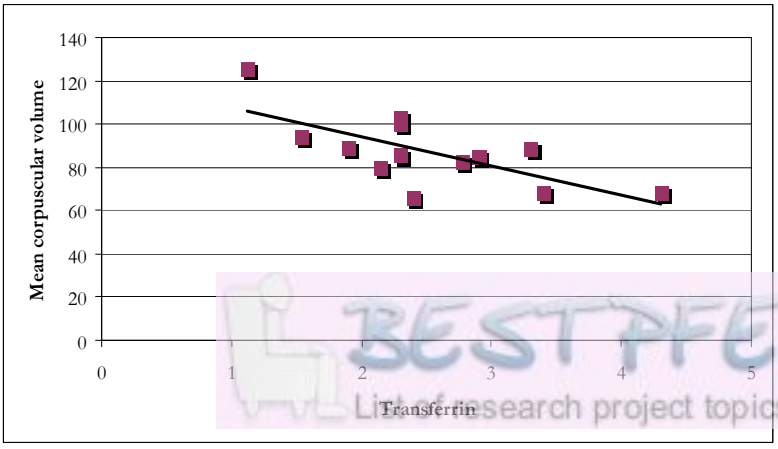

Figure 5.
Correlation between transferrin and the mean corpuscular volume in the group of Kalafong patients with normal neopterin (r-value = 0.70, p-value = 0.008).

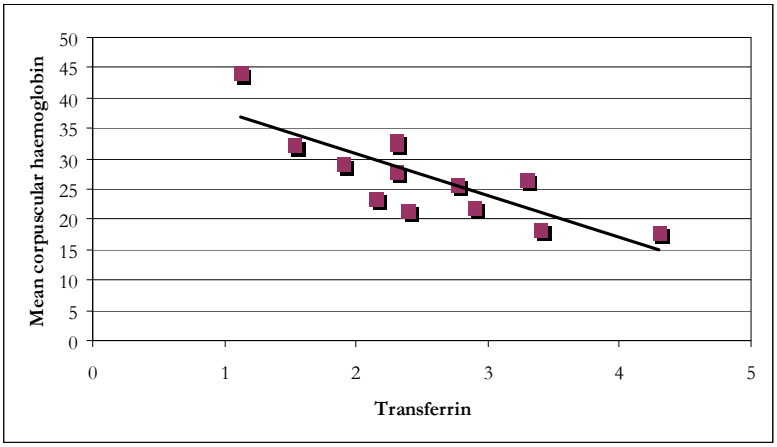

Figure 6.
Correlation between transferrin and the mean corpuscular haemoglobin in the group of Kalafong patients with normal neopterin (r-value = 0.80, p-value = 0.001).

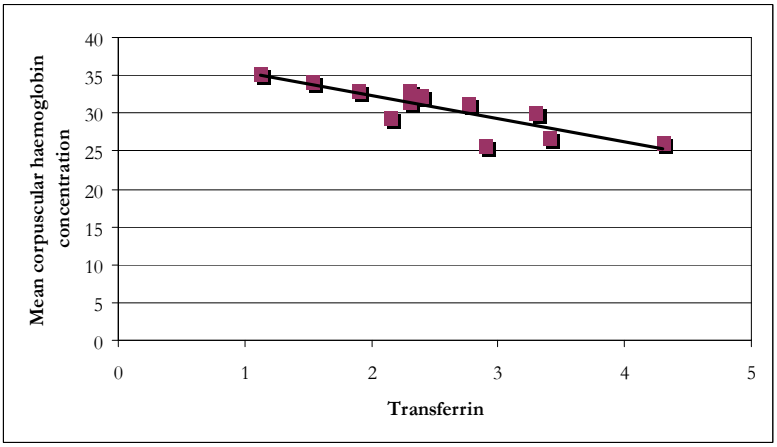

Figure 7.
Correlation between transferrin and the mean corpuscular haemoglobin concentration in the group of Kalafong patients with normal neopterin (r-value = 0.84, p-value = 0.0003).

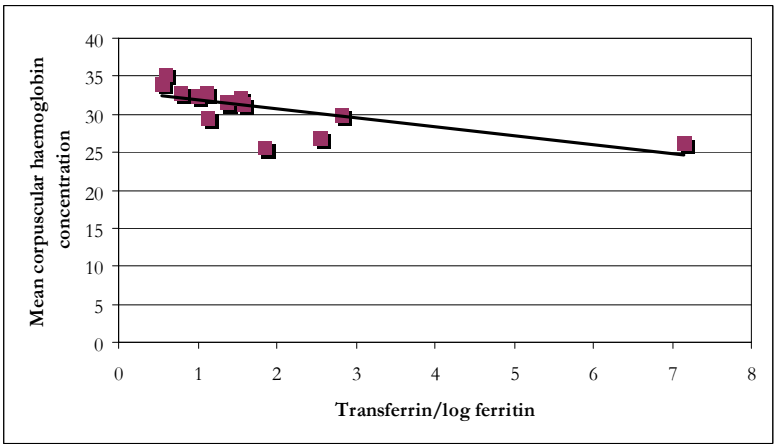

Figure 8.
Correlation between the transferrin/log ferritin ratio and the mean corpuscular haemoglobin concentration in the group of Kalafong patients with normal neopterin (r-value = 0.68, p-value = 0.01).

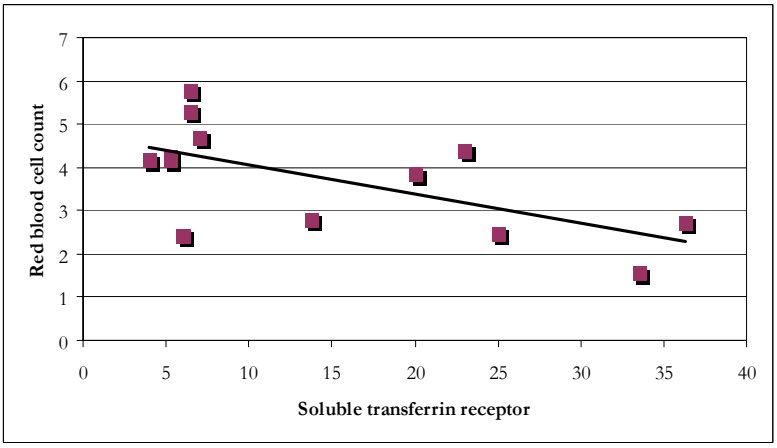

Figure 9.
Correlation between the soluble transferrin receptor and the red blood cell count in the group of Kalafong patients with normal neopterin (r-value = 0.63, p-value = 0.021).

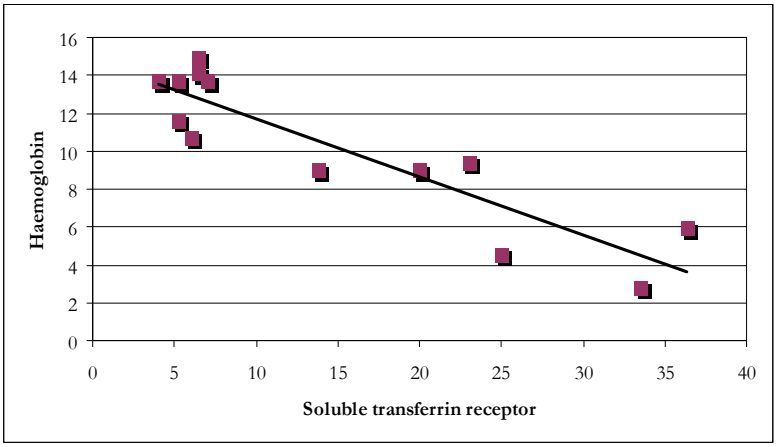

Figure 10.
Correlation between the soluble transferrin receptor and haemoglobin in the group of Kalafong patients with normal neopterin (r-value = 0.90, p-value < 0.0001).

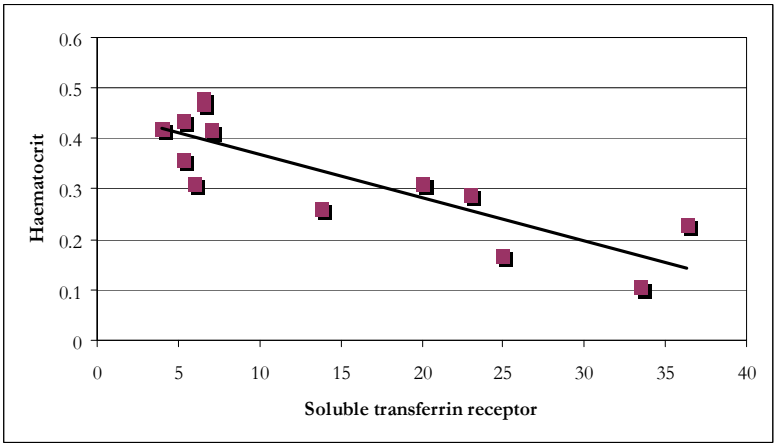

Figure 11.
Correlation between the soluble transferrin receptor and haematocrit in the group of Kalafong patients with normal neopterin (r-value = 0.84, p-value = 0.0003).

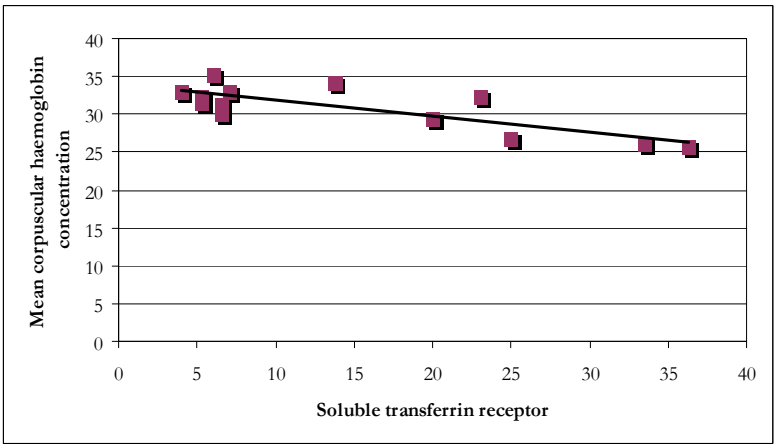

Figure 12.
Correlation between the soluble transferrin receptor and the mean corpuscular haemoglobin concentration in the group of Kalafong patients with normal neopterin (r-value = 0.79, p-value = 0.001).

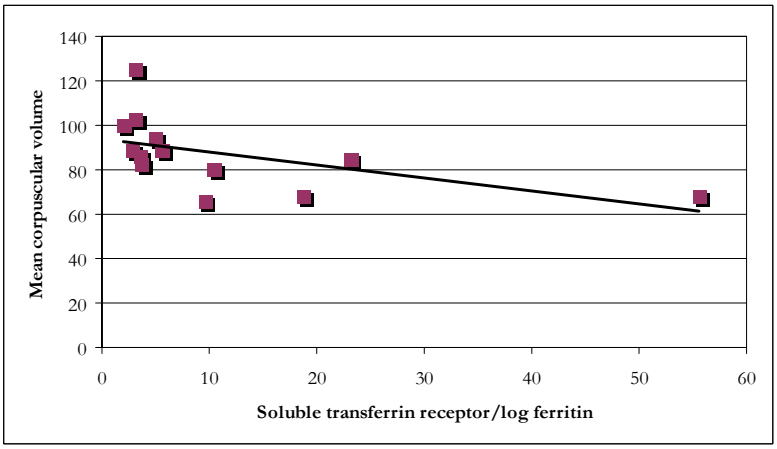

Figure 13.
Correlation between the soluble transferrin receptor/log ferritin ratio and the mean corpuscular volume in the group of Kalafong patients with normal neopterin (r-value = 0.53, p-value = 0.06).

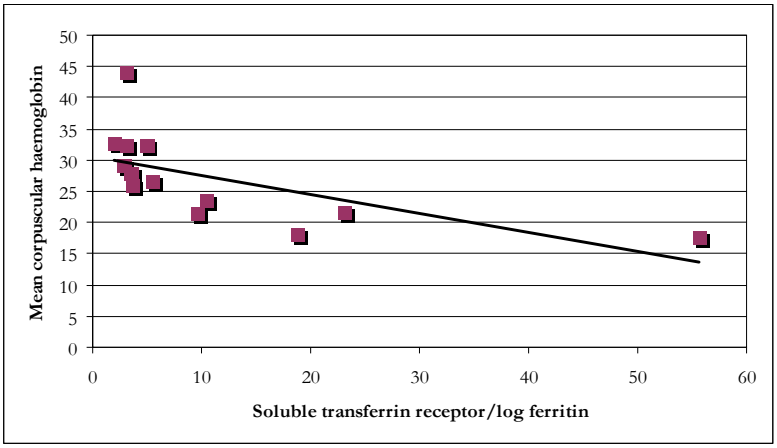

Figure 14.
Correlation between the soluble transferrin receptor/log ferritin ratio and the mean corpuscular haemoglobin in the group of Kalafong patients with normal neopterin (r-value = 0.63, p-value = 0.021).

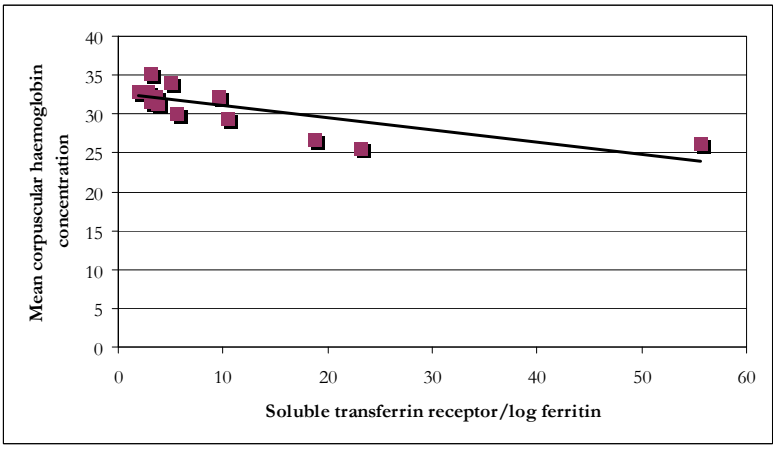

Figure 15.
Correlation between the soluble transferrin receptor/log ferritin ratio and the mean corpuscular haemoglobin concentration in the group of Kalafong patients with normal neopterin (r-value = 0.75, p-value = 0.003).

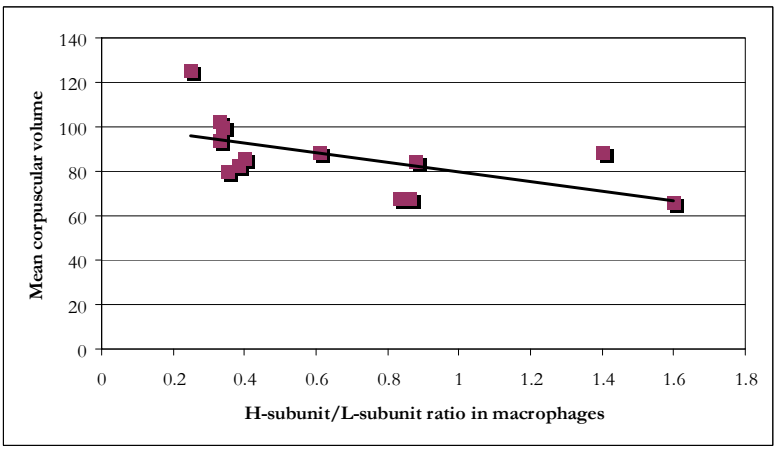

Figure 16.
Correlation between the H-subunit/L-subunit ratio in macrophages and the mean corpuscular volume in the group of Kalafong patients with normal neopterin (r-value = 0.58, p-value = 0.037).

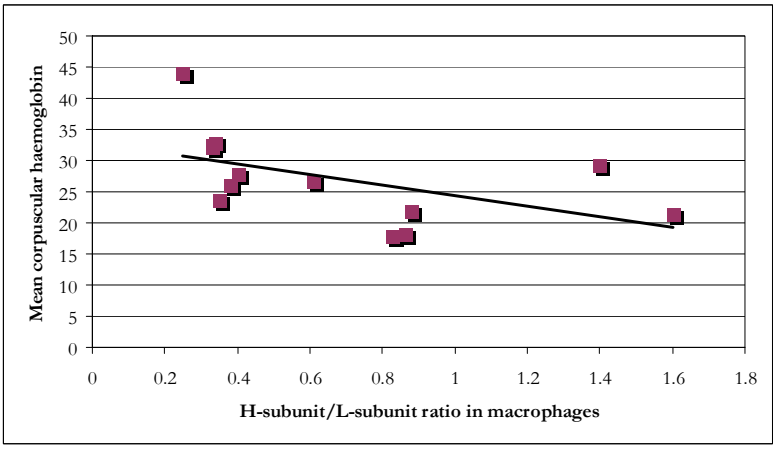

Figure 17.
Correlation between the H-subunit/L-subunit ratio in macrophages and the mean corpuscular haemoglobin in the group of Kalafong patients with normal neopterin (r-value = 0.51, p-value = 0.072).

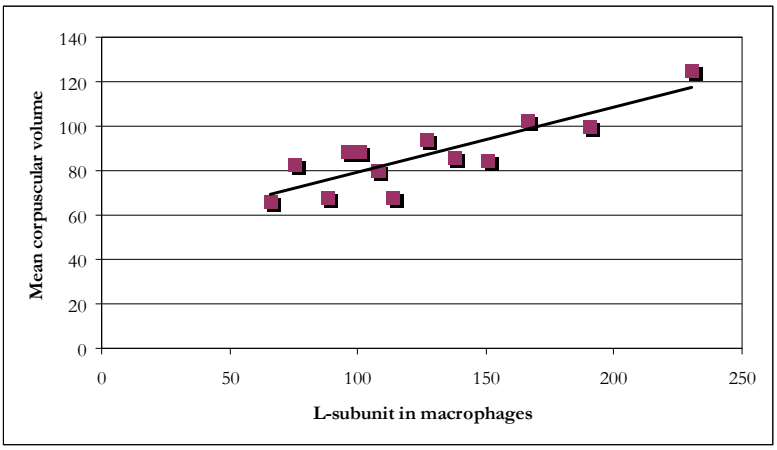

Figure 18.
Correlation between the L-subunit in macrophages and the mean corpuscular volume in the group of Kalafong patients with normal neopterin (r-value = 0.85, p-value = 0.0002).

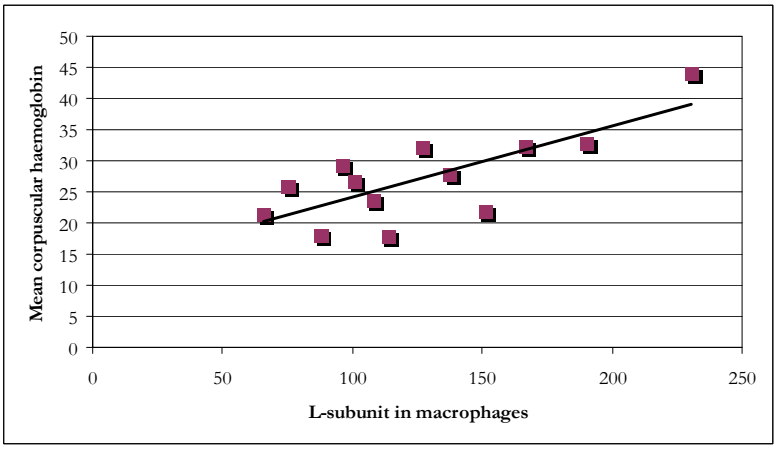

Figure 19.
Correlation between the L-subunit in macrophages and the mean corpuscular haemoglobin in the group of Kalafong patients with normal neopterin (r-value = 0.76, p-value = 0.003).

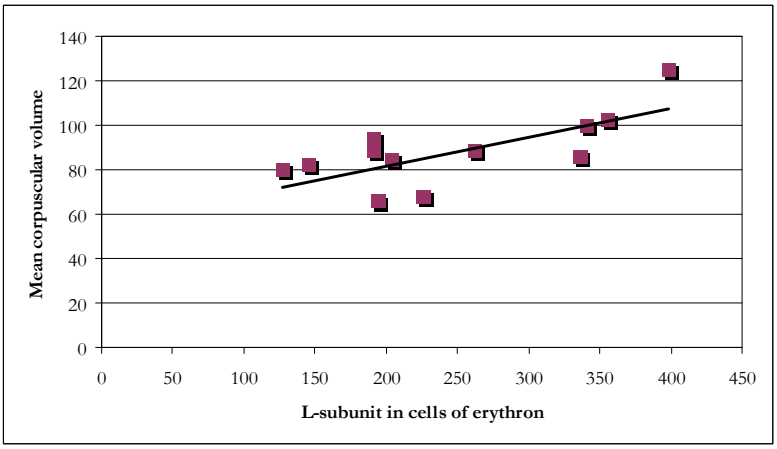

Figure 20.
Correlation between the L-subunit in cells of the erythron and the mean corpuscular volume in the group of Kalafong patients with normal neopterin (r-value = 0.69, p-value = 0.01).

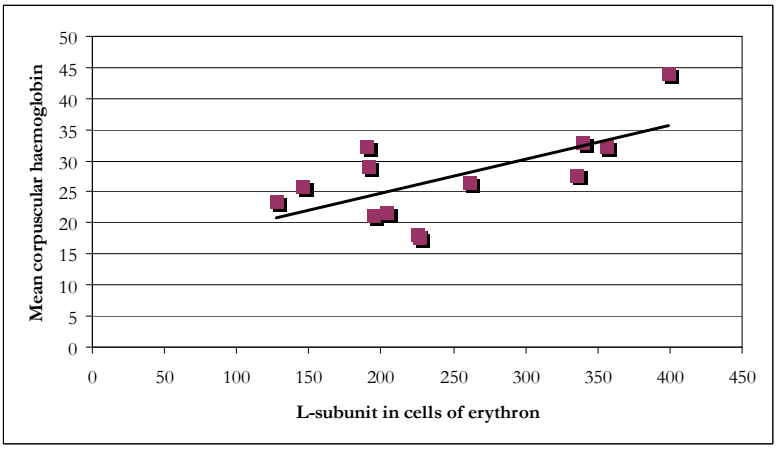

Figure 21.
Correlation between the L-subunit in cells of the erythron and the mean corpuscular haemoglobin in the group of Kalafong patients with normal neopterin (r-value = 0.65, p-value = 0.016).

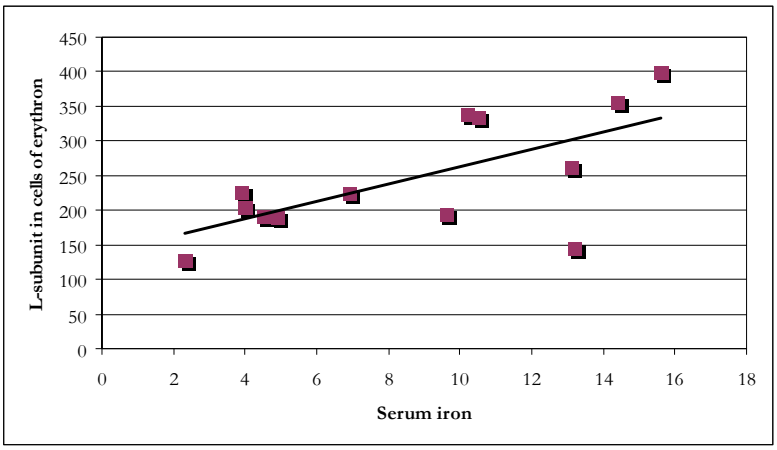

Figure 22.
Correlation between serum iron and the L-subunit in cells of the erythron in the group of Kalafong patients with normal neopterin (r-value = 0.66, p-value = 0.014).

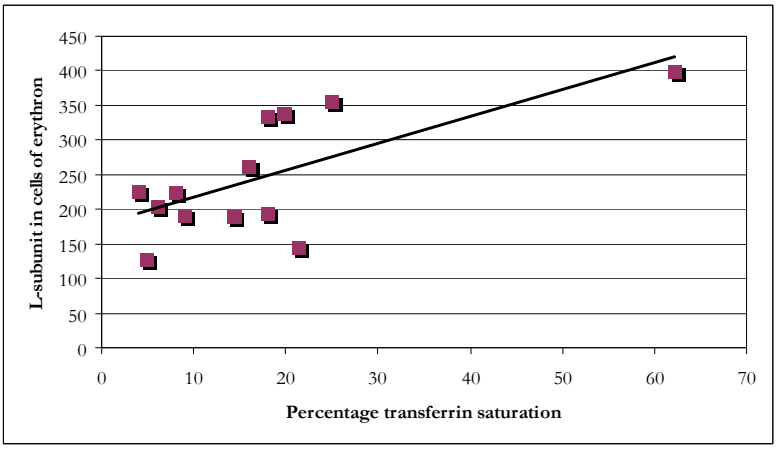

Figure 23.
Correlation between percentage transferrin saturation and the L-subunit in cells of the erythron in the group of Kalafong patients with normal neopterin (r-value = 0.68, p-value = 0.01).

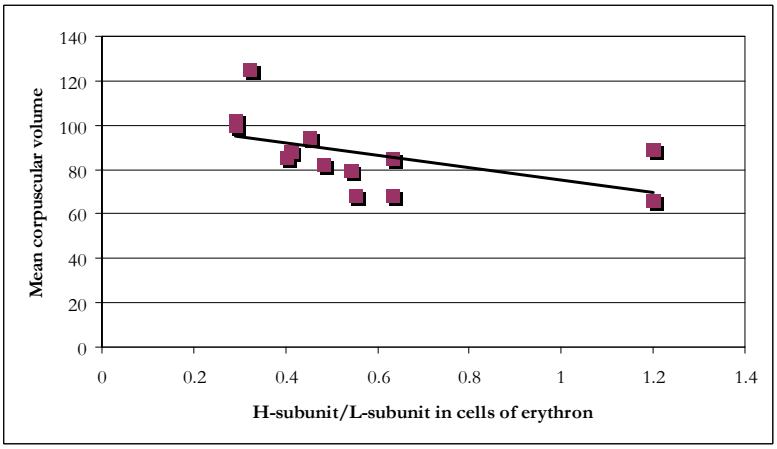

Figure 24.
Correlation between the H-subunit/L-subunit ratio in cells of the erythron and the mean corpuscular volume in the group of Kalafong patients with normal neopterin (r-value = 0.52, p-value = 0.069).

5.3) Correlations in the group of Kalafong patients with no iron transfer block

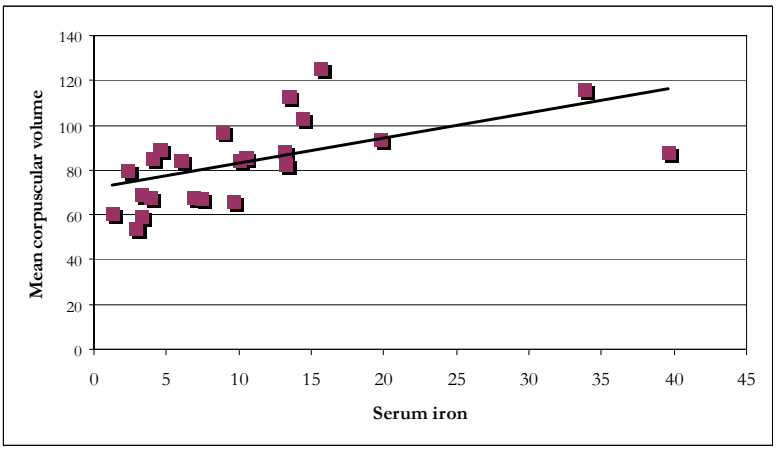

Figure 1.
Correlation between serum iron and the mean corpuscular volume in the group of Kalafong patients with no iron transfer block (r-value = 0.57, p-value = 0.004).

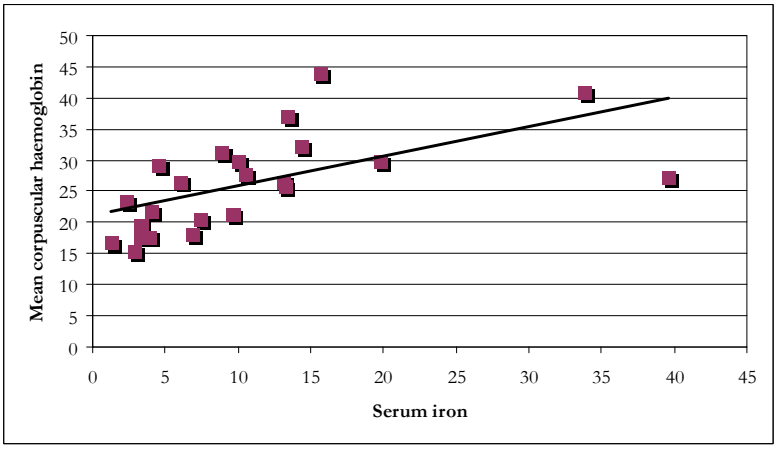

Figure 2.
Correlation between serum iron and the mean corpuscular haemoglobin in the group of Kalafong patients with no iron transfer block (r-value = 0.59, p-value = 0.003).

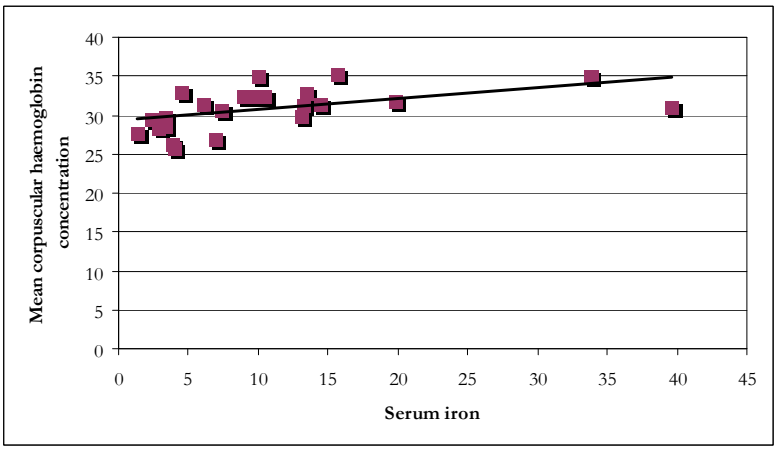

Figure 3.
Correlation between serum iron and the mean corpuscular haemoglobin concentration in the group of Kalafong patients with no iron transfer block (r-value = 0.50, p-value = 0.016).

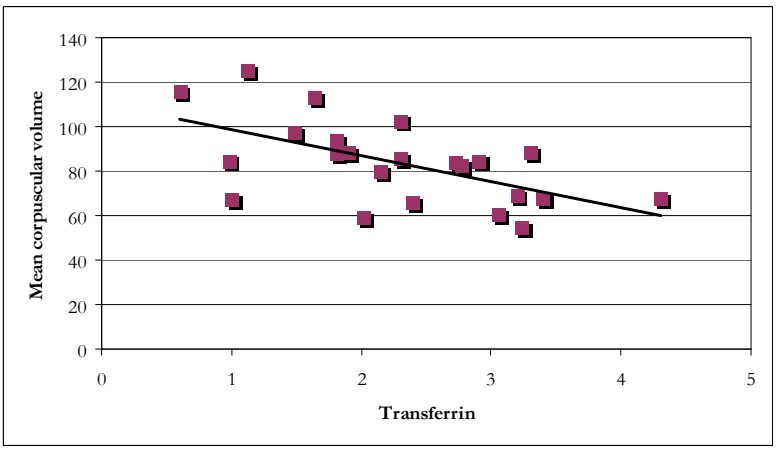

Figure 4.
Correlation between transferrin and the mean corpuscular volume in the group of Kalafong patients with no iron transfer block (r-value = 0.58, p-value = 0.004).

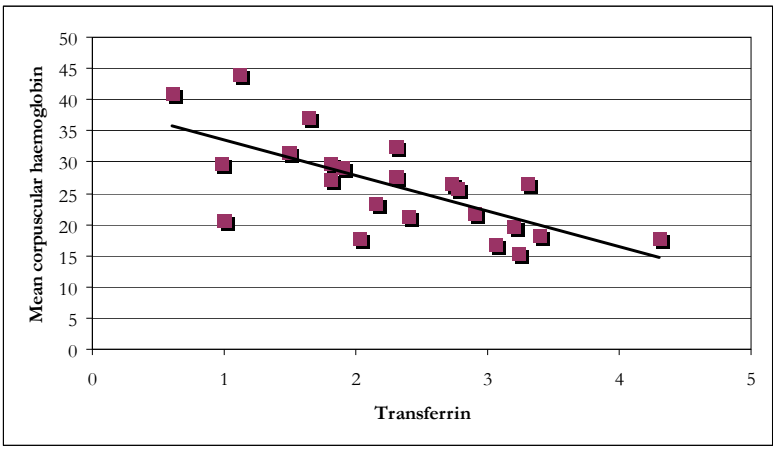

Figure 5.
Correlation between transferrin and the mean corpuscular haemoglobin in the group of Kalafong patients with no iron transfer block (r-value = 0.69, p-value = 0.0003).

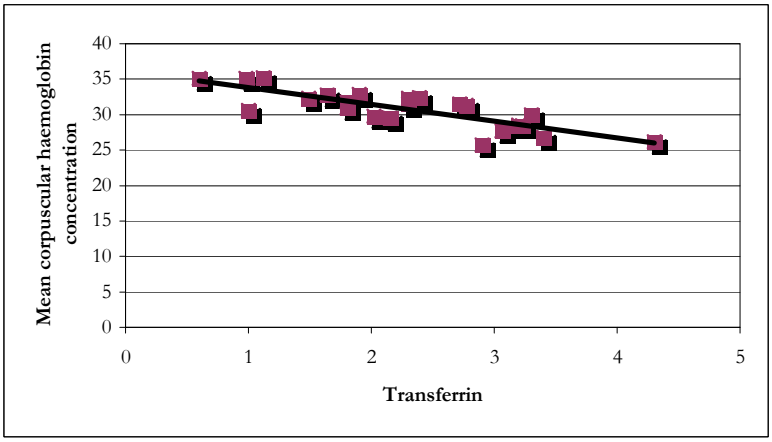

Figure 6.
Correlation between transferrin and the mean corpuscular haemoglobin concentration in the group of Kalafong patients with no iron transfer block (r-value = 0.82, p-value < 0.0001).

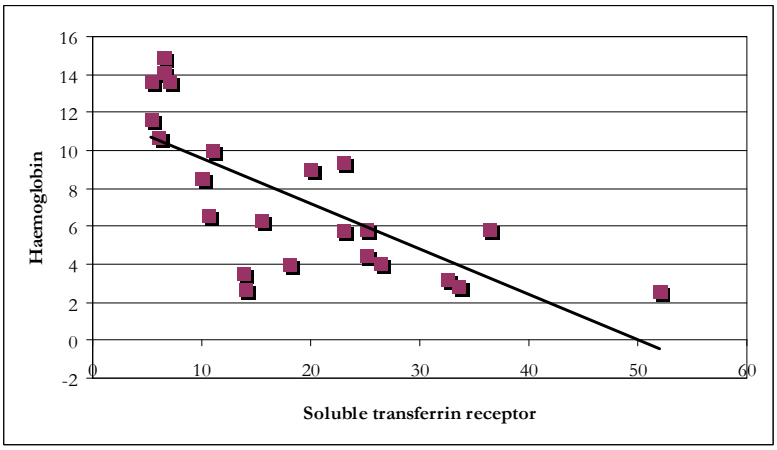

Figure 7.
Correlation between the soluble transferrin receptor and haemoglobin in the group of Kalafong patients with no iron transfer block (r-value = 0.71, p-value = 0.0001).

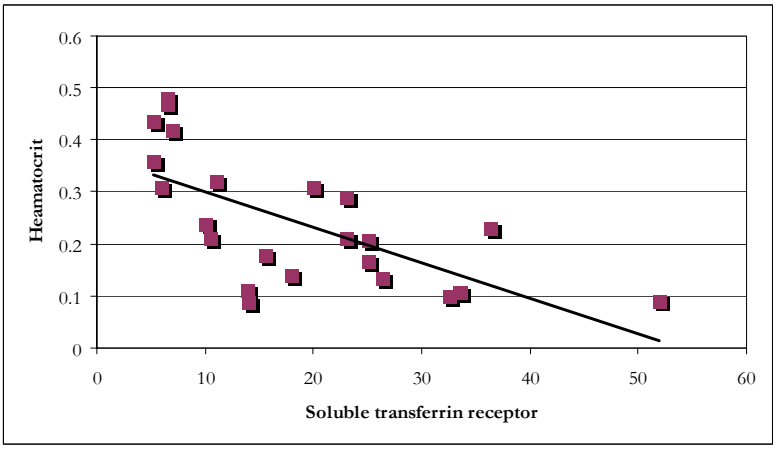

Figure 8.
Correlation between the soluble transferrin receptor and haematocrit in the group of Kalafong patients with no iron transfer block (r-value = 0.66, p-value = 0.0006).

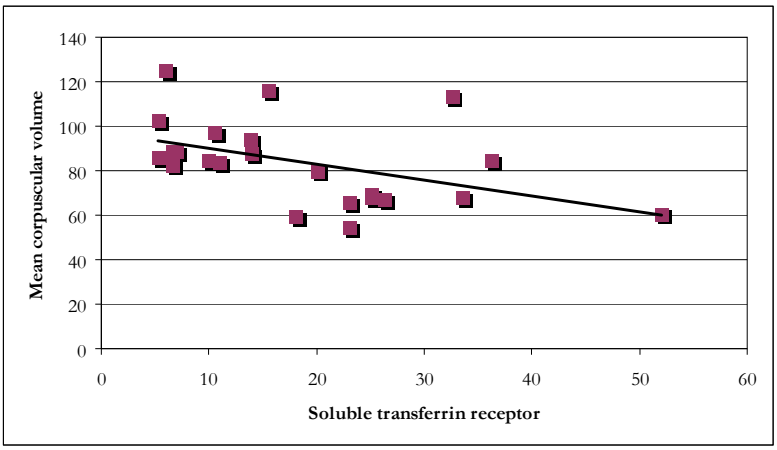

Figure 9.
Correlation between the soluble transferrin receptor and the mean corpuscular volume in the group of Kalafong patients with no iron transfer block (r-value = 0.46, p-value = 0.027).

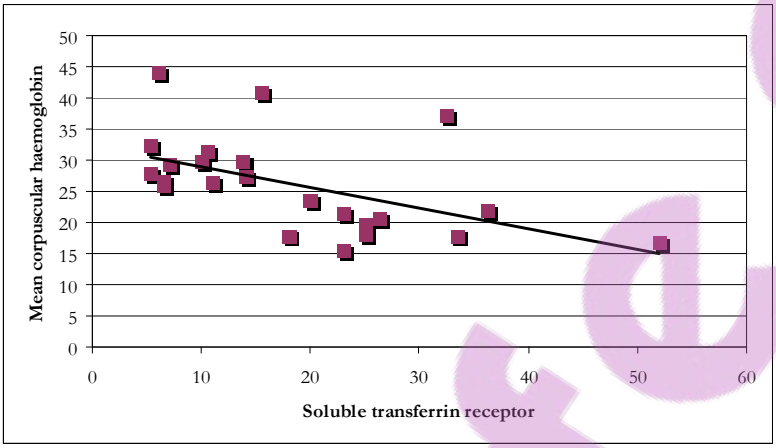

Figure 10.
Correlation between the soluble transferrin receptor and the mean corpuscular haemoglobin in the group of Kalafong patients with no iron transfer block (r-value = 0.53, p-value = 0.01).

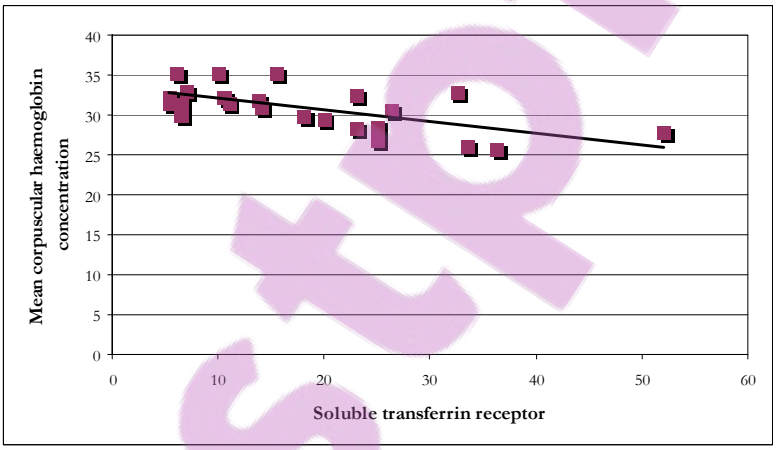

Figure 11.
Correlation between the soluble transferrin receptor and the mean corpuscular haemoglobin concentration in the group of Kalafong patients with no iron transfer block (r-value = 0.64, p-value = 0.001).

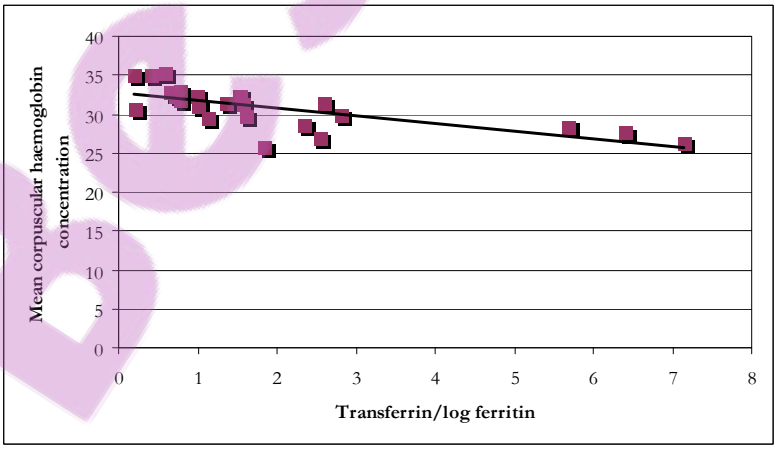

Figure 12.
Correlation between the transferrin/log ferritin ratio and the mean corpuscular haemoglobin concentration in the group of Kalafong patients with no iron transfer block (r-value = 0.69, p-value = 0.0003).

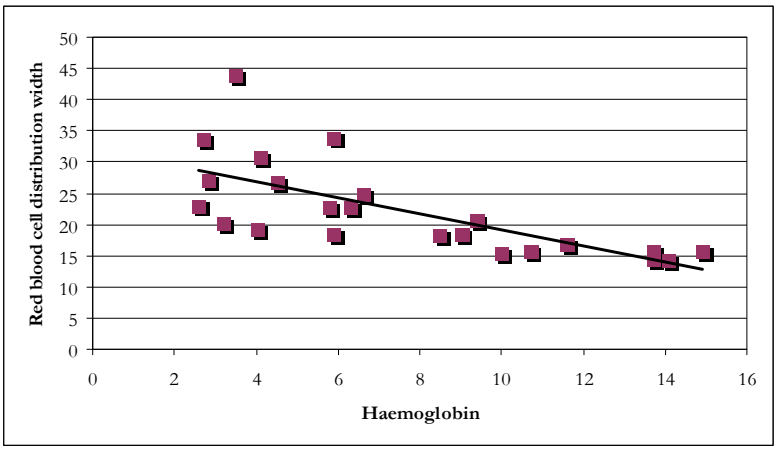

Figure 13.
Correlation between haemoglobin and the red blood cell distribution width in the group of Kalafong patients with no iron transfer block (r-value = 0.70, p-value = 0.0002).

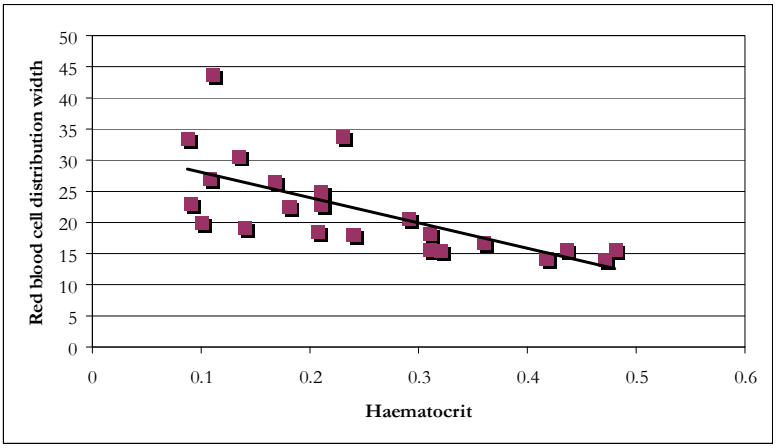

Figure 14.
Correlation between haematocrit and the red blood cell distribution width in the group of Kalafong patients with no iron transfer block (r-value = 0.68, p-value = 0.0003).

5.4) Correlations in the group of Kalafong patients with high C-reactive protein

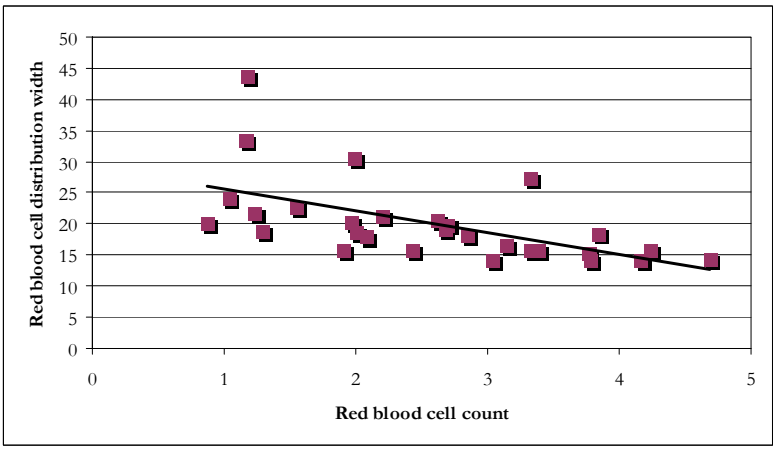

Figure 1.
Correlation between the red blood cell count and the red blood cell distribution width in the group of Kalafong patients with high CRP (r-value = 0.57, p-value = 0.001).

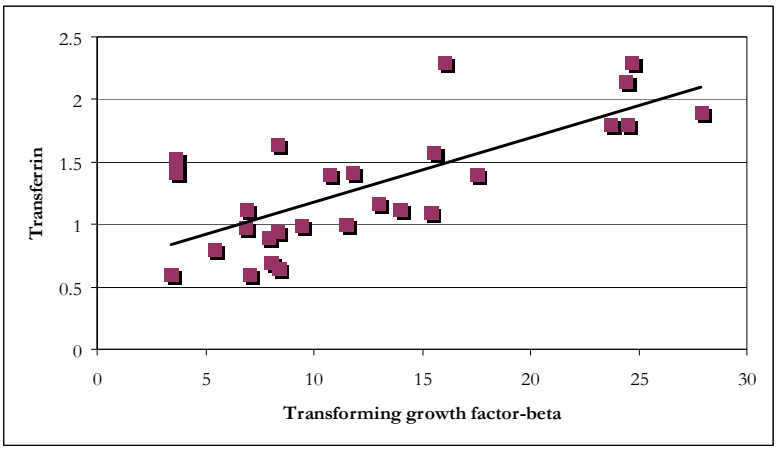

Figure 2.
Correlation between transforming growth factor-beta and transferrin in the group of Kalafong patients with high CRP (r-value = 0.73, p-value < 0.0001).

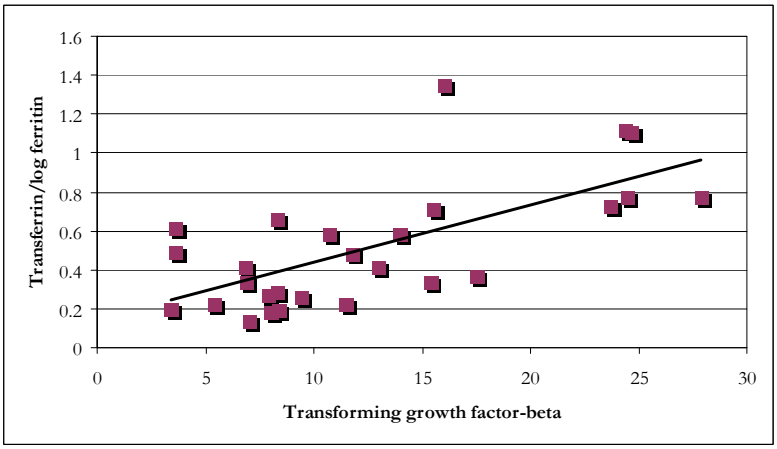

Figure 3.
Correlation between transforming growth factor-beta and the transferrin/log ferritin ratio in the group of Kalafong patients with high CRP (r-value = 0.67, p-value = 0.0001).

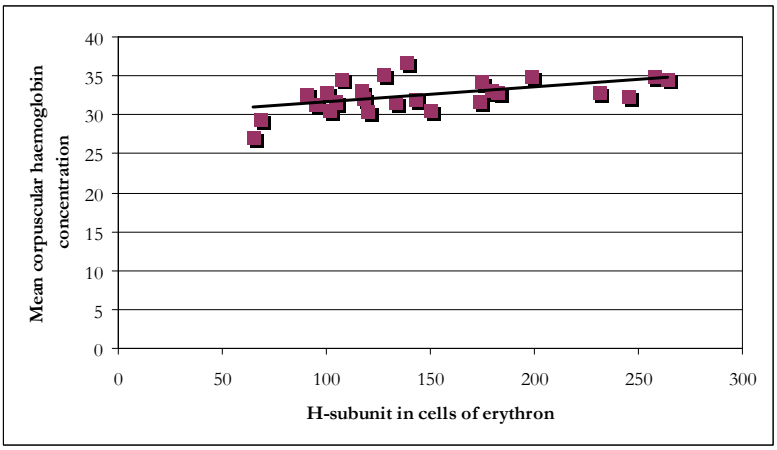

Figure 4.
Correlation between the H-subunit in cells of the erythron and the mean corpuscular haemoglobin concentration in the group of Kalafong patients with high CRP (r-value = 0.51, p-value = 0.007).

5.5) Correlations in the group of Kalafong patients with high neopterin

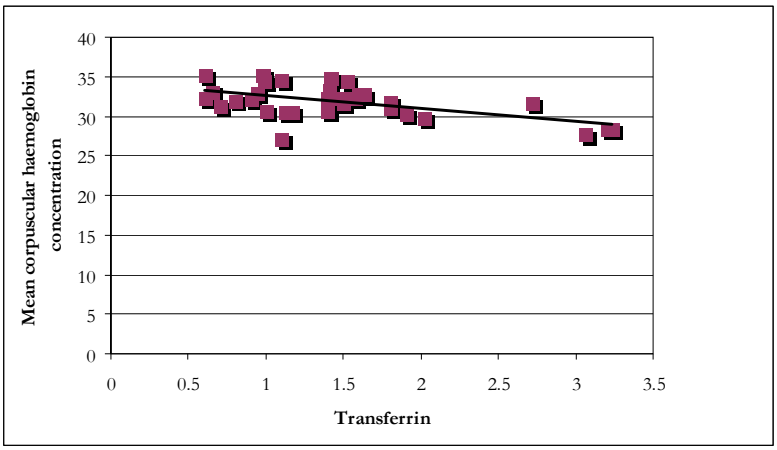

Figure 1.
Correlation between transferrin and the mean corpuscular haemoglobin concentration in the group of Kalafong patients with high neopterin (r-value = 0.56, p-value = 0.0006).

5.6) Correlations in the group of Kalafong patients with iron transfer block

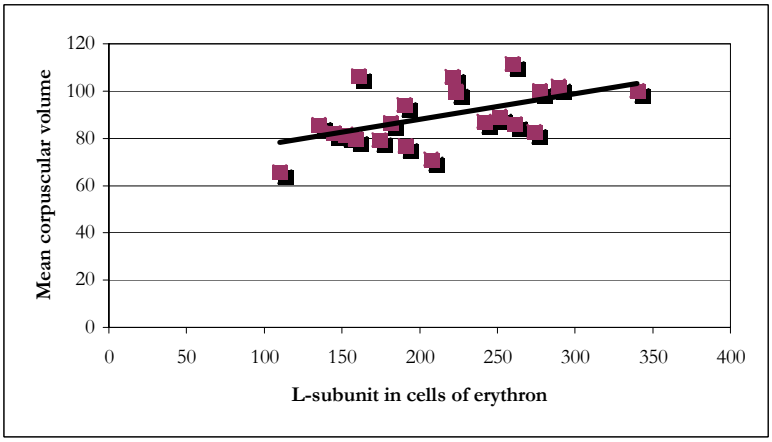

Figure 1.
Correlation between the L-subunit in cells of the erythron and the mean corpuscular volume in the group of Kalafong patients with iron transfer block (r-value = 0.53, p-value = 0.014).

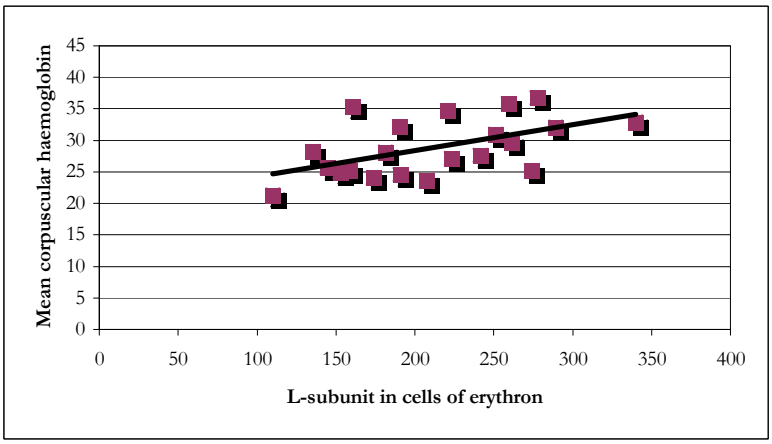

Figure 2.
Correlation between the L-subunit in cells of the erythron and the mean corpuscular haemoglobin in the group of Kalafong patients with iron transfer block (r-value = 0.53, p-value = 0.013).

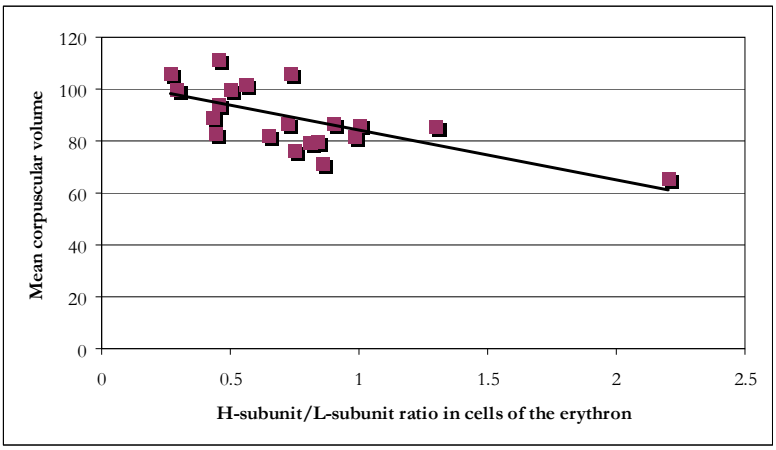

Figure 3.
Correlation between the H-subunit/L-subunit ratio in cells of the erythron and the mean corpuscular volume in the group of Kalafong patients with iron transfer block (r-value = 0.55, p-value = 0.008).

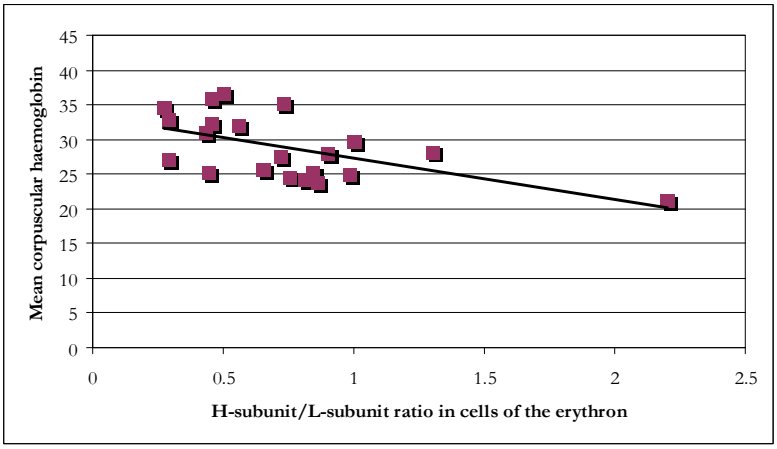

Figure 4.
Correlation between the H-subunit/L-subunit ratio in cells of the erythron and the mean corpuscular haemoglobin in the group of Kalafong patients with iron transfer block (r-value = 0.42, p-value = 0.049).

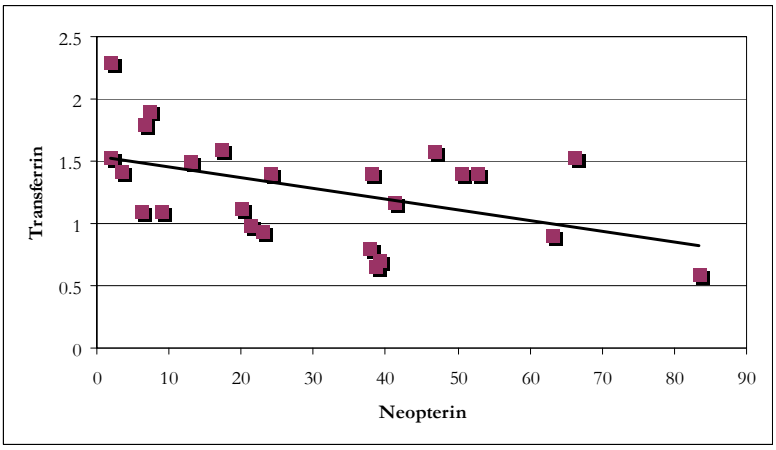

Figure 5.
Correlation between neopterin and transferrin in the group of Kalafong patients with iron transfer block (r-value = 0.47, p-value = 0.019).

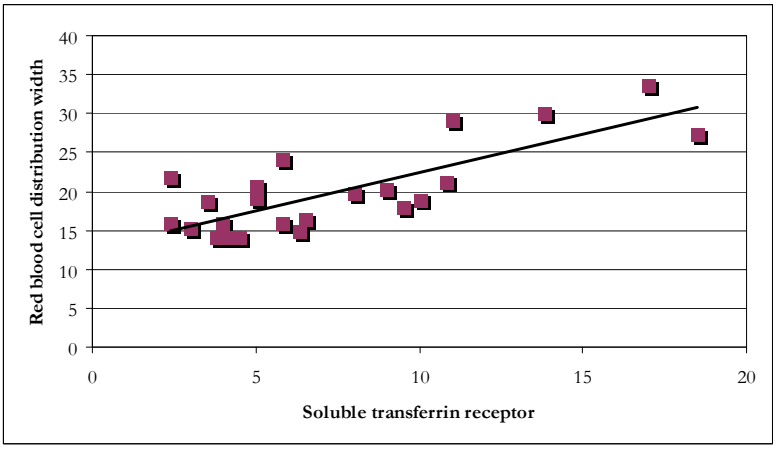

Figure 6.
Correlation between the soluble transferrin receptor and the red blood cell distribution width in the group of Kalafong patients with iron transfer block (r-value = 0.79, p-value < 0.0001).

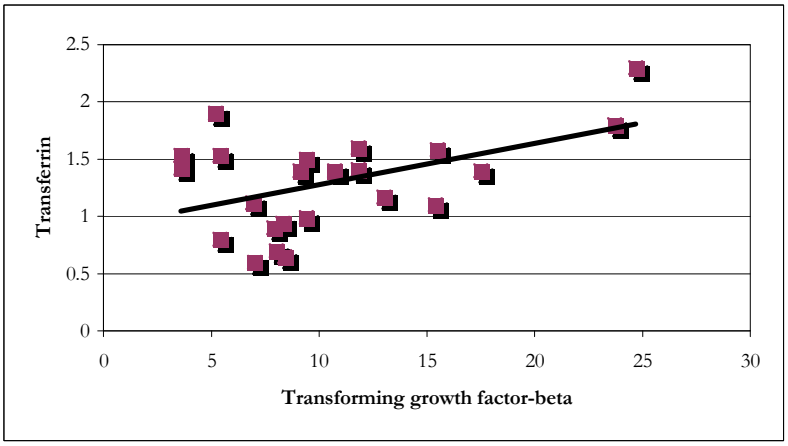

Figure 7.
Correlation between transforming growth factor-beta and transferrin in the group of Kalafong patients with iron transfer block (r-value = 0.48, p-value = 0.02).

5.7) Correlations in the group of osteoarthritis patients

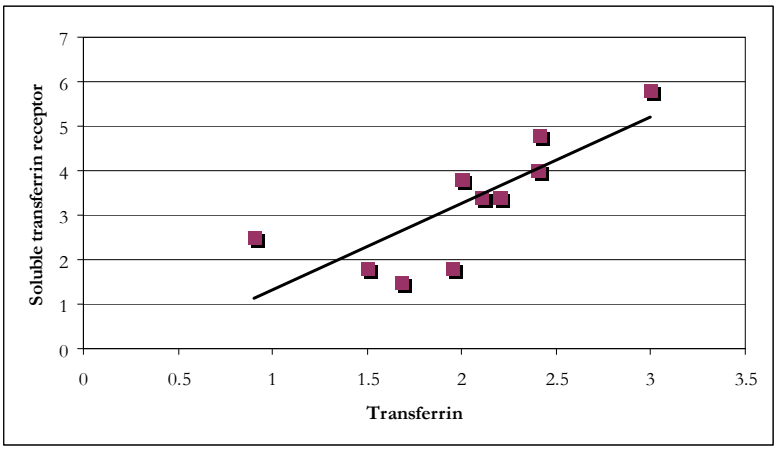

Figure 1.
Correlation between transferrin and the soluble transferrin receptor in the group of osteoarthritis patients (r-value = 0.79, p-value = 0.006).

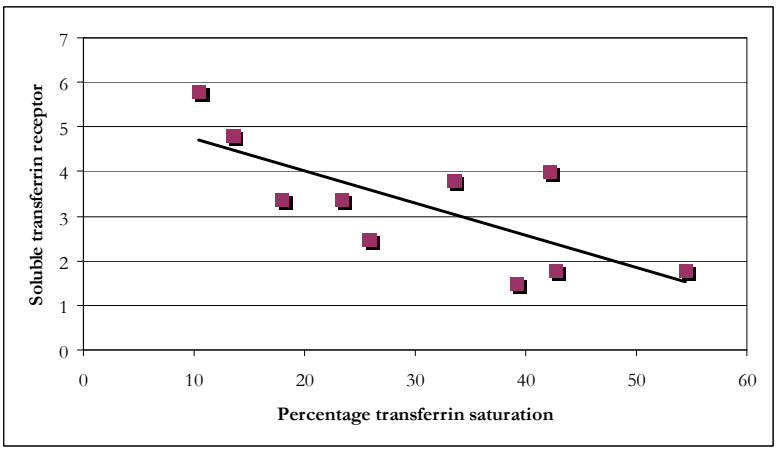

Figure 2.
Correlation between the percentage transferrin saturation and the soluble transferrin receptor in the group of osteoarthritis patients (r-value = 0.74, p-value = 0.014).

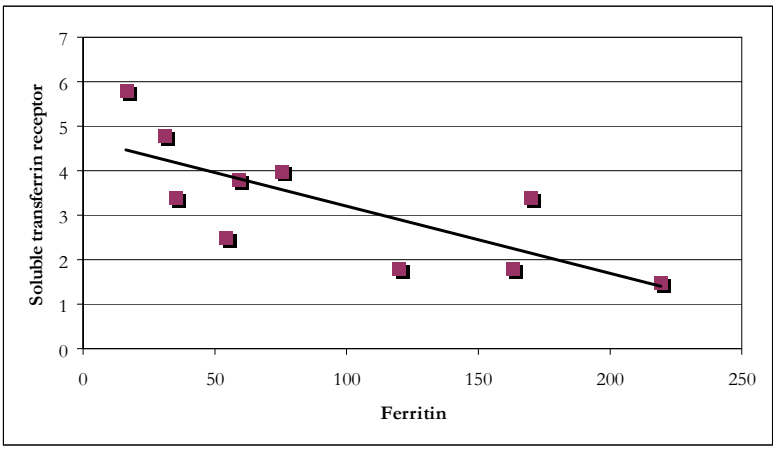

Figure 3.
Correlation between ferritin and the soluble transferrin receptor in the group of osteoarthritis patients (r-value = 0.75, p-value = 0.013).

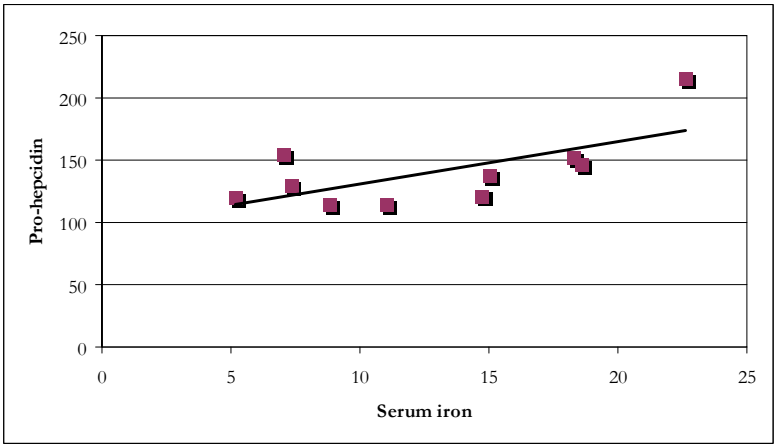

Figure 4.
Correlation between serum iron and pro-hepcidin in the group of osteoarthritis patients (r-value = 0.67, p-value = 0.034).

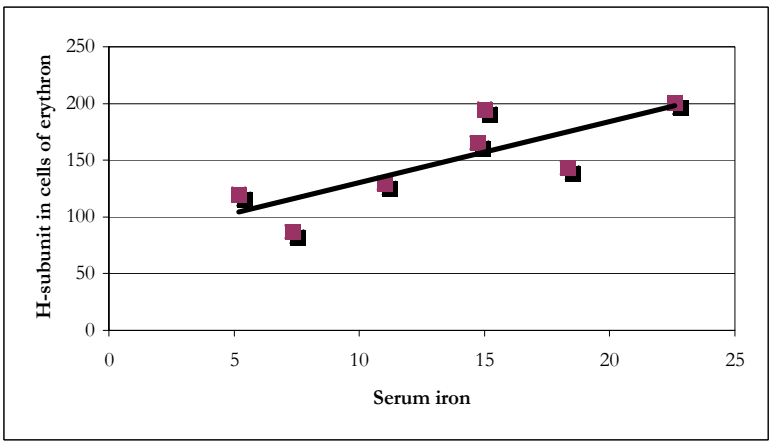

Figure 5.
Correlation between serum iron and the H-subunit in cells of the erythron in the group of osteoarthritis patients (r-value = 0.80, p-value = 0.031).

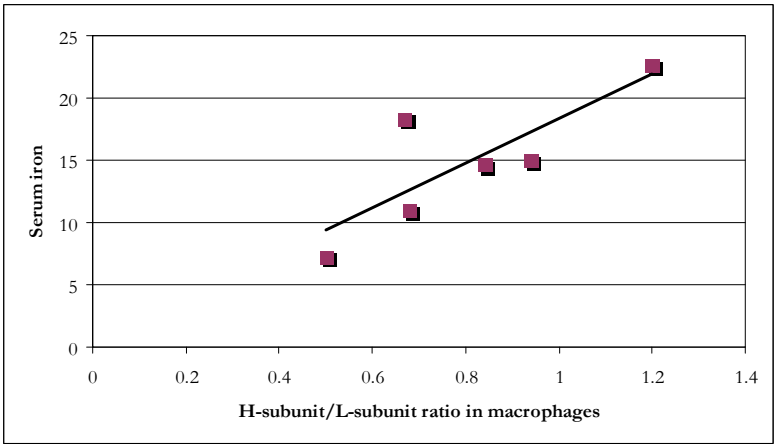

Figure 6.
Correlation between the H-subunit/L-subunit ratio in macrophages and serum iron in the group of osteoarthritis patients (r-value = 0.82, p-value = 0.047).

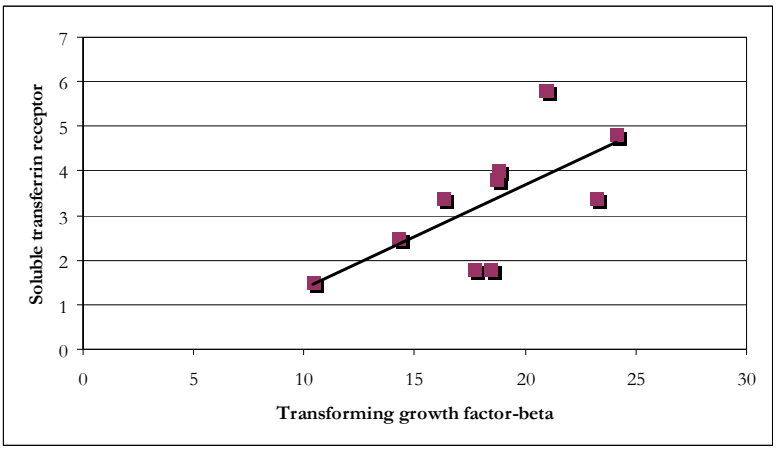

Figure 7.
Correlation between transforming growth factor-beta and the soluble transferrin receptor in the group of osteoarthritis patients (r-value = 0.67, p-value = 0.034).

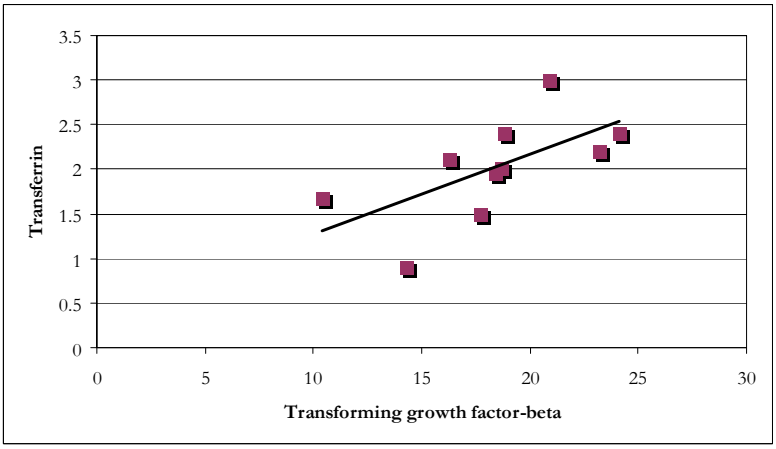

Figure 8.
Correlation between transforming growth factor-beta and transferrin in the group of osteoarthritis patients (r-value = 0.63, p-value = 0.05).

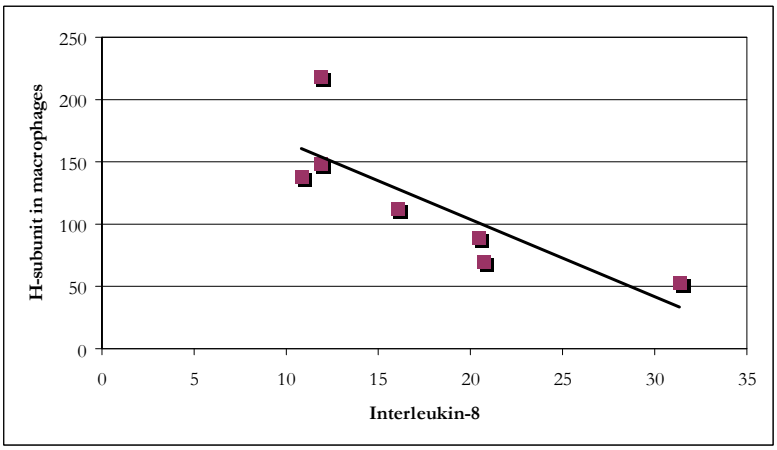

Figure 9.
Correlation between interleukin-8 and the H-subunit in macrophages in the group of osteoarthritis patients (r-value = 0.81, p-value = 0.026).

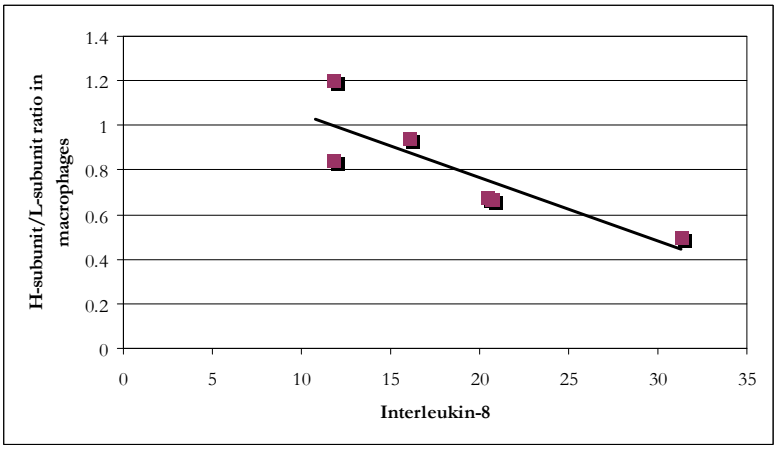

Figure 10.
Correlation between interleukin-8 and the H-subunit/L-subunit ratio in macrophages in the group of osteoarthritis patients (r-value = 0.84, p-value = 0.037).

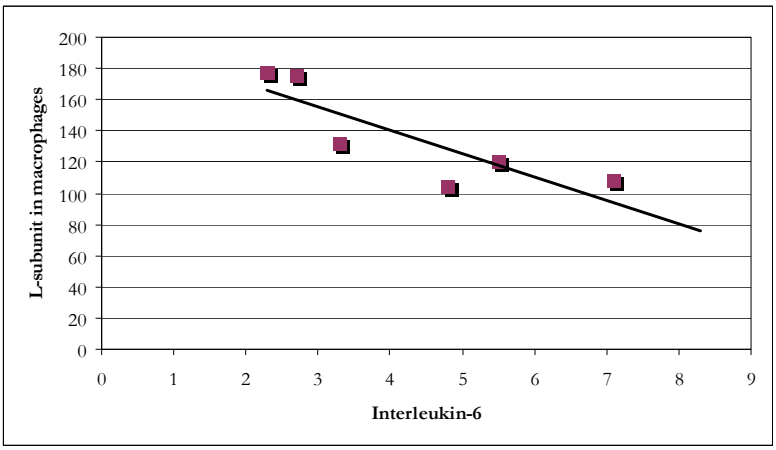

Figure 11.
Correlation between interleukin-6 and the L-subunit in macrophages in the group of osteoarthritis patients (r-value = 0.85, p-value = 0.034).

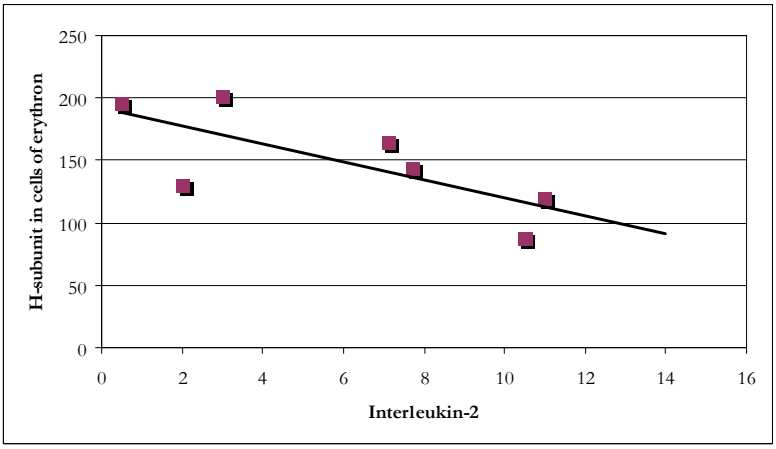

Figure 12.
Correlation between interleukin-2 and the H-subunit in cells of the erythron in the group of osteoarthritis patients (r-value = 0.73, p-value = 0.064).

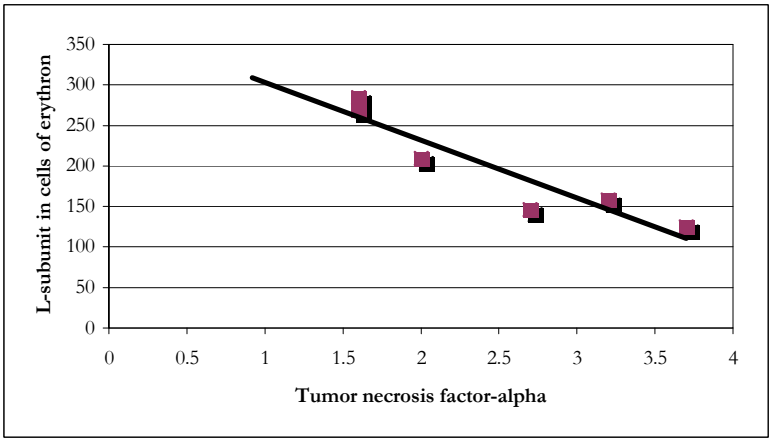

Figure 13.
Correlation between tumor necrosis factor-alpha and the L-subunit in cells of the erythron in the group of osteoarthritis patients (r-value = 0.94, p-value = 0.006).

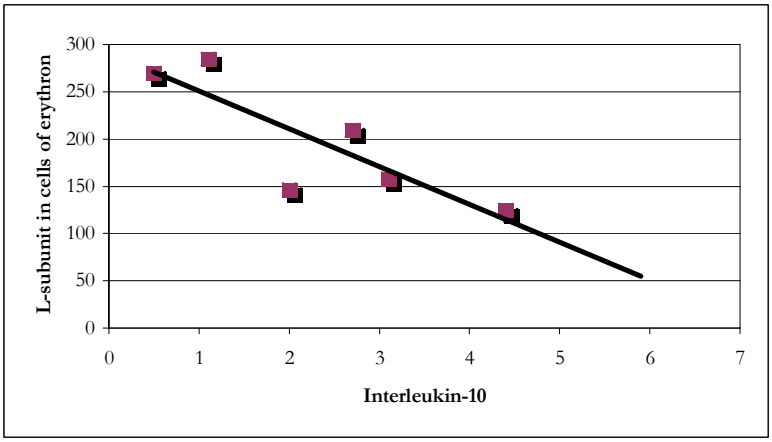

Figure 14.
Correlation between interleukin-10 and the L-subunit in cells of the erythron in the group of osteoarthritis patients (r-value = 0.85, p-value = 0.03).

Electron micrographs and raw data of immunolabelling of H-subunit and L-subunit of ferritin, photographs of the Prussian blue iron stains and the presence or absence of an iron transfer block are contained in volume 2, chapter 6.

CHAPTER 4

DISCUSSION

1) INTRODUCTION

Ferritin is the intracellular protein responsible for the sequestration, storage and release of iron. Ferritin can accumulate up to 4500 iron atoms as a ferrihydrite mineral in a protein shell and releases these iron atoms when there is an increase in the cell's need for bio-available iron (1). The ferritin protein shell consists of 24 protein subunits of two types, the H-subunit and the L-subunit. These ferritin subunits perform different functions in the mineralization process of iron (2). The ferritin protein shell can exist as various combinations of these two subunit types, giving rise to heteropolymers or isoferritins. Isoferritins are functionally distinct and it would appear that characteristic populations of isoferritins are found depending on the type of cell, the proliferation status of the cell and the presence of disease (3). The synthesis of ferritin is regulated both transcriptionally and translationally. Translation of ferritin subunit mRNA is increased or decreased, depending on the labile iron pool and is controlled by an iron-responsive element present in the 5'-untranslated region of the ferritin subunit mRNA (4). The transcription of the genes for the H-subunit and L-subunit of ferritin is controlled by hormones and cytokines, which can result in a change in the pool of translatable mRNA (5). The levels of intracellular ferritin are determined by the balance between synthesis and degradation. Degradation of ferritin in the cytosol results in complete release of iron, while degradation in secondary lysosomes results in the formation of haemosiderin and protection against iron toxicity (6). The majority of

ferritin is found in the cytosol. However, ferritin with slightly different properties can also be found in organelles such as nuclei and mitochondria (7, 8).

Most of the ferritin produced intracellularly is harnessed for the regulation of iron bio-availability, however some of the ferritin is secreted and internalized by other cells (9). In addition to the regulation of iron bio-availability ferritin may contribute to the control of myelopoiesis and immunological responses (10).

Plasma ferritin is increased as an acute phase protein during conditions of infection, inflammation and malignancies, but its expression is also up-regulated in the cytosol of various cells in conditions with uncontrolled cellular proliferation, in any condition marked by excessive production of toxic oxygen radicals, and by infectious and inflammatory processes (11). Under such conditions ferritin up-regulation is predominantly stimulated by increased reactive oxygen radical production and by cytokines (5, 12). The major function of ferritin in these conditions is to reduce the bio-availability of iron in order to stem uncontrolled cellular proliferation and excessive production of reactive oxygen radicals (13). Ferritin is, however, not indiscriminately up-regulated in these conditions as a marked shift towards a predominance in H-subunit rich ferritins would appear to occur (14, 15, 16, 17, 18, 19, 20, 21, 22).

In the present study ultrastructural immunolocalisation of the H-subunit and L-subunit of ferritin in different cells of the bone marrow was undertaken to quantitatively measure the expression of the subunits of ferritin at the single cell level. In this study the quantitative expression of the H-subunit and L-subunit of ferritin in bone marrow macrophages and cells of the erythron was ultrastructurally evaluated by post-embedding immunolocalisation with immunogold transmission electron microscopy in combination with the inflammatory status of patients with chronic immune stimulation.

2) EXPERIMENTAL GROUPS

Forty-eight patients attending the Department of Internal Medicine, Kalafong Hospital for treatment of chronic diseases, with a high prevalence of human immunodeficiency virus (HIV) infection were included in the study. Ten patients scheduled for hip replacement at the Department of Orthopaedics at the Pretoria Academic Hospital were included in the study as a group of patients with less severe immune stimulation. These patients were all diagnosed with osteoarthritis and were HIV-negative.

The diagnosis of the patients from Kalafong Hospital were diverse and included various types of infections (tuberculosis (TB), malaria, HIV), cancers (lung, breast), pancytopenias as a result of bone marrow suppression or peripheral destruction of blood cells, organ failures including renal failure, heart failure and liver failure, anaemias with different etiologies and various other pathologies that resulted in inflammatory reactions. This resulted in an extremely heterogenous group of patients. For the purpose of this study the immune status and iron status, respectively, were used to group these patients. The osteoarthritis patients were treated as a separate group.

3) AIM OF THE STUDY

The primary aim of the present study was to quantitatively measure the expression of the H-subunit and L-subunit of ferritin in the bone marrow macrophage and cells of the erythron in patients with chronic immune stimulation. A second aim was to investigate the possible role that the expression of the H-subunit and L-subunit of ferritin may have in the establishment and maintenance of an iron transfer block in patients with chronic immune stimulation.

The discussion will be presented in the following sections:

1) Subdivision of the patients according to their immune status.

2) Expression of the H-subunit and L-subunit of ferritin in the bone marrow macrophage and cells of the erythron in patients with a pro-inflammatory immune status.

3) Prevalence of the iron transfer block in patients with a pro-inflammatory immune status.

4) Expression of the H-subunit and L-subunit of ferritin in a group of Kalafong patients with iron transfer block.

5) Expression of the H-subunit and L-subunit of ferritin in the group of osteoarthritis patients.

4) SUBDIVISION OF THE PATIENTS ACCORDING TO THEIR IMMUNE STATUS

In order to investigate the expression of the H-subunit and L-subunit of ferritin it was necessary to subdivide the patients in groups according to their immune status. The immune status is determined to a major extent by cytokines and it has been shown that certain cytokines can influence the expression of the H-subunits and L-subunits to different extents. Patients were subdivided according to their immune status based firstly on C-reactive protein levels and secondly based on neopterin levels. In order to validate the subdivisions in terms of C-reactive protein and neopterin and to investigate more specifically the cytokines that may contribute to changes in the expression of the H-subunit and L-subunit of ferritin the cytokine profiles of these patients were determined.

4.1) C-reactive protein as an indicator of immune stimulation

C-reactive protein is an acute phase protein and rises sharply with the onset of inflammation reaching peak concentrations within 24-48 hours. Inflammatory processes accompanying tissue injury, infection, malignancy, autoimmune diseases and cardiovascular diseases can all result in an increase in C-reactive protein levels (23). Not

only does C-reactive protein correlate with the progression of the inflammatory process but C-reactive protein also reflects the resolution of inflammation. C-reactive protein is synthesised and secreted by hepatocytes upon stimulation by acute phase protein-inducing cytokines such as interleukin-6 (Il-6) (24). C-reactive protein is a pattern recognition molecule and binds to specific molecular configurations that are typically exposed during cell death or found on the surfaces of pathogens (25). By binding to the molecules exposed with cell death C-reactive protein increases the clearance of apoptotic cells. C-reactive protein binds to the stimulatory receptors, FcgammaRI and FcgammaRII, increasing phagocytosis and the release of inflammatory cytokines. In addition, C-reactive protein binds to the inhibitory receptor FcgammaRIIb, blocking activating signals (26). C-reactive protein is therefore clearly not only a by-stander molecule during inflammation but actively takes part in pro-inflammatory, as well as anti-inflammatory, processes. C-reactive protein levels are seen by some as the most accurate reflection of the inflammatory state.

In the present study, in order to subdivide the Kalafong patients into groups, C-reactive protein was determined as an overall indicator of the inflammatory status. A value of 10 mg/l and less was taken as normal C-reactive protein levels, whereas a value of more than 10 mg/l as elevated C-reactive protein levels. For the group of Kalafong patients (n = 19) with normal C-reactive protein the mean and SD was 2.8 ± 2.8 mg/l, whereas for the group of Kalafong patients (n = 29) with elevated C-reactive protein the mean and SD was 82.2 ± 76.2 mg/l. The mean and SD for C-reactive protein for the osteoarthritis group was 3.4 ± 5.1 mg/l (n = 10). The C-reactive protein was significantly higher (p-value < 0.0001) in the group of Kalafong patients with elevated C-reactive protein than in the group of osteoarthritis patients. There was no significant difference between the group of Kalafong patients with normal C-reactive protein and the osteoarthritis patients.

This subdivision of the Kalafong patients clearly showed a group of patients with increased C-reactive protein and a group with normal C-reactive protein. The group of osteoarthritis patients showed C-reactive protein levels similar to that of the group of Kalafong patients with normal C-reactive protein levels.

An increase in C-reactive protein is seen as an indicator of the involvement of the classically activated macrophage (pro-inflammatory macrophage) in the orchestration of the immune reponse. In the group of Kalafong patients with elevated C-reactive protein, the macrophage takes on a pro-inflammatory role, which is characteristic of a T-helper cell type-1 immune response.

Not all Kalafong patients with elevated C-reactive protein necessarily had elevated neopterin and *vice versa*. However, the group of Kalafong patients with elevated C-reactive protein showed a significantly higher level for neopterin (p-value = 0.0002), (29.5 ± 24.8 ng/ml; n = 29) than the group of Kalafong patients with normal C-reactive protein (7.7 ± 11.7 ng/ml; n = 19). Compared to the osteoarthritis patients (2.2 ± 0.52 ng/ml; n = 10), both the group of Kalafong patients with elevated C-reactive protein (p-value < 0.0001) and the group of Kalafong patients with normal C-reactive protein (p-value = 0.017) showed significantly higher neopterin levels.

4.2) Neopterin as an indicator of immune stimulation

The group of Kalafong patients were subsequently subdivided according to another immunological indicator namely neopterin. Neopterin is synthesised by macrophages upon stimulation with the T-helper cell type-1 secretory product, interferon-γ (INF-γ). Consequently, neopterin has thus been used as a measure of both macrophage activity and cell-mediated immunity. In the pro-inflammatory macrophage neopterin is produced from guanosine triphosphate (GTP). Activation of GTP cyclohydrolase I

results in an accumulation of 7,8-dihydroneopterin triphosphate, followed by the conversion of 7,8-dihydroneopterin triphosphate to neopterin and 7,8-dihydroneopterin by phosphatases (27). The rate of rise of neopterin is slower than that for C-reactive protein, peaking at 9-12 days after contraction of viral infection. Although IFN-γ is the major cytokine responsible for neopterin production (28), IFN-γ mediated neopterin production can be superinduced by lipopolysaccharide (LPS) and tumor necrosis factor-α (TNF-α) (27). Various other cytokines such as interleukin-2 (Il-2) which are able to induce IFN-γ release from T-helper cell type-1 cells can also provoke neopterin release (27). Furthermore, increasing the number of monocytes/macrophages by administration of granulocyte macrophage-colony stimulating factor (GM-CSF) also results in increased neopterin production (27). However, it has also been shown that IFN-γ is not essential for neopterin production. For instance, patients suffering from Mendelian susceptibility to mycobacterial disease (MSMD), characterised by impaired or absent IFN-γ production or function, show neopterin production when challenged by mycobacterium (29).

Neopterin production does not only indicate macrophage activation, but neopterin levels are also shown to correlate with the degree of macrophage activation. Therefore, neopterin levels in plasma can be employed to monitor the magnitude of cellular immune activation/involvement during an immune response (27). When cell-mediated immunity dominates, high neopterin levels will be present and when humoral immunity takes the lead, neopterin levels will be low (27). *In vivo* increased neopterin production was demonstrated in patients suffering from infections with viruses and intracellular bacterial or protozoal pathogens, in patients with rheumatoid arthritis, systemic lupus erythromatosus and in patients with acute cellular graft rejection or graft-versus-host disease (28).

In the present study neopterin was determined in order to indicate the involvement of cell-mediated immunity orchestrated by the classically activated macrophage (pro-inflammatory macrophage). In this study a value of less than 3.4 ng/ml was taken as normal neopterin and a value equal to and more than 3.4 ng/ml as elevated neopterin. This resulted in a group of 13 Kalafong patients with normal neopterin (2.2 ± 0.47 ng/ml) and a group of 35 Kalafong patients with elevated neopterin (27.9 ± 23.5 ng/ml). For the osteoarthritis patients neopterin was 2.2 ± 0.52 ng/ml (n = 10). The neopterin values were significantly higher (p-value < 0.0001) in the group of Kalafong patients with elevated neopterin than in the group of osteoarthritis patients. There was no significant difference for neopterin between the osteoarthritis patients and the group of Kalafong patients with normal neopterin.

As for the C-reactive protein subdivision, the subdivision of the Kalafong patients based on neopterin clearly showed a group of patients with increased neopterin and a group with normal neopterin. The group of osteoarthritis patients showed neopterin levels similar to that of the group of Kalafong patients with normal neopterin.

The group of Kalafong patients with elevated neopterin showed a significantly higher level for C-reactive protein (p-value = 0.001), (64.7 ± 77.2 mg/l; n = 35) than the group of Kalafong patients with normal neopterin (13.1 ± 24.4 mg/l; n = 13). Compared to the osteoarthritis patients (3.4 ± 5.1 mg/l; n = 10), only the group of Kalafong patients with elevated neopterin showed a significantly increased C-reactive protein (p-value < 0.0001).

C-reactive protein and neopterin correlated positively for the Kalafong patients (r = 0.48, p-value = 0.0006). However, not all Kalafong patients with elevated C-reactive protein necessarily had elevated neopterin and *vice versa*. Specific disease types show characteristic elevations in C-reactive protein and/or neopterin (25, 28, 30). Therefore,

depending on the type and stage of immune/inflammatory process and resolution thereoff, C-reactive protein and neopterin might be elevated to different extents and may be cleared at different time-points. Consequently, it was considered feasible to continue the investigation based on both the subdivision according to C-reactive protein and the subdivision according to neopterin. For the rest of the discussion reference will often be made to groups with elevated or normal C-reactive protein and groups with elevated or normal neopterin with the understanding that the reference is made to subdivisions according to C-reactive protein and neopterin and that there are overlapping in patients between the groups.

5) THE CYTOKINE RESPONSE OF PATIENTS WITH ELEVATED C-REACTIVE PROTEIN AND PATIENTS WITH ELEVATED NEOPTERIN

In order to validate the subdivision according to C-reactive protein and neopterin and to investigate more specifically the cytokines that may contribute to changes in the expression of the H-subunit and L-subunit of ferritin, cytokine profiles of these patients were determined. The cytokines investigated included interferon-γ (INF-γ), tumor necrosis factor-α (TNF-α), interleukin-1β (Il-1β), interleukin-6 (Il-6), interleukin-12 (Il-12), interleukin-2 (Il-2), interleukin-8 (Il-8), granulocyte macrophage-colony stimulating factor (GM-CSF), interleukin-4 (Il-4), interleukin-5 (Il-5), transforming growth factor-β (TGF-β) and interleukin-10 (Il-10).

5.1) Background

Macrophage activation has many phenotypes during an immune response. These macrophage phenotypes can be classified into three major types of activated macrophages, each with distinguishable, but also some overlapping functions. These different macrophage phenotypes are sequentially encountered during an immune

response. During the first phase of an immune response the macrophage (type-1 activated macrophage – classically activated macrophage) takes on a pro-inflammatory role. The function of the type-1 activated macrophage is as an effector cell in T-helper cell type-1 cellular immune responses. The type-2 activated macrophage is anti-inflammatory and preferentially induces T-helper cell type-2 humoral immune responses to antigen. The third type of activated macrophage, the alternatively activated macrophage appears to be involved in immunosuppression and tissue repair in the last phase of the immune response (31, 32, 33). The magnitude and duration of each of these phases of an immune response, orchestrated by one of the three types of activated macrophages, depend on the complexity of the signalling pattern encountered by the macrophage. Signal complexity depends on the type, combination and quantity of stimuli (such as cytokines) and the temporal sequence in which the stimuli (such as cytokines) are presented to the macrophage (34).

The activating signals for the classically activated macrophage (type-1 activated macrophage) include INF-γ, TNF-α and Il-2 with the secretory products TNF-α, Il-12, Il-1β, Il-6 and Il-8 (31, 34, 35). IFN-γ is the cytokine of major importance in the classical activation of the macrophage. IFN-γ has been shown to augment the activation of macrophages in response to bacterial products, such as LPS, pro-inflammatory cytokines including TNF-α, Il-1β and Il-12, or activated T-lymphocytes through the CD40 ligand (36). When the macrophage is activated by one of these stimuli without IFN-γ being present, the absolute amount of cytokines and toxic nitrogen radicals released are many-fold lower than for macrophages that have been exposed to activating stimuli with IFN-γ (36). Il-6 tends to be more of a secondary mediator, fundamental for the acute phase response in the liver and has a regulatory function in the immune response (35). The chemokine, Il-8, is responsible for the recruitment of leukocytes such as the neutrophil to the inflammatory site (37).

The activating signals for the type-2 activated macrophage include IgG complexes and Toll-like receptor (TLR) ligation with the secretory products Il-10, TNF-α and Il-6. The activating signals for the alternatively activated macrophage include Il-4, TGF-β and glucocorticoids with the secretory products Il-1 receptor antagonist (Il-1RA) and Il-10 (31). The T-helper cell type-2 cytokines Il-4, Il-10 and transforming growth factor-β (TGF-β) induces type-2 macrophage phenotypes. Type-2 macrophages are not simply deactivated macrophages but are macrophages that display anti-inflammatory properties together with the ability to bring about a more mature type-2 immune response characterised by up-regulated humoral activities. Therefore, none of these T-helper cell type-2 cytokines can be categorised as purely macrophage deactivating since they also need to exert macrophage-activating effects in order for the macrophage to orchestrate a type-2 immune response (38). T-helper cell type-2 activated macrophages show enhanced capacity for antigen presentation and enhanced phagocytosis of debris and particles, but not to pathogens. Furthermore, the T-helper cell type-2 activated macrophage generates anti-inflammatory cytokines, suppresses the synthesis of pro-inflammatory cytokines and is resistant to re-activation (36). Both Il-10 and TGF-β are shown to reduce the potential for inflammation in the local microenvironment, down-regulate ongoing inflammation and polarize adaptive immunity towards anti-inflammatory and/or humoral responses (39). TGF-β, Il-4 and Il-10 deactivate macrophages in numerous ways including indirectly by suppression of T-cell proliferation and/or directly by decreasing IFN-γ production. Furthermore, they can each induce antagonists of cytokines released by macrophages such as Il-2 receptor antagonist. Il-4 preferentially stimulates type-2 T-helper cells in an autocrine function. These type-2 T-helper cells produce Il-10 a potent inhibitor of monocyte/macrophage-dependent IFN-γ production by type-1 T-helper cells, cytotoxic T-cells and natural killer cells. TGF-β and Il-4 also suppress IFN-γ production by T-lymphocytes, human blood

mononuclear cells, or natural killer cells (38). Not only does these type-2 cytokines bring about alternatively activated macrophages during an immune response, but can also cause naïve macrophages to become resistant to type-1 cytokine exposure and the attainment of a pro-inflammatory status. When naïve macrophages are exposed to T-helper cell type-2 lymphokines such as Il-4 or TGF-β, cytokines Il-10 and Il-13 and glucocorticoids, the macrophage does not attain the classically activated (pro-inflammatory) phenotype, even when such macrophages are challenged with pro-inflammatory cytokines (36). These T-helper cell type-2 cytokines can all suppress nitric oxide (NO) production by various mechanisms including inducible nitric oxide synthase (iNOS) down-regulation and a decrease in iNOS substrate availability (40).

TGF-β is a potent anti-inflammatory cytokine, which plays a central role in the resolution of inflammation and tissue repair. It has been shown that TGF-β production can be stimulated early in the inflammatory response (41). TGF-β is the most potent inhibitor of the iNOS pathway and generation of NO. TGF-β has been shown to inhibit the synthesis of the iNOS protein and to destabilize iNOS mRNA (40). Furthermore, TGF-β suppresses the production of pro-inflammatory cytokines by macrophages including Il-8, GM-CSF and TNF-α (41, 42). TGF-β appears to be further involved in the reparative phase of inflammation due to its ability to stimulate formation of matrix components by fibroblasts. This enhanced production of matrix proteins coupled with the unique ability of TGF-β to both inhibit matrix-degrading enzymes and increase the secretion of protease inhibitors results in a pronounced pro-fibrotic influence of TGF-β (43).

5.2) Cytokine profiles of the Kalafong and osteoarthritis patients

The cytokines are presented in groups in the following order. Firstly, cytokines involved in the pro-inflammatory immune state, followed by the cytokines mostly involved in an alternative T-helper cell type-2 driven immune reaction (predominantly anti-inflammatory) and lastly, the cytokines most probably involved in the resolution of the immune response and tissue repair.

5.2.1) Cytokine levels in patients with elevated C-reactive protein, patients with normal C-reactive protein and osteoarthritis patients

Specific cytokines determine the production of C-reactive protein and others are raised concomitantly, but independently. Various cytokines both pro-inflammatory and anti-inflammatory were determined in the patients. As shown below, significant differences for the pro-inflammatory cytokines were found between the group of Kalafong patients with elevated C-reactive protein levels and the group of Kalafong patients with normal C-reactive protein levels, while the osteoarthritis group's pro-inflammatory cytokines largely corresponded with that of the group of Kalafong patients with normal C-reactive protein.

Pro-inflammatory cytokines

INF-γ was

- significantly higher (p-value = 0.0008) in the group of Kalafong patients with elevated C-reactive protein (25.6 ± 73.8 pg/ml; n = 28) compared to the group of Kalafong patients with normal C-reactive protein (1 ± 2.6 pg/ml; n = 19),
- significantly higher (p-value = 0.0008) in the group of Kalafong patients with elevated C-reactive protein compared to the osteoarthritis patients (0.1 ± 0 pg/ml; n = 10) and

- not significantly different between the group of Kalafong patients with normal C-reactive protein and the osteoarthritis patients.

Similar to INF-γ, TNF-α was also

- significantly higher (p-value = 0.007) in the group of Kalafong patients with elevated C-reactive protein (4.1 ± 2.9 pg/ml; n = 29) compared to the group of Kalafong patients with normal C-reactive protein (2.5 ± 0.97 pg/ml; n = 19),
- significantly higher (p-value = 0.014) in the group of Kalafong patients with elevated C-reactive protein compared to the osteoarthritis patients (2.5 ± 0.96 pg/ml; n = 10) and
- not significantly different between the group of Kalafong patients with normal C-reactive protein and the osteoarthritis patients.

Furthermore, the pro-inflammatory secretory product Il-1β was

- significantly higher (p-value = 0.013) in the group of Kalafong patients with elevated C-reactive protein (6.5 ± 10.3 pg/ml; n = 29) compared to the group of Kalafong patients with normal C-reactive protein (1.3 ± 2.3 pg/ml; n = 19),
- significantly higher (p-value = 0.029) in the group of Kalafong patients with elevated C-reactive protein compared to the osteoarthritis patients (1.6 ± 3.3 pg/ml; n = 10) and
- not significantly different between the group of Kalafong patients with normal C-reactive protein and the osteoarthritis patients.

Another of the pro-inflammatory secretory products, Il-6, was

- significantly higher (p-value < 0.0001) in the group of Kalafong patients with elevated C-reactive protein (807.6 ± 2384.6 pg/ml; n = 29) compared to the

group of Kalafong patients with normal C-reactive protein (7.2 ± 12.6 pg/ml; n = 19),

- significantly higher (p-value < 0.0001) in the group of Kalafong patients with elevated C-reactive protein compared to the osteoarthritis patients (5 ± 2.1 pg/ml; n = 10) and
- not significantly different between the group of Kalafong patients with normal C-reactive protein and the osteoarthritis patients.

The only pro-inflammatory secretory product not higher in the group of Kalafong patients with elevated C-reactive protein compared to the group of Kalafong patients with normal C-reactive protein was Il-12. However, the osteoarthritis patients differed from both the groups of Kalafong patients. Il-12 was

- not significantly different between the group of Kalafong patients with elevated C-reactive protein (4.6 ± 4 pg/ml; n = 29) and the group of Kalafong patients with normal C-reactive protein (4.7 ± 3.8 pg/ml; n = 19) and
- significantly higher in both the group of Kalafong patients with elevated C-reactive protein (p-value = 0.0001) and the group of Kalafong patients with normal C-reactive protein (p-value = 0.001) compared to the osteoarthritis patients (1.1 ± 1.3 pg/ml; n = 10).

The above may perhaps be explained by the reduced concentration of CD4 cells present in the group of Kalafong patients with elevated C-reactive protein, since Il-12 is produced by T-helper cell type-1 lymphocytes. The CD4 count was marginally lower (p-value = 0.072) in the group of Kalafong patients with elevated C-reactive protein (293 ± 397.7 x 10^6/l; n = 20) compared to the group of Kalafong patients with normal C-reactive protein (449.3 ± 664.9 x 10^6/l; n = 10). However, the CD4 counts were not

determined in all patients that were HIV-negative. If the CD4 counts of these patients were included the group of Kalafong patients with normal C-reactive protein are very likely to have had a higher mean CD4 count. Normal ranges for CD4 counts are 500-2010 x 10^6/l.

In addition, Il-2 was

- not significantly different between the group of Kalafong patients with elevated C-reactive protein (10.7 ± 6.3 pg/ml; n = 29) and the group of Kalafong patients with normal C-reactive protein (9.9 ± 8.2 pg/ml; n = 19),
- marginaly higher (p-value = 0.051) in the group of Kalafong patients with elevated C-reactive protein compared to the osteoarthritis patients (6.7 ± 4.9 pg/ml; n = 10) and
- not significantly different between the group of Kalafong patients with normal C-reactive protein and the osteoarthritis patients.

The finding of no significant difference between the group of Kalafong patients with elevated C-reactive protein and the group of Kalafong patients with normal C-reactive protein for Il-2 is also possibly accounted for by the low CD4 counts in the group of Kalafong patients with elevated C-reactive protein.

The chemokine Il-8 was

- significantly higher (p-value < 0.0001) in the group of Kalafong patients with elevated C-reactive protein (334.6 ± 845.2 pg/ml; n = 29) compared to the group of Kalafong patients with normal C-reactive protein (20.1 ± 19.9 pg/ml; n = 19),

- significantly higher (p-value = 0.0009) in the group of Kalafong patients with elevated C-reactive protein compared to the osteoarthritis patients (18.9 ± 6.4 pg/ml; n = 10) and
- not significantly different between the group of Kalafong patients with normal C-reactive protein and the osteoarthritis patients.

In the present study GM-CSF was

- not significantly different between the group of Kalafong patients with elevated C-reactive protein (6.1 ± 9.4 pg/ml; n = 28), the group of Kalafong patients with normal C-reactive protein (23.4 ± 55.5 pg/ml; n = 19) and the osteoarthritis patients (3.6 ± 6.2 pg/ml; n = 10).

GM-CSF is a hemopoietic cytokine involved in differentiation and activation of cells in the myeloid compartment (44). GM-CSF was originally defined by its ability to generate *in vitro* granulocyte and macrophage colonies from bone marrow precursor cells. It now appears more likely that its major role lies in its ability to govern the properties of the more mature myeloid cells of the granulocyte and macrophage lineages, particularly during host defence and inflammatory reactions (45). As it was previously shown that GM-CSF could contribute to inflammation through recruitment, increased survival and/or priming of monocytes/macrophages for activation (45), GM-CSF was determined in this study. However, no differences were seen between any of the groups.

T-helper cell type-2 cytokines

The T-helper cell type-2 (predominantly anti-inflammatory) cytokines are involved during the later phase of an immune response. These cytokines were evaluated for the groups of patients. As shown below, and in contrast to the findings on pro-inflammatory cytokines, the level of only Il-10 was marginally higher in the group of

Kalafong patients with elevated C-reactive protein compared to the group of Kalafong patients with normal C-reactive protein.

Il-4 was

- not significantly different between the group of Kalafong patients with elevated C-reactive protein (2.5 ± 1.8 pg/ml; n = 29), the group of Kalafong patients with normal C-reactive protein (2.4 ± 2.2 pg/ml; n = 19) and the osteoarthritis patients (2.5 ± 2.2 pg/ml; n = 10).

Il-5 was

- not significantly different between the group of Kalafong patients with elevated C-reactive protein (2.8 ± 1.5 pg/ml; n = 29), the group of Kalafong patients with normal C-reactive protein (4.1 ± 5 pg/ml; n = 19) and the osteoarthritis patients (2.4 ± 1.6 pg/ml; n = 10).

TGF-β was

- not significantly different between the group of Kalafong patients with elevated C-reactive protein (12.4 ± 7.1 ng/ml; n = 28) and the group of Kalafong patients with normal C-reactive protein (10.5 ± 7.1 ng/ml; n = 19),
- significantly lower (p-value = 0.003) in the group of Kalafong patients with elevated C-reactive protein compared to the osteoarthritis patients (18.3 ± 4.1 ng/ml; n = 10) and
- significantly lower (p-value = 0.0007) in the group of Kalafong patients with normal C-reactive protein compared to the osteoarthritis patients.

Il-10 was

- marginally higher (p-value = 0.059) in the group of Kalafong patients with elevated C-reactive protein (28.1 ± 61.6 pg/ml; n = 29) compared to the group of Kalafong patients with normal C-reactive protein (5.6 ± 3.3 pg/ml; n = 19),
- significantly higher (p-value = 0.035) in the group of Kalafong patients with elevated C-reactive protein compared to the osteoarthritis patients (2.7 ± 1.5 pg/ml; n = 10) and
- significantly higher (p-value = 0.004) in the group of Kalafong patients with normal C-reactive protein compared to the osteoarthritis patients.

In the present study there were no significant differences for the T-helper cell type-2 cytokines Il-4 and Il-5 between the group of Kalafong patients with elevated C-reactive protein and the group of Kalafong patients with normal C-reactive protein. However, the T-helper cell type-2 cytokine, Il-10, was increased in the group of Kalafong patients with elevated C-reactive protein compared to the group of Kalafong patients with normal C-reactive protein. In addition, TGF-β was not significantly different between the group of Kalafong patients with elevated C-reactive protein and the group of Kalafong patients with normal C-reactive protein.

In summary on the cytokine profiles of the C-reactive protein subdivision

The above cytokine results confirm the presence of a pro-inflammatory immune state in the group of Kalafong patients with elevated C-reactive protein levels. This was shown by the increase in various pro-inflammatory cytokines including INF-γ, TNF-α, Il-1β, Il-6 and Il-8. Nevertheless, Il-2 and Il-12 were not significantly different between the group of Kalafong patients with elevated C-reactive protein and the group of Kalafong patients with normal C-reactive protein. These cytokines are both produced by T-helper

type-1 cells (CD4 cells). A lower CD4 count than that of normal was shown in the group of Kalafong patients with elevated C-reactive protein. A decrease in CD4 cells would result in the production of less Il-2 and Il-12. With a pro-inflammatory immune state it would be expected that the T-helper cell type-2 cytokines involved in predominantly anti-inflammatory processes will not be increased. The T-helper cell type-2 cytokines, Il-4, Il-5 and TGF-β, were not significantly different between the group of Kalafong patients with elevated C-reactive protein and the group of Kalafong patients with normal C-reactive protein. However, the T-helper cell type-2 cytokine, Il-10, was marginally higher in the group of Kalafong patients with elevated C-reactive protein compared to the group of Kalafong patients with normal C-reactive protein.

5.2.2) Cytokine levels in patients with elevated neopterin, patients with normal neopterin and osteoarthritis patients

C-reactive protein and neopterin correlated positively for the Kalafong patients ($r = 0.48$, p-value = 0.0006). However, as previously mentioned, not all Kalafong patients with elevated C-reactive protein necessarily had elevated neopterin and *vice versa*. In the following paragraphs cytokines for the neopterin subdivision are evaluated. As shown below, significant differences for the pro-inflammatory cytokines were found between the group of Kalafong patients with elevated neopterin levels and the group of Kalafong patients with normal neopterin levels, while the osteoarthritis group's pro-inflammatory cytokines largely corresponded with that of the group of Kalafong patients with normal neopterin.

Pro-inflammatory cytokines

The major pro-inflammatory cytokine INF-γ was

- marginally higher (p-value = 0.056) in the group of Kalafong patients with elevated neopterin (21 ± 67.4 pg/ml; n = 34) compared to the group of Kalafong patients with normal neopterin (1.6 ± 3.3 pg/ml; n = 13),
- significantly higher (p-value = 0.003) in the group of Kalafong patients with elevated neopterin compared to the osteoarthritis patients (0.1 ± 0 pg/ml; n = 10) and
- not significantly different between the group of Kalafong patients with normal neopterin and the osteoarthritis patients.

The pro-inflammatory secreted cytokine TNF-α was

- significantly higher (p-value = 0.048) in the group of Kalafong patients with elevated neopterin (3.8 ± 2.8 pg/ml; n = 35) compared to the group of Kalafong patients with normal neopterin (2.7 ± 0.89 pg/ml; n = 13),
- significantly higher (p-value = 0.035) in the group of Kalafong patients with elevated neopterin compared to the osteoarthritis patients (2.5 ± 0.96 pg/ml; n = 10) and
- not significantly different between the group of Kalafong patients with normal neopterin and the osteoarthritis patients.

Furthermore, Il-1β was

- marginally higher (p-value = 0.075) in the group of Kalafong patients with elevated neopterin (5.4 ± 9.7 pg/ml; n = 35) compared to the group of Kalafong patients with normal neopterin (2 ± 2.8 pg/ml; n = 13),

- marginally higher (p-value = 0.057) in the group of Kalafong patients with elevated neopterin compared to the osteoarthritis patients (1.6 ± 3.3 pg/ml; n = 10) and
- not significantly different between the group of Kalafong patients with normal neopterin and the osteoarthritis patients.

Il-6 was

- significantly higher (p-value = 0.0003) in the group of Kalafong patients with elevated neopterin (661.1 ± 2187.6 pg/ml; n = 35) compared to the group of Kalafong patients with normal neopterin (32.3 ± 93.6 pg/ml; n = 13),
- significantly higher (p-value = 0.0005) in the group of Kalafong patients with elevated neopterin compared to the osteoarthritis patients (5 ± 2.1 pg/ml; n = 10) and
- not significantly different between the group of Kalafong patients with normal neopterin and the osteoarthritis patients.

Similar to what was found for the C-reactive protein subdivision, Il-12 was

- not significantly different between the group of Kalafong patients with elevated neopterin (4.5 ± 4.2 pg/ml; n = 35) and the group of Kalafong patients with normal neopterin (5.1 ± 3.1 pg/ml; n = 13) and
- significantly higher (p-value = 0.0001) in the group of Kalafong patients with elevated neopterin and in the group of Kalafong patients with normal neopterin (p-value = 0.0005) compared to the osteoarthritis patients (1.1 ± 1.3 pg/ml; n = 10).

In addition, similar to the C-reactive protein subdivision, Il-2 was

- not significantly different between the group of Kalafong patients with elevated neopterin (10.7 ± 7.1 pg/ml; n = 35) and the group of Kalafong patients with normal neopterin (9.3 ± 7.1 pg/ml; n = 13),
- significantly higher (p-value = 0.049) in the group of Kalafong patients with elevated neopterin compared to the osteoarthritis patients (6.7 ± 4.9 pg/ml; n = 10) and
- not significantly different between the group of Kalafong patients with normal neopterin and the osteoarthritis patients.

Il-8 was

- significantly higher (p-value = 0.0001) in the group of Kalafong patients with elevated neopterin (282.4 ± 775.9 pg/ml; n = 35) compared to the group of Kalafong patients with normal neopterin (15.4 ± 8.3 pg/ml; n = 13),
- significantly higher (p-value = 0.007) in the group of Kalafong patients with elevated neopterin compared to the osteoarthritis patients (18.9 ± 6.4 pg/ml; n = 10) and
- not significantly different between the group of Kalafong patients with normal neopterin and the osteoarthritis patients.

GM-CSF was

- not significantly different between the group of Kalafong patients with elevated neopterin (10.2 ± 15.6 pg/ml; n = 34) and the group of Kalafong patients with normal neopterin (20.8 ± 65.9 pg/ml; n = 13),

- marginally higher (p-value = 0.054) in the group of Kalafong patients with elevated neopterin compared to the osteoarthritis patients (3.6 ± 6.2 pg/ml; n = 10) and
- not significantly different between the group of Kalafong patients with normal neopterin and the osteoarthritis patients.

T-helper cell type-2 cytokines

As shown below, and in contrast to the findings on the T-helper cell type-2 cytokines for the C-reactive protein subdivision, the level of Il-5 was significantly higher in the group of Kalafong patients with elevated neopterin compared to the group of Kalafong patients with normal neopterin.

Il-4 was

- not significantly different between the group of Kalafong patients with elevated neopterin (2.6 ± 1.8 pg/ml; n = 35), the group of Kalafong patients with normal neopterin (2.1 ± 2.3 pg/ml; n = 13) and the osteoarthritis patients (2.5 ± 2.2 pg/ml; n = 10).

However, different from the C-reactive protein subdivision, Il-5 was

- significantly higher (p-value = 0.011) in the group of Kalafong patients with elevated neopterin (3.9 ± 3.7 pg/ml; n = 35) compared to the group of Kalafong patients with normal neopterin (1.9 ± 1.4 pg/ml; n = 13),
- marginally higher (p-value = 0.072) in the group of Kalafong patients with elevated neopterin compared to the osteoarthritis patients (2.4 ± 1.6 pg/ml; n = 10) and

- not significantly different between the group of Kalafong patients with normal neopterin and the osteoarthritis patients.

Il-10 was

- significantly higher (p-value = 0.032) in the group of Kalafong patients with elevated neopterin (24.9 ± 56.3 pg/ml; n = 35) compared to the group of Kalafong patients with normal neopterin (3.6 ± 2.1 pg/ml; n = 13),
- significantly higher (p-value = 0.026) in the group of Kalafong patients with elevated neopterin compared to the osteoarthritis patients (2.7 ± 1.5 pg/ml; n = 10) and
- not significantly different between the group of Kalafong patients with normal neopterin and the osteoarthritis patients.

TGF-β was

- marginally lower (p-value = 0.082) in the group of Kalafong patients with elevated neopterin (10.2 ± 5.8 ng/ml; n = 34) compared to the group of Kalafong patients with normal neopterin (15.2 ± 8.9 ng/ml; n = 13),
- significantly lower (p-value = 0.0001) in the group of Kalafong patients with elevated neopterin compared to the osteoarthritis patients (18.3 ± 4.1 ng/ml; n = 10) and
- not significantly different between the group of Kalafong patients with normal neopterin and the osteoarthritis patients.

In summary on the cytokine profiles of the neopterin subdivision

The pro-inflammatory cytokines for the group of Kalafong patients with elevated neopterin was increased similar to the group of Kalafong patients with elevated C-

reactive protein. However, significant differences, not shown in the subdivision according to C-reactive protein, were shown for T-helper cell type-2 cytokines between the group of Kalafong patients with elevated neopterin and the group of Kalafong patients with normal neopterin. The increase in these cytokines may have included a more mature immune response in the group of Kalafong patients with elevated neopterin. The pro-inflammatory cytokines for which significant increases were shown in the group of Kalafong patients with elevated neopterin compared to the group of Kalafong patients with normal neopterin included INF-γ, TNF-α, Il-1β, Il-6 and Il-8. Furthermore, similar to the C-reactive protein subdivision, Il-2 and Il-12 were not significantly different between the group of Kalafong patients with elevated neopterin and the group of Kalafong patients with normal neopterin. This may also have been as a result of the decreased CD4 count in the group of Kalafong patients with elevated neopterin. Il-5, a T-helper cell type-2 cytokine, was significantly increased in the group of Kalafong patients with elevated neopterin. Furthermore, Il-10 with predominantly anti-inflammatory properties was significantly increased in the group of Kalafong patients with elevated neopterin. For TGF-β, a decrease was shown for the group of Kalafong patients with elevated neopterin compared to the group of Kalafong patients with normal neopterin.

5.2.3) Osteoarthritis patients

Osteoarthritis is a disease of articular joints with the progression characterised by the destruction of articular cartilage, sclerosis of underlying bone and osteophyte formation (46). It has been suggested that osteoarthritis is induced by mechanical stress manifested by cartilage destruction with minimal involvement of the immune response as compared to that of rheumatoid arthritis (47). Although osteoarthritis is considered to be a largely non-inflammatory disease, there is compelling evidence that subclinical inflammation is a common event, even in the absence of acute inflammatory flares (48). It has previously

been shown that the secretion of tumor necrosis factor-α (TNF-α) and interleukin-6 (Il-6) by stimulated blood cells of osteoarthritis patients was increased, similar to that of rheumatoid arthritis patients. However, in contrast to the rheumatoid arthritis patients no increased production was shown for interleukin-1β (Il-1β) (49).

Controversial opinions exist about cytokine involvement in osteoarthritis. This is mostly due to differences in the levels found for these substances in the general circulation. Nevertheless, they do play a significant role at the tissue level. Osteoarthritis is characterised by the involvement of both catabolic and anabolic cytokines in the progression of the disease (46). The catabolic cytokines, Il-1β and TNF-α, have been shown to be involved in primary cartilage damage, whereas the anabolic cytokine, TGF-β, is implicated in promotion of the repair and integrity of cartilage with osteoarthritis (46). Both these catabolic and anabolic cytokines play an important part in the maintenance of articular cartilage homeostasis and it is suggested that the balance between the signalling pathways of the catabolic cytokines, Il-1β and TNF-α, and the anabolic cytokine, TGF-β, is disrupted with osteoarthritis (50). The catabolic effects of Il-1β and TNF-α are exerted by enzymatic destruction through activation of metalloproteinases of cartilage matrix. Furthermore, inadequate synthesis of inhibitors of the actions for Il-1β and TNF-α can contribute to cartilage destruction with osteoarthritis (51). An increase in the expression of the anabolic cytokine, TGF-β, has been reported early in osteoarthritis with an increase in extracellular matrix production (52). This anabolic cytokine, TGF-β, causes the synthesis of proteoglycans and other cartilage matrix components in osteoarthritis patients (46) and is said to counteract the effects of the catabolic cytokines in the later stages of disease progression. Although TGF-β results in an anabolic state it is believed not to compensate for the overall catabolic insult to cartilage with disease progression (52).

In summary on the cytokine profiles of the osteoarthritis patients

The group of osteoarthritis patients showed C-reactive protein and neopterin levels similar to the group of Kalafong patients with normal C-reactive protein and the group of Kalafong patients with normal neopterin, respectively. It is therefore suggested that the osteoarthritis patients did not have any pronounced pro-inflammatory immune stimulation. Furthermore, the cytokine profile of the osteoarthritis patients was, with one major exception, similar to the groups of Kalafong patients with normal C-reactive protein/normal neopterin. The exception was a significantly higher TGF-β level in the osteoarthritis patients.

In the present study no significantly higher levels were shown for the catabolic cytokines, Il-1β and TNF-α, in the osteoarthritis patients compared to the group of Kalafong patients with normal C-reactive protein and to the group of Kalafong patients with normal neopterin, respectively. In addition, no significantly higher levels for various other catabolic (pro-inflammatory) cytokines including INF-γ, Il-6, Il-8, Il-12, Il-2 and GM-CSF were shown in the osteoarthritis patients compared to the group of Kalafong patients with normal C-reactive protein and to the group of Kalafong patients with normal neopterin, respectively. Furthermore, no significantly higher levels for any of the following T-helper cell type-2 cyokines – Il-4, Il-5 or Il-10 – were shown in the osteoarthritis patients compared to either the group of Kalafong patients with normal C-reactive protein or to the group of Kalafong patients with normal neopterin. It should perhaps be stressed that circulating levels of cytokines do not necessarily reflect levels of cytokine activity at the tissue level (46). However, a significantly higher level was shown for TGF-β in the osteoarthritis patients compared to both the group of Kalafong patients with normal C-reactive protein and the group of Kalafong patients with elevated C-reactive protein, respectively. In addition, a significantly higher level was shown for TGF-β in the osteoarthritis patients compared to the group of Kalafong patients with

elevated neopterin. However, the group of Kalafong patients with normal neopterin showed TGF-β levels similar to that of the osteoarthritis patients.

TGF-β, a cytokine with pleiotropic functions, does not only play a paramount role as an anti-inflammatory cytokine during an immune response but also stimulates the production of extracellular matrix proteins in joints with osteoarthritis. In the present study TGF-β was significantly higher in the group of osteoarthritis patients without any significantly higher levels for any of the pro-inflammatory or T-helper cell type-2 cytokines compared to the group of Kalafong patients with normal C-reactive protein and the group of Kalafong patients with normal neopterin, respectively. It is therefore suggested that TGF-β was increased in the group of osteoarthritis patients in line with its pro-fibrotic role with disease progression of osteoarthritis. This significantly higher level for the anabolic cytokine TGF-β in the osteoarthritis patients resulted in a group of patients with a cytokine profile close to normal, but with a pronounced increase in one cytokine. The expression of the H-subunit and L-subunit of ferritin was thus investigated separately for this group and will be discussed in the last section on osteoarthritis patients.

6) EXPRESSION OF THE H-SUBUNIT AND L-SUBUNIT OF FERRITIN IN THE BONE MARROW MACROPHAGE AND CELLS OF THE ERYTHRON IN PATIENTS WITH A PRO-INFLAMMATORY IMMUNE STATUS COMPARED TO PATIENTS WITH NO PRONOUNCED IMMUNE ACTIVATION

The expression of the H-subunit and L-subunit and the relationship between these subunits depend not only on the type of cell, but also on the role of the cell in iron homeostasis and various other factors that can influence the expression of the H-subunit and L-subunit of ferritin. Since the role that the macrophage on the one hand, and the

cells of the erythron on the other, play in iron homeostasis is to a great extent different, it is expected that these subunits would be expressed differently. In this study the expression of the H-subunit and L-subunit of ferritin was determined in the bone marrow macrophage and in the cells of the erythron in patients.

6.1) H-subunit and L-subunit expression in the macrophage in the Kalafong patients with a pro-inflammatory immune status

Both the group of Kalafong patients with elevated C-reactive protein levels and the group of Kalafong patients with elevated neopterin levels displayed a predominantly pro-inflammatory state orchestrated by classically activated macrophages. Both groups showed significantly higher levels for the pro-inflammatory (T-helper cell type-1) cytokines, but not similar increases for the T-helper cell type-2 cytokines. In the group of Kalafong patients with elevated neopterin some of the T-helper cell type-2 cytokines were increased whereas for the group of Kalafong patients with elevated C-reactive protein these cytokines were mostly not significantly different from the group of Kalafong patients with normal C-reactive protein.

When the expression of the H-subunit and L-subunit of ferritin was determined in the bone marrow macrophage it was found that the expression of the H-subunit of ferritin was marginally higher (p-value = 0.074) in the group of Kalafong patients with elevated C-reactive protein (96.9 ± 40.6 counts/μm^2; n = 25) than in the group of Kalafong patients with normal C-reactive protein (76.5 ± 30 counts/μm^2; n = 19). No significant difference was shown for the expression of the L-subunit of ferritin between the group of Kalafong patients with elevated C-reactive protein (117.8 ± 45.9 counts/μm^2; n = 26) and the group of Kalafong patients with normal C-reactive protein (107.7 ± 26.8 counts/μm^2; n = 19). The H-subunit/L-subunit ratio in the macrophage was marginally higher (p-value = 0.086) in the group of Kalafong patients with elevated C-reactive

protein (0.99 ± 0.58; n = 25) than in the group of Kalafong patients with normal C-reactive protein (0.73 ± 0.29; n = 19). Therefore, for the group of Kalafong patients with increased C-reactive protein, for every one H-subunit there was one L-subunit. However, for the group of Kalafong patients with normal C-reactive protein, for every one H-subunit there was almost one and a half times as many L-subunits. This probably reflects isoferritins containing a higher quantity of H-subunits in the group of Kalafong patients with increased C-reactive protein compared to the group of Kalafong patients with normal C-reactive protein with isoferritins containing a lower quantity of H-subunits.

With the subdivision based on C-reactive protein levels there were indications of an increase in the expression of the H-subunit in the macrophage of the bone marrow during chronic pro-inflammatory stimulation. With the subdivision based on neopterin levels, the increase in the expression of the H-subunit of ferritin in the macrophage was pronounced for the group of patients with chronic pro-inflammatory immune stimulation. In the subdivision according to neopterin the expression of the H-subunit of ferritin in the bone marrow macrophage was significantly higher (p-value = 0.037) in the group of Kalafong patients with elevated neopterin (94.7 ± 37.3 counts/μm^2; n = 31) than in the group of Kalafong patients with normal neopterin (72.4 ± 34.0 counts/μm^2; n = 13). As was the case for the subdivision according to C-reactive protein, no difference was shown for the expression of the L-subunit in the bone marrow macrophage between the group of Kalafong patients with elevated neopterin (108.1 ± 34.3 counts/μm^2; n = 32) and the group of Kalafong patients with normal neopterin (126.8 ± 47.5 counts/μm^2; n = 13). The H-subunit/L-subunit ratio in the macrophage was significantly higher (p-value = 0.023) in the group of Kalafong patients with elevated neopterin (0.97 ± 0.49; n = 31) than in the group of Kalafong patients with normal neopterin (0.66 ± 0.43; n =

13). Therefore, similar to the C-reactive protein subdivision the group of Kalafong patients with elevated neopterin had one L-subunit for every H-subunit. Furthermore, in comparison to the C-reactive protein subdivision the group of Kalafong patients with normal neopterin had one and a half as many L-subunits for every one H-subunit. Similar to the C-reactive protein subdivision this probably reflects isoferritins containing a higher quantity of H-subunits in the group of Kalafong patients with elevated neopterin compared to the group of Kalafong patients with normal neopterin with isoferritins containing a lower quantity of H-subunits.

6.2) H-subunit and L-subunit expression in cells of the erythron in the Kalafong patients with a pro-inflammatory immune status

The expression of the H-subunit and L-subunit of ferritin was not only determined in the macrophages of the bone marrow but also in the cells of the erythron. For the C-reactive protein subdivision there was no significant difference for the expression of the H-subunit of ferritin in the cells of the erythron between the group of Kalafong patients with elevated C-reactive protein (144.4 ± 57.6 counts/μm^2; n = 25) and the group of Kalafong patients with normal C-reactive protein (128.1 ± 48.7 counts/μm^2; n = 19). In addition, there was no significant difference for the expression of the L-subunit of ferritin in the cells of the erythron between the group of Kalafong patients with elevated C-reactive protein (212.3 ± 76.6 counts/μm^2; n = 26) and the group of Kalafong patients with normal C-reactive protein (215.6 ± 54.4 counts/μm^2; n = 19). Furthermore, there was no significant difference for the H-subunit/L-subunit ratio in the cells of the erythron between the group of Kalafong patients with elevated C-reactive protein (0.78 ± 0.47; n = 25) and the group of Kalafong patients with normal C-reactive protein (0.61 ± 0.24; n = 19).

Similar to the C-reactive protein subdivision, the neopterin subdivision also showed no significant difference for the expression of the H-subunit of ferritin in the cells of the erythron between the group of Kalafong patients with elevated neopterin (141.4 ± 54.6 counts/μm^2; n = 31) and the group of Kalafong patients with normal neopterin (127.8 ± 53.3 counts/μm^2; n = 13). In addition, there was no significant difference for the expression of the L-subunit of ferritin in the cells of the erythron between the group of Kalafong patients with elevated neopterin (200.7 ± 54.9 counts/μm^2; n = 31) and the group of Kalafong patients with normal neopterin (245.7 ± 85.7 counts/μm^2; n = 13). However, different from the C-reactive protein subdivision the H-subunit/L-subunit ratio in the cells of the erythron was marginally higher (p-value = 0.062) in the group of Kalafong patients with elevated neopterin (0.77 ± 0.42; n = 31) than in the group of Kalafong patients with normal neopterin (0.57 ± 0.31; n = 13). This could possibly indicate isoferritins in cells of the erythron with marginally increased H-subunits in the group of Kalafong patients with elevated neopterin.

6.3) Discussion of the expression of the H-subunit and L-subunit of ferritin in patients with a pro-inflammatory immune status

Several *in vitro* studies which point towards the differential expression of the H-subunit and L-subunit of ferritin in a number of tissues in conditions marked by the excessive production of toxic oxygen radicals, and by infectious and/or inflammatory processes have been published. The present study focuses on the intracellular expression of the H-subunit and L-subunit of ferritin. In no previous study was the expression of the H-subunit and L-subunit of ferritin measured quantitatively in the macrophage of the bone marrow in combination with the inflammatory status of patients. A few studies have none the less been published that relate to the present study. One study exists in which the expression of the H-subunit and L-subunit of ferritin in liver biopsies from three

patients were investigated by ultrastructural immunolocalisation. However, no attempt was made to quantify the level of expression of these two subunits (53). In this particular study it was shown that the denatured H-ferritin subunit is a major constituent of haemosiderin in the liver of patients with iron overload. This is similar to the finding of another study which showed that antibodies directed against denatured human H-ferritin stain only reticuloendothelial cells within the bone marrow (54). However, ultrastructural immunolocalisation was not employed for the study. In a third related study the expression of the two subunits with different disease states was investigated in bone marrow aspirates with fluorescent immunolocalisation (55). However, due to the nature of the fluorescent immunolocalisation technique it was not possible to quantify the expression of the two subunits.

In the bone marrow, iron is differently metabolised by the cells of the erythron including erythroblasts, reticulocytes and red blood cells on the one hand and the macrophage on the other. Furthermore, iron is shuttled between the cells of the erythron and the macrophage to support erythropoiesis. Not only is iron metabolised differently by these various kinds of cells, but during conditions of chronic immune stimulation iron is retained by the macrophage resulting in an increase in storage iron and hypoferraemia – the so-called iron transfer block (56). In order to investigate the role of ferritin and more specifically the subunits of ferritin in the handling of iron by cells of the bone marrow it would be necessary to investigate the expression of the two subunits of ferritin, the H-subunit and L-subunit, at the single cell level.

The results of this study showed in patients with a predominantly pro-inflammatory immune status, governed by pro-inflammatory cytokines, the expression of the H-subunit of ferritin in the macrophage to be higher and the expression of the L-subunit of ferritin in the macrophage to be unaffected. In contrast, the expression of both the H-

subunit and the L-subunit in cells of the erythron was unaffected in the patients with a pro-inflammatory immune status.

The question now arises why the level of significance was higher with regard to the expression of the H-subunit of ferritin in the macrophage for the subdivision according to neopterin than for the subdivision according to C-reactive protein. Although both C-reactive protein and neopterin are commonly used as indicators of pro-inflammatory activity it is obvious that there are differences. One important difference is the time-points at which C-reactive protein and neopterin peak during an immune reaction. C-reactive protein peaks early in an immune reaction and neopterin peaks only later in the immune response (28). Furthermore, with regard to the cytokine profiles of these groups it could not be said that the group of Kalafong patients with elevated neopterin had purely a pro-inflammatory immune response since some of the T-helper cell type-2 cytokines were also increased.

The findings in the present study of the increased expression of the H-subunit of ferritin and unaffected expression of the L-subunit of ferritin in the macrophage are consistent with previous results in other cell types. Various pro-inflammatory cytokines have been reported to have the ability to induce ferritin expression including Il-1α, Il-1β, Il-2, Il-6, TNF-α and IFN-γ (Table 1, Chapter 1). These cytokines modulate ferritin expression by both transcriptional and translational mechanisms (57), but largely by an increase in the rate of transcription of the ferritin gene (19, 58). The expression of the ferritin subunits are, furthermore, differentially regulated by cytokines, and it is mostly the H-subunit of ferritin that is increased by cytokine induction at variance with the L-subunit (19). *In vitro* experiments with various cell types showed an increase in H-subunit expression relative to L-subunit expression upon cytokine activation (Table 1, Chapter 1).

The cytokine-induced increase in the expression of the H-subunit of ferritin is probably even higher than observed since two other processes induced by cytokines during an immune response can reduce the levels of the H-subunit of ferritin. Firstly, pro-inflammatory cytokines not only induce the expression of intracellular ferritin as part of the acute phase response, but also brings about an increase in the secretion of ferritin. For instance, the secretion of ferritin was shown to be stimulated by cytokines in a primary human hepatocyte culture where IL-1α and Il-6 induced a transient secretion of ferritin at 24 hours, followed by a decline to baseline, and TNF-α treatment resulted in a sustained increase in ferritin secretion (58). Therefore, in the present study, secretion of ferritin could very well have resulted in partially masking the response of an increase in the expression of the H-subunits of ferritin in macrophages during pro-inflammatory immune activation.

The second process, that could have brought about a lower observed increase in the H-subunit of ferritin, also induced by pro-inflammatory cytokines, is the degradation of ferritin (haemosiderin formation). It has been shown that activation of macrophages by cytokines such as TNF-α and Il-1β can result in the slower release of iron compared to the release by non-stimulated macrophages, thus supporting the proposed role of cytokines in ferritin-mediated iron sequestration by macrophages (59, 60). This increased formation of haemosiderin during immune stimulation with the subsequent with-holding of iron will be addressed in a following section.

The role of ferritin in inflammatory conditions can be summarised by saying that pro-inflammatory cytokines increase the production of ferritin early in the inflammatory response and that H-subunit rich ferritins are preferentially up-regulated at variance with L-subunit rich ferritins. At this stage this process not only protects the body against

reactive oxygen species generation but, in addition reduces the bio-availability of iron needed by pathogenic microorganisms.

The results of this study showed the expression of the H-subunit and L-subunit of ferritin in the cells of the erythron not to be influenced by the cytokines as was the case for the macrophage. The increase in the expression of the H-subunit of ferritin in the macrophage with immune stimulation is consistent with the role of ferritin in with-holding of iron. The accumulation of iron with chronic immune stimulation has been shown to occur in the macrophages (56). This brings about haemosiderosis of the macrophage and a reduction in serum iron. Due to this hypoferraemic state less iron will reach the cells of the erythron resulting in the subsequent depletion of iron in the cells of the erythron for the production of haemoglobin. In the present study it seems that in the cells of the erythron the H-subunit of ferritin is not up-regulated in order to contribute to the withholding of iron from haemoglobin production during a pro-inflammatory immune reaction.

However, the H-subunit/L-subunit ratio in the cells of the erythron was higher in the group of Kalafong patients with elevated neopterin than in the group of Kalafong patients with normal neopterin. This possible increase in H-subunit rich isoferritins in cells of the erythron in the group of Kalafong patients with elevated neopterin could play a role in the regulation of bio-available iron for haemoglobin production. It has been shown in a previous study that an increase in H-subunit rich ferritins in erythroid cells could result in chelation of the labile iron pool (61).

6.4) H-subunit and L-subunit expression in the macrophage and cells of the erythron in the osteoarthritis patients

The expression of the H-subunit and L-subunit of ferritin in the macrophage and cells of the erythron in the osteoarthritis patients was subsequently compared to the expression of these subunits in the Kalafong patients. Comparisons were made for both the C-reactive protein subdivision and the neopterin subdivision.

Osteoarthritis patients and the subdivision according to C-reactive protein

When the osteoarthritis patients were compared to the group of Kalafong patients with normal C-reactive protein the osteoarthritis patients showed a significantly higher (p-value = 0.02) H-subunit expression in the macrophage (118.8 ± 56.1 counts/μm^2; n = 7). There was no difference for the expression of the H-subunit in the macrophage between the osteoarthritis patients and the group of Kalafong patients with high C-reactive protein. When the expression of the L-subunit in the macrophage of the osteoarthritis patients (136.2 ± 32.8 counts/μm^2; n = 6) was compared to the group of Kalafong patients with normal C-reactive protein it was also seen that the osteoarthritis group had significantly higher (p-value = 0.042) L-subunit counts. The expression of the L-subunit of ferritin in the macrophage in the osteoarthritis patients was not significantly different from the group of Kalafong patients with elevated C-reactive protein. There was no significant difference for the H-subunit/L-subunit ratio in the macrophage between the group of osteoarthritis patients (0.81 ± 0.26; n = 6) and either the group of Kalafong patients with normal C-reactive protein or the group of Kalafong patients with elevated C-reactive protein.

The expression of the H-subunit of ferritin in the cells of the erythron for the osteoarthritis patients (148.8 ± 41.2 counts/μm^2; n = 7) was similar to that of the group of Kalafong patients with elevated C-reactive protein and to the group of Kalafong

patients with normal C-reactive protein. The expression of the L-subunit of ferritin in the cells of the erythron for the osteoarthritis patients (198.8 ± 66.8 counts/μm^2; n = 6) was also similar to the group of Kalafong patients with elevated C-reactive protein and the group of Kalafong patients with normal C-reactive protein. However, the osteoarthritis patients (0.83 ± 0.31; n = 6) showed a marginally higher H-subunit/L-subunit ratio (p-value = 0.075) in the cells of the erythron compared to the group of Kalafong patients with normal C-reactive protein. No difference was shown for the H-subunit/L-subunit ratio in the cells of the erythron between the osteoarthritis patients and the group of Kalafong patients with elevated C-reactive protein.

Osteoarthritis patients and the subdivision according to neopterin

When the expression of the H-subunit of ferritin in the macrophage in the osteoarthritis patients was compared to that of the Kalafong patient groups, subdivided according to their neopterin values, a very similar outcome was found as for the C-reactive protein subdivision. The expression of the H-subunit of ferritin in the macrophage was significantly higher (p-value 0.033) in the osteoarthritis patients (118.8 ± 56.1 counts/μm^2; n = 7) than in the group of Kalafong patients with normal neopterin and not significantly different from that in the group of Kalafong patients with elevated neopterin. There was no significant difference between the expression of the L-subunit of ferritin in the macrophages of the osteoarthritis patients and the Kalafong patients with normal neopterin. A marginally higher (p-value = 0.073) expression of the L-subunit of ferritin was seen in the macrophage of the osteoarthritis patients (136.2 ± 32.8 counts/μm^2; n = 6) compared to the group of Kalafong patients with elevated neopterin. There was no significant difference between the osteoarthritis patients and the group of Kalafong patients with normal neopterin for the expression of the L-subunit of ferritin in the macrophage. No difference was shown between the H-subunit/L-subunit ratio in

the macrophages of the osteoarthritis patients (0.81 ± 0.26; n = 6) and either of the group of Kalafong patients with elevated neopterin or the group of Kalafong patients with normal neopterin.

When the H-subunit and L-subunit expression in cells of the erythron of the osteoarthritis patients were compared to that of the Kalafong patient groups subdivided according to neopterin levels there was no significant difference between the expression of the H-subunit of ferritin in the cells of the erythron in the osteoarthritis patients (148.8 ± 41.2 counts/μm^2; n = 7) and that of either the group of Kalafong patients with elevated neopterin or the group of Kalafong patients with normal neopterin. Furthermore, no significant difference was seen between the expression of the L-subunit of ferritin in the cells of the erythron in the osteoarthritis patients (198.8 ± 66.8 counts/μm^2; n = 6) and that of either the group of Kalafong patients with elevated neopterin or the group of Kalafong patients with normal neopterin. However, the H-subunit/L-subunit ratio in the cells of the erythron was significantly increased (p-value = 0.035) in the osteoarthritis patients (0.83 ± 0.31; n = 6) compared to that of the group of Kalafong patients with normal neopterin. No significant difference was shown for the H-subunit/L-subunit ratio in the cells of the erythron between the osteoarthritis patients and the group of Kalafong patients with elevated neopterin.

In summary on the osteoarthritis patients

- their cytokine profile largely corresponded to that of the group of Kalafong patients with normal C-reactive protein and to that of the group of Kalafong patients with normal neopterin, therefore they did not show overt inflammatory activity.

- their TGF-β was significantly higher than in the group of Kalafong patients with normal C-reactive protein and significantly higher than in the group of Kalafong patients with elevated C-reactive protein.
- their TGF-β was significantly higher than in the group of Kalafong patients with normal neopterin but not significantly different from the group of Kalafong patients with normal neopterin.
- the expression of the H-subunit of ferritin in the bone marrow macrophage was significantly higher than that for the Kalafong patient groups with no pronounced pro-inflammatory activity – in fact, it corresponded to that of the Kalafong patient groups with overt pro-inflammatory activity.
- the expression of the H-subunit and the L-subunit of ferritin in the erythron was similar to all the groups of Kalafong patients, irrespective of immune status.
- the H-subunit/L-subunit ratio in the cells of the erythron was higher than that for the Kalafong patient groups with no pronounced pro-inflammatory activity – in fact, it corresponded to that of the Kalafong patient groups with overt pro-inflammatory activity.

6.5) Discussion of the expression of the H-subunit and L-subunit of ferritin in osteoarthritis patients

Osteoarthritis is a disease of articular joints and results in destruction of articular cartilage, sclerosis of underlying bone and osteophyte formation (46). Cytokines are implicated in the disease progression of osteoarthritis. Il-1β and TNF-α have been shown to be involved in primary cartilage damage, whereas TGF-β is implicated in the promotion of the repair and integrity of cartilage with osteoarthritis (46). However, in the present study the only cytokine elevated in the osteoarthritis patients compared to the group of Kalafong patients with normal C-reactive protein and to the group of Kalafong

patients with normal neopterin was TGF-β. The results of this study could thus implicate TGF-β in the increased expression of the H-subunit of ferritin in the macrophages of the osteoarthritis patients. However, the significance of this possible stimulation of the expression of the H-subunit in the macrophage by TGF-β is not known and can only be speculated on.

TGF-β as for many other cytokines has pleiotropic functions in many tissues and can play a role in various physiological processes. It is known that TGF-β plays an anabolic role in cartilage formation and it has been shown that TGF-β supplementation enhances cartilage repair. It is therefore sometimes used as a therapeutic tool. However, application of TGF-β provides problems in other tissues of the joints and results in fibrosis and osteophyte formation (52). The TGF-β family consists of over 35 members and includes, besides TGF-βs, activins and bone morphogenetic proteins (BMPs). They regulate cell proliferation, differentiation, apoptosis and migration, as well as control extracellular matrix synthesis and degradation of various tissues (52). Furthermore, they mediate cell and tissue responses to injury and modulate immune functions (52).

Due to the role that TGF-β plays in the differentiation of various cell types and the up-regulation of the expression of the H-subunit of ferritin upon cellular differentiation it is possible that TGF-β could cause an increase in the expression of the H-subunit of ferritin. In various cell types including pre-adipocytes, erythroid cells and neuronal cells the expression of the H-subunit of ferritin was shown to be up-regulated upon differentiation (62, 63, 64). This increase in the expression of the H-subunit of ferritin was also found with differentiation of monocytes to macrophages. Similarly differentiation of, for instance colon carcinoma cells is, as for normal cells, accompanied by an increased expression of the H-subunit of ferritin (65). TGF-β was first identified

for promoting the transformation of non-neoplastic cells (43). For instance, TGF-β has been shown to suppress erythropoiesis, not by inhibiting the proliferation of red blood cell precursors, but by initiating differentiation of the red blood cell precursors (66). It is thus speculated that TGF-β could possibly bring about differentiation of cells by up-regulating the expression of the H-subunit of ferritin. This is supported by the results of a previous study, which showed that TGF-β selectively increased the expression of the H-subunits of ferritin in malignant H-ras transformed cells (67).

TGF-β has been shown to have both stimulatory and inhibitory effects upon monocytes/macrophages. Stimulatory effects include chemotaxis of monocytes, induction of FcγRIII and induction of the transcription and translation of Il-1β, TNF-α, platelet-derived growth factor (PDGF) and basic fibroblast growth factor (bFGF). The inhibitory effects include a reduction in TGF-β receptors and deactivation of hydrogen peroxide and superoxide anion production (43). Therefore, monocytes/macrophages are responsive to TGF-β at different time-points during an immune reaction and it is possible that some of these effects of TGF-β on the monocyte/macrophage could be brought about by an up-regulation of the expression of the H-subunit of ferritin.

The suppression of proliferation and induction of differentation are regulated by intracellular iron (labile iron pool). Iron is a necessary element for cellular proliferation and it is generally accepted that rapidly dividing cells require more iron for their growth and metabolism than resting cells. It is also known that cells normally display an increase in cellular proliferation upon an increase in the labile iron pool (13). The reason for the high need for iron is that iron is necessary for the functioning of different enzymes involved in cellular proliferation, including ribonucleotide reductase, which controls a rate-limiting step in DNA synthesis, and for various mitochondrial enzymes involved in

the metabolism of the cell (68, 69). One way in which to bring about an increase in the cellular labile iron pool is by suppression of ferritin synthesis. The expression of the H-subunit gene is shown to be down-regulated by c-MYC and to be essential for the control of cellular proliferation and transformation by c-MYC (70). This is in agreement with the fact that the H-subunit is responsible for controlling the labile iron pool and that down-regulation of H-subunit expression would result in an increase in the labile iron pool. Therefore, in line with TGF-β's role in cellular growth it could be speculated that TGF-β could regulate proteins involved in iron homeostasis such as the H-subunit of ferritin. Furthermore, has it been shown that administration of BMP-2 (member of the TGF-β family) increases hepcidin expression and decreases serum iron levels *in vivo* (71). This increased expression of hepcidin has been shown to occur by the activation of the TGF-β/SMAD4 signalling pathway (72).

In the present section of the study it was seen that an increase in the expression of the H-subunit of ferritin occurred in the bone marrow macrophage in groups of Kalafong patients with a pro-inflammatory immune status and also in a group of osteoarthritis patients with no overt pro-inflammatory activity, but with high TGF-β levels. It is now of interest to investigate whether this increase in the expression of the H-subunit of ferritin could play a role in entrapment of iron in the macrophage and in the resulting reduction in serum iron.

7) PREVALENCE OF THE IRON TRANSFER BLOCK IN PATIENTS WITH A PRO-INFLAMMATORY IMMUNE STATUS COMPARED TO PATIENTS WITH NO PRONOUNCED IMMUNE ACTIVATION

In the next sections the possibility that the H-subunit and L-subunit of ferritin may play a role in an increase in macrophage storage iron and in the resulting hypoferraemia, are investigated. As pro-inflammatory cytokines are involved in the development of an iron

transfer block the first step was to investigate the prevalence of an iron transfer block in the groups of Kalafong patients with high pro-inflammatory activity.

7.1) Iron transfer block

A decrease in serum iron is often found in patients with immune activation. This hypoferraemic state is predominantly orchestrated by cytokines. Various iron homeostatic processes are affected by these cytokines with the combined actions resulting in entrapment of iron in the macrophage and a decrease in serum iron. This process is known as the iron transfer block (73).

The so-called iron transfer block is generally associated with chronic inflammatory conditions. Inflammation, mediated by cytokines, produces a shift in iron handling by the macrophage in favour of iron storage, in time leading to haemosiderosis of the macrophage (74, 75, 76), hypoferraemia (56, 76, 77) and the anaemia of chronic disease. The latter is, however, only partly due to a decrease in iron available for haemotopoiesis. Ferritin plays a major part in the establishment and maintenance of an iron transfer block and thus in the hypoferraemic state of the inflammatory reaction. TNF-α, Il-1β, Il-6 and Il-10 have all been shown to directly stimulate the transcription and translation of ferritin (73, 78). Furthermore, has it been shown that ferritin up-regulation precedes the reduction in serum iron. However, other iron homeostasis proteins also contribute to the reduction in serum iron. These include not only proteins responsible for the handling of macrophage iron but also many others responsible for body iron homeostasis. These proteins involved in the acquisition, storage and release of iron are all influenced, to different extents, at different time-points during the inflammatory reaction, by both pro- and anti-inflammatory cytokines. With an inflammatory reaction the cytokine Il-6 has been shown to stimulate the hepatic expression of the acute-phase protein hepcidin. In turn hepcidin inhibits duodenal absorption of iron by down-

regulating ferroportin expression thus reducing serum iron (79). By increasing the expression of the divalent metal transporter 1, IFN-γ has been shown to stimulate the uptake of ferrous iron by macrophages. However, not only pro-inflammatory cytokines are involved in the establishment of an iron transfer block, but it has also been shown that the anti-inflammatory cytokines, Il-4 and Il-10, can up-regulate transferrin receptor expression, resulting in an increase in transferrin receptor-mediated uptake of iron by the macrophage (73, 78). Furthermore, an increase in the phagocytosis and degradation of senescent erythrocytes is known to occur with an inflammatory reaction. This process is directly up-regulated by TNF-α stimulation as a result of the increase in the expression of C3bi (CD11b/CD18) receptors responsible for the recognition and uptake of damaged erythrocytes. In addition, it has been shown that TNF-α can also indirectly up-regulate this process by damaging circulating erythrocytes. These damaged erythrocytes are then phagocytosed upon binding to C3bi (CD11b/CD18) receptors followed by degradation (73, 78). Not only is haemoglobin iron obtained by degradation of red blood cells, but free plasma haemoglobin is taken up by the haemoglobin scavenger receptor, CD163. It has been shown that Il-10 and Il-6 contribute to macrophage haemoglobin acquisition by stimulating the expression of the haemoglobin scavenger receptor, CD163 (78). INF-γ down-regulates the expression of ferroportin, the major transmembrane protein responsible for the release of macrophage iron, thus inhibiting iron export from macrophages (78), a process that is also affected by hepcidin (80). Down-regulation of ferroportin occurs only later in the inflammatory response after the onset of hypoferremia. It is therefore suggested that the down-regulation of ferroportin is not responsible for the development of the iron transfer block, but that it plays a major role in the maintenance of the iron transfer block (78). In addition, many of these pro-inflammatory mediated effects on iron homeostasis are counterbalanced by anti-inflammatory cytokines such as IL-4 and IL-13 (78).

7.2) Diagnosis of iron transfer block

In the present study iron transfer block was diagnosed by examining various factors known to be associated with an iron transfer block. In general, the presence of an iron transfer block is diagnosed by haematologists as a reduction in the amount of sideroblasts relative to the amount of macrophage storage iron seen with Prussian Blue iron staining of a bone marrow aspirate. However, various serum iron markers can also be employed to assess the presence or absence of an iron transfer block. These include serum iron, transferrin, transferrin saturation, ferritin and soluble transferrin receptor. The transferrin/log ferritin ratio and the soluble transferrin receptor/log ferritin ratio also show changes characteristic of an iron transfer block. The evaluation of various red blood cell indices, influenced negatively by an iron transfer block, also contributes to the evaluation of a patient's iron status.

Normal serum iron levels range from 10-30 μmol/l and normal transferrin saturation between 15-60%. Both serum iron and transferrin saturation are decreased with true iron deficiency and are increased with iron overload (81). These changes relate to the changes in storage iron and depend on the size of the storage iron compartment. In the presence of an iron transfer block, serum iron and transferrin saturation are also decreased. Serum iron and transferrin saturation are decreased to below the normal ranges for these serum iron markers. However, the decrease in these values in the presence of an iron transfer block depends on the size of the storage iron compartment and the duration of the iron transfer block. Therefore, similar to the Prussian blue iron stains, the serum iron concentration and transferrin saturation are decreased relative to the size of the storage iron compartment. For the quantitative, non-invasive determination of iron stores, the plasma ferritin concentration is determined (81). It has been well established that each microgram of ferritin per litre of serum represents 8-10 milligrams of stored iron. In healthy iron-replete adult males the plasma ferritin is about

100 ± 60 µg/l, reflecting an average store of about 1000 mg iron. When the body iron reserve is completely exhausted the plasma ferritin is less than 12 µg/l. In women the average store is about one-third of that in men (82). However, with iron transfer block ferritin is elevated, since ferrtin is an acute phase protein and is therefore increased in various chronic diseases and thus do not reflect the size of the iron stores anymore. Therefore, in the presence of an iron transfer block only a Prussian blue iron stain of a bone marrow aspirate could give a reliable evaluation of the size of the storage iron compartment. Serum transferrin, the protein responsible for the transport of iron in the blood, is usually increased in iron deficiency and decreased in iron overload. Normal serum transferrin levels are between 2-3.5 g/l (81). In the presence of iron transfer block, serum transferrin levels will be decreased. Transferrin, in contrast to ferritin is a negative acute phase protein and decreased with inflammation. In order to determine to what extent the functional iron compartment is reduced the soluble transferrin receptor is determined. The soluble transferrin receptor is increased when the amount of iron reaching the red blood cell precursors is decreased (83). In addition, since haemoglobin contains the greatest part of the functional iron, can the haemoglobin concentration be determined to give an indication of the decrease in the functional iron compartment (82). Of the soluble transferrin receptor and haemoglobin concentration it is the increase in soluble transferrin receptor that would occur before the subsequent reduction in haemoglobin concentration. The haemoglobin concentration for males ranges between 130-180 g/l and for females between 120-160 g/l (81). These various factors are usually measured together to give the best indication of the iron status of the patient. Furthermore, two ratios, transferrin/log ferritin and soluble transferrin receptor/log ferritin can also be employed to assist in the differentiation between an iron transfer block and true iron deficiency. These ratios employ two factors, i.e., transferrin and transferrin receptor. Transferrin is decreased in the face of an inflammatory reaction and increased with true iron deficiency. Whereas, the soluble transferrin receptor is markedly

increased with true iron deficiency and with inflammation the soluble transferrin receptor is only slightly increased or normal (84). The denominator of these ratios, ferritin, is increased with an inflammatory reaction and decreased with true iron deficiency. Therefore, these ratios are expected to decrease with an inflammatory reaction and iron transfer block, whereas it is expected to increase with true iron deficiency.

As pro-inflammatory cytokines are generally presumed to be major role players in the development and maintenance of an iron transfer block, and as it was shown in the previous section of this study that the groups of patients with high pro-inflammatory activity have increased levels of the H-subunit of ferritin in the bone marrow macrophage, the prevalence of iron transfer block was investigated in these groups of Kalafong patients. Thereafter, the expression of the H-subunit and L-subunit of ferritin was examined in a group of Kalafong patients with iron transfer block, irrespective of their cytokine profiles.

7.3) Iron status of the C-reactive protein and neopterin subdivisions

The presence or absence of an iron transfer block was evaluated for individual Kalafong patients of both the subdivision according to C-reactive protein levels and the subdivision according to neopterin levels. In an attempt to identify the presence of an iron transfer block and to differentiate between an iron transfer block and true iron deficiency, bone marrow iron stains of the aspirate and the core, various serum iron markers and various red blood cell indices were assessed. This categorisation is discussed in volume 2, chapter 6.

7.3.1) Body iron stores as evaluated by Prussian blue iron stains of the bone marrow aspirates and cores of the C-reactive protein and neopterin subdivisions

To assess total body iron stores a Prussian blue iron stain was performed on the bone marrow aspirates and bone marrow cores. The magnitude of blue iron deposits formed in the bone marrow reticuloendothelial cells are known to correspond to total body iron stores. The findings for these iron stains are presented in volume 2, chapter 6. Iron stores for the group of Kalafong patients with elevated C-reactive protein were normal for 22% of the patients, increased for 59% and for 19% of the patients in this group the iron stores were reduced. Iron stores for the group of Kalafong patients with elevated neopterin were normal for 15% of the patients, increased for 52% and for 33% of the patients in this group the iron stores were reduced. Iron stores for the group of Kalafong patients with normal C-reactive protein were normal for 21% of the patients, increased for 16% and for 63% of the patients in this group the iron stores were reduced. Iron stores for the group of Kalafong patients with normal neopterin were normal for 38% of the patients, increased for 15% and for 46% of the patients in this group the iron stores were reduced.

7.3.2) Serum iron markers and determination of the iron status of the C-reactive protein and neopterin subdivisions

In the following section the iron status for the C-reactive protein and neopterin subdivisions was assessed by means of their serum iron markers. A summary of the findings is in this section provided in small print in order to facilitate the reading of the chapter.

Serum iron was

- not significantly different between the group of Kalafong patients with elevated C-reactive protein (9 ± 6.9 µmol/l; n = 29) and the group of

Kalafong patients with normal C-reactive protein (11.3 ± 10.6 µmol/l; n = 19) and
- not significantly different between the group of Kalafong patients with elevated neopterin (10.4 ± 9.6 µmol/l; n = 35) and the group of Kalafong patients with normal neopterin (8.7 ± 4.5 µmol/l; n = 13).
- The laboratory values for normal serum iron are between 10-30 µmol/l.

Serum iron was low-normal for the group of Kalafong patients with normal C-reactive protein and low for the group of Kalafong patients with normal neopterin. For these two patient groups the Prussian blue iron stains showed that the majority of the patients had low or absent iron stores. Therefore, the low mean serum iron for these groups was as a result of true iron deficiency. In the group of Kalafong patients with elevated C-reactive protein and the group of Kalafong patients with elevated neopterin the mean serum iron was also low. However, in these patient groups the Prussian blue iron stains showed that the iron stores for these patients were mostly normal or elevated. This situation is characteristic of an iron transfer block.

Serum transferrin was
- significantly lower (p-value < 0.0001) in the group of Kalafong patients with elevated C-reactive protein (1.3 ± 0.5 g/l; n = 28) compared to the group of Kalafong patients with normal C-reactive protein (2.5 ± 0.83 g/l; n = 19) and
- significantly lower (p-value = 0.0008) in the group of Kalafong patients with elevated neopterin (1.5 ± 0.70 g/l; n = 34) compared to the group of Kalafong patients with normal neopterin (2.5 ± 0.84 g/l; n = 13).
- The laboratory values for normal serum transferrin are between 2-3.6 g/l.

In the group of Kalafong patients with normal C-reactive protein and the group of Kalafong patients with normal neopterin the transferrin was normal as a result of the storage iron compartments that were low, normal and increased for these patients. The decrease in serum transferrin in the presence of low/deficient serum iron in the group of Kalafong patients with elevated C-reactive protein and the group of Kalafong patients with elevated neopterin are characteristic of an iron transfer block. Transferrin is a negative acute phase protein and is decreased with an iron transfer block.

Percentage transferrin saturation was

- not significantly different between the group of Kalafong patients with elevated C-reactive protein (34.2 ± 47.7%; n = 26) and the group of Kalafong patients with normal C-reactive protein (24.3 ± 26.5%; n = 19) and
- marginally lower (p-value = 0.058) in the group of Kalafong patients with normal neopterin (17.41 ± 15.1%; n = 13) compared to the group of Kalafong patients with elevated neopterin (35.2 ± 45.8%; n = 32).
- The laboratory values for normal percentage transferrin saturation are between 15-50% in females and between 20-50% in males.

For the group of Kalafong patients with normal neopterin the average transferrin saturation of 17.41% is as a result of the decrease in serum iron together with an increase in transferrin. Since, the percentage transferrin saturation is determined not only by serum iron but also by serum transferrin levels. The group of Kalafong patients with normal C-reactive protein showed similar transferrin levels but higher serum iron levels than the group of Kalafong patients with normal neopterin. This resulted in a smaller decrease in transferrin saturation in this group of patients. In the group of Kalafong patients with elevated C-reactive protein and the group of Kalafong patients with elevated neopterin serum transferrin saturation was thus normal for both groups. This is as a result of the low serum iron and low transferrin.

Serum ferritin was

- significantly higher (p-value = 0.033) in the group of Kalafong patients with elevated C-reactive protein (3903.1 ± 8942.6 µg/l; n = 29) compared to the group of Kalafong patients with normal C-reactive protein (166.8 ± 270.3 µg/l; n = 19) and
- significantly higher (p-value = 0.03) in the group of Kalafong patients with elevated neopterin (3277.4 ± 8236 µg/l; n = 35) compared to the group of Kalafong patients with normal neopterin (126.8 ± 164.5 µg/l; n = 13).
- The laboratory values for normal serum ferritin are between 11-306.8 µg/l in females and between 23.9-336.2 µg/l in males.

Serum ferritin is an acute phase protein and was markedly increased in the group of Kalafong patients with elevated C-reactive protein and the group of Kalafong patients with elevated neopterin. This increase in serum ferritin is characteristic of an iron transfer block.

The transferrin/log ferritin ratio was

- significantly lower (p-value = 0.002) in the group of Kalafong patients with elevated C-reactive protein (0.51 ± 0.31; n = 28) compared to the group of Kalafong patients with normal C-reactive protein (2.2 ± 2; n = 19) and
- significantly lower (p-value = 0.0008) in the group of Kalafong patients with elevated neopterin (0.96 ± 1.4; n = 34) compared to the group of Kalafong patients with normal neopterin (1.8 ± 1.7; n = 13).

The transferrin/log ferritin ratio was less than one for both the group of Kalafong patients with elevated C-reactive protein and the group of Kalafong patients with elevated neopterin. A transferrin/log ferritin ratio of less than one is characteristic of patients with an iron transfer block. This confirms the iron transfer block in patients with a pro-inflammatory, T-helper cell type-1 immune reaction.

Soluble transferrin receptor was

- significantly lower (p-value = 0.023) in the group of Kalafong patients with elevated C-reactive protein (9.5 ± 7.4 μg/ml; n = 29) compared to the group of Kalafong patients with normal C-reactive protein (17.3 ± 12.9 μg/ml; n = 19) and
- not significantly different between the group of Kalafong patients with elevated neopterin (11.8 ± 10.2 μg/ml; n = 35) and the group of Kalafong patients with normal neopterin (14.8 ± 11.5 μg/ml; n = 13).
- The ELISA kit's values for normal soluble transferrin receptor are between 2.9-8.3 μg/ml.

Soluble transferrin receptor was significantly lower in the group of Kalafong patients with elevated C-reactive protein than in the group of Kalafong patients with normal C-reactive protein. However, soluble transferrin receptor was higher for both groups compared to the normal range for soluble transferrin receptor. It has been shown in previous studies that soluble transferrin receptor is normal or slightly increased in the presence of an iron transfer block and markedly elevated with true iron deficiency. For patients with a possible iron transfer block together with true iron deficiency soluble transferrin receptor will be significantly elevated and not normal or slightly increased (73). A different result was shown for the neopterin subdivision. Soluble transferrin receptor was not significantly different between the group of Kalafong patients with

elevated neopterin and the group of Kalafong patients with normal neopterin. Nevertheless, similar to the C-reactive protein subdivision, soluble transferrin receptor was higher for both the group of Kalafong patients with elevated neopterin and the group of Kalafong patients with normal neopterin compared to the normal range for soluble transferrin receptor.

Soluble transferrin receptor in anaemia of chronic disease and iron deficiency anaemia

Transferrin receptors are expressed on the cell surface of many cell types and can be detected in serum (soluble transferrin receptors) as a result of cleavage from the cell surface (83). Although different cell types contribute to the serum soluble transferrin receptor concentration, erythroblasts provide more than 80% of the total concentration of serum soluble transferrin receptor (83). The erythroid marrow is the major site for iron uptake to support haemoglobin production with transferrin receptor numbers and iron uptake by developing erythroid cells maximal at the basophilic normoblast stage. When the erythroid cells cease dividing and mature into reticulocytes the transferrin receptor numbers decrease, and with the attainment of the circulating erythrocyte stages all transferrin receptors will have disappeared (85). Two factors can influence the amount of transferrin receptors expressed on the cell surface of the erythroid cells. Firstly, the rate of proliferation, with an increase in the rate of proliferation resulting in an up-regulation of transferrin receptors on the membranes of the erythroid cells. The second factor is the amount of available intracellular iron (85). The translation of transferrin receptor mRNA is regulated by the iron-responsive protein/iron-responsive element (IRP/IRE) with an increase in intracellular iron resulting in the down-regulation of transferrin receptors and a decrease in intracellular iron resulting in an increase in transferrin receptors. Since the proliferation of cells is dependent on the availability of intracellular iron, the effects of the increase in the proliferative rate are possibly a

consequence of the increased iron requirements with proliferation and thus another manifestation of the regulation of transferrin receptor synthesis through iron availability (86). Therefore, the serum soluble transferrin receptor concentration largely reflects the size of the erythroid marrow and the transferrin receptor number on the erythroblast surface (83).

In both the anaemia of chronic disease (ACD) and iron deficiency anaemia (IDA) sideropenia is shown with a bone marrow iron stain (83). Therefore, in both ACD and IDA the iron delivered to the erythroid marrow is suboptimal. However, with ACD this can be in the face of either normal or increased macrophage storage iron. Due to the suboptimal intracellular iron in the erythroblasts, an increase in the soluble transferrin receptor concentration is expected. Clearly it becomes increased earlier in the development of functional iron depletion than any of the red blood cell related parameters (84). However, this is only true for IDA. With ACD soluble transferrin receptor concentrations are normal or only slightly increased. This is as a result of the general suppression of erythropoiesis in ACD. With the suppression of the proliferative rate of the erythroblasts a decrease in transferrin receptor expression occurs. However, the coexistence of true iron deficiency with chronic disease is associated with an increase in both the efficiency and number of erythroblast transferrin receptors and a highly significant rise in soluble transferrin receptor numbers. Therefore, with ACD in the presence of true iron deficiency soluble transferrin receptor concentrations are increased (83). It has been suggested that soluble transferrin receptor levels can distinguish between ACD and IDA. Despite low serum iron levels, in both ACD and IDA, serum soluble transferrin receptor values remain largely within the normal range for ACD but are elevated in IDA, even in the presence of inflammatory disease (83, 84).

In this study soluble transferrin receptor/log ferritin ratio was

- significantly lower (p-value = 0.025) in the group of Kalafong patients with elevated C-reactive protein (3.4 ± 2.9; n = 29) compared to the group of Kalafong patients with normal C-reactive protein (18.1 ± 26.1; n = 19) and
- marginally lower (p-value = 0.065) in the group of Kalafong patients with elevated neopterin (8.5 ± 19; n = 35) compared to the group of Kalafong patients with normal neopterin (11.2 ± 14.9; n = 13).

With a pro-inflammatory immune reaction ferritin is known to be indiscriminately increased. Together with this increase in ferritin it is known that the soluble transferrin receptor levels are normal or slightly elevated. Therefore, with a pro-inflammatory immune reaction the soluble transferrin receptor/log ferritin ratio would decrease. In contrast, with true iron deficiency this ratio is supposed to increase. The soluble transferrin receptor/ferritin ratio was lower in both the group of Kalafong patients with elevated C-reactive protein and the group of Kalafong patients with elevated neopterin compared to the group of Kalafong patients with normal C-reactive protein and the group of Kalafong patients with normal neopterin, respectively. This lower soluble transferrin receptor/log ferritin ratio in the groups of patients with a pro-inflammatory immune reaction is characteristic for an iron transfer block.

7.3.3) Red blood cell indices of the C-reactive protein and neopterin subdivisions

The evaluation of various red blood cell indices, influenced negatively by an iron transfer block, also contributes to the evaluation of a patient's iron status.

The red blood cell count was

- significantly lower (p-value = 0.0008) in the group of Kalafong patients with elevated C-reactive protein (2.6 ± 1.1 x 10^{12}/l; n = 29) compared to the group of Kalafong patients with normal C-reactive protein (2.9 ± 1.4 x 10^{12}/l; n = 19) and
- significantly lower (p-value = 0.002) in the group of Kalafong patients with elevated neopterin (2.3 ± 0.95 x 10^{12}/l; n = 35) compared to the group of Kalafong patients with normal neopterin (3.7 ± 1.2 x 10^{12}/l; n = 13).
- The laboratory values for normal red blood cell count are between 4.13-5.67 x 10^{12}/l in females and between 4.89-6.11 x 10^{12}/l in males.

Anaemia was present in the majority of Kalafong patients. The anaemias had various etiologies including anaemia due to blood loss, haemolytic anaemia, iron deficiency anaemia, megaloblastic anaemia and anaemia of inflammation. Furthermore, the etiologies of anaemia in some of the Kalafong patients were multi-factorial.

The haemoglobin was

- significantly lower (p-value = 0.004) in the group of Kalafong patients with normal C-reactive protein (7.2 ± 3.8 g/dl; n = 19) compared to the group of Kalafong patients with elevated C-reactive protein (7.6 ± 3.5 g/dl; n = 29) and
- significantly lower (p-value = 0.005) in the group of Kalafong patients with elevated neopterin (6.4 ± 2.9 g/dl; n = 35) compared to the group of Kalafong patients with normal neopterin (10.2 ± 3.9 g/dl; n = 13).
- The laboratory values for normal haemoglobin are 12.1-16.3 g/dl for females and 14.3-18.3 g/dl for males.

Most of the Kalafong patients showed a decrease in haemoglobin. The patients had multifactorial causes for the reduction in haemoglobin.

The haematocrit was

- significantly lower (p-value = 0.001) in the group of Kalafong patients with elevated C-reactive protein (0.23 ± 0.1 l/l; n = 29) compared to the group of Kalafong patients with normal C-reactive protein (0.24 ± 0.12 l/l; n = 19) and
- significantly lower (p-value = 0.002) in the group of Kalafong patients with elevated neopterin (0.2 ± 0.08 l/l; n = 35) compared to the group of Kalafong patients with normal neopterin (0.33 ± 0.12 l/l; n = 13).
- The laboratory values for normal haematocrit are 0.370-0.490 l/l in females and 0.430-0.550 l/l in males.

Most of the Kalafong patients showed a decrease in haematocrit.

The mean corpuscular volume was

- significantly higher in the group of Kalafong patients with elevated C-reactive protein (91.3 ± 15.6 fl; n = 29) compared to that of the group of Kalafong patients with normal C-reactive protein (80.3 ± 14.9 fl; n = 19) and
- not significantly different between the group of Kalafong patients with elevated neopterin (86.8 ± 16.2 fl; n = 35) and the group of Kalafong patients with normal neopterin (87.3 ± 16.3 fl; n = 13).
- The laboratory values for normal mean corpuscular volume are 79.1-98.9 fl.

In the group of Kalafong patients with normal C-reactive protein and the group of Kalafong patients with normal neopterin the inclusion of patients with different iron storage compartments and different red blood cell pathologies such as macrocytic anaemias resulted in a normal average mean corpuscular volume. The average for the mean corpuscular volume for both the group of Kalafong patients with elevated C-reactive protein and the group of Kalafong patients with elevated neopterin showed the presence of normocytic red blood cells. It is known that most patients with an iron transfer block have a normocytic, normochromic anaemia (73, 87). The patients with an iron transfer block are mostly seen in medical care facilities at the time when they display the presence of a normocytic, normochromic anaemia. With further development of anaemia of chronic disease the patients develop a microcytic, hypochromic anaemia.

The mean corpuscular haemoglobin was

- significantly lower in the group of Kalafong patients with normal C-reactive protein (24.5 ± 5.9 pg; n = 19) compared to the group of Kalafong patients with elevated C-reactive protein (29.8 ± 6.1 pg; n = 29), and
- not significantly different between the group of Kalafong patients with elevated neopterin (27.9 ± 6.3 pg; n = 35) and the group of Kalafong patients with normal neopterin (27.2 ± 7.2 pg; n = 13).
- The laboratory values for normal mean corpuscular haemoglobin are between 27-32 pg.

The mean corpuscular haemoglobin concentration was

- significantly lower (p-value = 0.002) in the group of Kalafong patients with normal C-reactive protein (30.3 ± 2.4 g/dl; n = 19) compared to the group of Kalafong patients with elevated C-reactive protein (32.5 ± 2 g/dl; n = 29) and
- not significantly different between the group Kalafong patients with elevated neopterin (31.9 ± 2.2 g/dl; n = 35) and the group of Kalafong patients with normal neopterin (30.8 ± 3 g/dl; n = 13).
- The laboratory values for normal mean corpuscular haemoglobin concentration are between 32-36 g/dl.

The red blood cell distribution width (RDW) was

- not significantly different between the group of Kalafong patients with elevated C-reactive protein (20.2 ± 6.6%; n = 29) and the group of Kalafong patients with normal C-reactive protein (21.1 ± 8.2%; n = 19) and
- not significantly different between the group of Kalafong patients with elevated neopterin (20.6 ± 7.5%; n = 35) and the group of Kalafong patients with normal neopterin (20.3 ± 6.8%; n = 13).
- The laboratory values for normal red blood cell distribution width are between 11.6-14%.

The red blood cell distribution width is a measure of the variation of red blood cell width with an increase in the red blood cell distribution width known as anisocytosis. A greater variation in size occurs with iron deficient anaemia and anaemia of chronic inflammation. The red blood cells produced with iron deficiency anaemia initially show highly variable sizes therefore a markedly increased RDW, but with the development of a pronounced microcytic, hypochromic anaemia the RDW will decrease (88).

The reticulocyte production index (RPI) was

- significantly higher (p-value = 0.039) in the group of Kalafong patients with elevated C-reactive protein (0.81 ± 0.65; n = 11) compared to the group of Kalafong patients with normal C-reactive protein (0.47 ± 0.8; n = 11) and
- significantly higher (p-value = 0.047) in the group of Kalafong patients with elevated neopterin (0.75 ± 0.8; n = 17) compared to the group of Kalafong patients with normal neopterin (0.28 ± 0.23; n = 5).

A decrease in the reticulocyte production index to below 2.5 is as a result of hypoproliferative anaemias or anaemias due to ineffective erythropoiesis. The majority of patients for which the reticulocyte production index were determined had a value of less than 2.5. The decrease in the reticulocyte production index was as a result of various factors such as suppression of erythropoiesis by cytokines and/or nutritional deficiencies.

7.3.4) Prevalence of iron transfer block in patients with a pro-inflammatory immune status

In a previous section it was shown that the cytokine profiles of both the elevated neopterin and elevated C-reactive protein groups were predominantly pro-inflammatory (T-helper cell type-1). When the results of the Prussian blue iron stains of the bone marrow aspirate and core, the serum iron markers and the red blood cell indices were evaluated for each individual patient (volume 2, chapter 6) the prevalence of an iron transfer block in the subdivision according to C-reactive protein and the subdivision according to neopterin was as follows.

Iron status categorisation of patients for the C-reactive protein subdivision showed that

- 20 of the 29 patients (69%) with elevated C-reactive protein had an iron transfer block while
- 14 of the 19 patients (74%) with normal C-reactive protein did not have an iron transfer block, only five of the 19 patients (26%) with normal C-reactive protein had an iron transfer block.

Iron status categorisation of patients for the neopterin subdivision showed that

- 23 of the 35 patients (66%) with elevated neopterin had an iron transfer block while
- 11 of the 13 patients (85%) with normal neopterin did not have an iron transfer block, only two of the 13 patients (15%) with normal neopterin had an iron transfer block.

The above results supported the notion that T-helper cell type-1/pro-inflammatory cytokines are major role players in the development of an iron transfer block. However, it also showed that T-helper cell type-1/pro-inflammatory cytokines are not the only mediators for the development of an iron transfer block. In view of the pleiotropic nature of cytokines, the intracellular signalling cross-talk between cytokines, the many interactions between factors such as transmembrane iron transporters, hepcidin and others, it is difficult to predict the development of an iron transfer block merely on the basis of isolated factors such as the pro-inflammatory status. Despite the predominant role of pro-inflammatory cytokines in the development of an iron transfer block it was, for instance, previously shown that T-helper cell type-2 cytokines can also play a role in the development of an iron transfer block (73, 78). It was thus not a surprising finding that all patients with a pro-inflammatory cytokine profile did not have an iron transfer block. Neither was it a surprising finding that a small percentage of patients with a

relatively normal cytokine profile had an iron transfer block. Furthermore, although the cytokine profiles were very similar for the group of Kalafong patients with elevated C-reactive protein and the group of Kalafong patients with elevated neopterin, there was one notable exception. Together with the increase in the T-helper cell type-1 cytokines it was found that Il-5 was significantly higher in the group of Kalafong patients with elevated neopterin. Il-5 is, in essence, a T-helper cell type-2 cytokine, but belongs to the GM-CSF/Il-3 subgroup (89). In contrast to GM-CSF and Il-3 no effect on monocytes for Il-5 has been shown (90). However, it has been shown that Il-5, as for GM-CSF and Il-3, displayed proliferative effects on both microglia and macrophage cell lines (91). Furthermore, both Il-5 and Il-3 have been shown to bind and activate the GM-CSF receptor present on monocytes (44). It is therefore suggested that Il-5 could have contributed to the establishment of inflammation. Other confounding factors in the prediction of whether an iron transfer block will develop or not, are the activity of ferroportin and hepcidin (80). It has been shown that hepcidin production is increased in inflammation and that hepcidin plays a major role in iron transfer block (79). Hepcidin was shown to bind to ferroportin (major iron transporter involved in the export of cellular iron) resulting in the internalization of ferroportin and a decrease in the release of macrophage iron. However, it has also been shown that hepcidin's role in the iron transfer block involves, not the development of the block, but the maintenance of the iron transfer block (78).

In summary on the iron status of the groups of Kalafong patients with a pro-inflammatory immune status and the groups of Kalafong patients with no pronounced immune activation

The group of Kalafong patients with elevated C-reactive protein and the group of Kalafong patients with elevated neopterin displayed a pro-inflammatory cytokine profile. For these two groups of patients a high prevalence of an iron transfer block was found

when evaluating their Prussian blue iron stains for the bone marrow aspirate and core, their serum iron markers and their red blood cell indices. The prevalence of an iron transfer block was 69% for the group of Kalafong patients with elevated C-reactive protein and 66% for the group of Kalafong patients with elevated neopterin. The majority of the patients in these two groups of Kalafong patients had serum iron profiles characteristic of patients with an iron transfer block. A decrease in serum iron, an increase in ferritin, a decrease in transferrin, a small increase in soluble transferrin receptor, a decrease in transferrin/log ferritin ratio and a decrease in soluble transferrin receptor/log ferritin ratio all characteristic of the presence of an iron transfer block (73). On the other hand, for the group of Kalafong patients with normal C-reactive protein and the group of Kalafong patients with normal neopterin, no excessive pro-inflammatory immune activation was found. As was expected most of the patients in the group of Kalafong patients with normal C-reactive protein and in the group of Kalafong patients with normal neopterin did not have serum iron profiles characteristic of an iron transfer block. However, these groups of patients did not have normal iron status but a high incidence of true iron deficiency. For these groups of patients a decreased serum iron, normal ferritin, normal transferrin, a marked increase in soluble transferrin receptor, an increase in transferrin/log ferritin ratio and an increase in the soluble transferrin receptor/log ferritin ratio were shown. In the presence of an iron transfer block and in the presence of true iron deficiency a marked decrease in red blood cell production is known to occur (84). In the presence of an iron transfer block a negative effect on red blood cell production occurs as a result of the decrease in bio-available iron for haemoglobin production and various other factors resulting in a decrease in red blood cell production. These factors include suppression of the proliferation of erythroid progenitor cells, decrease in the synthesis of erythropoietin, decrease in the sensitivity of erythroblasts to erythropoietin and a decrease in red blood cell life span (73). The anaemia of inflammation, is therefore on the one hand a result of a decrease in

iron reaching the erythron and on the other as a result of the suppression of red blood cell synthesis (92, 93, 94). Il-1, TNF-α and TGF-β have all been shown to inhibit erythropoietin synthesis and action during an inflammatory reaction (92).

In the next few sections important observations derived from the investigation of the prevalence of an iron transfer block in the subdivision of the Kalafong patients based on C-reactive protein and the subdivision of the Kalafong patients based on neopterin are discussed.

7.4) Loss of the relationship between storage iron, bio-available iron and red blood cell production in patients with a pro-inflammatory, T-helper cell type-1 immune response

Normally a close relationship exists between bio-available iron and red blood cell production. In the present study, this close relationship has been shown to exist for the groups of Kalafong patients with no pronounced immune activation. In the following paragraphs it will be shown that this relationship was disturbed in the group of patients with a pro-inflammatory, T-helper cell type-1 immune response.

Serum iron and percentage transferrin saturation reflect the amount of iron that is available to bind to the transferrin receptors of the red blood cell precusors. Therefore, a decrease in serum iron and a decrease in percentage transferrin saturation are usually associated with a decrease in haemoglobin production. This was seen in both the group of Kalafong patients with normal C-reactive protein and the group of Kalafong patients with normal neopterin.

In the group of Kalafong patients with normal C-reactive protein a decrease in percentage transferrin saturation was shown to correlate with

- a decrease in mean corpuscular volume ($r = 0.62$, p-value = 0.005),
- a decrease in mean corpuscular haemoglobin ($r = 0.64$, p-value = 0.003) and
- a decrease in mean corpuscular haemoglobin concentration ($r = 0.49$, p-value = 0.033).

In the group of Kalafong patients with normal neopterin a decrease in percentage transferrin saturation was shown to correlate with

- a decrease in mean corpuscular haemoglobin concentration (r = 0.65, p-value = 0.015).

In the group of Kalafong patients with normal neopterin a decrease in serum iron was shown to correlate with

- a decrease in mean corpuscular volume (r = 0.55, p-value = 0.053),
- a decrease in mean corpuscular haemoglobin (r = 0.57, p-value = 0.040) and
- a decrease in mean corpuscular haemoglobin concentration (r = 0.49, p-value = 0.091).

When the available iron is reduced in the plasma due to decreased iron stores transferrin will normally be up-regulated. An increase in serum transferrin is known to occur in patients where the iron stores are deficient. An increase in transferrin in these patients was related to iron-deficient iron stores resulting in iron-deficient erythropoiesis. This was seen in both the group of Kalafong patients with normal C-reactive protein and the group of Kalafong patients with normal neopterin.

In the group of Kalafong patients with normal C-reactive protein an increase in serum transferrin was shown to correlate with

- a decrease in mean corpuscular volume (r = 0.62, p-value = 0.005),
- a decrease in mean corpuscular haemoglobin (r = 0.74, p-value = 0.0003) and
- a decrease in mean corpuscular haemoglobin concentration (r = 0.79, p-value = 0.0001).

In the group of Kalafong patients with normal neopterin an increase in serum transferrin was shown to correlate with

- a decrease in mean corpuscular volume (r = 0.70, p-value = 0.008),
- a decrease in mean corpuscular haemoglobin (r = 0.80, p-value = 0.001) and
- a decrease in mean corpuscular haemoglobin concentration (r = 0.84, p-value = 0.0003).

Furthermore, in the group of Kalafong patients with normal C-reactive protein an increase in the transferrin/log ferritin ratio was shown to correlate with

- a decrease in mean corpuscular volume (r = 0.66, p-value = 0.002),
- a decrease in mean corpuscular haemoglobin (r = 0.72, p-value = 0.0005) and
- a decrease in mean corpuscular haemoglobin concentration (r = 0.70, p-value = 0.001).

In the group of Kalafong patients with normal neopterin an increase in the transferrin/log ferritin ratio was shown to correlate with

- a decrease in mean corpuscular haemoglobin concentration (r = 0.68, p-value = 0.01).

With a decrease in iron reaching the red blood cell precursors these cells normally produce more transferrin receptors in attempt to take up more iron. This was seen in both the group of Kalafong patients with normal C-reactive protein and the group of Kalafong patients with normal neopterin.

In the group of Kalafong patients with normal C-reactive protein an increase in soluble transferrin receptor was shown to correlate with

- a decrease in serum iron (r = 0.52, p-value = 0.024),
- an increase in serum transferrin (r = 0.59, p-value = 0.007), an increase in serum transferrin indicates decreased iron stores as a result too little iron reached the erythroblasts for red blood cell production,
- a decrease in mean corpuscular volume (r = 0.65, p-value = 0.002),
- a decrease in mean corpuscular haemoglobin (r = 0.75, p-value = 0.0002) and
- a decrease in mean corpuscular heamaglobin concentration (r = 0.75, p-value = 0.0002).

In the group of Kalafong patients with normal neopterin an increase in soluble transferrin receptor was shown to correlate with

- a decrease in the red blood cell count (r = 0.63, p-value = 0.021),
- a decrease in haemoglobin (r = 0.90, p-value < 0.0001),
- a decrease in haematocrit (r = 0.84, p-value = 0.0003) and
- a decrease in mean corpuscular heamoglobin concentration (r = 0.79, p-value = 0.001).

Furthermore, in the group of Kalafong patients with normal C-reactive protein an increase in the soluble transferrin receptor/log ferritin ratio was shown to correlate with

- a decrease in mean corpuscular volume (r = 0.60, p-value = 0.007),
- a decrease in mean corpuscular haemoglobin (r = 0.65, p-value = 0.003) and
- a decrease in mean corpuscular haemoglobin concentration(r = 0.61, p-value = 0.005).

In the group of Kalafong patients with normal neopterin an increase in the soluble transferrin receptor/log ferritin ratio was shown to correlate with

- a decrease in mean corpuscular volume (r = 0.53, p-value = 0.06),
- a decrease in mean corpuscular haemoglobin (r = 0.63, p-value = 0.021) and
- a decrease in mean corpuscular haemoglobin concentration (r = 0.75, p-value = 0.003).

These relationships between red blood cell production and iron was not shown to exist in the group of Kalafong patients with elevated C-reactive protein and the group of Kalafong patients with elevated neopterin. Only the following correlations were indicated. In the group of Kalafong patients with elevated C-reactive protein a decrease in the red blood cell count was shown to correlate with an increase in the red blood cell distribution width (r = 0.57, p-value = 0.001). For the group of patients with elevated neopterin an increase in serum transferrin correlated with a decrease in mean corpuscular haemoglobin concentration (r = 0.56, p-value = 0.0006).

The results of the present study showed that in the group of Kalafong patients with normal C-reactive protein and the group of Kalafong patients with normal neopterin (patients with relatively normal pro-inflammatory activation) the availability of iron was

the most important factor for regulating red blood cell production. In contrast, in the groups of Kalafong patients with a pronounced pro-inflammatory cytokine profile (group of Kalafong patients with elevated C-reactive protein and group of Kalafong patients with elevated neopterin) this role of bio-available iron in the regulation of proper red blood cell production was lost.

7.5) Possible role of the anti-inflammatory cytokine, transforming growth factor-β, in resolving the iron transfer block

No direct correlation of any of the pro-inflammatory cytokines was shown between any of the serum iron markers or between any of the red blood cell indices in either the group of Kalafong patients with elevated C-reactive protein or the group of Kalafong patients with elevated neopterin. However, in the group of Kalafong patients with elevated C-reactive protein a possible role for the anti-inflammatory cytokine TGF-β was shown in resolving the iron transfer block. In the group of Kalafong patients with elevated C-reactive protein an increase in TGF-β correlated with an increase in serum transferrin ($r = 0.73$, p-value < 0.0001) and an increase in the transferrin/log ferritin ratio ($r = 0.67$, p-value $= 0.0001$). TGF-β is an anti-inflammatory cytokine and could perhaps contribute (directly or indirectly) to the increase in the negative acute phase protein transferrin.

7.6) Relationship between storage iron, bio-available iron, expression of the H-subunit and L-subunit of ferritin and red blood cell production in the group of Kalafong patients with normal neopterin

In the group of Kalafong patients with normal neopterin indications for a possible regulatory role for the H-subunit and L-subunit of ferritin was shown in the production of red blood cells. In the group of Kalafong patients with normal neopterin an increase in the H-subunit/L-subunit ratio in the macrophage correlated with a decrease in mean

corpuscular volume (r = 0.58, p-value = 0.037). A correlation was also seen between an increase in the H-subunit/L-subunit ratio in the macrophage with a decrease in mean corpuscular haemoglobin (r = 0.51, p-value = 0.072). Therefore, with an increase in the amount of H-subunits relative to the amount of L-subunits in the macrophage (increase in H-subunit rich ferritins) a decrease in efficient red blood cell production was shown. It has already been established by previous studies that a reduced amount of iron reaches the red blood cell precursors with an iron transfer block (95). An increase in the H-subunit/L-subunit ratio in the macrophage could contribute to the reduction in iron that reached the red blood cell precursors since H-subunit rich ferritins are more prone to conversion into haemosiderin. Once H-subunit rich ferritins are converted into haemosiderin, the iron that was contained in ferritin is trapped. In support of the trapping of iron in these patients it was shown that with an increase in the expression of the L-subunit of ferritin in the macrophage the mean corpuscular volume (r = 0.85, p-value = 0.0002) and the mean corpuscular haemoglobin (r = 0.76, p-value = 0.003) were increased. The L-subunit of ferritin is more likely to be influenced by iron and therefore is indicative of an increase in the labile iron pool of the macrophage. An increase in the labile iron pool of the macrophage is likely to result in more iron being delivered to the red blood cell precursors. Furthermore, an increase in the L-subunit of ferritin in the cells of the erythron correlated with an increase in the mean corpuscular volume (r = 0.69, p-value = 0.01) and an increase in the mean corpuscular haemoglobin (r = 0.65, p-value = 0.016). An increase in the L-subunit of ferritin in cells of the erythron most probably reflects an increase in the labile iron pool of these cells. It has been shown in previous studies that when iron accumulates in erythroid cells due to an increase in the cellular uptake of iron, the L-subunit rich ferritins seem to increase and to be closely related to the iron status of the cells (55, 96). An increase in the labile iron pool would furnish the cells of the erythron with more iron for haemoglobin synthesis. This increase in the intracellular labile iron pool in the cells of the erythron reflected by an increase in

the expression of the L-subunit of ferritin was most likely as a result of an increase in bio-available iron since the L-subunit of ferritin in the cells of the erythron was shown to correlate with an increase in serum iron ($r = 0.66$, p-value = 0.014) and an increase in the percentage transferrin saturation ($r = 0.68$, p-value = 0.01).

7.7) Relationship between the H-subunit/L-subunit ratio in cells of the erythron and the mean corpuscular volume in the group of Kalafong patients with normal neopterin

Similar to what was shown for the H-subunit/L-subunit ratio in the macrophage an increase in the H-subunit/L-subunit ratio in the cells of the erythron correlated with a decrease in the mean corpuscular volume ($r = 0.52$, p-value = 0.069) in the group of Kalafong patients with normal neopterin. The mean corpuscular volume of red blood cells is closely related to the amount of haemoglobin in these cells. Therefore, a reduction in the mean corpuscular volume reflects a decrease in the amount of iron reaching the red blood cell precursors (97). The importance of an increase in the H-subunit/L-subunit ratio in the cells of the erythron in terms of iron bio-availability is not known. It could be that an increase in the H-subunit/L-subunit ratio in the cells of the erythron, similar to the macrophage, can result in the un-availability of cellular iron for red blood cell production. Red blood cell precursors obtain iron for haemoglobin production possibly by the following two routes – transferrin iron via the transferrin receptor and as ferritin during the process of rhopheocytosis (98). Once the iron reaches the intracellular labile iron pool it is either incorporated into ferritin or used for haemoglobin production. The expression of the H-subunit and L-subunit of ferritin plays an important role in the sequestration and the release of bio-avalable iron for the production of haemoglobin. The erythroid cells contain mainly H-subunit rich ferritins, which play a major role in the intracellular transport and donation of iron for the active synthesis of haem (99), particularly in immature erythroid cell precursors such as

proerythroblasts and basophilic erythroblasts (55). However, it has been shown that an increase in H-subunit rich isoferritins can result in the rapid chelation of labile iron in erythroid cells (61). Therefore, the increase in the H-subunit/L-subunit ratio in the red blood cell precursors could result in the reduction in the red blood cell volume as a result of the withholding of iron by these H-subunit rich ferritins.

7.8) Relationship between the H-subunit of ferritin in the cells of the erythron and the mean corpuscular haemoglobin concentration in the group of Kalafong patients with elevated C-reactive protein

In the group of Kalafong patients with elevated C-reactive protein a decrease in the H-subunit of ferritin in the cells of the erythron correlated with a decrease in the mean corpuscular haemoglobin concentration ($r = 0.51$, p-value = 0.007). The intracellular labile iron pool of the red blood cell precursors is regulated by the expression of the H-subunit and L-subunit of ferritin (61). It is suggested by previous studies that in the red blood cell precursors the expression of the H-subunit of ferritin plays an important role in the release of bio-available iron for the production of haemoglobin. It has been shown that H-subunit rich ferritins accumulate and release iron faster than do L-subunit rich ferritins (2, 3, 76, 100) and it is suggested that the H-subunit rich ferritins permit more dynamic intracellular traffic of iron (3, 101). Therefore, this correlation of a decrease in the expression of the H-subunit in the cells of the erythron together with the decrease in the mean corpuscular haemoglobin concentration points to a role for the decrease in H-subunit resulting in a reduction in the release of bio-available iron. It was shown, *in vitro*, that a too great proportion of H-subunits in the ferritin protein shell result in ferritin aggregation. This may be due to the inadequacy of the ferritin protein shell to retain the formed Fe^{3+} resulting in the loss of Fe^{3+} and hydrolysis of Fe^{3+} on the outside of the ferritin molecule (4). Upon ferritin aggregation, the iron contained in the

ferritin protein shell may be trapped and therefore no longer available to support haemoglobin production.

7.9) Pro-hepcidin and caeruloplasmin levels for the C-reactive protein and neopterin subdivisions

Pro-hepcidin is the precursor of the hormone hepcidin that plays a role in the mediation of the homeostasis of extracellular iron. Hepcidin synthesis is physiologically increased by elevated plasma iron, decreased by erythropoietic activity and pathologically increased by inflammation. Hepcidin acts by regulating iron influx into plasma from duodenal enterocytes, hepatocytes and macrophages. Hepcidin binds to the transmembrane iron-transporter, ferroportin, responsible for the movement of iron from the cytoplasm of these cells to the plasma. An increase in hepcidin results in the internalization of ferrroportin and a reduction in the release of iron from enterocytes, hepatocytes and macrophages. Due to the role of hepcidin in the regulation of the release of iron from macrophages, it has been suggested that hepcidin could play a role in the development of the iron transfer block with inflammation (79).

At the time of the study the newly developed hepcidin ELISA from DRG Diagnostics, Germany was not avaliable for purchase and therefore only pro-hepcidin could be measured. In this study pro-hepcidin was significantly decreased (p-value = 0.039) for the group of Kalafong patients with elevated C-reactive protein (135.2 ± 48.2 ng/ml; n = 28) compared to the group of Kalafong patients with normal C-reactive protein (159.3 ± 38.6 ng/ml; n = 19). Similar to what was found for the C-reactive protein subdivision pro-hepcidin was significantly decreased (p-value = 0.02) in the group of Kalafong patients with elevated neopterin (135.6 ± 40 ng/ml; n = 34) compared to the group of Kalafong patients with normal neopterin (169.2 ± 52.2 ng/ml; n = 13).

Although it was previously shown that pro-hepcidin is increased during an inflammatory reaction (102), the results of the present study showed the opposite to occur in the groups of Kalafong patients with a pro-inflammatory immune reaction. Nevertheless, pro-hepcidin might be reduced in this study due to an increase in the conversion to hepcidin. This could, however, only be clarified by the measurement of hepcidin.

Caeruloplasmin is a multi-copper binding protein that acts as a serum ferroxidase and is essential for the mobilization of iron from storage tissues (103). Caeruloplasmin is situated on the extracellular side of the cell membrane and oxidizes Fe^{2+} to Fe^{3+} to facilitate the binding to transferrin. Therefore, caeruloplasmin plays an important role in the export of iron from tissue storage sites. In the present study, there was no significant difference for caeruloplasmin between the group of Kalafong patients with elevated C-reactive protein (0.47 ± 0.15 g/l; n = 27) and the group of Kalafong patients with normal C-reactive protein (0.46 ± 0.16 g/l; n = 19). There was also no difference for caeruloplasmin between the group of Kalafong patients with elevated neopterin (0.47 ± 0.16 g/l; n = 33) and the group of Kalafong patients with normal neopterin (0.47 ± 0.14 g/l; n = 13).

8) EXPRESSION OF THE H-SUBUNIT AND L-SUBUNIT OF FERRITIN IN A GROUP OF KALAFONG PATIENTS WITH IRON TRANSFER BLOCK COMPARED TO A GROUP OF KALAFONG PATIENTS WITH NO IRON TRANSFER BLOCK

In order to investigate the possibility that the H-subunit and L-subunit of ferritin may play a role in the development and maintenance of an iron transfer block the Kalafong patients were subdivided in a group of patients with iron transfer block and a group of patients with no iron transfer block.

8.1) Iron status of the iron transfer block subdivision of the Kalafong patients

For the next section the presence or absence of an iron transfer block was evaluated for all Kalafong patients irrespective of their immune status. In an attempt to identify the presence of an iron transfer block and to differentiate between an iron transfer block and true iron deficiency, bone marrow iron stains of the aspirate and the core, various serum iron markers and various red blood cell indices were assessed. This categorisation was discussed in the results chapter (volume 2, chapter 6) and will be summarised in the following section.

8.1.1) Body iron stores as evaluated by Prussian blue iron stains of the bone marrow aspirates and cores of the iron transfer block subdivision of the Kalafong patients

The iron stores for the group of Kalafong patients with no iron transfer block were normal for 7 of 23 (30%) of the patients, increased for 3 of 23 (13%) of the patients and for 13 of 23 (57%) of the patients in this group the iron stores were reduced. The iron stores for the group of Kalafong patients with iron transfer block were normal for 3 of 23 (13%) of the patients, increased for 16 of 23 (70%) of the patients and for 4 of 23 (17%) of the patients in this group the iron strores were reduced. Not all patients with an iron transfer block had increased iron stores. This can be ascribed to the concomitant existence of true iron deficiency.

8.1.2) Serum iron markers and determination of the iron status of the iron transfer block subdivision of the Kalafong patients

The following serum iron markers were evaluated; serum iron, transferrin, transferrin saturation, ferritin, soluble transferrin receptor, transferrin/log ferritin and soluble transferrin receptor/log ferritin.

Serum iron was

- not significantly different between the group of Kalafong patients with iron transfer block (9.1 ± 7.5 µmol/l; n = 25) and the group of Kalafong patients without iron transfer block (10.8 ± 9.6 µmol/l; n = 23).
- The laboratory values for normal serum iron are between 10-30 µmol/l.

The group of Kalafong patients without iron transfer block had low serum iron due to the inclusion of many patients with true iron deficiency.

Serum transferrin was

- significantly lower (p-value < 0.0001) in the group of Kalafong patients with iron transfer block (1.3 ± 0.42 g/l; n = 24) compared to the group of Kalafong patients without iron transfer block (2.3 ± 0.92 g/l; n = 23).
- The laboratory values for normal serum transferrin are between 2-3.6 g/l.

Transferrin is a negative acute phase protein and a decrease in transferrin is characteristic of the presence of iron transfer block.

Percentage transferrin saturation was

- not significantly different between the group of Kalafong patients with iron transfer block (27.7 ± 21.7%; n = 22) and the group of Kalafong patients without iron transfer block (32.3 ± 52.5%; n = 23).
- The laboratory values for normal percentage transferrin saturation are between 15-50% in females and between 20-50% in males.

The percentage transferrin saturation is determined not only by serum iron but also by serum transferrin levels. In the group of Kalafong patients with iron transfer block the percentage transferrin saturation was thus normal because of the low serum iron and low transferrin.

Serum ferritin was

- significantly higher (p-value < 0.0001) in the group of Kalafong patients with iron transfer block (2709.6 ± 4210.9 µg/l; n = 25) compared to the group of Kalafong patients without iron transfer block (2113.8 ± 9465 µg/l; n = 23).
- The laboratory values for normal serum ferritin are between 11-306.8 µg/l in females and between 23.9-336.2 µg/l in males.

Serum ferritin is an acute phase protein and is elevated in the presence of an inflammatory reaction. The high mean for serum ferritin in the group of Kalafong patients with no iron transfer block was as a result of a patient included in this group with a serum ferritin value of more than 45500 µg/l.

Transferrin/log ferritin ratio was

- significantly lower (p-value = 0.002) in the group of Kalafong patients with iron transfer block (0.48 ± 0.28; n = 24) compared to the group of Kalafong patients without iron transfer block (2 ± 1.9; n = 23).

A decrease in the transferrin/log ferritin ratio is characteristic of an iron transfer block.

The soluble transferrin receptor was

- significantly lower (p-value < 0.0001) in the group of Kalafong patients with iron transfer block (7.1 ± 4.4 µg/ml; n = 25) compared to the group of Kalafong patients without iron transfer block (18.5 ± 12.1 µg/ml; n = 23).
- The ELISA kit's values for normal soluble transferrin receptor are between 2.9-8.3 µg/ml.

The soluble transferrin receptor is normal or only slightly increased in the presence of an iron transfer block but with true iron deficiency it is markely elevated (83). In the group of Kalafong patients without the iron transfer block a pronounced elevation of the soluble transferrin receptor was shown indicating the presence of true iron deficiency. This underlines the fact that many of the Kalafong patients without iron transfer block did not have normal iron status, but true iron deficiency.

The soluble transferrin receptor/log ferritin ratio was

- significantly lower (p-value = 0.011) in the group of Kalafong patients with iron transfer block (2.6 ± 1.9; n = 25) compared to the group of Kalafong patients without iron transfer block (16.5 ± 23.9; n = 23).

A decrease in the soluble transferrin receptor/log ferritin ratio is characteristic of an iron transfer block, whereas the tremendously increased soluble transferrin receptor/log ferritin ratio is characteristic for true iron deficiency. This once again indicated the

presence of true iron deficiency in many of the Kalafong patients without iron transfer block.

8.1.3) Red blood cell indices of the iron transfer block subdivision of the Kalafong patients

The evaluation of various red blood cell indices, influenced negatively by an iron transfer block, also contributes to the evaluation of a patient's iron status.

The red blood cell count was

- not significantly different between the group of Kalafong patients with iron transfer block (2.5 ± 0.95 x 10^{12}/l; n = 25) and the group of Kalafong patients without iron transfer block (2.9 ± 1.4 x 10^{12}/l; n = 23).
- The red blood cell counts were low compared to the normal ranges of 4.13-5.67 x 10^{12}/l for females and 4.89-6.11 x 10^{12}/l for males.

The low red blood cell counts was as a result of not only functional iron deficiency, with or without the presence of an iron transfer block, but was also the result of many other pathologies found in the Kalafong patients.

Haemoglobin was

- not significantly different between the group of Kalafong patients with iron transfer block (7.3 ± 3.2 g/dl; n = 25) and the group of Kalafong patients without iron transfer block (7.5 ± 4.1 g/dl; n = 23).
- The laboratory values for normal haemoglobin are between 12.1-16.3 g/dl for females and between 14.3-18.3 g/dl for males.

Haematocrit was

- not significantly different between the group of Kalafong patients with iron transfer block (0.22 ± 0.09 l/l; n = 25) and the group of Kalafong patients without iron transfer block (0.24 ± 0.13 l/l; n = 23).
- The laboratory values for normal haematocrit are between 0.370-0.490 l/l for females and between 0.430-0.550 l/l for males.

The mean corpuscular volume was

- not significantly different between the group of Kalafong patients with iron transfer block (89.8 ± 13 fl; n = 25) and the group of Kalafong patients without iron transfer block (83.9 ± 18.6 fl; n = 23).
- The laboratory values for normal mean corpuscular volume are between 79.1-98.9 fl.

The mean corpuscular volume for the group of Kalafong patients was normal when compared to the normal laboratory values. It is known that the anaemia of chronic disease is mostly normocytic and normochromic (73, 87).

The mean corpuscular haemoglobin was

- not significantly different between the group of Kalafong patients with iron transfer block (29.1 ± 5 pg; n = 25) and the group of Kalafong patients without iron transfer block (26.2 ± 7.7 pg; n = 23).
- The laboratory values for normal mean corpuscular haemoglobin are between 27-32 pg.

The mean corpuscular haemoglobin was normal for the group of Kalafong patients with iron transfer block, but below normal for the group of Kalafong patients without iron transfer block. Many patients with true iron deficiency were included in the group of Kalafong patients with no iron transfer block. The anaemia of true iron deficiency is mostly a microcytic, hypochromic anaemia with the anaemia of chronic disease mostly a normocytic, normochromic anaemia.

The mean corpuscular haemoglobin concentration was

- significantly higher (p-value = 0.024) in the group of Kalafong patients with iron transfer block (32.4 ± 1.9 g/dl; n = 25) compared to the group of Kalafong patients without iron transfer block (30.8 ± 2.7 g/dl; n = 23).
- The normal ranges for the mean corpuscular haemoglobin concentration are between 32-36 g/dl.

Similar to the mean corpuscular haemoglobin the mean corpuscular haemoglobin concentration was low-normal for the group of Kalafong patients with iron transfer block and below normal for the group of Kalafong patients with no iron transfer block.

The red blood cell distribution width was

- not significantly different between the group of Kalafong patients with iron transfer block (19.7 ± 5.5%; n = 24) and the group of Kalafong patients without iron transfer block (22.3 ± 7.5%; n = 23).
- The laboratory values for normal red blood cell distribution width are between 11.6-14 %.

The red blood cell distribution width was above normal for both the group of Kalafong patients with iron transfer block and the group of Kalafong patients with no iron transfer block. An increase in the red blood cell distribution width occurs for both anaemia of chronic disease and for the anaemia of true iron deficiency.

The RPI was

- not significantly different between the group of Kalafong patients with iron transfer block (0.41 ± 0.41; n = 10) and the group of Kalafong patients without iron transfer block (0.84 ± 0.89; n = 12).

The reticulocyte production index was below 2.5 for both the group of Kalafong patients with iron transfer block and the group of Kalafong patients with no iron transfer block. A reticulocyte production index of below 2.5 indicates a suppressed bone marrow response.

In this section the Prussian blue iron stains of the bone marrow aspirates and cores, the serum iron markers and the red blood cell indices were used to subdivide the Kalafong patients into a group of patients with iron transfer block and a group of patients without iron transfer block. This was done irrespective of their immune status. This subdivision will be used to investigate the expression of the H-subunit and L-subunit of ferritin in bone marrow macrophages and the cells of the erythron with an iron transfer block.

8.2) Loss of the relationship between storage iron, bio-available iron and red blood cell production in the group of Kalafong patients with an iron transfer block

In the group of Kalafong patients with no iron transfer block the role that iron play in red blood cell production was clearly shown.

An increase in serum iron correlated with

- an increase in mean corpuscular volume (r = 0.57, p-value = 0.004),

- an increase in mean corpuscular haemoglobin (r = 0.59, p-value = 0.003) and
- an increase in mean corpuscular haemoglobin concentration (r = 0.50, p-value = 0.016).

An increase in transferrin correlated with

- a decrease in mean corpuscular volume (r = 0.58, p-value = 0.004),
- a decrease in mean corpuscular haemoglobin (r = 0.69, p-value = 0.0003) and
- a decrease in mean corpuscular haemoglobin concentration (r = 0.82, p-value < 0.0001).

An increase in soluble transferrin receptor correlated with

- an increase in haemoglobin (r = 0.71, p-value = 0.0001),
- an increase in haematocrit (r = 0.66, p-value = 0.0006),
- an increase in mean corpuscular volume (r = 0.46, p-value = 0.027),
- an increase in mean corpuscular haemoglobin (r = 0.53, p-value = 0.01) and
- an increase in mean corpuscular haemoglobin concentration (r = 0.64, p-value = 0.001).

A decrease in transferrin/log ferritin ratio correlated with

- an increase in mean corpuscular haemoglobin concentration (r = 0.69, p-value = 0.0003).

A decrease in the red blood cell distribution width correlated with

- an increase in haemoglobin (r = 0.70, p-value = 0.0002) and
- an increase in haematocrit (r = 0.68, p-value = 0.0003).

In the group of Kalafong patients with an iron transfer block no direct role was indicated for iron in red blood cell production as was shown for the group of Kalafong patients with no iron transfer block. The results showed that with an iron transfer block the iron status is only one of the factors that contribute to the decrease in red blood cell production. The other factors that play a role include suppression of the proliferation of erythroid progenitor cells, decrease in the synthesis of erythropoietin, decrease in the sensitivity of erythroblasts to erythropoietin and a decrease in red blood cell life span (73). Iron status is therefore not the major determinant of proper red blood cell production in patients with an iron transfer block.

8.3) Expression of the H-subunit and L-subunit of ferritin in macrophages and cells of the erythron in the group of Kalafong patients with an iron transfer block compared to the group of Kalafong patients with no iron transfer block

In this study the expression of the H-subunit in the macrophages of the bone marrow in the group of Kalafong patients with an iron transfer block (99.5 ± 41 counts/μm^2; n = 22) was marginally higher (p-value = 0.06) than in the group of Kalafong patients without an iron transfer block (78.5 ± 30.8 counts/μm^2; n = 23). For the expression of the L-subunit in the macrophages there was no difference between the group of Kalafong patients with an iron transfer block (113.1 ± 39.4 counts/μm^2; n = 21) and the group of Kalafong patients without an iron transfer block (113.6 ± 40.3 counts/μm^2; n = 23). There was no significant difference for the H-subunit/L-subunit ratio in the macrophages between the group of Kalafong patients with an iron transfer block (1 ± 0.57; n = 21) and the group of Kalafong patients without an iron transfer block (0.76 ± 0.39; n =23).

There were no significant differences for the expression of the H-subunit of ferritin in the cells of the erythron between the group of Kalafong patients with an iron transfer block (141.5 ± 50.9 counts/μm^2; n = 22) and the group of Kalafong patients without an iron transfer block (135.1 ± 57.1 counts/μm^2; n = 23). For the expression of the L-subunit of ferritin in the cells of the erythron there was no significant difference between the group of Kalafong patients with iron transfer block (211.5 ± 59.6 counts/μm^2; n = 21) and the group of Kalafong patients without an iron transfer block (217.5 ± 76.1 counts/μm^2; n = 23). There was no significant difference for the H-subunit/L-subunit ratio in the cells of the erythron between the group of Kalafong patients with iron

transfer block (0.74 ± 0.44; n = 21) and the group of Kalafong patients without an iron transfer block (0.68 ± 0.36; n = 23).

The increase in only the H-subunit of ferritin in the macrophage in the group of Kalafong patients with iron transfer block was similar to the group of Kalafong patients with elevated C-reactive protein and to the group of Kalafong patients with elevated neopterin. Both the group of Kalafong patients with elevated C-reactive protein and the group of Kalafong patients with elevated neopterin showed a pro-inflammatory, T-helper cell type-1 response. The immune status for the the group of Kalafong patients with iron transfer block and the group of Kalafong patients with no iron transfer block is discussed in a following section.

8.4) Relationship between the H-subunit/L-subunit ratio in cells of the erythron and the mean corpuscular volume and the mean corpuscular haemoglobin in the group of Kalafong patients with an iron transfer block

In the group of Kalafong patients with an iron transfer block an increase in the H-subunit/L-subunit ratio in cells of the erythron correlated with a decrease in mean corpuscular volume ($r = 0.55$, p-value = 0.008) and a decrease in mean corpuscular haemoglobin ($r = 0.42$, p-value = 0.049). This suggests that an increase in H-subunit rich ferritins in the cells of the erythron might play a role in the amount of iron available for haemoglobin synthesis.

Iron taken up by the red blood cell precursors either as ferritin with rhopheocytosis or as transferrin via the transferrin receptor pathway is incorporated into ferritin in the red blood cell precursors before this iron is used for haemoglobin production (9, 104). In the present study it was shown that with an increase in H-subunit rich ferritins in red

blood cell precursors less haemoglobin was produced. Therefore, it could be said that these H-subunit rich ferritins withholds iron from haemoglobin production.

8.5) Relationship between the L-subunit of ferritin in cells of the erythron and the mean corpuscular volume and the mean corpuscular haemoglobin in the group of Kalafong patients with an iron transfer block

In the group of Kalafong patients with an iron transfer block a positive correlation was shown between the L-subunit of ferritin in the cells of the erythron and the mean corpuscular volume ($r = 0.53$, p-value = 0.014) and the mean corpuscular haemoglobin ($r = 0.53$, p-value = 0.013). This correlation might reflect an increase in iron reaching the cells of the erythron. It is known that the expression of the L-subunit of ferritin is closely related to the intracellular labile iron pool. Translation of the L-subunit mRNA is increased by binding of iron to the iron responsive protein resulting in an unoccupied iron responsive element site on the L-subunit mRNA which is then available for binding of the translation complex (58). This results in an increase in the expression of the L-subunit of ferritin with an increase in the labile iron pool.

8.6) Relationship between the soluble transferrin receptor and the red blood cell distribution width in the group of Kalafong patients with an iron transfer block

Different factors play a role in the anaemia of chronic disease including an iron transfer block (73). That the iron transfer block could be a contributing factor in the anaemia associated with chronic inflammation was shown for the group of Kalafong patients with an iron transfer block. A correlation was shown between an increase in soluble transferrin receptor with an increase in the red blood cell distribution width ($r = 0.79$, p-value < 0.0001) for the group of Kalafong patients with an iron transfer block. An increase in the soluble transferrin receptor is known to occur with a reduction in the

amount of iron reaching the red blood cell precursors (83). The resulting increase in the red blood cell distribution width occurs as a result of differences in the amount of haemoglobin in the red blood cells and the subsequent variation in the red blood cell's volume (88).

8.7) Cytokine levels of the iron transfer block subdivision of the Kalafong patients

When the pro-inflammatory immune status as reflected by C-reactive protein and neopterin was compared between the group of Kalafong patients with iron transfer block and the group of Kalafong patients without iron transfer block it was found that the group of Kalafong patients with iron transfer block showed a significantly higher level of pro-inflammatory activity. C-reactive protein was significantly higher (p-value = 0.0004) in the group of Kalafong patients with an iron transfer block (84.1 ± 83.2 mg/l; n = 25) compared to the group of Kalafong patients without an iron transfer block (14.5 ± 22.3 mg/l; n = 23). Neopterin was also significantly higher (p-value = 0.0004) in the group of Kalafong patients with an iron transfer block (31.7 ± 24.5 ng/ml; n = 25) compared to the group of Kalafong patients without an iron transfer block (9.2 ± 14.5 ng/ml; n = 23). Furthermore, it was found that an increase in neopterin correlated with a decrease in transferrin (r = 0.47, p-value = 0.019). Therefore with an increase in cellular immune activation (T-helper cell type-1 response) a decrease in transferrin was shown. A decrease in transferrin is characteristic of iron transfer block.

This pronounced pro-inflammatory immune status indicated by the significantly elevated C-reactive protein and neopterin levels for the group of Kalafong patients with iron transfer block was reflected in the cytokine profile of these patients. Cytokines have previously been shown to play a significant role in the establishment of an iron transfer block (56, 74, 75, 76, 77). Various cytokines are known to contribute to the

establishment and maintenance of an iron transfer block whereas some cytokines are known to play a major part in resolving the iron transfer block (78). Cytokines make use of different intracellular pathways but also overlapping pathways resulting in cross-talk between different cytokines where specific cytokines can augment or down-regulate the effects of other cytokines (34). Therefore, the establishment and the maintenance of an iron transfer block depend not only on the type of cytokines but also on the combination of these cytokines. In the group of Kalafong patients with an iron transfer block compared to the group of Kalafong patients with no iron transfer block the pro-inflammatory cytokines that were significantly higher included INF-γ, Il-6, Il-8 and Il-2. No significant increases were shown for Il-12 and GM-CSF in the group of Kalafong patients with iron transfer block compared to the group of Kalafong patients with no iron transfer block.

INF-γ was

- significantly higher (p-value = 0.0007) in the group of Kalafong patients with iron transfer block (14.8 ± 33.7 pg/ml; n = 24) compared to the group of Kalafong patients with no iron transfer block (16.5 ± 76.2 pg/ml; n = 23),
- significantly higher (p-value = 0.043) in the group of Kalafong patients with iron transfer block compared to the osteoarthritis patients (0.1 ± 0 pg/ml; n = 10) and
- not significantly different between the group of Kalafong patients with no iron transfer block and the osteoarthritis patients.

Il-6 was

- significantly higher (p-value = 0.002) in the group of Kalafong patients with iron transfer block (525.4 ± 1782.4 pg/ml; n = 25) compared to the group of Kalafong patients with no iron transfer block (453.1 ± 2025.5 pg/ml; n = 23),
- significantly higher (p-value = 0.0005) in the group of Kalafong patients with iron transfer block compared to the osteoarthritis patients (5 ± 2.1 pg/ml; n = 10) and
- not significantly different between the group of Kalafong patients with no iron transfer block and the osteoarthritis patients.

Il-8 was

- significantly higher (p-value = 0.0001) in the group of Kalafong patients with iron transfer block (321.1 ± 893.6 pg/ml; n = 25) compared to the group of Kalafong patients with no iron transfer block (89.4 ± 246.5 pg/ml; n = 23),
- significantly higher (p-value = 0.0007) in the group of Kalafong patients with iron transfer block compared to the osteoarthritis patients (18.9 ± 6.4; n = 10) and
- not significantly different between the group of Kalafong patients with no iron transfer block and the osteoarthritis patients.

Il-2 was

- not significantly different between the group of Kalafong patients with iron transfer block (11 ± 6.9 pg/ml; n = 25) and the group of Kalafong patients with no iron transfer block (9.6 ± 7.3 pg/ml; n = 23),
- significantly higher (p-value = 0.047) in the group of Kalafong patients with iron transfer block compared to the osteoarthritis patients (6.7 ± 4.9 pg/ml; n = 10) and
- not significantly different between the group of Kalafong patients with no iron transfer block and the osteoarthritis patients.

Il-12 was

- not significantly different between the group of Kalafong patients with iron transfer block (4 ± 3.4 pg/ml; n = 25) and the group of Kalafong patients with no iron transfer block (5.4 ± 4.3 pg/ml; n = 23),
- significantly higher (p-value = 0.0009) in the group of Kalafong patients with iron transfer block compared to the osteoarthritis patients (1.1 ± 1.3 pg/ml; n = 10) and
- significantly higher (p-value = 0.0001) in the group of Kalafong patients with no iron transfer block compared to the osteoarthritis patients.

GM-CSF was

- not significantly different between the group of Kalafong patients with iron transfer block (15.2 ± 48.6 pg/ml; n = 24) and the group of Kalafong patients with no iron transfer block (10.9 ± 17.4 pg/ml; n = 23),
- not significantly different between the group group of Kalafong patients with iron transfer block and the osteoarthritis patients (3.6 ± 6.2; n = 10) and
- marginally higher (p-value = 0.085) in the group of Kalafong patients with no iron transfer block compared to the osteoarthritis patients.

These pro-inflammatory cytokines could all contribute to the establishment and maintenance, either directly or indirectly, of the iron transfer block. The role of Il-6 in the establishment and maintenance of an iron transfer block is complicated. Il-6 is generally seen as a pro-inflammatory cytokine although Il-6 does not bring about NO production and can bring about an anti-inflammatory macrophage phenotype (40). Il-6 utilises the JAK/Stat signalling pathway involving the Janus family of tyrosine kinases (JAK kinases). Stimulation of this pathway by Il-6, similar to Il-1β, results in activation of the Stat3 transcription factor (105). Stat3 results in transcription of genes of inhibitory pathways, which brings about an anti-inflammatory macrophage phenotype (106). However, Il-6 possibly plays a role in the establishment of the iron transfer block by the stimulation of the secretion of hepcidin by hepatocytes (79). A major role for hepcidin has been proposed in causing an iron transfer block during an inflammatory reaction (79). Hepcidin results in an increase in iron retainment in macrophages and enterocytes

by decreasing the availability of the transmembrane protein, ferroportin, on the cellular membranes. Ferroportin is responsible for the efflux of iron from macrophages and enterocytes and thus when ferroportin is not available on the cell membrane less iron is released into the circulation. In the macrophage this will significantly contribute to the increased amounts of storage iron during an inflammatory reaction (79).

The pro-inflammatory cytokine, TNF-α, was not significantly different between the group of Kalafong patients with iron transfer block and the group of Kalafong patients with no iron transfer block, but marginally higher in the group of Kalafong patients with iron transfer block when compared to the osteoarthritis patients. TNF-α is able to mediate macrophage activation along one of two pathways. One pathway plays a role in wound repair and is characterised by the induction of insulin-like growth factor. The second pathway is involved in macrophage cytocidal activation and is characterised by the induction of the inducible form of nitric oxide synthase (iNOS). It is this second pathway, which would predominate during a pro-inflammatory immune reaction with the production of iNOS. However, TNF-α only activates this pathway in the presence of INF-γ whereas the first pathway can be activated by TNF-α without the presence of INF-γ (107). Therefore, TNF-α is perhaps redundant for the establishment and maintenance of an iron transfer block since INF-γ is the most potent activator of iNOS (40).

TNF-α was

- not significantly different between the group of Kalafong patients with iron transfer block (3.8 ± 2.9 pg/ml; n = 25) and the group of Kalafong patients with no iron transfer block (3.2 ± 1.9 pg/ml; n = 23),
- marginally higher (p-value = 0.071) in the group of Kalafong patients with iron transfer block compared to the osteoarthritis patients (2.5 ± 0.96 pg/ml; n = 10) and
- not significantly different between the group of Kalafong patients with no iron transfer block and the osteoarthritis patients.

The cytokine, Il-1β, was not significantly different between any of the groups. Il-1β is also generally known as a pro-inflammatory cytokine. However, Il-1β has been shown to bring about an anti-inflammatory macrophage phenotype. Il-1β utilises the JAK/Stat signalling pathway involving the Janus family of tyrosine kinases (JAK kinases). Stimulation of this pathway by Il-1β, similar to Il-6, results in activation of the Stat3 transcription factor (105). Stat3 results in transcription of genes of inhibitory pathways, which brings about an anti-inflammatory macrophage phenotype (40, 106). Therefore, it is very likely that Il-1β did not contribute to the establishment and maintenance of an iron transfer block in the Kalafong patients.

Il-1β was

- not significantly different between the group of Kalafong patients with iron transfer block (5.5 ± 10.3 pg/ml; n = 25), the group of Kalafong patients without iron transfer block (3.4 ± 6.1 pg/ml; n = 23) and the osteoarthritis patients (1.6 ± 3.3 pg/ml; n = 10).

The cytokine, Il-5, was the only T-helper cell type-2 cytokine that was significantly higher in the group of Kalafong patients with an iron transfer block compared to the group of Kalafong patients with no iron transfer block. Il-5 is, in essence, a T-helper cell type-2 cytokine, but belongs to the GM-CSF/Il-3 subgroup (89). In contrast to GM-CSF and Il-3 no effect on monocytes for Il-5 has been shown (90). However, it has been shown that Il-5, as for GM-CSF and Il-3, displayed proliferative effects on both microglia and macrophage cell lines (91). Furthermore, both Il-5 and Il-3 has been shown to bind and activate the GM-CSF receptor present on monocytes (44). It is therefore suggested that Il-5 could have contributed to the establishment of the iron transfer block.

Il-5 was

- significantly higher (p-value = 0.045) in the group of Kalafong patients with iron transfer block (4.2 ± 4.3 pg/ml; n = 25) compared to the group of Kalafong patients with no iron transfer block (2.3 ± 1.3 pg/ml; n = 23),
- marginally higher (p-value = 0.07) in the group of Kalafong patients with iron transfer block compared to the osteoarthritis patients (2.4 ± 1.6 pg/ml; n= 10) and
- not significantly different between the group of Kalafong patients with no iron transfer block and the osteoarthritis patients.

The T-helper cell type-2 cytokine, Il-10, was not significantly different between the group of Kalafong patients with iron transfer block and the group of Kalafong patients with no iron transfer block, but was significantly higher for both these groups compared to the osteoarthritis group. The anti-inflammatory cytokine, Il-10, results in decreased production of pro-inflammatory cytokines (transcriptional repression perhaps through the up-regulation of the formation of p50 homodimers of NF-κB and/or the expression of Bcl-3, which preferentially recruits p50 homodimers of NF-κB – negative effect on pro-inflammatory gene transcription) into the nucleus (41). Therefore, the role that Il-10 plays in the establishment and maintenance of the iron transfer block as an anti-inflammatory cytokine is perhaps not clear. However, in previous studies it has been shown that Il-10 can up-regulate the transferrin receptor on the cell membrane of the macrophage resulting in an increase in transferrin receptor-mediated uptake of iron (73, 78). Furthermore, has it been shown that Il-10 contributes to macrophage haemoglobin acquisition by stimulating the expression of the haemoglobin scavenger receptor, CD163 (78).

Il-10 was

- not significantly different between the group of Kalafong patients with iron transfer block (15.2 ± 19.9 pg/ml; n = 25) and the group of Kalafong patients with no iron transfer block (23.5 ± 68 pg/ml; n = 23),
- significantly higher (p-value = 0.005) in the group of Kalafong patients with iron transfer block compared to the osteoarthritis patients (2.7 ± 1.5 pg/ml; n = 10) and
- significantly higher (p-value = 0.014) in the group of Kalafong patients with no iron transfer block compared to the osteoarthritis patients.

The anti-inflammatory cytokine Il-4 is able to markedly suppress transcriptional activation of INF-γ responsive genes and the promoter sequences required for both INF-γ and Il-4 sensitivity are identical. INF-γ activates Stat1 and Il-4 activates Stat6, where Stat1 promotes transcription and Stat6 is inactive. Therefore, Il-4 appears to suppress INF-γ-inducible pro-inflammatory gene expression through the ability of Stat6 to compete with Stat1 for occupancy of promoter sites necessary for INF-γ-induced

transcriptional initiation (108). In the present study, Il-4 was neither higher in the group of Kalafong patients with iron transfer block, nor in the group of Kalafong patients with no iron transfer block compared to the osteoarthritis patients.

Il-4 was

- not significantly different between the group of Kalafong patients with iron transfer block (2.7 ± 1.9 pg/ml; n = 25), the group of Kalafong patients with no iron transfer block (2.2 ± 2 pg/ml; n = 23) and the osteoarthritis patients (2.5 ± 2.2 pg/ml; n = 10).

There was no significant difference for TGF-β between the group of Kalafong patients with iron transfer block and the group of Kalafong patients with no iron transfer block. However, TGF-β was significantly lower for both these groups when compared to the osteoarthritis patients. This significant increase of TGF-β in the osteoarthritis patients was discussed in a previous section.

TGF-β was

- not significantly different between the group of Kalafong patients with iron transfer block (10.4 ± 5.6 ng/ml; n = 24) and the group of Kalafong patients with no iron transfer block (12.8 ± 8.3 ng/ml; n = 23),
- significantly lower (p-value = 0.0001) in the group of Kalafong patients with iron transfer block compared to the osteoarthritis patients (18.3 ± 4.1 ng/ml; n = 10) and
- significantly lower (p-value = 0.016) in the group of Kalafong patients with no iron transfer block compared to the osteoarthritis patients.

The question now remains whether any relationship could be expected between specific cytokines and any of the serum iron markers or red blood cell indices. In the group of Kalafong patients with an iron transfer block no correlations was shown for any of the pro-inflammatory cytokines and serum iron markers or red blood cell indices. Although no direct role for any of the T-helper cell type-1 cytokines was shown, an increase in TGF-β (anti-inflammatory cytokine) correlated with an increase in transferrin (r = 0.48, p-value = 0.02). The opposite of what occurs with an iron transfer block.

8.8) Pro-hepcidin and caeruloplasmin levels for the iron transfer block subdivision

For pro-hepcidin there was no significant difference between the group of Kalafong patients with iron transfer block (194 ± 281 ng/ml; n = 25) and the group of Kalafong patients without iron transfer block (151.6 ± 44.7 ng/ml; n = 23). As was previously mentioned, pro-hepcidin levels not necessarily reflect the hepcidin levels. The pro-hepcidin/hepcidin relationship can only be established when a suitable commercial ELISA kit is available.

There was no significant difference for caeruloplasmin between the group of Kalafong patients with iron transfer block (0.44 ± 0.16 g/l; n = 23) and the group of Kalafong patients without iron transfer block (0.49 ± 0.14 g/l; n = 23).

8.9) In summary on the expression of the H-subunit and L-subunit of ferritin in the iron transfer block subdivision of the Kalafong patients

The expression of the H-subunit of ferritin in the bone marrow macrophage was marginally higher in the group of Kalafong patients with iron transfer block compared to the group of Kalafong patients with no iron transfer block. The expression of the L-subunit of ferritin in the bone marrow macrophage was not significantly different between the group of Kalafong patients with iron transfer block and the group of Kalafong patients with no iron transfer block. Furthermore, the expression of the H-subunit and L-subunit of ferritin in the cells of the erythron was not significantly different between the group of Kalafong patients with iron transfer block and the group of Kalafong patients with no iron transfer block. These findings were similar to the C-reactive protein and neopterin subdivisions. The cytokine profile of the iron transfer block subdivision was similar to that of the neopterin subdivision – a pro-inflammatory

T-helper cell type-1 immune response, but for a significant increase in the T-helper cell type-2 cytokine, Il-5.

No correlation was shown between the expression of the H-subunit and L-subunit of ferritin in the bone marrow macrophage and any of the serum iron markers or red blood cell indices in iron transfer block. However, correlations were shown between the expression of the H-subunit and L-subunit of ferritin in the cells of the erythron and red blood cell indices in iron transfer block. An increase in the H-subunit/L-subunit ratio in cells of the erythron was shown to correlate with a decrease in the mean corpuscular volume ($r = 0.67$, p-value = 0.0009) and a decrease in the mean corpuscular haemoglobin ($r = 0.56$, p-value = 0.008) in the group of Kalafong patients with an iron transfer block. An increase in the H-subunit/L-subunit ratio showed a possible increase in H-subunit rich ferritins. These H-subunit rich ferritins could have resulted in withholding of the iron from haemoglobin production in the cells of the erythron. Furthermore, an increase in the L-subunit of ferritin in the cells of the erythron was shown to correlate with an increase in the mean corpuscular volume ($r = 0.53$, p-value = 0.014) and an increase in the mean corpuscular haemoglobin ($r = 0.53$, p-value = 0.013) in the group of Kalafong patients with an iron transfer block. The expression of the L-subunit of ferritin has been shown to be closely related to the amount of intracellular iron. Therefore, the increase in the expression of the L-subunit of ferritin in the cells of the erythron could have indicated an increase in intracellular iron available for haemoglobin production.

9) INCREASE IN THE EXPRESSION OF THE H-SUBUNIT OF FERRITIN IN THE MACROPHAGES OF OSTEOARTHRITIS PATIENTS AND IMPLICATIONS

In the group of osteoarthritis patients the expression of the H-subunit of ferritin in the bone marrow macrophage was similarly increased as for the group of Kalafong patients

with elevated C-reactive protein and the group of Kalafong patients with elevated neopterin. This increase in the expression of the H-subunit of ferritin in the macrophage was found despite the osteoarthritis patients not showing any pronounced pro-inflammatory activity as reflected by their C-reactive protein and neopterin levels. Furthermore, no increases were found for any of the pro-inflammatory cytokines. The only cytokine that was significantly increased for the group of osteoarthritis patients was the anti-inflammatory cytokine TGF-β. In this section the possible role that an increase in the H-subunit of ferritin in the macrophage can play in iron metabolism and possibly iron transfer block in osteoarthritis is addressed.

9.1) Iron status of the osteoarthritis patients

In order to investigate the possible role of the H-subunit of ferritin in an iron transfer block the iron status of the osteoarthritis patients were determined by Prussian blue iron stains for bone marrow cores, serum iron markers and red blood cell indices.

9.1.1) Body iron stores as evaluated by Prussian blue iron stains of the bone marrow cores of the osteoarthritis patients

Prussian blue iron stains were done for only six of the ten osteoarthritis patients. Four of these osteoarthritis patients had reduced iron stores, one had absent iron stores and one had normal iron stores. The body iron stores for the osteoarthritis patients were markedly low.

9.1.2) Serum iron markers and determination of the iron status of the osteoarthritis patients

The results on the serum iron markers are given in small print followed by a summary on the serum iron markers in osteoarthritis patients.

- Serum iron was low-normal for the group of osteoarthritis patients (12.9 ± 5.9 µmol/l; n = 10) and not significantly different from the group of Kalafong patients with normal C-reactive protein and the group of Kalafong patients with normal neopterin.
- Serum transferrin was low-normal for the group of osteoarthritis patients (2 ± 0.57 g/l; n = 10) and not significantly different from the group of Kalafong patients with normal C-reactive protein and the group of Kalafong patients with normal neopterin.
- Percentage transferrin saturation was normal for the osteoarthritis patients (30.3 ± 14.4%; n = 10) and not significantly different from the group of Kalafong patients with normal C-reactive protein but significantly higher (p-value = 0.049) compared to the group of Kalafong patients with normal neopterin.
- Ferritin was normal for the osteoarthritis patients (94.2 ± 69.6 µg/l; n = 10) and not significantly different from the group of Kalafong patients with normal C-reactive protein and the group of Kalafong patients with normal neopterin.
- The transferrin/log ferritin ratio was significantly lower (p-value = 0.044) in the osteoarthritis patients (1.2 ± 0.58; n = 10) compared to the group of Kalafong patients with normal C-reactive protein and significantly higher (p-value = 0.005) compared to the group of Kalafong patients with elevated C-reactive protein. When compared to the neopterin subdivision the transferrin/log ferritin ratio was significantly higher (p-value = 0.008) in the osteoarthritis patients compared to the group of Kalafong patients with elevated neopterin and not significantly different from the group of Kalafong patients with normal neopterin.
- The soluble transferrin receptor was significantly lower (p-value = 0.0002) in the osteoarthritis patients (3.3 ± 1.4 µg/ml; n = 10) compared to the group of Kalafong patients with normal C-reactive protein and significatly lower (p-value = 0.0001) compared to the group of Kalafong patients with elevated C-reactive protein. Compared to the neopterin subdivision the soluble transferrin receptor in the osteoarthritis patients was significantly lower (p-value = 0.004) compared to the group of Kalafong patients with normal neopterin and significantly lower (p-value < 0.0001) compared to the group of Kalafong patients with elevated neopterin.
- The soluble transferrin receptor/log ferritin ratio was significantly lower (p-value = 0.015) in the osteoarthritis patients (2 ± 1.3; n = 10) compared to the group of Kalafong patients with normal C-reactive protein and significantly lower (p-value = 0.04) compared to the group of Kalafong patients with elevated C-reactive protein. Compared to the neopterin subdivision the soluble transferrin receptor/log ferritin ratio in the osteoarthritis patients was significantly lower (p-value = 0.045) compared to the group of Kalafong patients with normal neopterin and significantly lower (p-value = 0.042) compared to the group of Kalafong patients with elevated neopterin.

In summary on the serum iron markers of the osteoarthritis patients

The osteoarthritis patients showed low/reduced body iron stores and low-normal serum iron. In this situation a marked increase in transferrin would be expected. However, the osteoarthritis patients showed low-normal transferrin. Furthermore, the osteoarthritis patients showed a transferrin/log ferritin ratio significantly lower than that in the group of Kalafong patients with normal C-reactive protein but still significantly higher than that in the group of Kalafong patients with elevated C-reactive protein. The transferrin/log

ferritin ratio was lower for the group of osteoarthritis patients when compared to the group of Kalafong patients with normal C-reactive protein. This decrease in the transferrin/log ferritin ratio is characteristic of iron transfer block. A marked decrease for soluble transferrin receptor was seen in the osteoarthritis patients. The soluble transferrin receptor was abnormally low in the face of low serum iron in the osteoarthritis patients. The soluble transferrin receptor was not only significantly lower in the osteoarthritis patients than in the groups of Kalafong patients with normal C-reactive protein and normal neopterin but was also significantly lower than in the group of Kalafong patients with elevated C-reactive protein and elevated neopterin. Such a reduced soluble transferrin receptor is expected in patients with an iron transfer block. In addition, the soluble transferrin receptor/log ferritin ratio in the osteoarthritis patients was not only significantly lower than in the groups of Kalafong patients with normal C-reactive protein and normal neopterin, but also significantly lower than in the groups of Kalafong patients with elevated C-reactive protein and elevated neopterin.

The group of osteoarthritis patients thus displayed some characteristics that could be expected for patients with a combination of true iron deficiency and iron transfer block. These factors were low-normal serum iron, reduced transferrin/log ferritin ratio, reduced soluble transferrin receptor and reduced soluble transferrin receptor/log ferritin ratio.

9.1.3) Red blood cell indices of the osteoarthritis patients

The results on the red blood cell indices are given in small print followed by a summary on the red blood cell indices in osteoarthritis patients.

- The red blood cell count was low-normal for the osteoarthritis patients (4.8 ± 0.67 x 10^{12}/l; n = 9) and significantly higher (p-value < 0.0001) compared to the group of Kalafong patients with normal C-reactive protein and marginally higher (p-value = 0.057) compared to the group of Kalafong patients with normal neopterin.

- The haemoglobin was normal in the osteoarthritis patients (14.9 ± 1.5 g/dl; n = 10) and significantly higher (p-value < 0.0001) compared to the group of Kalafong patients with normal C-reactive protein and significantly higher (p-value = 0.001) compared to the group of Kalafong patients with normal neopterin.
- The haematocrit was normal in the osteoarthritis patients (0.45 ± 0.05 l/l; n = 10) and significantly higher (p-value < 0.0001) compared to the group Kalafong patients with normal C-reactive protein and significantly higher (p-value = 0.003) compared to the group of Kalafong patients with normal neopterin.
- The mean corpuscular volume was normal in the osteoarthritis patients (94.2 ± 5.7 fl; n = 9) and significantly higher (p-value = 0.002) compared to the group Kalafong patients with normal C-reactive protein and marginally higher (p-value = 0.082) compared to the group of Kalafong patients with normal neopterin.
- The mean corpuscular haemoglobin was normal in the osteoarthritis patients (31.1 ± 2.2 pg; n = 9) and significantly higher (p-value = 0.0002) compared to the group of Kalafong patients with normal C-reactive protein and marginally higher (p-value 0.053) compared to the group of Kalafong patients with normal neopterin.
- The mean corpuscular haemoglobin concentration was normal in the osteoarthritis patients (33 ± 1.2 g/dl; n = 9) and significantly higher (p-value = 0.0003) compared to the group of Kalafong patients with normal C-reactive protein and significantly higher (p-value = 0.03) compared to group of the Kalafong patients with normal neopterin.
- The red blood cell distribution width was normal in the osteoarthritis patients (12.9 ± 0.64%; n = 9) and significantly lower (p-value = 0.0004) compared to the group of Kalafong patients with normal C-reactive protein and significantly lower (p-value = 0.002) compared the group of Kalafong patients with normal neopterin.

In summary on the red blood cell indices of the osteoarthritis patients

The red blood cell production was low-normal for the osteoarthritis patients. This was most probably as a result of the low body iron stores and serum iron. None of the red blood cell indices indicated that insufficient amounts of iron were reaching the erythron for haemoglobin production.

9.1.4) Iron status of the osteoarthritis patients

When the results of the Prussian blue iron stains of the bone marrow core, the serum iron markers and the red blood cell indices were evaluated for each individual osteoarthritis patient (volume 2, chapter 6) an iron transfer block was shown for some of the osteoarthritis patients. For 40% (four of ten patients) of the osteoarthritis patients an iron transfer block was shown and for 60% (six of ten patients) no iron transfer block was shown. The most pronounced changes shown for the osteoarthritis patients characteristic of an iron transfer block were low-normal serum iron, reduced

transferrin/log ferritin ratio, reduced soluble transferrin receptor and reduced soluble transferrin receptor/log ferritin ratio. In addition, a decrease in transferrin was related to an increase in the red blood cell distribution width (r = 0.67, p-value = 0.05). This is characteristic for an iron transfer block.

9.2) Relationship between storage iron, bio-available iron, expression of the H-subunit and L-subunit of ferritin and red blood cell production in the osteoarthritis patients

The soluble transferrin receptor/transferrin complex is responsible for the acquiring of iron for various cell types and especially so for the cells of the erythron (85). In the group of osteoarthritis patients the soluble transferrin receptor was closely related to the transferrin levels (r = 0.79, p-value = 0.006), negatively related to the percentage transferrin saturation (r = 0.74, p-value = 0.014) and negatively related to the ferritin levels (r = 0.75, p-value = 0.013). Therefore, with a decrease in body iron (decrease in ferritin, decrease in transferrin saturation and increase in transferrin) the amount of soluble transferrin receptors was probably increased in an attempt by the erythron to acquire more iron.

Hepcidin (formed from pro-hepcidin) decreases ferroportin availability in cell membranes. Ferroportin transports iron out of cells and is the major iron transmembrane channel for the movement of iron from the cytosol to the blood in enterocytes and macrophages. As body iron increases, hepcidin is induced, which then inhibits the efflux of iron through ferroportin down-regulation (109). This blocks intestinal iron absorption and iron recycling from erythrocytes by macrophages. In this study pro-hepcidin was closely related to the serum iron in the group of osteoarthritis patients (r = 0.67, p-value = 0.034).

The expression of the H-subunit of ferritin in the cells of the erythron was closely related to the serum iron (r = 0.80, p-value = 0.031). This might further be suggestive of the role that this subunit plays in rapid turnover of iron in the cells of the erythron. Due to the H-subunit rich ferritin's more dynamic ability of iron uptake and release it would appear to be largely found in cells having high iron requirements for metabolic activities and a non-existent role in iron storage (96).

The H-subunit/L-subunit ratio in the bone marrow macrophages was closely related to the serum iron level (r = 0.82, p-value = 0.047) in the osteoarthritis patients. Therefore, with an increase in serum iron and body iron the macrophages responded by increasing the expression of the H-subunits relative to that of the L-subunits. It is known that the H-subunit to L-subunit ratio of a specific type of cell does not remain constant and the proportion of the H-subunits and L-subunits present in the ferritin shell changes during differentiation and in various pathological states (110, 111, 112, 113).

9.3) Possible role for the anti-inflammatory cytokine, transforming growth factor-β, in resolving the iron transfer block in osteoarthritis patients

The osteoarthrtitis patients had a relatively normal cytokine profile similar to the group of Kalafong patients with normal C-reactive protein and the group of Kalafong patients with normal neopterin. However, an increase in TGF-β was found for the osteoarthritis patients. TGF-β is an anti-inflammatory cytokine (41) and could have brought about an increase in soluble transferrin receptor and transferrin (both are decreased by pro-inflammatory cytokines). This was found in the osteoarthritis patients where an increase in TGF-β correlated with an increase in soluble transferrin receptor (r = 0.67, p-value = 0.034) and an increase in transferrin (r = 0.63, p-value = 0.05).

9.4) Cytokines and the expression of the H-subunit and L-subunit of ferritin in osteoarthritis patients

It is generally assumed that cytokines play a major role in the expression of the H-subunit of ferritin not only by the up-regulation of transcription but also by inducing secretion and ferritin aggregation (58, 59, 60). In the present study on the osteoarthritis patients some cytokines were shown to correlate with a decrease in the expression of the subunits of ferritin. An increase in Il-8 correlated with a decrease in the H-subunit of ferritin ($r = 0.81$, p-value = 0.026) and a decrease in the H-subunit/L-subunit ratio in the macrophage ($r = 0.84$, p-value = 0.037). An increase in Il-6 correlated with a decrease in the L-subunit of ferritin in the macrophage ($r = 0.85$, p-value = 0.034). This is consistent with the role that ferritin plays in inflammation with possibly first the up-regulation of specifically the H-subunit of ferritin followed by a decrease in the H-subunit and L-subunit as a result of an increase in haemosiderin formation or secretion of ferritin. An increase in Il-2 correlated with a decrease in the H-subunit of ferritin in the cells of the erythron ($r = 0.73$, p-value = 0.064). An increase in TNF-α ($r = 0.94$, p-value = 0.006) and an increase in Il-10 ($r = 0.85$, p-value = 0.03) correlated with a decrease in the L-subunit of ferritin in the cells of the erythron. This negative correlation between different cytokines and the decrease in the expression of the ferritin subunits might point to a role for cytokines in the possible decrease of the ferritin subunits in osteoarthritis patients.

9.5) Pro-hepcidin and caeruloplasmin levels for the osteoarthritis patients

Pro-hepcidin was not significantly different between the osteoarthritis patients (140.6 ± 30.2 ng/ml; $n = 10$) and any of the groups of Kalafong patients with elevated C-reactive protein, normal C-reactive protein, elevated neopterin and normal neopterin. However, in the group of osteoarthritis patients an increase in pro-hepcidin correlated with an increase in serum iron ($r = 0.67$, p-value = 0.034). This finding is similar to the results of

previous studies where it has been shown that the production of pro-hepcidin is regulated by serum iron (79). Caeruloplasmin was not significantly different between the osteoarthritis patients (0.45 ± 0.14 g/l; n = 10) and any of the groups of Kalafong patients with elevated C-reactive protein, normal C-reactive protein, elevated neopterin and normal neopterin.

9.6) In summary on the osteoarthritis patients

The pro-inflammatory indicators, C-reactive protein and neopterin, of the osteoarthritis patients were not significantly different from the groups of Kalafong patients with no overt pro-inflammatory activity. The cytokine profiles of the osteoarthritis patients were also similar to the groups of Kalafong patients with no overt pro-inflammatory activity except for the significant increase in TGF-β levels in the osteoarthritis patients. However, the osteoarthritis patients had some serum iron markers characteristic of an iron transfer block including low-normal serum iron, reduced transferrin/log ferritin ratio, reduced soluble transferrin receptor and reduced soluble transferrin receptor/log ferritin ratio. In addition, a decrease in transferrin was related to an increase in the red blood cell distribution width. However, an increase in TGF-β correlated with an increase in soluble transferrin receptor and an increase in transferrin, both opposite for what occurs with an iron transfer block.

The expression of the H-subunit of ferritin in the bone marrow macrophage in the osteoarthritis patients was showed to be increased, similar to the group of Kalafong patients with a pronounced increase in pro-inflammatory activity. However, it is thought that this increase in the expression of the H-subunit of ferritin in the macrophage was caused by the increase in TGF-β in the osteoarthritis patients. A very interesting finding for the group of osteoarthritis patients was the correlation of the decrease in the expression of the H-subunit and L-subunit of ferritin with an increase in some cytokines.

Cytokines has been shown, in previous studies, to not only induce the transcription of mostly the H-subunit of ferritin, but also to cause an increase in the formation of haemosiderin and the secretion of ferritin (58, 59, 60).

In this chapter the results were discussed in five main sections a) subdivision of the patients according to their immune status where the Kalafong patients were subdivided firstly based on C-reactive protein levels and secondly on neopterin levels, b) the expression of the H-subunit and L-subunit of ferritin in the bone marrow macrophage and cells of the erythron in patients with a pro-inflammatory immune status where the expression of the H-subunit and L-subunit of ferritin was investigated in the groups of Kalafong patients with high C-reactive protein and high neopterin, respectively, c) the prevalence of iron transfer block in patients with a pro-inflammatory immune status where the iron status of the Kalafong patients and the possible role that the H-subunit and L-subunit of ferritin in macrophages and cells of the erythron play in iron transfer block were investigated, d) the expression of the H-subunit and L-subunit of ferritin in a group of Kalafong patients with iron transfer block and a group of Kalafong patients with no iron transfer block where the possible role that the H-subunit and L-subunit of ferritin in macrophages and cells of the erythron play in the establishment and maintenance of iron transfer block were investigated and finally e) a section on the osteoarthritis patients where the expression of the H-subunit and L-subunit of ferritin in macrophages and cells of the erythron were investigated. The next and final chapter will present a summation of the results, conclusions and suggestions for further study.

10) References

1) Chasteen ND. Ferritin. Uptake, storage, and release of iron. Metal Ions in Biological Systems 1998; 35: 479-514.

2) Arosio P, Levi S, Santambrogio P, Cozzi A, Luzzago A, Cesareni G *et al.* Structural and functional studies of human ferritin H and L chains. Current Studies in Hematology and Blood Transfusion 1991; 58: 127-131.

3) Chiancone E, Stefanini S. Heterogeneity of ferritin. I. Structural and functional aspects. In: Albertini A, Arosio P, Chiancone E, Drysdale J editors. Ferritins and isoferritins as biochemical markers. Amsterdam: Elsevier Science Publishers; 1984. p. 23-32.

4) Harrison PM, Arosio P. The ferritins: molecular properties, iron storage function and cellular regulation. Biochimica *et* Biophysica Acta 1996; 1275: 161-203.

5) Rogers J, Lacroix L, Durmowitz G, Kasschau K, Andriotakis J, Bridges KR. The role of cytokines in the regulation of ferritin expression. Advances in Experimental Medicine and Biology 1994; 356: 127-132.

6) Wixom RL, Prutkin L, Munro HN. Hemosiderin: Nature, Formation, and Significance. International Reviews in Experimental Pathology 1980; 22: 193-225.

7) Surguladze N, Patton S, Cozzi A, Fried MG, Connor JR. Characterization of nuclear ferritin and mechanism of translocation. Biochemical Journal 2005; 388: 731-740.

8) Levi S, Corsi B, Bosisio M, Invernizzi R, Volz A, Sanford D *et al.* A human mitochondrial ferritin encoded by an intronless gene. Journal of Biological Chemistry 2001; 270(27): 24437-24440.

9) Meyron-Holtz EG, Fibach E, Gelvan D, Konijn AM. Binding and uptake of exogenous isoferritins by cultured human erythroid precursor cells. British Journal of Haematology 1994; 86: 635-641.

10) Broxmeyer HE, Gentile P, Listowsky I, Cavanna F, Feickert HJ, Dorner MH *et al.* Acidic isoferritins in the regulation of hematopoiesis in vitro and in vivo. In: Albertini A, Arosio P, Chiancone E, Drysdale J editors. Ferritins and isoferritins as biochemical markers. Amsterdam: Elsevier Science Publishers; 1984. p. 97-111.

11) Torti SV, Torti FM. Iron and ferritin in inflammation and cancer. Advances in Inorganic Biochemistry 1994; 10: 119-137.

12) Tsuji Y, Ayaki H, Whitman SP, Morrow CS, Torti SV, Torti FM. Coordinate transcriptional and translational regulation of ferritin in response to oxidative stress. Molecular and Cellular Biology 2000; 20(16): 5818-5827.

13) Kakhlon O, Gruenbaum Y, Cabantchik ZI. Repression of ferritin expression increase the labile iron pool, oxidative stress, and short-term growth of human erythroleukemia cells. Blood 2001; 97(9): 2853-2871.

14) Bevilacqua MA, Costanzo F, Buonaguro L, Cimino F. Ferritin H and L mRNAs in human neoplastic tissues. Italian Journal of Biochemistry 1988; 37(1): 1-7.

15) Connor JR, Snyder BS, Arosio P, Loeffler DA, LeWitt P. A quantitative analysis of isoferritins in select regions of aged, parkinsonian, and alzheimer's diseased brains. Journal of Neurochemistry 1995; 65: 717-724.

16) Higgy NA, Salicioni AM, Russo IH, Zhang PL, Russo J. Differential expression of human ferritin H chain gene in immortal human breast epithelial MCF-10F cells. Molecular Carcinogenesis 1997; 20(4): 332-339.

17) Jones BM, Worwood M, Jacobs A. Serum ferritin in patients with cancer: determination with antibodies to HeLa cell and spleen ferritin. Clinica Chimica Acta 1980; 106: 203-214.

18) Lin F, Girotti AW. Elevated ferritin production, iron containment, and oxidant resistance in hemin-treated leukaemia cells. Archives of Biochemistry and Biophysics 1997; 346(1): 131-141.

19) Miller LL, Miller SC, Torti SV, Tsuji Y, Torti FM. Iron-independent induction of ferritin H chain by tumor necrosis factor. Proceedings of the National Academy of Sciences of the United States of America 1991; 88(11): 4946-4950.

20) Tripathi PK, Chatterjee SK. Elevated expression of ferritin H-chain mRNA in metastatic ovarian tumor. Cancer Investigation 1996; 14(6): 518-526.

21) Vernet M, Renversez JC, Lasne Y, Revenant MC, Charlier-de-Bressing C, Guillemin C *et al.* Comparison of six serum ferritin immunoassays and isoferritin spectrotypes in malignancies. Annales de Biologie Clinique 1995; 53: 419-427.

22) Whittaker D, Torrance JD, Kew MC. Isolation of ferritin from human hepatocellular carcinoma. Scandinavian Journal of Haematology 1984; 33(5): 432-439.

23) Rosalki SB. C-reactive protein. International Journal of Clinical Practice 2001; 55(4): 269-270.

24) Volanakis JE. Human C-reactive protein: expression, structure and function. Molecular Immunology 2001; 38(2-3): 189-197.

25) Black S, Kushner I, Samols D. C-reactive protein. Journal of Biological Chemistry 2004; 279(47): 48487-48490.

26) Marnell L, Mold C, Du Clos TW. C-reactive protein: ligands, receptors and role in inflammation. Clinical Immunology 2005; 117(2): 104-111.

27) Murr C, Widner B, Wirleitner B, Fuchs D. Neopterin as a marker for immune system activation. Current Drug Metabolism 2002; 3:175-187.

28) Huber C, Batchelor JR, Fuchs D, Hausen A, Lang A, Niederwieser D *et al.* Immune response-associated production of neopterin. Journal of Experimental Medicine 1984; 160: 310-316.

29) Sghiri R, Feinberg J, Thabet F, Dellagi K, Boukadida J, Casanova AB *et al.* Gamma interferon is dispensable for neopterin production. Clinical and Diagnostic Laboratory Immunology 2005; 12(12): 1437-1441.

30) Sheldon J, Riches PG, Soni N, Jurges E, Gore M, Dadian G *et al.* Plasma neopterin as an adjunct to C-reactive protein in assessment of infection. Clinical Chemistry 1991; 37(12): 2038-2042.

31) Mosser DM. The many faces of macrophage activation. Journal of Leukocyte Biology 2003; 73: 209-212.

32) McGrath MS, Kodelja V. Balanced macrophage activation hypothesis: a biological model for development of drugs targeted at macrophage functional states. Pathobiology 1999; 67: 277-281.

33) Correll PH, Morrison AC, Lutz MA. Receptor tyrosine kinases and the regulation of macrophage activation. Journal of Leukocyte Biology 2004; 75: 731-737.

34) Ohmori Y, Hamilton TA. Regulation of macrophage gene expression by T-cell derived lymphokines. Pharmaco Therapy 1994; 63: 235-264.

35) Montavani A, Sica A, Locati M. New vistas on macrophage differentiation and activation. European Journal of Immunology 2007; 37: 14-16.

36) Duffield JS. The inflammatory macrophage: a story of Jekyll and Hyde. Clinical Science 2003; 104: 27-38.

37) Keshav S, Chung L-P, Gordon S. Macrophage products in inflammation. Diagnostic Microbiology and Infectious Diseases 1990; 13: 439-447.

38) Bogdan C, Nathan C. Modulation of macrophage function by transforming growth factor-β, interleukin-4, and interleukin-10. Annals of the New York Academy of Sciences 1993; 685: 713-739.

39) Stoy N. Macrophage biology and pathobiology in the evolution of immune responses: a functional analysis. Pathobiology 2001; 69: 179-211.

40) Mills CD. Macrophage arginine metabolism to ornithine/urea or nitric oxide/citrulline: a life or death issue. Critical Reviews in Immunology 2001; 21(4): 399-426.

41) Butchar JP, Parsa KVL, Marsh CB, Tridandapani S. Negative regulators of Toll-like receptor 4-mediated macrophage inflammatory response. Current Pharmaceutical Design 2006; 12: 4143-4153.

42) Ashcroft GS. Bidirectional regulation of macrophage function by TGF-β. Microbes and Infection 1999; 1: 1275-1282.

43) Wahl SM, McCartney-Francis N, Allen JB, Dougherty EB, Dougherty SF. Macrophage production of TGF-β and regulation by TGF-β. Annals of the New York Academy of Sciences 1990; 593: 188-196.

44) Woodcock JM, Bagley CJ, Lopez AF. The functional basis of granulocyte-macrophage colony stimulating factor, interleukin-3 and interleukin-5 receptor activation, basic and clinical implications. International Journal of Biochemistry and Cell Biology 1999; 31: 1017-1025.

45) Fleetwood AJ, Cook AD, Hamilton JA. Functions of granulocyte-macrophage colony-stimulating factor. Critical Reviews in Immunology 2005; 25(5): 405-428.

46) Blom AB, van der Kraan PM, van den Berg WB. Cytokine targeting in osteoarthritis. Current Drug Targets 2007; 8: 283-292.

47) Leheita O, Abed Elrazek NY, Younes S, Mahmoud AZ. Lymphocyte subsets in osteoarthritis versus rheumatoid arthritis. Egyptian Journal of Immunology 2005; 12(2): 113-124.

48) Rollin R, Marco F, Jover JA, Garcia-Asenjo JA, Rodriguez L, Lopez-Duran L *et al.* Early lymphocyte activation in the synovial microenvironment in patients with osteoarthritis: comparison with rheumatoid arthritis patients and healthy controls. Rheumatology International 2008; 28(8): 757-764.

49) Zangerle PF, De Groote D, Lopez M, Meuleman RJ, Vrindts Y, Fauchet F *et al.* Direct stimulation of cytokines (Il-1 beta, TNF-alpha, Il-6, Il-2, IFN-gamma and GM-CSF) in whole blood: II. Application to rheumatoid arthritris and osteoarthritis. Cytokine 1992; 4(6): 568-572.

50) Roman-Blas JA, Stokes DG, Jimenez SA. Modulation of TGF-β signaling by proinflammatory cytokines in articular cartilage. Osteoarthritis and Cartilage 2007; 15: 1367-1377.

51) Iannone F, Lapadula G. The pathophysiology of osteoarthritis. Aging Clinical and Experimental Research 2003; 15(5): 364-372.

52) Blaney-Davidson EN, van der Kraan PM, van den Berg WB. TGF-β and osteoarthritis. Osteoarthritis and Cartilage 2007; 15: 597-604.

53) Miyazaki E, Kato J, Kobune M, Okumura K, Sasaki K, Shintani N *et al.* Denatured H-ferritin subunit is a major constituent of haemosiderin in the liver of patients with iron overload. Gut 2002; 50(3): 413-419.

54) Ruggeri G, Santambrogio P, Bonfiglio, Levi S, Bugari G, Verardi R *et al.* Antibodies for denatured human H-ferritin stain only reticuloendothelial cells within the bone marrow. British Journal of Haematology 1992; 81: 118-124.

55) Invernezzi R, Cazzola M, De Fazio P, Rosti V, Ruggeri G, Arosio P. Immunocytochemical detection of ferritin in human bone marrow and peripheral blood cells using monoclonal antibodies specific for the H and L subunit. British Journal of Haematology 1990; 76(30): 427-432.

56) Alvarez-Hernández X, Licéaga J, McKay IC, Brock JH. Induction of hypoferremia and modulation of macrophage iron metabolism by tumor necrosis factor. Laboratory Investigation 1989; 61(3): 319-322.

57) Piñero DJ, Hu J, Cook BM, Scaduto Jr RC, Connor JR. Interleukin-1β increases binding of the iron regulatory protein and the synthesis of ferritin by increasing the labile iron pool. Biochimica *et* Biophysica Acta 2000; 1497: 279-288.

58) Torti FM, Torti SV. Regulation of ferritin genes and protein. Blood 2002; 99(10): 3505-3516.

59) Alvarez-Hernández X, Felstein MV, Brock JH. The relationship between iron release, ferritin synthesis and intracellular iron distribution in mouse peritoneal

macrophages. Evidence for a reduced level of metabolically available iron in elicited macrophages. Biochimica *et* Biophysica Acta 1986; 886: 214-222.

60) Savarino A, Pescarmona GP, Boelaert JR. Iron metabolism and HIV infection: reciprocal interactions with potentially harmful consequences. Cell Biochemistry and Function 1999; 17: 279-287.

61) Picard V, Renaudie F, Porcher C, Hentze MW, Grandchamp B, Beaumont C. Overexpression of the ferritin H subunit in cultured erythroid cells changes the intracellular iron distribution. Blood 1996; 87(5): 2057-2064.

62) Festa M, Ricciardelli G, Mele G, Pietropaolo C, Ruffo A, Colonna A. Overexpression of H ferritin and up-regulation of iron regulatory protein genes during differentiation of 3T3-L1 pre-adipocytes. Journal of Biological Chemistry 2000; 275(47): 36708-36712.

63) Marziali G, Perrotti E, Ilari R, Testa U, Coccia EM, Battistini A. Transcriptional regulation of the ferritin heavy-chain gene: the activity of the CCAAT binding factor NF-Y is modulated in heme-treated Friend leukemia cells and during monocyte-to-macrophage differentiation. Molecular and Cellular Biology 1997; 17(3): 1387-1395.

64) Vanlandingham JW, Levenson CW. Effect of retinoic acid on ferritin H expression during brain development and neuronal differentiation. Nutritional Neuroscience 2003; 6(1): 39-45.

65) Bevilacqua MA, Faniello MC, D'Agostino P. Transcriptional activation of the H-ferritin gene in differentiated Caco-2 cells parallels a change in the activity of the nuclear factor Bbf. Biochemical Journal 1995; 311(Pt 3): 769-773.

66) Zermati Y, Fichelson S, Valensi F, Freyssinier JM, Rouyer-Fessard P, Cramer E *et al.* Transforming growth factor inhibits erythropoiesis by blocking proliferation and accelerating differentiation of erythroid progenitors. Experimental Hematology 2000; 28(8): 885-894.

67) Lo J, Hurta RAR. Transforming growth factor β_1 selectively regulates ferritin gene expression in malignant H-ras-transformed fibrosarcoma cell lines. Biohemistry and Cell Biology 2000; 78(4): 527-535.

68) Shterman N, Kupfer B, Moroz C. Comparison of transferrin receptors, iron content and isoferritn profile in normal and malignant human breast cell lines. Pathobiology 1991; 59(1): 19-25.

69) Yang DC, Wang F, Elliott RL, Head JF. Expression of transferrin receptor and ferritin H-chain mRNA are associated with clinical and histopathological prognostic indicators in breast cancer. Anticancer Research 2001; 21(1B): 541-549.

70) Wu KJ, Polack A, Dalla-Favera R. Coordinated regulation of iron-controlling genes, H-ferritin and IRP-2, by c-MYC. Science 1999; 283(5402): 676-679.

71) Babitt JL, Huang FW, Xia Y, Sidis Y, Andrews NC, Lin HY. Modulation of bone morphogenetic protein signaling *in vivo* regulates systemic iron balance. Journal of Clinical Investigation 2007; 117(7): 1933-1939.

72) Wang R-H, Li C, Xu X, Zheng Y, Xiao C, Zerfas P. A role of SMAD4 in iron metabolism through the positive regulation of hepcidin expression. Cell Metabolism 2005; 2: 399-409.

73) Weiss G, Goodnough LT. Anemia of chronic disease. New England Journal of Medicine 2005; 352(10): 1011-1023.

74) Finch CA, Huebers HA, Cazzola M, Bergamaschi G, Bellotti V. Storage iron. In: Albertini A, Arosio P, Chiancone E, Drysdale J editors. Ferritins and isoferritins as biochemical markers. Amsterdam: Elsevier Science Publishers; 1984. p. 3-21.

75) Lipschitz DA, Simon MO, Lynch SR, Dugard J, Bothwell TH, Charlton RW. Some factors affecting the release of iron from reticuloendothelial cells. British Journal of Haematology 1971; 21: 289-303.

76) Worwood M. Ferritin. Blood Reviews 1990; 4: 259-269.

77) Fahmy M, Young SP. Modulation of iron metabolism in monocyte cell line U937 by inflammatory cytokines: changes in transferrin uptake, iron handling and ferritin mRNA. Biochemical Journal 1993; 296: 175-181.

78) Ludwiczek S, Aigner E, Theurl I, Weiss G. Cytokine-mediated regulation of iron transport in human monocytic cells. Blood 2003; 101(10): 4148-4154.

79) Ganz T. Hepcidin in iron metabolism. Current Opinion in Hematology 2004; 11: 251-254.

80) Deicher R, Hörl WH. New insights into the regulation of iron homeostasis. European Journal of Clinical Investigation 2006; 36: 301-309.

81) Sherwood RA, Pippard MJ, Peters TJ. Iron homeostasis and the assessment of iron status. Annals of Clinical Biochemistry 1998; 35: 693-708.

82) Charlton RW, Bothwell TH. Definition, prevalence and prevention of iron deficiency. Clinics in Haematology 1982; 11(2): 309-325.

83) Mclintock LA, Fitzsimons EJ. Erythroblast iron metabolism in sideroblastic and sideropenic states. Hematology 2002; 7(3): 189-195.

84) Baynes RD. Iron deficiency. In: Brock JH, Halliday JW, Pippard MJ, Powell LW editors. Iron metabolism in health and disease. London: W.B. Saunders Company Ltd; 1994. p. 189-225.

85) Brittenham GM. The red cell cycle. In: Brock JH, Halliday JW, Pippard MJ, Powell LW editors. Iron metabolism in health and disease. London: W.B. Saunders Company Ltd; 1994. p. 31-62.

86) Harford JB, Rouault TA, Klausner RD. The control of cellular iron homeostasis. In: Brock JH, Halliday JW, Pippard MJ, Powell LW editors. Iron metabolism in health and disease. London: W.B. Saunders Company Ltd; 1994. p. 123-149.

87) Brock JH. Iron in infection, immunity, inflammation and neoplasia. In: Brock JH, Halliday JW, Pippard MJ, Powell LW editors. Iron metabolism in health and disease. London: W.B. Saunders Company Ltd; 1994. p. 353-389.

88) Uchida T. Change in red blood cell distribution width with iron deficiency. Clinical and Laboratory Haematology 1989; 11(2): 117-121.

89) Scott CL, Begley CG. The beta common chain (βc) of the granulocyte-colony stimulating factor, interleukin-3 and interleukin-5 receptors. International Journal of Biochemistry and Cell Biology 1999; 31: 1011-1015.

90) Miyajima A, Mui AL, Ogorochi T, Sakamaki K. Receptors for granulocyte-macrophage colony-stimulating factor, interleukin-3, and interleukin-5. Blood 1993; 82: 1960-1974.

91) Ringheim GE. Mitogenic effects of interleukin-5 on microglia. Neuroscience Letters 1995; 201(2): 131-134.

92) Pieracci FM, Barie PS. Diagnosis and management of iron-related anemias in critical illness. Critical Care Medicine 2006; 34(7): 1898-1905.

93) Fuchs D, Hausen A, Reibnegger G, Werner ER, Werner-Felmayer G, Dierich MP *et al.* Immune activation and the anaemia associated with chronic inflammatory disorders. European Journal of Haematology 1991; 46: 65-70.

94) Jongen-Lavrencic M, Peeters HRM, Vreugdenhil G, Swak AJG. Interaction of inflammatory cytokines and erythropoietin in iron metabolism and erythropoiesis in anaemia of chronic disease. Clinical rheumatology 1995; 14(5): 519-525.

95) Jurado RL. Iron, infections, and anemia of inflammation. Clinical Infectious Diseases 1997; 25: 888-895.

96) Cazzola M, Dezza L, Bergamaschi G, Barosi G, Bellotti V, Caldera D *et al.* Biologic and clinical significance of red cell ferritin. Blood 1983; 62(5): 1078-1087.

97) Perkins S. Diagnosis of anaemia. In: Kjeldsberg CR editor. Practical diagnosis of hematologic disorders. Chicago IL: American Society for Clinical Pathology Press; 2006. p. 1-16.

98) Gelvan D, Fibach E, Meyron-Holtz EG, Konijn AM. Ferritin uptake by human erythroid precursors is a regulated iron uptake pathway. Blood 1996; 88(8): 3200-3207.

99) Coccia EM, Profita V, Fiorucci G, Romeo G, Affabris E, Testa U *et al.* Modulation of ferritin H-chain expression in Friend erythroleukemia cells: transcriptional and translational regulation by hemin. Molecular and Cellular Biology 1992; 12(7): 3015-3022.

100) Wagstaff M, Worwood M, Jacobs A. Iron and isoferritins in iron overload. Clinical Science 1982; 62(5): 529-540.

101) Speyer BE, Fielding J. Ferritin as a cytosol iron transport intermediate in human reticulocytes. British Journal of Haematology 1979; 42: 255-267.

102) Ganz T. Hepcidin, a key regulator of iron metabolism and mediator of anemia of inflammation. Blood 2003; 102: 783-788.

103) Sharp P. The molecular basis of copper and iron interactions. Proceedings of the Nutrition Society 2004; 63: 563-569.

104) Konijn AM, Meyron-Holtz EG, Fibach E, Gelvan D. Cellular ferritin uptake: a highly regulated pathway for iron assimilation in human erythroid precursor cells. Advances in Experimental Medicine and Biology 1994; 356: 189-197.

105) Tietzel I, Mosser DM. The modulation of macrophage activation by tyrosine phosphorylation. Frontiers in Bioscience 2002; 7: d1494-d1502.

106) Lang R. Tuning of macrophage responses by Stat3-inducing cytokines: molecular mechanisms and consequences in infection. Immunobiology 2005; 210: 63-76.

107) Winston BW, Krein PM, Mowat C, Huang Y. Cytokine-induced macrophage differentiation: a tale of 2 genes. Clinical and Investigative Medicine 1999; 22(6): 236-255.

108) Hamilton TA, Ohmori Y, Tebo JM, Kishore R. Regulation of macrophage gene expression by pro- and anti-inflammatory cytokines. Pathobiology 1999; 67: 241-244.

109) Hugman A. Hepcidin: an important new regulator of iron homeostasis. Clinical and Laboratory Haematology 2006; 28: 75-83.

110) Arosio P, Yokota M, Drysdale JW. Structural and immunological relationships of isoferritins in normal and malignant cells. Cancer Research 1976; 36: 1735-1739.

111) Boyd D, Vecoli C, Belcher DM, Jain SK, Drysdale JW. Structural and functional relationships of human ferritin H and L chains deduced from cDNA clones. Journal of Biological Chemistry 1985; 260(21): 11755-11761.

112) Ponka P, Beaumont C, Richardson DR. Function and regulation of transferrin and ferritin. Seminars in Hematology 1998; 35(1): 35-54.

113) Theil EC. The ferritin family of iron storage proteins. Advances in Enzymology and Related Areas in Molecular Biology 1990; 63: 421-449.

CHAPTER 5

FINAL SUMMARY AND CONCLUSIONS

The primary aim of the present study was to quantitatively measure the expression of the H-subunit and L-subunit of ferritin in the bone marrow macrophage and cells of the erythron in patients with chronic immune stimulation – more specifically chronic T-helper cell type-1 stimulation. The expression of the H-subunit and L-subunit of ferritin has not previously been measured quantitatively in the bone marrow macrophage and cells of the erythron in relation to patients' immune status. A second aim was to investigate the possible role that the expression of the H-subunit and L-subunit of ferritin may have in the establishment and maintenance of an iron transfer block in patients with chronic immune stimulation.

The study subjects included 48 patients with chronic diseases from the Department of Internal Medicine, Kalafong Hospital and 10 patients with osteoarthritis, scheduled for hip replacement at the Department of Orthopaedics, Pretoria Academic Hospital. Bone marrow and blood samples were collected from each patient. The diagnoses of the patients from Kalafong Hospital were diverse and resulted in an extremely heterogenous group of patients. For the purpose of this study the immune status and iron status were used to group these patients.

The first objective of the study was to subdivide patients according to their immune status. Both neopterin and C-reactive protein levels are often used to assess the pro-

inflammatory status of patients. The Kalafong patients were thus subdivided, firstly based on C-reactive protein levels and secondly on neopterin levels. Although a significant correspondence was seen between the patients in whom high C-reactive protein and patients in whom high neopterin levels were recorded, it was found that there were patients in whom neopterin levels gave a different picture in terms of their inflammatory status from that assumed from their C-reactive protein values. This, for reasons explained in the relevant sections of the discussion, was not an unexpected finding. In view of potential subtle differences in immune status, the subdivision according to C-reactive protein and that according to neopterin were henceforth tested independently and were, despite the large overlap in patients, referred to as the C-reactive protein and neopterin groups or subdivisions.

The pro-inflammatory status of the C-reactive protein and neopterin subdivisions was subsequently examined by their cytokine profiles. The cytokine profiles were investigated in terms of the macrophage phenotype-associated cytokines, i.e., those related to the classically activated macrophage which is an effector in T-helper cell type-1 cellular immune responses, those related to the type-2 or anti-inflammatory macrophage that preferentially effects T-helper cell type-2 humoral responses, and those related to the alternatively activated macrophage predominantly involved in immunosuppression and tissue repair. The cytokine profiles confirmed that the subdivisions according to high C-reactive protein and high neopterin, respectively, did represent patient groups with high pro-inflammatory activity.

The osteoarthritis group showed no pronounced pro-inflammatory activity, similar to the group of Kalafong patients with normal C-reactive protein and the group of Kalafong patients with normal neopterin, but in contrast to these groups the osteoarthritis patients had a significantly higher plasma TGF-β level. The high TGF-β level in the

osteoarthritis group is not unexpected since TGF-β has, for instance, been shown to play an anabolic role in cartilage formation and to modulate cell and tissue responses to injury (1). TGF-β has, in addition, been shown to play a role in cell proliferation, differentiation, apoptosis and migration and is, despite its ability to contribute to fibrosis and osteophyte formation, sometimes used as a therapeutic tool in osteoarthritis (1). In view of their particular cytokine profile, the osteoarthritis patients were, for further analyses, subsequently treated as a separate group.

The expression of the H-subunit and L-subunit of ferritin in the bone marrow macrophage and cells of the erythron in patients with chronic pro-inflammatory activity, i.e., immune activity related to the classically activated macrophage was investigated separately for the subdivisions of Kalafong patients according to high C-reactive protein and high neopterin. The osteoarthritis patient group was treated as separate. The Kalafong patients with chronic immune stimulation, the subdivision according to C-reactive protein and that according to neopterin levels, showed similar changes in expression of the H-subunit and L-subunit of ferritin. The one major difference from normal found in expression of the ferritin subunits in the patient groups with overt pro-inflammatory activity was that of a significantly higher H-subunit expression in the macrophage of the bone marrow. The expression of the L-subunit in the bone marrow macrophage in the groups of Kalafong patients with high pro-inflammatory activity did not differ markedly from those with normal immune activity. The H-subunit/L-subunit ratio in the macrophage was also higher in the groups of Kalafong patients with pronounced pro-inflammatory activity possibly reflecting an increase in H-subunit rich isoferritins. These findings of increased H-subunit, but normal L-subunit expression of ferritin in the macrophage of the bone marrow are in line with previous indications that pro-inflammatory cytokines have the ability to modulate ferritin expression through both transcriptional and translational mechanisms, but that it is mostly the expression of the

H-subunit of ferritin that is increased by pro-inflammatory cytokines (2). From a functional point of view the observed increase in the expression of the H-subunit of ferritin in inflammatory conditions could have a physiological advantage as it may offer protection against increased oxidative onslaughts to the cell. The latter statement is based on the fact that pro-inflammatory conditions stimulate the production of reactive oxygen species (3) and that the H-subunit of ferritin can offer protection against oxidative damage through the withdrawal of iron (4).

There were no significant differences between the pro-inflammatory and normal Kalafong groups for either the H-subunit or L-subunit expression in the cells of the erythron. However, in the group of Kalafong patients with elevated neopterin the H-subunit/L-subunit ratio in the cells of the erythron was higher than in the group of Kalafong patients with normal neopterin. This could indicate that the expression of the H-subunit of ferritin in the cells of the erythron might be influenced by cytokines, but not to the same extent as for the macrophage. The cells of the erythron also handle large amounts of iron, but they do not play the same major role in the storage of iron as the macrophage.

When the expression of the subunits was examined in the osteoarthritis patients, a somewhat surprising observation was made. As previously discussed, the pro-inflammatory status of the osteoarthritis group was similar to that of the Kalafong patients with normal inflammatory status whether examined by C-reactive protein, neopterin or pro-inflammatory cytokines. The only marked cytokine difference from normal was seen in their TGF-β levels that were significantly higher in the group of osteoarthritis patients than in the other groups. However, when the ferritin subunits were examined, the osteoarthritis group's subunit profile corresponded to that of the Kalafong patient groups with overt pro-inflammatory activity. From these findings it is

tempting to imply a role for TGF-β in the enhanced expression of the H-subunit. However, it is obvious that further investigations are required to confirm or refute this possibility and that the results found here merely suggest further investigation into the relationship between TGF-β and H-subunit expression. Before embarking on such work one should perhaps ask whether a possible advantage exists for an increase in H-subunit expression in these patients or whether the co-occurrence of an increase in H-subunit expression and in TGF-β is merely an epiphenomenon.

The second aim of this study was to investigate a possible role for the expression of the H-subunit of ferritin in the macrophage in iron transfer block. The rationale for such an investigation can be found firstly, in the fact that inflammatory conditions can underlie iron retention by bone marrow macrophages, and – as seen from the results of this study – increased H-subunit expression, and secondly, that the H-subunit of ferritin is known to reduce the efflux of iron from cells (5, 6). As pro-inflammatory cytokines may not be the only factors involved in the development and maintenance of the iron transfer block the first step was to investigate the prevalence of the iron transfer block in the Kalafong patients – against the background of their pro-inflammatory activity. The second step in investigating a possible role for the H-subunit of ferritin in the macrophage in iron transfer block was to subdivide the Kalafong patients on the basis of the presence or absence of an iron transfer block – irrespective of their immune status.

In examining the prevalence of an iron transfer block in the presence of chronic pro-inflammatory activity the results showed almost 70% of the patients with high pro-inflammatory activity to exhibit the characteristics of an iron transfer block. However, between 15% and 26% of patients, depending on whether C-reactive protein or neopterin was used as indicator, who did not show overt pro-inflammatory activity, also had an iron transfer block. These results thus confirmed the strong association between

the development and maintenance of an iron transfer block on the one hand, and pro-inflammatory activity on the other. It does, however, also show that the chronic pro-inflammatory state cannot summarily be assumed to be accompanied by an iron transfer block and consequently with the associated anaemia of chronic disease. Whether the observation of an iron transfer block in a small number of patients without pronounced pro-inflammatory activity was due to the stage of the disease and therefore to the phase of the immune response, or some other factor, cannot at this point be deduced from the results. Other potential role players in the development and maintenance of the iron transfer block were discussed in the previous chapter.

In the second phase of investigating the possibility that the H-subunit of ferritin may play a role in the iron transfer block, the Kalafong patients were subdivided according to the presence or absence of an iron transfer block – irrespective of their immune status. The subdivision into patients with and patients without an iron transfer block was made on the grounds of assessment of the iron stores of Prussian blue stains of the bone marrow aspirates and cores, serum indicators of iron status and red blood cell profiles. The subdivision based solely on aspirates was made virtually impossible due to many of the patients, in addition to iron transfer block, also suffering from true iron deficiency. However, in addition to serum iron, serum transferrin, percentage serum transferrin saturation, transferrin/log ferritin ratio, other factors such as soluble transferrin receptor and soluble transferrin receptor/log ferritin ratio, as well as the red blood cell profiles, were employed in order to group the patients. A marginally higher expression of the H-subunit of ferritin was seen in the patients with an iron transfer block than in those without an iron transfer block. Although not the primary aim of this study, the results thus pointed towards a role for increased expression of the H-subunit in the bone marrow macrophage in iron transfer block.

The preceding paragraphs summarized the outcome of the main aims of the study. However, a number of important observations were made that warrant reporting and may point the way for further investigation. These are touched upon in the following paragraphs.

In investigating the relationship between the presence of an iron transfer block and immune activity the normal, expected relationships between storage iron, bio-available iron and red blood cell profile was seen. This normal relationship was present in the Kalafong groups with normal immune status, the Kalafong group with no iron transfer block and in the osteoarthritis patients. However, these relationships were largely lost in the immune-stimulated Kalafong patients. It would thus appear that, in conditions with chronic pro-inflammatory activity, iron availability loses its primary role in the establishment of the circulating red blood cell profile.

The study also provided indications that the H-subunit and L-subunit of ferritin may, in patients with normal immune status, play a role in the bio-availability of iron for haemoglobin synthesis. In the group of Kalafong patients with normal neopterin the possibility that the H-subunit and L-subunit of ferritin may play a role in the bio-availability of iron for haemoglobin synthesis was supported by a) the negative correlation between the H-subunit/L-subunit ratio in the macrophage and the MCV and MCH of the red blood cells, b) the negative correlation between the H-subunit/L-subunit ratio (increase in H-subunit rich isoferritins) in the cells of the erythron and the red blood cell MCV, c) the positive correlation between the expression of the L-subunit of ferritin in the macrophage (reflecting an increase in the labile iron pool in the macrophage and therefore a reduction in the shunting of iron to more stable pools) and the red blood cell MCV and MCH and d) the positive correlation between the bio-available serum iron (serum iron and percentage transferrin saturation) and the

expression of the L-subunit of ferritin in the cells of the erythron. Similar correlations were found in the Kalafong patients with an iron transfer block where it was seen that a) the H-subunit/L-subunit ratio in cells of the erythron correlated negatively with the MCV and MCH of the red blood cells and b) the expression of the L-subunit of ferritin in the cells of the erythron correlated positively with the MCV and MCH of the red blood cells. According to these results it would appear that an increase in H-subunit rich ferritins in the macrophage may result in less iron being released by the macrophage due to the possible shunting of iron to more stable pools and that an increase in the L-subunit of ferritin in the macrophage may reflect an increase in the labile iron pool in the macrophage and therefore a reduction in the shunting of iron to more stable pools and an increase in the bio-availability of iron. Although the possibility that the H-subunit and L-subunit of ferritin may play a role in the bio-availability of iron for haemoglobin synthesis has not before been investigated *in vivo,* there are indications from investigations in cell cultures that would appear to support the above correlations. The first of the above deductions is in line with the results of Picard *et al.* on cultured erythroid cells where it was shown that an increase in H-subunit rich isoferritins can result in the rapid chelation of the labile iron pool (7) and the second deduction with that of a study by Ruggeri *et al.* where it was shown that the concentration of L-subunit rich ferritins in liver, serum and cultured cells is related to iron levels (8). An, as yet, inexplicable, but opposing, relationship was found in the immune-stimulated Kalafong patients where a positive correlation was found between the expression of the H-subunit of ferritin in the cells of the erythron and red blood cell MCHC.

In the osteoarthritis patients the correlations between the H-subunit and L-subunit of ferritin and the bio-availability of iron was directly opposite to that of the Kalafong patients with normal immune status. The H-subunit/L-subunit ratio in the bone marrow macrophage and the H-subunit of ferritin in the cells of the erythron were closely related

to the serum iron level. This contradiction in results between the immunological normal Kalafong group and the osteoarthritis group needs further investigation. In fact, further studies on the H-subunit and L-subunit of ferritin, in general, would be of interest in osteoarthritis patients as several of the osteoarthritis patients showed characteristics of an iron transfer block while their circulating cytokine profiles were, except for TGF-β, relatively normal.

In the group of osteoarthritis patients a role for various cytokines in the regulation of the levels of the H-subunit and L-subunit of ferritin was shown. Some cytokines were shown to correlate with a decrease in the expression of the subunits of ferritin. An increase in Il-8 correlated with a decrease in the H-subunit of ferritin and a decrease in the H-subunit/L-subunit ratio in the macrophage. An increase in Il-6 correlated with a decrease in the L-subunit of ferritin in the macrophage. This is consistent with the role that ferritin plays in inflammation (9) with possibly first the up-regulation of specifically the H-subunit of ferritin followed by a decrease in the H-subunit and L-subunit as a result of an increase in haemosiderin formation or secretion of ferritin.

Some correlations were also found between the expression of the H-subunit and L-subunit of ferritin in cells of the erythron and cytokines. An increase in Il-2 correlated with a decrease in the H-subunit of ferritin in the cells of the erythron. An increase in TNF-α and an increase in Il-10 correlated with a decrease in the L-subunit of ferritin in the cells of the erythron. In view of the pleiotropic nature of cytokines, it would be unwarranted to make definitive assumptions on the role that cytokines play in the expression of the H-subunit and L-subunit of ferritin without further investigations.

Suggestions for further investigations

In no previous study was the expression of the H-subunit and L-subunit of ferritin measured quantitatively in bone marrow macrophages and cells of the erythron in combination with the inflammatory status of patients. This study investigated the influence of an overt pro-inflammatory state on the expression of the H-subunit and L-subunit of ferritin. The expression/levels of the H-subunit and L-subunit of ferritin are determined by various processes including transcription of the H-subunit and L-subunit genes, translation of the H-subunit and L-subunit mRNA, aggregation of ferritin and secretion of ferritin. It is suggested that the regulation of H-subunit/L-subunit levels during inflammatory processes be further investigated by measuring the mRNA levels, the amount of ferritin aggregation and the secretion of ferritin. By determining the mRNA levels the change in transcription could be evaluated. Measuring mRNA with ultrastructural *in situ* hybridisation is theoretically possible and was tried. However, the copies of mRNA transcripts were very few and even completely absent due to the harsh treatments of fixation, dehydration and embedding. It is suggested that *in situ* hybridisation of tissue prepared by cryo-fixation could be tried in order to retain more mRNA copies. The process of secretion can also contribute to the levels of the H-subunit and L-subunit of ferritin. By determining the plasma levels of the H-subunit and L-subunit of ferritin this process of secretion could be investigated.

References

1) Blaney-Davidson EN, van der Kraan PM, van den Berg WB. TGF-β and osteoarthritis. Osteoarthritis and Cartilage 2007; 15: 597-604.

2) Miller LL, Miller SC, Torti SV, Tsuji Y, Torti FM. Iron-independent induction of ferritin H chain by tumor necrosis factor. Proceedings of the National Academy of Sciences of the United States of America 1991; 88(11): 4946-4950.

3) Closa D, Folch-Puy E. Oxygen free radicals and the systemic inflammatory response. IUBMB Life 2004; 56(4): 185-191.

4) Lin F, Girotti AW. Elevated ferritin production, iron containment, and oxidant resistance in hemin-treated leukaemia cells. Archives of Biochemistry and Biophysics 1997; 346(1): 131-141.

5) Alvarez-Hernández X, Licéaga J, McKay IC, Brock JH. Induction of hypoferremia and modulation of macrophage iron metabolism by tumor necrosis factor. Laboratory Investigation 1989; 61(3): 319-322.

6) Fahmy M, Young SP. Modulation of iron metabolism in monocyte cell line U937 by inflammatory cytokines: changes in transferrin uptake, iron handling and ferritin mRNA. Biochemical Journal 1993; 296: 175-181.

7) Picard V, Renaudie F, Porcher C, Hentze MW, Grandchamp B, Beaumont C. Overexpression of the ferritin H subunit in cultured erythroid cells changes the intracellular iron distribution. Blood 1996; 87(5): 2057-2064.

8) Ruggeri G, Iacobello C, Albertini A, Brocchi E, Levi S, Gabri E *et al.* Studies of human isoferritins in tissues and body fluids. In: Albertini A, Arosio P, Chiancone E, Drysdale J editors. Ferritins and isoferritins as biochemical markers. Amsterdam: Elsevier Science Publishers; 1984. p. 67-78.

9) Alvarez-Hernández X, Felstein MV, Brock JH. The relationship between iron release, ferritin synthesis and intracellular iron distribution in mouse peritoneal

macrophages. Evidence for a reduced level of metabolically available iron in elicited macrophages. Biochimica *et* Biophysica Acta 1986; 886: 214-222.

CHAPTER 6

ELECTRON MICROGRAPHS AND RAW DATA OF IMMUNOLABELLING OF H-SUBUNIT AND L-SUBUNIT OF FERRITIN, PHOTOGRAPHS OF THE PRUSSIAN BLUE IRON STAINS AND THE PRESENCE OR ABSENCE OF AN IRON TRANSFER BLOCK

1) Electron micrographs of the immunolabelling of the H-subunit and L-subunit of ferritin

Figures 1 – 48 g, h and i contain electron micrographs for the immunolabelling of the H-subunit of ferritin for the Kalafong patient group and Figures 1 – 48 j, k and l contain electron micrographs for the immunolabelling of the L-subunit of ferritin for the Kalafong patient group. Figures 49 – 55 g, h and i contain electron micrographs for the immunolabelling of the H-sububnit of ferritin for the osteoarthritis group and Figures 49 – 55 j, k and l contain electron micrographs for the immunolabelling of the L-subunit of ferritin for the osteoarthritis group.

2) Photographs of the Prussian blue iron stains for the bone marrow aspirates and cores

Figures 1 – 48 a, b and c contain photographs for the Prussian blue iron stains of the bone marrow aspirates and Figures 1 – 48 d, e and f contain photographs for the

Prussian blue iron stains of the bone marrow cores. In comparison these two techniques gave similar results. For the osteoarthritis group a Prussian blue iron stain was only performed for the bone marrow cores. Figures 49 – 55 d, e and f contain the photographs for the Prussian blue iron stains of the bone marrow cores for the osteoarthritis group.

Figure 1

Kalafong patient 1

Figure 1a. A bone marrow fragment slightly stained blue with the Prussian blue iron stain – normal amount of storage iron.

Figure 1b and c. Bone marrow aspirate smears stained with the Prussian blue iron stain with no sideroblasts.

Figure 1g. An electron micrograph of a bone marrow macrophage immunolabelled with a monoclonal antibody to the H-subunit of ferritin, 10 nm gold particles and scale bar = 1 µm.

Figure 1h. An electron micrograph of a bone marrow red blood cell precursor immunolabelled with a monoclonal antibody to the H-subunit of ferritin, 10 nm gold particles and scale bar = 1 µm.

Figure 1i. An electron micrograph of a bone marrow red blood cell precursor immunolabelled with a monoclonal antibody to the H-subunit of ferritin, 10 nm gold particles and scale bar = 1 µm.

Figure 1j. An electron micrograph of a bone marrow macrophage immunolabelled with a monoclonal antibody to the L-subunit of ferritin, 10 nm gold particles and scale bar = 1 µm.

Figure 1k. An electron micrograph of a bone marrow red blood cell immunolabelled with a monoclonal antibody to the L-subunit of ferritin, 10 nm gold particles and scale bar = 1 µm.

Figure 1l. An electron micrograph of a bone marrow red blood cell precursor immunolabelled with a monoclonal antibody to the L-subunit of ferritin, 10 nm gold particles and scale bar = 1 µm.

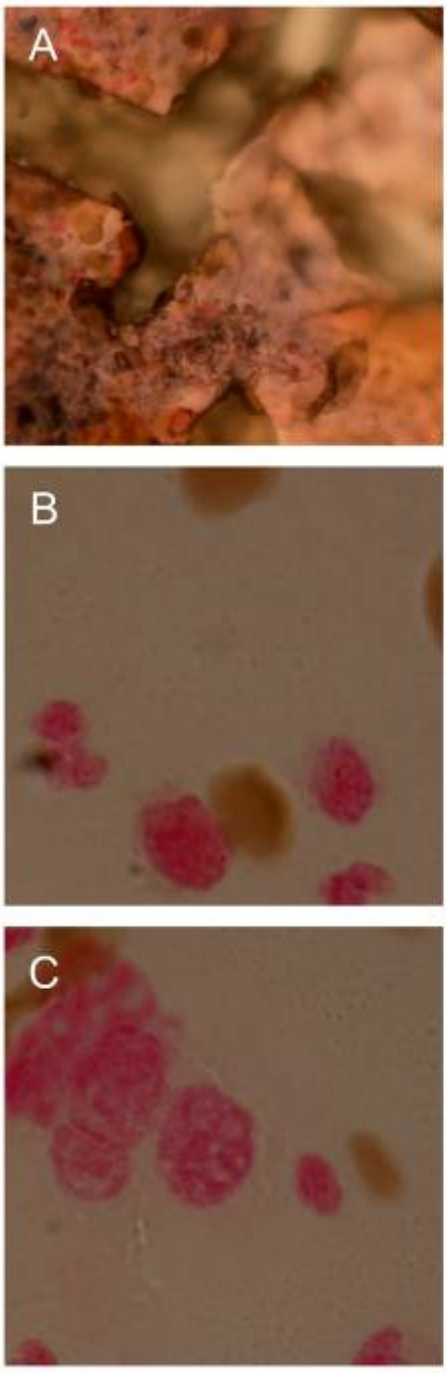
A
B
C

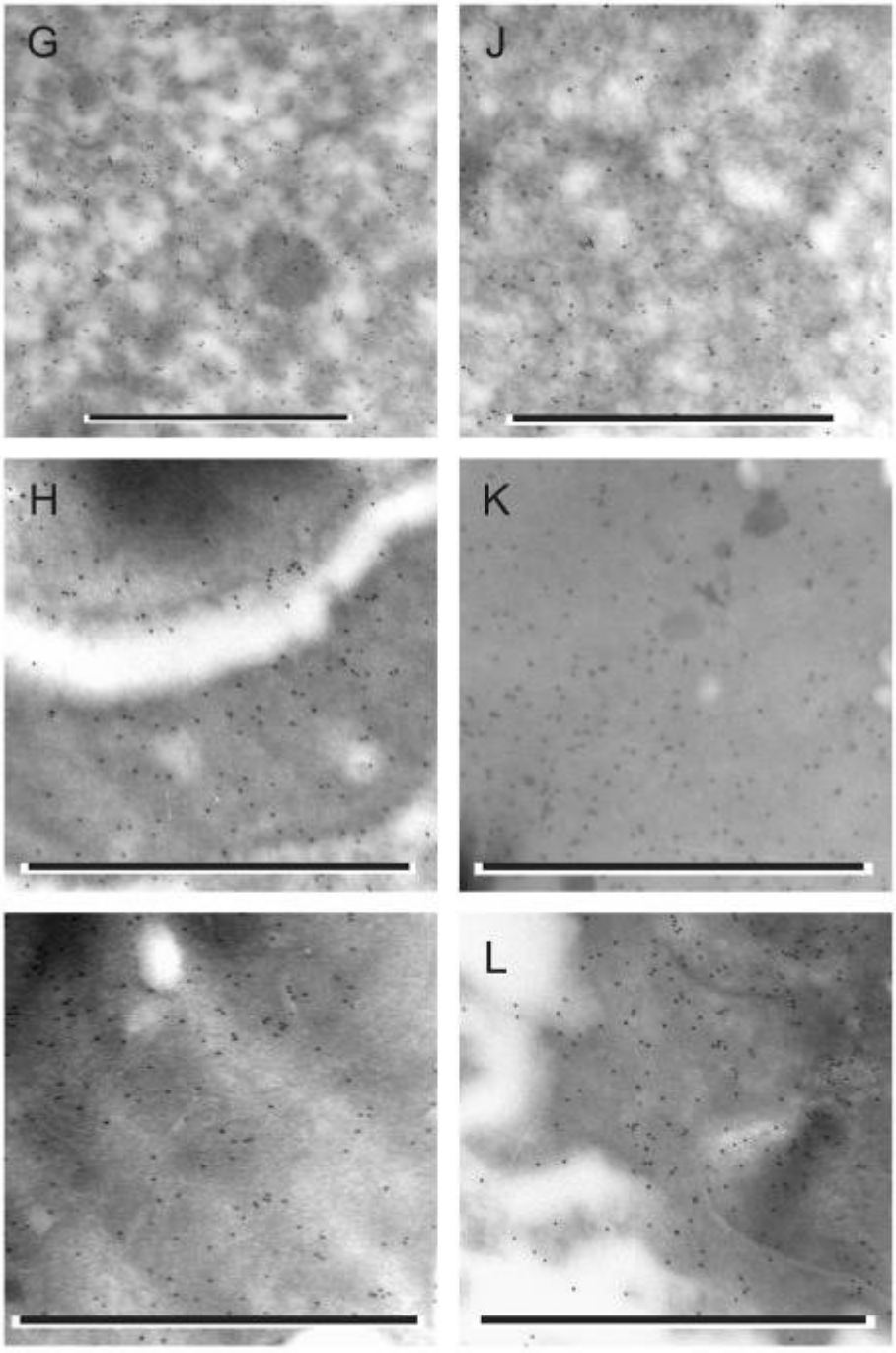
G
J
H
K
L

Figure 2

Kalafong patient 2

Figure 2a. A bone marrow fragment stained blue with the Prussian blue iron stain – increased amount of storage iron.

Figure 2b and c. Bone marrow aspirate smears stained with the Prussian blue iron stain with pathologically overloaded sideroblasts.

Figure 2d. A bone marrow macrophage stained blue with the Prussian blue iron stain – increased amount of storage iron.

Figure 2e and f. Bone marrow sections stained with the Prussian blue iron stain with pathologically overloaded sideroblasts.

Figure 2g. An electron micrograph of a bone marrow macrophage immunolabelled with a monoclonal antibody to the H-subunit of ferritin, 10 nm gold particles and scale bar = 1 µm.

Figure 2h. An electron micrograph of a bone marrow red blood cell precursor immunolabelled with a monoclonal antibody to the H-subunit of ferritin. Note the cluster of iron – haemosiderin near the nucleus, 10 nm gold particles and scale bar = 1 µm.

Figure 2i. An electron micrograph of a bone marrow red blood cell precursor immunolabelled with a monoclonal antibody to the H-subunit of ferritin. Note the cluster of iron – haemosiderin near the nucleus, 10 nm gold particles and scale bar = 1 µm.

Figure 2j. An electron micrograph of a bone marrow macrophage immunolabelled with a monoclonal antibody to the L-subunit of ferritin, 10 nm gold particles and scale bar = 1 µm.

Figure 2k. An electron micrograph of a bone marrow red blood cell precursor immunolabelled with a monoclonal antibody to the L-subunit of ferritin. Note the two clusters of iron – haemosiderin near the nucleus, 10 nm gold particles and scale bar = 1 µm.

Figure 2l. An electron micrograph of a bone marrow red blood cell precursor immunolabelled with a monoclonal antibody to the L-subunit of ferritin. Note the two clusters of iron – haemosiderin, 10 nm gold particles and scale bar = 1 µm.

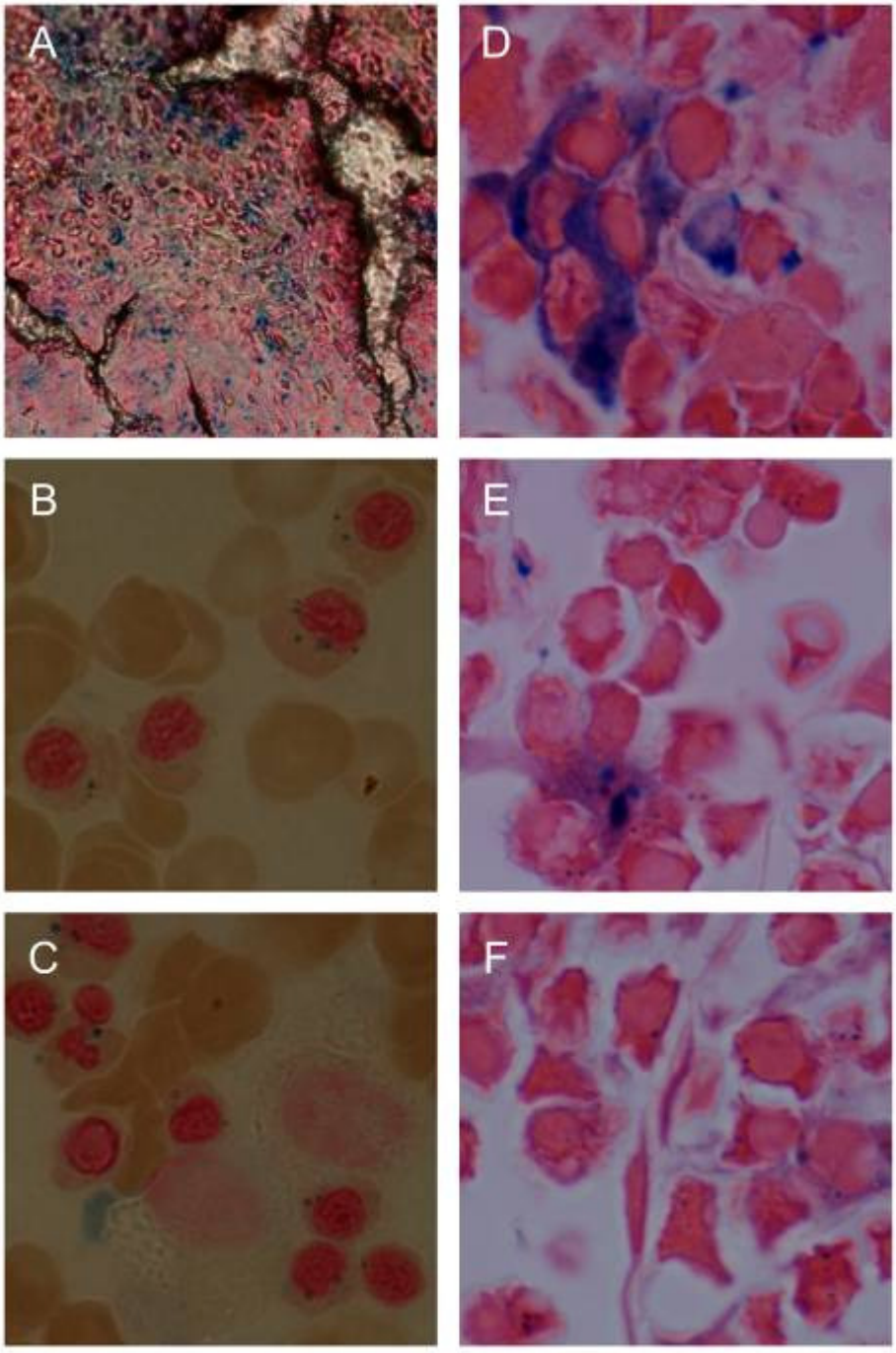
A
D
B
E
C
F

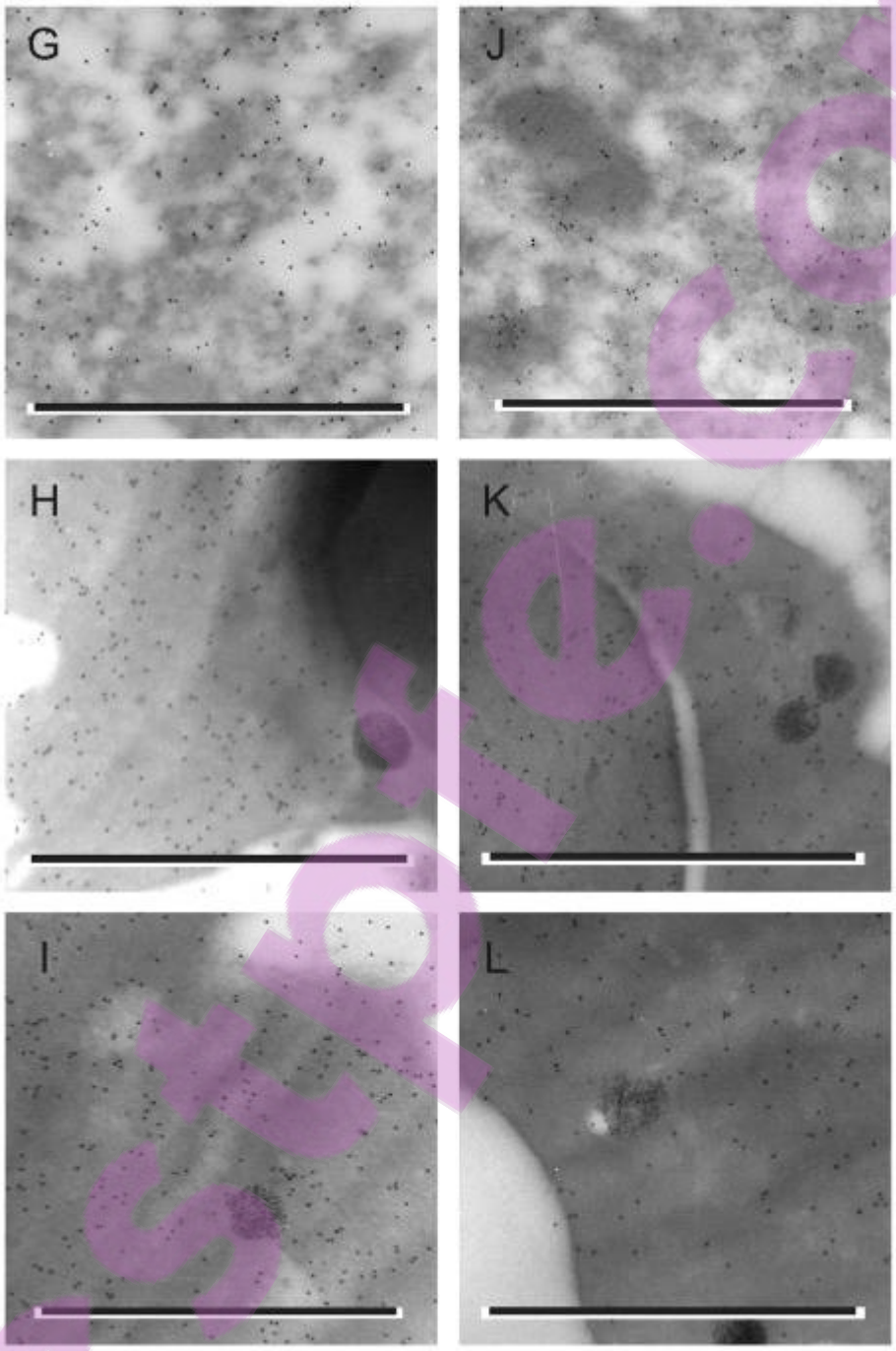

Figure 3

Kalafong patient 3

Figure 3a. A small bone marrow fragment stained partly blue with the Prussian blue iron stain – possibly increased amount of storage iron.

Figure 3b and c. Bone marrow aspirate smears stained with the Prussian blue iron stain with pathologically overloaded sideroblasts.

Figure 3d. A bone marrow section stained blue with the Prussian blue iron stain – no stainable macrophage iron.

Figure 3e and f. Bone marrow sections stained with the Prussian blue iron stain with some sideroblasts.

Figure 3g. An electron micrograph of a bone marrow macrophage immunolabelled with a monoclonal antibody to the H-subunit of ferritin, 10 nm gold particles and scale bar = 1 μm.

Figure 3h. An electron micrograph of two bone marrow reticulocytes immunolabelled with a monoclonal antibody to the H-subunit of ferritin. Note the contact between the two cell membranes of the reticulocytes, 10 nm gold particles and scale bar = 1 μm.

Figure 3i. An electron micrograph of two bone marrow reticulocytes immunolabelled with a monoclonal antibody to the H-subunit of ferritin, 10 nm gold particles and scale bar = 1 μm.

Figure 3j. An electron micrograph of a bone marrow macrophage immunolabelled with a monoclonal antibody to the L-subunit of ferritin, 10 nm gold particles and scale bar = 1 μm.

Figure 3k. An electron micrograph of a bone marrow red blood cell precursor immunolabelled with a monoclonal antibody to the L-subunit of ferritin. Note the two clusters of iron – haemosiderin, 10 nm gold particles and scale bar = 1 μm.

Figure 3l. An electron micrograph of two bone marrow reticulocytes immunolabelled with a monoclonal antibody to the L-subunit of ferritin, 10 nm gold particles and scale bar = 1 μm.

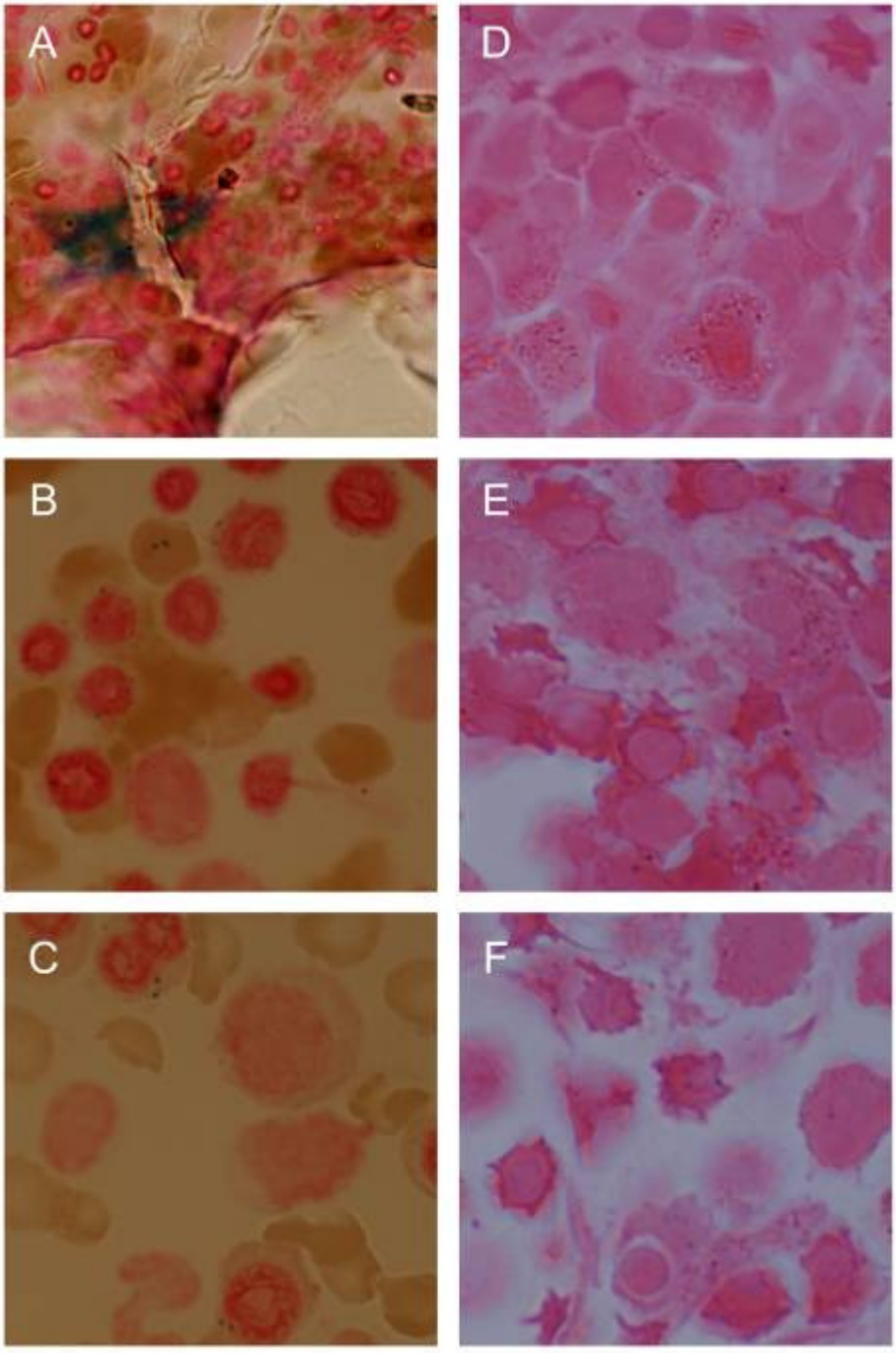

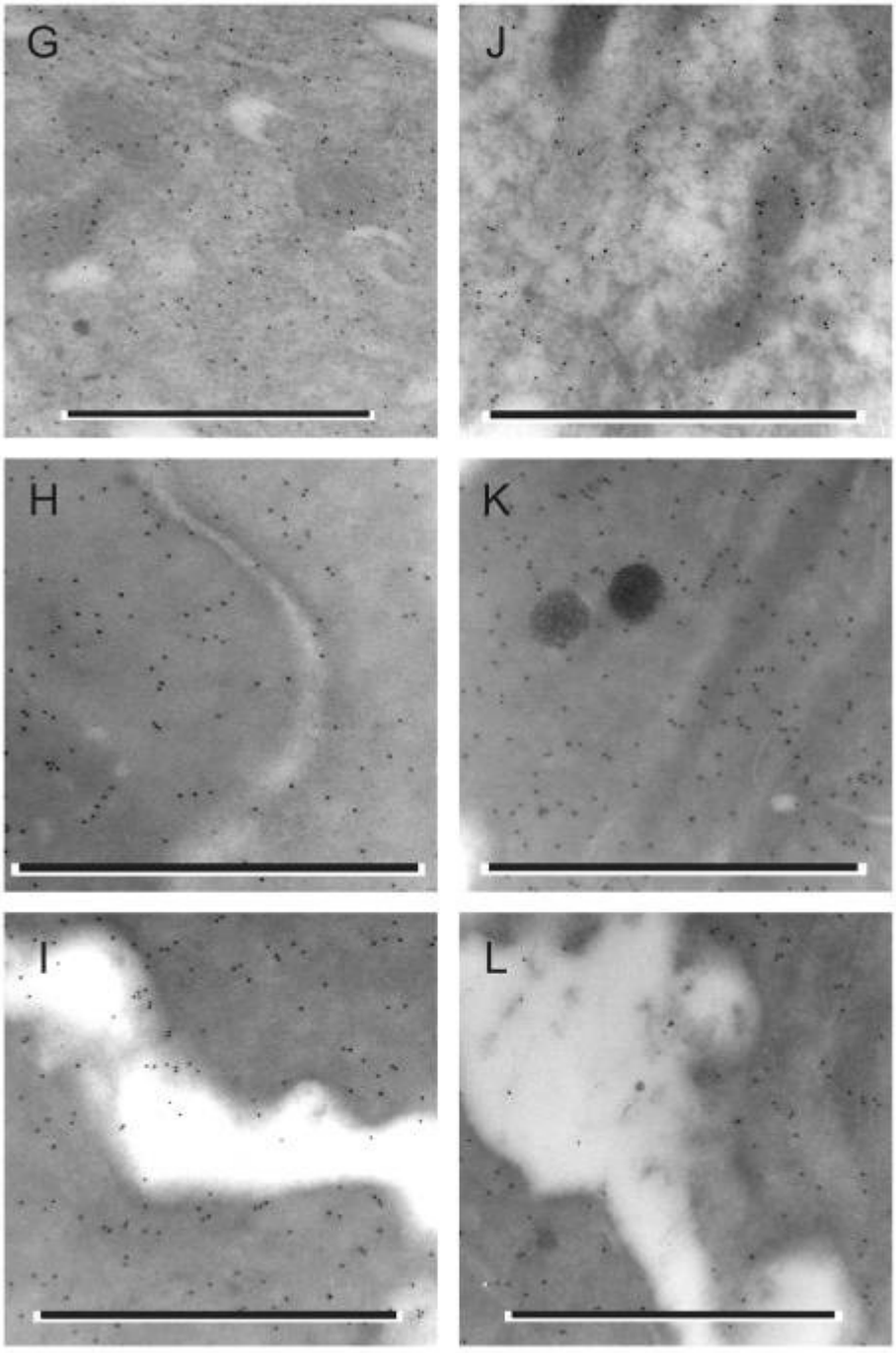
G
J
H
K
I
L

Figure 4

Kalafong patient 4

Figure 4j. An electron micrograph of a bone marrow macrophage immunolabelled with a monoclonal antibody to the L-subunit of ferritin, 10 nm gold particles and scale bar = 1 µm.

Figure 4k. An electron micrograph of a bone marrow reticulocyte immunoabelled with a monoclonal antibody to the L-subunit of ferritin, 10 nm gold particles and scale bar = 1 µm.

Figure 4l. An electron micrograph of a bone marrow reticulocyte immunolabelled with a monoclonal antibody to the L-subunit of ferritin, 10 nm gold particles and scale bar = 1 µm.

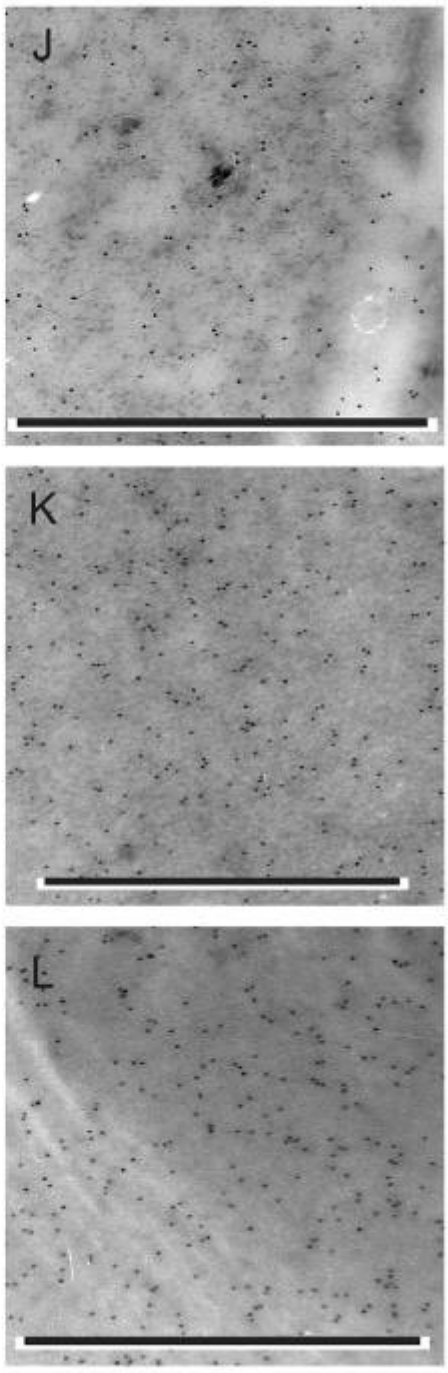
J
K
L

Figure 5

Kalafong patient 5

Figure 5d, e and f. Bone marrow sections stained blue with the Prussian blue iron stain – macrophage stained only slightly for storage iron with no sideroblasts.

Figure 5g. An electron micrograph of a bone marrow macrophage immunolabelled with a monoclonal antibody to the H-subunit of ferritin, 10 nm gold particles and scale bar = 1 μm.

Figure 5h. An electron micrograph of a bone marrow red blood cell precursor immunolabelled with a monoclonal antibody to the H-subunit of ferritin. Note the contact between the cell membrane of the red blood cell precursor and that of an iron-containing macrophage, 10 nm gold particles and scale bar = 1 μm.

Figure 5i. An electron micrograph of a bone marrow red blood cell precursor immunolabelled with a monoclonal antibody to the H-subunit of ferritin. Note the small cluster of ferritin - haemosiderin, 10 nm gold particles and scale bar = 1 μm.

Figure 5j. An electron micrograph of a bone marrow macrophage immunolabelled with a monoclonal antibody to the L-subunit of ferritin, 10 nm gold particles and scale bar = 1 μm.

Figure 5k. An electron micrograph of a bone marrow red blood cell precursor immunolabelled with a monoclonal antibody to the L-subunit of ferritin, 10 nm gold particles and scale bar = 1 μm.

Figure 5l. An electron micrograph of a bone marrow red blood cell precursor immunolabelled with a monoclonal antibody to the L-subunit of ferritin, 10 nm gold particles and scale bar = 1 μm.

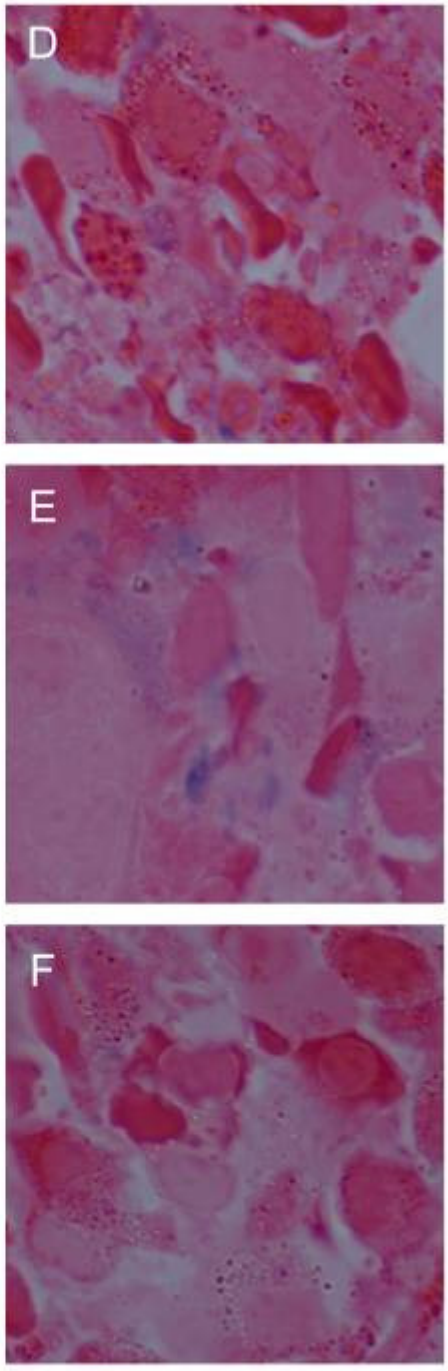
D
E
F

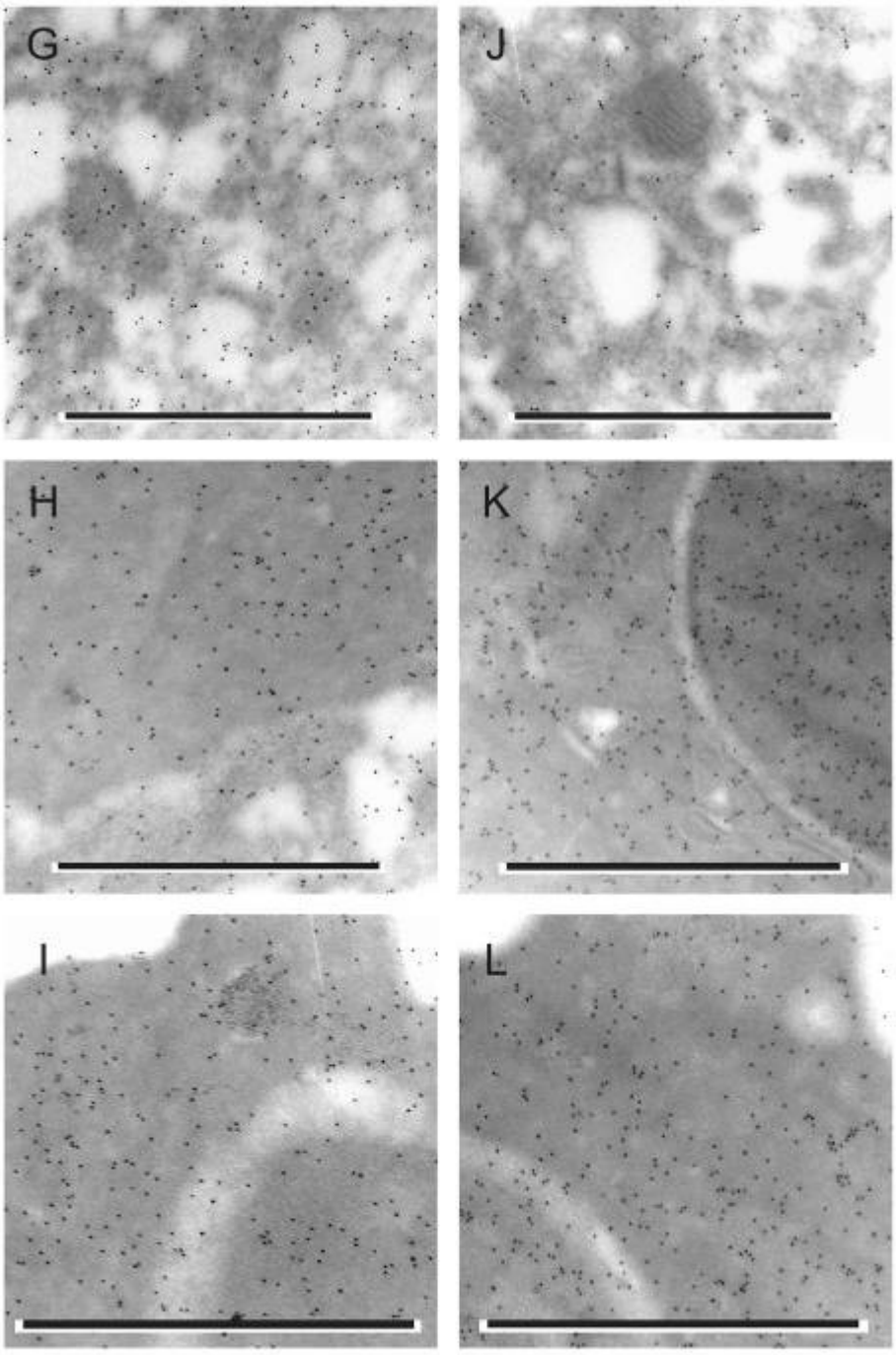
G
J
H
K
I
L

Figure 6

Kalafong patient 6

Figure 6d. A bone marrow macrophage stained blue with the Prussian blue iron stain.

Figure 6e. A bone marrow macrophage stained blue with the Prussian blue iron stain and a sideroblast.

Figure 6f. A bone marrow section stained with the Prussian blue iron stain with some sideroblasts.

Figure 6g. An electron micrograph of a bone marrow macrophage immunolabelled with a monoclonal antibody to the H-subunit of ferritin, 10 nm gold particles and scale bar = 1 μm.

Figure 6h. An electron micrograph of a bone marrow reticulocyte immunolabelled with a monoclonal antibody to the H-subunit of ferritin, 10 nm gold particles and scale bar = 1 μm.

Figure 6i. An electron micrograph of two bone marrow red blood cell precursors immunolabelled with a monoclonal antibody to the H-subunit of ferritin. Note the contact between the cell membranes of the two cells and the presence of ferritin in the space between the two membranes, 10 nm gold particles and scale bar = 1 μm.

Figure 6j. An electron micrograph of a bone marrow macrophage immunolabelled with a monoclonal antibody to the L-subunit of ferritin, 10 nm gold particles and scale bar = 1 μm.

Figure 6k. An electron micrograph of two bone marrow red blood cells immunolabelled with a monoclonal antibody to the L-subunit of ferritin, 10 nm gold particles and scale bar = 1 μm.

Figure 6l. An electron micrograph of a bone marrow red blood cell precursor immunolabelled with a monoclonal antibody to the L-subunit of ferritin. Note the ferritin present on the cell membrane and one endocytic vesicle containing ferritin, 10 nm gold particles and scale bar = 1 μm.

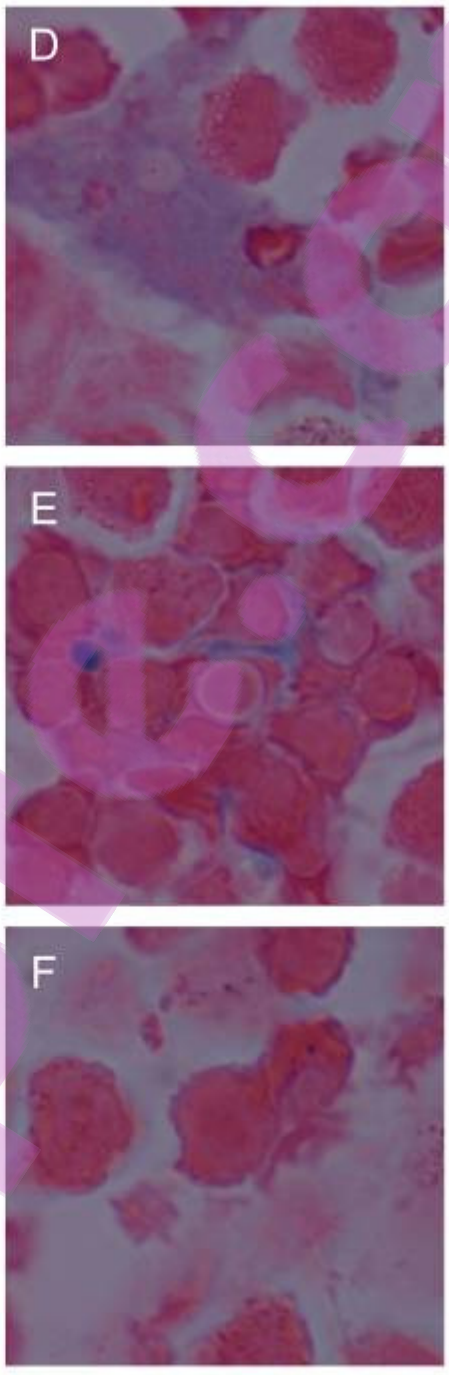

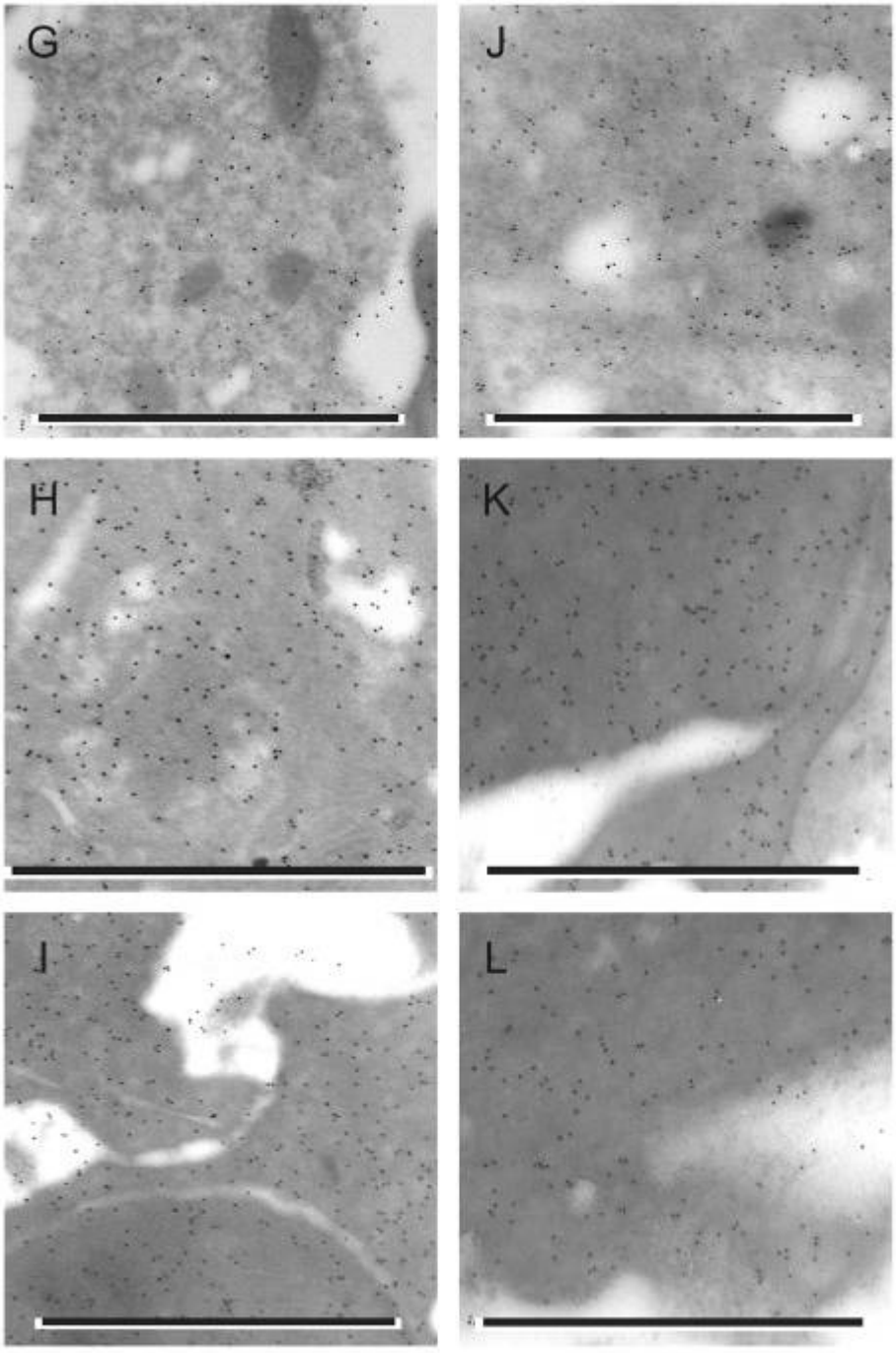
G
J
H
K
I
L

Figure 7

Kalafong patient 7

Figure 7a. A bone marrow fragment stained blue with the Prussian blue iron stain – normal amount of storage iron.

Figure 7b. A bone marrow aspirate smear stained with the Prussian blue iron stain with a macrophage stained positive for the presence of iron.

Figure 7c. A bone marrow aspirate smear stained with the Prussian blue iron stain with some pathologically overloaded sideroblasts.

Figure 7d, e and f. Bone marrow sections stained blue with the Prussian blue iron stain – macrophages stained positive for the presence of storage iron.

Figure 7g. An electron micrograph of a bone marrow macrophage immunolabelled with a monoclonal antibody to the H-subunit of ferritin, 10 nm gold particles and scale bar = 1 µm.

Figure 7h. An electron micrograph of two bone marrow red blood cell precursors immunolabelled with a monoclonal antibody to the H-subunit of ferritin. Note the contact between the two cell membranes of the red blood cell precursors and the presence of ferritin on the cell membranes and in endocytic vesicles, 10 nm gold particles and scale bar = 1 µm.

Figure 7i. An electron micrograph of a bone marrow red blood cell precursor immunolabelled with a monoclonal antibody to the H-subunit of ferritin. Note the cluster of ferritin – haemosiderin, 10 nm gold particles and scale bar = 1 µm.

Figure 7j. An electron micrograph of a bone marrow macrophage immunolabelled with a monoclonal antibody to the L-subunit of ferritin. Note the presence of iron loaded ferritin, 10 nm gold particles and scale bar = 1 µm.

Figure 7k. An electron micrograph of a bone marrow red blood cell precursor immunolabelled with a monoclonal antibody to the L-subunit of ferritin, 10 nm gold particles and scale bar = 1 µm.

Figure 7l. An electron micrograph of two bone marrow reticulocytes immunolabelled with a monoclonal antibody to the L-subunit of ferritin, 10 nm gold particles and scale bar = 1 µm.

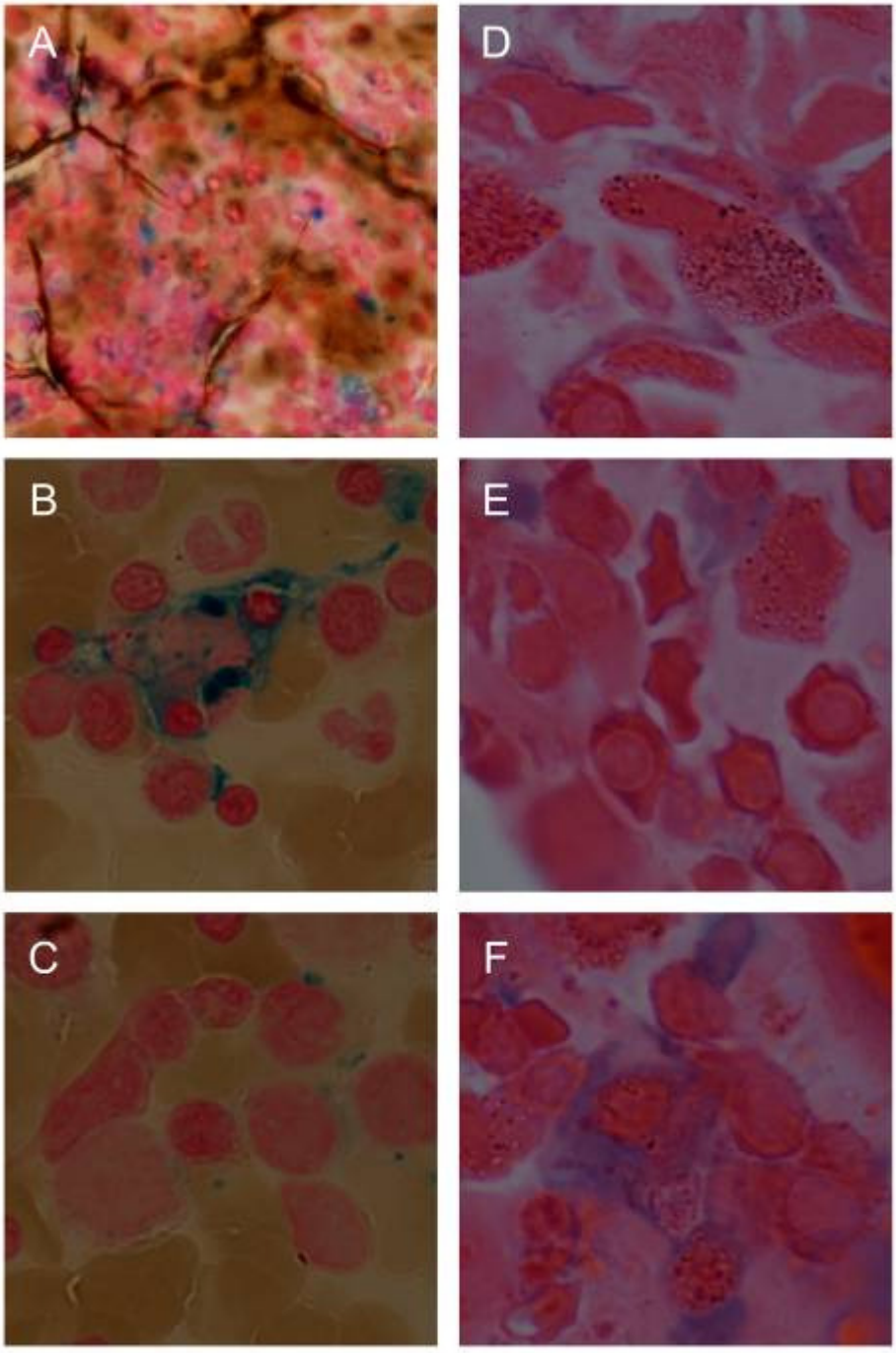
A
D
B
E
C
F

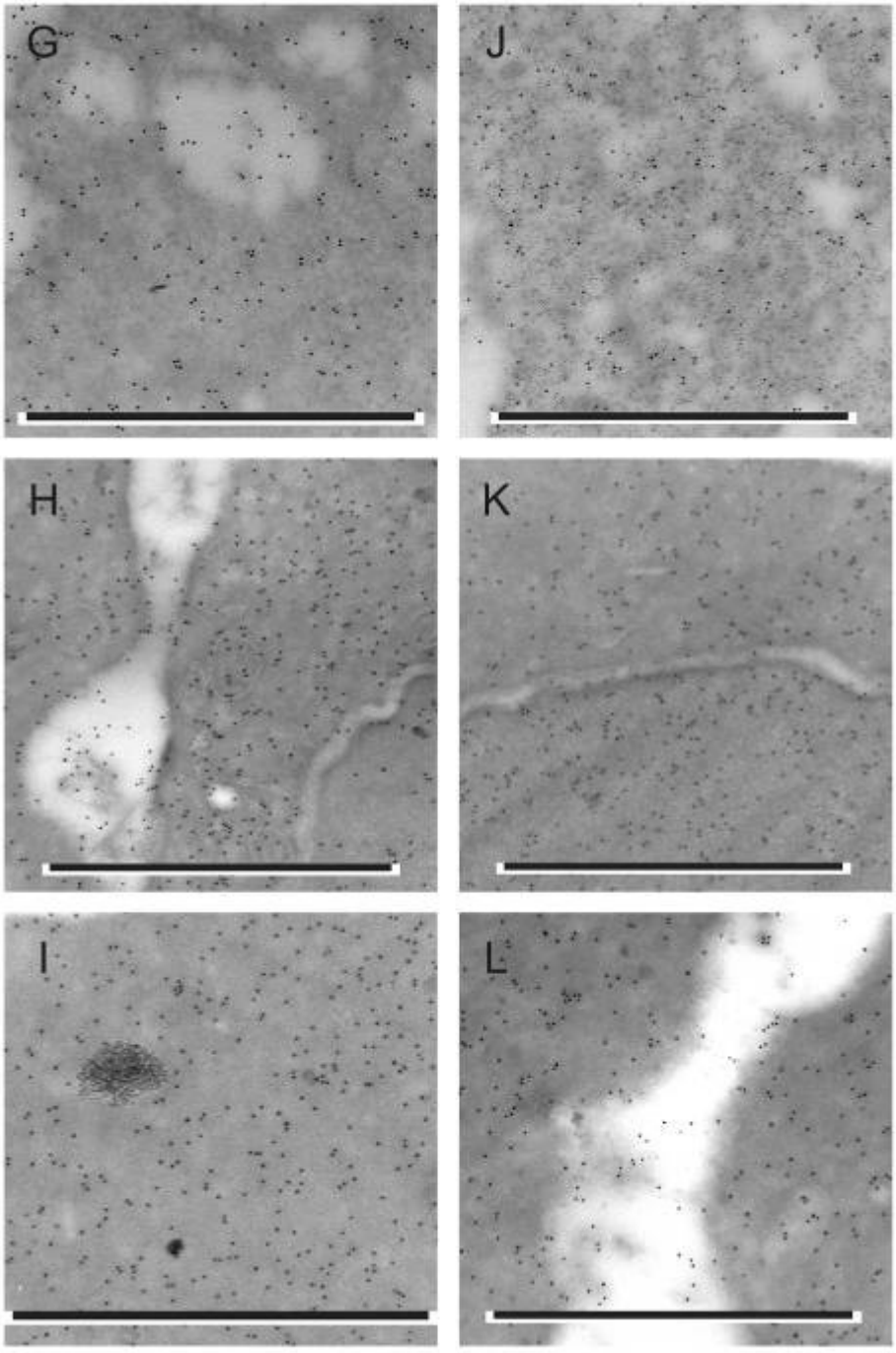
G
J
H
K
I
L

Figure 8

Kalafong patient 8

Figure 8a. A bone marrow fragment stained positive with the Prussian blue iron stain – severely increased amount of storage iron.

Figure 8b and c. Bone marrow aspirate smears stained with the Prussian blue iron stain with no sideroblasts.

Figure 8d. A bone marrow section stained blue with the Prussian blue iron stain – severely increased amount of storage iron.

Figure 8e and f. Bone marrow sections stained with the Prussian blue iron stain with no sideroblasts.

Figure 8g. An electron micrograph of a bone marrow macrophage immunolabelled with a monoclonal antibody to the H-subunit of ferritin, 10 nm gold particles and scale bar = 1 μm.

Figure 8h. An electron micrograph of a bone marrow red blood cell immunolabelled with a monoclonal antibody to the H-subunit of ferritin. Note the macrophage with the presence of siderosomes, 10 nm gold particles and scale bar = 1 μm.

Figure 8i. An electron micrograph of a bone marrow red blood cell precursor immunolabelled with a monoclonal antibody to the H-subunit of ferritin. Note the macrophage with the presence of siderosomes, 10 nm gold particles and scale bar = 1 μm.

Figure 8j. An electron micrograph of a bone marrow macrophage immunolabelled with a monoclonal antibody to the L-subunit of ferritin. Note the siderosomes, 10 nm gold particles and scale bar = 1 μm.

Figure 8k. An electron micrograph of a bone marrow red blood cell immunolabelled with a monoclonal antibody to the L-subunit of ferritin. Note the macrophage with siderosomes, 10 nm gold particles and scale bar = 1 μm.

Figure 8l. An electron micrograph of a bone marrow red blood cell precursor immunolabelled with a monoclonal antibody to the L-subunit of ferritin, 10 nm gold particles and scale bar = 1 μm.

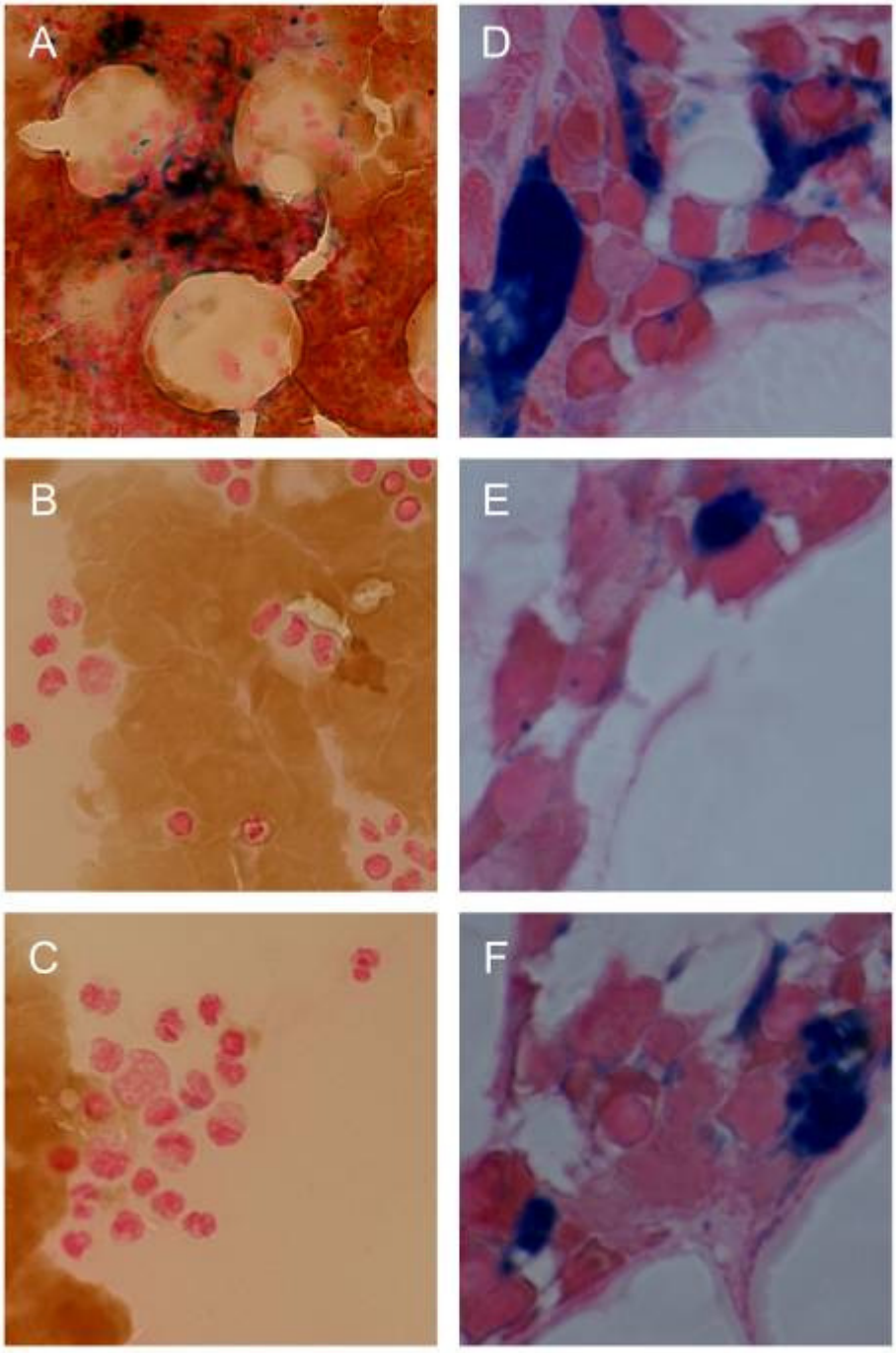
A
D
B
E
C
F

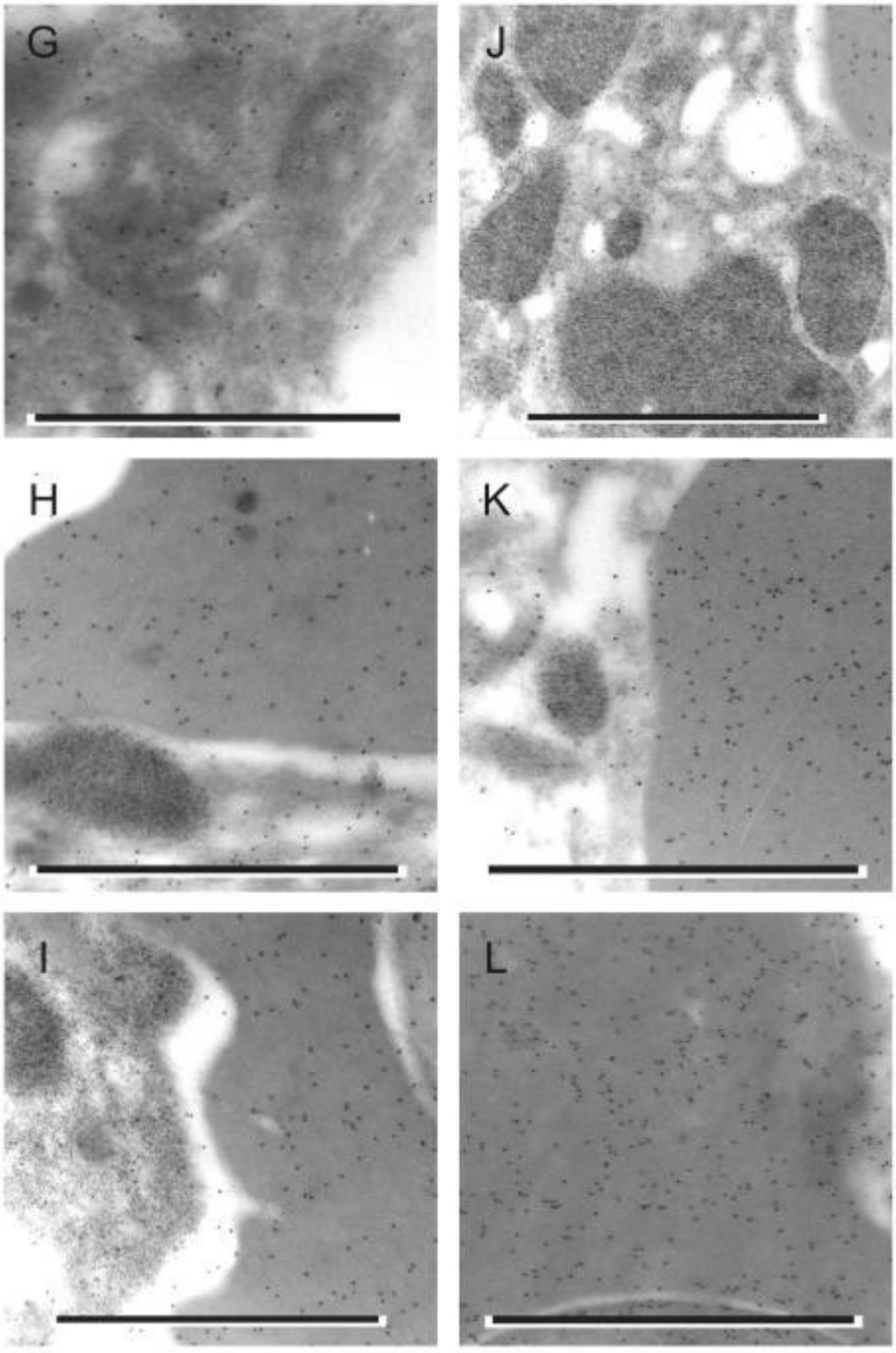
G
J
H
K
I
L

Figure 9

Kalafong patient 9

Figure 9a. A bone marrow fragment stained positive with the Prussian blue iron stain – severely increased amount of storage iron.

Figure 9b and c. Bone marrow aspirate smears stained with the Prussian blue iron stain with some sideroblasts.

Figure 9d. A bone marrow section stained blue with the Prussian blue iron stain – severely increased amount of storage iron.

Figure 9e and f. Bone marrow sections stained with the Prussian blue iron stain with no sideroblasts.

Figure 9g. An electron micrograph of a bone marrow macrophage immunolabelled with a monoclonal antibody to the H-subunit of ferritin, 10 nm gold particles and scale bar = 1 μm.

Figure 9h. An electron micrograph of two bone marrow red blood cells immunolabelled with a monoclonal antibody to the H-subunit of ferritin. Note the contact between the cell membranes of the two cells, 10 nm gold particles and scale bar = 1 μm.

Figure 9i. An electron micrograph of a bone marrow reticulocyte immunolabelled with a monoclonal antibody to the H-subunit of ferritin, 10 nm gold particles and scale bar = 1 μm.

Figure 9j. An electron micrograph of a bone marrow macrophage immunolabelled with a monoclonal antibody to the L-subunit of ferritin. Note the iron-loaded ferritin, 10 nm gold particles and scale bar = 1 μm.

Figure 9k. An electron micrograph of two bone marrow reticulocytes immunolabelled with a monoclonal antibody to the L-subunit of ferritin. Note the contact between the two cell membranes and the iron-loaded ferritin in the space between the membranes, 10 nm gold particles and scale bar = 1 μm.

Figure 9l. An electron micrograph of two bone marrow reticulocytes immunolabelled with a monoclonal antibody to the L-subunit of ferritin. Note the contact between the two cell membranes and the iron-loaded ferritin in the space between the membranes, 10 nm gold particles and scale bar = 1 μm.

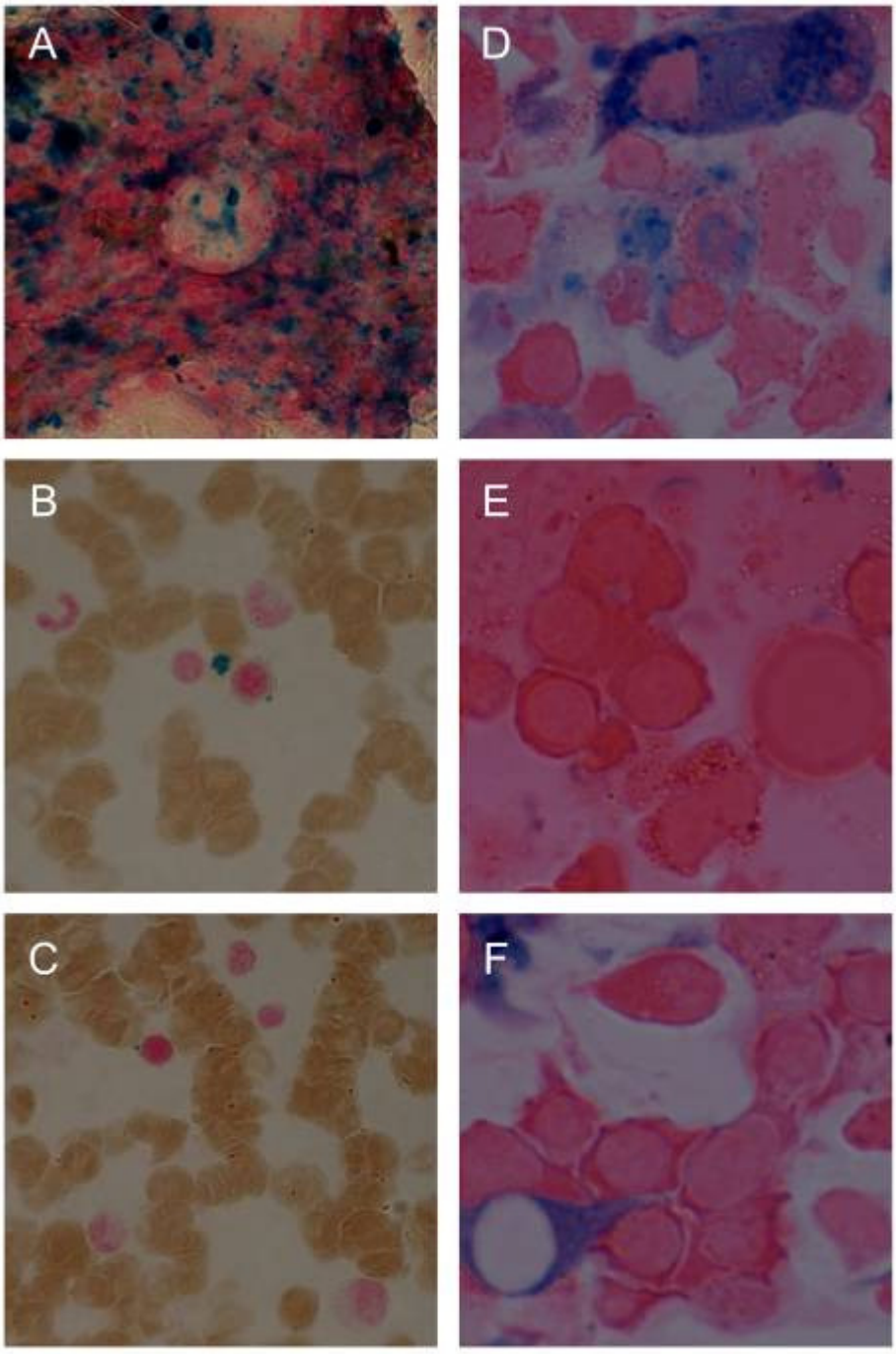
A
D
B
E
C
F

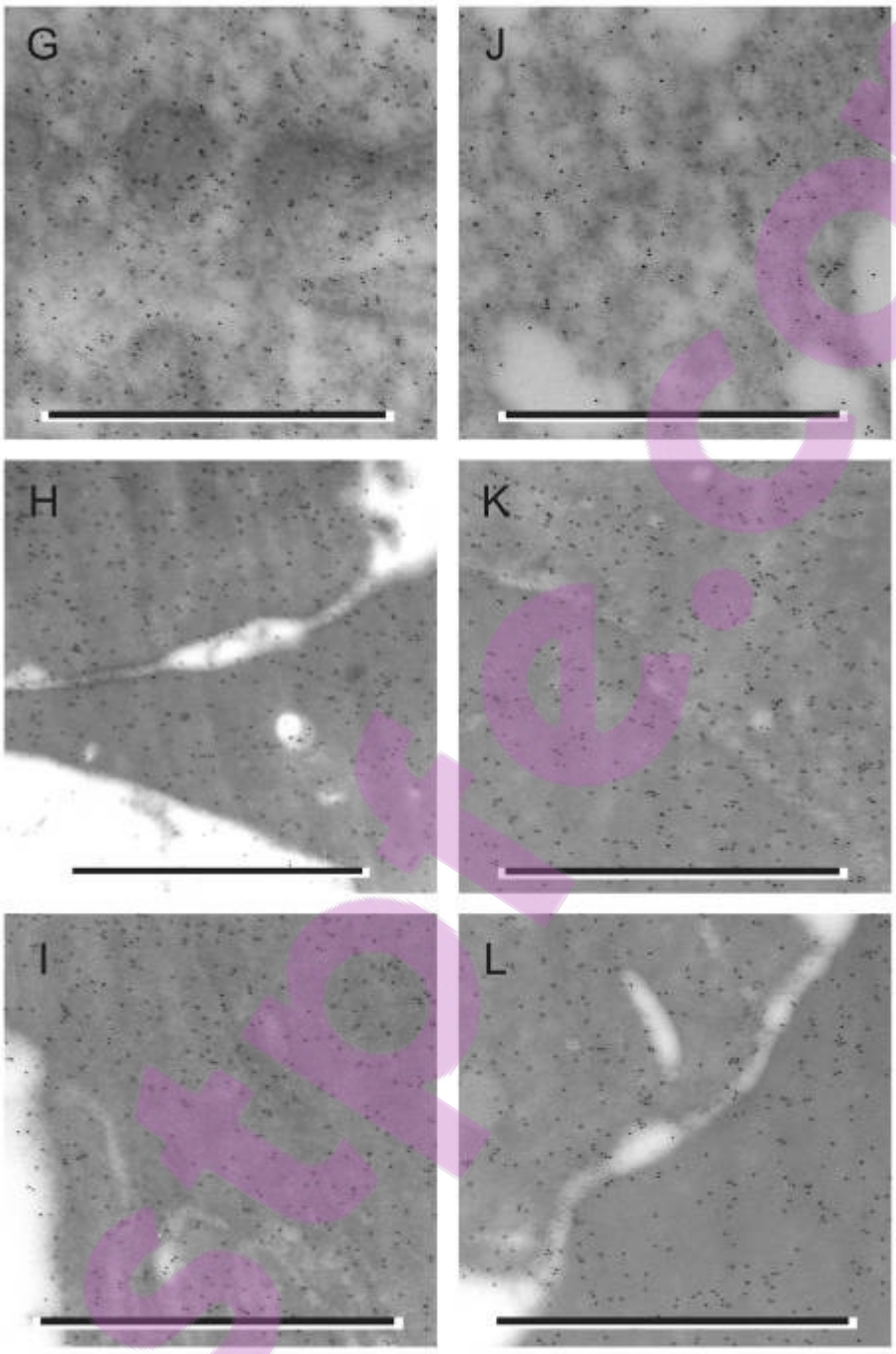

Figure 10

Kalafong patient 10

Figure 10a. A bone marrow fragment stained negative with the Prussian blue iron stain – no storage iron.

Figure 10b and c. Bone marrow aspirate smears stained with the Prussian blue iron stain with no sideroblasts.

Figure 10d. A bone marrow section stained negative with the Prussian blue iron stain – no amount of storage iron.

Figure 10e and f. Bone marrow sections stained with the Prussian blue iron stain with no sideroblasts.

Figure 10g. An electron micrograph of a bone marrow macrophage immunolabelled with a monoclonal antibody to the H-subunit of ferritin, 10 nm gold particles and scale bar = 1 μm.

Figure 10h. An electron micrograph of two bone marrow reticulocytes immunolabelled with a monoclonal antibody to the H-subunit of ferritin. Note the contact between the cell membranes of the two cells, 10 nm gold particles and scale bar = 1 μm.

Figure 10i. An electron micrograph of a bone marrow red blood cell precursor immunolabelled with a monoclonal antibody to the H-subunit of ferritin, 10 nm gold particles and scale bar = 1 μm.

Figure 10j. An electron micrograph of a bone marrow macrophage immunolabelled with a monoclonal antibody to the L-subunit of ferritin, 10 nm gold particles and scale bar = 1 μm.

Figure 10k. An electron micrograph of two bone marrow red blood cells immunolabelled with a monoclonal antibody to the L-subunit of ferritin. Note the contact between the two cell membranes, 10 nm gold particles and scale bar = 1 μm.

Figure 10l. An electron micrograph of a bone marrow reticulocyte immunolabelled with a monoclonal antibody to the L-subunit of ferritin, 10 nm gold particles and scale bar = 1 μm.

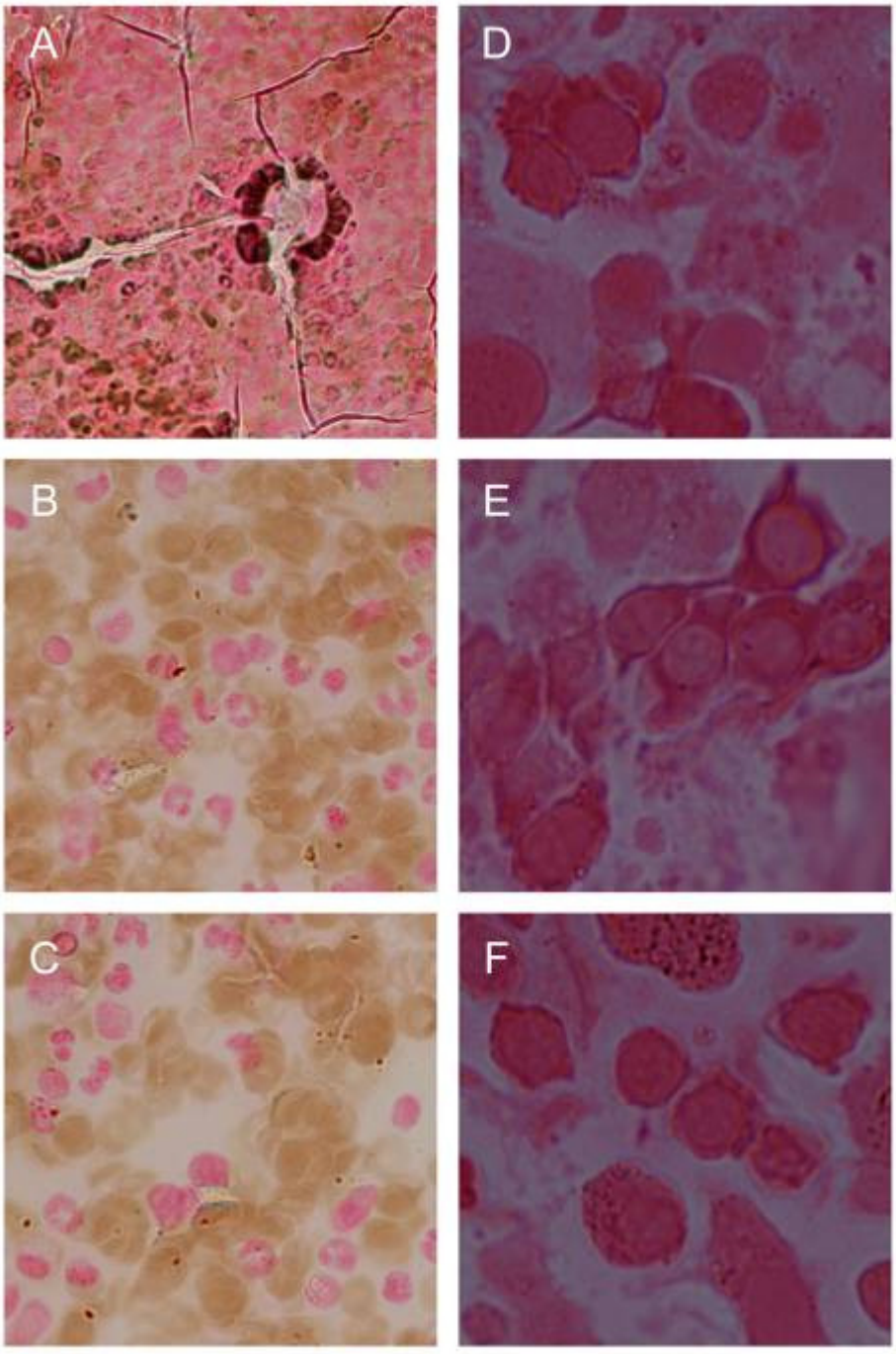

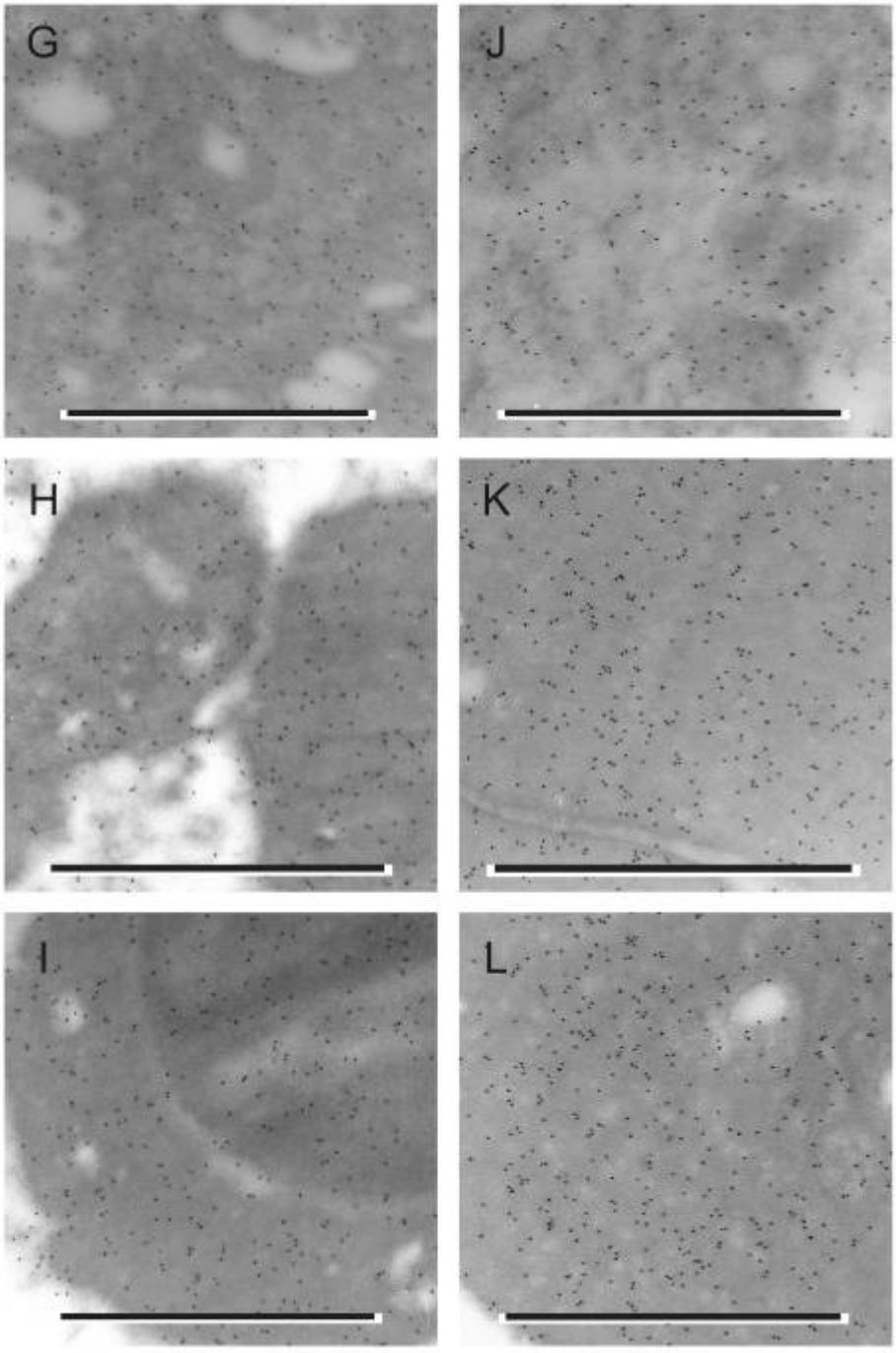
G
J
H
K
I
L

Figure 11

Kalafong patient 11

Figure 11a. A bone marrow fragment stained positive with the Prussian blue iron stain – severely increased amount of storage iron.

Figure 11b and c. Bone marrow aspirate smears stained with the Prussian blue iron stain with no sideroblasts.

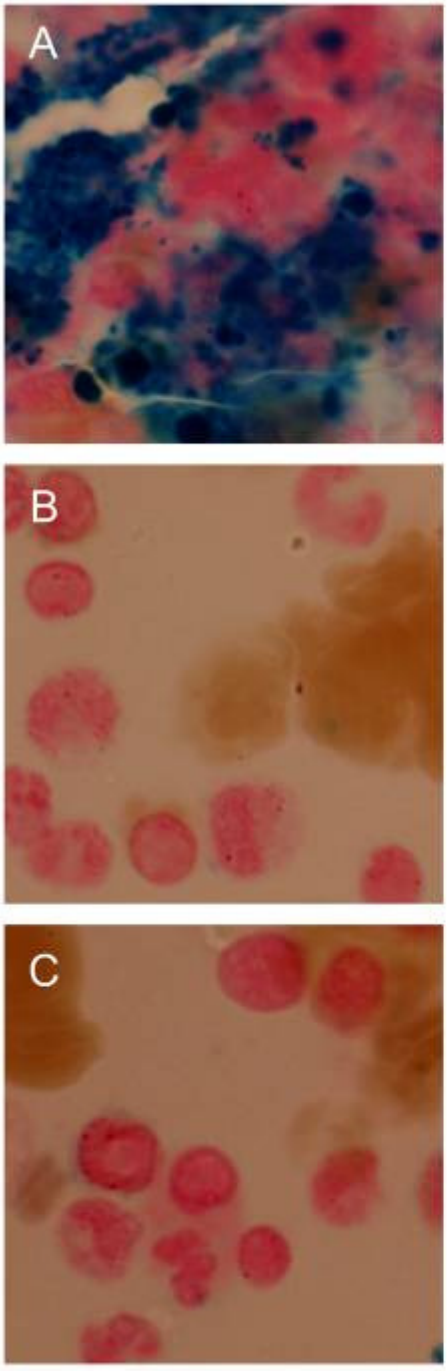
A
B
C

Figure 12

Kalafong patient 12

Figure 12a. A bone marrow fragment stained negative with the Prussian blue iron stain – no storage iron.

Figure 12b and c. Bone marrow aspirate smears stained with the Prussian blue iron stain with no sideroblasts.

Figure 12d. A bone marrow section stained blue with the Prussian blue iron stain – some storage iron.

Figure 12e and f. Bone marrow sections stained with the Prussian blue iron stain with no sideroblasts.

Figure 12g. An electron micrograph of a bone marrow macrophage immunolabelled with a monoclonal antibody to the H-subunit of ferritin, 10 nm gold particles and scale bar = 1 μm.

Figure 12h. An electron micrograph of two bone marrow red blood cells immunolabelled with a monoclonal antibody to the H-subunit of ferritin. Note the contact between the cell membranes of the two cells, 10 nm gold particles and scale bar = 1 μm.

Figure 12i. An electron micrograph of bone marrow red blood cells immunolabelled with a monoclonal antibody to the H-subunit of ferritin. Note the contact between the cell membranes of the cells with some iron-loaded ferritin in the space between the membranes, 10 nm gold particles and scale bar = 1 μm.

Figure 12j. An electron micrograph of a bone marrow macrophage immunolabelled with a monoclonal antibody to the L-subunit of ferritin, 10 nm gold particles and scale bar = 1 μm.

Figure 12k. An electron micrograph of two bone marrow reticulocytes immunolabelled with a monoclonal antibody to the L-subunit of ferritin. Note the contact between the two cell membranes and some iron-loaded ferritin in the space between the membranes, 10 nm gold particles and scale bar = 1 μm.

Figure 12l. An electron micrograph of a bone marrow reticulocyte immunolabelled with a monoclonal antibody to the L-subunit of ferritin, 10 nm gold particles and scale bar = 1 μm.

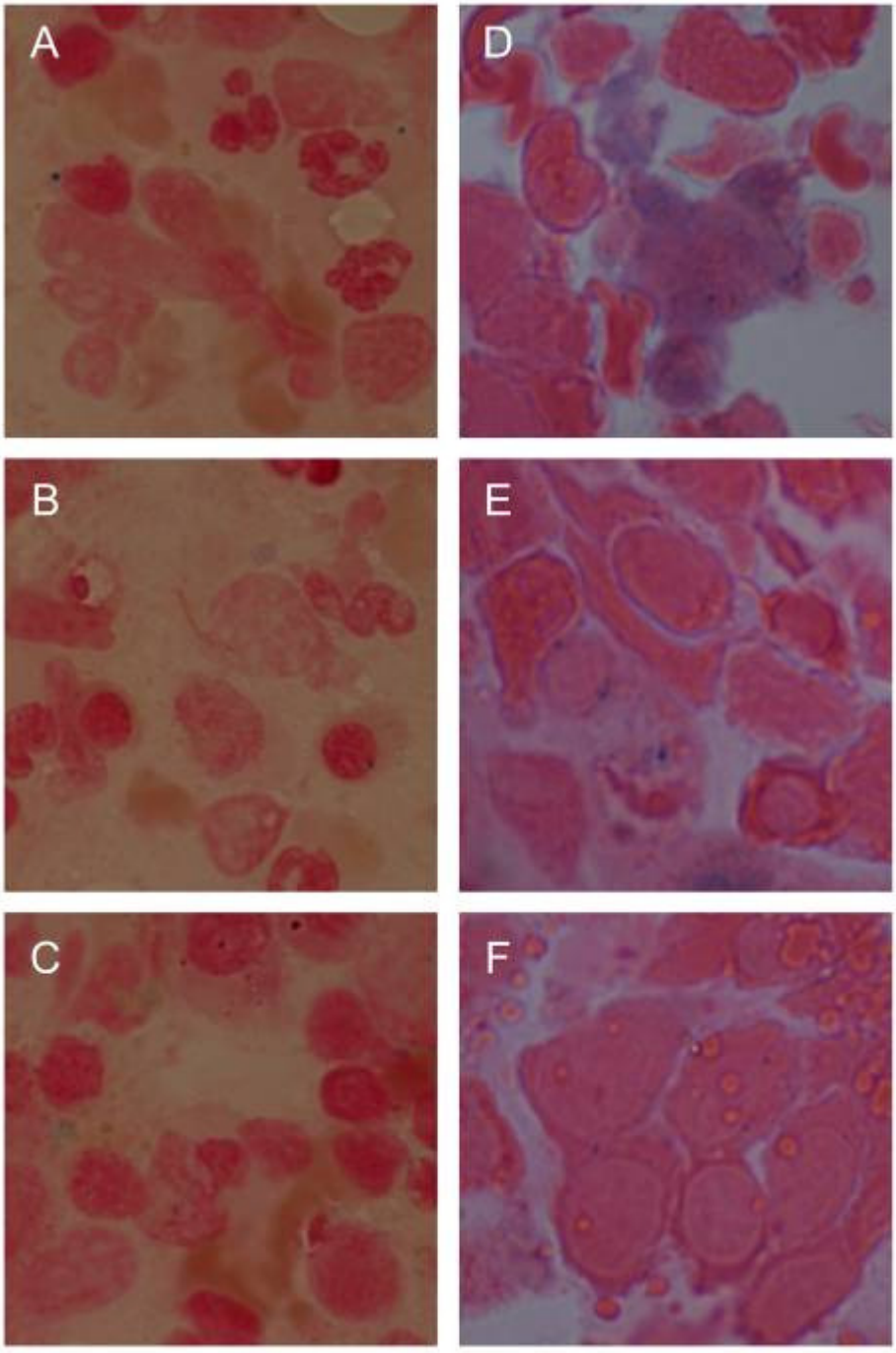
A
D
B
E
C
F

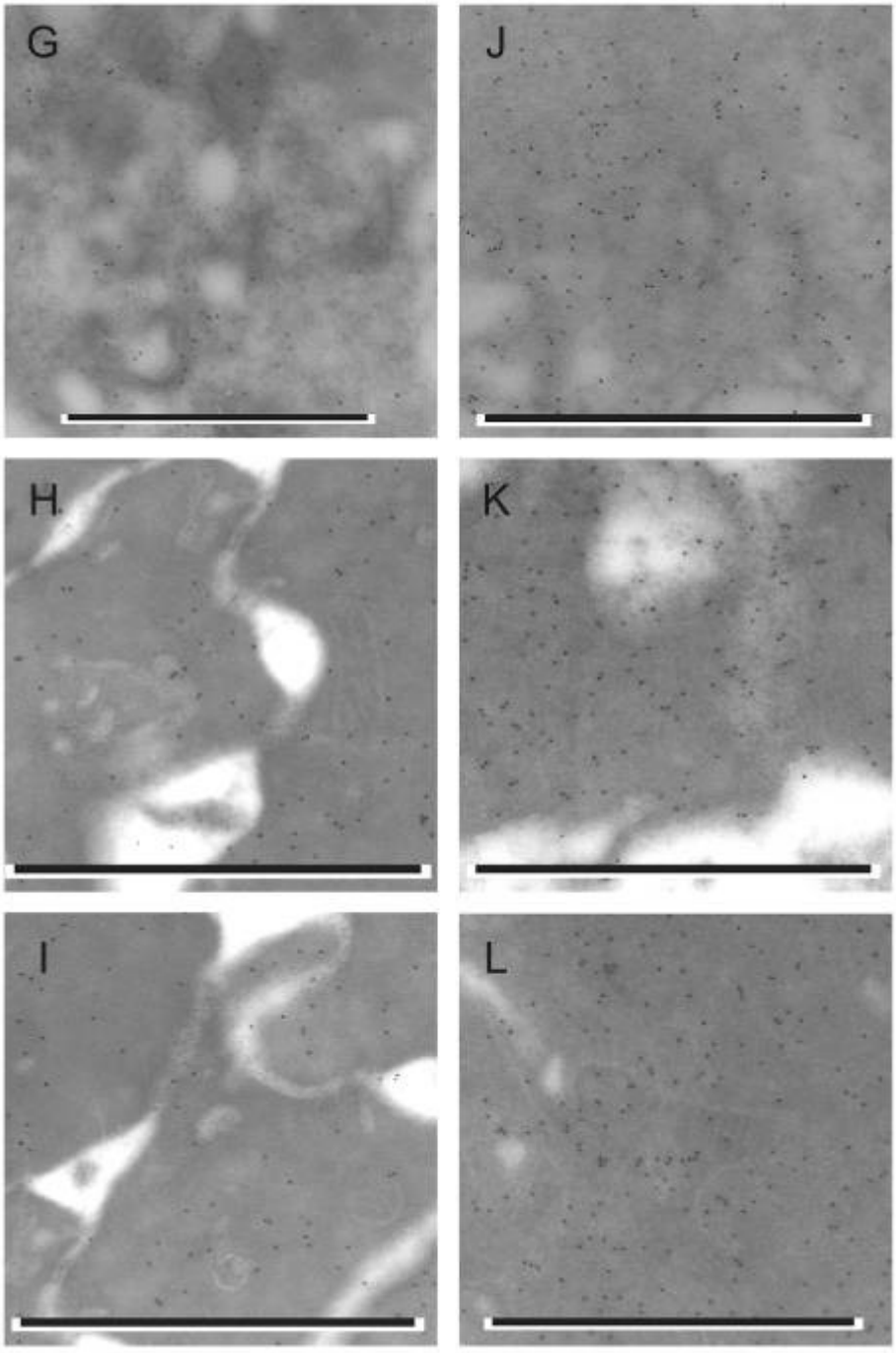
G
J
H
K
I
L

Figure 13

Kalafong patient 13

Figure 13d. A bone marrow section stained blue with the Prussian blue iron stain – severely increased amount of storage iron.

Figure 13e and f. Bone marrow sections stained with the Prussian blue iron stain with no sideroblasts.

Figure 13g. An electron micrograph of a bone marrow macrophage immunolabelled with a monoclonal antibody to the H-subunit of ferritin. Note the siderosomes and clusters of iron-loaded ferritin, 10 nm gold particles and scale bar = 1 μm.

Figure 13h. An electron micrograph of a bone marrow red blood cell precursor immunolabelled with a monoclonal antibody to the H-subunit of ferritin. Note the endocytic vesicle containing almost no iron-loaded ferritin, 10 nm gold particles and scale bar = 1 μm.

Figure 13i. An electron micrograph of a bone marrow red blood cell immunolabelled with a monoclonal antibody to the H-subunit of ferritin. Note the cluster of iron-loaded ferritin, 10 nm gold particles and scale bar = 1 μm.

Figure 13j. An electron micrograph of a bone marrow macrophage immunolabelled with a monoclonal antibody to the L-subunit of ferritin. Note the siderosomes and clusters of iron-loaded ferritin, 10 nm gold particles and scale bar = 1 μm.

Figure 13k. An electron micrograph of a bone marrow reticulocyte immunolabelled with a monoclonal antibody to the L-subunit of ferritin. Note the endocytic vesicle containing iron-loaded ferritin, 10 nm gold particles and scale bar = 1 μm.

Figure 13l. An electron micrograph of a bone marrow precursor immunolabelled with a monoclonal antibody to the L-subunit of ferritin. Note the endocytic vesicle containing some iron-loaded ferritin, 10 nm gold particles and scale bar = 1 μm.

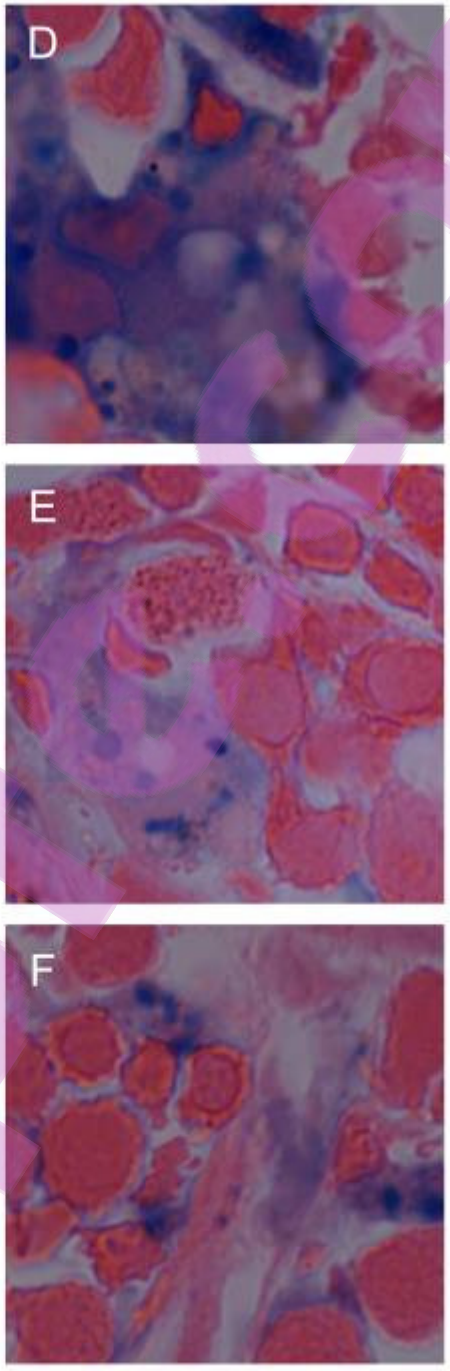

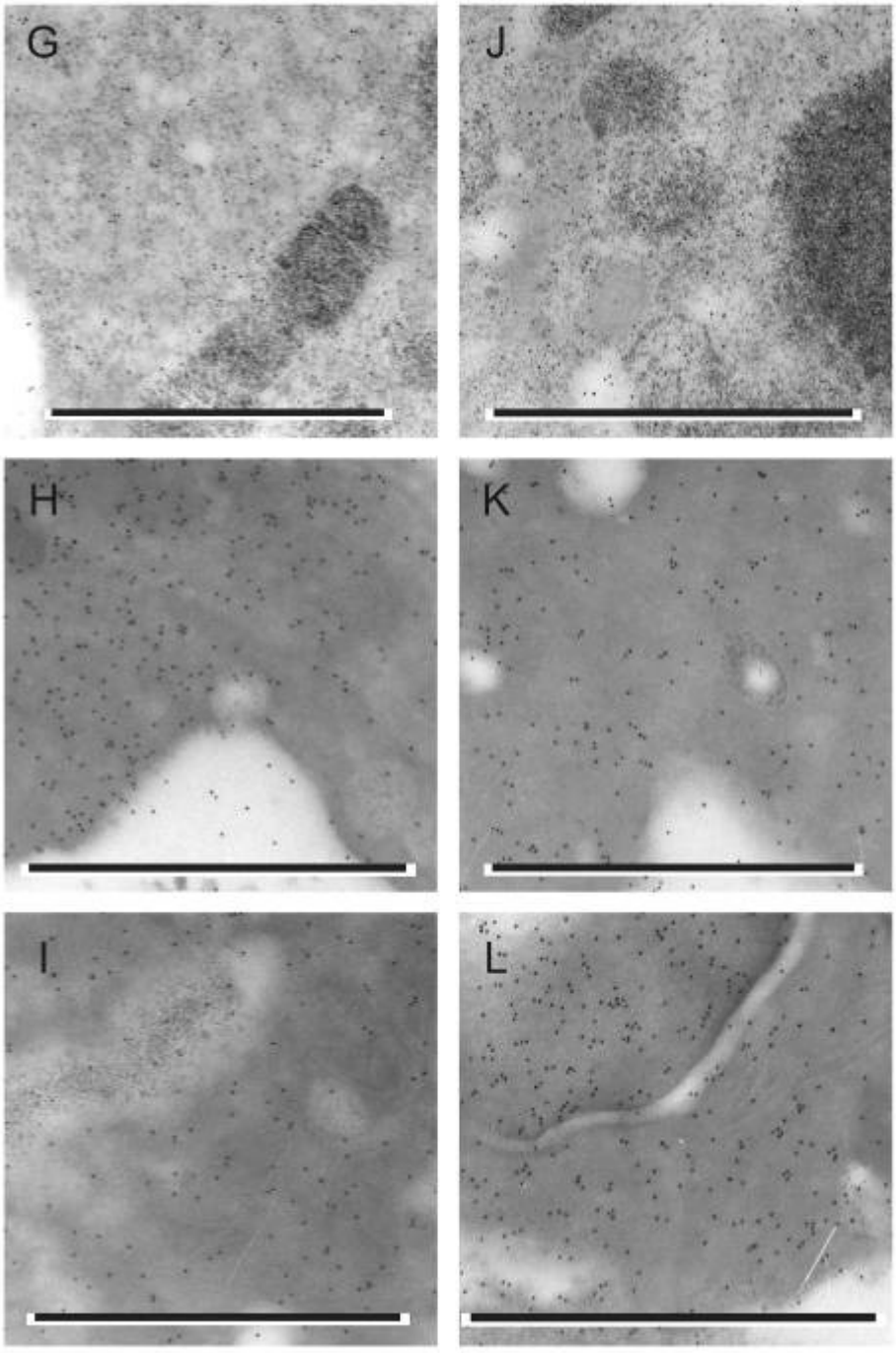
G
J
H
K
I
L

Figure 14

Kalafong patient 14

Figure 14d. A bone marrow section stained blue with the Prussian blue iron stain – increased amount of storage iron.

Figure 14e and f. Bone marrow sections stained with the Prussian blue iron stain with no sideroblasts.

Figure 14g. An electron micrograph of a bone marrow macrophage immunolabelled with a monoclonal antibody to the H-subunit of ferritin. Note the clusters of iron-loaded ferritin, 10 nm gold particles and scale bar = 1 μm.

Figure 14h. An electron micrograph of a bone marrow red blood cell precursor immunolabelled with a monoclonal antibody to the H-subunit of ferritin, 10 nm gold particles and scale bar = 1 μm.

Figure 14i. An electron micrograph of a bone marrow red blood cell immunolabelled with a monoclonal antibody to the H-subunit of ferritin, 10 nm gold particles and scale bar = 1 μm.

Figure 14j. An electron micrograph of a bone marrow macrophage immunolabelled with a monoclonal antibody to the L-subunit of ferritin, 10 nm gold particles and scale bar = 1 μm.

Figure 14k. An electron micrograph of a bone marrow reticulocyte and red blood cell immunolabelled with a monoclonal antibody to the L-subunit of ferritin. Note the contact between the two cell membranes and the iron-loaded ferritin in the space between the two cell membranes, 10 nm gold particles and scale bar = 1 μm.

Figure 14l. An electron micrograph of a bone marrow precursor immunolabelled with a monoclonal antibody to the L-subunit of ferritin. Note the endocytic vesicle containing iron-loaded ferritin, 10 nm gold particles and scale bar = 1 μm.

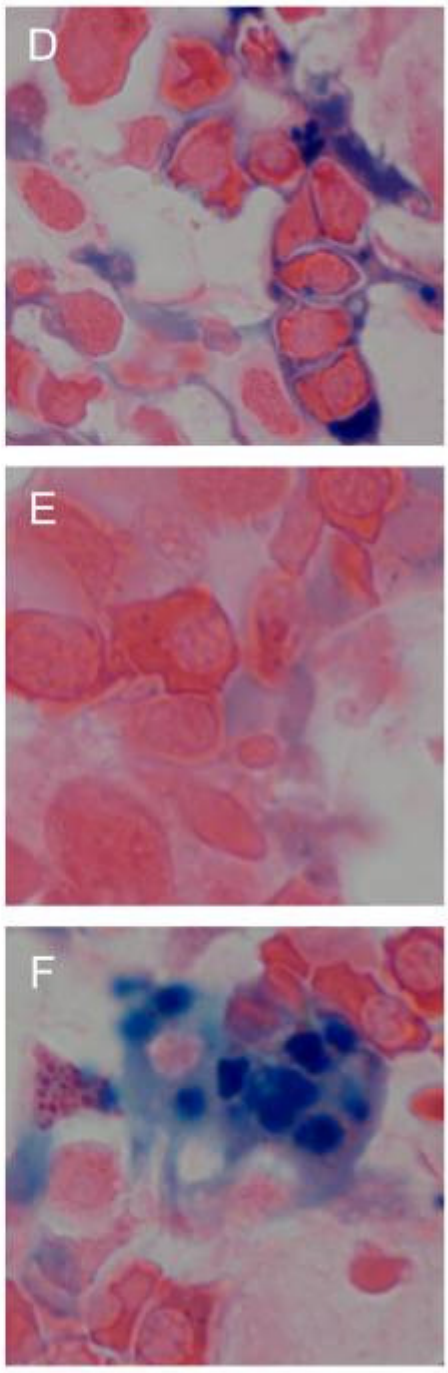
D
E
F

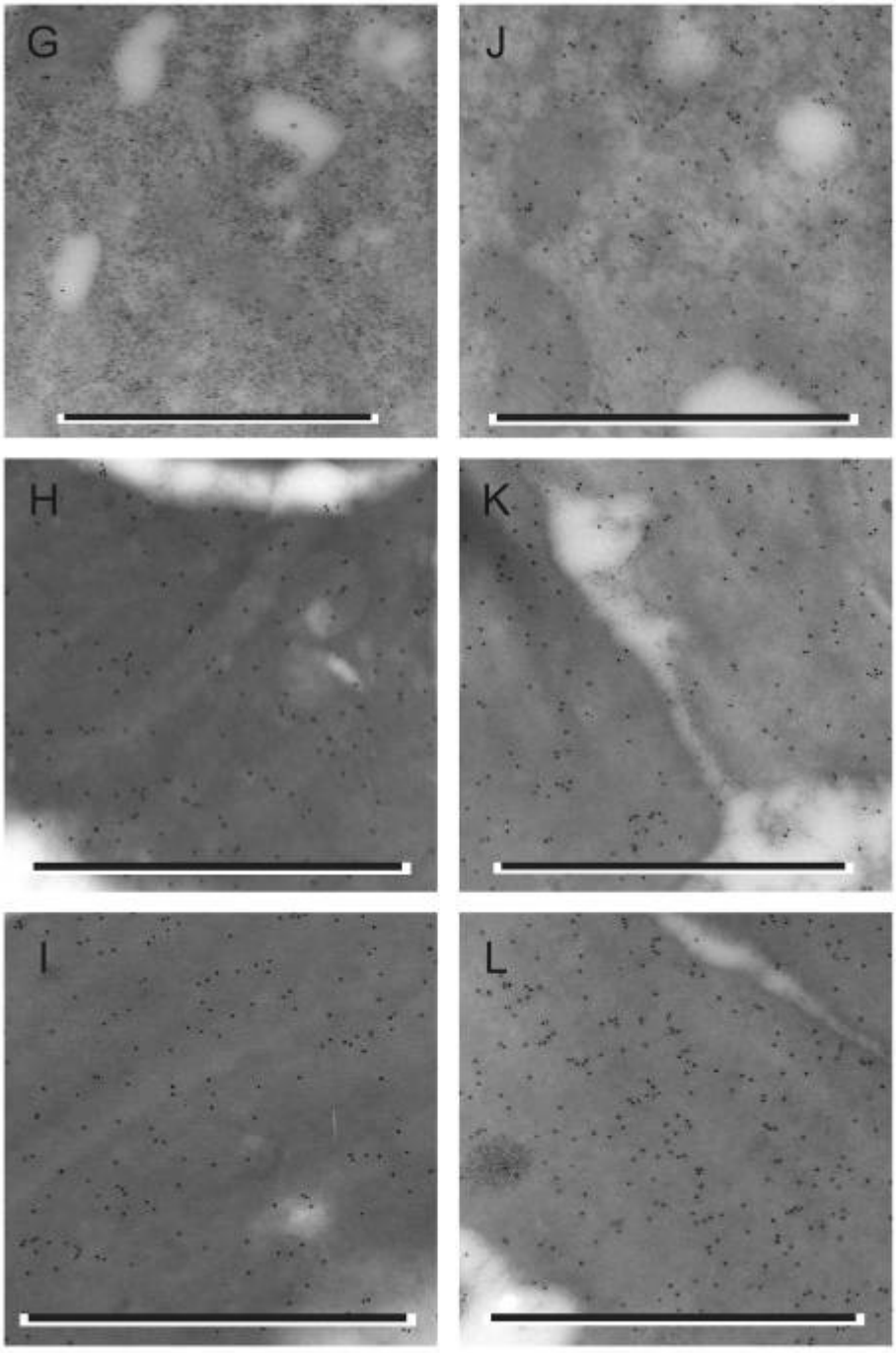
G
J
H
K
I
L

Figure 15

Kalafong patient 15

Figure 15a. A bone marrow fragment stained positive with the Prussian blue iron stain – increased amount of storage iron.

Figure 15b and c. Bone marrow aspirate smears stained with the Prussian blue iron stain with a few pathologically overloaded sideroblasts.

Figure 15d. A bone marrow section stained blue with the Prussian blue iron stain – some storage iron.

Figure 15e and f. Bone marrow sections stained with the Prussian blue iron stain with a few pathologically overloaded sideroblasts.

Figure 15g. An electron micrograph of a bone marrow macrophage immunolabelled with a monoclonal antibody to the H-subunit of ferritin, 10 nm gold particles and scale bar = 1 μm.

Figure 15h. An electron micrograph of a bone marrow red blood cell precursor immunolabelled with a monoclonal antibody to the H-subunit of ferritin, 10 nm gold particles and scale bar = 1 μm.

Figure 15i. An electron micrograph of a bone marrow red blood cell precursor immunolabelled with a monoclonal antibody to the H-subunit of ferritin, 10 nm gold particles and scale bar = 1 μm.

Figure 15j. An electron micrograph of a bone marrow macrophage immunolabelled with a monoclonal antibody to the L-subunit of ferritin, 10 nm gold particles and scale bar = 1 μm.

Figure 15k. An electron micrograph of two bone marrow red blood cell precursors immunolabelled with a monoclonal antibody to the L-subunit of ferritin. Note the contact between the two cell membranes and some iron-loaded ferritin in the space between the membranes, 10 nm gold particles and scale bar = 1 μm.

Figure 15l. An electron micrograph of a bone marrow reticulocyte immunolabelled with a monoclonal antibody to the L-subunit of ferritin. Note the cluster of ferritin – haemosiderin, 10 nm gold particles and scale bar = 1 μm.

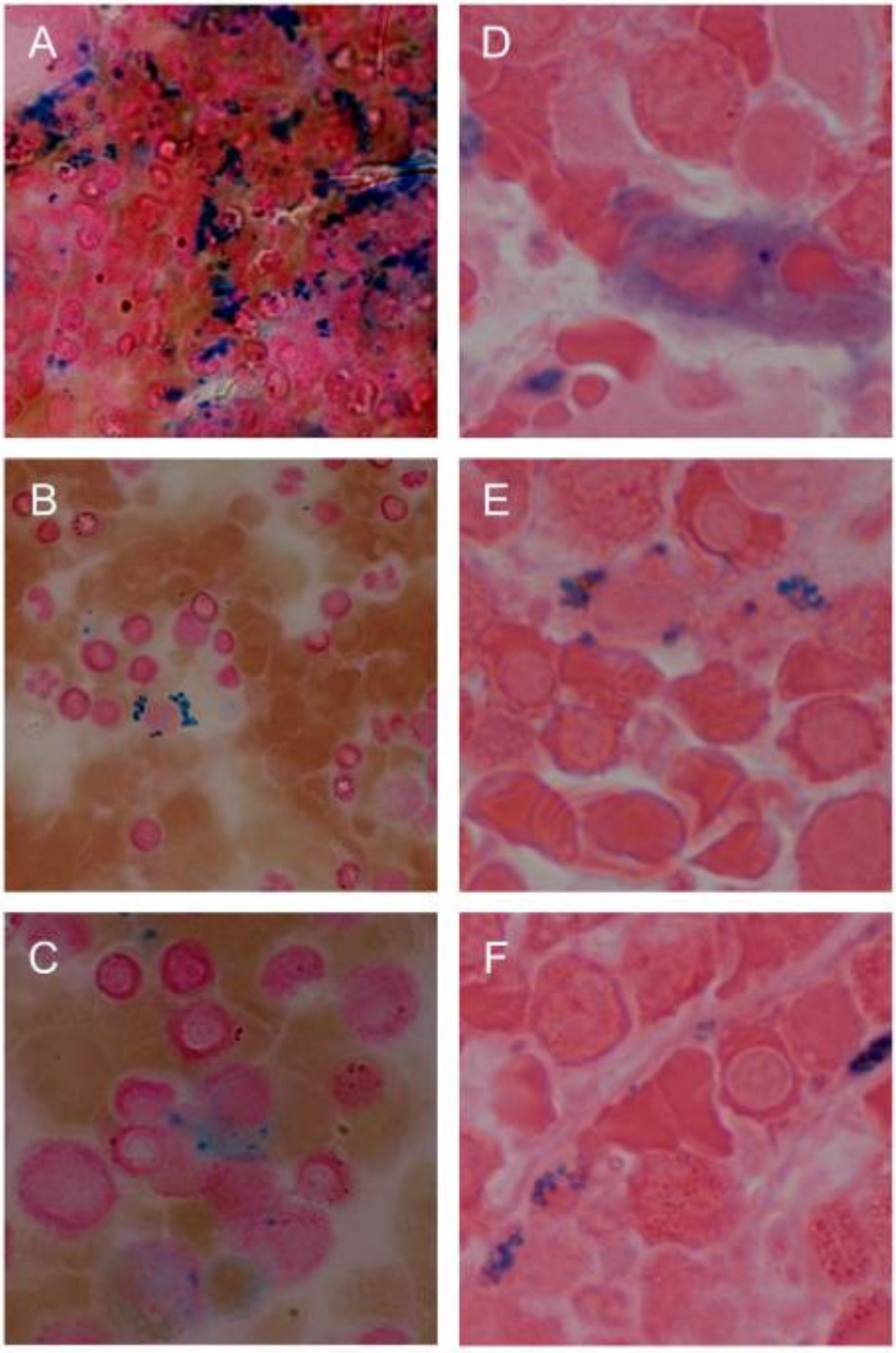
A
D
B
E
C
F

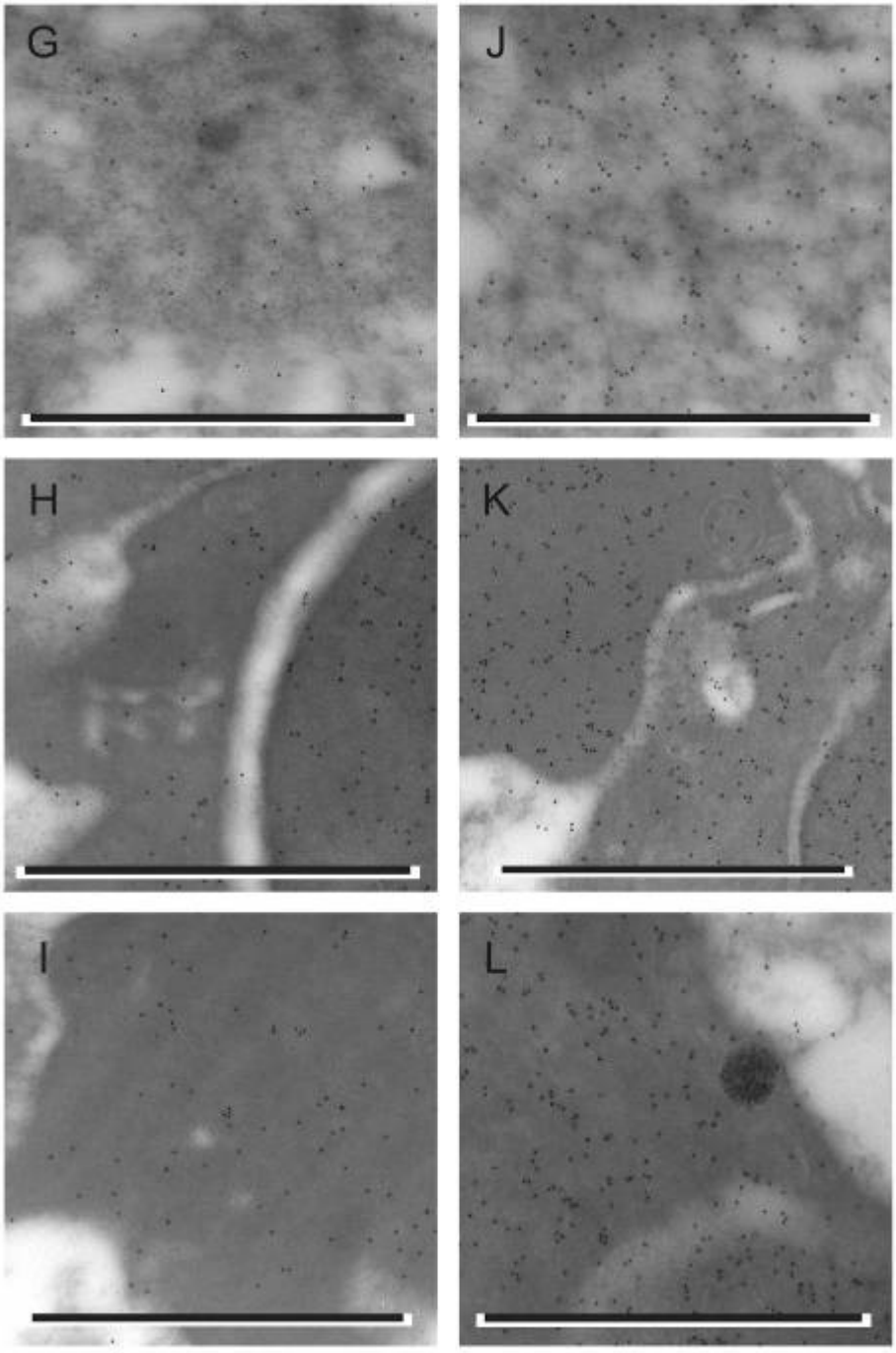
G
J
H
K
I
L

Figure 16

Kalafong patient 16

Figure 16a. A bone marrow fragment stained negative with the Prussian blue iron stain – absent storage iron.

Figure 16b and c. Bone marrow aspirate smears stained with the Prussian blue iron stain with no sideroblasts.

Figure 16d. A bone marrow section stained with the Prussian blue iron stain – absent storage iron.

Figure 16e and f. Bone marrow sections stained with the Prussian blue iron stain with no sideroblasts.

Figure 16g. An electron micrograph of a bone marrow macrophage immunolabelled with a monoclonal antibody to the H-subunit of ferritin, 10 nm gold particles and scale bar = 1 µm.

Figure 16h. An electron micrograph of two bone marrow red blood cell precursors immunolabelled with a monoclonal antibody to the H-subunit of ferritin. Note the iron-loaded ferritin in the space between the cell membranes, 10 nm gold particles and scale bar = 1 µm.

Figure 16i. An electron micrograph of two bone marrow red blood cell precursors immunolabelled with a monoclonal antibody to the H-subunit of ferritin. Note some iron-loaded ferritin in the space between the cell membranes, 10 nm gold particles and scale bar = 1 µm.

Figure 16j. An electron micrograph of a bone marrow macrophage immunolabelled with a monoclonal antibody to the L-subunit of ferritin, 10 nm gold particles and scale bar = 1 µm.

Figure 16k. An electron micrograph of a bone marrow red blood cell precursor immunolabelled with a monoclonal antibody to the L-subunit of ferritin. Note the absence of iron-loaded ferritin in the endocytic vesicle, 10 nm gold particles and scale bar = 1 µm.

Figure 16l. An electron micrograph of a bone marrow red blood cell precursor immunolabelled with a monoclonal antibody to the L-subunit of ferritin, 10 nm gold particles and scale bar = 1 µm.

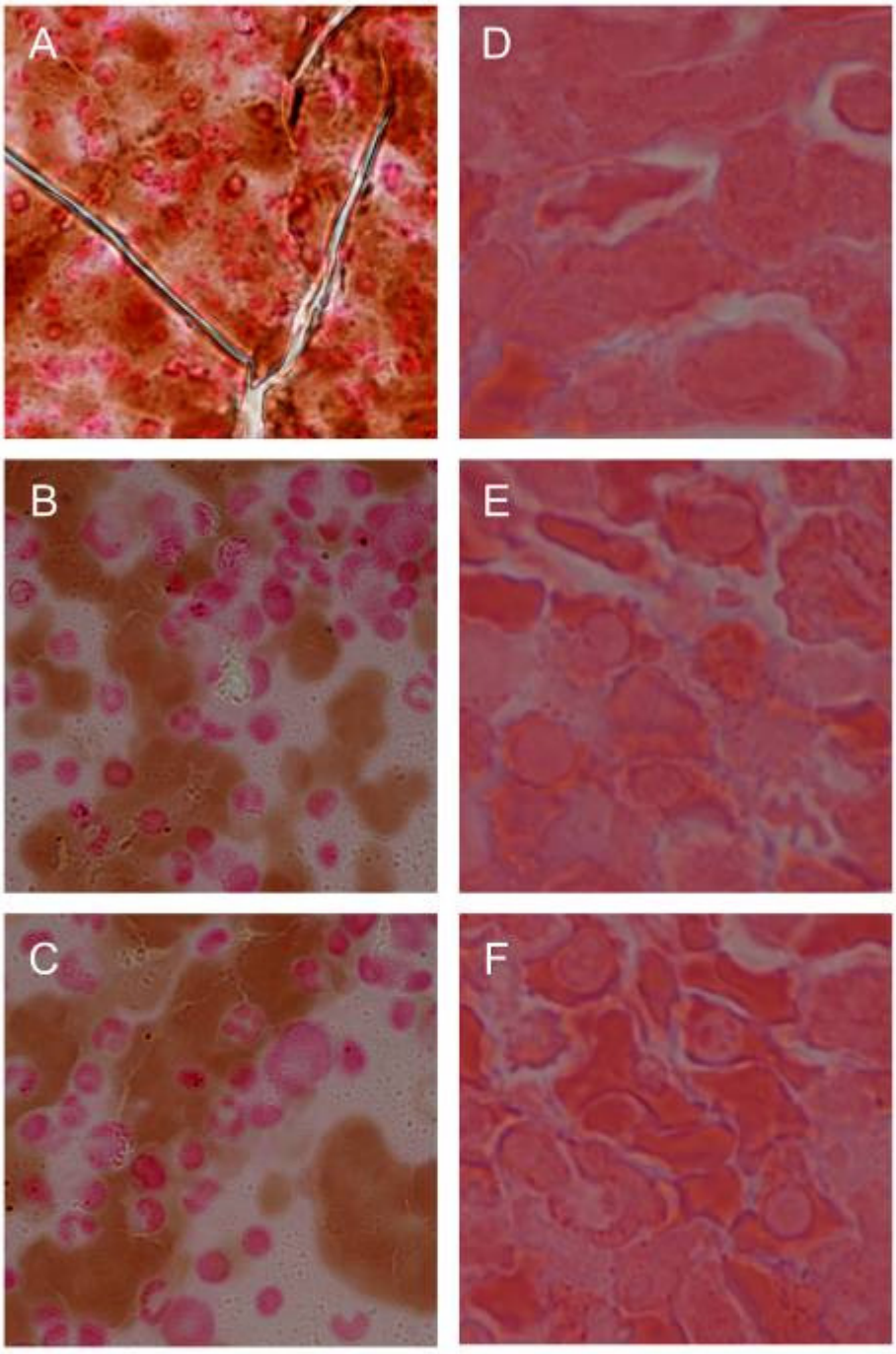
A
D
B
E
C
F

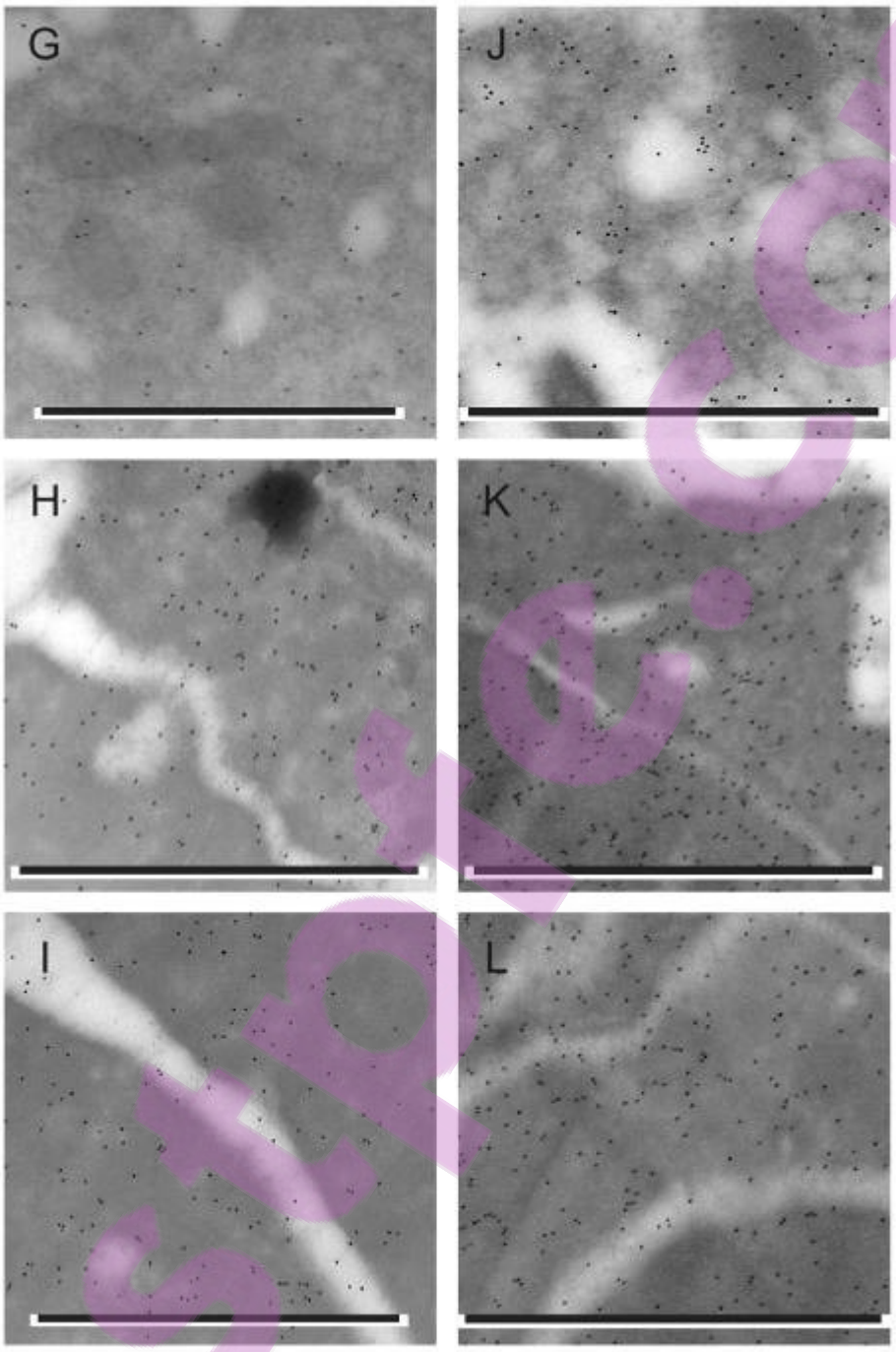

Figure 17

Kalafong patient 17

Figure 17d. A bone marrow section stained blue with the Prussian blue iron stain – some storage iron.

Figure 17e and f. Bone marrow sections stained with the Prussian blue iron stain with some sideroblasts.

Figure 17g. An electron micrograph of a bone marrow macrophage immunolabelled with a monoclonal antibody to the H-subunit of ferritin. Note the siderosome, 10 nm gold particles and scale bar = 1 μm.

Figure 17h. An electron micrograph of a bone marrow reticulocyte immunolabelled with a monoclonal antibody to the H-subunit of ferritin, 10 nm gold particles and scale bar = 1 μm.

Figure 17i. An electron micrograph of a bone marrow red blood cell precursor immunolabelled with a monoclonal antibody to the H-subunit of ferritin, 10 nm gold particles and scale bar = 1 μm.

Figure 17j. An electron micrograph of a bone marrow macrophage immunolabelled with a monoclonal antibody to the L-subunit of ferritin. Note the siderosomes, 10 nm gold particles and scale bar = 1 μm.

Figure 17k. An electron micrograph of a bone marrow red blood cell precursor immunolabelled with a monoclonal antibody to the L-subunit of ferritin, 10 nm gold particles and scale bar = 1 μm.

Figure 17l. An electron micrograph of a bone marrow red blood cell precursor immunolabelled with a monoclonal antibody to the L-subunit of ferritin, 10 nm gold particles and scale bar = 1 μm.

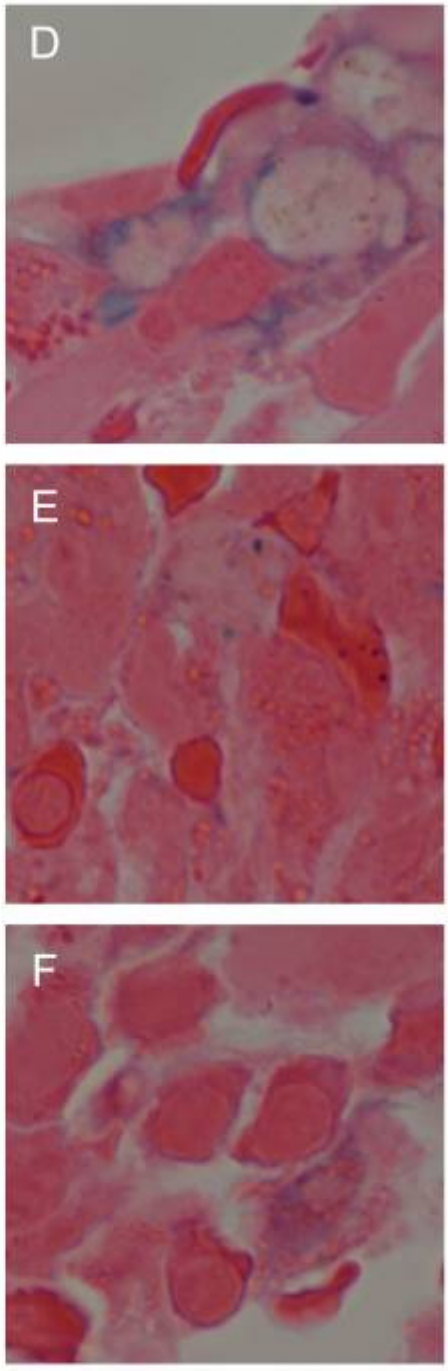

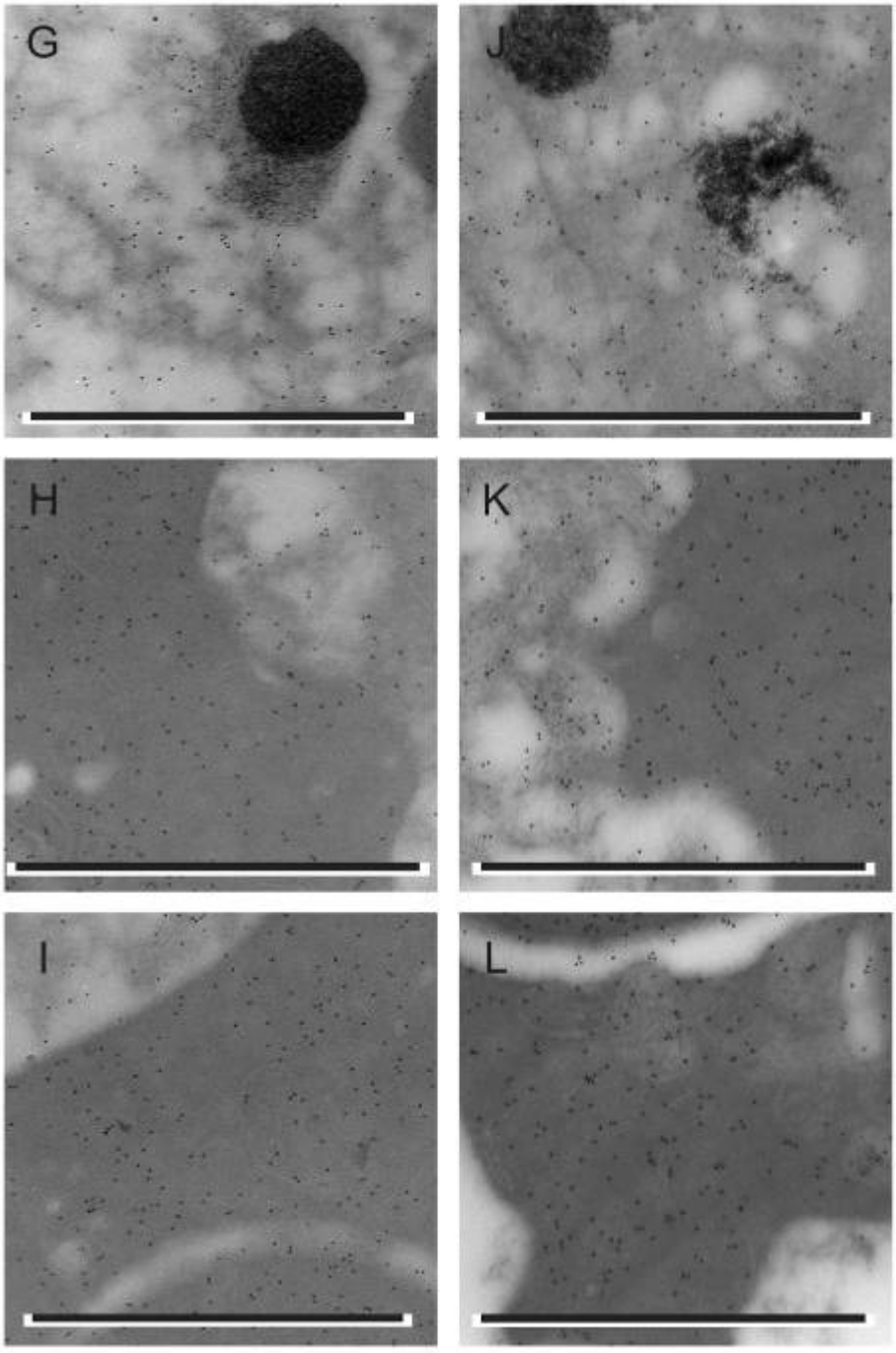
G
J
H
K
I
L

Figure 18

Kalafong patient 18

Figure 18d. A bone marrow section stained blue with the Prussian blue iron stain – some storage iron.

Figure 18e and f. Bone marrow sections stained with the Prussian blue iron stain with some sideroblasts.

Figure 18g. An electron micrograph of a bone marrow macrophage immunolabelled with a monoclonal antibody to the H-subunit of ferritin, 10 nm gold particles and scale bar = 1 μm.

Figure 18h. An electron micrograph of a bone marrow red blood cell precursor immunolabelled with a monoclonal antibody to the H-subunit of ferritin, 10 nm gold particles and scale bar = 1 μm.

Figure 18i. An electron micrograph of a bone marrow red blood cell precursor immunolabelled with a monoclonal antibody to the H-subunit of ferritin. Note the cluster of ferritin near the nucleus – haemosiderin, 10 nm gold particles and scale bar = 1 μm.

Figure 18j. An electron micrograph of a bone marrow macrophage immunolabelled with a monoclonal antibody to the L-subunit of ferritin. Note the presence of some iron-loaded ferritin, 10 nm gold particles and scale bar = 1 μm.

Figure 18k. An electron micrograph of a bone marrow red blood cell precursor immunolabelled with a monoclonal antibody to the L-subunit of ferritin, 10 nm gold particles and scale bar = 1 μm.

Figure 18l. An electron micrograph of a bone marrow reticulocyte immunolabelled with a monoclonal antibody to the L-subunit of ferritin. Note the small cluster of ferritin – haemosiderin, 10 nm gold particles and scale bar = 1 μm.

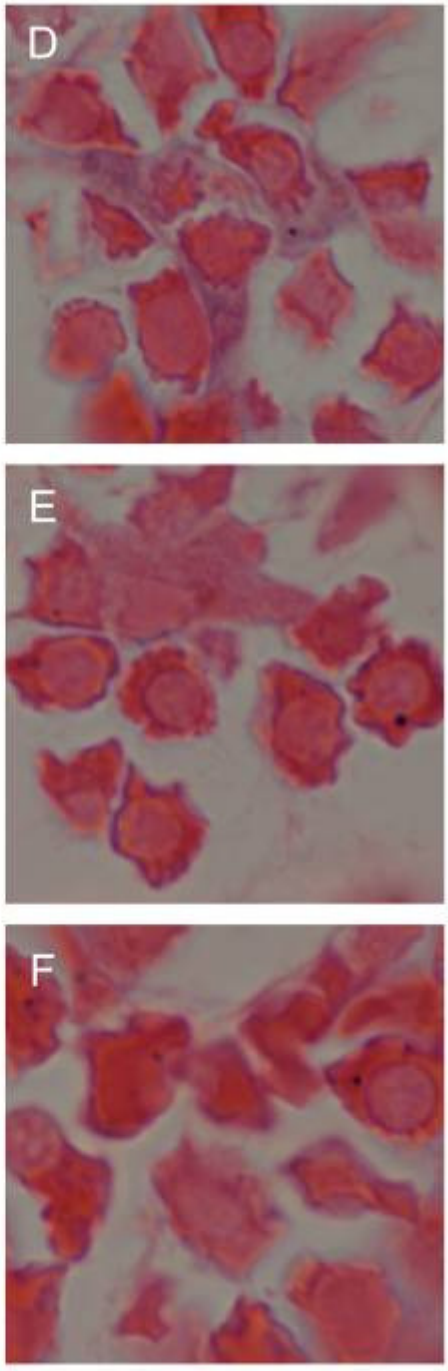
D
E
F

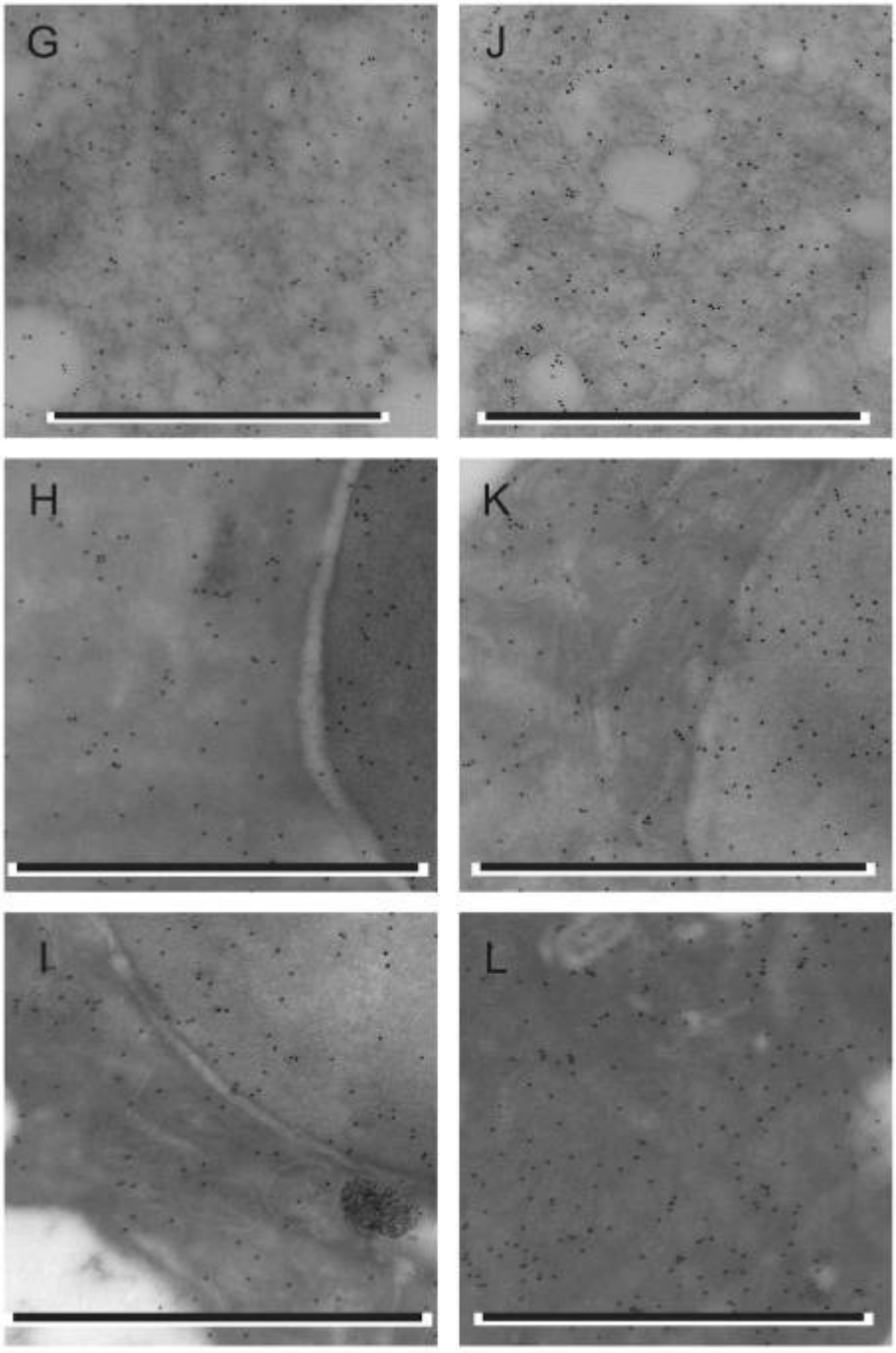
G
J
H
K
I
L

Figure 19

Kalafong patient 19

Figure 19d. A bone marrow section stained blue with the Prussian blue iron stain – increased amount of storage iron.

Figure 19e and f. Bone marrow sections stained with the Prussian blue iron stain with no sideroblasts.

Figure 19g. An electron micrograph of a bone marrow macrophage immunolabelled with a monoclonal antibody to the H-subunit of ferritin. Note the siderosomes, 10 nm gold particles and scale bar = 1 μm.

Figure 19h. An electron micrograph of a bone marrow reticulocyte immunolabelled with a monoclonal antibody to the H-subunit of ferritin, 10 nm gold particles and scale bar = 1 μm.

Figure 19i. An electron micrograph of two bone marrow red blood cell precursors immunolabelled with a monoclonal antibody to the H-subunit of ferritin, 10 nm gold particles and scale bar = 1 μm.

Figure 19j. An electron micrograph of a bone marrow macrophage immunolabelled with a monoclonal antibody to the L-subunit of ferritin. Note the presence of iron-loaded ferritin, 10 nm gold particles and scale bar = 1 μm.

Figure 19k. An electron micrograph of a bone marrow red blood cell precursor immunolabelled with a monoclonal antibody to the L-subunit of ferritin, 10 nm gold particles and scale bar = 1 μm.

Figure 19l. An electron micrograph of a bone marrow red blood cell precursor immunolabelled with a monoclonal antibody to the L-subunit of ferritin, 10 nm gold particles and scale bar = 1 μm.

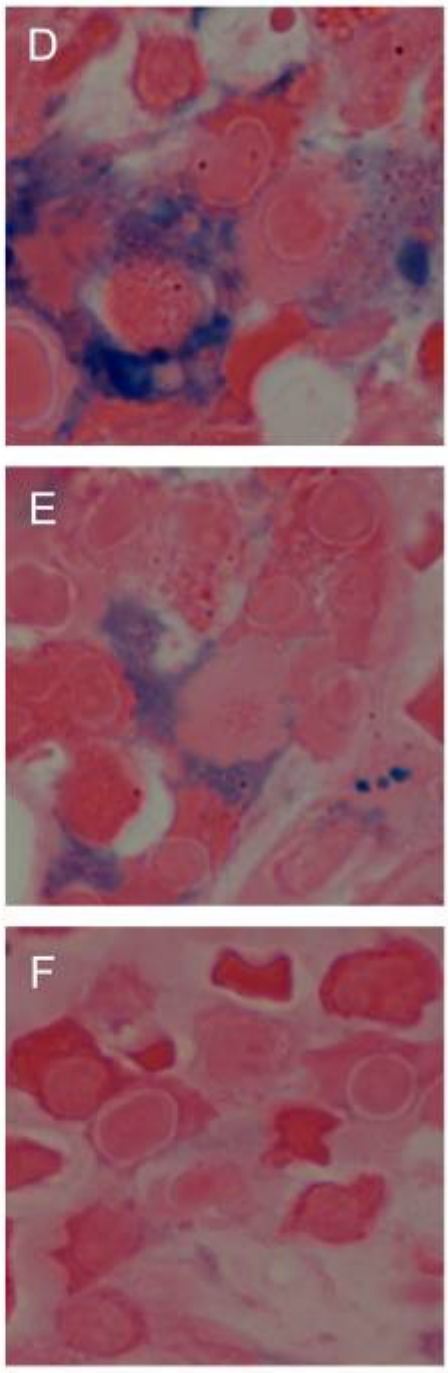
D
E
F

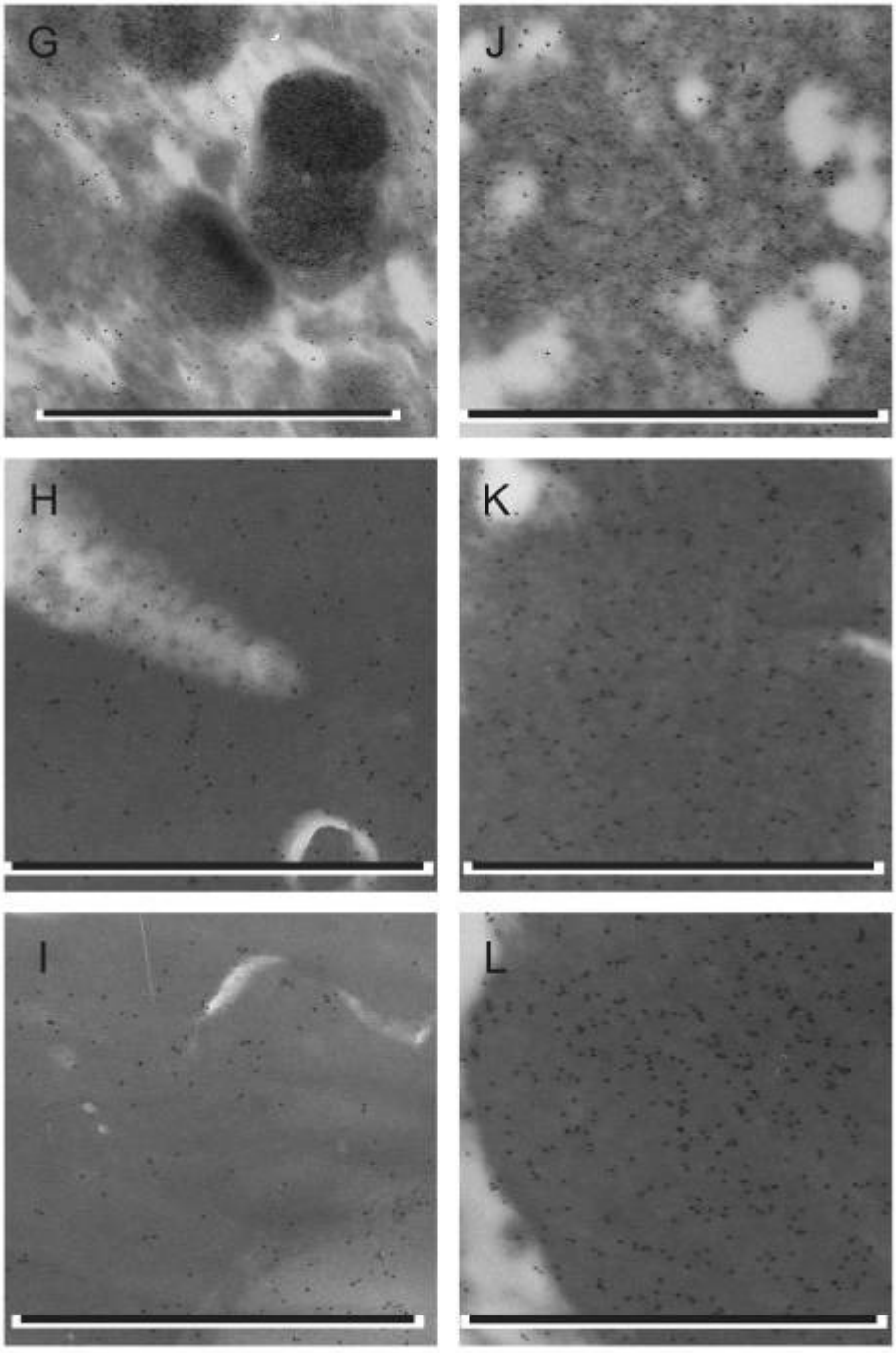
G
J
H
K
I
L

Figure 20

Kalafong patient 20

Figure 20a. A bone marrow fragment stained negative with the Prussian blue iron stain – absent storage iron.

Figure 20b and c. Bone marrow aspirate smears stained with the Prussian blue iron stain with no sideroblasts.

Figure 20d. A bone marrow section stained negative with the Prussian blue iron stain – absent storage iron.

Figure 20e and f. Bone marrow sections stained with the Prussian blue iron stain with no sideroblasts.

Figure 20g. An electron micrograph of a bone marrow macrophage immunolabelled with a monoclonal antibody to the H-subunit of ferritin, 10 nm gold particles and scale bar = 1 μm.

Figure 20h. An electron micrograph of two bone marrow red blood cell precursors immunolabelled with a monoclonal antibody to the H-subunit of ferritin, 10 nm gold particles and scale bar = 1 μm.

Figure 20i. An electron micrograph of two bone marrow reticulocytes immunolabelled with a monoclonal antibody to the H-subunit of ferritin, 10 nm gold particles and scale bar = 1 μm.

Figure 20j. An electron micrograph of a bone marrow macrophage immunolabelled with a monoclonal antibody to the L-subunit of ferritin, 10 nm gold particles and scale bar = 1 μm.

Figure 20k. An electron micrograph of two bone marrow red blood cell precursors immunolabelled with a monoclonal antibody to the L-subunit of ferritin. Note the contact between the two cell membranes and no iron-loaded ferritin in the space between the membranes, 10 nm gold particles and scale bar = 1 μm.

Figure 20l. An electron micrograph of a bone marrow reticulocyte immunolabelled with a monoclonal antibody to the L-subunit of ferritin, 10 nm gold particles and scale bar = 1 μm.

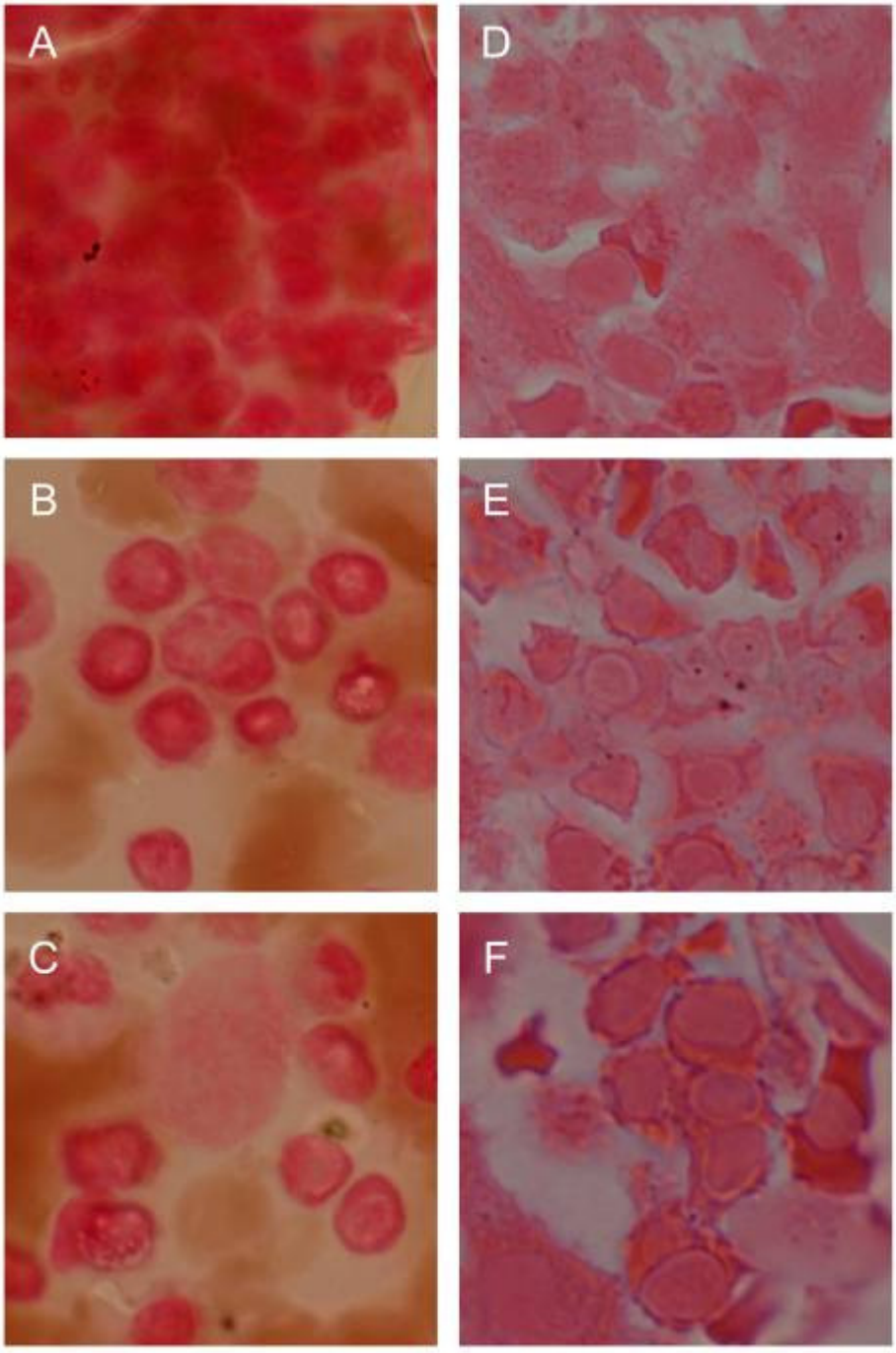
A
D
B
E
C
F

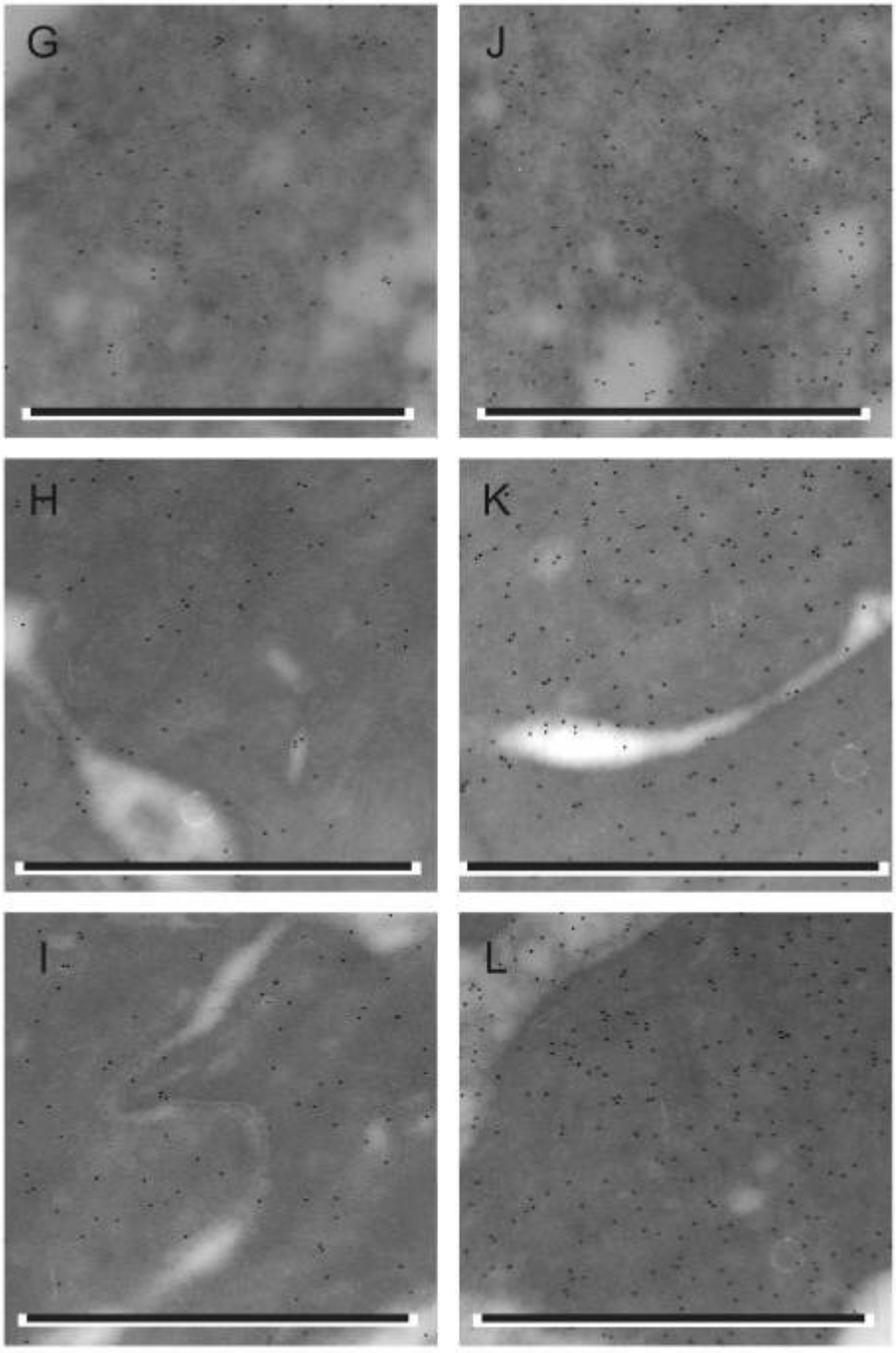

Figure 21

Kalafong patient 21

Figure 21a. A bone marrow fragment stained positive with the Prussian blue iron stain – severely increased amount of storage iron.

Figure 21b and c. Bone marrow aspirate smears stained with the Prussian blue iron stain with no sideroblasts.

Figure 21d. A bone marrow section stained blue with the Prussian blue iron stain – severely increased amount of storage iron.

Figure 21e and f. Bone marrow sections stained with the Prussian blue iron stain with some sideroblasts.

Figure 21g. An electron micrograph of a bone marrow macrophage immunolabelled with a monoclonal antibody to the H-subunit of ferritin, 10 nm gold particles and scale bar = 1 μm.

Figure 21h. An electron micrograph of a bone marrow red blood cell precursor immunolabelled with a monoclonal antibody to the H-subunit of ferritin, 10 nm gold particles and scale bar = 1 μm.

Figure 21i. An electron micrograph of a bone marrow red blood cell precursor immunolabelled with a monoclonal antibody to the H-subunit of ferritin, 10 nm gold particles and scale bar = 1 μm.

Figure 21j. An electron micrograph of a bone marrow macrophage immunolabelled with a monoclonal antibody to the L-subunit of ferritin, 10 nm gold particles and scale bar = 1 μm.

Figure 21k. An electron micrograph of a bone marrow red blood cell precursor immunolabelled with a monoclonal antibody to the L-subunit of ferritin, 10 nm gold particles and scale bar = 1 μm.

Figure 21l. An electron micrograph of a bone marrow reticulocyte immunolabelled with a monoclonal antibody to the L-subunit of ferritin. Note the small amount of iron-loaded ferritin in the endocytic vesicle, 10 nm gold particles and scale bar = 1 μm.

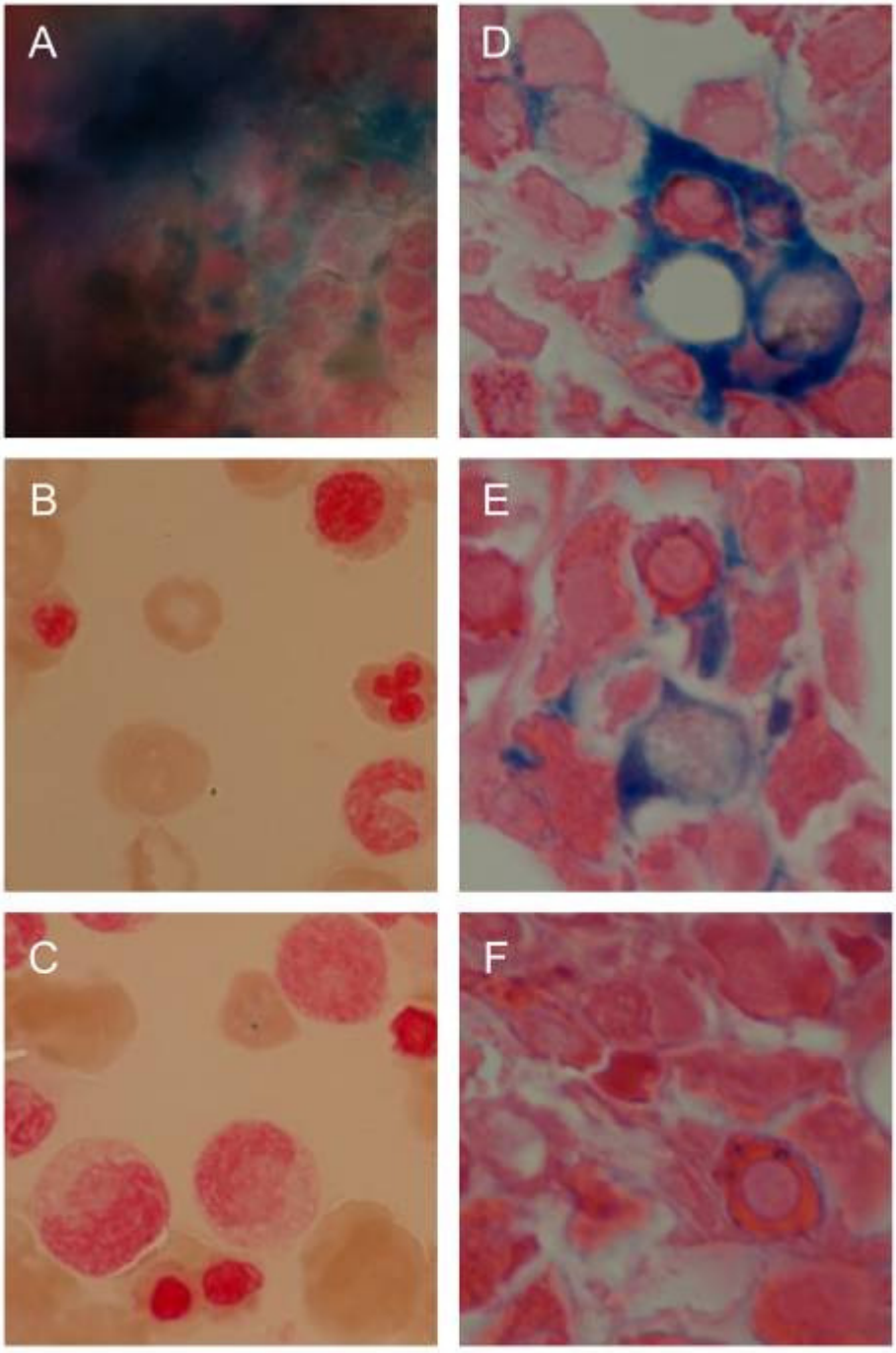
A
D
B
E
C
F

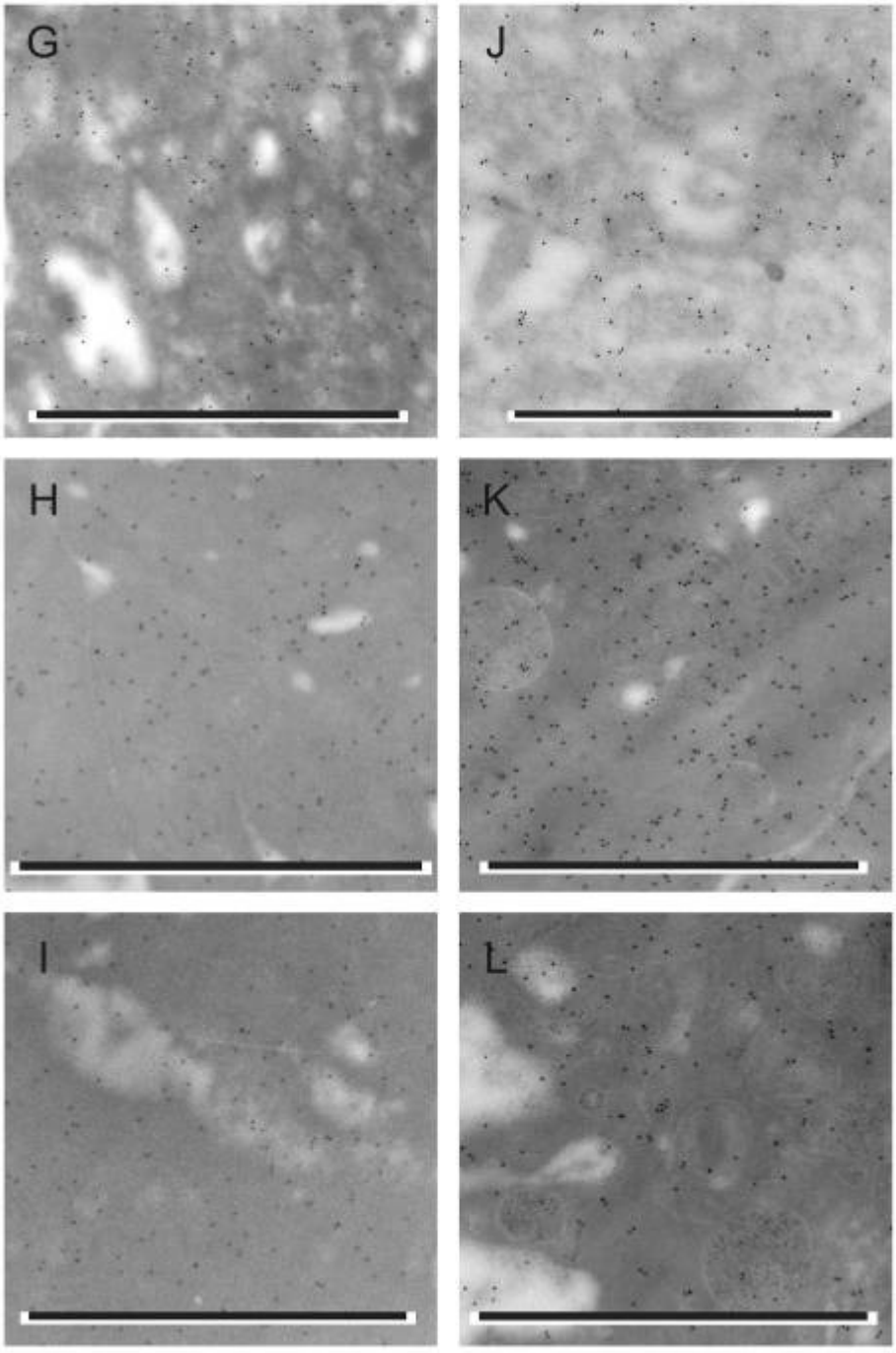
G
J
H
K
I
L

Figure 22

Kalafong patient 22

Figure 22a. A bone marrow fragment stained positive with the Prussian blue iron stain – increased amount of storage iron.

Figure 22b and c. Bone marrow aspirate smears stained with the Prussian blue iron stain with some sideroblasts.

Figure 22d. A bone marrow section stained blue with the Prussian blue iron stain – increased amount of storage iron.

Figure 22e and f. Bone marrow sections stained with the Prussian blue iron stain with some sideroblasts.

Figure 22g. An electron micrograph of a bone marrow macrophage immunolabelled with a monoclonal antibody to the H-subunit of ferritin, 10 nm gold particles and scale bar = 1 μm.

Figure 22h. An electron micrograph of a bone marrow red blood cell immunolabelled with a monoclonal antibody to the H-subunit of ferritin, 10 nm gold particles and scale bar = 1 μm.

Figure 22i. An electron micrograph of a bone marrow red blood cell immunolabelled with a monoclonal antibody to the H-subunit of ferritin, 10 nm gold particles and scale bar = 1 μm.

Figure 22j. An electron micrograph of a bone marrow macrophage immunolabelled with a monoclonal antibody to the L-subunit of ferritin, 10 nm gold particles and scale bar = 1 μm.

Figure 22k. An electron micrograph of a bone marrow red blood cell precursor immunolabelled with a monoclonal antibody to the L-subunit of ferritin. Note the cluster of iron-loaded ferritin, 10 nm gold particles and scale bar = 1 μm.

Figure 22l. An electron micrograph of a bone marrow reticulocyte immunolabelled with a monoclonal antibody to the L-subunit of ferritin, 10 nm gold particles and scale bar = 1 μm.

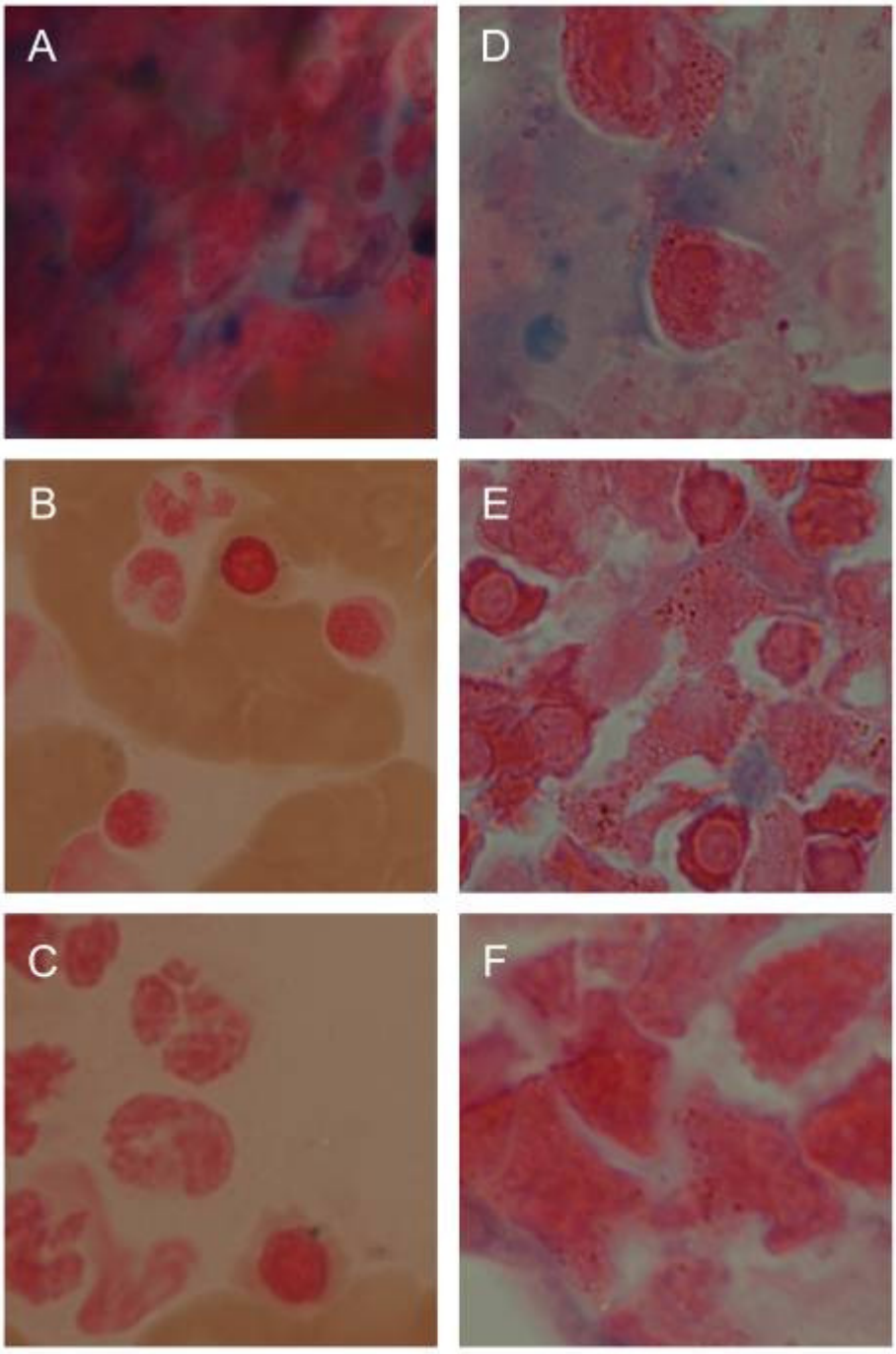
A
D
B
E
C
F

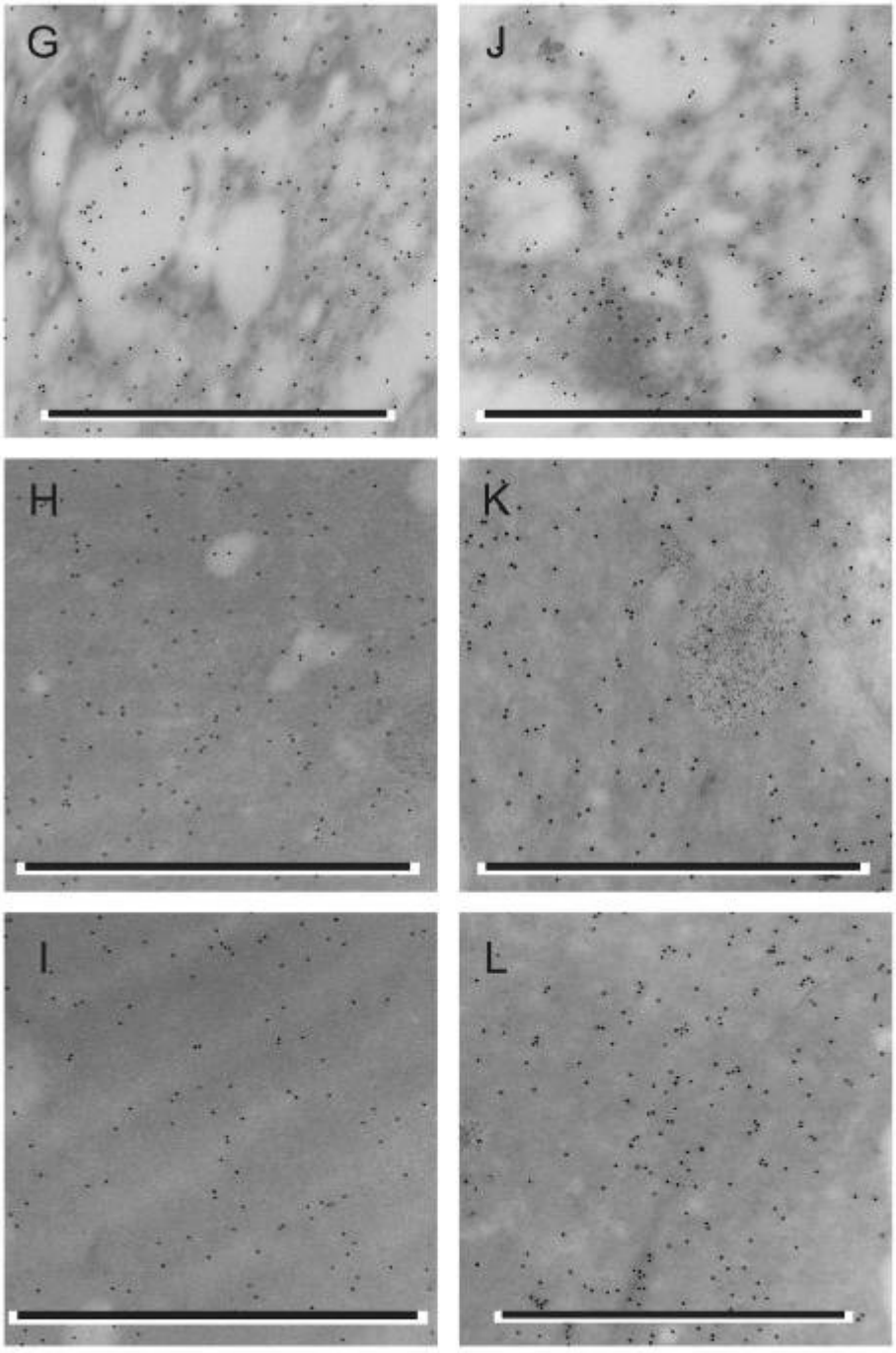
G
J
H
K
I
L

Figure 24

Kalafong patient 24

Figure 24a. A bone marrow fragment stained negative with the Prussian blue iron stain – absence of storage iron.

Figure 24b and c. Bone marrow aspirate smears stained with the Prussian blue iron stain with no sideroblasts.

Figure 24d. A bone marrow section stained negative with the Prussian blue iron stain – absence of storage iron.

Figure 24e and f. Bone marrow sections stained with the Prussian blue iron stain with no sideroblasts.

Figure 24g. An electron micrograph of a bone marrow macrophage immunolabelled with a monoclonal antibody to the H-subunit of ferritin, 10 nm gold particles and scale bar = 1 µm.

Figure 24h. An electron micrograph of a bone marrow red blood cell immunolabelled with a monoclonal antibody to the H-subunit of ferritin, 10 nm gold particles and scale bar = 1 µm.

Figure 24i. An electron micrograph of a bone marrow red blood cell precursor immunolabelled with a monoclonal antibody to the H-subunit of ferritin, 10 nm gold particles and scale bar = 1 µm.

Figure 24j. An electron micrograph of a bone marrow macrophage immunolabelled with a monoclonal antibody to the L-subunit of ferritin, 10 nm gold particles and scale bar = 1 µm.

Figure 24k. An electron micrograph of a bone marrow red blood cell immunolabelled with a monoclonal antibody to the L-subunit of ferritin, 10 nm gold particles and scale bar = 1 µm.

Figure 24l. An electron micrograph of a bone marrow red blood cell precursor immunolabelled with a monoclonal antibody to the L-subunit of ferritin, 10 nm gold particles and scale bar = 1 µm.

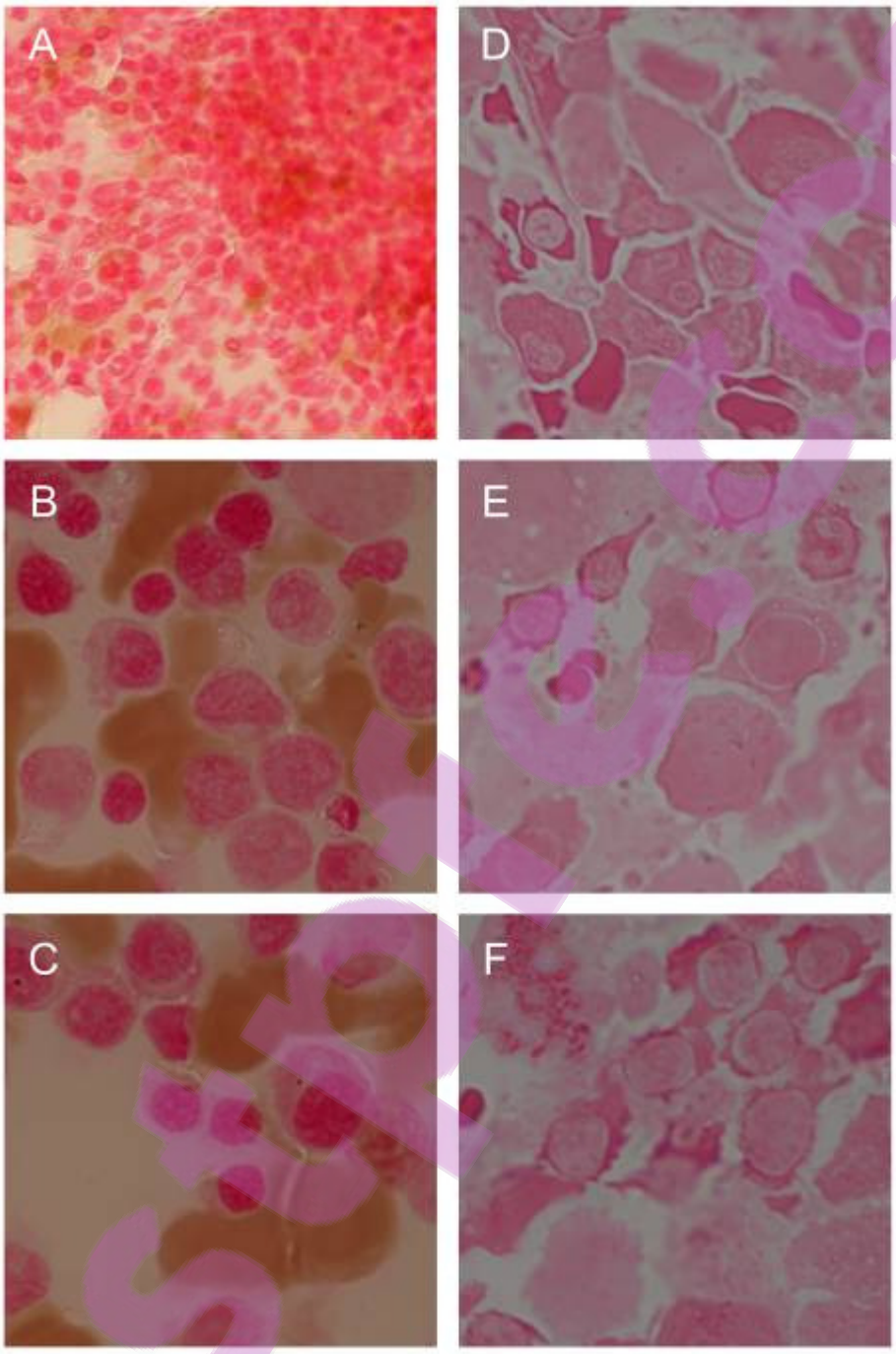

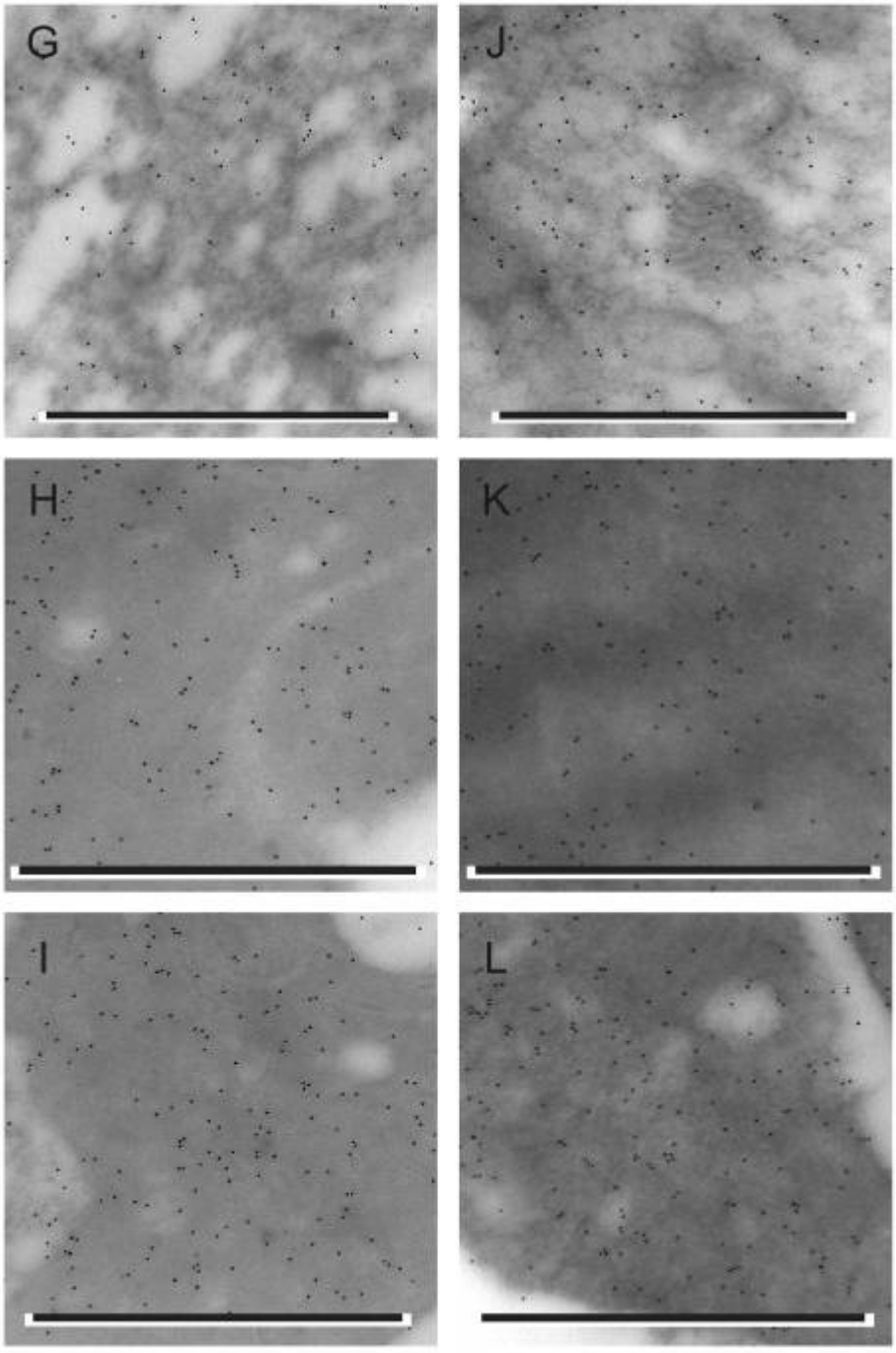
G
J
H
K
I
L

Figure 25

Kalafong patient 25

Figure 25a. A bone marrow fragment stained negative with the Prussian blue iron stain – absence of storage iron.

Figure 25b and c. Bone marrow aspirate smears stained with the Prussian blue iron stain with no sideroblasts.

Figure 25d. A bone marrow section stained negative with the Prussian blue iron stain – absence of storage iron.

Figure 25e and f. Bone marrow sections stained with the Prussian blue iron stain with no sideroblasts.

Figure 25g. An electron micrograph of a bone marrow macrophage immunolabelled with a monoclonal antibody to the H-subunit of ferritin, 10 nm gold particles and scale bar = 1 μm.

Figure 25h. An electron micrograph of a bone marrow red blood cell immunolabelled with a monoclonal antibody to the H-subunit of ferritin, 10 nm gold particles and scale bar = 1 μm.

Figure 25i. An electron micrograph of a bone marrow red blood cell precursor immunolabelled with a monoclonal antibody to the H-subunit of ferritin, 10 nm gold particles and scale bar = 1 μm.

Figure 25j. An electron micrograph of a bone marrow macrophage immunolabelled with a monoclonal antibody to the L-subunit of ferritin, 10 nm gold particles and scale bar = 1 μm.

Figure 25k. An electron micrograph of a bone marrow red blood cell immunolabelled with a monoclonal antibody to the L-subunit of ferritin, 10 nm gold particles and scale bar = 1 μm.

Figure 25l. An electron micrograph of a bone marrow red blood cell precursor immunolabelled with a monoclonal antibody to the L-subunit of ferritin, 10 nm gold particles and scale bar = 1 μm.

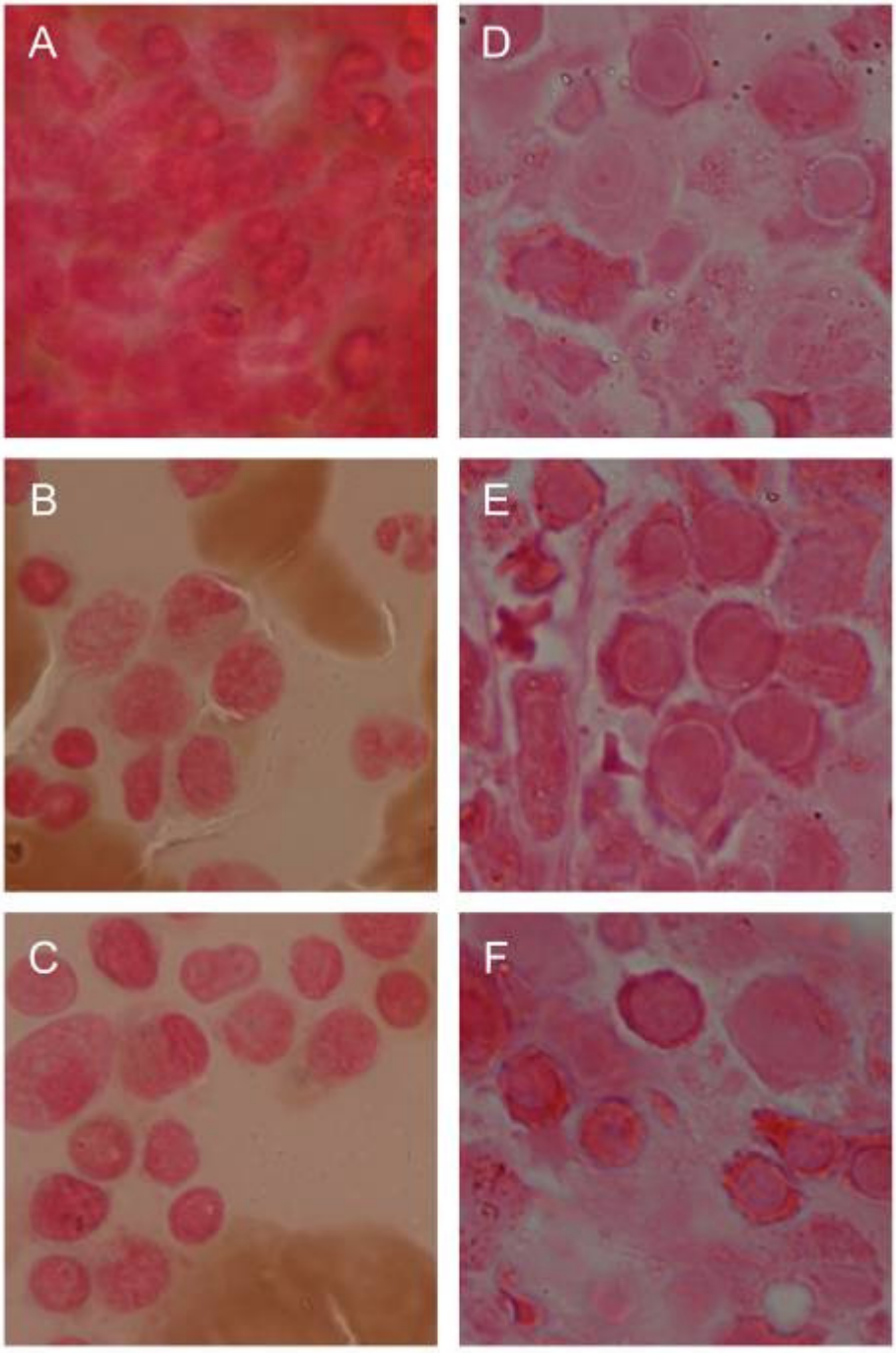
A
D
B
E
C
F

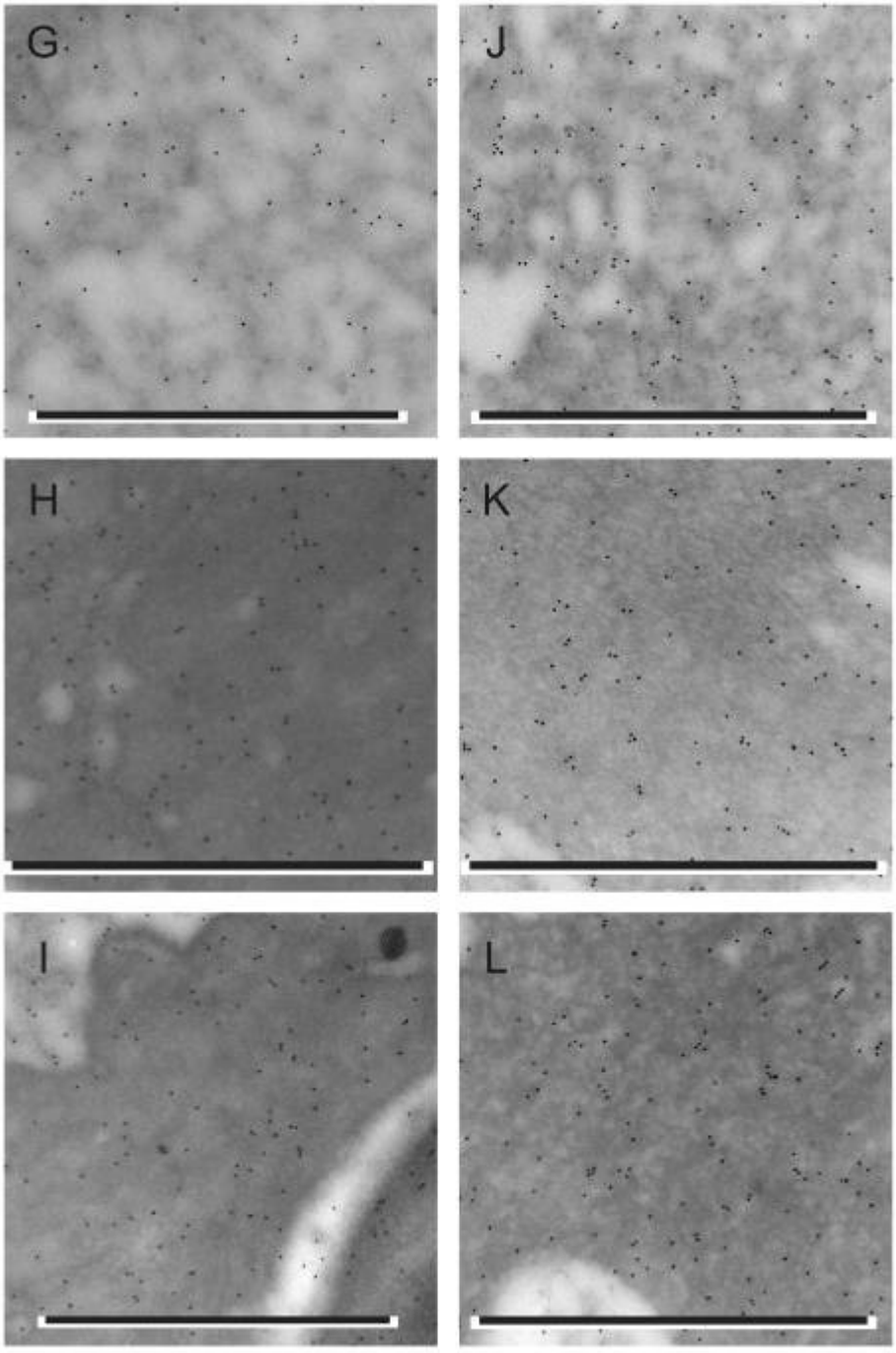
G
J
H
K
I
L

Figure 26

Kalafong patient 26

Figure 26d. A bone marrow section stained positive with the Prussian blue iron stain – normal amount of storage iron.

Figure 26e and f. Bone marrow sections stained with the Prussian blue iron stain with no sideroblasts.

Figure 26g. An electron micrograph of a bone marrow macrophage immunolabelled with a monoclonal antibody to the H-subunit of ferritin. Note the iron-loaded ferritin and the siderosome, 10 nm gold particles and scale bar = 1 μm.

Figure 26h. An electron micrograph of a bone marrow red blood cell immunolabelled with a monoclonal antibody to the H-subunit of ferritin, 10 nm gold particles and scale bar = 1 μm.

Figure 26i. An electron micrograph of two bone marrow red blood cell precursors immunolabelled with a monoclonal antibody to the H-subunit of ferritin. Note the contact between the two cell membranes and almost no iron-loaded ferritin, 10 nm gold particles and scale bar = 1 μm.

Figure 26j. An electron micrograph of a bone marrow macrophage immunolabelled with a monoclonal antibody to the L-subunit of ferritin, 10 nm gold particles and scale bar = 1 μm.

Figure 26k. An electron micrograph of a bone marrow red blood cell precursor immunolabelled with a monoclonal antibody to the L-subunit of ferritin, 10 nm gold particles and scale bar = 1 μm.

Figure 26l. An electron micrograph of a bone marrow red blood cell immunolabelled with a monoclonal antibody to the L-subunit of ferritin, 10 nm gold particles and scale bar = 1 μm.

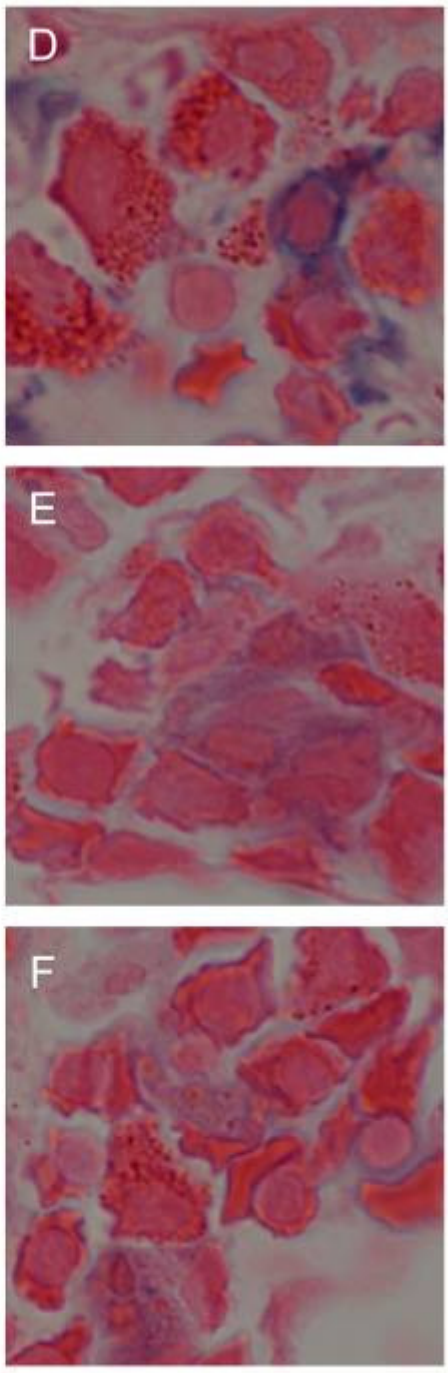
D
E
F

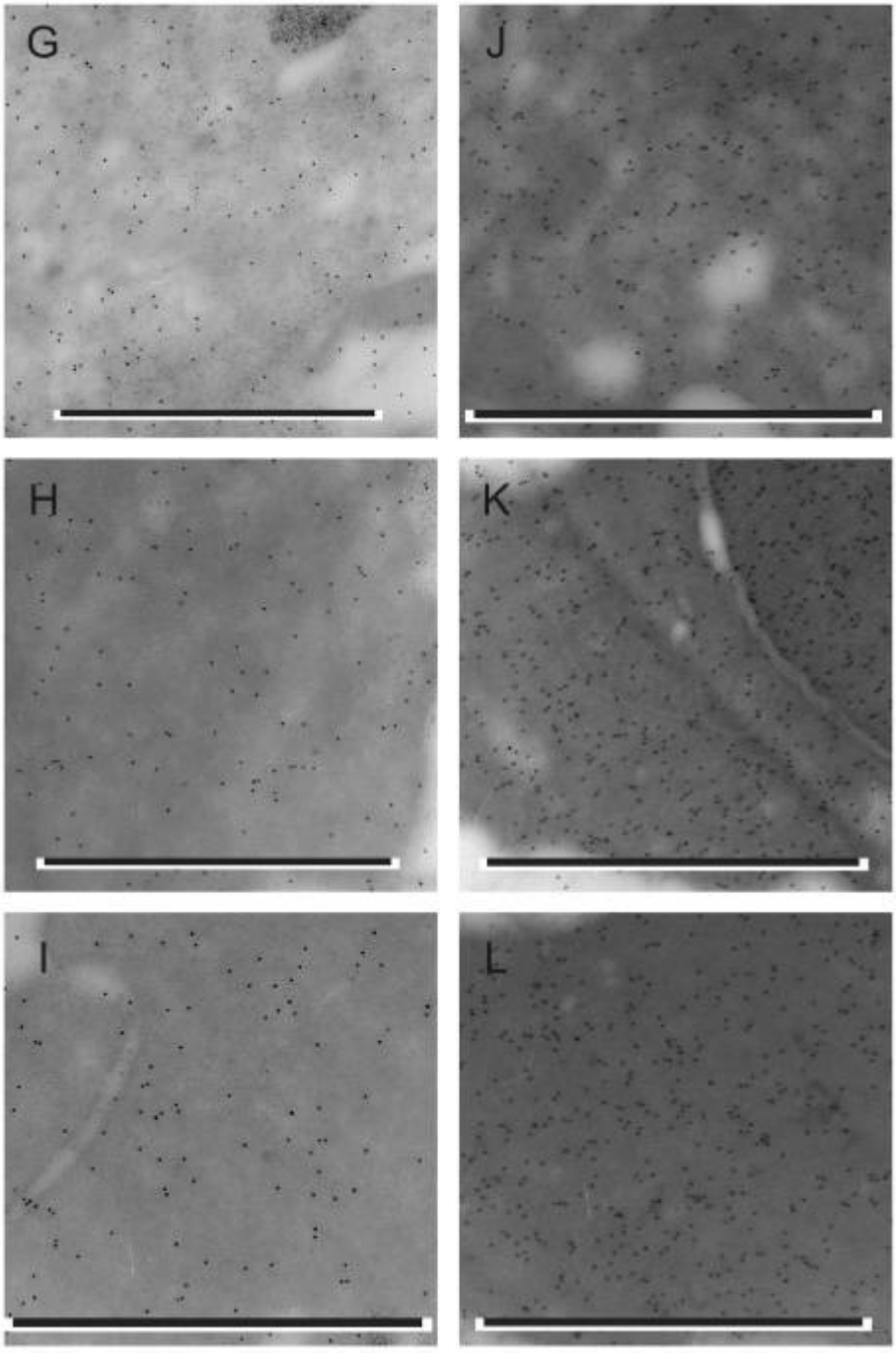
G
J
H
K
I
L

Figure 27

Kalafong patient 27

Figure 27d. A bone marrow section stained negative with the Prussian blue iron stain – absence of storage iron.

Figure 27e and f. Bone marrow sections stained with the Prussian blue iron stain with no sideroblasts.

Figure 27g. An electron micrograph of a bone marrow macrophage immunolabelled with a monoclonal antibody to the H-subunit of ferritin, 10 nm gold particles and scale bar = 1 µm.

Figure 27h. An electron micrograph of a bone marrow red blood cell immunolabelled with a monoclonal antibody to the H-subunit of ferritin, 10 nm gold particles and scale bar = 1 µm.

Figure 27i. An electron micrograph of a bone marrow reticulocyte immunolabelled with a monoclonal antibody to the H-subunit of ferritin, 10 nm gold particles and scale bar = 1 µm.

Figure 27j. An electron micrograph of a bone marrow macrophage immunolabelled with a monoclonal antibody to the L-subunit of ferritin, 10 nm gold particles and scale bar = 1 µm.

Figure 27k. An electron micrograph of a bone marrow red blood cell immunolabelled with a monoclonal antibody to the L-subunit of ferritin, 10 nm gold particles and scale bar = 1 µm.

Figure 27l. An electron micrograph of a bone marrow red blood cell immunolabelled with a monoclonal antibody to the L-subunit of ferritin, 10 nm gold particles and scale bar = 1 µm.

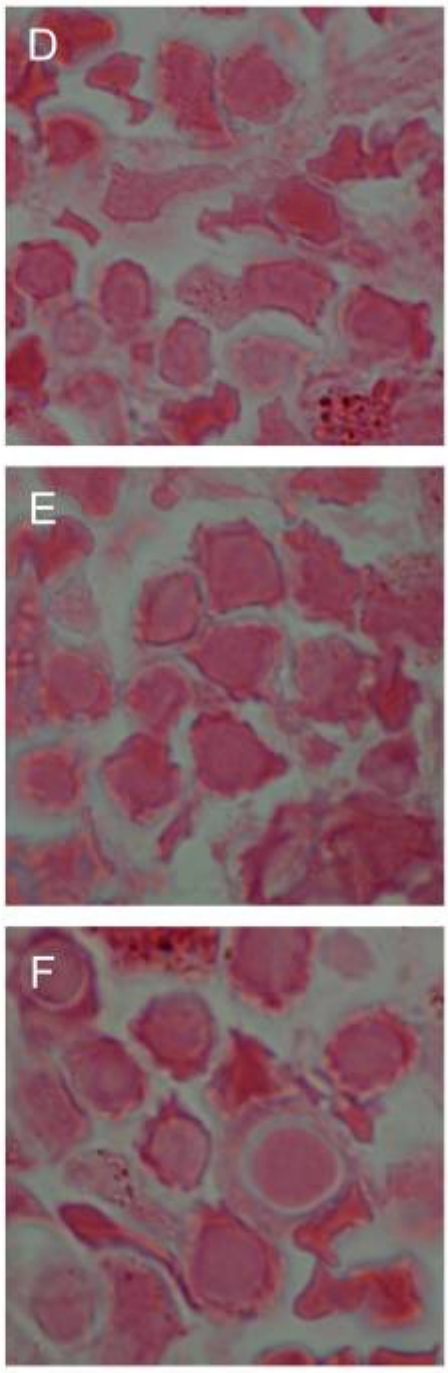
D
E
F

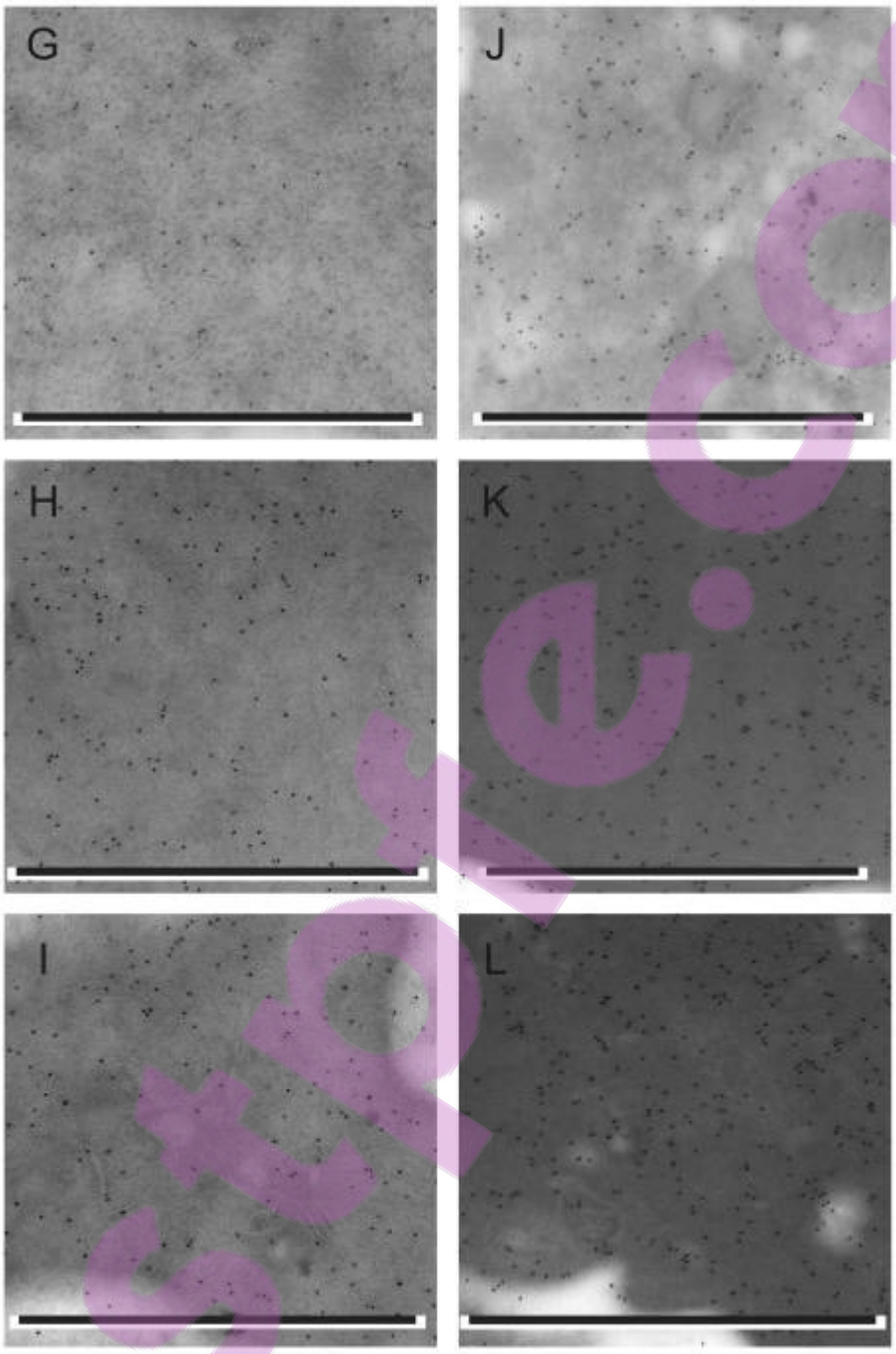

Figure 28

Kalafong patient 28

Figure 28d. A bone marrow section stained positive with the Prussian blue iron stain – normal amount of storage iron.

Figure 28e and f. Bone marrow sections stained with the Prussian blue iron stain with sideroblasts.

Figure 28g. An electron micrograph of a bone marrow macrophage immunolabelled with a monoclonal antibody to the H-subunit of ferritin. Note the iron-loaded ferritin, 10 nm gold particles and scale bar = 1 μm.

Figure 28h. An electron micrograph of a bone marrow red blood cell precursor immunolabelled with a monoclonal antibody to the H-subunit of ferritin. Note the cluster of iron-loaded ferritin – haemosiderin, 10 nm gold particles and scale bar = 1 μm.

Figure 28i. An electron micrograph of a bone marrow macrophage and reticulocyte immunolabelled with a monoclonal antibody to the H-subunit of ferritin, 10 nm gold particles and scale bar = 1 μm.

Figure 28j. An electron micrograph of a bone marrow macrophage immunolabelled with a monoclonal antibody to the L-subunit of ferritin. Note the iron-loaded ferritin and siderosome, 10 nm gold particles and scale bar = 1 μm.

Figure 28k. An electron micrograph of a bone marrow red blood cell immunolabelled with a monoclonal antibody to the L-subunit of ferritin, 10 nm gold particles and scale bar = 1 μm.

Figure 28l. An electron micrograph of a bone marrow red blood cell precursor immunolabelled with a monoclonal antibody to the L-subunit of ferritin, 10 nm gold particles and scale bar = 1 μm.

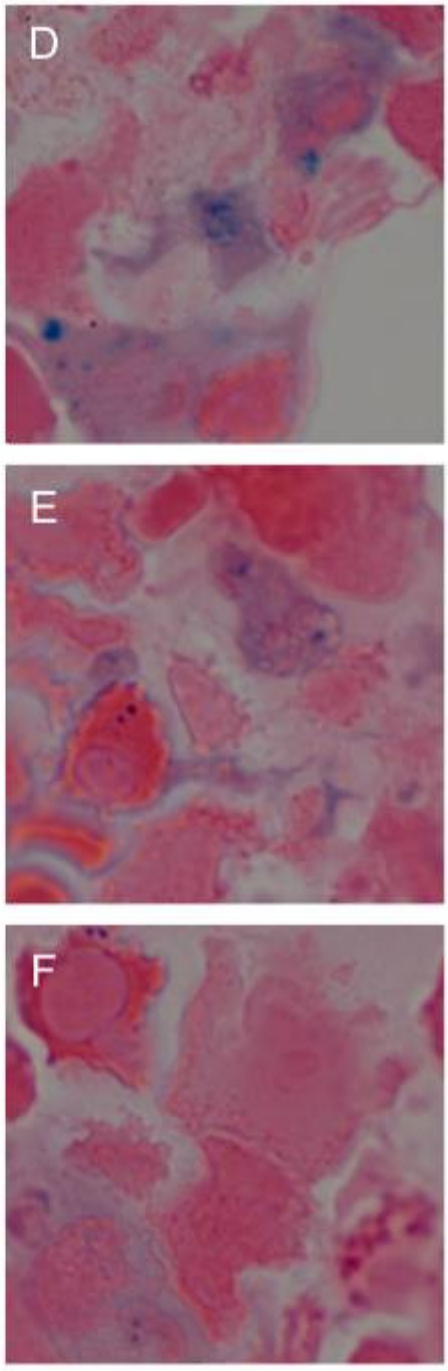

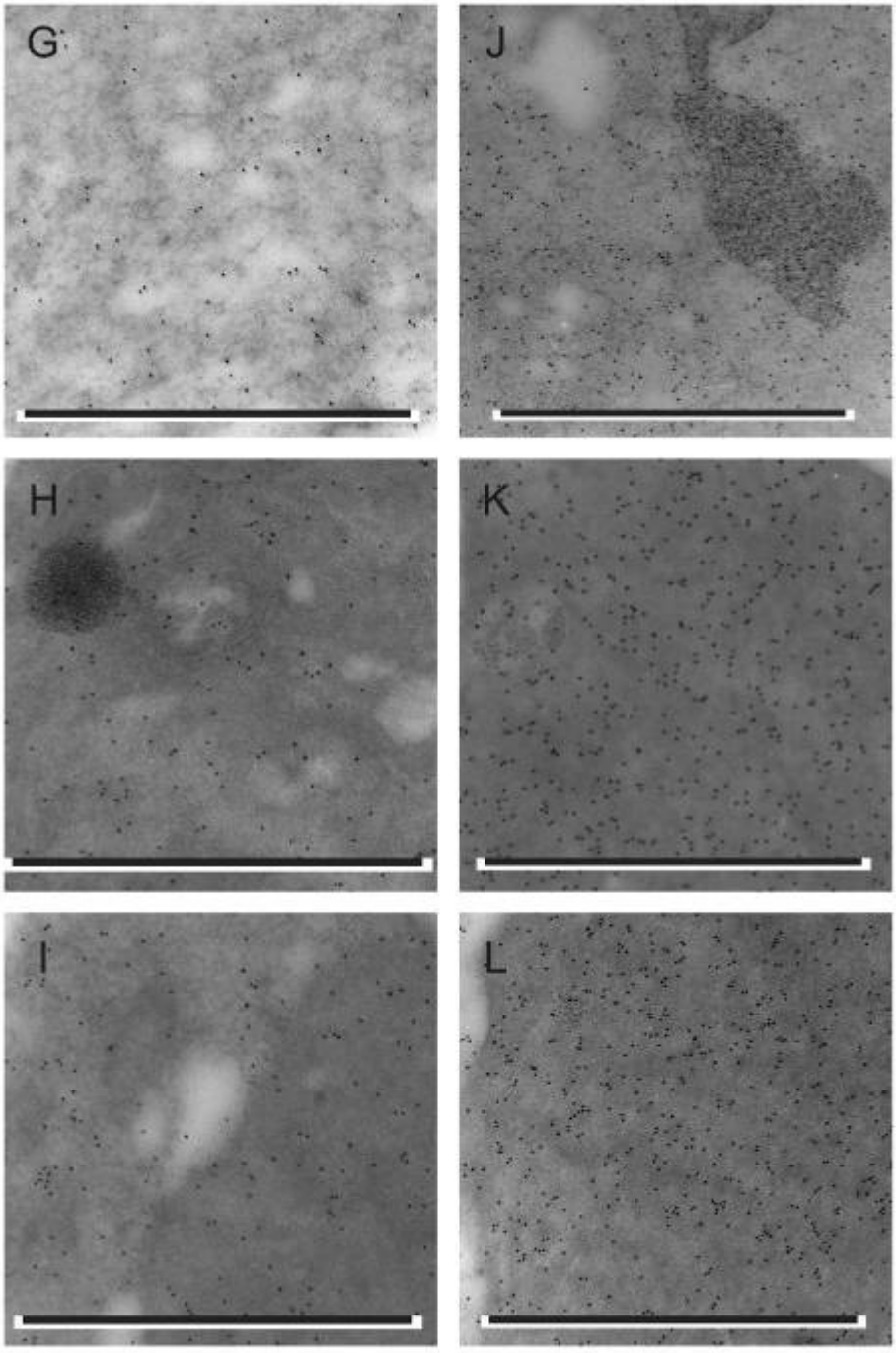
G
J
H
K
I
L

Figure 29

Kalafong patient 29

Figure 29d. A bone marrow section stained positive with the Prussian blue iron stain – normal amount of storage iron.

Figure 29e and f. Bone marrow sections stained with the Prussian blue iron stain with a few sideroblasts.

Figure 29g. An electron micrograph of a bone marrow macrophage immunolabelled with a monoclonal antibody to the H-subunit of ferritin, 10 nm gold particles and scale bar = 1 μm.

Figure 29h. An electron micrograph of a bone marrow red blood cell precursor immunolabelled with a monoclonal antibody to the H-subunit of ferritin, 10 nm gold particles and scale bar = 1 μm.

Figure 29i. An electron micrograph of a bone marrow red blood cell precursor immunolabelled with a monoclonal antibody to the H-subunit of ferritin, 10 nm gold particles and scale bar = 1 μm.

Figure 29j. An electron micrograph of a bone marrow macrophage immunolabelled with a monoclonal antibody to the L-subunit of ferritin. Note the presence of some iron-loaded ferritin, 10 nm gold particles and scale bar = 1 μm.

Figure 29k. An electron micrograph of a bone marrow red blood cell precursor immunolabelled with a monoclonal antibody to the L-subunit of ferritin, 10 nm gold particles and scale bar = 1 μm.

Figure 29l. An electron micrograph of a bone marrow red blood cell immunolabelled with a monoclonal antibody to the L-subunit of ferritin, 10 nm gold particles and scale bar = 1 μm.

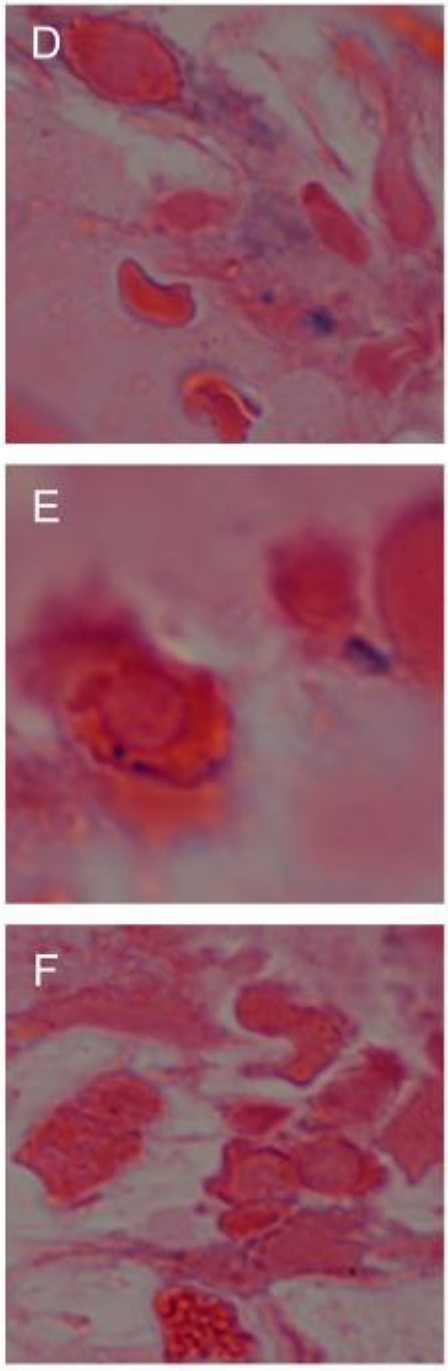
D
E
F

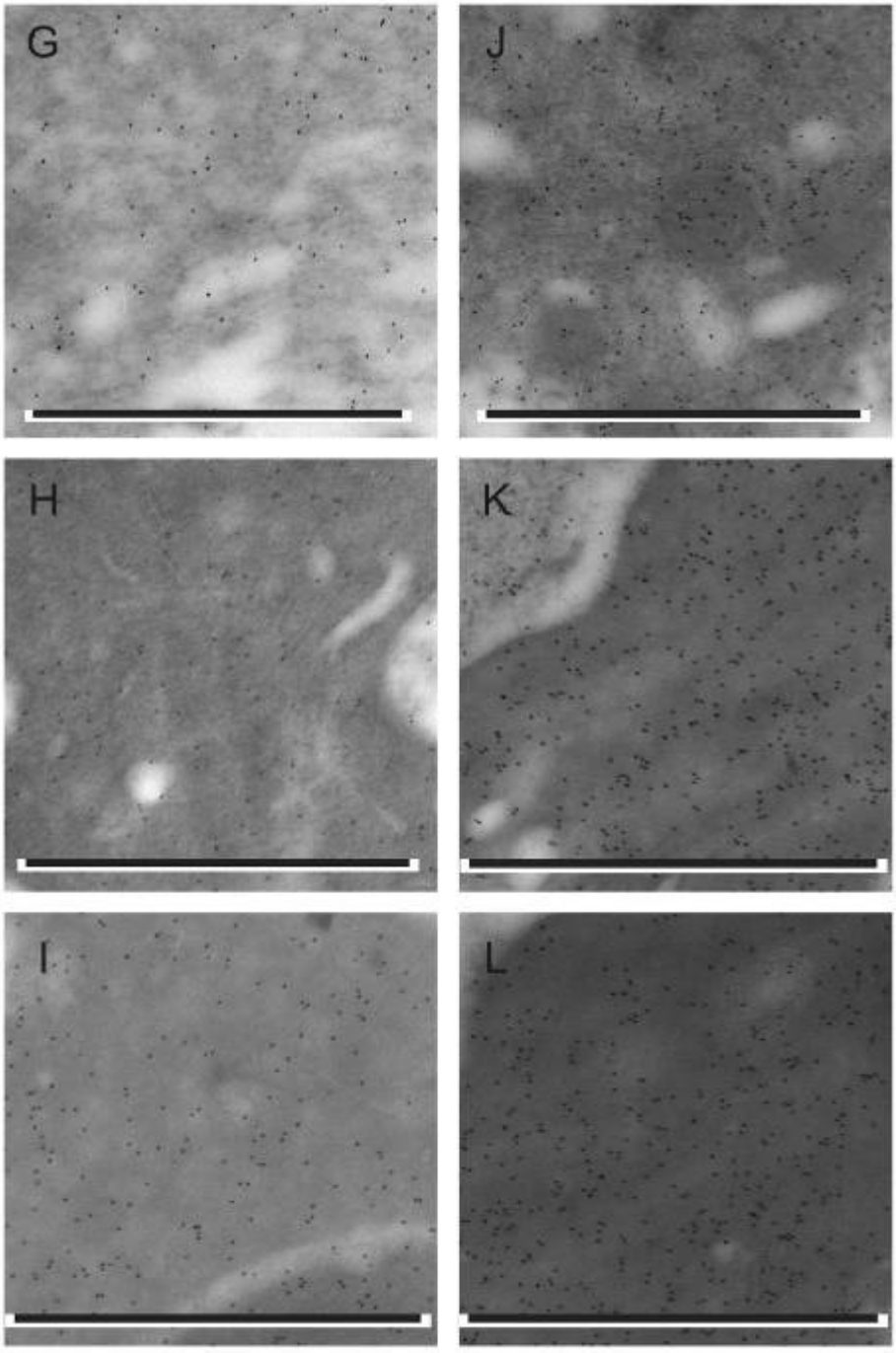
G
J
H
K
I
L

Figure 30

Kalafong patient 30

Figure 30a. A bone marrow fragment stained positive with the Prussian blue iron stain – normal amount of storage iron.

Figure 30b and c. Bone marrow aspirate smears stained with the Prussian blue iron stain with normal amount of sideroblasts.

Figure 30d. A bone marrow section stained negative with the Prussian blue iron stain – absence of storage iron.

Figure 30e and f. Bone marrow sections stained with the Prussian blue iron stain with no sideroblasts.

Figure 30g. An electron micrograph of a bone marrow macrophage immunolabelled with a monoclonal antibody to the H-subunit of ferritin. Note the presence of iron-loaded ferritin, 10 nm gold particles and scale bar = 1 μm.

Figure 30h. An electron micrograph of two bone marrow red blood cell precursors immunolabelled with a monoclonal antibody to the H-subunit of ferritin. Note the contact between the two cell membranes and the presence of iron-loaded ferritin in the space between the membranes, 10 nm gold particles and scale bar = 1 μm.

Figure 30i. An electron micrograph of two bone marrow red blood cell precursors immunolabelled with a monoclonal antibody to the H-subunit of ferritin. Note the contact between the two cell membranes and the presence of iron-loaded ferritin in the space between the membranes, 10 nm gold particles and scale bar = 1 μm.

Figure 30j. An electron micrograph of a bone marrow macrophage immunolabelled with a monoclonal antibody to the L-subunit of ferritin, 10 nm gold particles and scale bar = 1 μm.

Figure 30k. An electron micrograph of a bone marrow red blood cell precursor immunolabelled with a monoclonal antibody to the L-subunit of ferritin. Note the cluster of iron-loaded ferritin – haemosiderin, 10 nm gold particles and scale bar = 1 μm.

Figure 30l. An electron micrograph of a bone marrow red blood cell precursor immunolabelled with a monoclonal antibody to the L-subunit of ferritin, 10 nm gold particles and scale bar = 1 µm.

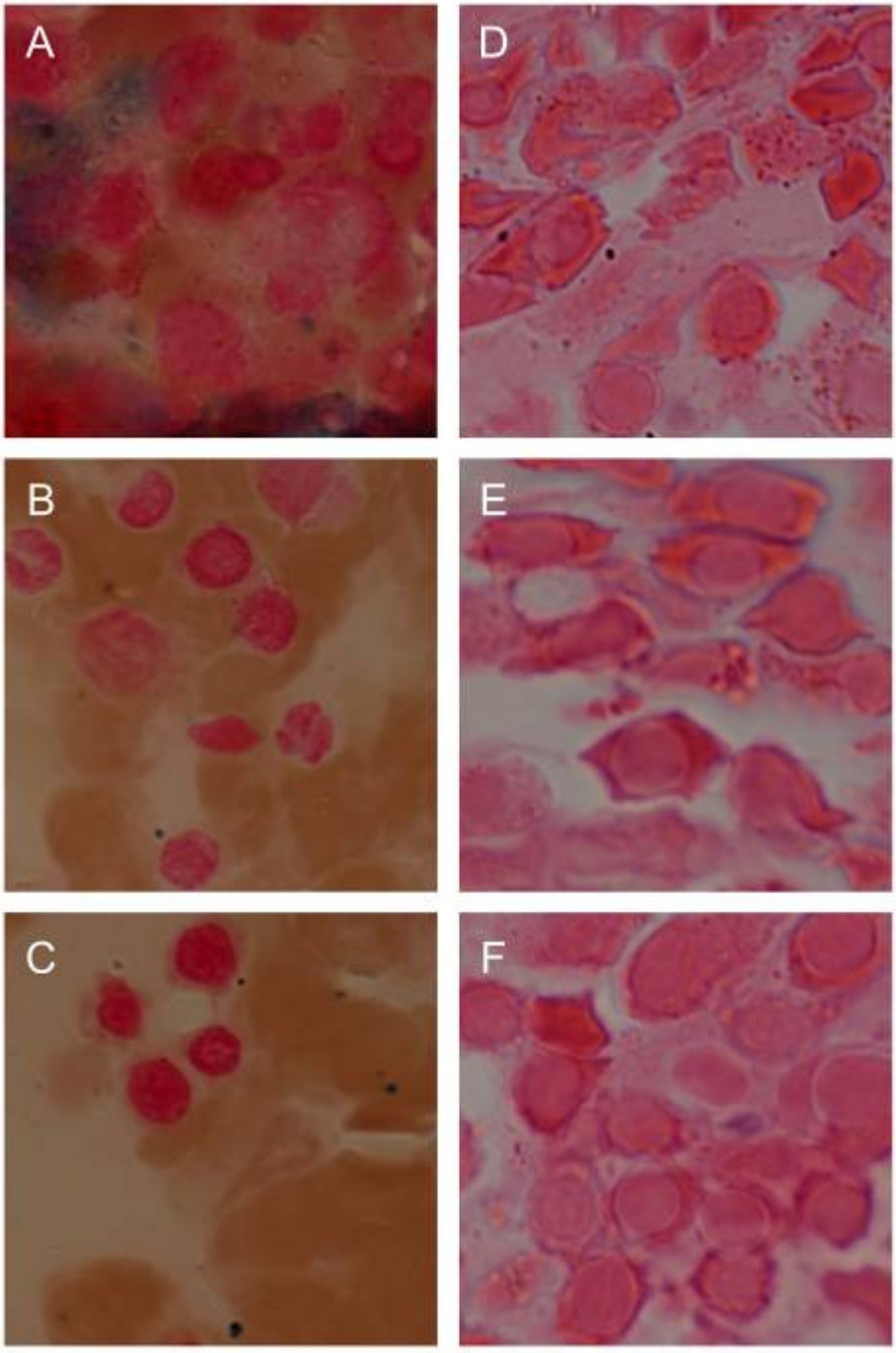
A
D
B
E
C
F

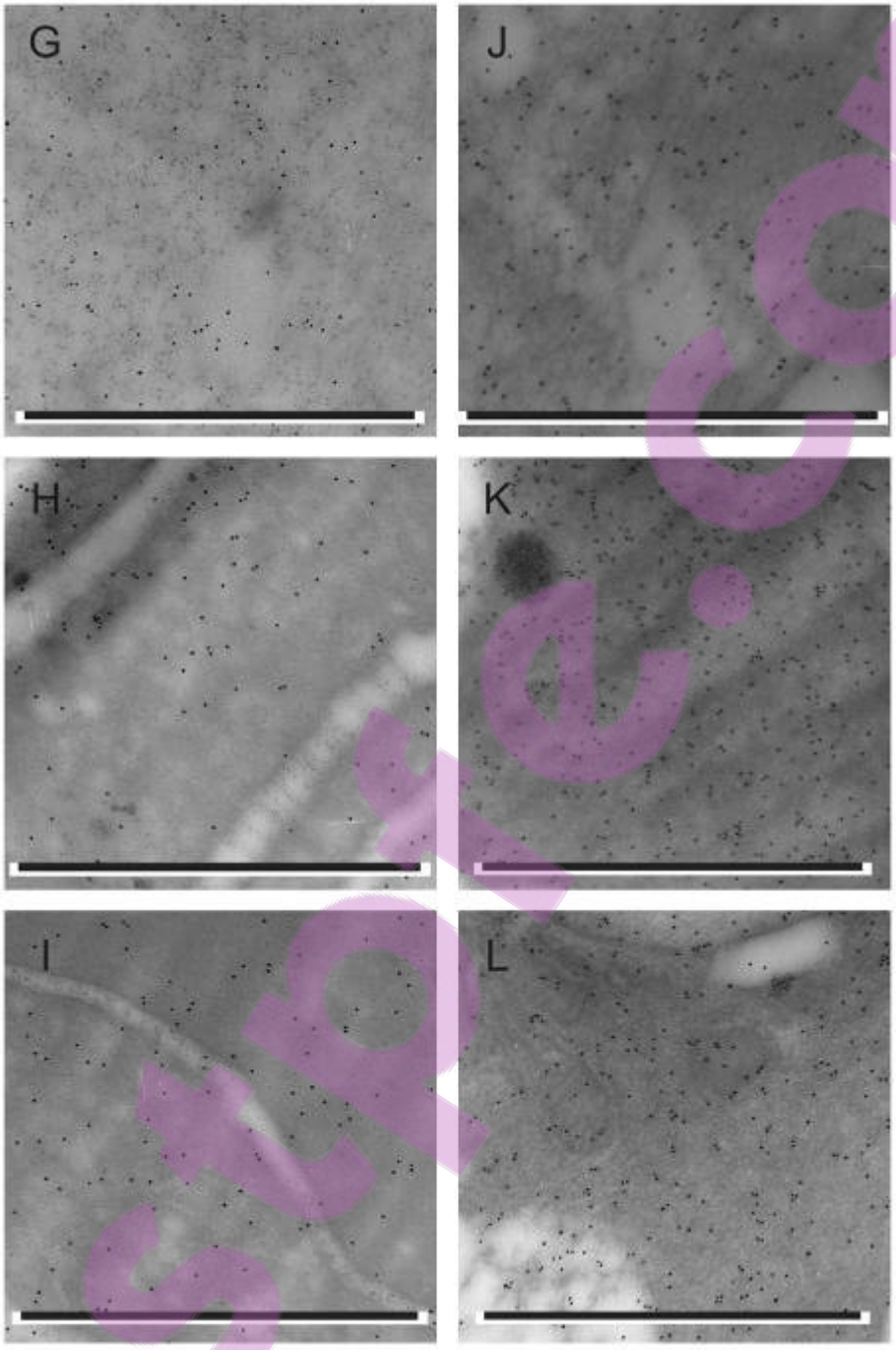

Figure 31

Kalafong patient 31

Figure 31d. A bone marrow section stained positive with the Prussian blue iron stain – increased amount of storage iron.

Figure 31e and f. Bone marrow sections stained with the Prussian blue iron stain with a sideroblast.

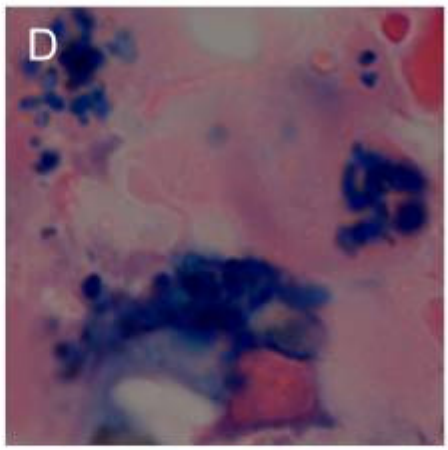

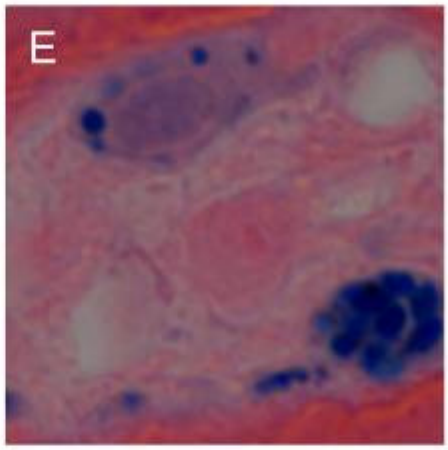

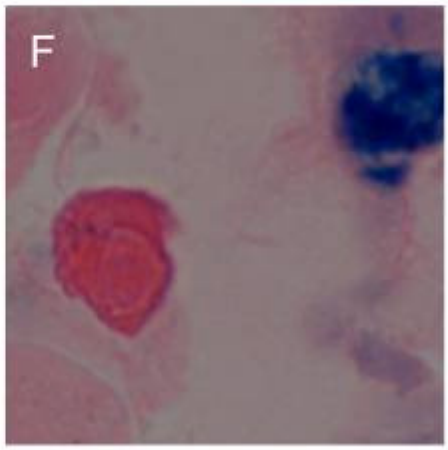

Figure 32

Kalafong patient 32

Figure 32a. A bone marrow fragment stained negative with the Prussian blue iron stain – absence of storage iron.

Figure 32b and c. Bone marrow aspirate smears stained with the Prussian blue iron stain with no sideroblasts.

Figure 32d. A bone marrow section stained negative with the Prussian blue iron stain – absence of storage iron.

Figure 32e and f. Bone marrow sections stained with the Prussian blue iron stain with no sideroblasts.

Figure 32g. An electron micrograph of a bone marrow macrophage immunolabelled with a monoclonal antibody to the H-subunit of ferritin, 10 nm gold particles and scale bar = 1 μm.

Figure 32h. An electron micrograph of two bone marrow red blood cell precursors immunolabelled with a monoclonal antibody to the H-subunit of ferritin. Note the contact between the two cell membranes and the absence of iron-loaded ferritin in the space between the membranes, 10 nm gold particles and scale bar = 1 μm.

Figure 32i. An electron micrograph of two bone marrow red blood cell precursors immunolabelled with a monoclonal antibody to the H-subunit of ferritin, 10 nm gold particles and scale bar = 1 μm.

Figure 32j. An electron micrograph of a bone marrow macrophage immunolabelled with a monoclonal antibody to the L-subunit of ferritin, 10 nm gold particles and scale bar = 1 μm.

Figure 32k. An electron micrograph of a bone marrow red blood cell immunolabelled with a monoclonal antibody to the L-subunit of ferritin, 10 nm gold particles and scale bar = 1 μm.

Figure 32l. An electron micrograph of a bone marrow red blood cell immunolabelled with a monoclonal antibody to the L-subunit of ferritin, 10 nm gold particles and scale bar = 1 μm.

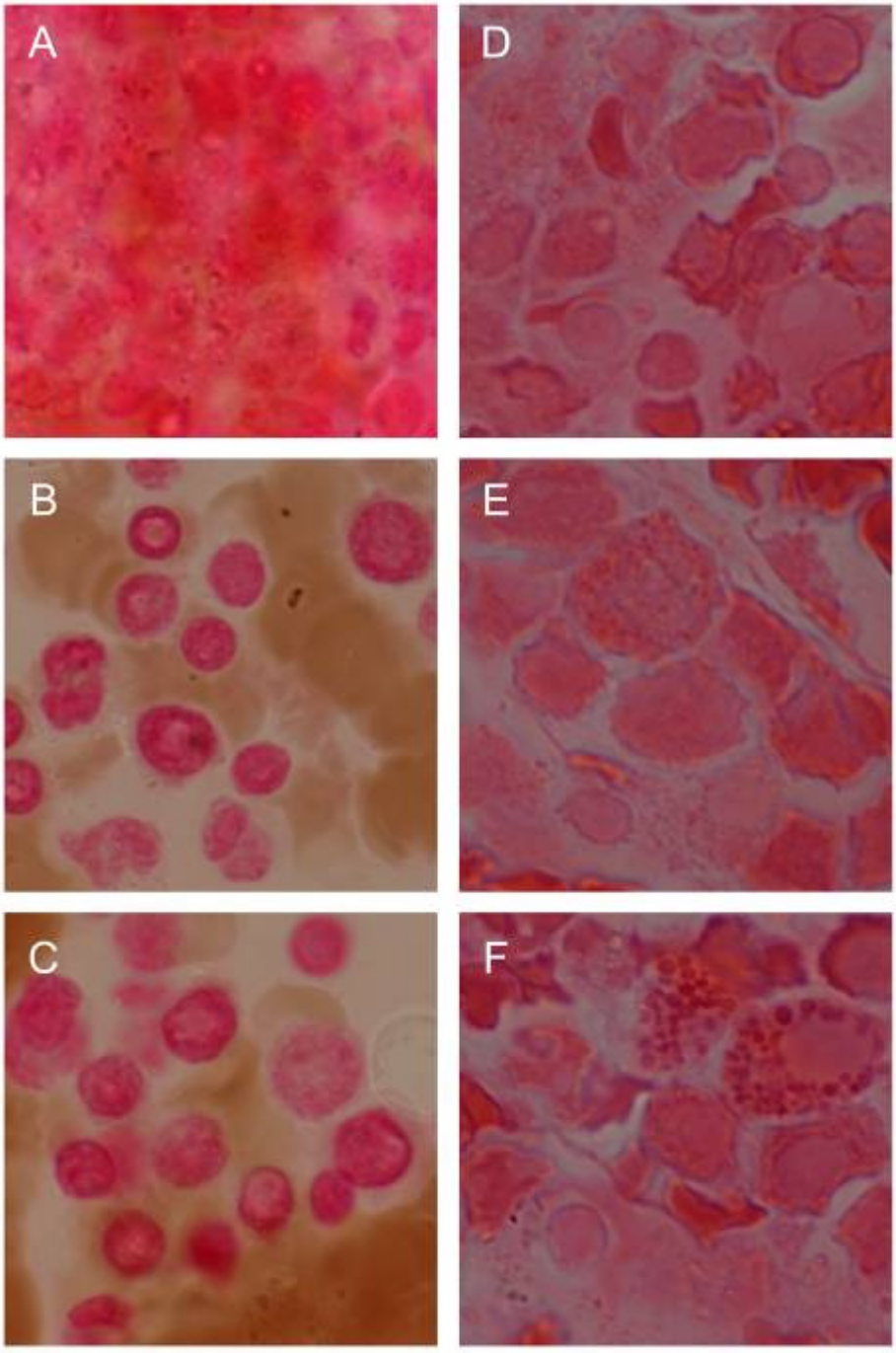
A
D
B
E
C
F

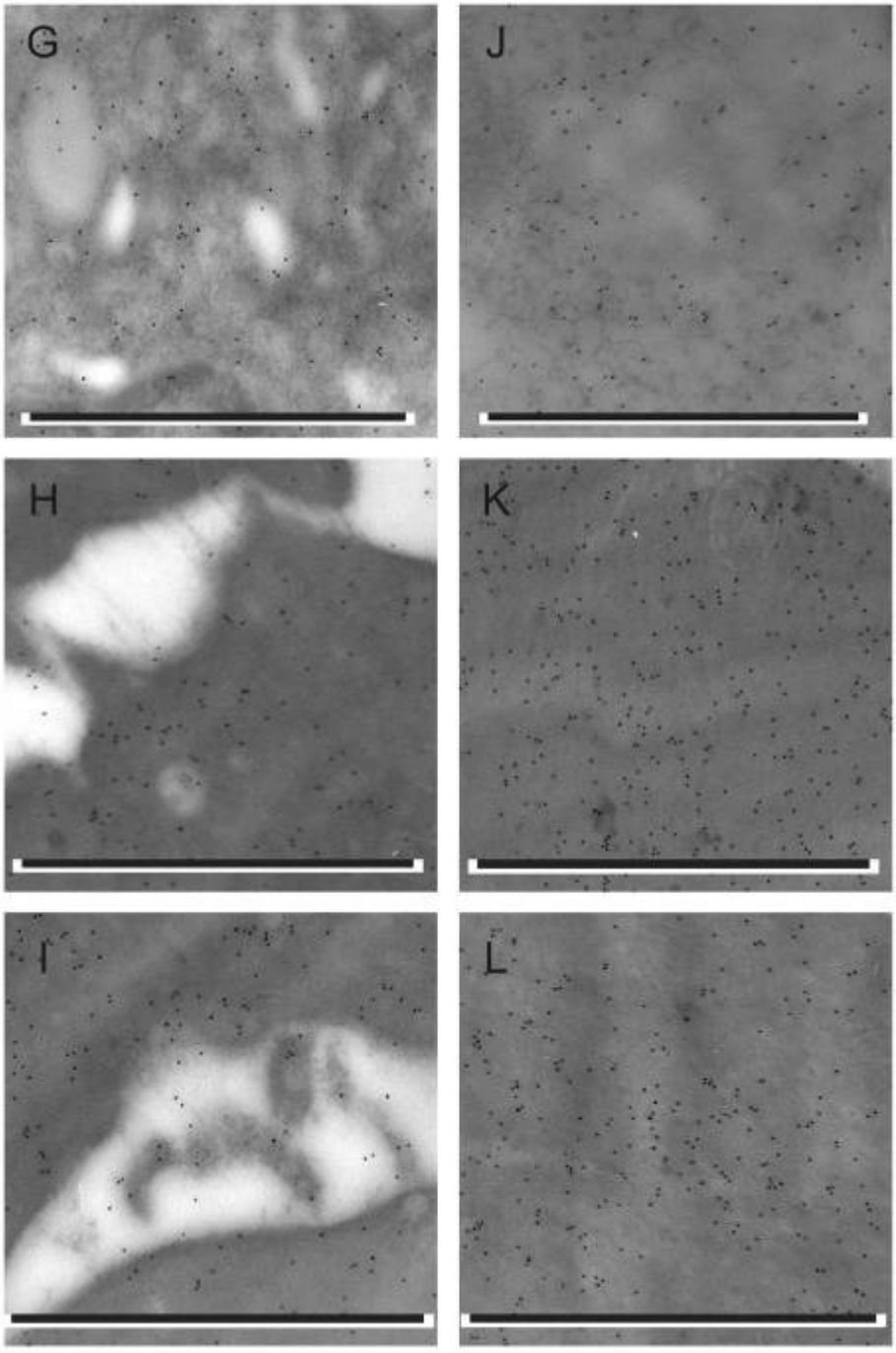
G
J
H
K
I
L

Figure 33

Kalafong patient 33

Figure 33a. A bone marrow fragment stained positive with the Prussian blue iron stain – normal amount of storage iron.

Figure 33b and c. Bone marrow aspirate smears stained with the Prussian blue iron stain with normal amount of sideroblasts.

Figure 33d. A bone marrow section stained positive with the Prussian blue iron stain – presence of storage iron.

Figure 33e and f. Bone marrow sections stained with the Prussian blue iron stain with some sideroblasts.

Figure 33g. An electron micrograph of a bone marrow macrophage immunolabelled with a monoclonal antibody to the H-subunit of ferritin, 10 nm gold particles and scale bar = 1 μm.

Figure 33h. An electron micrograph of a bone marrow red blood cell precursor immunolabelled with a monoclonal antibody to the H-subunit of ferritin, 10 nm gold particles and scale bar = 1 μm.

Figure 33i. An electron micrograph of two bone marrow red blood cell precursors immunolabelled with a monoclonal antibody to the H-subunit of ferritin. Note the contact between the two cell membranes and the presence of iron-loaded ferritin in the space between the membranes, 10 nm gold particles and scale bar = 1 μm.

Figure 33j. An electron micrograph of a bone marrow macrophage immunolabelled with a monoclonal antibody to the L-subunit of ferritin. Note the presence of iron-loaded ferritin, 10 nm gold particles and scale bar = 1 μm.

Figure 33k. An electron micrograph of two bone marrow red blood cells immunolabelled with a monoclonal antibody to the L-subunit of ferritin, 10 nm gold particles and scale bar = 1 μm.

Figure 33l. An electron micrograph of a bone marrow red blood cell precursor immunolabelled with a monoclonal antibody to the L-subunit of ferritin, 10 nm gold particles and scale bar = 1 μm.

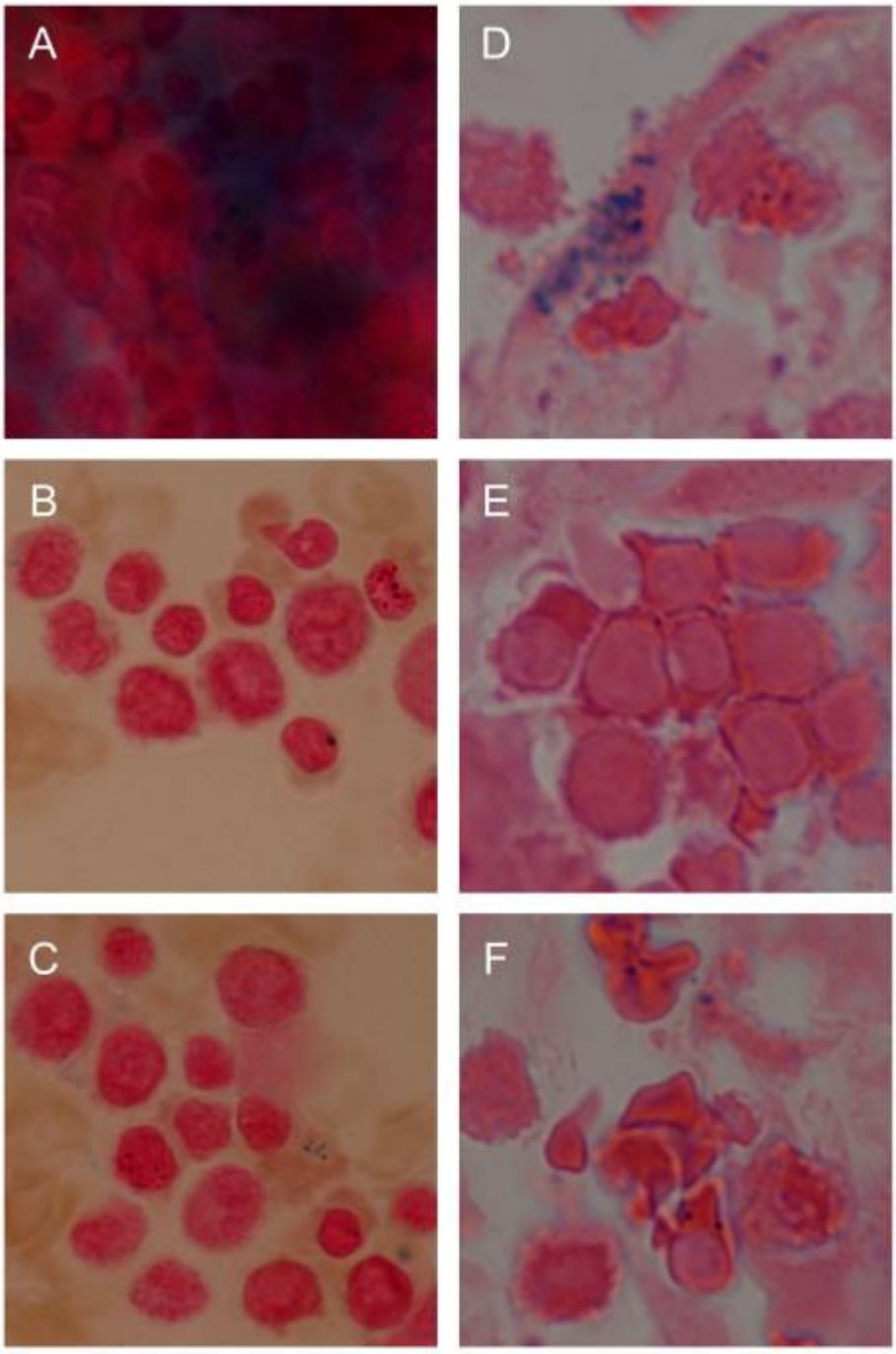
A
D
B
E
C
F

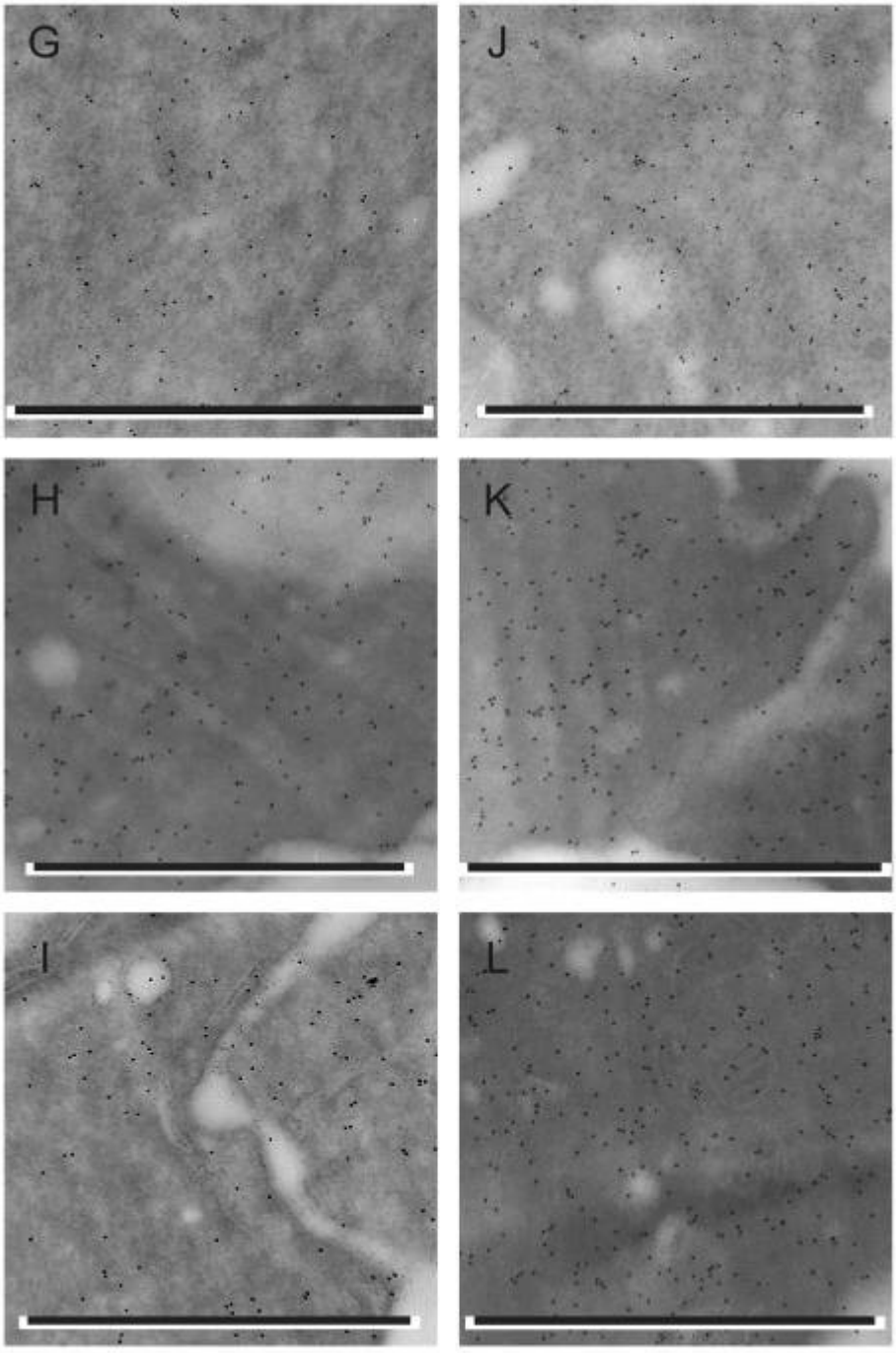
G
J
H
K
I
L

Figure 34

Kalafong patient 34

Figure 34d. A bone marrow section stained positive with the Prussian blue iron stain – increased amount of storage iron.

Figure 34e and f. Bone marrow sections stained with the Prussian blue iron stain with no sideroblasts.

Figure 34g. An electron micrograph of a bone marrow macrophage immunolabelled with a monoclonal antibody to the H-subunit of ferritin. Note the presence of iron-loaded ferritin, 10 nm gold particles and scale bar = 1 µm.

Figure 34h. An electron micrograph of a bone marrow red blood cell immunolabelled with a monoclonal antibody to the H-subunit of ferritin, 10 nm gold particles and scale bar = 1 µm.

Figure 34i. An electron micrograph of two bone marrow red blood cell precursors immunolabelled with a monoclonal antibody to the H-subunit of ferritin. Note the contact between the two cell membranes, 10 nm gold particles and scale bar = 1 µm.

Figure 34j. An electron micrograph of a bone marrow macrophage immunolabelled with a monoclonal antibody to the L-subunit of ferritin. Note the presence of iron-loaded ferritin, 10 nm gold particles and scale bar = 1 µm.

Figure 34k. An electron micrograph of a bone marrow red blood cell precursor immunolabelled with a monoclonal antibody to the L-subunit of ferritin, 10 nm gold particles and scale bar = 1 µm.

Figure 34l. An electron micrograph of a bone marrow red blood cell precursor immunolabelled with a monoclonal antibody to the L-subunit of ferritin. Note the presence of the endocytic vesicle with some iron-loaded ferritin, 10 nm gold particles and scale bar = 1 µm.

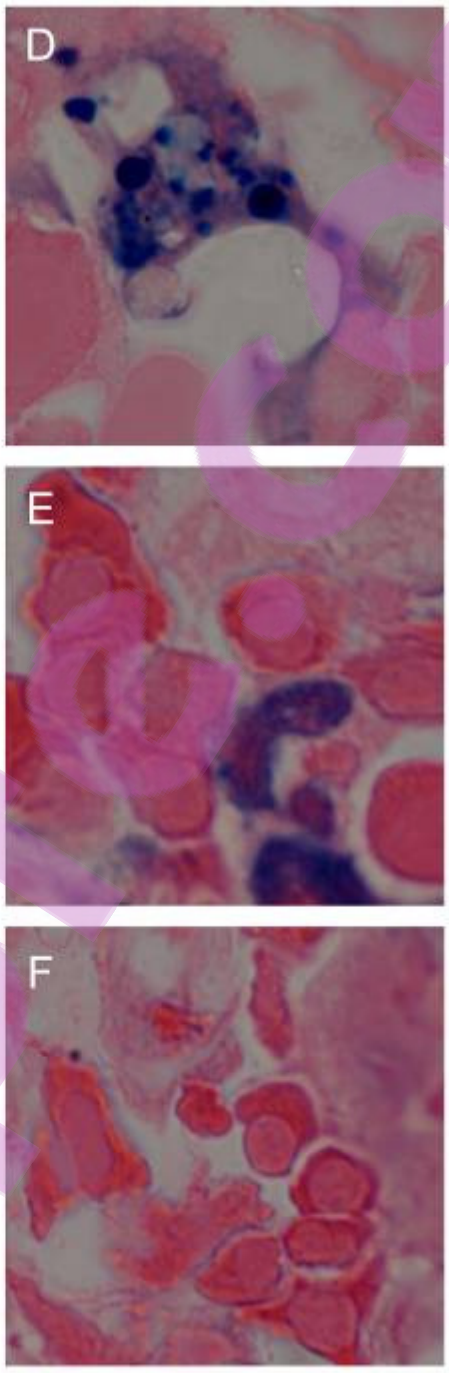

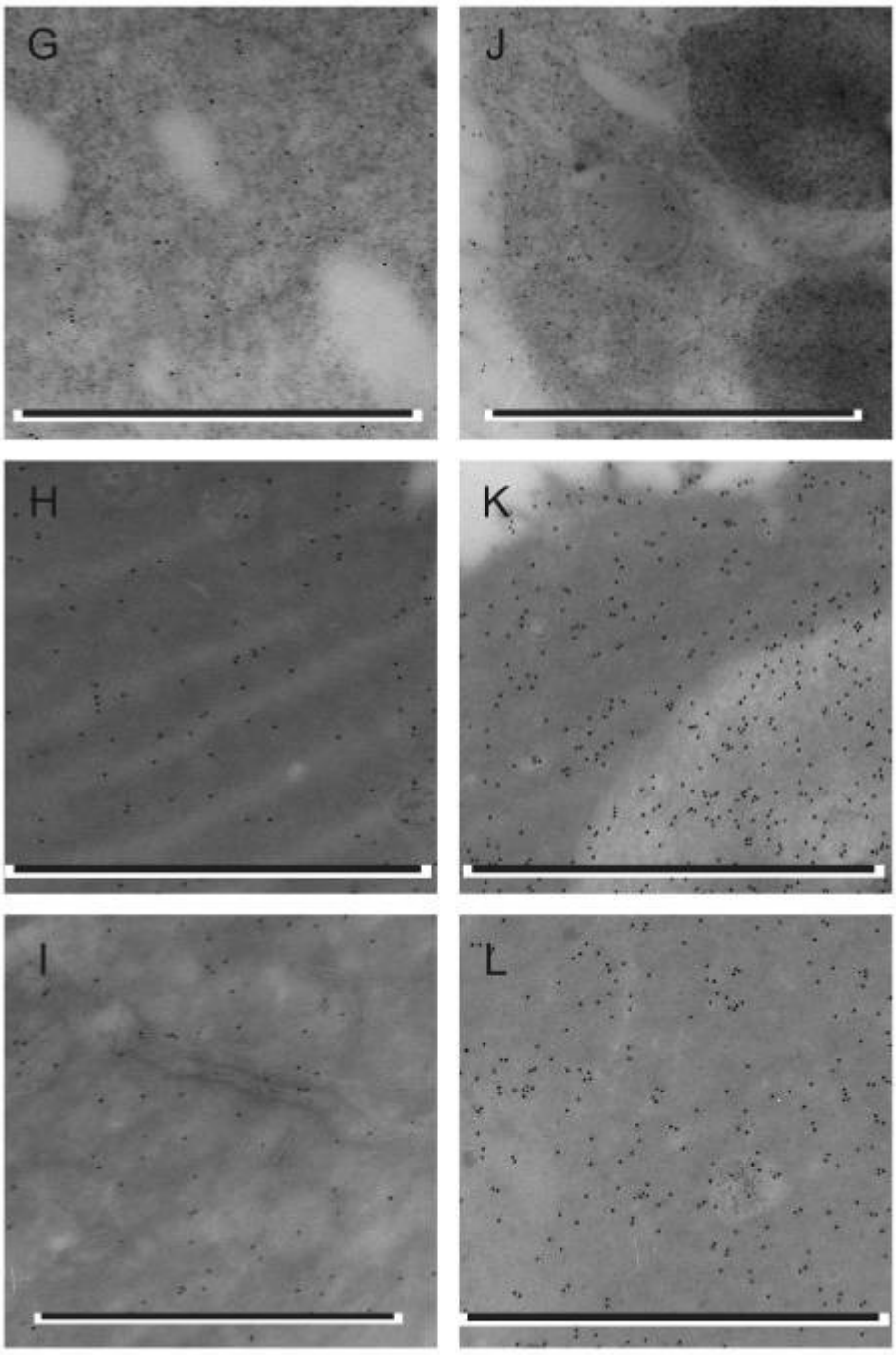
G
J
H
K
I
L

Figure 35

Kalafong patient 35

Figure 35a. A bone marrow fragment stained negative with the Prussian blue iron stain – absence of storage iron.

Figure 35b and c. Bone marrow aspirate smears stained with the Prussian blue iron stain with no sideroblasts.

Figure 35d. A bone marrow section stained negative with the Prussian blue iron stain – absence of storage iron.

Figure 35e and f. Bone marrow sections stained with the Prussian blue iron stain with no sideroblasts.

Figure 35g. An electron micrograph of a bone marrow macrophage immunolabelled with a monoclonal antibody to the H-subunit of ferritin, 10 nm gold particles and scale bar = 1 μm.

Figure 35h. An electron micrograph of a bone marrow red blood cell precursor immunolabelled with a monoclonal antibody to the H-subunit of ferritin, 10 nm gold particles and scale bar = 1 μm.

Figure 35i. An electron micrograph of a bone marrow red blood cell precursor immunolabelled with a monoclonal antibody to the H-subunit of ferritin, 10 nm gold particles and scale bar = 1 μm.

Figure 35j. An electron micrograph of a bone marrow macrophage immunolabelled with a monoclonal antibody to the L-subunit of ferritin, 10 nm gold particles and scale bar = 1 μm.

Figure 35k. An electron micrograph of a bone marrow red blood cell precursor immunolabelled with a monoclonal antibody to the L-subunit of ferritin, 10 nm gold particles and scale bar = 1 μm.

Figure 35l. An electron micrograph of a bone marrow reticulocyte immunolabelled with a monoclonal antibody to the L-subunit of ferritin, 10 nm gold particles and scale bar = 1 μm.

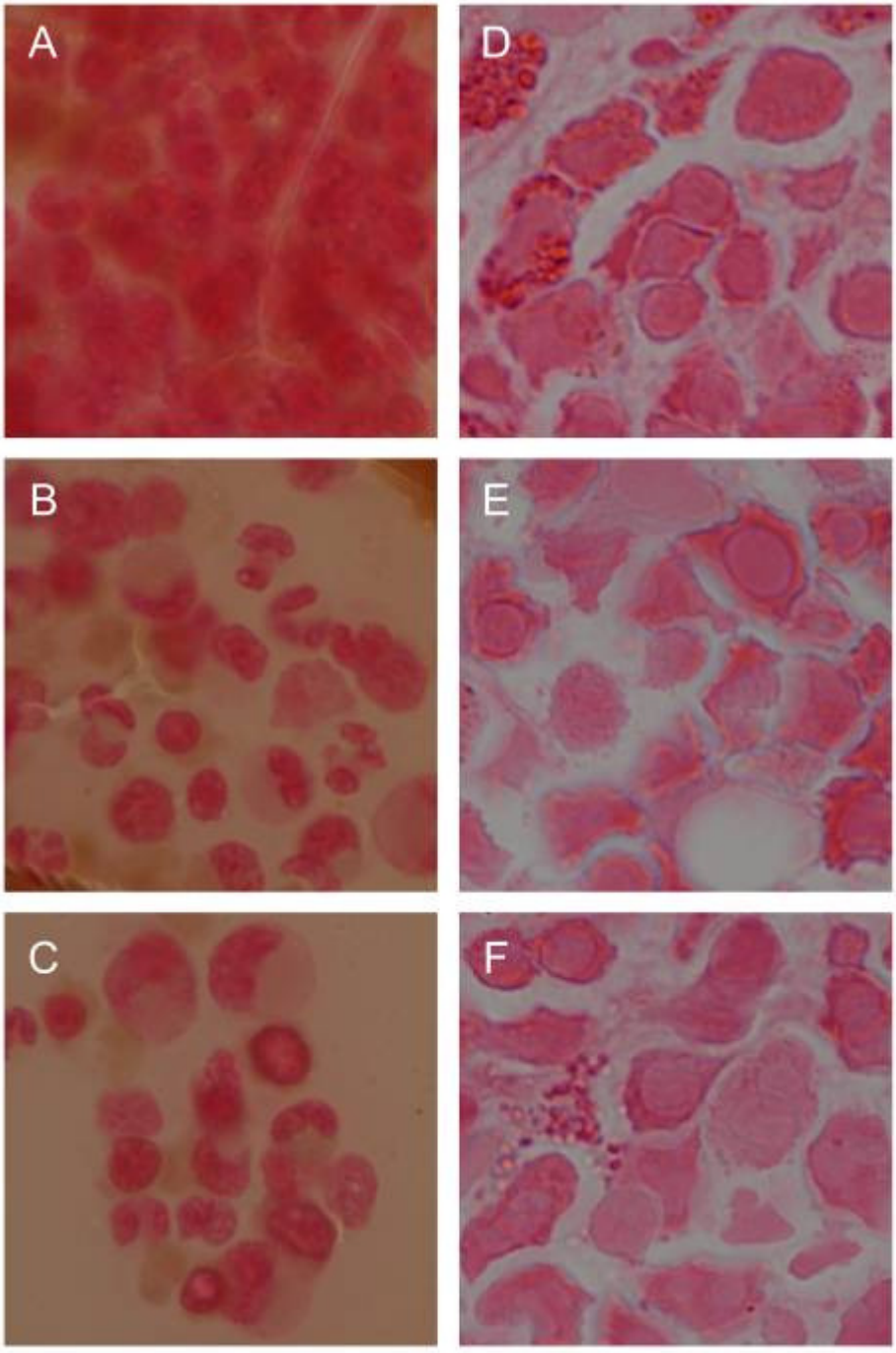
A
D
B
E
C
F

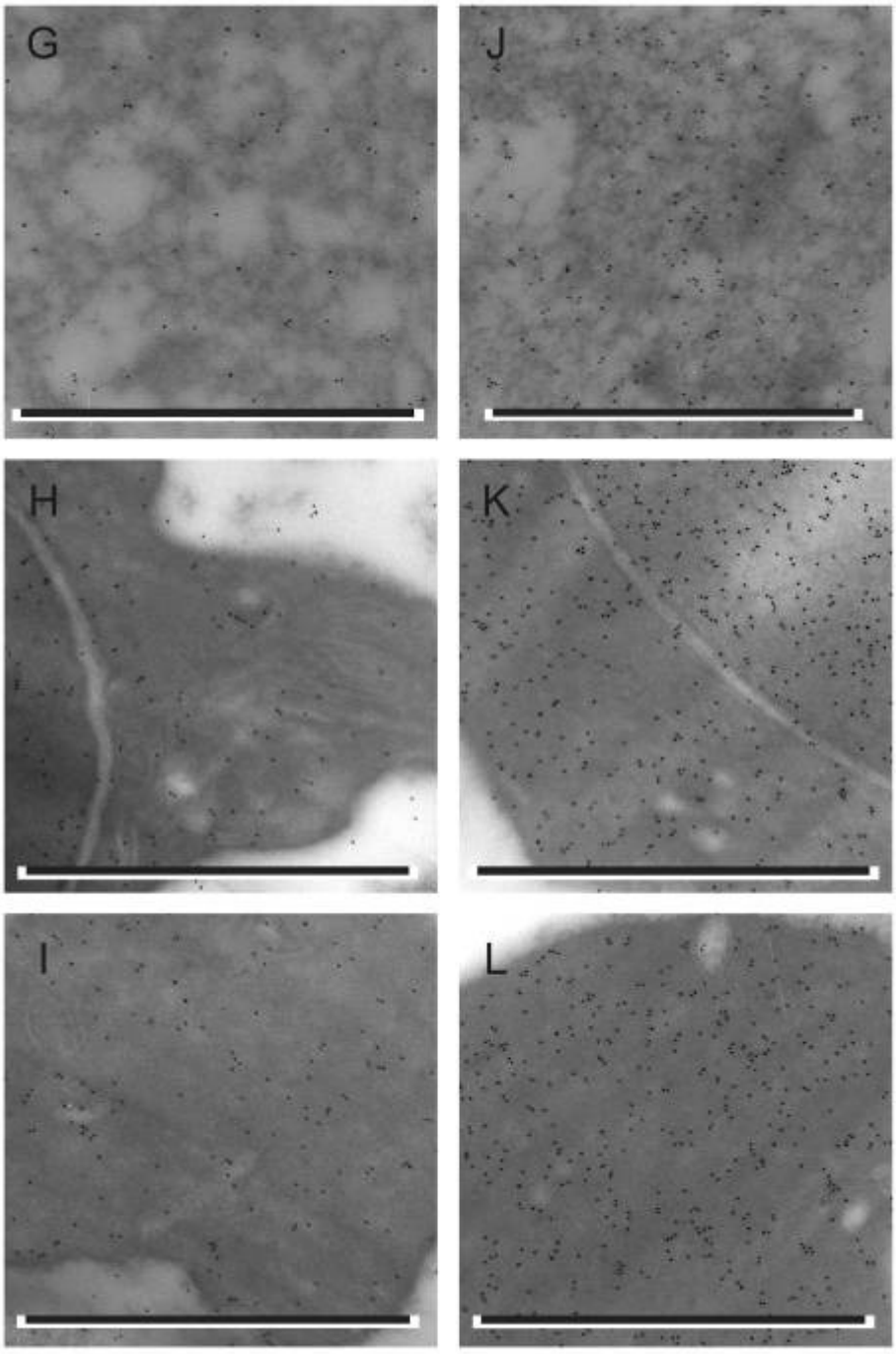
G
J
H
K
I
L

Figure 36

Kalafong patient 36

Figure 36a. A bone marrow fragment stained postive with the Prussian blue iron stain – increased amount of storage iron.

Figure 36b and c. Bone marrow aspirate smears stained with the Prussian blue iron stain with no sideroblasts.

Figure 36d. A bone marrow section stained positive with the Prussian blue iron stain – increased amount of storage iron.

Figure 36e and f. Bone marrow sections stained with the Prussian blue iron stain with pathologically overloaded sideroblasts.

Figure 36g. An electron micrograph of a bone marrow macrophage immunolabelled with a monoclonal antibody to the H-subunit of ferritin. Note the iron-loaded ferritin, 10 nm gold particles and scale bar = 1 μm.

Figure 36h. An electron micrograph of a bone marrow red blood cell precursor immunolabelled with a monoclonal antibody to the H-subunit of ferritin, 10 nm gold particles and scale bar = 1 μm.

Figure 36i. An electron micrograph of a bone marrow red blood cell precursor immunolabelled with a monoclonal antibody to the H-subunit of ferritin. Note the cluster of iron-loaded ferritin, 10 nm gold particles and scale bar = 1 μm.

Figure 36j. An electron micrograph of a bone marrow macrophage immunolabelled with a monoclonal antibody to the L-subunit of ferritin, 10 nm gold particles and scale bar = 1 μm.

Figure 36k. An electron micrograph of a bone marrow red blood cell immunolabelled with a monoclonal antibody to the L-subunit of ferritin, 10 nm gold particles and scale bar = 1 μm.

Figure 36l. An electron micrograph of a bone marrow reticulocyte immunolabelled with a monoclonal antibody to the L-subunit of ferritin, 10 nm gold particles and scale bar = 1 μm.

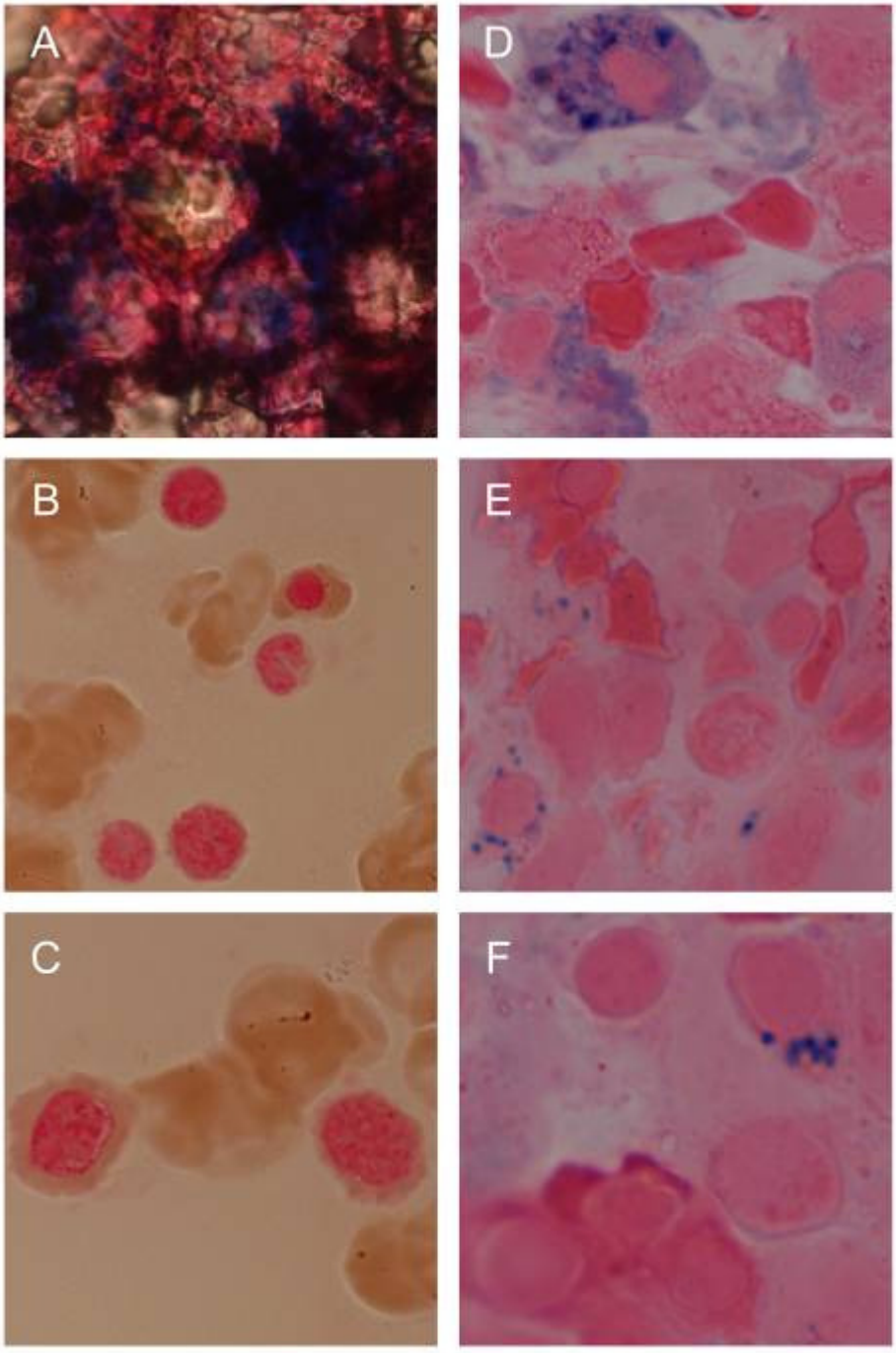
A
D
B
E
C
F

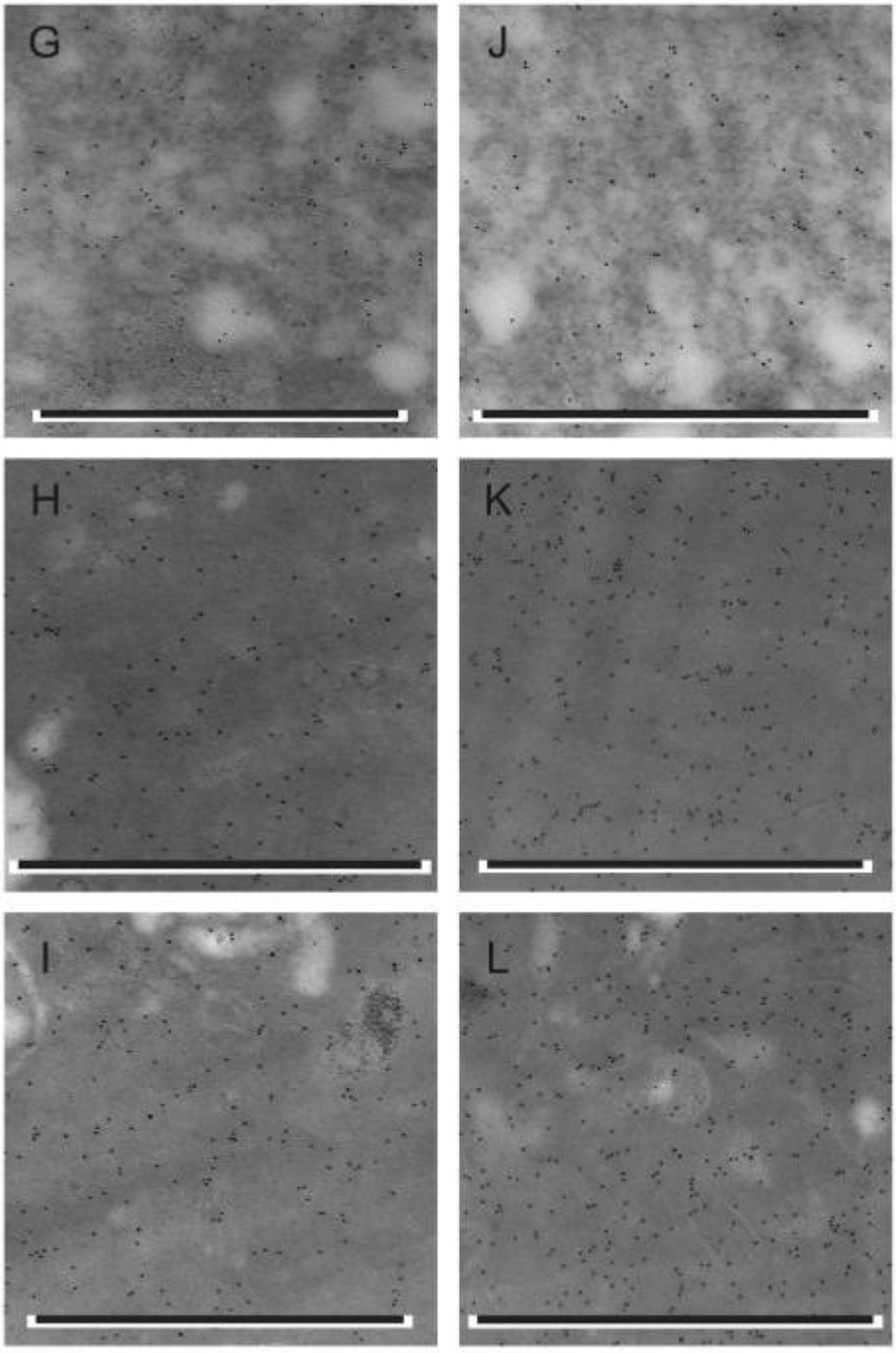
G
J
H
K
I
L

Figure 37

Kalafong patient 37

Figure 37a. A bone marrow fragment stained negative with the Prussian blue iron stain – absence of storage iron.

Figure 37b and c. Bone marrow aspirate smears stained with the Prussian blue iron stain with pathologically overloaded sideroblasts.

Figure 37d. A bone marrow section stained negative with the Prussian blue iron stain – absence of storage iron.

Figure 37e and f. Bone marrow sections stained with the Prussian blue iron stain with sideroblasts.

Figure 37g. An electron micrograph of a bone marrow macrophage immunolabelled with a monoclonal antibody to the H-subunit of ferritin, 10 nm gold particles and scale bar = 1 µm.

Figure 37h. An electron micrograph of a bone marrow red blood cell immunolabelled with a monoclonal antibody to the H-subunit of ferritin, 10 nm gold particles and scale bar = 1 µm.

Figure 37i. An electron micrograph of a bone marrow red blood cell immunolabelled with a monoclonal antibody to the H-subunit of ferritin, 10 nm gold particles and scale bar = 1 µm.

Figure 37j. An electron micrograph of a bone marrow macrophage immunolabelled with a monoclonal antibody to the L-subunit of ferritin, 10 nm gold particles and scale bar = 1 µm.

Figure 37k. An electron micrograph of a bone marrow red blood cell immunolabelled with a monoclonal antibody to the L-subunit of ferritin. Note the presence of iron-loaded ferritin on the surface of the cell membrane, 10 nm gold particles and scale bar = 1 µm.

Figure 37l. An electron micrograph of a bone marrow red blood cell precursor immunolabelled with a monoclonal antibody to the L-subunit of ferritin, 10 nm gold particles and scale bar = 1 µm.

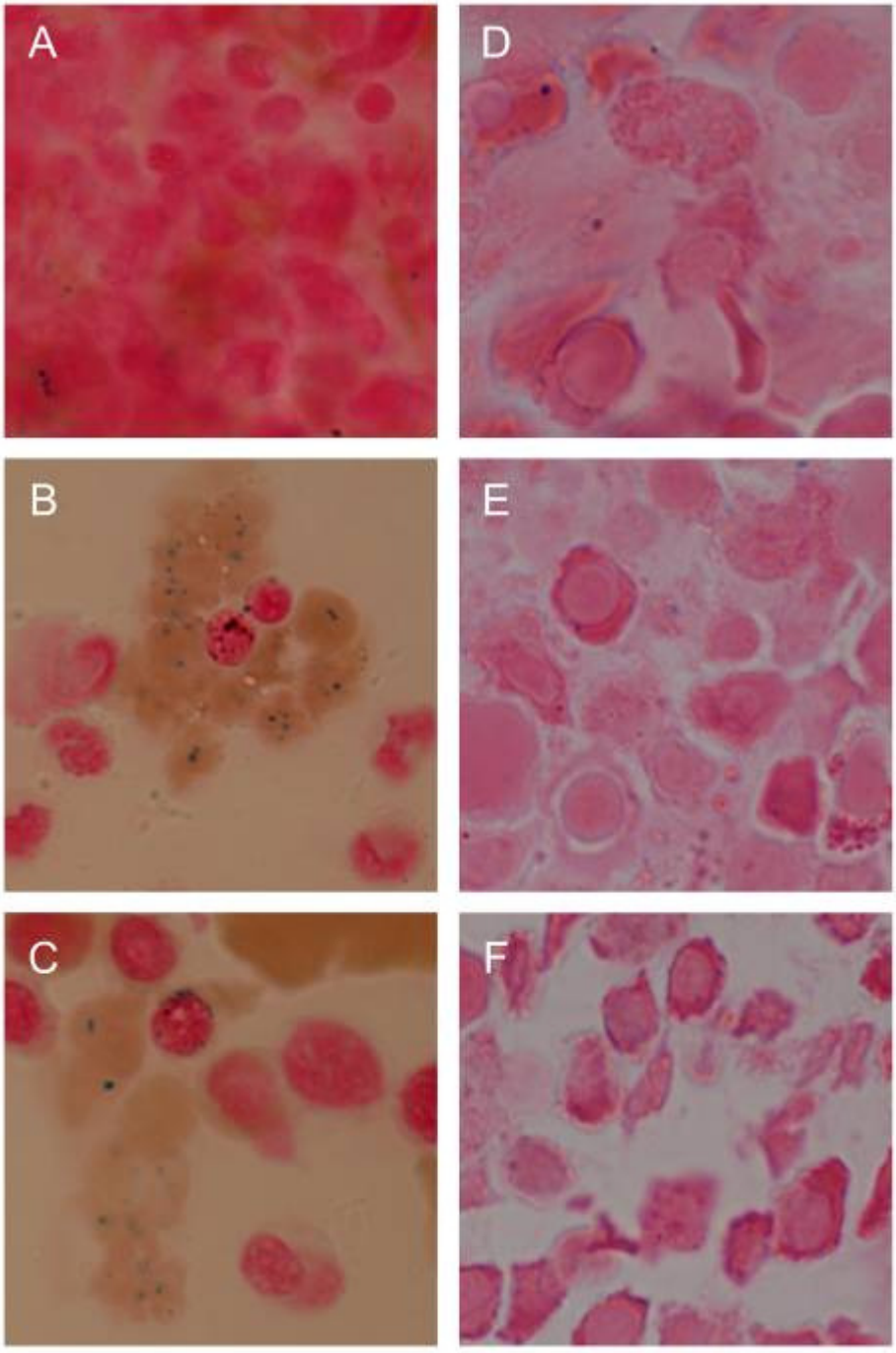
A
D
B
E
C
F

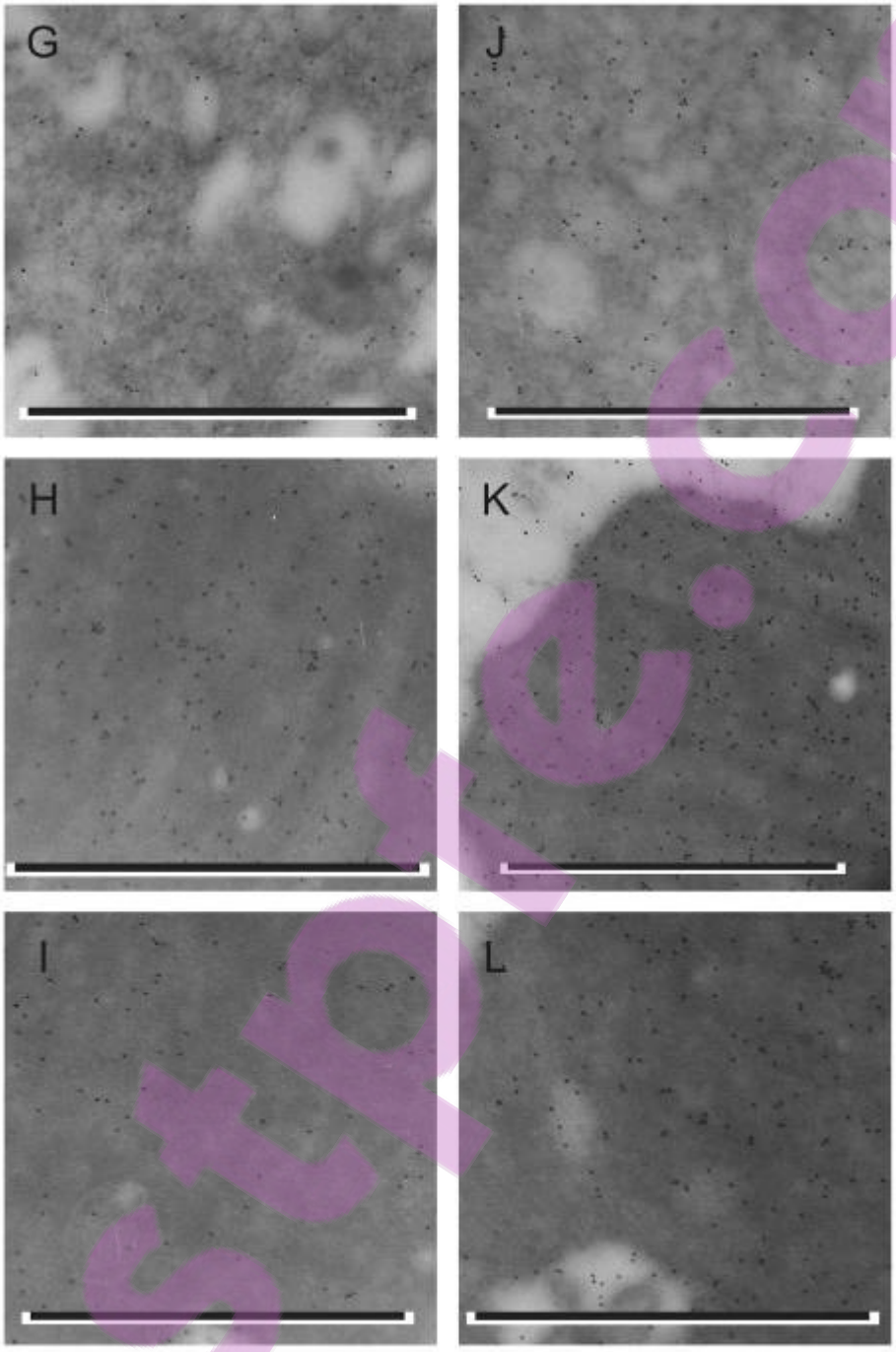

Figure 38

Kalafong patient 38

Figure 38d. A bone marrow section stained positive with the Prussian blue iron stain – presence of storage iron.

Figure 38e and f. Bone marrow sections stained with the Prussian blue iron stain with some sideroblasts.

Figure 38g. An electron micrograph of a bone marrow macrophage immunolabelled with a monoclonal antibody to the H-subunit of ferritin. Note the presence of iron-loaded ferritin, 10 nm gold particles and scale bar = 1 μm.

Figure 38h. An electron micrograph of a bone marrow red blood cell immunolabelled with a monoclonal antibody to the H-subunit of ferritin, 10 nm gold particles and scale bar = 1 μm.

Figure 38i. An electron micrograph of a bone marrow red blood cell immunolabelled with a monoclonal antibody to the H-subunit of ferritin, 10 nm gold particles and scale bar = 1 μm.

Figure 38j. An electron micrograph of a bone marrow macrophage immunolabelled with a monoclonal antibody to the L-subunit of ferritin. Note the siderosomes, 10 nm gold particles and scale bar = 1 μm.

Figure 38k. An electron micrograph of a bone marrow red blood cell immunolabelled with a monoclonal antibody to the L-subunit of ferritin, 10 nm gold particles and scale bar = 1 μm.

Figure 38l. An electron micrograph of a bone marrow reticulocyte immunolabelled with a monoclonal antibody to the L-subunit of ferritin. Note the presence of the cluster of ferritin – haemosiderin, 10 nm gold particles and scale bar = 1 μm.

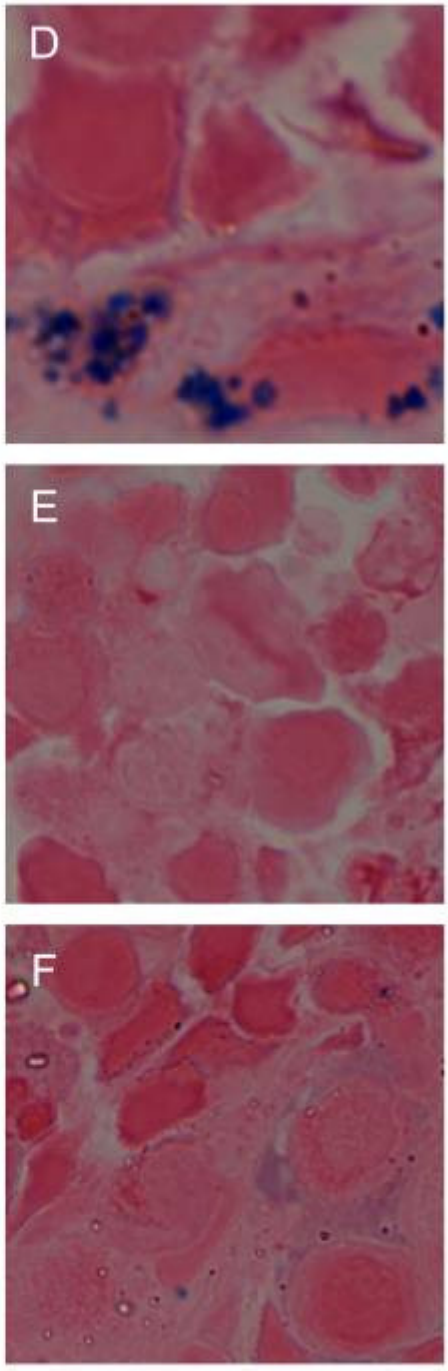

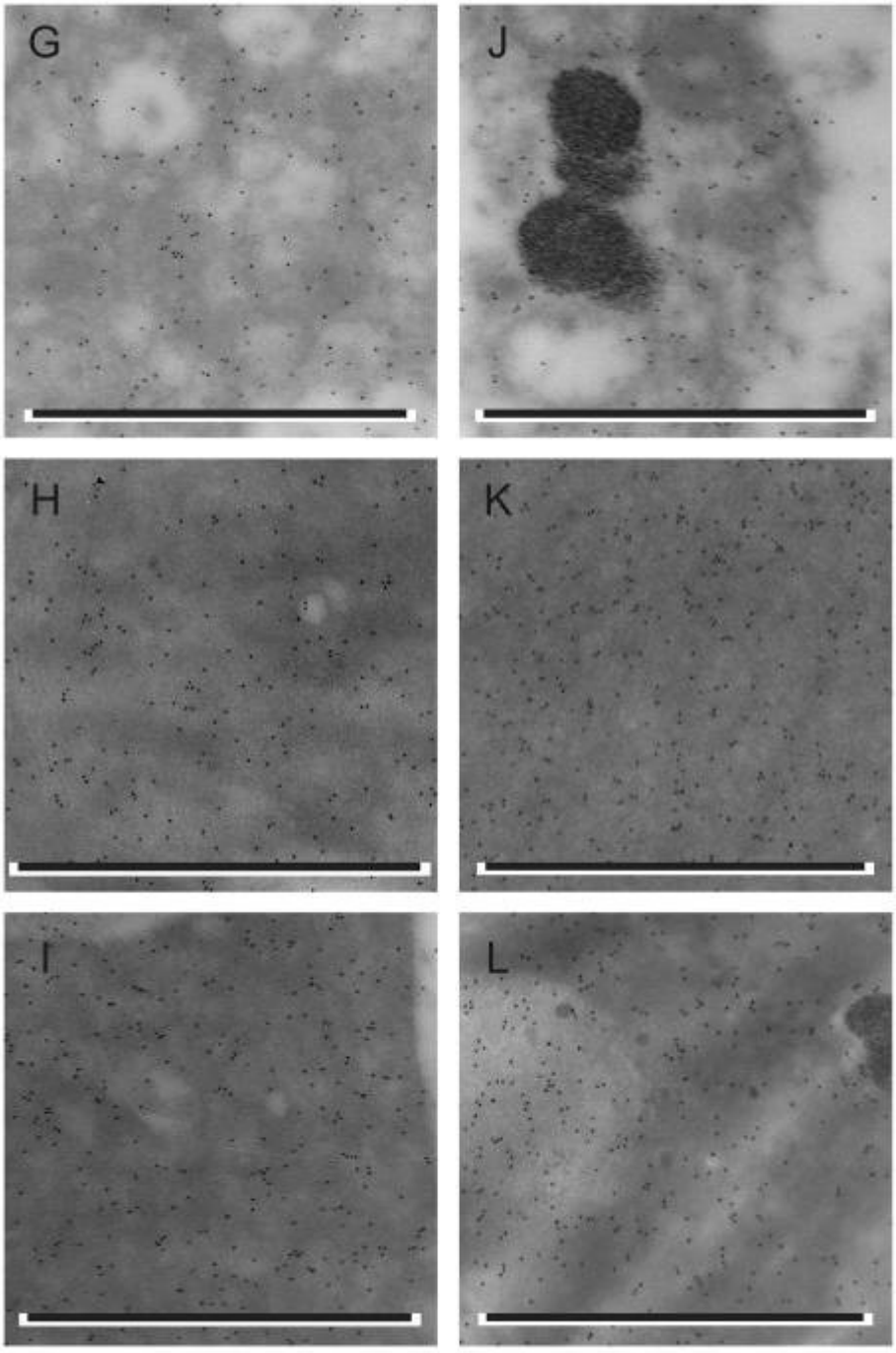
G
J
H
K
I
L

Figure 39

Kalafong patient 39

Figure 39a. A bone marrow fragment stained positive with the Prussian blue iron stain – severely increased amount of storage iron.

Figure 39b and c. Bone marrow aspirate smears stained with the Prussian blue iron stain with no sideroblasts.

Figure 39d. A bone marrow section stained positive with the Prussian blue iron stain – severely increased amount of storage iron.

Figure 39e and f. Bone marrow sections stained with the Prussian blue iron stain with some sideroblasts.

Figure 39g. An electron micrograph of a bone marrow macrophage immunolabelled with a monoclonal antibody to the H-subunit of ferritin. Note the presence of iron-loaded ferritin and the siderosome, 10 nm gold particles and scale bar = 1 μm.

Figure 39h. An electron micrograph of two bone marrow red blood cell precursors immunolabelled with a monoclonal antibody to the H-subunit of ferritin. Note the contact between the two cell membranes and the iron-loaded ferritin in the space between the membranes, 10 nm gold particles and scale bar = 1 μm.

Figure 39i. An electron micrograph of a bone marrow red blood cell precursor immunolabelled with a monoclonal antibody to the H-subunit of ferritin. Note the presence of iron-loaded ferritin in the endocytic vesicle and on the cell membrane, 10 nm gold particles and scale bar = 1 μm.

Figure 39j. An electron micrograph of a bone marrow macrophage immunolabelled with a monoclonal antibody to the L-subunit of ferritin. Note the presence of iron-loaded ferritin and the siderosome, 10 nm gold particles and scale bar = 1 μm.

Figure 39k. An electron micrograph of a bone marrow red blood cell precursor immunolabelled with a monoclonal antibody to the L-subunit of ferritin. Note the presence of iron-loaded ferritin on the surface of the cell membrane, 10 nm gold particles and scale bar = 1 μm.

Figure 39l. An electron micrograph of a bone marrow red blood cell precursor immunolabelled with a monoclonal antibody to the L-subunit of ferritin, 10 nm gold particles and scale bar = 1 µm.

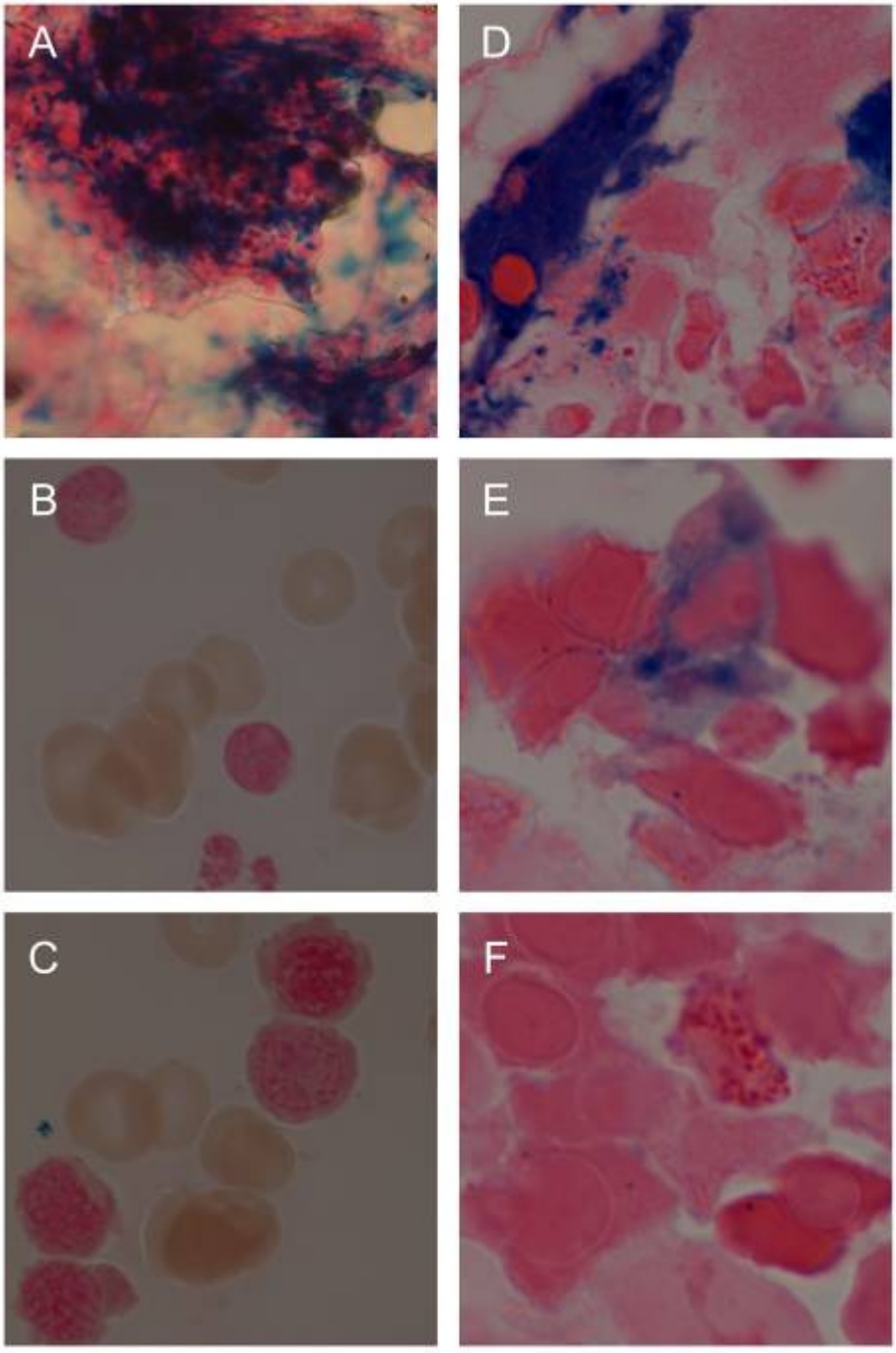
A
D
B
E
C
F

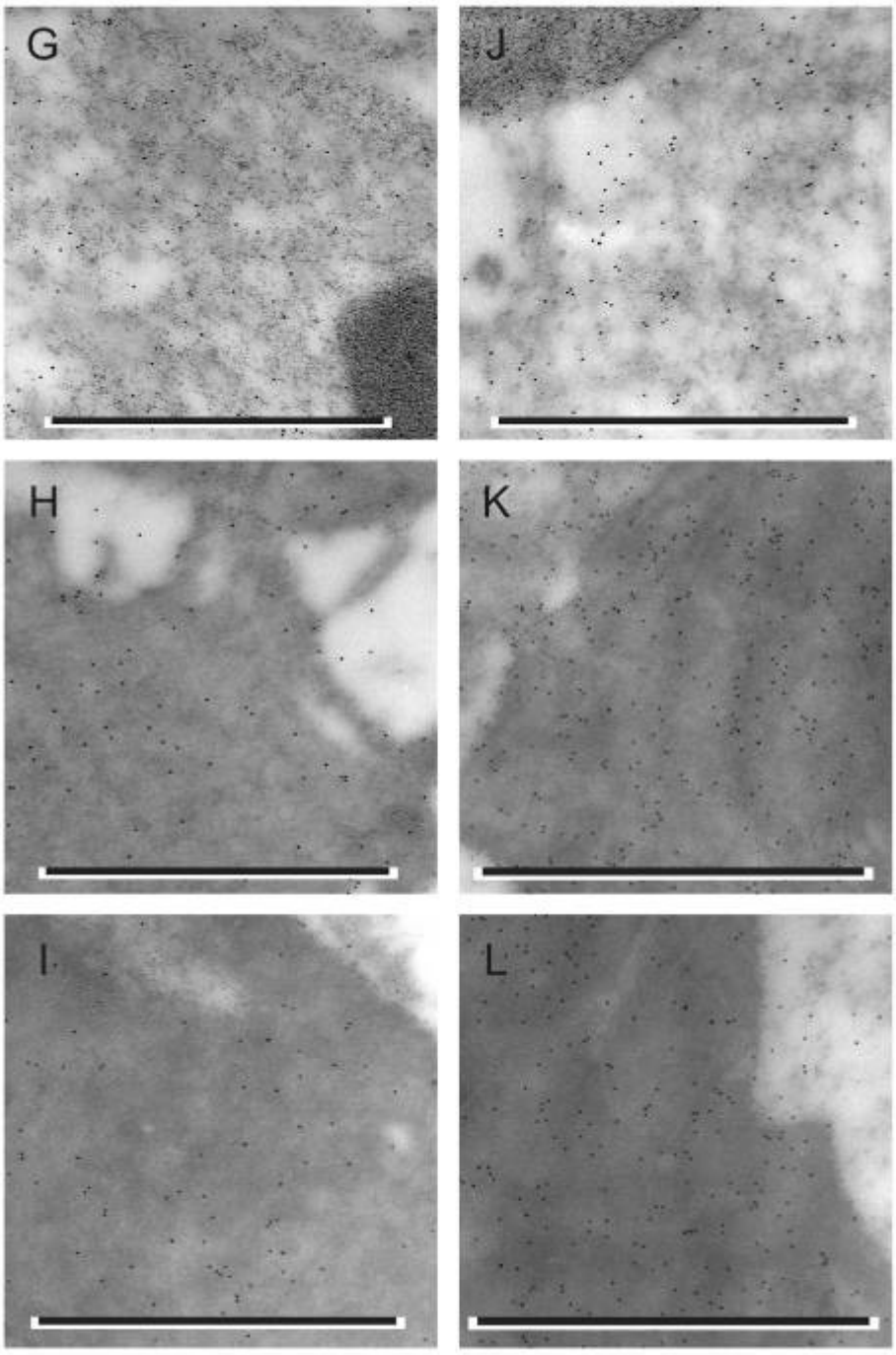
G
J
H
K
I
L

Figure 40

Kalafong patient 40

Figure 40a. A bone marrow fragment stained positive with the Prussian blue iron stain – severely increased amount of storage iron.

Figure 40b and c. Bone marrow aspirate smears stained with the Prussian blue iron stain with reduced amount of sideroblasts.

Figure 40d. A bone marrow section stained positive with the Prussian blue iron stain – severely increased amount of storage iron.

Figure 40e and f. Bone marrow sections stained with the Prussian blue iron stain with no sideroblasts.

Figure 40g. An electron micrograph of a bone marrow macrophage immunolabelled with a monoclonal antibody to the H-subunit of ferritin, 10 nm gold particles and scale bar = 1 μm.

Figure 40h. An electron micrograph of a bone marrow reticulocyte immunolabelled with a monoclonal antibody to the H-subunit of ferritin, 10 nm gold particles and scale bar = 1 μm.

Figure 40i. An electron micrograph of a bone marrow red blood cell precursor immunolabelled with a monoclonal antibody to the H-subunit of ferritin. Note the presence of some iron-loaded ferritin on the cell membrane, 10 nm gold particles and scale bar = 1 μm.

Figure 40j. An electron micrograph of a bone marrow macrophage immunolabelled with a monoclonal antibody to the L-subunit of ferritin, 10 nm gold particles and scale bar = 1 μm.

Figure 40k. An electron micrograph of a bone marrow red blood cell immunolabelled with a monoclonal antibody to the L-subunit of ferritin, 10 nm gold particles and scale bar = 1 μm.

Figure 40l. An electron micrograph of a bone marrow red blood cell immunolabelled with a monoclonal antibody to the L-subunit of ferritin, 10 nm gold particles and scale bar = 1 μm.

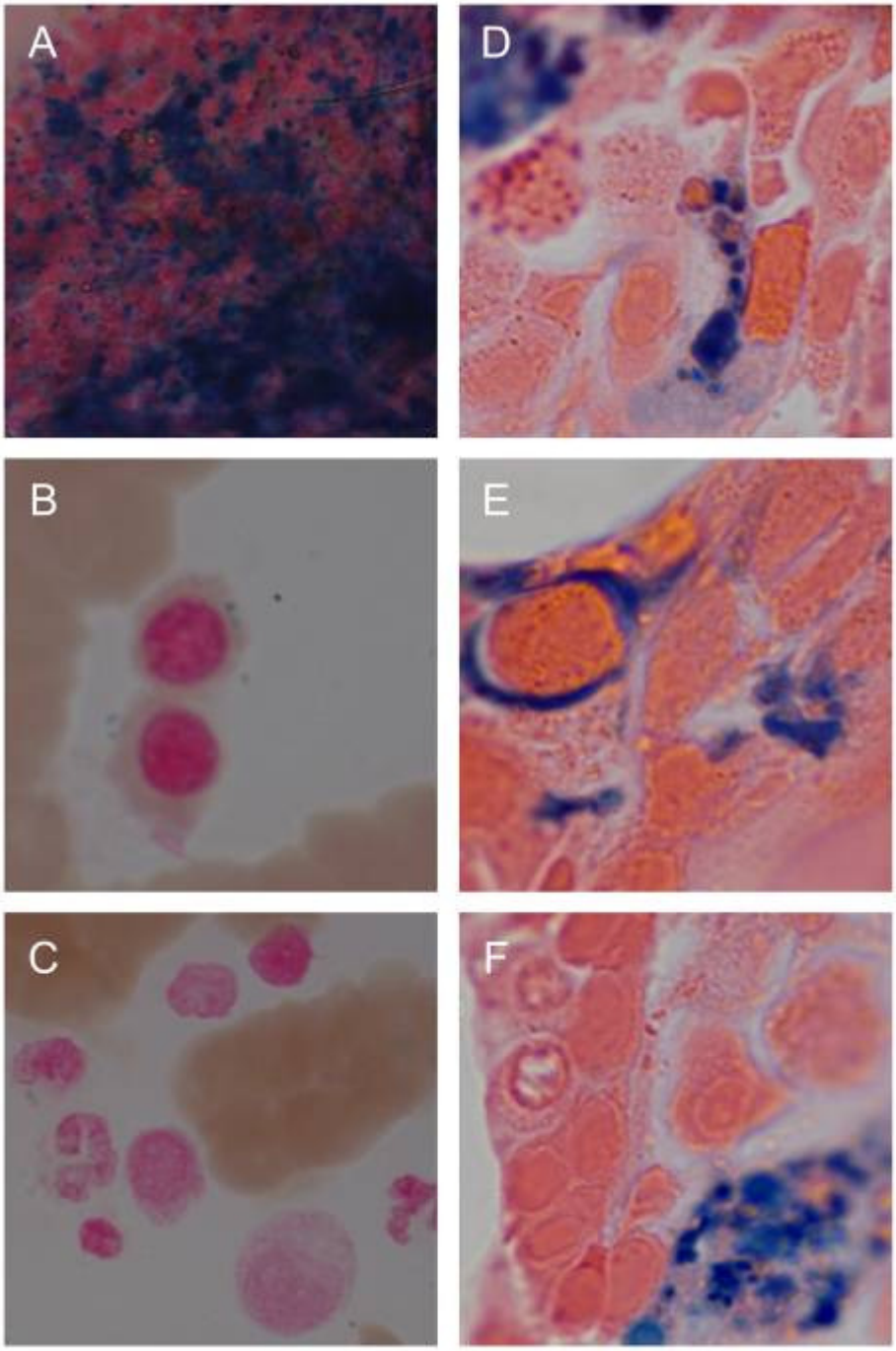
A
D
B
E
C
F

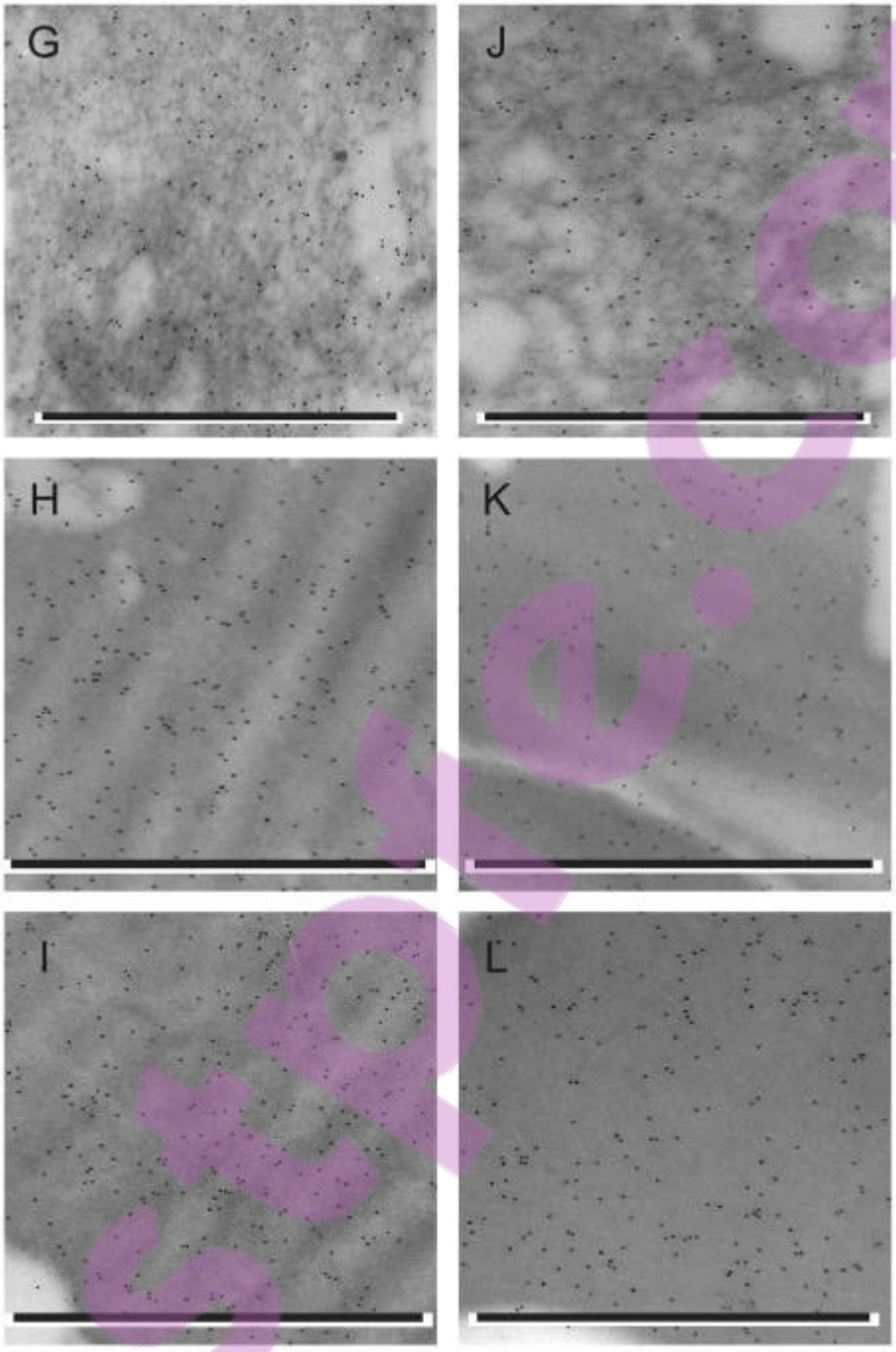

Figure 41

Kalafong patient 41

Figure 41a. A bone marrow fragment stained negative with the Prussian blue iron stain – absence of storage iron.

Figure 41b and c. Bone marrow aspirate smears stained with the Prussian blue iron stain with no sideroblasts.

Figure 41d. A bone marrow section stained negative with the Prussian blue iron stain – absence of storage iron.

Figure 41e and f. Bone marrow sections stained with the Prussian blue iron stain with no sideroblasts.

Figure 41g. An electron micrograph of a bone marrow macrophage immunolabelled with a monoclonal antibody to the H-subunit of ferritin, 10 nm gold particles and scale bar = 1 μm.

Figure 41h. An electron micrograph of a bone marrow red blood cell precursor immunolabelled with a monoclonal antibody to the H-subunit of ferritin. Note the presence of the endocytic vesicle with no iron-loaded ferritin, 10 nm gold particles and scale bar = 1 μm.

Figure 41i. An electron micrograph of a bone marrow red blood cell precursor immunolabelled with a monoclonal antibody to the H-subunit of ferritin. Note the presence of the endocytic vesicle with no iron-loaded ferritin, 10 nm gold particles and scale bar = 1 μm.

Figure 41j. An electron micrograph of a bone marrow macrophage immunolabelled with a monoclonal antibody to the L-subunit of ferritin, 10 nm gold particles and scale bar = 1 μm.

Figure 41k. An electron micrograph of a bone marrow red blood cell precursor immunolabelled with a monoclonal antibody to the H-subunit of ferritin. Note the presence of the endocytic vesicle with no iron-loaded ferritin, 10 nm gold particles and scale bar = 1 μm.

Figure 41l. An electron micrograph of a bone marrow red blood cell precursor immunolabelled with a monoclonal antibody to the H-subunit of ferritin. Note the presence of the endocytic vesicle with no iron-loaded ferritin, 10 nm gold particles and scale bar = 1 μm.

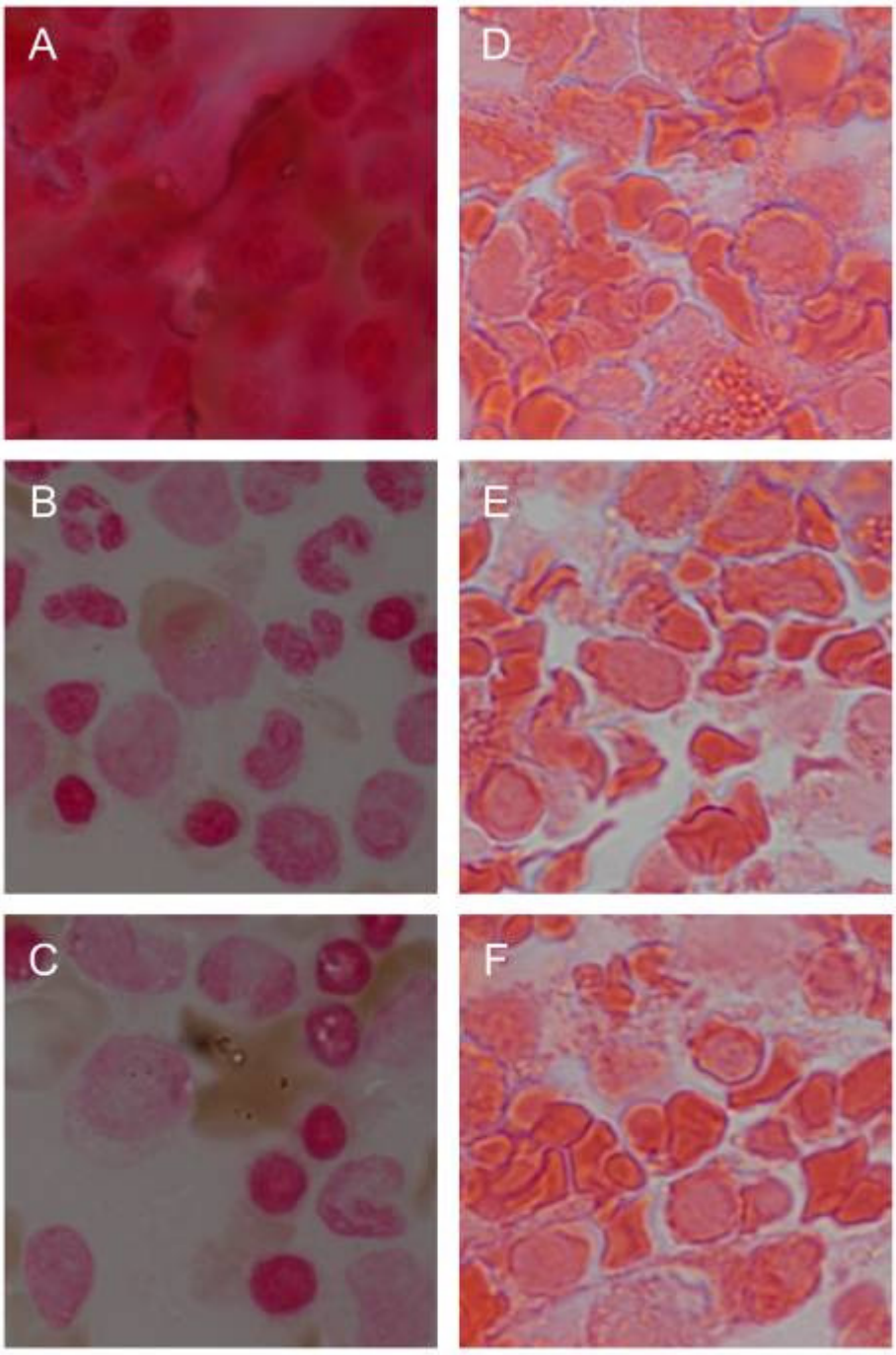

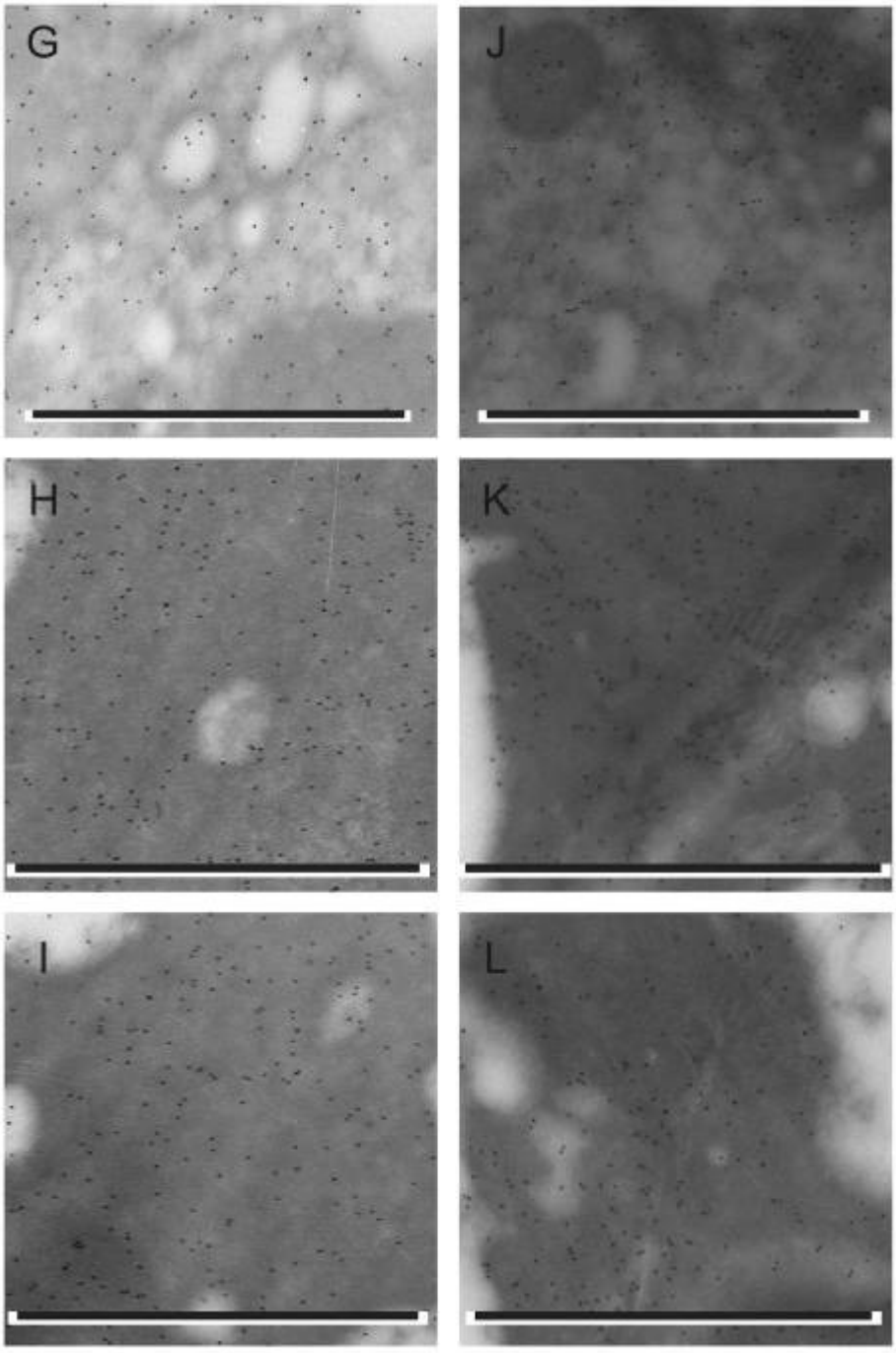
G
J
H
K
I
L

Figure 42

Kalafong patient 42

Figure 42a. A bone marrow fragment stained negative with the Prussian blue iron stain – absence of storage iron.

Figure 42b and c. Bone marrow aspirate smears stained with the Prussian blue iron stain with some sideroblasts.

Figure 42d. A bone marrow section stained negative with the Prussian blue iron stain – absence of storage iron.

Figure 42e and f. Bone marrow sections stained with the Prussian blue iron stain with some sideroblasts.

Figure 42g. An electron micrograph of a bone marrow macrophage immunolabelled with a monoclonal antibody to the H-subunit of ferritin, 10 nm gold particles and scale bar = 1 μm.

Figure 42h. An electron micrograph of a bone marrow macrophage and red blood cell precursor immunolabelled with a monoclonal antibody to the H-subunit of ferritin, 10 nm gold particles and scale bar = 1 μm.

Figure 42i. An electron micrograph of a bone marrow red blood cell precursor immunolabelled with a monoclonal antibody to the H-subunit of ferritin. Note the presence of the endocytic vesicle with no iron-loaded ferritin, 10 nm gold particles and scale bar = 1 μm.

Figure 42j. An electron micrograph of a bone marrow macrophage immunolabelled with a monoclonal antibody to the L-subunit of ferritin, 10 nm gold particles and scale bar = 1 μm.

Figure 42k. An electron micrograph of a bone marrow red blood cell precursor immunolabelled with a monoclonal antibody to the H-subunit of ferritin, 10 nm gold particles and scale bar = 1 μm.

Figure 42l. An electron micrograph of a bone marrow reticulocyte immunolabelled with a monoclonal antibody to the H-subunit of ferritin, 10 nm gold particles and scale bar = 1 μm.

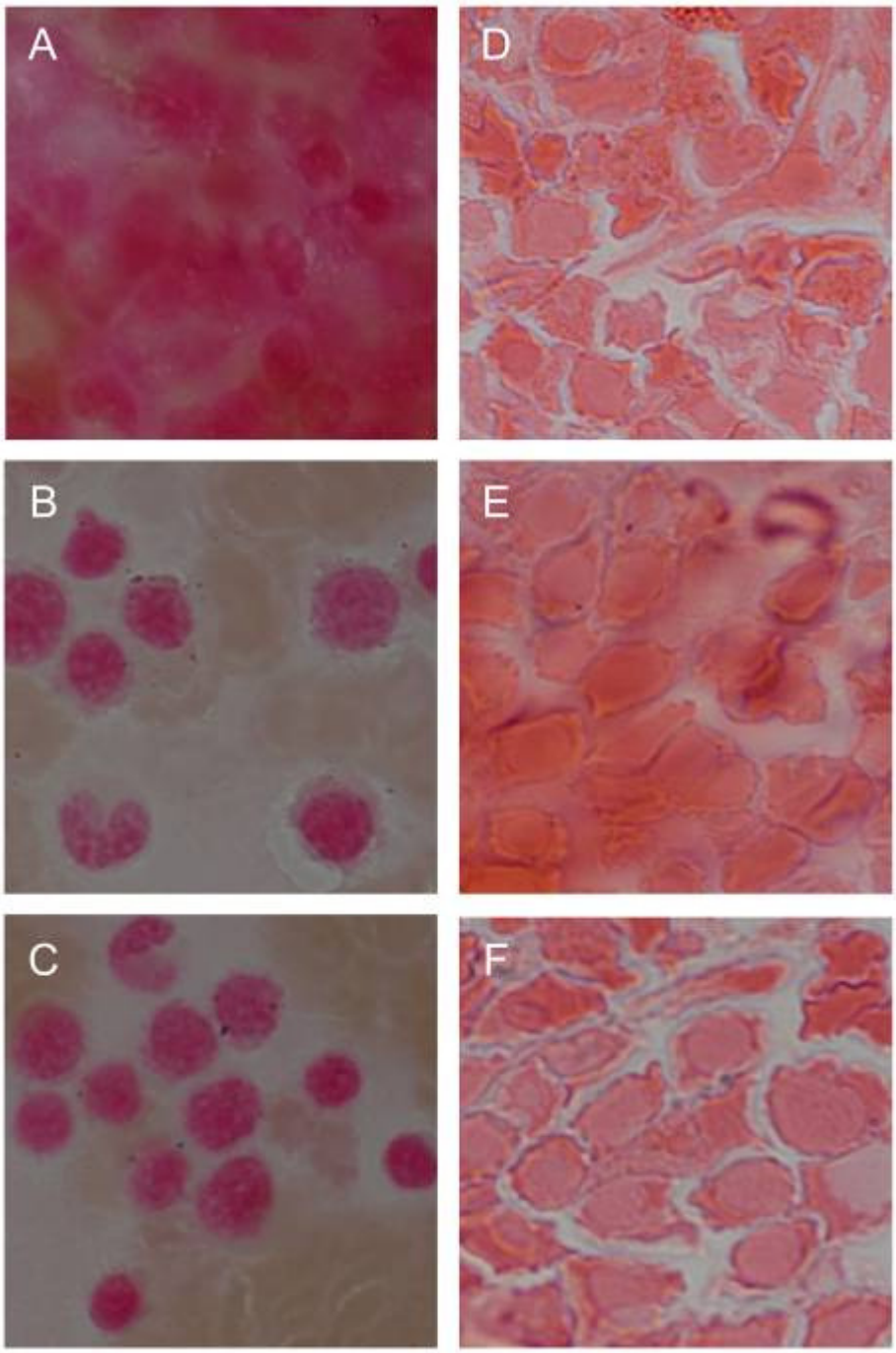
A
D
B
E
C
F

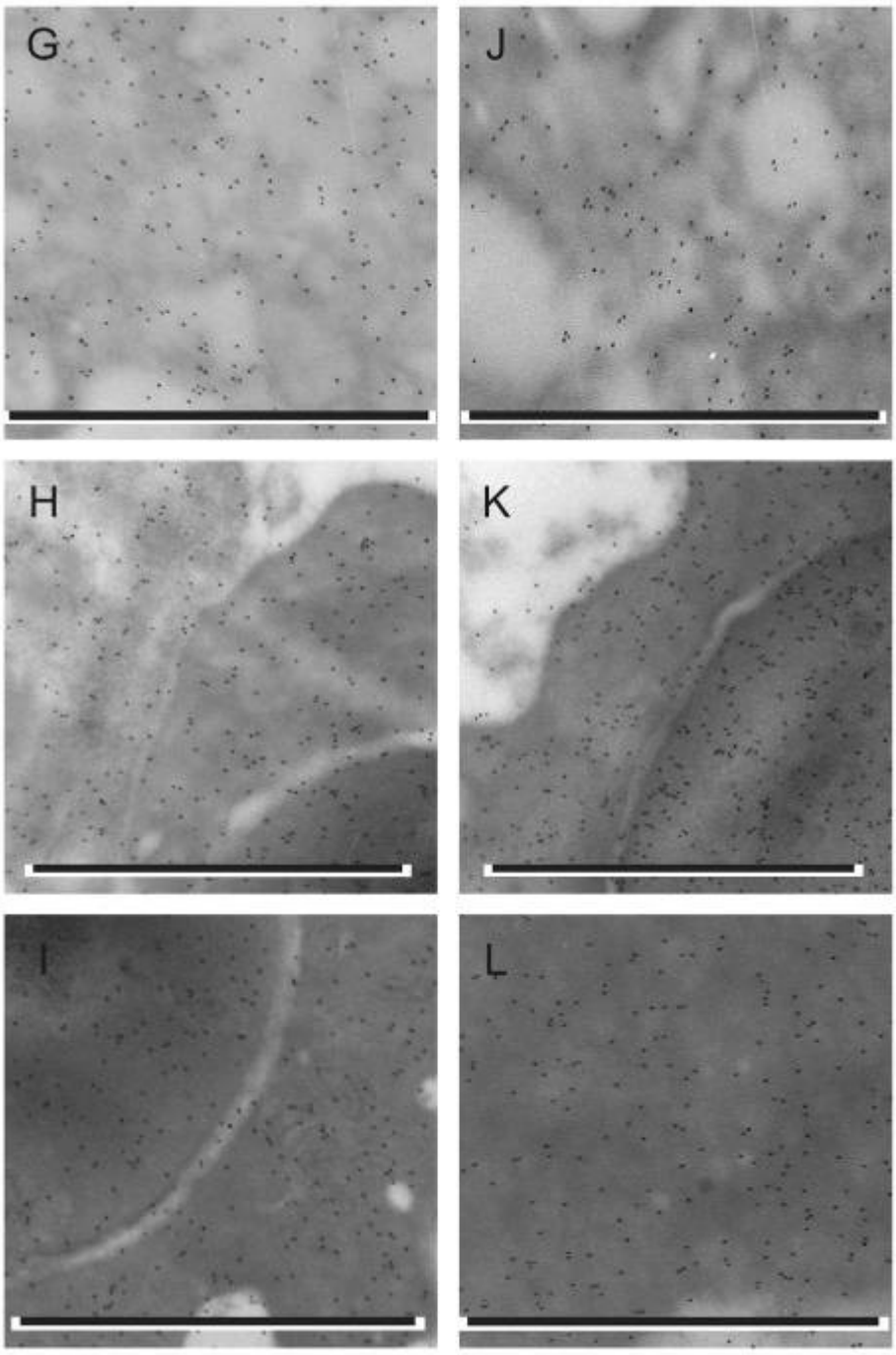
G
J
H
K
I
L

Figure 43

Kalafong patient 43

Figure 43a. A bone marrow fragment stained negative with the Prussian blue iron stain – absence of storage iron.

Figure 43b and c. Bone marrow aspirate smears stained with the Prussian blue iron stain with no sideroblasts.

Figure 43d. A bone marrow section stained negative with the Prussian blue iron stain – absence of storage iron.

Figure 43e and f. Bone marrow sections stained with the Prussian blue iron stain with no sideroblasts.

Figure 43g. An electron micrograph of a bone marrow macrophage immunolabelled with a monoclonal antibody to the H-subunit of ferritin, 10 nm gold particles and scale bar = 1 μm.

Figure 43h. An electron micrograph of a bone marrow red blood cell precursor immunolabelled with a monoclonal antibody to the H-subunit of ferritin, 10 nm gold particles and scale bar = 1 μm.

Figure 43i. An electron micrograph of a bone marrow red blood cell immunolabelled with a monoclonal antibody to the H-subunit of ferritin, 10 nm gold particles and scale bar = 1 μm.

Figure 43j. An electron micrograph of a bone marrow macrophage immunolabelled with a monoclonal antibody to the L-subunit of ferritin, 10 nm gold particles and scale bar = 1 μm.

Figure 43k. An electron micrograph of a bone marrow red blood cell precursor immunolabelled with a monoclonal antibody to the H-subunit of ferritin, 10 nm gold particles and scale bar = 1 μm.

Figure 43l. An electron micrograph of a bone marrow reticulocyte immunolabelled with a monoclonal antibody to the H-subunit of ferritin, 10 nm gold particles and scale bar = 1 μm.

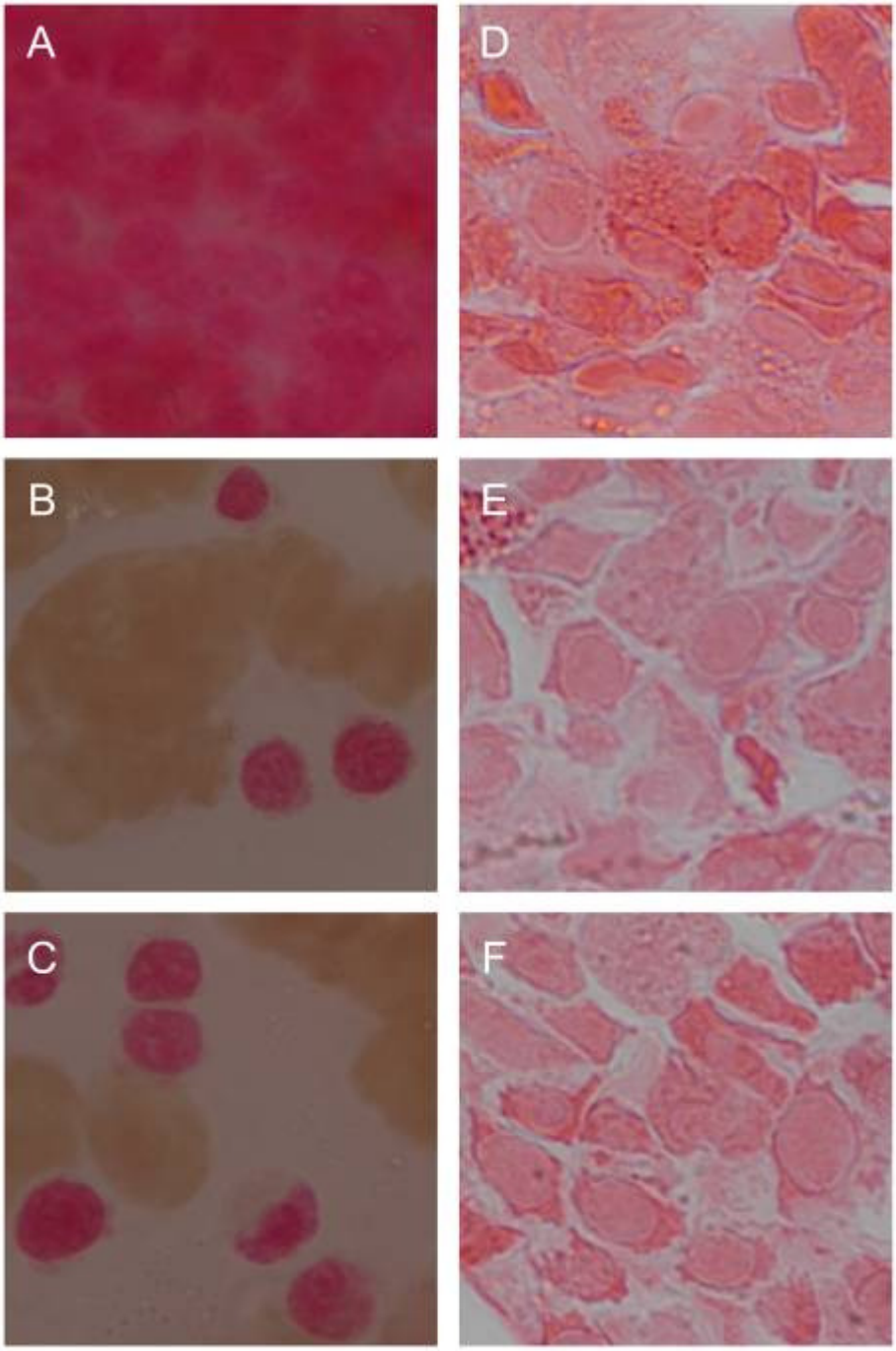
A
D
B
E
C
F

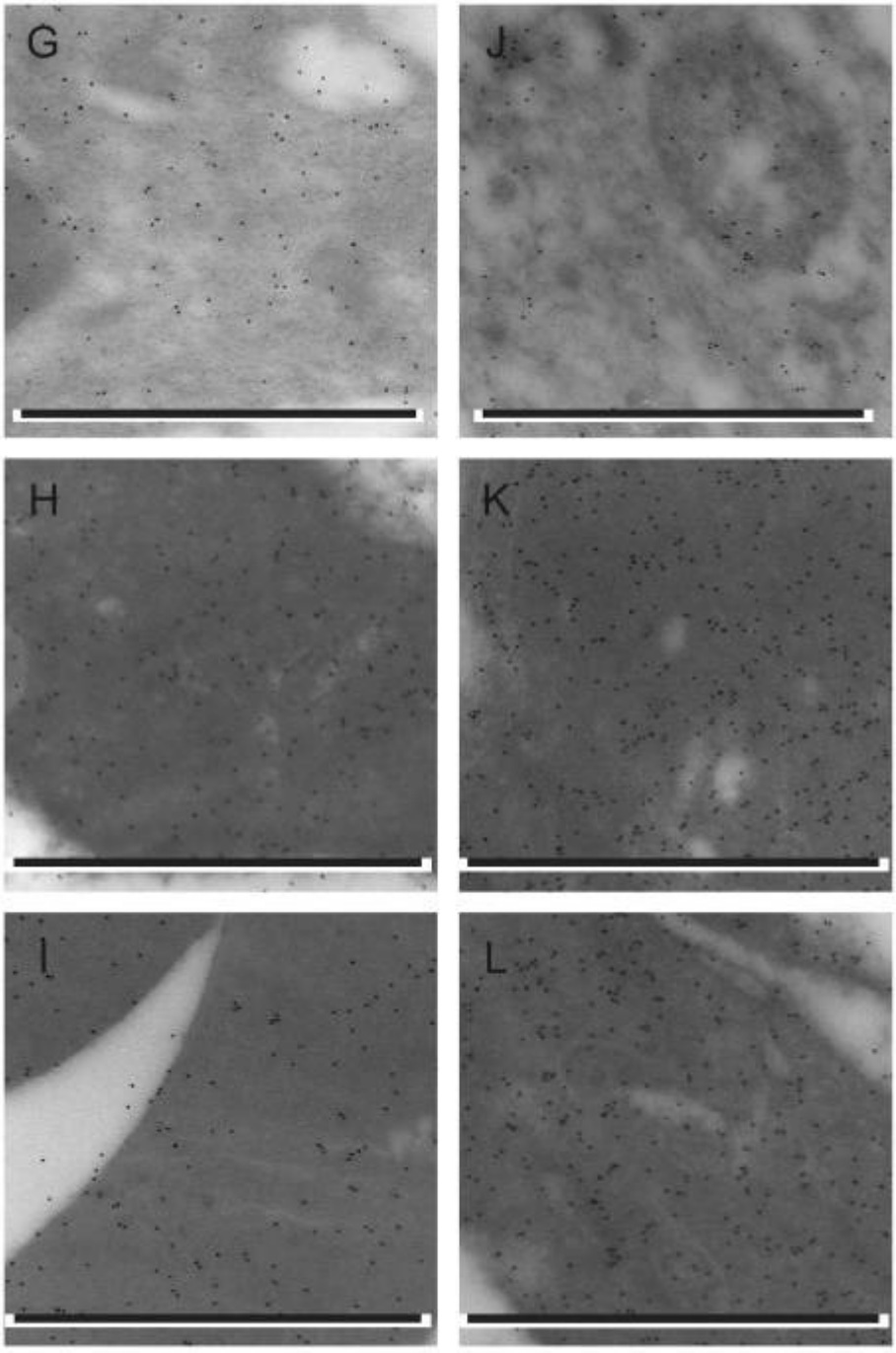
G
J
H
K
I
L

Figure 44

Kalafong patient 44

Figure 44a. A bone marrow fragment stained positive with the Prussian blue iron stain – increased amount of storage iron.

Figure 44b and c. Bone marrow aspirate smears stained with the Prussian blue iron stain with no sideroblasts.

Figure 44d. A bone marrow section stained positive with the Prussian blue iron stain – increased amount of storage iron.

Figure 44e and f. Bone marrow sections stained with the Prussian blue iron stain with no sideroblasts.

Figure 44g. An electron micrograph of a bone marrow macrophage immunolabelled with a monoclonal antibody to the H-subunit of ferritin, 10 nm gold particles and scale bar = 1 μm.

Figure 44h. An electron micrograph of a bone marrow red blood cell precursor immunolabelled with a monoclonal antibody to the H-subunit of ferritin, 10 nm gold particles and scale bar = 1 μm.

Figure 44i. An electron micrograph of a bone marrow red blood cell precursor immunolabelled with a monoclonal antibody to the H-subunit of ferritin, 10 nm gold particles and scale bar = 1 μm.

Figure 44j. An electron micrograph of a bone marrow macrophage immunolabelled with a monoclonal antibody to the L-subunit of ferritin, 10 nm gold particles and and scale bar = 1 μm.

Figure 44k. An electron micrograph of two bone marrow red blood cell precursors immunolabelled with a monoclonal antibody to the H-subunit of ferritin. Note the contact between the two cell membranes and the presence of iron-loaded ferritin in the space between the membranes, 10 nm gold particles and scale bar = 1 μm.

Figure 44l. An electron micrograph of a bone marrow red blood cell precursor immunolabelled with a monoclonal antibody to the H-subunit of ferritin. Note the cluster of iron-loaded ferritin and the iron-loaded ferritin on the cell membrane, 10 nm gold particles and scale bar = 1 μm.

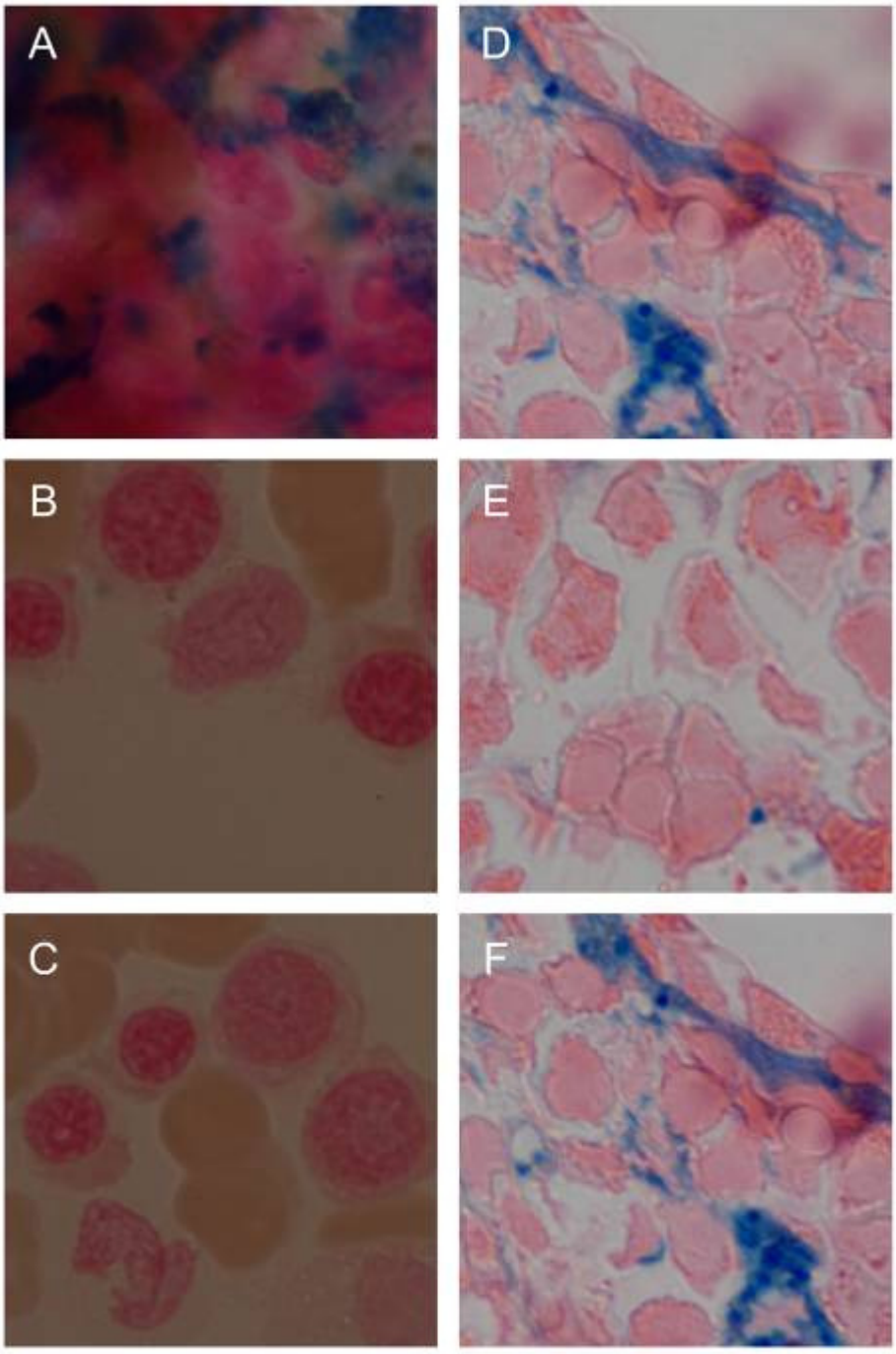
A
D
B
E
C
F

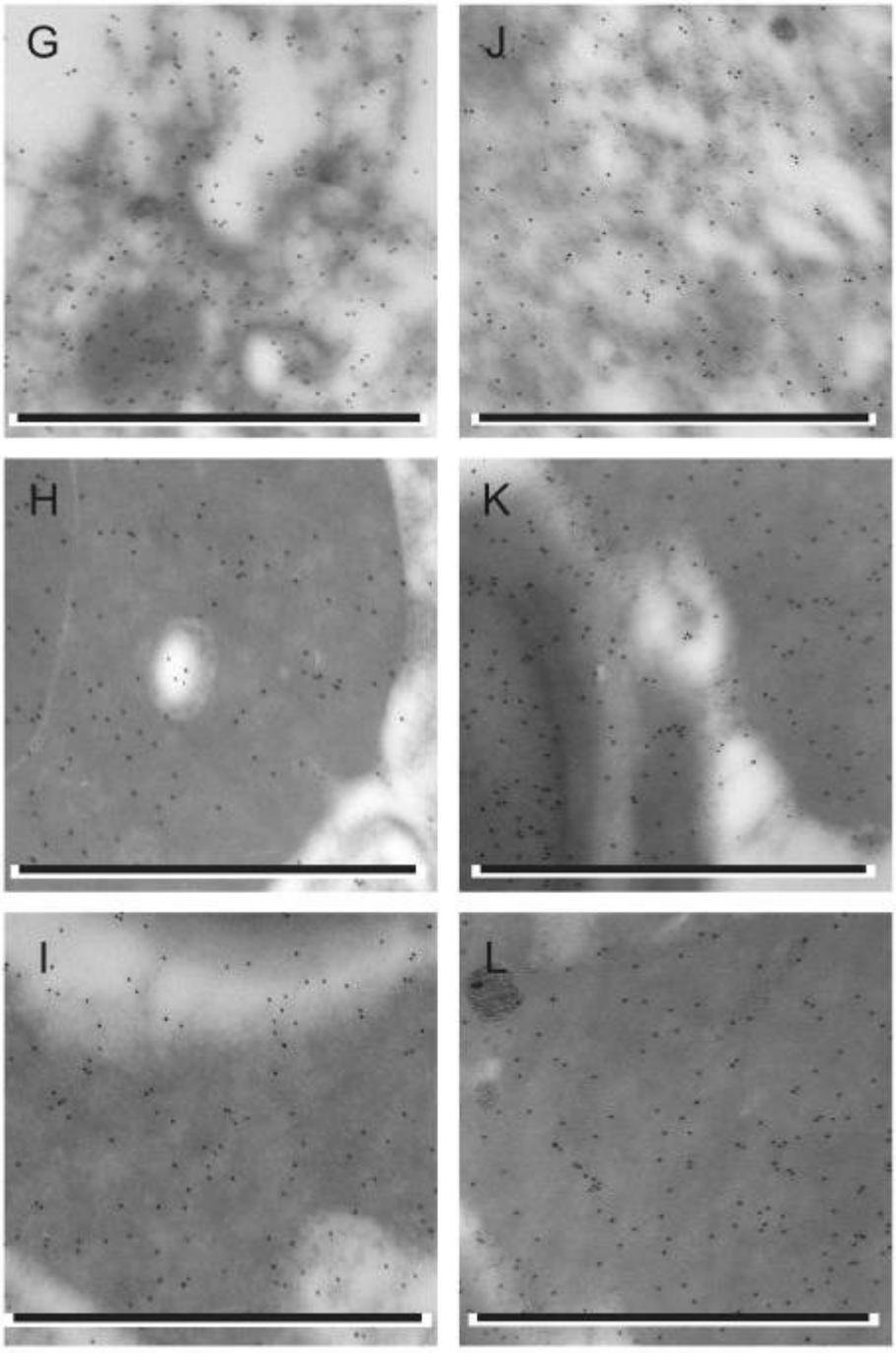

Figure 45

Kalafong patient 45

Figure 45d. A bone marrow section stained positive with the Prussian blue iron stain – severely increased amount of storage iron.

Figure 45e and f. Bone marrow sections stained with the Prussian blue iron stain with no sideroblasts.

Figure 45g. An electron micrograph of a bone marrow macrophage immunolabelled with a monoclonal antibody to the H-subunit of ferritin. Note the iron-loaded ferritin, 10 nm gold particles and scale bar = 1 μm.

Figure 45h. An electron micrograph of a bone marrow reticulocyte immunolabelled with a monoclonal antibody to the H-subunit of ferritin, 10 nm gold particles and scale bar = 1 μm.

Figure 45i. An electron micrograph of a bone marrow red blood cell precursor immunolabelled with a monoclonal antibody to the H-subunit of ferritin. Note the presence of the cluster of iron-loaded ferritin, 10 nm gold particles and scale bar = 1 μm.

Figure 45j. An electron micrograph of a bone marrow macrophage immunolabelled with a monoclonal antibody to the L-subunit of ferritin. Note the iron-loaded ferritin and the siderosomes, 10 nm gold particles and scale bar = 1 μm.

Figure 45k. An electron micrograph of a bone marrow red blood cell precursor immunolabelled with a monoclonal antibody to the H-subunit of ferritin, 10 nm gold particles and scale bar = 1 μm.

Figure 45l. An electron micrograph of a bone marrow red blood cell and part of a macrophage immunolabelled with a monoclonal antibody to the H-subunit of ferritin, 10 nm gold particles and scale bar = 1 μm.

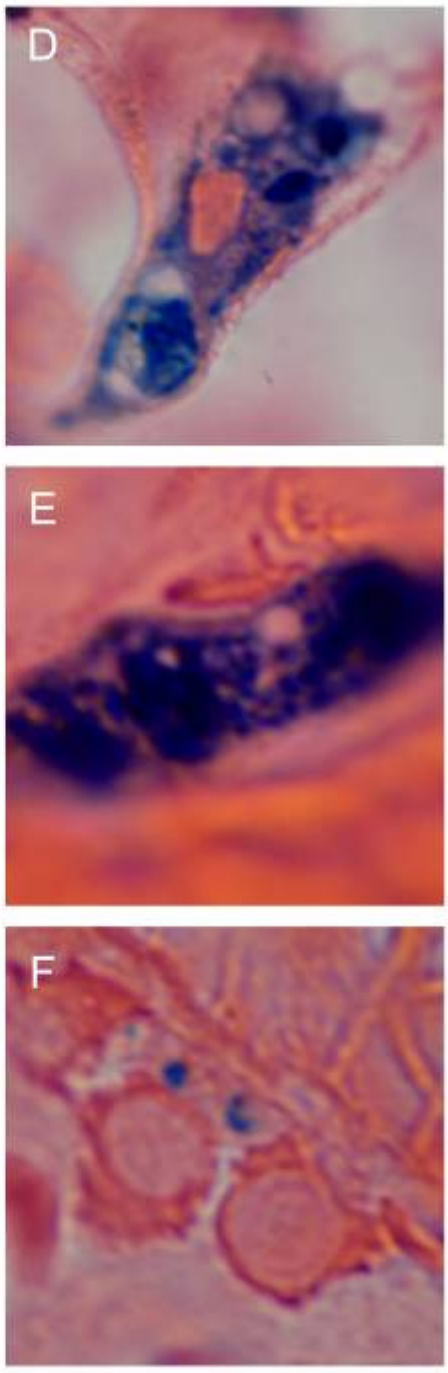
D
E
F

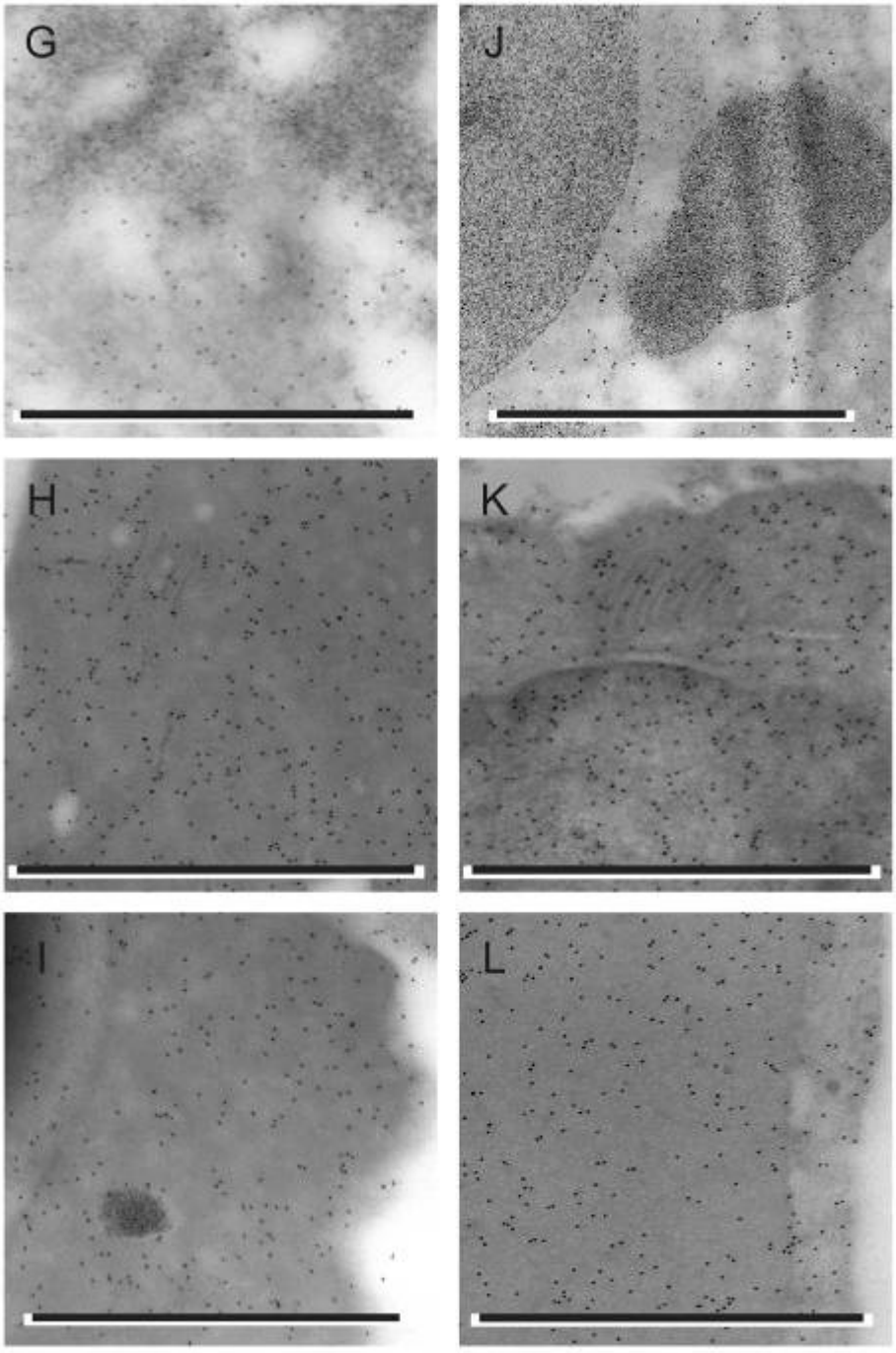
G
J
H
K
I
L

Figure 46

Kalafong patient 46

Figure 46a. A bone marrow fragment stained positive with the Prussian blue iron stain – severely increased amount of storage iron.

Figure 46b and c. Bone marrow aspirate smears stained with the Prussian blue iron stain with some sideroblasts.

Figure 46d. A bone marrow section stained positive with the Prussian blue iron stain – increased amount of storage iron.

Figure 46e and f. Bone marrow sections stained with the Prussian blue iron stain with no sideroblasts.

Figure 46g. An electron micrograph of a bone marrow macrophage immunolabelled with a monoclonal antibody to the H-subunit of ferritin, 10 nm gold particles and scale bar = 1 μm.

Figure 46h. An electron micrograph of two bone marrow red blood cell precursors immunolabelled with a monoclonal antibody to the H-subunit of ferritin. Note the contact between the two cell membranes and the iron-loaded ferritin in the space between the membranes, 10 nm gold particles and scale bar = 1 μm.

Figure 46i. An electron micrograph of two bone marrow reticulocytes immunolabelled with a monoclonal antibody to the H-subunit of ferritin. Note the contact between the two cell membranes and the iron-loaded ferritin in the space between the mebranes, 10 nm gold particles and scale bar = 1 μm.

Figure 46j. An electron micrograph of a bone marrow macrophage immunolabelled with a monoclonal antibody to the L-subunit of ferritin, 10 nm gold particles and scale bar = 1 μm.

Figure 46k. An electron micrograph of a bone marrow red blood cell immunolabelled with a monoclonal antibody to the H-subunit of ferritin. Note the presence of iron-loaded ferritin on the cell membranes, 10 nm gold particles and scale bar = 1 μm.

Figure 46l. An electron micrograph of a bone marrow red blood cell and part of a macrophage immunolabelled with a monoclonal antibody to the H-subunit of ferritin. Note the cluster of

iron-loaded ferritin and the iron-loaded ferritin on the cell membrane, 10 nm gold particles and scale bar = 1 μm.

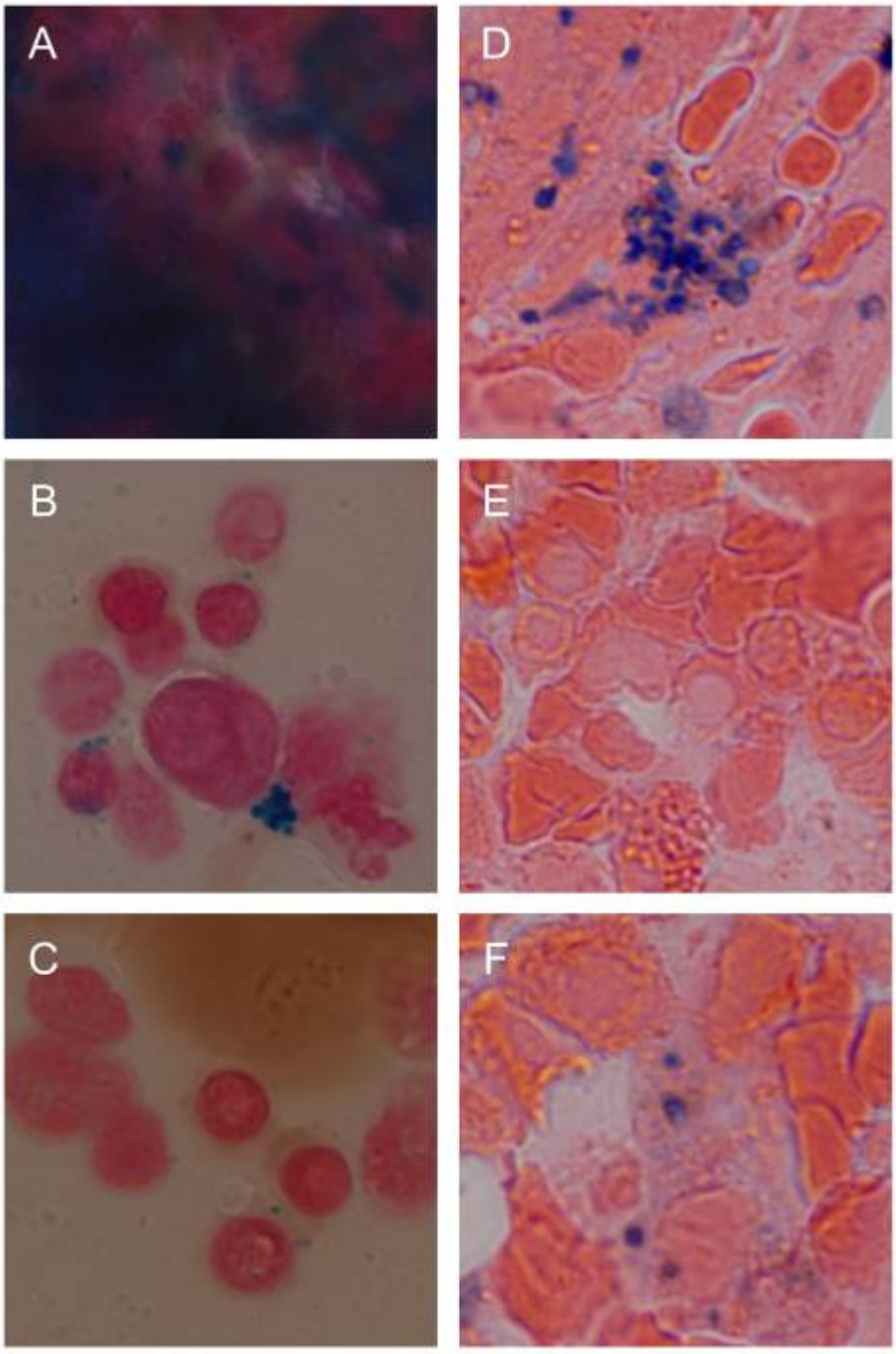
A
D
B
E
C
F

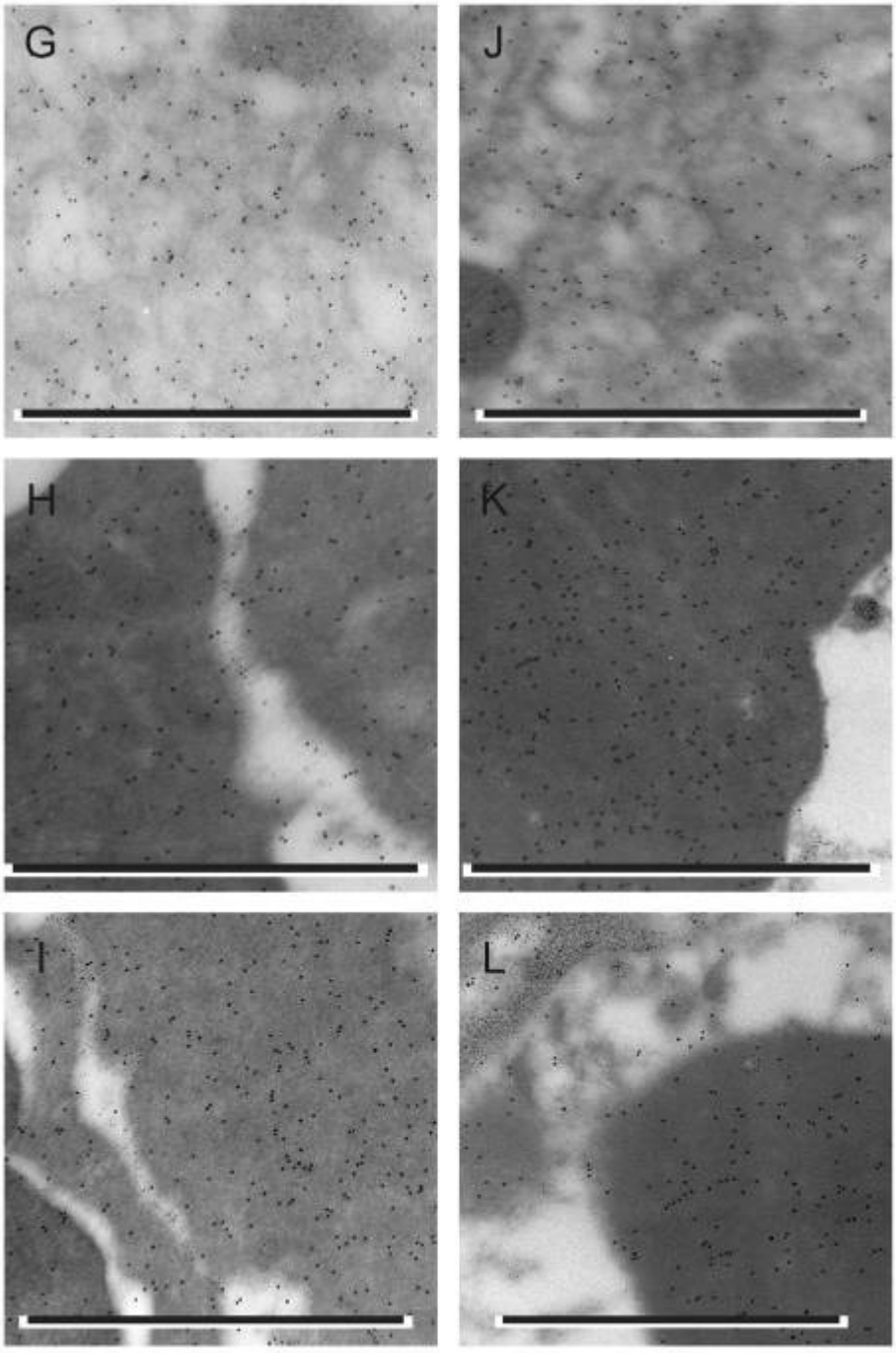
G
J
H
K
I
L

Figure 47

Kalafong patient 47

Figure 47d. A bone marrow section stained negative with the Prussian blue iron stain – absence of storage iron.

Figure 47e and f. Bone marrow sections stained with the Prussian blue iron stain with no sideroblasts.

Figure 47g. An electron micrograph of a bone marrow macrophage immunolabelled with a monoclonal antibody to the H-subunit of ferritin. Note the presence of iron-loaded ferritin, 10 nm gold particles and scale bar = 1 µm.

Figure 47h. An electron micrograph of a bone marrow red blood cell precursor immunolabelled with a monoclonal antibody to the H-subunit of ferritin, 10 nm gold particles and scale bar = 1 µm.

Figure 47i. An electron micrograph of a bone marrow red blood cell precursor immunolabelled with a monoclonal antibody to the H-subunit of ferritin, 10 nm gold particles and scale bar = 1 µm.

Figure 47j. An electron micrograph of a bone marrow macrophage immunolabelled with a monoclonal antibody to the L-subunit of ferritin, 10 nm gold particles and scale bar = 1 µm.

Figure 47k. An electron micrograph of a bone marrow red blood cell precursor immunolabelled with a monoclonal antibody to the H-subunit of ferritin, 10 nm gold particles and scale bar = 1 µm.

Figure 47l. An electron micrograph of two bone marrow red blood cell precursors immunolabelled with a monoclonal antibody to the H-subunit of ferritin. Note the contact between the two cell membranes and the absence of iron-loaded ferritin in the space between the cell membranes, 10 nm gold particles and scale bar = 1 µm.

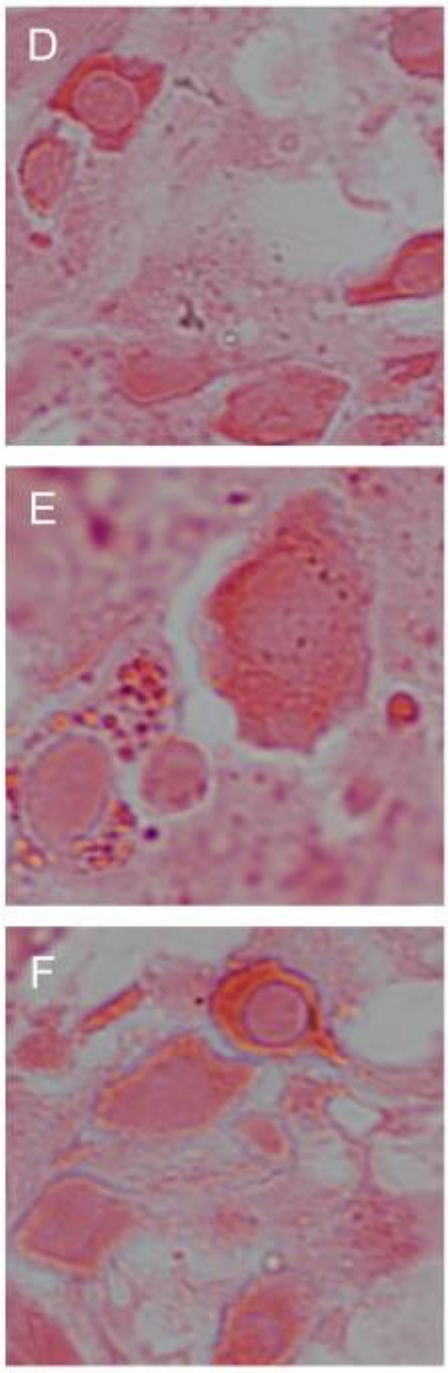
D
E
F

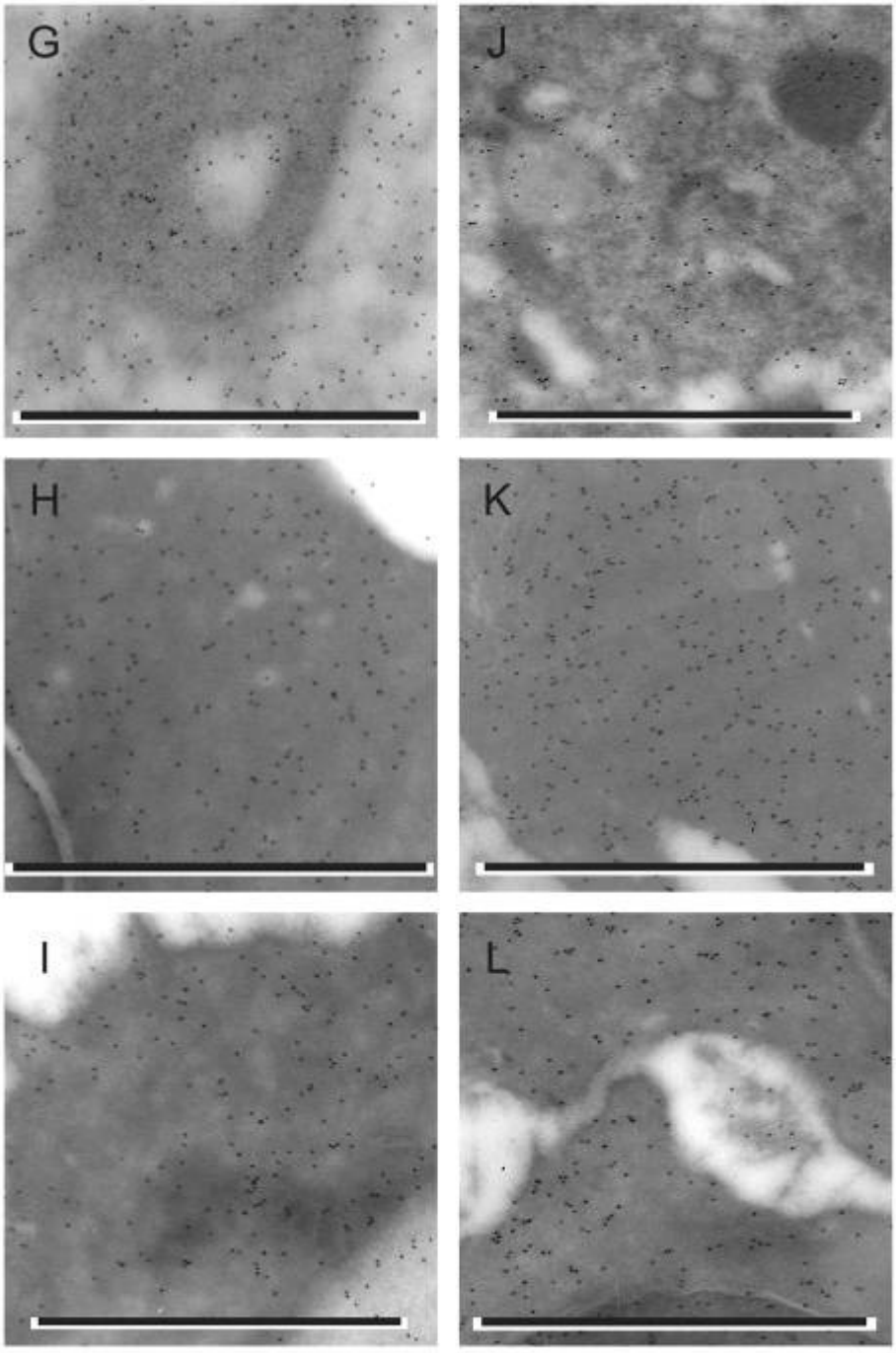

Figure 48

Kalafong patient 48

Figure 48a. A bone marrow fragment stained negative with the Prussian blue iron stain – absence of storage iron.

Figure 48b and c. Bone marrow aspirate smears stained with the Prussian blue iron stain with some sideroblasts.

Figure 48d. A bone marrow section stained negative with the Prussian blue iron stain – absence of storage iron.

Figure 48e and f. Bone marrow sections stained with the Prussian blue iron stain with no sideroblasts.

Figure 48g. An electron micrograph of a bone marrow macrophage immunolabelled with a monoclonal antibody to the H-subunit of ferritin, 10 nm gold particles and scale bar = 1 µm.

Figure 48h. An electron micrograph of a bone marrow red blood cell immunolabelled with a monoclonal antibody to the H-subunit of ferritin, 10 nm gold particles and scale bar = 1 µm.

Figure 48i. An electron micrograph of a bone marrow red blood cell precursor immunolabelled with a monoclonal antibody to the H-subunit of ferritin, 10 nm gold particles and scale bar = 1 µm.

Figure 48j. An electron micrograph of a bone marrow macrophage immunolabelled with a monoclonal antibody to the L-subunit of ferritin, 10 nm gold particles and scale bar = 1 µm.

Figure 48k. An electron micrograph of a bone marrow red blood cell precursor immunolabelled with a monoclonal antibody to the L-subunit of ferritin. Note the cluster of iron-loaded ferritin near the nucleus – haemosiderin, 10 nm gold particles and scale bar = 1 µm.

Figure 48l. An electron micrograph of a bone marrow red blood cell precursor immunolabelled with a monoclonal antibody to the L-subunit of ferritin, 10 nm gold particles and scale bar = 1 µm.

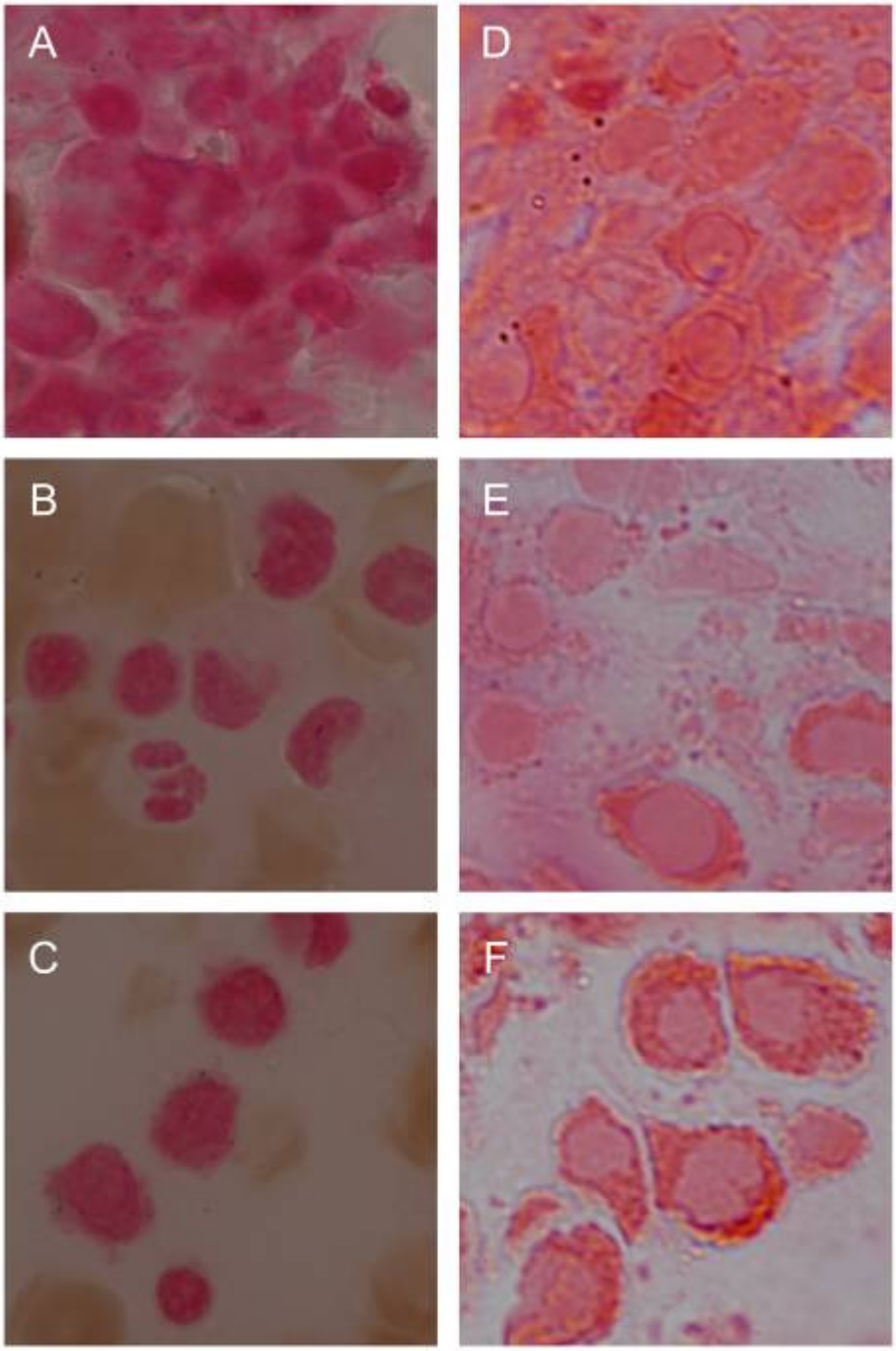
A
D
B
E
C
F

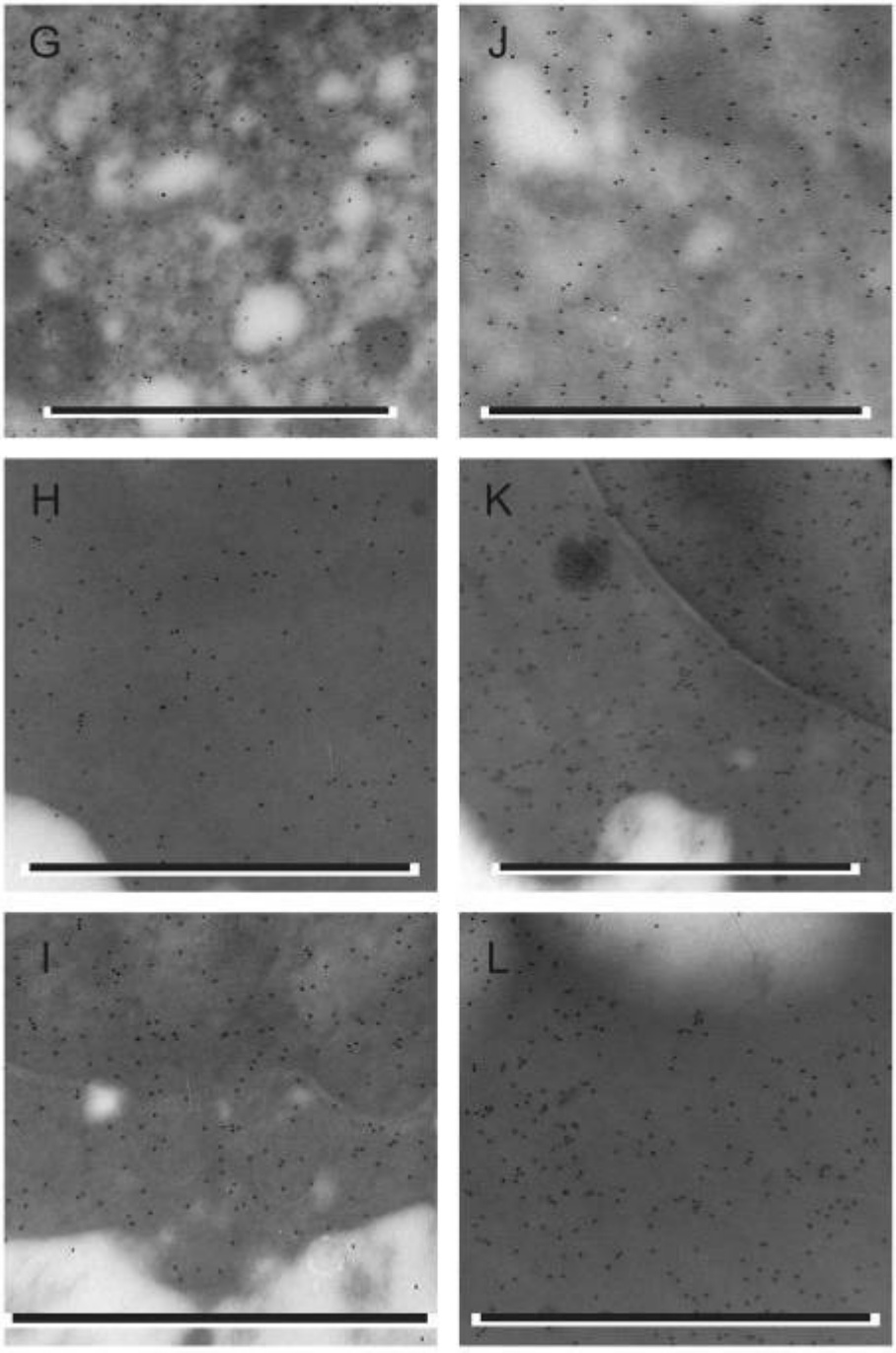
G
J
H
K
I
L

Figure 49

Osteoarthritis patient 1

Figure 49d. A bone marrow section stained negative with the Prussian blue iron stain – absence of storage iron.

Figure 49e and f. Bone marrow sections stained with the Prussian blue iron stain with no sideroblasts.

Figure 49g. An electron micrograph of a bone marrow macrophage immunolabelled with a monoclonal antibody to the H-subunit of ferritin. Note the cluster of iron-loaded ferritin, 10 nm gold particles and scale bar = 1 μm.

Figure 49h. An electron micrograph of a bone marrow red blood cell immunolabelled with a monoclonal antibody to the H-subunit of ferritin, 10 nm gold particles and scale bar = 1 μm.

Figure 49j. An electron micrograph of a bone marrow macrophage immunolabelled with a monoclonal antibody to the L-subunit of ferritin, 10 nm gold particles and scale bar = 1 μm.

Figure 49k. An electron micrograph of a bone marrow red blood cell precursor immunolabelled with a monoclonal antibody to the L-subunit of ferritin, 10 nm gold particles and scale bar = 1 μm.

Figure 49l. An electron micrograph of a bone marrow red blood cell precursor immunolabelled with a monoclonal antibody to the L-subunit of ferritin, 10 nm gold particles and scale bar = 1 μm.

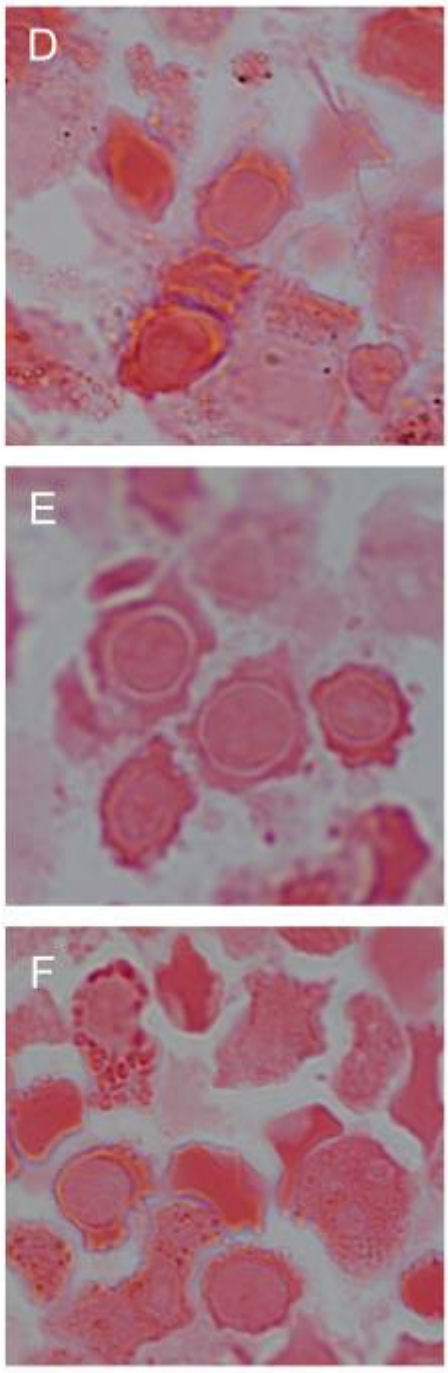
D
E
F

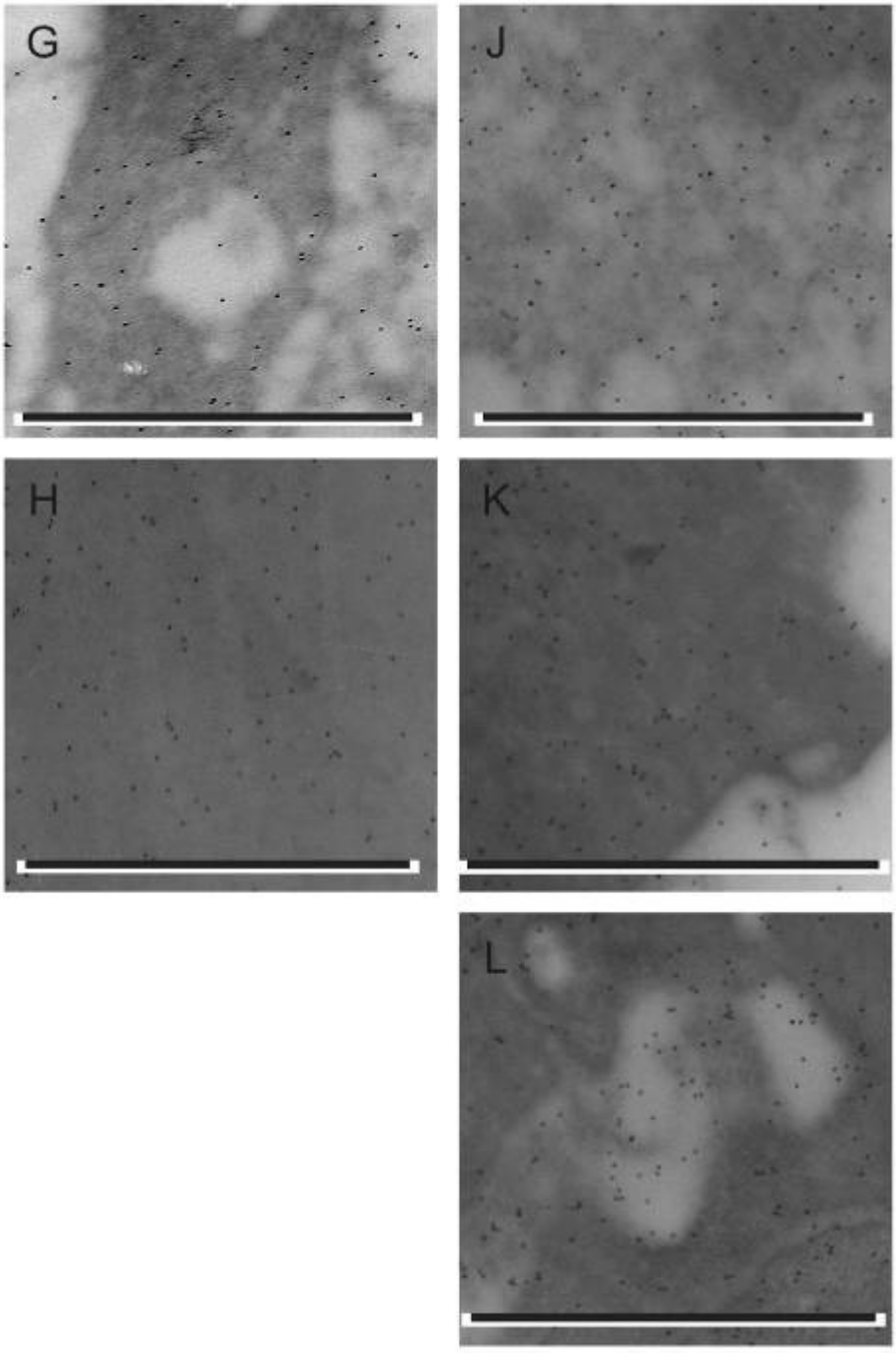
G
J
H
K
L

Figure 50

Osteoarthritis patient 3

Figure 50d. A bone marrow section stained positive with the Prussian blue iron stain – some storage iron.

Figure 50e and f. Bone marrow sections stained with the Prussian blue iron stain with some sideroblasts.

Figure 50g. An electron micrograph of a bone marrow macrophage immunolabelled with a monoclonal antibody to the H-subunit of ferritin. Note the iron-loaded ferritin, 10 nm gold particles and scale bar = 1 μm.

Figure 50h. An electron micrograph of a bone marrow red blood cell precursor immunolabelled with a monoclonal antibody to the H-subunit of ferritin, 10 nm gold particles and scale bar = 1 μm.

Figure 50i. An electron micrograph of a bone marrow red blood cell precursor immunolabelled with a monoclonal antibody to the H-subunit of ferritin, 10 nm gold particles and scale bar = 1 μm.

Figure 50j. An electron micrograph of a bone marrow macrophage immunolabelled with a monoclonal antibody to the L-subunit of ferritin, 10 nm gold particles and scale bar = 1 μm.

Figure 50k. An electron micrograph of a bone marrow red blood cell precursor immunolabelled with a monoclonal antibody to the L-subunit of ferritin, 10 nm gold particles and scale bar = 1 μm.

Figure 50l. An electron micrograph of a bone marrow red blood cell precursor immunolabelled with a monoclonal antibody to the L-subunit of ferritin, 10 nm gold particles and scale bar = 1 μm.

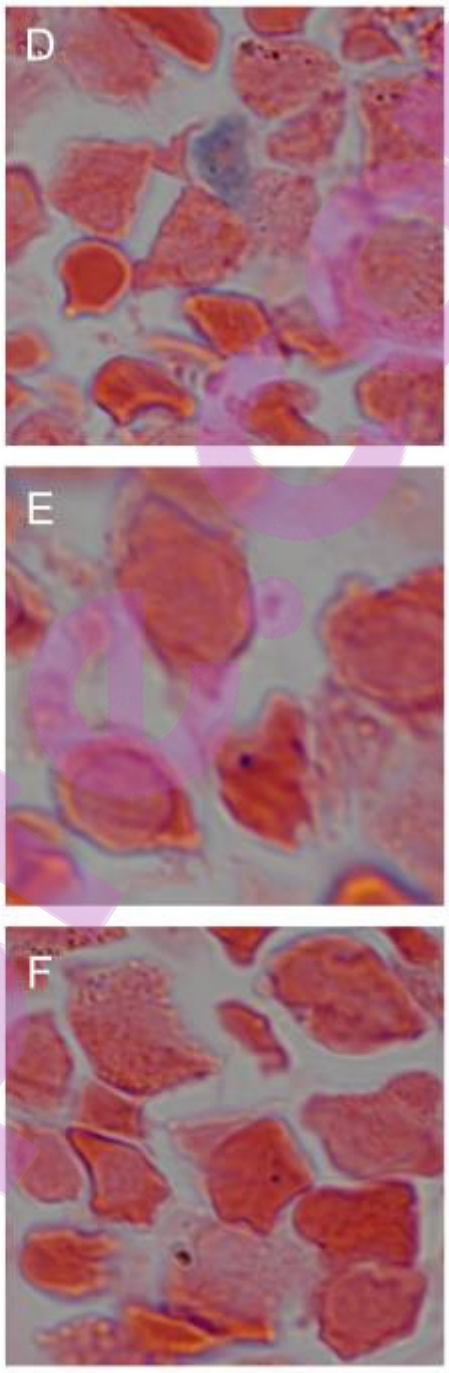

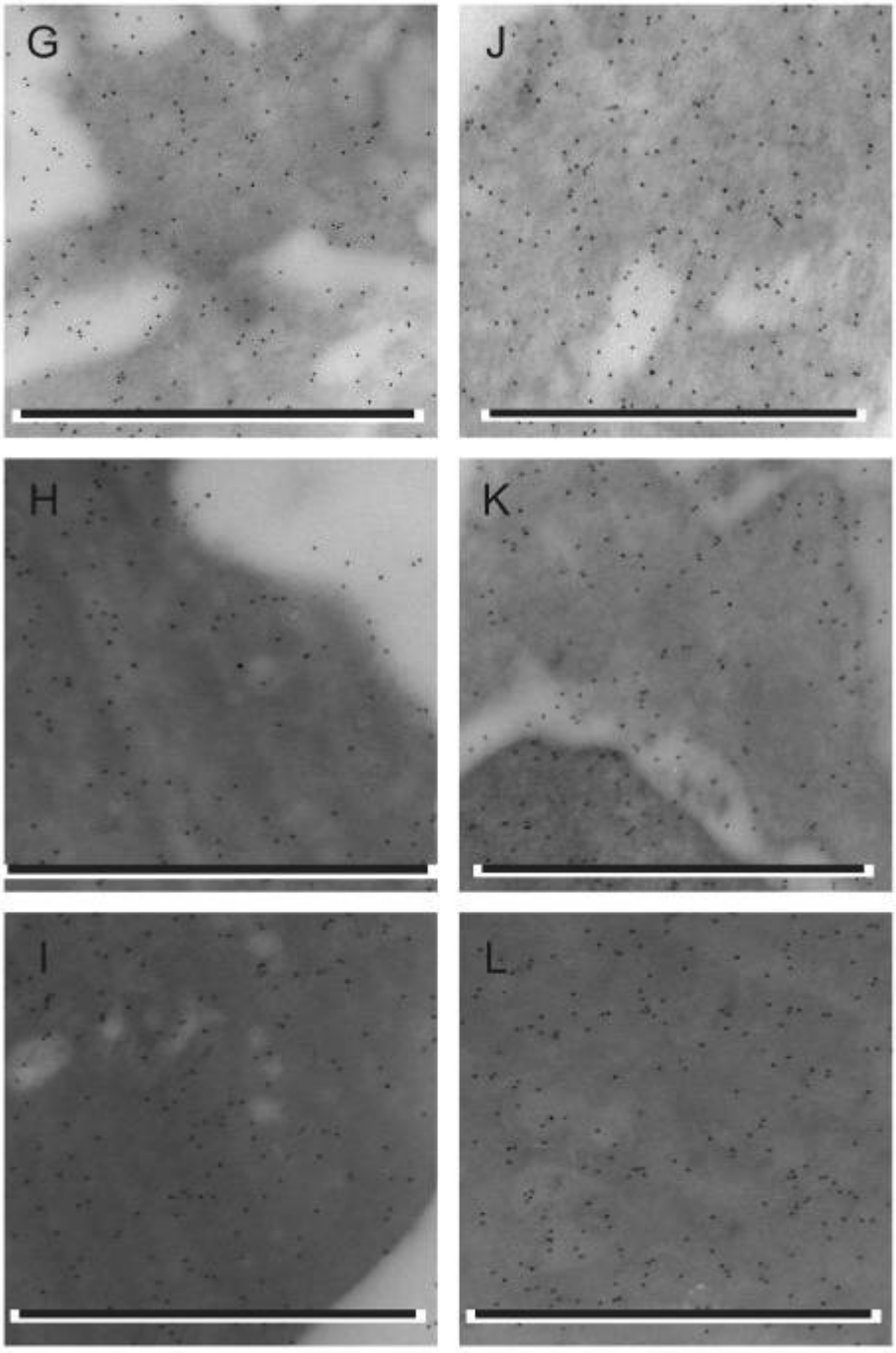
G
J
H
K
I
L

Figure 51

Osteoarthritis patient 5

Figure 51d. A bone marrow section stained negative with the Prussian blue iron stain – absence of storage iron.

Figure 51e and f. Bone marrow sections stained with the Prussian blue iron stain with no sideroblasts.

Figure 51g. An electron micrograph of a bone marrow macrophage immunolabelled with a monoclonal antibody to the H-subunit of ferritin, 10 nm gold particles and scale bar = 1 μm.

Figure 51h. An electron micrograph of a bone marrow red blood cell precursor immunolabelled with a monoclonal antibody to the H-subunit of ferritin. Note the iron-loaded ferritin on the cell membrane, 10 nm gold particles and scale bar = 1 μm.

Figure 51i. An electron micrograph of a bone marrow red blood cell precursor immunolabelled with a monoclonal antibody to the H-subunit of ferritin, 10 nm gold particles and scale bar = 1 μm.

Figure 51j. An electron micrograph of a bone marrow macrophage immunolabelled with a monoclonal antibody to the L-subunit of ferritin, 10 nm gold particles and scale bar = 1 μm.

Figure 51k. An electron micrograph of two bone marrow red blood cell precursors immunolabelled with a monoclonal antibody to the L-subunit of ferritin. Note the iron-loaded ferritin on the cell membranes, 10 nm gold particles and scale bar = 1 μm.

Figure 51l. An electron micrograph of a bone marrow red blood cell precursor immunolabelled with a monoclonal antibody to the L-subunit of ferritin, 10 nm gold particles and scale bar = 1 μm.

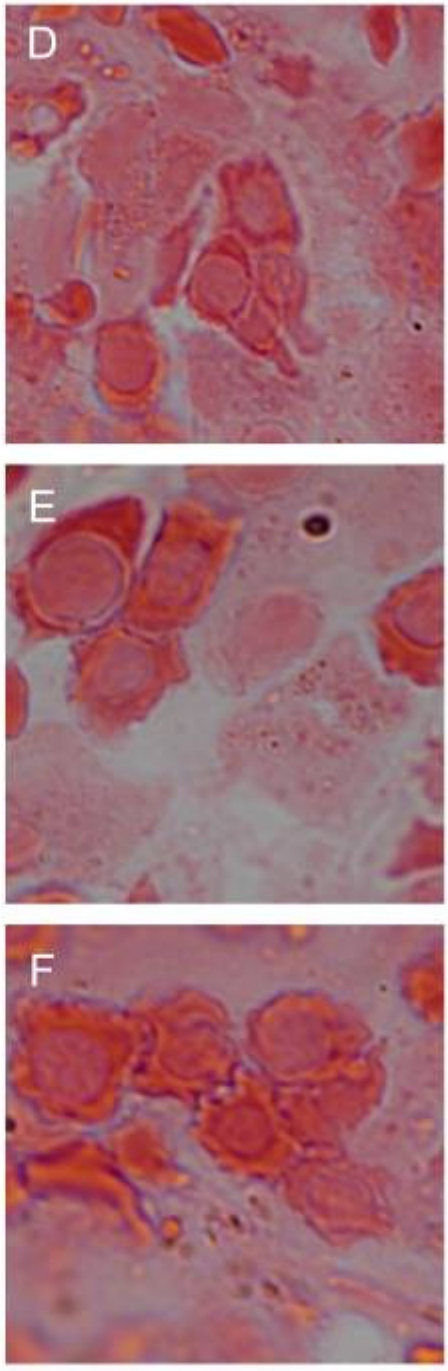
D
E
F

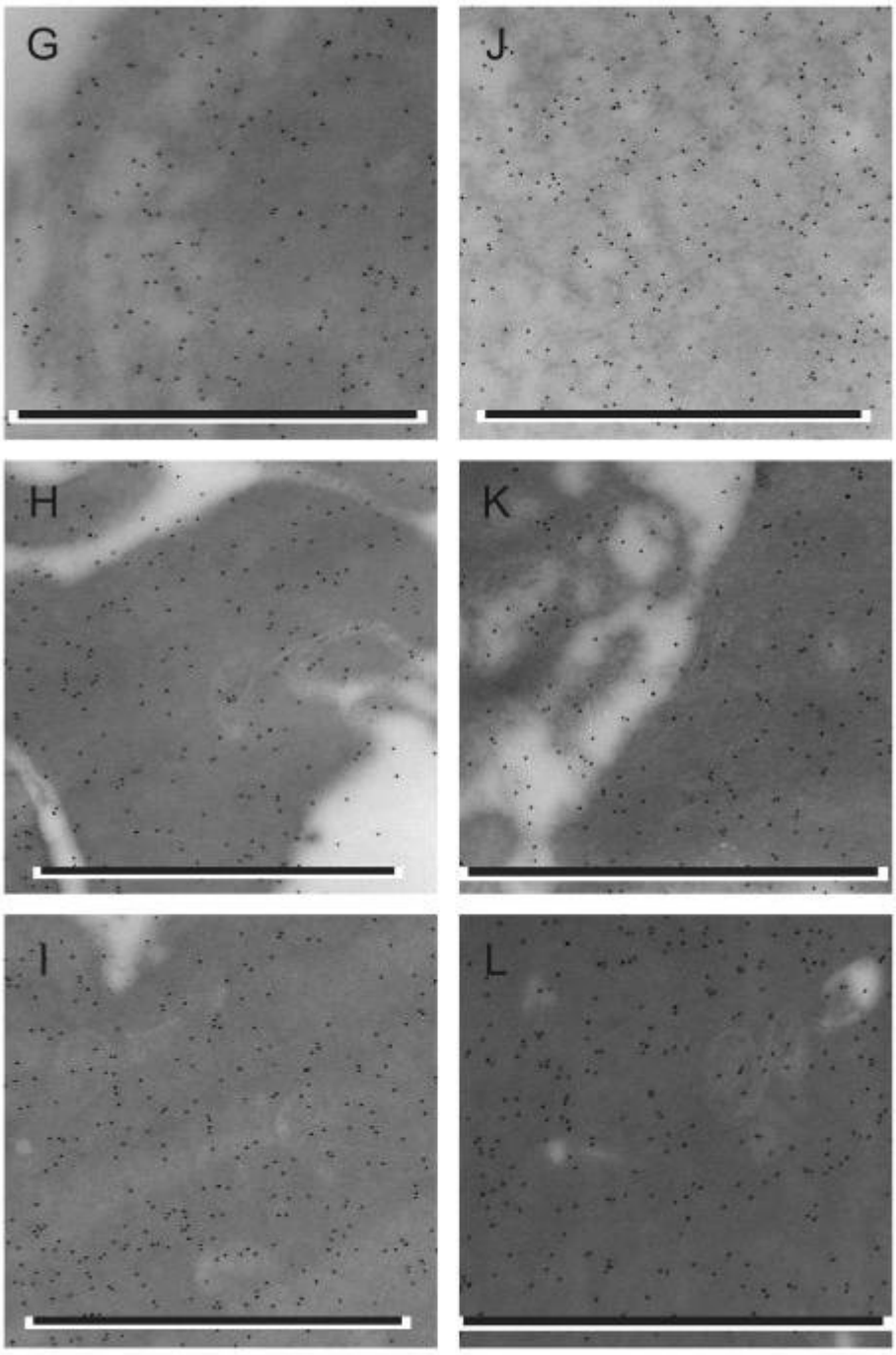
G
J
H
K
I
L

Figure 52

Osteoarthritis patient 6

Figure 52d. A bone marrow section stained negative with the Prussian blue iron stain – absence of storage iron.

Figure 52e and f. Bone marrow sections stained with the Prussian blue iron stain with no sideroblasts.

Figure 52g. An electron micrograph of a bone marrow macrophage immunolabelled with a monoclonal antibody to the H-subunit of ferritin. Note the iron-loaded ferritin, 10 nm gold particles and scale bar = 1 µm.

Figure 52h. An electron micrograph of a bone marrow red blood cell precursor immunolabelled with a monoclonal antibody to the H-subunit of ferritin, 10 nm gold particles and scale bar = 1 µm.

Figure 52i. An electron micrograph of a bone marrow red blood cell precursor immunolabelled with a monoclonal antibody to the H-subunit of ferritin, 10 nm gold particles and scale bar = 1 µm.

Figure 52j. An electron micrograph of a bone marrow macrophage immunolabelled with a monoclonal antibody to the L-subunit of ferritin, 10 nm gold particles and scale bar = 1 µm.

Figure 52k. An electron micrograph of a bone marrow reticulocyte immunolabelled with a monoclonal antibody to the L-subunit of ferritin, 10 nm gold particles and scale bar = 1 µm.

Figure 52l. An electron micrograph of a bone marrow red blood cell precursor immunolabelled with a monoclonal antibody to the L-subunit of ferritin, 10 nm gold particles and scale bar = 1 µm.

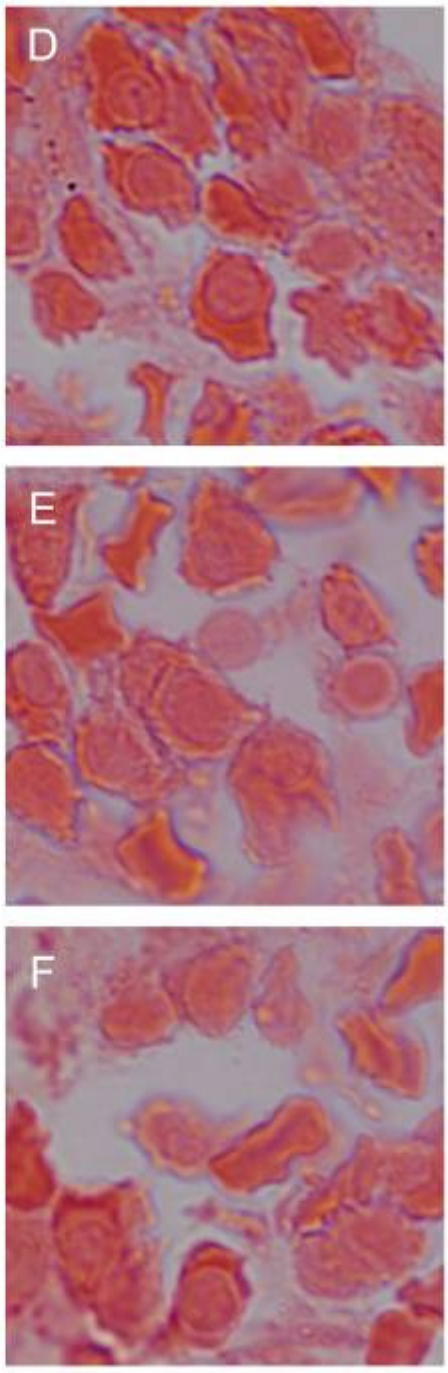
D
E
F

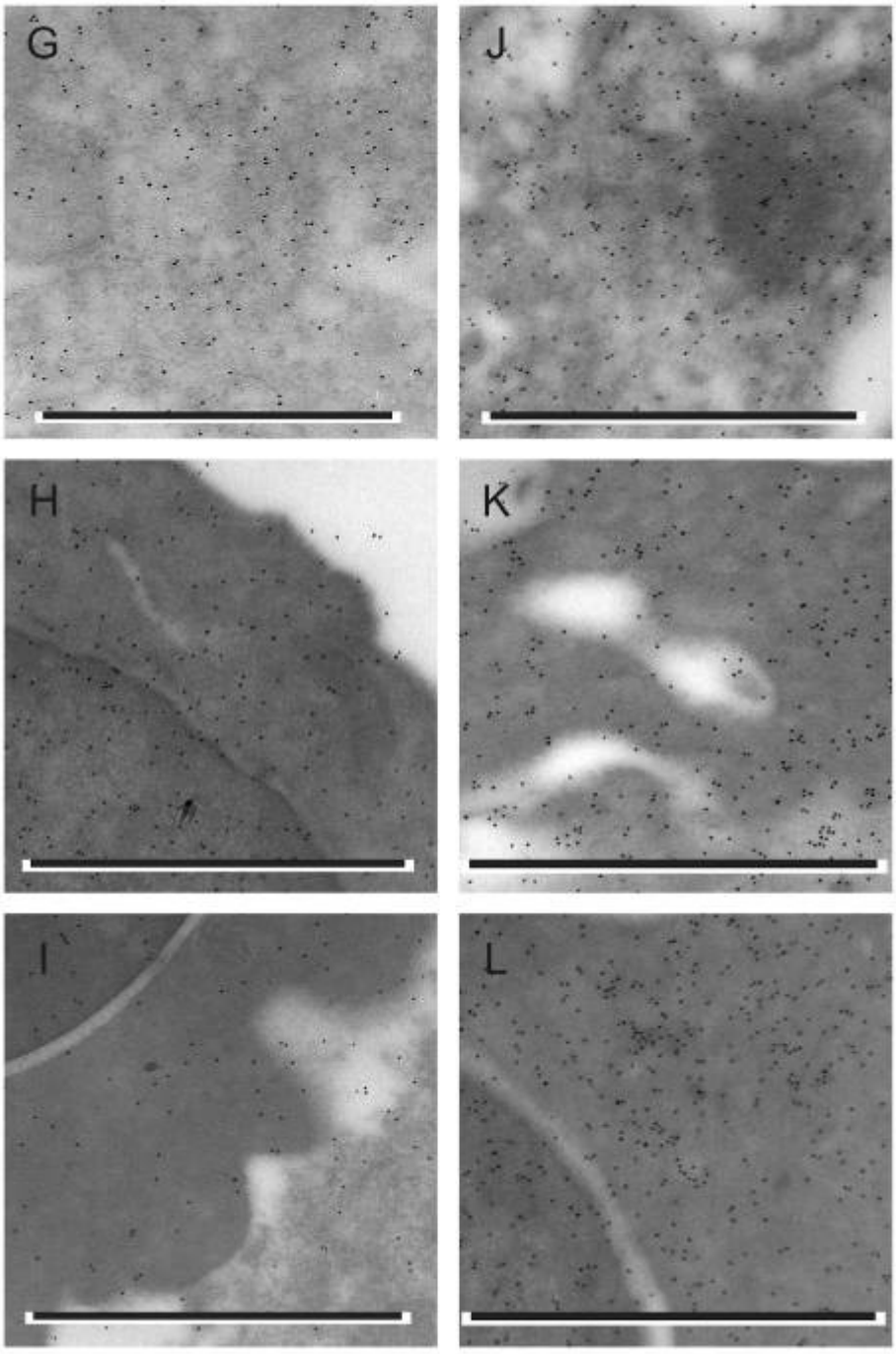
G
J
H
K
I
L

Figure 53

Osteoarthritis patient 7

Figure 53g. An electron micrograph of a bone marrow macrophage immunolabelled with a monoclonal antibody to the H-subunit of ferritin, 10 nm gold particles and scale bar = 1 µm.

Figure 53h. An electron micrograph of a bone marrow red blood cell immunolabelled with a monoclonal antibody to the H-subunit of ferritin, 10 nm gold particles and scale bar = 1 µm.

Figure 53i. An electron micrograph of a bone marrow red blood cell immunolabelled with a monoclonal antibody to the H-subunit of ferritin, 10 nm gold particles and scale bar = 1 µm.

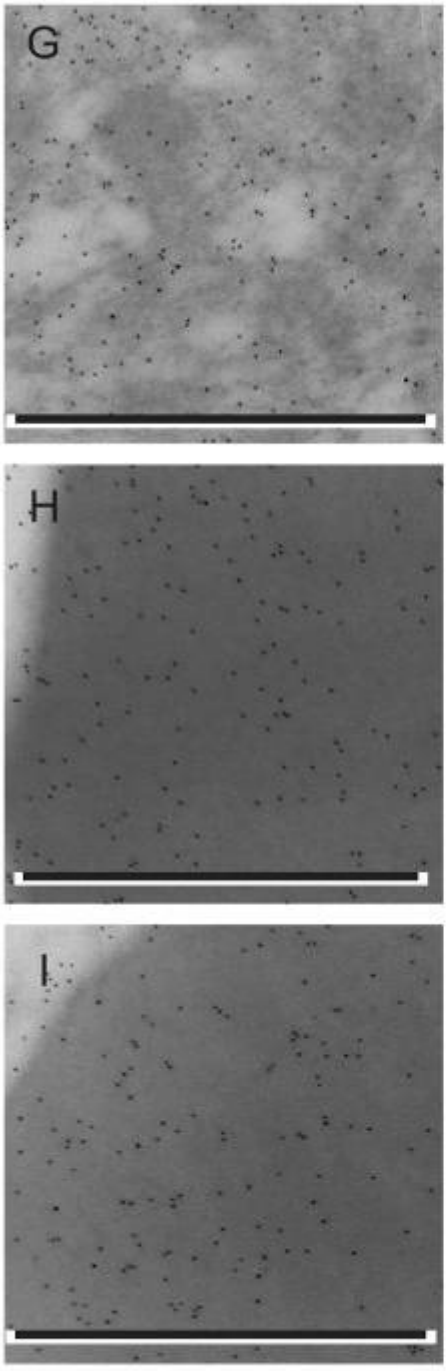
G
H
I

Figure 54

Osteoarthritis patient 8

Figure 54d. A bone marrow section stained positive with the Prussian blue iron stain – presence of storage iron.

Figure 54e and f. Bone marrow sections stained with the Prussian blue iron stain with no sideroblasts.

Figure 54g. An electron micrograph of a bone marrow macrophage immunolabelled with a monoclonal antibody to the H-subunit of ferritin. Note the iron-loaded ferritin, 10 nm gold particles and scale bar = 1 μm.

Figure 54h. An electron micrograph of a bone marrow reticulocyte immunolabelled with a monoclonal antibody to the H-subunit of ferritin. Note the cluster of iron-loaded ferritin, 10 nm gold particles and scale bar = 1 μm.

Figure 54i. An electron micrograph of two bone marrow red blood cell precursors immunolabelled with a monoclonal antibody to the H-subunit of ferritin. Note the contact between the two cell membranes and the iron-loaded ferritin in the space between the membranes, 10 nm gold particles and scale bar = 1 μm.

Figure 54j. An electron micrograph of a bone marrow macrophage immunolabelled with a monoclonal antibody to the L-subunit of ferritin, 10 nm gold particles and scale bar = 1 μm.

Figure 54k. An electron micrograph of a bone marrow reticulocyte immunolabelled with a monoclonal antibody to the L-subunit of ferritin, 10 nm gold particles and scale bar = 1 μm.

Figure 54l. An electron micrograph of a bone marrow red blood cell precursor immunolabelled with a monoclonal antibody to the L-subunit of ferritin, 10 nm gold particles and scale bar = 1 μm.

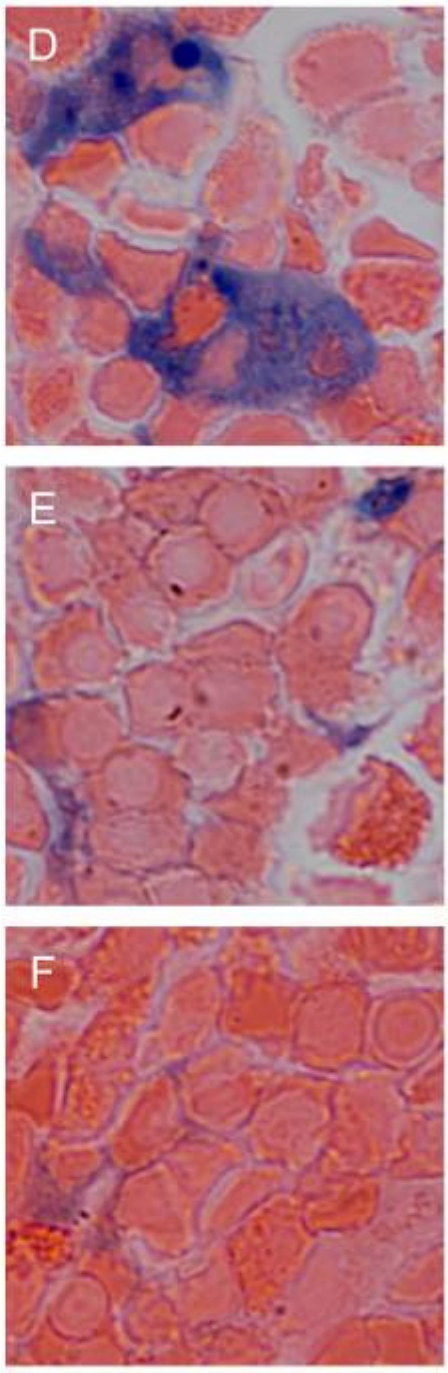
D
E
F

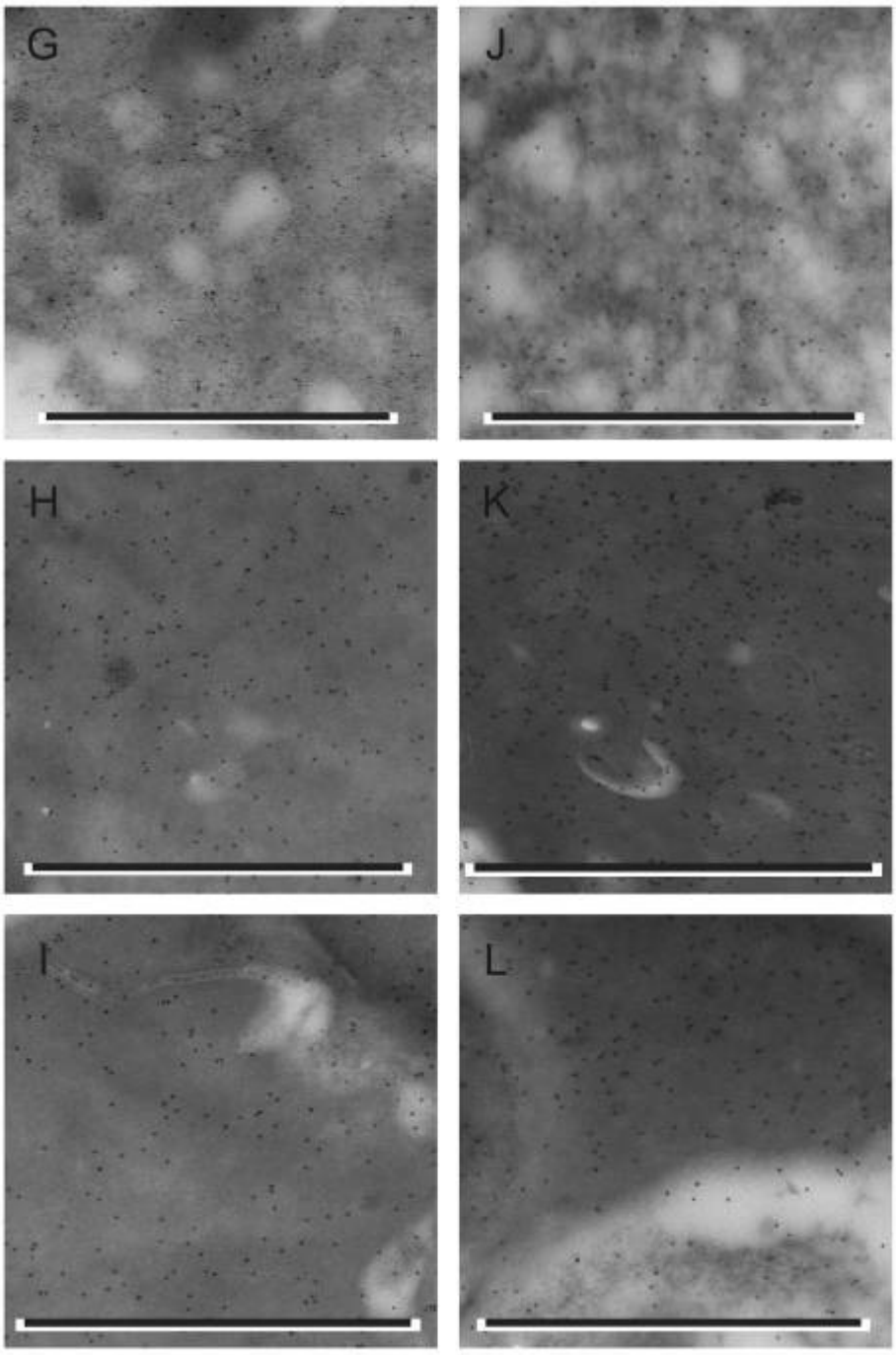

Figure 55

Osteoarthritis patient 10

Figure 55d. A bone marrow section stained negative with the Prussian blue iron stain – absence of storage iron.

Figure 55e and f. Bone marrow sections stained with the Prussian blue iron stain with no sideroblasts.

Figure 55g. An electron micrograph of a bone marrow macrophage immunolabelled with a monoclonal antibody to the H-subunit of ferritin, 10 nm gold particles and scale bar = 1 μm.

Figure 55h. An electron micrograph of a bone marrow red blood cell precursor immunolabelled with a monoclonal antibody to the H-subunit of ferritin, 10 nm gold particles and scale bar = 1 μm.

Figure 55i. An electron micrograph of two bone marrow red blood cell precursors immunolabelled with a monoclonal antibody to the H-subunit of ferritin. Note the contact between the two cell membranes and some iron-loaded ferritin in the space between the membranes, 10 nm gold particles and scale bar = 1 μm.

Figure 55j. An electron micrograph of a bone marrow macrophage immunolabelled with a monoclonal antibody to the L-subunit of ferritin. Note the iron-loaded ferritin, 10 nm gold particles and scale bar = 1 μm.

Figure 55k. An electron micrograph of a bone marrow reticulocyte immunolabelled with a monoclonal antibody to the L-subunit of ferritin, 10 nm gold particles and scale bar = 1 μm.

Figure 55l. An electron micrograph of a bone marrow red blood cell precursor immunolabelled with a monoclonal antibody to the L-subunit of ferritin. Note the endocytic vesicle containing some iron-loaded ferritin, 10 nm gold particles and scale bar = 1 μm.

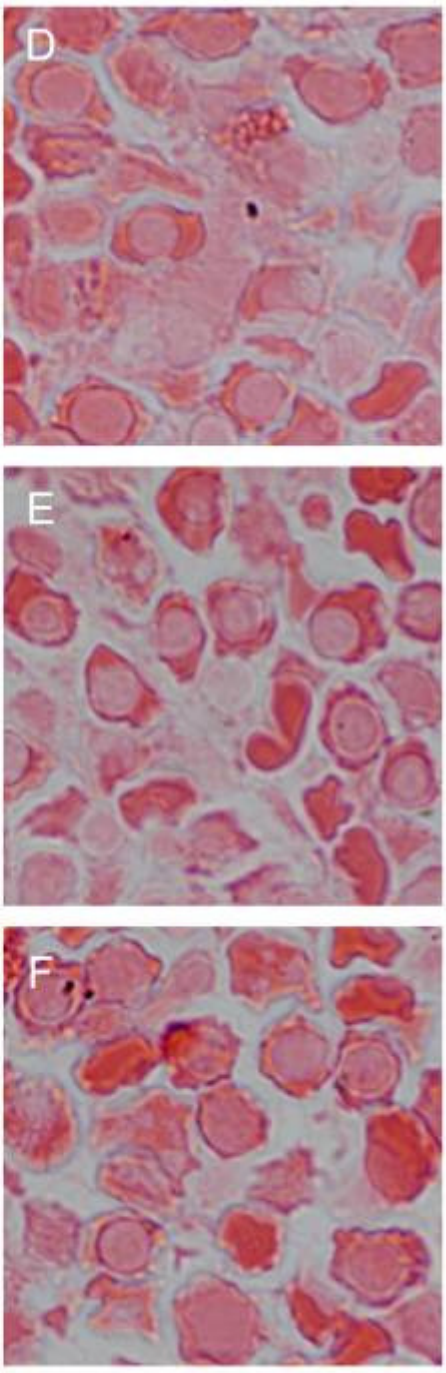
D
E
F

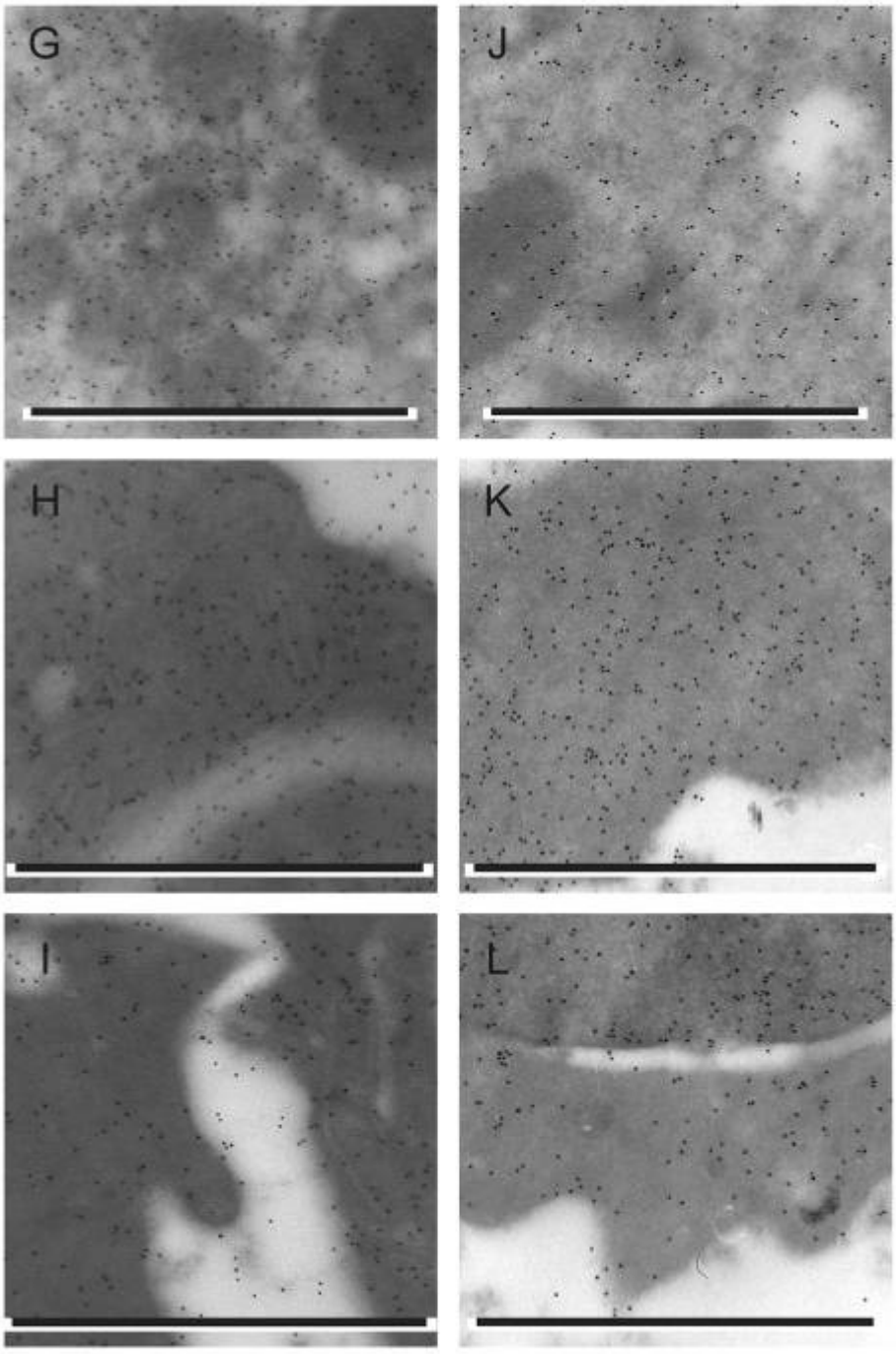
G
J
H
K
I
L

3) Evaluation of the presence or absence of an iron transfer block

3.1) Prussian blue iron stains of bone marrow aspirates and core bone marrow biopsies

A panel of serum iron markers can be employed to evaluate a patient's iron status, however these serum iron markers can be misleading with many chronic diseases since different cytokines can influence the levels of these iron markers. Therefore, when evaluating a patient's iron status a bone marrow aspirate followed by Prussian blue staining of haemosiderin iron is considered to be the gold standard for directly assessing body iron status (1). The haemosiderin iron content of a bone marrow aspirate or biopsy, graded histologically, serves as an index of the whole body storage iron level (1). However, histological techniques are semi-quantitative at best. Comparison of histologic techniques with chemical determination of iron in bone marrow shows a substantial amount of overlap in iron concentrations between the histological grades. Furthermore, individuals with no visible haemosiderin may have normal iron contents while the amount of iron in those assigned to the highest grade may vary by a factor of 10 or more (1).

A bone marrow Prussian blue iron stain was performed to evaluate the amount of storage iron and sideroblasts. For the Kalafong patient group a bone marrow aspirate was taken for a Prussian blue iron stain to be graded histologically by haematologists at the National Health Laboratory Services, Pretoria, South Africa. However, not all aspirates were suitable for this procedure. Therefore, in addition to the Prussian blue iron stain of the bone marrow aspirate a second Prussian blue iron stain was performed on LR White sections of the core bone marrow biopsy.

3.1.1) Comparison of stainable iron in a bone marrow aspirate smear and a bone marrow core section

Studies comparing the amount of stainable marrow iron between a bone marrow aspirate and a bone marrow core biopsy come to different conclusions as to the superiority of the aspirate iron stain to the bone marrow core iron stain. In a study conducted by Krause *et al.* it was shown that in general, iron tended to be less in the bone marrow aspirate compared to the bone marrow core biopsy (2). Furthermore, significant differences occurred when iron was assessed as absent in the aspirated smear with only 35% of the corresponding bone marrow core biopsies showing absent storage iron. However, correlations were better when iron stores were being assessed as present or increased in the aspirated smears, since stainable iron in the bone marrow core biopsy was always present in equal or greater amounts. A very good correlation was shown between haemosiderotic aspirate smears (increased stainable iron) and bone marrow core biopsies of a 3+ to a 4+ grading (2). In another study by Fong *et al.* the opposite was found when the amount of stainable iron was compared between a bone marrow aspirate and a bone marrow core biopsy (3). The usual difference consisted of significantly less stainable iron in the bone marrow core as compared to the aspirated smears. Of clinical importance was the finding of absent stainable iron in 8% of the bone marrow core sections in contrast to the definite deposits observed in the corresponding aspirated smear. Of similar interest was the observation that 6% of the bone marrow core sections had significantly less stainable iron than the corresponding haemosiderotic smears (3). One possible explanation for less iron in the bone marrow core section is the loss of iron during the decalcification step of the bone marrow core biopsy. Decalcification results in decreased recovery of stainable iron when aspirate histiocytic iron was minimal or moderate. There was no significant difference in recovery when large quantities of histiocytic iron were present prior to the decalcification step (4). In another study by

Stuart-Smith *et al.* iron was present in 44% of cases where iron was being assessed as absent from the bone marrow core biopsy (5). However, 61% of cases with unaccessible aspirate samples had a positive bone marrow core Prussian blue iron stain which could contribute to useful clinical information about iron status (5).

3.2) Presence or absence of an iron transfer block

The following procedure was used in order to determine the presence or absence of an iron transfer block. In the first place, the gold standard, a Prussian blue iron stain of the bone marrow aspirate, was used. With a Prussian blue iron stain of the bone marrow aspirate, both the storage iron in the macrophage and the amount of sideroblasts are noted. Normal and increased storage iron in the presence of a reduction in the amount of sideroblasts are indicative of the presence of an iron transfer block. However, with true iron deficiency with no stainable iron in the aspirate it is not possible to make use of the Prussian blue iron stain to indicate the presence or absence of an iron transfer block. In these situations it is impossible to discriminate between reduced supply of iron to the erythron as a result of true iron deficiency or of true iron deficiency and the existence of an iron transfer block. In these situations, soluble transferrin receptor determinations were used. A substantial increase in the soluble transferrin receptor value indicates the existence of true iron deficiency with normal to slightly increased soluble transferrin receptor of true iron deficiency and the existence of an iron transfer block. In this study the Prussian blue iron stain and haematologist's evaluation was used to determine the presence or absence of an iron transfer block. Where not available, the Prussian blue iron stain of the bone marrow core (no decalcification step) was used together with the available serum iron markers.

3.2.1) Reference ranges for the determination of the iron status of the Kalafong patient group and osteoarthritis patient group

3.2.1.1) Serum iron markers

Iron	10 – 30 µmol/l
Transferrin	2 – 3.6 g/l
Transferrin saturation	15 – 50 % for females and 20 – 50 % for males
Ferritin	11 – 306.8 µg/l for females and 23.9 – 336.2 µg/l for males
Soluble transferrin receptor	2.9 – 8.3 µg/ml
Transferrin:log ferritin	
Soluble transferrin receptor:log ferritin	

3.2.1.2) Red blood cell production

RCC	4.13 – 5.67 x 10^{12}/l for females and 4.89 – 6.11 x 10^{12}/l for males
HB	12.1 – 16.3 g/dl for females and 14.3 – 18.3 g/dl for males
HCT	0.370 – 0.490 l/l for females and 0.430 – 0.550 l/l for males
MCV	79.1 – 98.9 fl
MCH	27 – 32 pg
MCHC	32 – 36 g/dl
RDW	11.6 – 14 %
RPI	> 2.5 – normal bone marrow response and < 2.5 – suppressed bone marrow response

3.2.2) The haematology reports on the bone marrow aspirates, serum iron markers, red blood cell production and the presence or absence of an iron transfer block for the Kalafong patient group and osteoarthritis patient group

Kalafong patient 1

Bone marrow iron stain – haematology report

Normal amount of iron in bone marrow fragment (only one fragment on smear)

Reduced amount of sideroblasts

Reduced erythropoietic activity

Iron block

Anaemia could be multi-factorial

Serum iron markers

Iron	2.4 µmol/l	decreased
Transferrin	1.58 g/l	decreased
Transferrin saturation	6.8%	decreased
Ferritin	171.0 µg/l	normal
Soluble transferrin receptor	5.0 µg/ml	normal
Transferrin:log ferritin	0.71	
Soluble transferrin receptor:log ferritin	2.24	

Red blood cell production

RCC	2.62 x 10^{12}/l	anaemia
HB	5.6 g/dl	decreased
HCT	0.17 l/l	decreased
MCV	65.7 fl	microcytic

MCH	21.3 pg	hypochromic
MCHC	32.4 g/dl	normochromic
RDW	20.6 %	increased
RPI	0.15	suppressed bone marrow

- Normal amount of storage iron with reduced amount of sideroblasts according to bone marrow aspirate iron stain.
- Severely decreased serum iron.
- Normal serum ferritin.
- Reduced supply of iron to erythroblasts according to red blood cell production.
- Iron transfer block.

Kalafong patient 2

Bone marrow iron stain – haematology report

Increased amount of iron in bone marrow fragments

Pathologically overloaded sideroblasts

Hyperactive and megaloblastic erythropoiesis

Megaloblastic anaemia – suggests vitamin B_{12} and RBC folate evaluation

Serum iron markers

Iron	33.8 µmol/l	increased
Transferrin	0.60 g/l	decreased
Transferrin saturation	252.2 %	increased
Ferritin	1139.0 µg/l	increased
Soluble transferrin receptor	15.5 µg/ml	increased
Transferrin:log ferritin	0.20	
Soluble transferrin receptor:log ferritin	5.07	

Red blood cell production

RCC	1.55 x 10^{12}/l	anaemia
HB	6.3 g/dl	decreased
HCT	0.18 l/l	decreased
MCV	116.2 fl	macrocytic
MCH	40.9 pg	hyperchromic
MCHC	35.1 g/dl	normochromic
RDW	22.7 %	increased
RPI	0.19	suppressed bone marrow

- Increased amount of storage iron with pathologically overloaded sideroblasts according to bone marrow aspirate iron stain.
- Severely increased serum iron concentration.
- Severely increased ferritin.
- Normal supply of iron to erythroblasts according to red blood cell production with megaloblastic changes.
- No iron transfer block.

Kalafong patient 3

Bone marrow iron stain – haematology report

No bone marrow fragments – iron appears increased

Pathologically overloaded sideroblasts

Increased erythropoietic activity, normoblastic

Iron overload

Serum iron markers

Iron	19.8 µmol/l	normal
Transferrin	1.80 g/l	decreased

Transferrin saturation	45 %	normal
Ferritin	224.0 µg/l	normal
Soluble transferrin receptor	13.8 µg/ml	increased
Transferrin:log ferritin	0.77	
Soluble transferrin receptor:log ferritin	5.87	

Red blood cell production

RCC	1.17 x 10^{12}/l	anaemia
HB	3.5 g/dl	decreased
HCT	0.11 l/l	decreased
MCV	93.7 fl	normocytic
MCH	29.8 pg	normochromic
MCHC	31.8 g/dl	hypochromic
RDW	43.8 %	increased
RPI	1.72	suppressed bone marrow

- Pathologically overloaded sideroblasts according to the bone marrow aspirate iron stain.
- Normal serum iron concentration.
- Normal serum ferritin.
- Normal supply of iron to erythroblasts according to red blood cell production.
- No iron transfer block.

Kalafong patient 4

Haematology report

No iron stain

Depressed erythropoiesis, mildly megaloblastic

Serum iron markers

Iron	5.6 µmol/l	decreased
Transferrin	0.99 g/l	decreased
Transferrin saturation	25.2 %	normal
Ferritin	7756.0 µg/l	increased
Soluble transferrin receptor	3.8 µg/ml	normal
Transferrin:log ferritin	0.26	
Soluble transferrin receptor:log ferritin	0.98	

Red blood cell production

RCC	3.03 x 10^{12}/l	anaemia
HB	11.8 g/dl	decreased
HCT	0.35 l/l	decreased
MCV	114 fl	macrocytic
MCH	39.1 pg	hyperchromic
MCHC	34.3 g/dl	normochromic
RDW	14.2 %	slightly increased
RPI	1.72	suppressed bone marrow

- No bone marrow iron stains.
- Decreased serum iron concentration.
- Severely increased serum ferritin.
- Normal supply of iron to erythroblasts according to red blood cell production with megaloblastic changes.
- Decreased transferrin concentration.
- Normal soluble transferrin receptor concentration.
- Low soluble transferrin receptor/log ferritin ratio.

- Iron transfer block.

Kalafong patient 5

Unsuitable smear

Serum iron markers

Iron	3.3 µmol/l	decreased
Transferrin	1.41 g/l	decreased
Transferrin saturation	10.5 %	decreased
Ferritin	888.0 µg/l	increased
Soluble transferrin receptor	18.5 µg/ml	increased
Transferrin:log ferritin	0.48	
Soluble transferrin receptor:log ferritin	6.28	

Red blood cell production

RCC	3.33 x 10^{12}/l	anaemia
HB	7.9 g/dl	decreased
HCT	0.24 l/l	decreased
MCV	71.3 fl	microcytic
MCH	23.7 pg	hypochromic
MCHC	33.2 g/dl	normochromic
RDW	27.3 %	increased
RPI	0.24	suppressed bone marrow

- No bone marrow aspirate iron stain. Decreased amount of storage iron according to bone marrow core iron stain.
- Decreased serum iron concentration.
- Increased serum ferritin.

- Reduced supply of iron to erythroblasts according to red blood cell production.
- Decreased transferrin concentration.
- Increased soluble transferrin receptor.
- Iron transfer block.

Kalafong patient 6

Haematology report

No iron stain

Active erythropoiesis with decreased hemoglobinization – suggests iron deficiency

Serum iron markers

Iron	9.6 µmol/l	decreased
Transferrin	2.39 g/l	normal
Transferrin saturation	17.9 %	normal
Ferritin	262.0 µg/l	normal
Soluble transferrin receptor	23.0 µg/ml	increased
Transferrin:log ferritin	0.99	
Soluble transferrin receptor:log ferritin	9.51	

Red blood cell production

RCC	4.4 x 10^{12}/l	normal
HB	9.4 g/dl	decreased
HCT	0.29 l/l	decreased
MCV	66 fl	microcytic
MCH	21.4 pg	hypochromic
MCHC	32.4 g/dl	normochromic
RDW	20.6 %	increased
RPI	0.42	suppressed bone marrow

- No bone marrow aspirate iron stains, but suggests true iron deficiency. Slightly reduced storage iron with some erythroblasts according to iron stain of bone marrow core.
- Slightly reduced serum iron concentration.
- Normal serum ferritin.
- Reduced supply of iron to erythroblasts according to red blood cell production.
- Severely increased soluble transferrin receptor concentration.
- No iron transfer block.

Kalafong patient 7

Bone marrow iron stain – haematology report

Normal amount of iron in bone marrow fragments

Occasional pathologically overloaded sideroblasts

Very active erythropoiesis, normoblastic

Anaemia may be due to haemolysis or hypersplenism

Serum iron markers

Iron	10.0 µmol/l	normal
Transferrin	0.98 g/l	decreased
Transferrin saturation	45.7 %	normal
Ferritin	234.0 µg/l	normal
Soluble transferrin receptor	10.0 µg/ml	increased
Transferrin:log ferritin	0.41	
Soluble transferrin receptor:log ferritin	4.22	

Red blood cell production

RCC	2.85 x 10^{12}/l	anaemia
HB	8.5 g/dl	decreased

HCT	0.24 l/l	decreased
MCV	84.7 fl	normocytic
MCH	29.8 pg	normochromic
MCHC	35.1 g/dl	normochromic
RDW	18.2 %	increased
RPI	1.08	suppressed bone marrow

- Normal amount of storage iron with occasional pathologically overloaded sideroblasts according to bone marrow aspirate iron stain.
- Normal serum iron concentration.
- Normal serum ferritin.
- Normal supply of iron to erythroblasts according to red blood cell production.
- No iron transfer block.

Kalafong patient 8

Bone marrow iron stain – haematology report

Severely increased amount of iron in bone marrow fragments

Normal amount of sideroblasts

Active erythropoiesis, normoblastic

Iron overload

Serum iron markers

Iron	6.0 µmol/l	decreased
Transferrin	1.42 g/l	decreased
Transferrin saturation	18.9 %	decreased
Ferritin	780.0 µg/l	increased
Soluble transferrin receptor	2.4 µg/ml	decreased
Transferrin:log ferritin	0.49	

Soluble transferrin receptor:log ferritin 0.83

Red blood cell production

RCC	3.33 x 10^{12}/l	anaemia
HB	10.3 g/dl	decreased
HCT	0.30 l/l	decreased
MCV	89.4 fl	normocytic
MCH	31.0 pg	normochromic
MCHC	34.7 g/dl	normochromic
RDW	15.9 %	increased
RPI	0.36	suppressed bone marrow

- Severely increased amount of storage iron with normal amount of sideroblasts according to bone marrow aspirate iron stain.
- Reduced serum iron concentration.
- Increased serum ferritin.
- Normal supply of iron to erythroblasts according to red blood cell production.
- Reduced soluble transferrin receptor/log ferritin ratio.
- Iron transfer block.

Kalafong patient 9

Bone marrow iron stain – haematology report

Increased amount of iron in bone marrow fragments

Reduced amount of sideroblasts

Active erythropoiesis, normoblastic

Iron block (chronic disease)

Suggests vitamin B_{12} and RBC folate investigations

Serum iron markers

Iron	5.4 µmol/l	decreased
Transferrin	1.10 g/l	decreased
Transferrin saturation	20.0 %	normal
Ferritin	1657.0 µg/l	increased
Soluble transferrin receptor	6.5 µg/ml	normal
Transferrin:log ferritin	0.34	
Soluble transferrin receptor:log ferritin	2.02	

Red blood cell production

RCC	3.14 x 10^{12}/l	anaemia
HB	9.4 g/dl	decreased
HCT	0.27 l/l	decreased
MCV	86.2 fl	normocytic
MCH	29.8 pg	normochromic
MCHC	34.6 g/dl	normochromic
RDW	16.5 %	increased

- Increased amount of storage iron with reduced amount of sideroblasts according to bone marrow aspirate iron stain.
- Decreased serum iron concentration.
- Severely increased ferritin.
- Normal supply of iron to erythroblasts according to red blood cell production.
- Iron transfer block.

Kalafong patient 10

Bone marrow iron stain – haematology report

Absent iron in bone marrow fragments

Reduced amount of sideroblasts

Active erythropoiesis, normoblastic

Iron deficiency

Serum iron markers

Iron	1.3 µmol/l	decreased
Transferrin	3.06 g/l	normal
Transferrin saturation	1.9 %	decreased
Ferritin	3.0 µg/l	decreased
Soluble transferrin receptor	52.0 µg/ml	increased
Transferrin:log ferritin	6.41	
Soluble transferrin receptor:log ferritin	108.99	

Red blood cell production

RCC	1.54 x 10^{12}/l	anaemia
HB	2.6 g/dl	decreased
HCT	0.09 l/l	decreased
MCV	60.8 fl	microcytic
MCH	16.8 pg	hypochromic
MCHC	27.7 g/dl	hypochromic
RDW	23.0 %	increased

- Absent storage iron with reduced amount of sideroblasts in bone marrow aspirate iron stain.
- Severely decreased serum iron concentration.
- Decreased serum ferritin.
- Reduced supply of iron to erythroblasts according to red blood cell production.
- Severely increased soluble transferrin receptor.

- No iron transfer block.

Kalafong patient 11

Bone marrow iron stain – haematology report

Severely increased amount of iron in bone marrow fragments

Few pathologically overloaded sideroblasts

Active erythropoiesis, normoblastic, irregular hemoglobinization

Serum iron markers

Iron	5.4 µmol/l	decreased
Transferrin	1.53 g/l	decreased
Transferrin saturation	15.8 %	decreased
Ferritin	334.0 µg/l	normal
Soluble transferrin receptor	2.4 µg/ml	decreased
Transferrin:log ferritin	0.61	
Soluble transferrin receptor:log ferritin	0.95	

Red blood cell production

RCC	1.23 x 10^{12}/l	anaemia
HB	4.2 g/dl	decreased
HCT	0.12 l/l	decreased
MCV	99.1 fl	macrocytic
MCH	34.1 pg	hyperchromic
MCHC	34.4 g/dl	normohromic
RDW	21.8 %	increased
RPI	0.8	suppressed bone marrow

- Severely increased amount of storage iron with few pathologically overloaded sideroblasts according to bone marrow aspirate iron stain.
- Decreased serum iron concentration.
- Normal serum ferritin.
- Normal supply of iron to erythroblasts according to red blood cell production with megaloblastic changes.
- Iron transfer block.

Kalafong patient 12

Bone marrow iron stain – haematology report

No bone marrow fragments

Normal amount of sideroblasts

Active erythropoiesis, normoblastic

Serum iron markers

Iron	13.2 µmol/l	normal
Transferrin	2.77 g/l	normal
Transferrin saturation	21.3 %	normal
Ferritin	58.6 µg/l	normal
Soluble transferrin receptor	6.5 µg/ml	normal
Transferrin:log ferritin	1.57	
Soluble transferrin receptor:log ferritin	3.68	

Red blood cell production

RCC	5.77 x 10^{12}/l	normal
HB	14.9 g/dl	normal
HCT	0.48 l/l	normal
MCV	82.4 fl	normocytic

MCH	25.9 pg	hypochromic
MCHC	31.3 g/dl	hypohromic
RDW	15.7 %	increased

- Normal amount of sideroblasts according to bone marrow aspirate iron stain. Normal to slightly reduced amount of storage iron according to bone marrow core iron stain.
- Normal serum iron concentration.
- Normal serum ferritin.
- Reduced supply of iron to erythroblasts according to red blood cell production.
- No iron transfer block.

Kalafong patient 13

Haematology report

Smear unsuitable for iron stain, no bone marrow fragments

Active erythropoiesis

Serum iron markers

Iron	1.8 µmol/l	decreased
Transferrin	0.80 g/l	decreased
Transferrin saturation	9.0 %	decreased
Ferritin	3975.0 µg/l	increased
Soluble transferrin receptor	4.0 µg/ml	normal
Transferrin:log ferritin	0.22	
Soluble transferrin receptor:log ferritin	1.11	

Red blood cell production

RCC	1.91 x 10^{12}/l	anaemia
HB	4.7 g/dl	decreased

HCT	0.15 l/l	decreased
MCV	76.8 fl	microcytic
MCH	24.6 pg	hypochromic
MCHC	32.0 g/dl	normohromic
RDW	15.8 %	increased

- Severely increased amount of storage iron with no sideroblasts according to the bone marrow core iron stain.
- Severely decreased serum iron concentration.
- Severely increased seum ferritin.
- Reduced supply of iron to erythroblasts according to red blood cell production.
- Iron transfer block.

Kalafong patient 14

Haematology report

No iron stain

Active erythropoiesis, normoblastic

Serum iron markers

Iron	7.1 µmol/l	decreased
Transferrin	0.94 g/l	decreased
Transferrin saturation	33.8 %	normal
Ferritin	2096.0 µg/l	increased
Soluble transferrin receptor	5.8 µg/ml	normal
Transferrin:log ferritin	0.28	
Soluble transferrin receptor:log ferritin	1.75	

Red blood cell production

RCC	3.38 x 10^{12}/l	anaemia
HB	9.5 g/dl	decreased
HCT	0.29 l/l	decreased
MCV	85.8 fl	normocytic
MCH	28.2 pg	normochromic
MCHC	32.9 g/dl	normohromic
RDW	15.8 %	increased

- Increased amount of storage iron with no sideroblasts according to the bone marrow core iron stain.
- Decreased serum iron concentration.
- Severely increased serum ferritin.
- Normal supply of iron to erythroblasts according to red blood cell production.
- Decreased transferrin concentration.
- Normal soluble transferrin receptor concentration.
- Iron transfer block.

Kalafong patient 15

Bone marrow iron stain – haematology report

Abundant iron in bone marrow fragments (4/6)

Few pathologically overloaded sideroblasts

Active erythropoiesis, megaloblastic

Mild iron overload

Serum iron markers

Iron	4.9 µmol/l	decreased
Transferrin	1.53 g/l	decreased

Transferrin saturation	14.3 %	decreased
Ferritin	581.0 µg/l	increased
Soluble transferrin receptor	13.8 µg/ml	increased
Transferrin:log ferritin	0.55	
Soluble transferrin receptor:log ferritin	4.99	

Red blood cell production

RCC	2.79 x 10^{12}/l	anaemia
HB	9.0 g/dl	decreased
HCT	0.26 l/l	decreased
MCV	94.3 fl	normocytic
MCH	32.2 pg	hyperchromic
MCHC	34.1 g/dl	normochromic
RDW	30.1 %	increased
RPI	0.10	suppressed bone marrow

- Increased amount of storage iron with few pathologically overloaded sideroblasts according to bone marrow aspirate iron stain.
- Decreased serum iron concentration.
- Increased serum ferritin.
- Normal supply of iron to erythroblasts according to red blood cell production.
- Iron transfer block.

Kalafong patient 16

Bone marrow iron stain – haematology report

No iron in bone marrow fragment

Reduced amount of sideroblasts

Active erythropoiesis

Iron deficiency

Suggests vitamin B_{12} and folate supplementation

Serum iron markers

Iron	8.9 µmol/l	decreased
Transferrin	1.49 g/l	decreased
Transferrin saturation	26.7 %	normal
Ferritin	124.0 µg/l	normal
Soluble transferrin receptor	10.5 µg/ml	increased
Transferrin:log ferritin	0.71	
Soluble transferrin receptor:log ferritin	5.02	

Red blood cell production

RCC	2.12 x 10^{12}/l	anaemia
HB	6.6 g/dl	decreased
HCT	0.21 l/l	decreased
MCV	97.4 fl	normocytic
MCH	31.4 pg	normochromic
MCHC	32.3 g/dl	normochromic
RDW	25.0 %	increased
RPI	2.80	normal bone marrow response

- Absent storage iron with reduced amount of sideroblasts according to the bone marrow aspirate iron stain.
- Decreased serum iron concentration.
- Normal serum ferritin.
- Decreased transferrin concentration.
- Slightly increased soluble transferrin receptor concentration.

- Normal supply of iron to erythroblasts according to red blood cell production.
- No iron transfer block.

Kalafong patient 17

Haematology report

No iron stain

Active erythropoiesis, slight megaloblastc changes

Serum iron markers

Iron	16.6 µmol/l	normal
Transferrin	1.40 g/l	decreased
Transferrin saturation	53.0 %	increased
Ferritin	241.0 µg/l	normal
Soluble transferrin receptor	4.3 µg/ml	normal
Transferrin:log ferritin	0.59	
Soluble transferrin receptor:log ferritin	1.81	

Red blood cell production

RCC	3.63 x 10^{12}/l	anaemia
HB	10.2 g/dl	decreased
HCT	0.32 l/l	decreased
MCV	86.6 fl	normocytic
MCH	28.1 pg	normochromic
MCHC	32.4 g/dl	normochromic
RDW	14.2 %	increased

- Normal to slightly decreased amount of storage iron with few sideroblasts according to bone marrow core iron stain.

- Normal serum iron concentration.
- Normal serum ferritin.
- Normal supply of iron to erythroblasts according to red blood cell production.
- Normal soluble transferrin receptor.
- Iron transfer block.

Kalafong patient 18

Unsuitable smears

Serum iron markers

Iron	13.4 µmol/l	normal
Transferrin	1.64 g/l	decreased
Transferrin saturation	36.5 %	normal
Ferritin	304.0 µg/l	normal
Soluble transferrin receptor	32.5 µg/ml	increased
Transferrin:log ferritin	0.66	
Soluble transferrin receptor:log ferritin	13.09	

Red blood cell production

RCC	0.87 x 10^{12}/l	anaemia
HB	3.2 g/dl	decreased
HCT	0.1 l/l	decreased
MCV	113.1 fl	macrocytic
MCH	37.1 pg	hyperchromic
MCHC	32.8 g/dl	normochromic
RDW	20.1 %	increased
RPI	2.04	suppressed bone marrow response

- Decreased amount of storage iron with present sideroblasts according to the bone marrow core iron stain.
- Normal serum iron concentration.
- Normal serum ferritin.
- Normal supply of iron to erythroblasts according to red blood cell production.
- Severely increased soluble transferrin receptor.
- No iron transfer block.

Kalafong patient 19

Bone marrow iron stain – haematology report

Increased amount of iron in bone marrow fragments

Reduced amount of sideroblasts

Active erythropoiesis with poor hemoglobinization of precursors

Iron block

Serum iron markers

Iron	1.7 µmol/l	decreased
Transferrin	1.17 g/l	decreased
Transferrin saturation	6.5 %	decreased
Ferritin	669.0 µg/l	increased
Soluble transferrin receptor	9.0 µg/ml	increased
Transferrin:log ferritin	0.41	
Soluble transferrin receptor:log ferritin	3.19	

Red blood cell production

RCC	1.96 x 10^{12}/l	anaemia
HB	4.9 g/dl	decreased

HCT	0.16 l/l	decreased
MCV	83.0 fl	normocytic
MCH	25.2 pg	hypochromic
MCHC	30.4 g/dl	hypochromic
RDW	20.3 %	increased
RPI	0.26	suppressed bone marrow response

- Severely increased amount of storage iron with reduced amount of sideroblasts according to the bone marrow aspirate iron stain.
- Severely reduced serum iron concentration.
- Increased serum ferritin.
- Reduced supply of iron to erythroblasts according to red blood cell production.
- Iron transfer block.

Kalafong patient 20

Bone marrow iron stain – haematology report

Slight amount of iron in bone marrow fragments

No sideroblasts

Active erythropoiesis, poor hemoglobinization of precursors

Iron deficiency

Serum iron markers

Iron	2.3 µmol/l	decreased
Transferrin	2.15 g/l	normal
Transferrin saturation	4.8 %	decreased
Ferritin	83.1 µg/l	normal
Soluble transferrin receptor	20.0 µg/ml	increased
Transferrin:log ferritin	1.12	

Soluble transferrin receptor:log ferritin 10.42

Red blood cell production

RCC	3.84 x 10^{12}/l	anaemia
HB	9.0 g/dl	decreased
HCT	0.31 l/l	decreased
MCV	79.8 fl	normocytic
MCH	23.5 pg	hypochromic
MCHC	29.5 g/dl	hypochromic
RDW	18.4 %	increased

- Reduced amount of storage iron with reduced amount of sideroblasts according to bone marrow aspirate iron stain.
- Severely reduced serum iron concentration.
- Normal serum ferritin.
- Severely increased soluble transferrin receptor.
- Reduced supply of iron to erythroblasts according to red blood cell production.
- No iron transfer block.

Kalafong patient 21

Bone marrow iron stain – haematology report

Increased amount of iron in bone marrow fragments (4/6)

Normal amount of sideroblasts

Active erythropoiesis with dysplastic forms and signs of poor hemoglobinization

Serum iron markers

Iron	16.4 µmol/l	normal
Transferrin	0.70 g/l	decreased

Transferrin saturation		
Ferritin	7316.0 µg/l	increased
Soluble transferrin receptor	8.0 µg/ml	normal
Transferrin:log ferritin	0.18	
Soluble transferrin receptor:log ferritin	2.07	

Red blood cell production

RCC	2.7 x 10^{12}/l	anaemia
HB	6.9 g/dl	decreased
HCT	0.22 l/l	decreased
MCV	82.3 fl	normocytic
MCH	25.7 pg	hypochromic
MCHC	31.3 g/dl	hypochromic
RDW	19.8 %	increased

- Increased amount of storage iron with normal amount of sideroblasts according to bone marrow aspirate iron stain.
- Normal serum iron concentration.
- Severely increased serum ferritin.
- Normal soluble transferrin receptor.
- Reduced supply of iron to erythroblasts according to red blood cell production.
- Iron transfer block.

Kalafong patient 22

Bone marrow iron stain – haematology report

Increased amount of iron in bone marrow fragments (4/6)

Normal amount of sideroblasts

Active erythropoiesis, normoblastic

Mild iron overload

Serum iron markers

Iron	9.5 µmol/l	decreased
Transferrin	0.65 g/l	decreased
Transferrin saturation		
Ferritin	2855.0 µg/l	increased
Soluble transferrin receptor	4.5 µg/ml	normal
Transferrin:log ferritin	0.19	
Soluble transferrin receptor:log ferritin	1.30	

Red blood cell production

RCC	3.78 x 10^{12}/l	anaemia
HB	13.3 g/dl	normal
HCT	0.4 l/l	normal
MCV	106.5 fl	macrocytic
MCH	35.3 pg	hyperchromic
MCHC	33.1 g/dl	normochromic
RDW	14.2 %	increased

- Increased amount of storage iron with normal amount of sideroblasts according to bone marrow aspirate iron stain.
- Slightly decreased serum iron concentration.
- Severely increased serum ferritin.
- Normal supply of iron to erythroblasts according to red blood cell production.
- Iron transfer block.

Kalafong patient 23

Haematology report

No iron stain

Slightly hypocellular

Serum iron markers

Iron	16.7 µmol/l	normal
Transferrin	1.12 g/l	decreased
Transferrin saturation	66.5 %	increased
Ferritin	2016.0 µg/l	increased
Soluble transferrin receptor	5.0 µg/ml	normal
Transferrin:log ferritin	0.34	
Soluble transferrin receptor:log ferritin	1.51	

Red blood cell production

RCC	2.67 x 10^{12}/l	anaemia
HB	6.9 g/dl	decreased
HCT	0.23 l/l	decreased
MCV	84.5 fl	normocytic
MCH	25.7 pg	hypochromic
MCHC	30.4 g/dl	hypochromic
RDW	19.1 %	increased

- Normal serum iron concentration.
- Increased serum ferritin.
- Reduced supply of iron to erythroblasts according to red blood cell production.
- Iron transfer block.

Kalafong patient 24

Bone marrow iron stain – haematology report

No iron in bone marrow fragments

Severely reduced amount of sideroblasts

Active erythropoiesis with poor hemoglobinization of precursors

Iron deficiency anaemia

Serum iron markers

Iron	3.3 µmol/l	decreased
Transferrin	2.02 g/l	normal
Transferrin saturation	7.3 %	decreased
Ferritin	17.6 µg/l	normal
Soluble transferrin receptor	18.0 µg/ml	increased
Transferrin:log ferritin	1.62	
Soluble transferrin receptor:log ferritin	14.45	

Red blood cell production

RCC	2.26 x 10^{12}/l	anaemia
HB	4.0 g/dl	decreased
HCT	0.14 l/l	decreased
MCV	59.6 fl	microcytic
MCH	17.8 pg	hypochromic
MCHC	29.8 g/dl	hypochromic
RDW	19.2 %	increased

- No storage iron with severely reduced amount of sideroblasts according to bone marrow aspirate iron stain.
- Severely decreased serum iron concentration.

- Normal serum ferritin.
- Normal transferrin concentration.
- Severely increased soluble transferrin receptor.
- Reduced supply of iron to erythroblasts according to red blood cell production.
- No iron transfer block.

Kalafong patient 25

Bone marrow iron stain – haematology report

No iron in bone marrow fragments

Occasional pathologically overloaded sideroblasts, very occasional ring sideroblasts

Exceptionally active erythropoiesis, features of poor hemoglobinization and occasional dysplastic forms

Serum iron markers

Iron	2.9 µmol/l	decreased
Transferrin	3.23 g/l	normal
Transferrin saturation	4.0 %	decreased
Ferritin	3.7 µg/l	decreased
Soluble transferrin receptor	23.0 µg/ml	increased
Transferrin:log ferritin	5.69	
Soluble transferrin receptor:log ferritin	40.48	

Red blood cell production

RCC	3.77 x 10^{12}/l	anaemia
HB	5.8 g/dl	decreased
HCT	0.21 l/l	decreased
MCV	54.4 fl	microcytic
MCH	15.4 pg	hypochromic

MCHC	28.4 g/dl	hypochromic
RDW	22.8 %	increased
RPI	0.24	suppressed bone marrow response

- No storage iron with occasional pathologically overloaded sideroblasts according to bone marrow aspirate iron stain.
- Severely decreased serum iron concentration.
- Severely decreased serum ferritin.
- Reduced supply of iron to erythroblasts according to red blood cell production.
- Severely increased soluble transferrin receptor.
- No iron transfer block.

Kalafong patient 26

Haematology report

No iron stain

Active erythropoiesis, normoblastic

Serum iron markers

Iron	10.2 µmol/l	normal
Transferrin	2.30 g/l	normal
Transferrin saturation	19.8 %	normal
Ferritin	116.0 µg/l	normal
Soluble transferrin receptor	4.0 µg/ml	normal
Transferrin:log ferritin	1.11	
Soluble transferrin receptor:log ferritin	1.94	

Red blood cell production

RCC	4.16 x 10^{12}/l	normal
HB	13.7 g/dl	normal
HCT	0.42 l/l	normal
MCV	100.1 fl	macrocytic
MCH	32.9 pg	hyperchromic
MCHC	32.9 g/dl	normochromic
RDW	14.2 %	increased

- Normal to decreased amount of storage iron with no sideroblasts according to bone marrow core iron stain.
- Normal serum iron concentration.
- Normal serum ferritin.
- Normal supply of iron to erythroblasts according to red blood cell production.
- Iron transfer block.

Kalafong patient 27

No bone marrow aspirate evaluation

Serum iron markers

Iron	6.0 µmol/l	decreased
Transferrin	2.72 g/l	normal
Transferrin saturation	9.9 %	decreased
Ferritin	11.0 µg/l	normal
Soluble transferrin receptor	11.0 µg/ml	increased
Transferrin:log ferritin	2.61	
Soluble transferrin receptor:log ferritin	10.56	

Red blood cell production

RCC	3.76 x 10^{12}/l	anaemia
HB	10.0 g/dl	decreased
HCT	0.32 l/l	decreased
MCV	84.2 fl	normocytic
MCH	26.5 pg	hypochromic
MCHC	31.5 g/dl	hypochromic
RDW	15.4 %	increased
RPI	0.59	suppressed bone marrow response

- Reduced amount of storage iron according to core bone marrow iron stain.
- Decreased serum iron concentration.
- Normal but low serum ferritin.
- Normal transferrin concentration.
- Increased soluble transferrin receptor.
- Reduced supply of iron to erythroblasts according to red blood cell production.
- No iron transfer block.

Kalafong patient 28

Haematology report

No iron stain

Active erythropoiesis, megaloblastic

Serum iron markers

Iron	15.6 µmol/l	normal
Transferrin	1.12 g/l	decreased
Transferrin saturation	62.2 %	increased
Ferritin	87.3 µg/l	normal

Soluble transferrin receptor	6.0 µg/ml	normal
Transferrin:log ferritin	0.58	
Soluble transferrin receptor:log ferritin	3.09	

Red blood cell production

RCC	2.43 x 10^{12}/l	anaemia
HB	10.7 g/dl	decreased
HCT	0.31 l/l	decreased
MCV	125.3 fl	macrocytic
MCH	44.1 pg	hyperchromic
MCHC	35.2 g/dl	normochromic
RDW	15.7 %	increased

- Normal to decreased amount of storage iron with some sideroblasts according to bone marrow core iron stain.
- Normal serum iron concentration.
- Normal serum ferritin.
- Normal supply of iron to erythroblasts according to red blood cell production.
- No iron transfer block.

Kalafong patient 29

No iron stain

Serum iron markers

Iron	11.4 µmol/l	normal
Transferrin		
Transferrin saturation		
Ferritin	5672.0 µg/l	increased

Soluble transferrin receptor	10.8 µg/ml	increased
Transferrin:log ferritin		
Soluble transferrin receptor:log ferritin	2.88	

Red blood cell production

RCC	2.2 x 10^{12}/l	anaemia
HB	8.1 g/dl	decreased
HCT	0.22 l/l	decreased
MCV	100.2 fl	macrocytic
MCH	36.8 pg	hyperchromic
MCHC	36.7 g/dl	hyperchromic (spherocytosis)
RDW	21.3 %	increased

- Decreased amount of storage iron according to bone marrow core iron stain.
- Normal but low serum iron concentration.
- Severely increased serum ferritin.
- Slightly increased soluble transferrin receptor concentration.
- Normal supply of iron to erythroblasts according to red blood cell production.
- Iron transfer block.

Kalafong patient 30

Bone marrow iron stain – haematology report

Normal amount of iron in bone marrow fragments

Normal amount of sideroblasts

Active erythropoiesis with some erythroblasts larger than usual but not megaloblastic, occasional poor hemoglobinization

Serum iron markers

Iron	14.4 µmol/l	normal
Transferrin	2.30 g/l	normal
Transferrin saturation	25.0 %	normal
Ferritin	50.0 µg/l	normal
Soluble transferrin receptor	5.3 µg/ml	normal
Transferrin:log ferritin	1.35	
Soluble transferrin receptor:log ferritin	3.12	

Red blood cell production

RCC	4.23 x 10^{12}/l	normal
HB	13.7 g/dl	normal
HCT	0.435 l/l	normal
MCV	102.8 fl	macrocytic
MCH	32.4 pg	hyperchromic
MCHC	31.5 g/dl	hypochromic
RDW	15.7 %	increased

- Normal amount of storage iron with normal amount of sideroblasts according to the bone marrow aspirate iron stain.
- Normal serum iron concentration.
- Normal serum ferritin.
- Normal transferrin concentration.
- Normal soluble transferrin receptor concentration.
- Reduced supply of iron to erythroblasts according to red blood cell production.
- No iron transfer block.

Kalafong patient 31

Haematology report

No iron stain

Active erythropoiesis with dyserythropoiesis, poor hemoglobinization of late normoblasts

Anaemia is probably multifactorial with ineffective erythropoiesis, decreased red blood cell life span and iron transfer block

Serum iron markers

Iron	7.8 µmol/l	decreased
Transferrin	0.60 g/l	decreased
Transferrin saturation	49.0 %	normal
Ferritin	19644.0 µg/l	increased
Soluble transferrin receptor	3.5 µg/ml	normal
Transferrin:log ferritin	0.14	
Soluble transferrin receptor:log ferritin	0.82	

Red blood cell production

RCC	2 x 10^{12}/l	anaemia
HB	4.6 g/dl	decreased
HCT	0.142 l/l	decreased
MCV	71.0 fl	microcytic
MCH	23.0 pg	hypochromic
MCHC	32.4 g/dl	normochromic
RDW	18.7 %	increased

- Increased amount of storage iron according to bone marrow core iron stain.
- Decreased serum iron concentration.
- Severely increased serum ferritin.

- Reduced supply of iron to erythroblasts according to red blood cell production.
- Iron transfer block.

Kalafong patient 32

Bone marrow iron stain – haematology report

Reduced iron present in bone marrow fragments (1/6)

No sideroblasts

Active erythropoiesis, normoblastic

Serum iron markers

Iron	13.1 µmol/l	normal
Transferrin	3.30 g/l	normal
Transferrin saturation	16.0 %	normal
Ferritin	15.0 µg/l	normal
Soluble transferrin receptor	6.5 µg/ml	normal
Transferrin:log ferritin	2.81	
Soluble transferrin receptor:log ferritin	5.53	

Red blood cell production

RCC	5.3 x 10^{12}/l	normal
HB	14.1 g/dl	normal
HCT	0.47 l/l	normal
MCV	88.7 fl	normocytic
MCH	26.6 pg	hypochromic
MCHC	30.0 g/dl	hypochromic
RDW	14.1 %	increased

- Reduced amount of storage iron with no sideroblasts according to bone marrow aspirate iron stain.
- Normal serum iron concentration.
- Normal serum ferritin.
- Reduced supply of iron to erythroblasts according to red blood cell production.
- No iron transfer block.

Kalafong patient 33

Bone marrow iron stain – haematology report

Normal amount of iron in bone marrow fragments

Normal amount of sideroblasts

Serum iron markers

Iron	7.4 µmol/l	decreased
Transferrin	1.00 g/l	decreased
Transferrin saturation	29.0 %	normal
Ferritin	45519.0 µg/l	increased
Soluble transferrin receptor	26.3 µg/ml	increased
Transferrin:log ferritin	0.22	
Soluble transferrin receptor:log ferritin	5.65	

Red blood cell production

RCC	1.99 x 10^{12}/l	anaemia
HB	4.1 g/dl	decreased
HCT	0.134 l/l	decreased
MCV	67.3 fl	microcytic
MCH	20.6 pg	hypochromic
MCHC	30.6 g/dl	hypochromic

RDW	30.7 %	increased

- Normal amount of storage iron with normal amount of sideroblasts according to bone marrow aspirate iron stain.
- Decreased serum iron concentration.
- Severely increased serum ferritin.
- Reduced supply of iron to erythroblasts according to red blood cell production.
- No iron transfer block.

Kalafong patient 34

Bone marrow iron stain – haematology report

Increased amount of iron in bone marrow fragments

Serum iron markers

Iron	4.8 µmol/l	decreased
Transferrin	1.10 g/l	decreased
Transferrin saturation	18.0 %	normal
Ferritin	913.0 µg/l	increased
Soluble transferrin receptor	10.0 µg/ml	increased
Transferrin:log ferritin	0.37	
Soluble transferrin receptor:log ferritin	3.38	

Red blood cell production

RCC	1.29 x 10^{12}/l	anaemia
HB	3.5 g/dl	decreased
HCT	0.129 l/l	decreased
MCV	100.0 fl	macrocytic
MCH	27.1 pg	normochromic

MCHC	27.1 g/dl	hypochromic
RDW	18.9 %	increased

- Increased amount of storage iron according to bone marrow aspirate iron stain.
- Increased amount of storage iron with no sideroblasts according to bone marrow core iron stain.
- Decreased serum iron concentration.
- Increased serum ferritin.
- Reduced supply of iron to erythroblasts according to red blood cell production.
- Iron transfer block.

Kalafong patient 35

Bone marrow iron stain – haematology report

Normal amount of iron in bone marrow fragments

Reduced amount of sideroblasts

Active erythropoiesis with poor hemoglobinization

Iron block

The haematology report was eliminated since it is not consistent with the aspirate iron stain and bone marrow core iron stain.

Serum iron markers

Iron	10.5 µmol/l	normal
Transferrin	2.30 g/l	normal
Transferrin saturation	18.0 %	normal
Ferritin	32.0 µg/l	normal
Soluble transferrin receptor	5.3 µg/ml	normal
Transferrin:log ferritin	1.53	

Soluble transferrin receptor:log ferritin 3.52

Red blood cell production

RCC	4.18 x 10^{12}/l	normal
HB	11.6 g/dl	decreased
HCT	0.359 l/l	decreased
MCV	85.9 fl	normocytic
MCH	27.8 pg	normochromic
MCHC	32.3 g/dl	normochromic
RDW	16.9 %	increased

- Absent storage iron with no sideroblasts according to bone marrow core iron stain.
- Normal but low serum iron concentration.
- Normal but low serum ferritin.
- Normal supply of iron to erythroblasts according to red blood cell production.
- No iron transfer block.

Kalafong patient 36

Bone marrow iron stain – haematology report

Increased amount of iron in bone marrow fragments (5/6)

Increased amount of sideroblasts with pathologically overloaded forms

Active erythropoiesis with dyserythropoiesis and megaloblasts

Serum iron markers

Iron	8.7 µmol/l	decreased
Transferrin	0.90 g/l	decreased
Transferrin saturation	39.0 %	normal
Ferritin	2073.0 µg/l	increased

Soluble transferrin receptor	5.8 µg/ml	normal
Transferrin:log ferritin	0.27	
Soluble transferrin receptor:log ferritin	1.75	

Red blood cell production

RCC	1.03 x 10^{12}/l	anaemia
HB	3.7 g/dl	decreased
HCT	0.115 l/l	decreased
MCV	111.7 fl	macrocytic
MCH	35.9 pg	hyperchromic
MCHC	32.2 g/dl	normochromic
RDW	24.1 %	increased

- Increased amount of storage iron with increased amount of sideroblasts according to bone marrow aspirate iron stain.
- Decreased serum iron concentration.
- Severely increased serum ferritin.
- Normal supply of iron to erythroblasts according to red blood cell production.
- The pathologically overloaded sideroblasts do not indicate the presence of an iron transfer block, but the severely increased amount of storage iron and the decreased serum iron concentration are synonymous with iron transfer block.
- Iron transfer block.

Kalafong patient 37

Bone marrow iron stain – haematology report

Reduced amount of iron in bone marrow fragments (1/6)

Pathologically overloaded sideroblasts are noted

Active erythropoiesis with dyserythropoiesis and uneven hemoglobinization, nuclear budding

Serum iron markers

Iron	16.9 µmol/l	normal
Transferrin	1.90 g/l	decreased
Transferrin saturation	35.0 %	normal
Ferritin	29.1 µg/l	normal
Soluble transferrin receptor	11.0 µg/ml	increased
Transferrin:log ferritin	1.30	
Soluble transferrin receptor:log ferritin	7.51	

Red blood cell production

RCC	1.66 x 10^{12}/l	anaemia
HB	4.0 g/dl	decreased
HCT	0.132 l/l	decreased
MCV	79.5 fl	normocytic
MCH	24.1 pg	hypochromic
MCHC	30.3 g/dl	hypochromic
RDW	29.0 %	increased
RPI	0.080	suppressed bone marrow response

- Reduced amount of storage iron with pathologically overloaded sideroblasts according to bone marrow aspirate iron stain.
- Normal serum iron concentration.
- Normal but low serum ferritin.
- Reduced supply of iron to erythroblasts according to red blood cell production.
- Iron transfer block.

Kalafong patient 38

Haematology report

No iron stain

Active erythropoiesis, megaloblastic, poor hemoglobinization of normoblasts

Suggests vitamin B_{12} and red blood cell folate investigations

Megaloblastic anaemia – concurrent iron deficiency

Serum iron markers

Iron	39.6 µmol/l	increased
Transferrin	1.80 g/l	decreased
Transferrin saturation	88.0 %	increased
Ferritin	63.1 µg/l	normal
Soluble transferrin receptor	14.0 µg/ml	increased
Transferrin:log ferritin	1.00	
Soluble transferrin receptor:log ferritin	7.78	

Red blood cell production

RCC	0.99 x 10^{12}/l	anaemia
HB	2.7 g/dl	decreased
HCT	0.087 l/l	decreased
MCV	87.9 fl	normocytic
MCH	27.3 pg	normochromic
MCHC	31.0 g/dl	hypochromic
RDW	33.6 %	increased
RPI	0.06	suppressed bone marrow response

- Normal/decreased amount of storage iron according to bone marrow core iron stain.
- Severely increased serum iron concentration.

- Normal serum ferritin.
- Reduced supply of iron to erythroblasts according to red blood cell production.
- No iron transfer block.

Kalafong patient 39

Bone marrow iron stain – haematology report

Increased amount of iron in bone marrow fragments (4/6)

Decreased amount of sideroblasts

Hypoactive erythropoiesis, megaloblastic changes

Iron block

Serum iron markers

Iron	36.6 µmol/l	increased
Transferrin	1.60 g/l	decreased
Transferrin saturation	91.0 %	increased
Ferritin	782.8 µg/l	increased
Soluble transferrin receptor	4.5 µg/ml	normal
Transferrin:log ferritin	0.55	
Soluble transferrin receptor:log ferritin	1.56	

Red blood cell production

RCC	0.95 x 10^{12}/l	anaemia
HB	3.3 g/dl	decreased
HCT	0.101 l/l	decreased
MCV	106.3 fl	macrocytic
MCH	34.7 pg	hyperchromic
MCHC	32.7 g/dl	normochromic
RDW	0.0 %	decreased

RPI	0.010	suppressed bone marrow response

- Increased amount of storage iron with reduced amount of sideroblasts according to bone marrow aspirate iron stain.
- Severely increased serum iron concentration.
- Increased serum ferritin.
- Normal supply of iron to erythroblasts.
- Iron transfer block.

Kalafong patient 40

Bone marrow iron stain – haematology report

Markedly increased amount of iron in bone marrow fragments (6/6)

Reduced amount of sideroblasts

Active erythropoiesis, precursors show dyserythropoiesis while some late erythrobasts show uneven hemoglobinization

Iron block

The haemoglobin level suggests that the anaemia is multifactorial with ineffective erythropoiesis and reduced red blood cell life span

Serum iron markers

Iron	8.9 µmol/l	decreased
Transferrin	1.40 g/l	decreased
Transferrin saturation	25.0 %	normal
Ferritin	5760.0 µg/l	increased
Soluble transferrin receptor	9.5 µg/ml	increased
Transferrin:log ferritin	0.37	
Soluble transferrin receptor:log ferritin	2.53	

Red blood cell production

RCC	2.08 x 10^{12}/l	anaemia
HB	5.2 g/dl	decreased
HCT	0.170 l/l	decreased
MCV	81.7 fl	normocytic
MCH	25.0 pg	hypochromic
MCHC	30.6 g/dl	hypochromic
RDW	18.0 %	increased

- Severely increased amount of storage iron with reduced amount of sideroblasts according to bone marrow aspirate iron stain.
- Reduced serum iron concentration.
- Severely increased serum ferritin.
- Reduced supply of iron to erythroblasts according to red blood cell production.
- Iron transfer block.

Kalafong patient 41

Bone marrow iron stain – haematology report

No iron in bone marrow fragments

Active erythropoiesis with dyserythropoiesis and poor hemoglobinization

Iron deficient marrow

Serum iron markers

Iron	3.9 µmol/l	decreased
Transferrin	4.30 g/l	increased
Transferrin saturation	4.0 %	decreased
Ferritin	4.0 µg/l	decreased
Soluble transferrin receptor	33.5 µg/ml	increased

Transferrin:log ferritin	7.14
Soluble transferrin receptor:log ferritin	55.64

Red blood cell production

RCC	1.57 x 10^{12}/l	anaemia
HB	2.8 g/dl	decreased
HCT	0.107 l/l	decreased
MCV	68.2 fl	microcytic
MCH	17.8 pg	hypochromic
MCHC	26.2 g/dl	hypochromic
RDW	27.1 %	increased
RPI	0.150	suppressed bone marrow response

- Absent storage iron with no sideroblasts according to bone marrow aspirate iron stain.
- Severely decreased serum iron concentration.
- Severely decreased serum ferritin.
- Increased transferrin concentration.
- Severely increased soluble transferrin receptor.
- Reduced supply of iron to erythroblasts according to red blood cell production.
- No iron transfer block.

Kalafong patient 42

Bone marrow iron stain – haematology report

No iron in bone marrow fragments

Occasional sideroblasts

Hyperactive erythropoiesis with some dyserythropoiesis and poor hemoglobinization of late normoblasts

Iron deficient marrow

Serum iron markers

Iron	4.0 µmol/l	decreased
Transferrin	2.90 g/l	normal
Transferrin saturation	6.0 %	decreased
Ferritin	37.0 µg/l	normal
Soluble transferrin receptor	36.3 µg/ml	increased
Transferrin:log ferritin	1.85	
Soluble transferrin receptor:log ferritin	23.15	

Red blood cell production

RCC	2.71 x 10^{12}/l	anaemia
HB	5.9 g/dl	decreased
HCT	0.230 l/l	decreased
MCV	84.9 fl	normocytic
MCH	21.8 pg	hypochromic
MCHC	25.7 g/dl	hypochromic
RDW	33.9 %	increased
RPI	0.630	suppressed bone marrow response

- No storage iron with occasional sideroblasts according to bone marrow aspirate iron stain.
- Severely decreased serum iron concentration.
- Normal serum ferritin.
- Normal transferrin concentration.
- Severely increased soluble transferrin receptor.
- Reduced supply of iron to erythroblasts according to red blood cell production.
- No iron transfer block.

Kalafong patient 43

Bone marrow iron stain – haematology report

No iron in bone marrow fragments

No sideroblasts

Active erythropoiesis with dyserythropoietic features (uneven hemoglobinization, intercytoplasmic bridging)

Iron deficient marrow

Serum iron markers

Iron	3.3 µmol/l	decreased
Transferrin	3.20 g/l	normal
Transferrin saturation	4.0 %	decreased
Ferritin	23.4 µg/l	decreased
Soluble transferrin receptor	25.0 µg/ml	increased
Transferrin:log ferritin	2.34	
Soluble transferrin receptor:log ferritin	18.26	

Red blood cell production

RCC	2.99 x 10^{12}/l	anaemia
HB	5.9 g/dl	decreased
HCT	0.207 l/l	decreased
MCV	69.2 fl	microcytic
MCH	19.7 pg	hypochromic
MCHC	28.5 g/dl	hypochromic
RDW	18.5 %	increased

- Absent storage iron with no sideroblasts according to bone marrow iron stain.
- Severely reduced serum iron concentration.

- Decreased serum ferritin.
- Normal transferrin concentration.
- Severely increased soluble transferrin receptor.
- Reduced supply of iron to erythroblasts according to red blood cell production.
- No iron transfer block.

Kalafong patient 44

Bone marrow iron stain – haematology report

Increased amount of iron in bone marrow fragments (4/6)

No pathologically overloaded or ring sideroblasts

Active erythropoiesis with dyserythropoietic features (uneven hemoglobinization, intercytoplasmic bridging)

Serum iron markers

Iron	4.8 µmol/l	decreased
Transferrin	1.80 g/l	decreased
Transferrin saturation	11.0 %	decreased
Ferritin	289.1 µg/l	normal
Soluble transferrin receptor	3.0 µg/ml	normal
Transferrin:log ferritin	0.73	
Soluble transferrin receptor:log ferritin	1.22	

Red blood cell production

RCC	3.77 x 10^{12}/l	anaemia
HB	5.9 g/dl	decreased
HCT	0.301 l/l	decreased
MCV	79.8 fl	normocytic
MCH	25.2 pg	hypochromic

MCHC	31.6 g/dl	hypochromic
RDW	15.4 %	increased

- Increased amount of storage iron with no pathologically overloaded or ring sideroblasts according to bone marrow aspirate iron stain.
- Decreased serum iron concentration.
- Normal serum ferritin.
- Reduced supply of iron to erythroblasts according to red blood cell production.
- Iron transfer block.

Kalafong patient 45

Haematology report

No iron stain

Dyserythropoiesis

Serum iron markers

Iron	13.5 µmol/l	normal
Transferrin	1.50 g/l	decreased
Transferrin saturation	36.0 %	normal
Ferritin	859.8 µg/l	increased
Soluble transferrin receptor	6.3 µg/ml	normal
Transferrin:log ferritin	0.51	
Soluble transferrin receptor:log ferritin	2.15	

Red blood cell production

RCC	2.99 x 10^{12}/l	anaemia
HB	9.6 g/dl	decreased
HCT	0.305 l/l	decreased

MCV	102.0 fl	macrocytic
MCH	32.1 pg	hyperchromic
MCHC	31.5 g/dl	hypochromic
RDW	14.9 %	increased

- Increased amount of storage iron according to bone marrow core iron stain.
- Normal but low serum iron concentration.
- Increased serum ferritin.
- Reduced supply of iron to erythroblasts according to red blood cell production.
- Iron transfer block

Kalafong patient 46

Bone marrow iron stain – haematology report

Increased amount of iron in bone marrow fragments (5/6)

Sideroblasts present

Active erythropoiesis, uneven hemoglobinization

Serum iron markers

Iron	4.5 µmol/l	decreased
Transferrin	1.90 g/l	decreased
Transferrin saturation	9.0 %	decreased
Ferritin	301.1 µg/l	normal
Soluble transferrin receptor	7.0 µg/ml	normal
Transferrin:log ferritin	0.77	
Soluble transferrin receptor:log ferritin	2.82	

Red blood cell production

RCC	4.69 x 10^{12}/l	normal

HB	13.7 g/dl	normal
HCT	0.417 l/l	normal
MCV	88.9 fl	normocytic
MCH	29.2 pg	normochromic
MCHC	32.9 g/dl	normochromic
RDW	14.4 %	increased

- Increased amount of storage iron with sideroblasts according to bone marrow aspirate iron stain.
- Decreased serum iron concentration.
- Normal serum ferritin.
- Normal supply of iron to erythroblasts according to red blood cell production.
- No iron transfer block.

Kalafong patient 47

Unsuitable bone marrow aspirate

Serum iron markers

Iron	1.7 µmol/l	decreased
Transferrin	1.40 g/l	decreased
Transferrin saturation	5.0 %	decreased
Ferritin	266.9 µg/l	normal
Soluble transferrin receptor	17.0 µg/ml	increased
Transferrin:log ferritin	0.58	
Soluble transferrin receptor:log ferritin	7.01	

Red blood cell production

RCC	1.16 x 10^{12}/l	anaemia

HB	3.2 g/dl	decreased
HCT	0.101 l/l	decreased
MCV	87.1 fl	normocytic
MCH	27.6 pg	normochromic
MCHC	31.7 g/dl	hypochromic
RDW	33.6 %	increased
RPI	0.730	suppressed bone marrow response

- No storage iron according to bone marrow core iron stain.
- Severely decreased serum iron concentration.
- Normal serum ferritin.
- Reduced supply of iron to erythroblasts according to red blood cell production.
- Increased soluble transferrin receptor concentration.
- Iron transfer block.

Kalafong patient 48

Bone marrow iron stain – haematology report

Decreased amount of iron in bone marrow fragments

Sideroblasts present

Hyperactive erythropoiesis, mildly magaloblastic

Iron deficiency

Suggests vitamin B_{12} and RBC folate investigation

Serum iron markers

Iron	6.9 µmol/l	decreased
Transferrin	3.40 g/l	normal
Transferrin saturation	8.0 %	decreased
Ferritin	21.6 µg/l	normal

Soluble transferrin receptor	25.0 µg/ml	increased
Transferrin:log ferritin	2.55	
Soluble transferrin receptor:log ferritin	18.73	

Red blood cell production

RCC	2.47 x 10^{12}/l	anaemia
HB	4.5 g/dl	decreased
HCT	0.168 l/l	decreased
MCV	68.0 fl	microcytic
MCH	18.2 pg	hypochromic
MCHC	26.8 g/dl	hypochromic
RDW	26.7 %	increased
RPI	0.110	suppressed bone marrow response

- Reduced amount of storage iron with sideroblasts according to bone marrow aspirate iron stain.
- Decreased serum iron concentration.
- Normal serum ferritin.
- Normal transferrin concentration.
- Reduced supply of iron to erythroblasts according to red blood cell production.
- Severely increased soluble transferrin receptor.
- No iron transfer block.

Osteoarthritis patient 1

Serum iron markers

Iron	7.3 µmol/l	decreased
Transferrin	2.41 g/l	normal
Transferrin saturation	13.5 %	decreased

Ferritin	30.8 µg/l	normal
Soluble transferrin receptor	4.8 µg/ml	normal
Transferrin:log ferritin	1.62	
Soluble transferrin receptor:log ferritin	3.23	

Red blood cell production

RCC	4.06 x 10^{12}/l	anaemia
HB	13.5 g/dl	normal
HCT	0.41 l/l	normal
MCV	101.2 fl	macrocytic
MCH	33.3 pg	hyperchromic
MCHC	32.9 g/dl	normochromic
RDW	12.9 %	normal

- Reduced amount of storage iron with no sideroblasts according to bone marrow core iron stain.
- Reduced serum iron concentration.
- Normal ferritin.
- Normal transferrin.
- Normal supply of iron to erythroblasts according to red blood cell production.
- Normal soluble transferrin receptor.
- Ratio of soluble transferrin receptor/log ferritin >2.
- No Iron transfer block.

Osteoarthritis patient 2

Serum iron markers

Iron	18.6 µmol/l	normal

Transferrin	1.95 g/l	decreased
Transferrin saturation	42.7 %	normal
Ferritin	120 µg/l	normal
Soluble transferrin receptor	1.8 µg/ml	decreased
Transferrin:log ferritin	0.94	
Soluble transferrin receptor:log ferritin	0.87	

Red blood cell production

RCC	4.22 x 10^{12}/l	normal
HB	14 g/dl	normal
HCT	0.41 l/l	normal
MCV	97.4 fl	normocytic
MCH	33.2 pg	hyperchromic
MCHC	34 g/dl	normochromic
RDW	12.7 %	normal

- No iron stains.
- Normal serum iron concentration.
- Normal ferritin.
- Decreased transferrin.
- Decreased soluble transferrin receptor.
- Normal supply of iron to erythroblasts according to red blood cell production.
- Ratio of soluble transferrin receptor/log ferritin <1.
- Iron transfer block.

Osteoarthritis patient 3

Serum iron markers

Iron	14.7 µmol/l	normal
Transferrin	1.68 g/l	decreased
Transferrin saturation	39.1 %	normal
Ferritin	219 µg/l	normal
Soluble transferrin receptor	1.5 µg/ml	decreased
Transferrin:log ferritin	0.72	
Soluble transferrin receptor:log ferritin	0.64	

Red blood cell production

HB	14.9 g/dl	normal
HCT	0.44 l/l	normal

- Reduced amount of storage iron with no sideroblasts according to bone marrow core iron stain.
- Normal serum iron concentration.
- Normal ferritin.
- Decreased transferrin.
- Decreased soluble transferrin receptor.
- Ratio of soluble transferrin receptor/log ferritin <1.
- Iron transfer block.

Osteoarthritis patient 4

Serum iron markers

Iron	8.8 µmol/l	decreased
Transferrin	2.2 g/l	normal

Transferrin saturation	17.9 %	decreased
Ferritin	170 µg/l	normal
Soluble transferrin receptor	3.4 µg/ml	normal
Transferrin:log ferritin	0.99	
Soluble transferrin receptor:log ferritin	1.52	

Red blood cell production

RCC	4.62 x 10^{12}/l	anaemia
HB	16.1 g/dl	normal
HCT	0.481 l/l	normal
MCV	104.2 fl	macrocytic
MCH	35 pg	hyperchromic
MCHC	33.6 g/dl	normochromic
RDW	12.4 %	normal

- No iron stains.
- Decreased serum iron concentration.
- Normal ferritin.
- Normal transferrin.
- Normal soluble transferrin receptor.
- Normal supply of iron to erythroblasts according to red blood cell production.
- Ratio of soluble transferrin receptor/log ferritin >1 and <2.
- No iron transfer block.

Osteoarthritis patient 5

Serum iron markers

Iron	15 µmol/l	normal

Transferrin	2 g/l	normal
Transferrin saturation	33.5 %	normal
Ferritin	59 µg/l	normal
Soluble transferrin receptor	3.8 µg/ml	normal
Transferrin:log ferritin	1.13	
Soluble transferrin receptor:log ferritin	2.15	

Red blood cell production

RCC	5.17 x 10^{12}/l	normal
HB	16.1 g/dl	normal
HCT	0.461 l/l	normal
MCV	88.8 fl	normocytic
MCH	31.2 pg	normochromic
MCHC	35.1 g/dl	normochromic
RDW	12.8 %	normal

- Reduced amount of storage iron with no sideroblasts according to bone marrow core iron stain.
- Normal serum iron concentration.
- Normal ferritin.
- Normal transferrin.
- Normal soluble transferrin receptor.
- Normal supply of iron to erythroblasts according to red blood cell production.
- No iron transfer block.

Osteoarthritis patient 6

Serum iron markers

Iron	11 µmol/l	normal
Transferrin	2.1 g/l	normal
Transferrin saturation	23.4 %	normal
Ferritin	35 µg/l	normal
Soluble transferrin receptor	3.4 µg/ml	normal
Transferrin:log ferritin	1.36	
Soluble transferrin receptor:log ferritin	2.2	

Red blood cell production

RCC	3.91 x 10^{12}/l	anaemia
HB	11.8 g/dl	decreased
HCT	0.359 l/l	decreased
MCV	91.9 fl	normocytic
MCH	30.2 pg	normochromic
MCHC	32.9 g/dl	normochromic
RDW	12.6 %	normal

- Reduced amount of storage iron with no sideroblasts according to bone marrow core iron stain.
- Normal serum iron concentration.
- Normal ferritin.
- Normal transferrin.
- Normal soluble transferrin receptor.
- Normal supply of iron to erythroblasts according to red blood cell production.
- No iron transfer block.

Osteoarthritis patient 7

Serum iron markers

Iron	5.2 µmol/l	decreased
Transferrin	0.9 g/l	decreased
Transferrin saturation	25.9 %	normal
Ferritin	54 µg/l	normal
Soluble transferrin receptor	2.5 µg/ml	decreased
Transferrin:log ferritin	0.52	
Soluble transferrin receptor:log ferritin	1.44	

Red blood cell production

RCC	5.2 x 10^{12}/l	normal
HB	15.1 g/dl	normal
HCT	0.49 l/l	normal
MCV	94.3 fl	normocytic
MCH	29.2 pg	normochromic
MCHC	30.9 g/dl	normochromic
RDW	14.1 %	normal

- No iron stains.
- Reduced serum iron concentration.
- Normal ferritin.
- Decreased transferrin.
- Decreased soluble transferrin receptor.
- Normal supply of iron to erythroblasts according to red blood cell production.
- Iron transfer block.

Osteoarthritis patient 8

Serum iron markers

Iron	18.3 µmol/l	normal
Transferrin	1.5 g/l	decreased
Transferrin saturation	54.5 %	increased
Ferritin	163 µg/l	normal
Soluble transferrin receptor	1.8 µg/ml	decreased
Transferrin:log ferritin	0.68	
Soluble transferrin receptor:log ferritin	0.81	

Red blood cell production

RCC	6 x 10^{12}/l	normal
HB	17.2 g/dl	normal
HCT	0.535 l/l	normal
MCV	89.2 fl	normocytic
MCH	28.7 pg	normochromic
MCHC	32.2 g/dl	normochromic
RDW	13.8 %	normal

- Normal amount of storage iron with no sideroblasts according to bone marrow core iron stain.
- Normal serum iron concentration.
- Normal ferritin.
- Decreased transferrin.
- Decreased soluble transferrin receptor.
- Normal supply of iron to erythroblasts according to red blood cell production.
- Ratio of soluble transferrin receptor/log ferritin <1.

- Iron transfer block.

Osteoarthritis patient 9

Serum iron markers

Iron	7 µmol/l	decreased
Transferrin	3 g/l	normal
Transferrin saturation	10.4 %	decreased
Ferritin	16 µg/l	decreased
Soluble transferrin receptor	5.8 µg/ml	normal
Transferrin:log ferritin	2.49	
Soluble transferrin receptor:log ferritin	4.82	

Red blood cell production

RCC	5.04 x 10^{12}/l	normal
HB	14.7 g/dl	normal
HCT	0.444 l/l	normal
MCV	88.1 fl	normocytic
MCH	29.1 pg	normochromic
MCHC	33 g/dl	normochromic
RDW	13.1 %	normal

- No iron stains.
- Decreased serum iron concentration.
- Decreased ferritin.
- Normal transferrin.
- Normal soluble transferrin receptor.
- Normal supply of iron to erythroblasts according to red blood cell production.

- Ratio of soluble transferrin receptor/log ferritin >2.
- No iron transfer block.

Osteoarthritis patient 10

Serum iron markers

Iron	22.6 µmol/l	normal
Transferrin	2.4 g/l	normal
Transferrin saturation	42.1 %	normal
Ferritin	75 µg/l	normal
Soluble transferrin receptor	4 µg/ml	normal
Transferrin:log ferritin	1.28	
Soluble transferrin receptor:log ferritin	2.13	

Red blood cell production

RCC	5.06 x 10^{12}/l	normal
HB	15.2 g/dl	normal
HCT	0.467 l/l	normal
MCV	92.3 fl	normocytic
MCH	30.1 pg	normochromic
MCHC	32.6 g/dl	normochromic
RDW	12.1 %	normal

- No storage iron with no sideroblasts according to bone marrow core iron stain.
- Normal serum iron concentration.
- Normal ferritin.
- Normal transferrin.
- Normal soluble transferrin receptor.

- Normal supply of iron to erythroblasts according to red blood cell production.
- Ratio of soluble transferrin receptor/log ferritin >2.
- No iron transfer block.

4) Raw data of the immunolabelling of the H-subunit and L-subunit of ferritin

Table 1. The count/μm^2 for the immunolabelling of the H-subunit and L-subunit of ferritin in the different cell types for the Kalafong patients (patients 1-48) and the osteoarthritis patients (patients 1001-1010)

Patient	Cell type	Subunit	Count/μm^2	Mean for cell type
1	Red blood cell precursor	H	145	145
1	Late red blood cell precursor	H	123	123
1	Late red blood cell precursor/Reticulocyte	H	258	258
1	Red blood cell	H	291	
1	Red blood cell	H	330	
1	Red blood cell	H	322	314.3
1	Macrophage	H	135	
1	Macrophage	H	172	
1	Macrophage	H	109	
1	Macrophage	H	95	127.8
1	Red blood cell precursor	L	122	
1	Red blood cell precursor	L	115	118.5
1	Late red blood cell precursor	L	121	121
1	Reticulocyte	L	81	81
1	Macrophage	L	73	
1	Macrophage	L	73	
1	Macrophage	L	59	68.3
2	Red blood cell precursor	H	276	
2	Red blood cell precursor	H	236	256
2	Latish red blood cell precursor	H	259	259
2	Reticulocyte	H	159	
2	Reticulocyte	H	182	
2	Reticulocyte	H	127	156
2	Red blood cell	H	208	
2	Red blood cell	H	161	
2	Red blood cell	H	176	181.7
2	Macrophage	H	112	
2	Macrophage	H	90	
2	Macrophage	H	121	107.7
2	Red blood cell precursor	L	128	
2	Red blood cell precursor	L	174	
2	Red blood cell precursor	L	137	146.3
2	Late red blood cell precursor	L	146	
2	Late red blood cell precursor	L	124	135
2	Reticulocyte	L	102	
2	Reticulocyte	L	140	
2	Reticulocyte	L	114	118.7
2	Red blood cell	L	118	
2	Red blood cell	L	139	128.5
2	Macrophage	L	51	
2	Macrophage	L	78	

2	Macrophage	L	75	68
3	Red blood cell precursor	H	108	
3	Red blood cell precursor	H	80	
3	Red blood cell precursor	H	112	
3	Red blood cell precursor	H	85	96.3
3	Reticulocyte	H	91	
3	Reticulocyte	H	103	
3	Reticulocyte	H	143	112.3
3	Reticulocyte/Red blood cell	H	120	120
3	Red blood cell	H	123	
3	Red blood cell	H	82	102.5
3	Macrophage	H	78	
3	Macrophage	H	90	
3	Macrophage	H	79	82.3
3	Red blood cell precursor	L	110	
3	Red blood cell precursor	L	106	
3	Red blood cell precursor	L	85	100.3
3	Late red blood cell precursor	L	120	
3	Late red blood cell precursor	L	112	116
3	Late red blood cell precursor/Reticulocyte	L	149	149
3	Reticulocyte	L	117	
3	Reticulocyte	L	186	
3	Reticulocyte	L	69	
3	Reticulocyte	L	84	114
3	Red blood cell	L	173	173
3	Macrophage	L	55	
3	Macrophage	L	62	
3	Macrophage	L	71	62.7
4	Late red blood cell precursor/Reticulocyte	L	130	130
4	Reticulocyte	L	158	158
4	Red blood cell	L	234	234
4	Macrophage	L	103	
4	Macrophage	L	135	119
5	Red blood cell precursor	H	155	
5	Red blood cell precursor	H	185	170
5	Late red blood cell precursor	H	139	
5	Late red blood cell precursor	H	141	140
5	Late red blood cell precursor/Reticulocyte	H	142	
5	Late red blood cell precursor/Reticulocyte	H	212	177
5	Reticulocyte	H	139	
5	Reticulocyte	H	188	163.5
5	Red blood cell	H	269	
5	Red blood cell	H	223	246
5	Macrophage	H	160	
5	Macrophage	H	100	
5	Macrophage	H	124	128
5	Red blood cell precursor	L	244	
5	Red blood cell precursor	L	173	208.5
5	Late red blood cell precursor	L	222	
5	Late red blood cell precursor	L	213	217.5
5	Reticulocyte	L	195	
5	Reticulocyte	L	133	
5	Reticulocyte	L	106	144.7
5	Red blood cell	L	224	
5	Red blood cell	L	259	

5	Red blood cell	L	305	262.7
5	Macrophage	L	57	
5	Macrophage	L	37	
5	Macrophage	L	63	52.3
6	Red blood cell precursor	H	160	
6	Red blood cell precursor	H	227	
6	Red blood cell precursor	H	268	
6	Red blood cell precursor	H	267	
6	Red blood cell precursor	H	266	
6	Red blood cell precursor	H	310	249.7
6	Late red blood cell precursor/Reticulocyte	H	268	268
6	Reticulocyte	H	159	
6	Reticulocyte	H	222	
6	Reticulocyte	H	223	
6	Reticulocyte	H	201	201.3
6	Red blood cell	H	274	
6	Red blood cell	H	290	282
6	Macrophage	H	104	
6	Macrophage	H	115	
6	Macrophage	H	94	104.3
6	Red blood cell precursor	L	177	
6	Red blood cell precursor	L	143	160
6	Latish red blood cell precursor	L	225	225
6	Late red blood cell precursor	L	200	200
6	Reticulocyte	L	207	
6	Reticulocyte	L	230	218.5
6	Reticulocyte/Red blood cell	L	212	212
6	Red blood cell	L	160	160
6	Macrophage	L	35	
6	Macrophage	L	94	
6	Macrophage	L	69	66
7	Red blood cell precursor	H	223	
7	Red blood cell precursor	H	310	266.5
7	Late red blood cell precursor	H	204	
7	Late red blood cell precursor	H	241	
7	Late red blood cell precursor	H	281	242
7	Late red blood cell precursor/Reticulocyte	H	179	179
7	Reticulocyte	H	306	
7	Reticulocyte	H	289	
7	Reticulocyte	H	333	309.3
7	Reticulocyte/Red blood cell	H	309	309
7	Red blood cell	H	250	
7	Red blood cell	H	163	206.5
7	Macrophage	H	186	
7	Macrophage	H	154	
7	Macrophage	H	99	146.3
7	Red blood cell precursor	L	172	
7	Red blood cell precursor	L	135	
7	Red blood cell precursor	L	138	
7	Red blood cell precursor	L	183	157
7	Late red blood cell precursor	L	128	
7	Late red blood cell precursor	L	199	
7	Late red blood cell precursor	L	216	181
7	Reticulocyte	L	242	
7	Reticulocyte	L	160	201

7	Red blood cell	L	194	
7	Red blood cell	L	152	
7	Red blood cell	L	198	181.3
7	Macrophage	L	151	
7	Macrophage	L	120	
7	Macrophage	L	138	136.3
8	Red blood cell precursor	H	114	114
8	Latish red blood cell precursor	H	119	119
8	Late red blood cell precursor	H	84	
8	Late red blood cell precursor	H	83	83.5
8	Late red blood cell precursor/Reticulocyte	H	109	
8	Late red blood cell precursor/Reticulocyte	H	118	113.5
8	Reticulocyte/Red blood cell	H	111	111
8	Red blood cell	H	111	
8	Red blood cell	H	120	115.5
8	Macrophage	H	77	
8	Macrophage	H	52	
8	Macrophage	H	70	66.3
8	Red blood cell precursor	L	179	
8	Red blood cell precursor	L	235	207
8	Latish red blood cell precursor	L	263	263
8	Reticulocyte	L	304	304
8	Reticulocyte/Red blood cell	L	355	
8	Reticulocyte/Red blood cell	L	189	
8	Reticulocyte/Red blood cell	L	221	255
8	Red blood cell	L	308	
8	Red blood cell	L	235	
8	Red blood cell	L	223	255.3
8	Macrophage	L	98	
8	Macrophage	L	45	
8	Macrophage	L	62	
8	Macrophage	L	74	69.8
9	Red blood cell precursor	H	230	
9	Red blood cell precursor	H	321	275.5
9	Late red blood cell precursor	H	232	
9	Late red blood cell precursor	H	256	
9	Late red blood cell precursor	H	283	257
9	Reticulocyte	H	219	
9	Reticulocyte	H	250	
9	Reticulocyte	H	294	254.3
9	Red blood cell	H	281	
9	Red blood cell	H	273	277
9	Macrophage	H	114	
9	Macrophage	H	154	
9	Macrophage	H	183	
9	Macrophage	H	171	
9	Macrophage	H	181	160.6
9	Red blood cell precursor	L	194	
9	Red blood cell precursor	L	211	202.5
9	Latish red blood cell precursor	L	372	372
9	Late red blood cell precursor	L	236	
9	Late red blood cell precursor	L	237	236.5
9	Reticulocyte	L	334	
9	Reticulocyte	L	272	
9	Reticulocyte	L	275	

9	Reticulocyte	L	270	287.8
9	Red blood cell	L	254	
9	Red blood cell	L	269	
9	Red blood cell	L	211	244.7
9	Macrophage	L	152	
9	Macrophage	L	165	
9	Macrophage	L	72	129.7
10	Red blood cell precursor	H	175	
10	Red blood cell precursor	H	84	
10	Red blood cell precursor	H	175	144.7
10	Latish red blood cell precursor	H	138	
10	Latish red blood cell precursor	H	164	151
10	Reticulocyte	H	300	
10	Reticulocyte	H	93	196.5
10	Red blood cell	H	249	
10	Red blood cell	H	390	
10	Red blood cell	H	356	
10	Red blood cell	H	429	356
10	Macrophage	H	66	
10	Macrophage	H	86	
10	Macrophage	H	134	95.3
10	Red blood cell precursor	L	221	
10	Red blood cell precursor	L	185	
10	Red blood cell precursor	L	211	205.7
10	Late red blood cell precursor	L	258	258
10	Reticulocyte	L	260	
10	Reticulocyte	L	220	240
10	Reticulocyte/Red blood cell	L	258	258
10	Red blood cell	L	209	
10	Red blood cell	L	227	218
10	Macrophage	L	131	
10	Macrophage	L	112	
10	Macrophage	L	208	150.3
12	Red blood cell precursor	H	90	
12	Red blood cell precursor	H	76	83
12	Late red blood cell precursor	H	80	
12	Late red blood cell precursor	H	50	65
12	Late red blood cell precursor/Reticulocyte	H	85	85
12	Reticulocyte	H	78	
12	Reticulocyte	H	68	
12	Reticulocyte	H	63	
12	Reticulocyte	H	71	
12	Reticulocyte	H	64	68.8
12	Reticulocyte/Red blood cell	H	56	
12	Reticulocyte/Red blood cell	H	82	69
12	Red blood cell	H	53	
12	Red blood cell	H	68	60.5
12	Macrophage	H	30	
12	Macrophage	H	24	
12	Macrophage	H	33	29
12	Red blood cell precursor	L	125	
12	Red blood cell precursor	L	151	
12	Red blood cell precursor	L	132	136
12	Late red blood cell precursor	L	136	136
12	Late red blood cell precursor/Reticulocyte	L	123	123

12	Reticulocyte	L	159	
12	Reticulocyte	L	143	151
12	Reticulocyte/Red blood cell	L	186	186
12	Red blood cell	L	156	156
12	Macrophage	L	91	
12	Macrophage	L	68	
12	Macrophage	L	67	75.3
13	Red blood cell precursor	H	248	
13	Red blood cell precursor	H	115	181.5
13	Late red blood cell precursor	H	102	102
13	Reticulocyte	H	94	
13	Reticulocyte	H	183	
13	Reticulocyte	H	119	
13	Reticulocyte	H	176	143
13	Red blood cell	H	167	
13	Red blood cell	H	132	
13	Red blood cell	H	118	
13	Red blood cell	H	131	
13	Red blood cell	H	129	135.4
13	Macrophage	H	73	
13	Macrophage	H	56	
13	Macrophage	H	56	
13	Macrophage	H	61	61.5
13	Red blood cell precursor	L	186	
13	Red blood cell precursor	L	222	204
13	Late red blood cell precursor	L	184	
13	Late red blood cell precursor	L	161	172.5
13	Reticulocyte	L	168	
13	Reticulocyte	L	139	153.5
13	Reticulocyte/Red blood cell	L	169	169
13	Red blood cell	L	238	
13	Red blood cell	L	248	243
13	Macrophage	L	148	
13	Macrophage	L	158	
13	Macrophage	L	140	148.7
14	Red blood cell precursor	H	202	
14	Red blood cell precursor	H	132	
14	Red blood cell precursor	H	188	174
14	Late red blood cell precursor	H	161	161
14	Reticulocyte	H	222	
14	Reticulocyte	H	126	
14	Reticulocyte	H	132	
14	Reticulocyte	H	235	
14	Reticulocyte	H	200	
14	Reticulocyte	H	233	
14	Reticulocyte	H	238	
14	Reticulocyte	H	279	208.1
14	Reticulocyte/Red blood cell	H	99	99
14	Red blood cell	H	170	
14	Red blood cell	H	145	
14	Red blood cell	H	179	
14	Red blood cell	H	202	
14	Red blood cell	H	139	167
14	Macrophage	H	59	
14	Macrophage	H	55	

14	Macrophage	H	69	61
14	Red blood cell precursor	L	129	
14	Red blood cell precursor	L	112	
14	Red blood cell precursor	L	127	122.7
14	Late red blood cell precursor	L	121	121
14	Late red blood cell precursor/Reticulocyte	L	107	107
14	Reticulocyte	L	135	
14	Reticulocyte	L	139	137
14	Red blood cell	L	136	
14	Red blood cell	L	123	
14	Red blood cell	L	161	
14	Red blood cell	L	196	154
14	Macrophage	L	113	
14	Macrophage	L	115	
14	Macrophage	L	127	118.3
15	Red blood cell precursor	H	68	
15	Red blood cell precursor	H	65	
15	Red blood cell precursor	H	59	64
15	Late red blood cell precursor	H	71	
15	Late red blood cell precursor	H	90	
15	Late red blood cell precursor	H	141	100.7
15	Reticulocyte	H	90	
15	Reticulocyte	H	66	
15	Reticulocyte	H	116	90.7
15	Red blood cell	H	72	
15	Red blood cell	H	108	90
15	Macrophage	H	40	
15	Macrophage	H	46	
15	Macrophage	H	38	
15	Macrophage	H	43	41.8
15	Red blood cell precursor	L	195	
15	Red blood cell precursor	L	216	
15	Red blood cell precursor	L	194	201.7
15	Late red blood cell precursor	L	194	
15	Late red blood cell precursor	L	188	
15	Late red blood cell precursor	L	156	179.3
15	Reticulocyte	L	210	
15	Reticulocyte	L	222	
15	Reticulocyte	L	158	196.7
15	Reticulocyte/Red blood cell	L	154	
15	Reticulocyte/Red blood cell	L	182	168
15	Red blood cell	L	212	212
15	Macrophage	L	137	
15	Macrophage	L	105	
15	Macrophage	L	139	
15	Macrophage	L	125	126.5
16	Red blood cell precursor	H	118	
16	Red blood cell precursor	H	167	142.5
16	Reticulocyte	H	101	
16	Reticulocyte	H	68	
16	Reticulocyte	H	132	
16	Reticulocyte	H	120	
16	Reticulocyte	H	106	105.4
16	Red blood cell	H	109	
16	Red blood cell	H	105	

16	Red blood cell	H	100	104.7
16	Macrophage	H	40	
16	Macrophage	H	46	
16	Macrophage	H	111	65.7
16	Red blood cell precursor	L	255	
16	Red blood cell precursor	L	225	240
16	Latish red blood cell precursor	L	189	
16	Latish red blood cell precursor	L	180	184.5
16	Late red blood cell precursor	L	243	243
16	Late red blood cell precursor/Reticulocyte	L	153	
16	Late red blood cell precursor/Reticulocyte	L	222	187.5
16	Reticulocyte	L	176	
16	Reticulocyte	L	192	
16	Reticulocyte	L	186	184.7
16	Reticulocyte/Red blood cell	L	164	
16	Reticulocyte/Red blood cell	L	252	208
16	Red blood cell	L	171	
16	Red blood cell	L	189	180
16	Macrophage	L	122	
16	Macrophage	L	132	
16	Macrophage	L	119	124.3
17	Red blood cell precursor	H	205	
17	Red blood cell precursor	H	135	170
17	Late red blood cell precursor	H	120	
17	Late red blood cell precursor	H	195	157.5
17	Late red blood cell precursor/Reticulocyte	H	189	189
17	Reticulocyte	H	167	167
17	Red blood cell	H	144	
17	Red blood cell	H	157	150.5
17	Macrophage	H	115	
17	Macrophage	H	112	
17	Macrophage	H	151	126
17	Red blood cell precursor	L	159	
17	Red blood cell precursor	L	189	
17	Red blood cell precursor	L	138	162
17	Late red blood cell precursor	L	210	
17	Late red blood cell precursor	L	171	190.5
17	Reticulocyte	L	154	
17	Reticulocyte	L	207	180.5
17	Red blood cell	L	174	
17	Red blood cell	L	233	203.5
17	Macrophage	L	126	
17	Macrophage	L	117	
17	Macrophage	L	89	
17	Macrophage	L	145	119.3
18	Red blood cell precursor	H	69	
18	Red blood cell precursor	H	100	
18	Red blood cell precursor	H	62	77
18	Late red blood cell precursor	H	72	72
18	Reticulocyte	H	124	
18	Reticulocyte	H	80	
18	Reticulocyte	H	113	105.7
18	Red blood cell	H	88	
18	Red blood cell	H	117	
18	Red blood cell	H	78	94.3

18	Macrophage	H	88	
18	Macrophage	H	57	
18	Macrophage	H	48	64.3
18	Red blood cell precursor	L	121	
18	Red blood cell precursor	L	128	
18	Red blood cell precursor	L	150	133
18	Late red blood cell precursor	L	122	
18	Late red blood cell precursor	L	203	162.5
18	Late red blood cell precursor/Reticulocyte	L	224	224
18	Reticulocyte	L	188	
18	Reticulocyte	L	206	197
18	Red blood cell	L	209	
18	Red blood cell	L	303	
18	Red blood cell	L	238	250
18	Macrophage	L	100	
18	Macrophage	L	109	
18	Macrophage	L	100	103
19	Red blood cell precursor	H	105	
19	Red blood cell precursor	H	142	123.5
19	Late red blood cell precursor	H	95	
19	Late red blood cell precursor	H	114	104.5
19	Reticulocyte	H	102	102
19	Reticulocyte/Red blood cell	H	86	
19	Reticulocyte/Red blood cell	H	142	
19	Reticulocyte/Red blood cell	H	119	115.7
19	Red blood cell	H	145	
19	Red blood cell	H	128	
19	Red blood cell	H	136	136.3
19	Macrophage	H	124	
19	Macrophage	H	126	
19	Macrophage	H	113	
19	Macrophage	H	200	140.8
19	Red blood cell precursor	L	125	
19	Red blood cell precursor	L	184	154.5
19	Late red blood cell precursor	L	651	
19	Late red blood cell precursor	L	314	482.5
19	Late red blood cell precursor/Reticulocyte	L	157	157
19	Reticulocyte	L	260	260
19	Reticulocyte/Red blood cell	L	315	
19	Reticulocyte/Red blood cell	L	247	
19	Reticulocyte/Red blood cell	L	209	257
19	Red blood cell	L	327	
19	Red blood cell	L	222	274.5
19	Macrophage	L	163	
19	Macrophage	L	155	
19	Macrophage	L	128	148.7
20	Red blood cell precursor	H	46	
20	Red blood cell precursor	H	53	
20	Red blood cell precursor	H	56	51.7
20	Latish red blood cell precursor	H	53	
20	Latish red blood cell precursor	H	62	57.5
20	Late red blood cell precursor	H	142	142
20	Reticulocyte	H	82	
20	Reticulocyte	H	62	
20	Reticulocyte	H	58	67.3

20	Reticulocyte/Red blood cell	H	70	70
20	Red blood cell	H	63	
20	Red blood cell	H	73	68
20	Macrophage	H	42	
20	Macrophage	H	33	37.5
20	Red blood cell precursor	L	114	
20	Red blood cell precursor	L	106	
20	Red blood cell precursor	L	105	108.3
20	Latish red blood cell precursor	L	128	128
20	Late red blood cell precursor	L	103	
20	Late red blood cell precursor	L	168	
20	Late red blood cell precursor	L	110	127
20	Reticulocyte	L	151	151
20	Reticulocyte/Red blood cell	L	117	
20	Reticulocyte/Red blood cell	L	122	119.5
20	Red blood cell	L	172	
20	Red blood cell	L	170	171
20	Macrophage	L	108	
20	Macrophage	L	126	
20	Macrophage	L	89	107.7
21	Red blood cell precursor	H	93	
21	Red blood cell precursor	H	103	98
21	Late red blood cell precursor	H	124	
21	Late red blood cell precursor	H	92	108
21	Reticulocyte	H	105	
21	Reticulocyte	H	114	
21	Reticulocyte	H	65	94.7
21	Reticulocyte/Red blood cell	H	82	82
21	Red blood cell	H	71	
21	Red blood cell	H	96	83.5
21	Macrophage	H	100	
21	Macrophage	H	106	
21	Macrophage	H	84	96.7
21	Red blood cell precursor	L	146	
21	Red blood cell precursor	L	95	120.5
21	Latish red blood cell precursor	L	129	
21	Latish red blood cell precursor	L	135	132
21	Late red blood cell precursor	L	218	218
21	Late red blood cell precursor/Reticulocyte	L	154	154
21	Reticulocyte	L	118	
21	Reticulocyte	L	94	
21	Reticulocyte	L	244	152
21	Red blood cell	L	117	
21	Red blood cell	L	141	129
21	Macrophage	L	67	
21	Macrophage	L	104	85.5
22	Red blood cell precursor	H	108	
22	Red blood cell precursor	H	110	109
22	Late red blood cell precursor	H	89	
22	Late red blood cell precursor	H	121	105
22	Reticulocyte	H	128	128
22	Reticulocyte/Red blood cell	H	100	100
22	Red blood cell	H	122	
22	Red blood cell	H	174	
22	Red blood cell	H	87	

22	Red blood cell	H	131	128.5
22	Macrophage	H	112	
22	Macrophage	H	118	
22	Macrophage	H	100	110
22	Red blood cell precursor	L	205	
22	Red blood cell precursor	L	119	162
22	Latish red blood cell precursor	L	136	136
22	Late red blood cell precursor	L	119	119
22	Reticulocyte	L	262	
22	Reticulocyte	L	142	
22	Reticulocyte	L	136	180
22	Red blood cell	L	137	
22	Red blood cell	L	141	
22	Red blood cell	L	208	162
22	Macrophage	L	103	
22	Macrophage	L	86	
22	Macrophage	L	106	
22	Macrophage	L	83	94.5
24	Red blood cell precursor	H	85	
24	Red blood cell precursor	H	83	
24	Red blood cell precursor	H	62	76.7
24	Late red blood cell precursor	H	73	
24	Late red blood cell precursor	H	81	77
24	Reticulocyte	H	95	
24	Reticulocyte	H	61	
24	Reticulocyte	H	104	
24	Reticulocyte	H	129	97.3
24	Red blood cell	H	76	
24	Red blood cell	H	72	
24	Red blood cell	H	105	
24	Red blood cell	H	109	90.5
24	Macrophage	H	52	
24	Macrophage	H	54	
24	Macrophage	H	23	
24	Macrophage	H	45	43.5
24	Red blood cell precursor	L	125	125
24	Late red blood cell precursor	L	148	148
24	Reticulocyte	L	109	
24	Reticulocyte	L	122	
24	Reticulocyte	L	129	120
24	Reticulocyte/Red blood cell	L	135	135
24	Red blood cell	L	179	
24	Red blood cell	L	127	153
24	Macrophage	L	45	
24	Macrophage	L	60	
24	Macrophage	L	68	57.7
25	Red blood cell precursor	H	93	
25	Red blood cell precursor	H	55	74
25	Late red blood cell precursor	H	61	
25	Late red blood cell precursor	H	53	57
25	Reticulocyte	H	66	
25	Reticulocyte	H	84	
25	Reticulocyte	H	81	
25	Reticulocyte	H	82	78.3
25	Red blood cell	H	98	

25	Red blood cell	H	70	
25	Red blood cell	H	99	89
25	Macrophage	H	55	
25	Macrophage	H	34	
25	Macrophage	H	92	60.3
25	Red blood cell precursor	L	115	
25	Red blood cell precursor	L	167	
25	Red blood cell precursor	L	182	154.7
25	Late red blood cell precursor	L	109	
25	Late red blood cell precursor	L	246	177.5
25	Reticulocyte	L	142	
25	Reticulocyte	L	105	
25	Reticulocyte	L	119	122
25	Red blood cell	L	181	
25	Red blood cell	L	190	
25	Red blood cell	L	158	176.3
25	Macrophage	L	132	
25	Macrophage	L	151	
25	Macrophage	L	124	
25	Macrophage	L	114	
25	Macrophage	L	98	123.8
26	Red blood cell precursor	H	68	
26	Red blood cell precursor	H	96	
26	Red blood cell precursor	H	118	
26	Red blood cell precursor	H	82	91
26	Late red blood cell precursor	H	92	92
26	Reticulocyte	H	97	
26	Reticulocyte	H	94	95.5
26	Red blood cell	H	80	
26	Red blood cell	H	157	
26	Red blood cell	H	117	118
26	Macrophage	H	53	
26	Macrophage	H	65	
26	Macrophage	H	75	64.3
26	Red blood cell precursor	L	394	
26	Red blood cell precursor	L	295	344.5
26	Latish red blood cell precursor	L	404	404
26	Late red blood cell precursor	L	289	
26	Late red blood cell precursor	L	265	277
26	Reticulocyte	L	329	
26	Reticulocyte	L	340	334.5
26	Red blood cell	L	312	
26	Red blood cell	L	431	371.5
26	Macrophage	L	200	
26	Macrophage	L	228	
26	Macrophage	L	142	190
27	Red blood cell precursor	H	92	
27	Red blood cell precursor	H	136	114
27	Late red blood cell precursor	H	119	
27	Late red blood cell precursor	H	108	113.5
27	Reticulocyte	H	60	
27	Reticulocyte	H	117	
27	Reticulocyte	H	124	100.3
27	Reticulocyte/Red blood cell	H	100	100
27	Red blood cell	H	118	118

27	Macrophage	H	86	
27	Macrophage	H	71	
27	Macrophage	H	72	76.3
27	Red blood cell precursor	L	210	
27	Red blood cell precursor	L	243	
27	Red blood cell precursor	L	177	210
27	Late red blood cell precursor	L	192	192
27	Reticulocyte	L	190	
27	Reticulocyte	L	212	201
27	Reticulocyte/Red blood cell	L	118	
27	Reticulocyte/Red blood cell	L	276	197
27	Red blood cell	L	206	
27	Red blood cell	L	150	178
27	Macrophage	L	81	
27	Macrophage	L	156	
27	Macrophage	L	140	
27	Macrophage	L	95	118
28	Latish red blood cell precursor	H	160	
28	Latish red blood cell precursor	H	83	
28	Latish red blood cell precursor	H	130	
28	Latish red blood cell precursor	H	126	124.8
28	Late red blood cell precursor	H	148	148
28	Reticulocyte	H	140	
28	Reticulocyte	H	118	
28	Reticulocyte	H	136	131.3
28	Red blood cell	H	143	
28	Red blood cell	H	86	114.5
28	Macrophage	H	55	
28	Macrophage	H	74	
28	Macrophage	H	47	58.7
28	Red blood cell precursor	L	300	
28	Red blood cell precursor	L	403	351.5
28	Late red blood cell precursor	L	385	385
28	Reticulocyte	L	392	392
28	Reticulocyte/Red blood cell	L	365	
28	Reticulocyte/Red blood cell	L	454	
28	Reticulocyte/Red blood cell	L	502	440.3
28	Red blood cell	L	348	
28	Red blood cell	L	440	394
28	Macrophage	L	194	
28	Macrophage	L	298	
28	Macrophage	L	199	230.3
29	Red blood cell precursor	H	171	171
29	Latish red blood cell precursor	H	177	177
29	Late red blood cell precursor	H	111	111
29	Reticulocyte	H	102	102
29	Reticulocyte/Red blood cell	H	82	82
29	Red blood cell	H	183	
29	Red blood cell	H	216	
29	Red blood cell	H	63	154
29	Macrophage	H	94	
29	Macrophage	H	35	64.5
29	Red blood cell precursor	L	184	184
29	Late red blood cell precursor/Reticulocyte	L	351	
29	Late red blood cell precursor/Reticulocyte	L	365	

29	Late red blood cell precursor/Reticulocyte	L	240	318.7
29	Reticulocyte	L	320	320
29	Reticulocyte/Red blood cell	L	169	169
29	Red blood cell	L	312	312
29	Macrophage	L	208	
29	Macrophage	L	166	
29	Macrophage	L	196	190
30	Red blood cell precursor	H	82	
30	Red blood cell precursor	H	86	
30	Red blood cell precursor	H	88	
30	Red blood cell precursor	H	75	82.8
30	Late red blood cell precursor	H	138	
30	Late red blood cell precursor	H	112	125
30	Reticulocyte/Red blood cell	H	116	
30	Reticulocyte/Red blood cell	H	127	121.5
30	Red blood cell	H	98	
30	Red blood cell	H	116	
30	Red blood cell	H	108	107.3
30	Macrophage	H	63	
30	Macrophage	H	46	54.5
30	Red blood cell precursor	L	388	
30	Red blood cell precursor	L	295	341.5
30	Late red blood cell precursor	L	327	
30	Late red blood cell precursor	L	211	269
30	Reticulocyte	L	369	
30	Reticulocyte	L	363	366
30	Reticulocyte/Red blood cell	L	373	373
30	Red blood cell	L	313	
30	Red blood cell	L	562	437.5
30	Macrophage	L	169	
30	Macrophage	L	164	
30	Macrophage	L	166	166.3
32	Red blood cell precursor	H	107	
32	Red blood cell precursor	H	108	
32	Red blood cell precursor	H	108	107.7
32	Late red blood cell precursor	H	99	
32	Late red blood cell precursor	H	113	106
32	Reticulocyte	H	96	
32	Reticulocyte	H	132	
32	Reticulocyte	H	116	114.7
32	Red blood cell	H	106	
32	Red blood cell	H	90	98
32	Macrophage	H	79	
32	Macrophage	H	42	
32	Macrophage	H	63	61.3
32	Red blood cell precursor	L	265	
32	Red blood cell precursor	L	284	
32	Red blood cell precursor	L	254	267.7
32	Reticulocyte	L	271	
32	Reticulocyte	L	181	226
32	Reticulocyte/Red blood cell	L	250	
32	Reticulocyte/Red blood cell	L	297	273.5
32	Red blood cell	L	263	
32	Red blood cell	L	288	275.5
32	Macrophage	L	103	

32	Macrophage	L	93	
32	Macrophage	L	106	100.7
33	Red blood cell precursor	H	112	
33	Red blood cell precursor	H	84	
33	Red blood cell precursor	H	90	95.3
33	Late red blood cell precursor	H	102	
33	Late red blood cell precursor	H	115	
33	Late red blood cell precursor	H	96	104.3
33	Reticulocyte	H	101	
33	Reticulocyte	H	110	
33	Reticulocyte	H	85	98.7
33	Reticulocyte/Red blood cell	H	117	117
33	Red blood cell	H	104	104
33	Macrophage	H	68	
33	Macrophage	H	113	
33	Macrophage	H	119	
33	Macrophage	H	134	
33	Macrophage	H	81	
33	Macrophage	H	53	
33	Macrophage	H	75	91.9
33	Red blood cell precursor	L	284	
33	Red blood cell precursor	L	237	
33	Red blood cell precursor	L	254	
33	Red blood cell precursor	L	183	239.5
33	Latish red blood cell precursor	L	305	305
33	Late red blood cell precursor	L	190	190
33	Reticulocyte	L	407	
33	Reticulocyte	L	244	
33	Reticulocyte	L	242	297.7
33	Red blood cell	L	330	
33	Red blood cell	L	291	310.5
33	Macrophage	L	156	
33	Macrophage	L	166	
33	Macrophage	L	134	152
34	Red blood cell precursor	H	66	
34	Red blood cell precursor	H	45	
34	Red blood cell precursor	H	52	54.3
34	Latish red blood cell precursor	H	73	73
34	Late red blood cell precursor	H	63	63
34	Reticulocyte	H	81	
34	Reticulocyte	H	64	72.5
34	Reticulocyte/Red blood cell	H	79	79
34	Red blood cell	H	72	
34	Red blood cell	H	50	61
34	Macrophage	H	41	
34	Macrophage	H	49	
34	Macrophage	H	45	45
34	Red blood cell precursor	L	234	
34	Red blood cell precursor	L	247	240.5
34	Late red blood cell precursor	L	270	
34	Late red blood cell precursor	L	160	
34	Late red blood cell precursor	L	167	199
34	Reticulocyte	L	170	170
34	Red blood cell	L	210	
34	Red blood cell	L	297	

34	Red blood cell	L	254	253.7
34	Macrophage	L	167	
34	Macrophage	L	170	
34	Macrophage	L	154	163.7
35	Red blood cell precursor	H	138	
35	Red blood cell precursor	H	145	141.5
35	Latish red blood cell precursor	H	125	125
35	Late red blood cell precursor	H	147	147
35	Reticulocyte	H	115	
35	Reticulocyte	H	156	135.5
35	Reticulocyte/Red blood cell	H	144	
35	Reticulocyte/Red blood cell	H	138	141
35	Red blood cell	H	122	
35	Red blood cell	H	112	
35	Red blood cell	H	124	119.3
35	Macrophage	H	46	
35	Macrophage	H	57	
35	Macrophage	H	60	54.3
35	Red blood cell precursor	L	376	
35	Red blood cell precursor	L	315	345.5
35	Reticulocyte	L	177	
35	Reticulocyte	L	334	255.5
35	Reticulocyte/Red blood cell	L	365	365
35	Red blood cell	L	295	
35	Red blood cell	L	354	
35	Red blood cell	L	410	
35	Red blood cell	L	395	363.5
35	Macrophage	L	141	
35	Macrophage	L	140	
35	Macrophage	L	131	137.3
36	Red blood cell precursor	H	128	
36	Red blood cell precursor	H	91	
36	Red blood cell precursor	H	83	100.7
36	Late red blood cell precursor	H	116	116
36	Late red blood cell precursor/Reticulocyte	H	190	190
36	Reticulocyte	H	96	96
36	Reticulocyte/Red blood cell	H	108	108
36	Red blood cell	H	155	
36	Red blood cell	H	92	123.5
36	Macrophage	H	48	
36	Macrophage	H	64	
36	Macrophage	H	62	58
36	Red blood cell precursor	L	176	
36	Red blood cell precursor	L	282	
36	Red blood cell precursor	L	276	244.7
36	Late red blood cell precursor	L	234	
36	Late red blood cell precursor	L	210	222
36	Reticulocyte	L	267	
36	Reticulocyte	L	348	307.5
36	Reticulocyte/Red blood cell	L	348	348
36	Red blood cell	L	205	
36	Red blood cell	L	248	226.5
36	Macrophage	L	82	
36	Macrophage	L	18	
36	Macrophage	L	78	59.3

37	Red blood cell precursor	H	166	
37	Red blood cell precursor	H	83	124.5
37	Late red blood cell precursor	H	135	
37	Late red blood cell precursor	H	222	178.5
37	Reticulocyte	H	103	
37	Reticulocyte	H	70	86.5
37	Reticulocyte/Red blood cell	H	144	144
37	Red blood cell	H	151	
37	Red blood cell	H	193	
37	Red blood cell	H	137	160.3
37	Macrophage	H	64	
37	Macrophage	H	53	
37	Macrophage	H	62	59.7
37	Red blood cell precursor	L	182	182
37	Late red blood cell precursor	L	204	
37	Late red blood cell precursor	L	128	166
37	Late red blood cell precursor/Reticulocyte	L	131	131
37	Reticulocyte	L	155	
37	Reticulocyte	L	299	
37	Reticulocyte	L	123	192.3
37	Red blood cell	L	204	
37	Red blood cell	L	137	170.5
37	Macrophage	L	115	
37	Macrophage	L	88	
37	Macrophage	L	117	106.7
38	Red blood cell precursor	H	157	
38	Red blood cell precursor	H	151	154
38	Late red blood cell precursor	H	87	87
38	Late red blood cell precursor/Reticulocyte	H	156	156
38	Reticulocyte	H	175	
38	Reticulocyte	H	144	
38	Reticulocyte	H	206	175
38	Red blood cell	H	135	
38	Red blood cell	H	180	157.5
38	Macrophage	H	52	
38	Macrophage	H	44	
38	Macrophage	H	114	70
38	Red blood cell precursor	L	147	147
38	Late red blood cell precursor	L	99	99
38	Late red blood cell precursor/Reticulocyte	L	227	227
38	Reticulocyte	L	288	
38	Reticulocyte	L	254	
38	Reticulocyte	L	141	227.7
38	Red blood cell	L	273	
38	Red blood cell	L	279	276
38	Macrophage	L	88	
38	Macrophage	L	81	
38	Macrophage	L	79	
38	Macrophage	L	123	92.8
39	Red blood cell precursor	H	57	
39	Red blood cell precursor	H	51	
39	Red blood cell precursor	H	79	62.3
39	Late red blood cell precursor/Reticulocyte	H	68	
39	Late red blood cell precursor/Reticulocyte	H	66	67
39	Reticulocyte	H	52	

39	Reticulocyte	H	62	57
39	Red blood cell	H	48	
39	Red blood cell	H	50	49
39	Macrophage	H	61	
39	Macrophage	H	44	
39	Macrophage	H	50	
39	Macrophage	H	112	66.8
39	Red blood cell precursor	L	249	
39	Red blood cell precursor	L	165	207
39	Late red blood cell precursor	L	152	
39	Late red blood cell precursor	L	189	170.5
39	Reticulocyte	L	217	
39	Reticulocyte	L	224	220.5
39	Red blood cell	L	266	
39	Red blood cell	L	245	
39	Red blood cell	L	280	263.7
39	Macrophage	L	67	
39	Macrophage	L	75	
39	Macrophage	L	97	79.7
40	Red blood cell precursor	H	93	
40	Red blood cell precursor	H	158	125.5
40	Late red blood cell precursor	H	182	
40	Late red blood cell precursor	H	122	
40	Late red blood cell precursor	H	171	158.3
40	Reticulocyte	H	127	
40	Reticulocyte	H	188	
40	Reticulocyte	H	240	185
40	Red blood cell	H	147	
40	Red blood cell	H	133	
40	Red blood cell	H	112	
40	Red blood cell	H	125	129.3
40	Macrophage	H	148	
40	Macrophage	H	178	
40	Macrophage	H	157	161
40	Red blood cell precursor	L	125	
40	Red blood cell precursor	L	158	
40	Red blood cell precursor	L	166	149.7
40	Late red blood cell precursor/Reticulocyte	L	119	119
40	Reticulocyte	L	128	
40	Reticulocyte	L	126	127
40	Reticulocyte/Red blood cell	L	197	197
40	Red blood cell	L	202	202
40	Macrophage	L	127	
40	Macrophage	L	103	115
41	Red blood cell precursor	H	98	
41	Red blood cell precursor	H	220	159
41	Late red blood cell precursor	H	171	171
41	Reticulocyte	H	212	
41	Reticulocyte	H	125	
41	Reticulocyte	H	128	155
41	Reticulocyte/Red blood cell	H	121	121
41	Red blood cell	H	111	
41	Red blood cell	H	114	
41	Red blood cell	H	111	112
41	Macrophage	H	96	

41	Macrophage	H	83	
41	Macrophage	H	102	93.7
41	Red blood cell precursor	L	236	
41	Red blood cell precursor	L	185	
41	Red blood cell precursor	L	212	211
41	Latish red blood cell precursor	L	219	219
41	Late red blood cell precursor/Reticulocyte	L	239	239
41	Reticulocyte	L	240	
41	Reticulocyte	L	241	240.5
41	Red blood cell	L	218	
41	Red blood cell	L	241	229.5
41	Macrophage	L	137	
41	Macrophage	L	90	113.5
42	Red blood cell precursor	H	84	
42	Red blood cell precursor	H	155	119.5
42	Late red blood cell precursor	H	127	
42	Late red blood cell precursor	H	171	149
42	Late red blood cell precursor/Reticulocyte	H	131	131
42	Reticulocyte	H	90	
42	Reticulocyte	H	187	
42	Reticulocyte	H	110	
42	Reticulocyte	H	98	121.3
42	Reticulocyte/Red blood cell	H	152	152
42	Red blood cell	H	137	
42	Red blood cell	H	127	
42	Red blood cell	H	95	119.7
42	Macrophage	H	79	
42	Macrophage	H	188	133.5
42	Red blood cell precursor	L	160	
42	Red blood cell precursor	L	176	
42	Red blood cell precursor	L	309	215
42	Late red blood cell precursor	L	184	184
42	Reticulocyte	L	263	
42	Reticulocyte	L	202	
42	Reticulocyte	L	215	226.7
42	Red blood cell	L	160	
42	Red blood cell	L	224	
42	Red blood cell	L	159	
42	Red blood cell	L	194	
42	Red blood cell	L	205	
42	Red blood cell	L	199	190.2
42	Macrophage	L	170	
42	Macrophage	L	134	
42	Macrophage	L	149	151
43	Red blood cell precursor	H	86	86
43	Late red blood cell precursor	H	90	
43	Late red blood cell precursor	H	88	89
43	Reticulocyte	H	160	
43	Reticulocyte	H	129	
43	Reticulocyte	H	128	139
43	Red blood cell	H	73	
43	Red blood cell	H	90	
43	Red blood cell	H	109	
43	Red blood cell	H	121	98.3
43	Macrophage	H	52	

43	Macrophage	H	87	
43	Macrophage	H	61	66.7
43	Red blood cell precursor	L	343	
43	Red blood cell precursor	L	278	
43	Red blood cell precursor	L	289	303.3
43	Late red blood cell precursor	L	396	
43	Late red blood cell precursor	L	314	355
43	Reticulocyte	L	383	
43	Reticulocyte	L	374	
43	Reticulocyte	L	274	343.7
43	Reticulocyte/Red blood cell	L	255	
43	Reticulocyte/Red blood cell	L	310	282.5
43	Macrophage	L	65	
43	Macrophage	L	81	
43	Macrophage	L	132	92.7
44	Red blood cell precursor	H	136	
44	Red blood cell precursor	H	78	107
44	Latish red blood cell precursor	H	156	156
44	Late red blood cell precursor	H	90	90
44	Reticulocyte	H	105	
44	Reticulocyte	H	148	
44	Reticulocyte	H	213	
44	Reticulocyte	H	179	161.3
44	Reticulocyte/Red blood cell	H	150	150
44	Red blood cell	H	96	
44	Red blood cell	H	144	
44	Red blood cell	H	102	114
44	Macrophage	H	101	
44	Macrophage	H	191	
44	Macrophage	H	148	146.7
44	Red blood cell precursor	L	134	134
44	Late red blood cell precursor	L	164	
44	Late red blood cell precursor	L	188	176
44	Reticulocyte	L	155	
44	Reticulocyte	L	164	
44	Reticulocyte	L	113	
44	Reticulocyte	L	131	140.8
44	Red blood cell	L	175	
44	Red blood cell	L	157	
44	Red blood cell	L	168	
44	Red blood cell	L	196	174
44	Macrophage	L	109	
44	Macrophage	L	91	
44	Macrophage	L	87	95.7
45	Red blood cell precursor	H	191	
45	Red blood cell precursor	H	163	
45	Red blood cell precursor	H	224	192.7
45	Reticulocyte	H	329	
45	Reticulocyte	H	81	
45	Reticulocyte	H	91	
45	Reticulocyte	H	113	
45	Reticulocyte	H	127	148.2
45	Red blood cell	H	160	
45	Red blood cell	H	238	
45	Red blood cell	H	86	

45	Red blood cell	H	137	
45	Red blood cell	H	152	154.6
45	Macrophage	H	109	
45	Macrophage	H	140	
45	Macrophage	H	142	130.3
45	Red blood cell precursor	L	272	272
45	Latish red blood cell precursor	L	210	210
45	Late red blood cell precursor	L	314	314
45	Reticulocyte	L	312	312
45	Reticulocyte/Red blood cell	L	377	377
45	Red blood cell	L	246	
45	Red blood cell	L	294	270
45	Macrophage	L	79	
45	Macrophage	L	156	
45	Macrophage	L	133	122.7
46	Red blood cell precursor	H	186	
46	Red blood cell precursor	H	267	
46	Red blood cell precursor	H	268	
46	Red blood cell precursor	H	263	
46	Red blood cell precursor	H	198	236.4
46	Latish red blood cell precursor	H	240	240
46	Late red blood cell precursor	H	170	
46	Late red blood cell precursor	H	307	238.5
46	Reticulocyte	H	251	251
46	Red blood cell	H	221	
46	Red blood cell	H	166	
46	Red blood cell	H	233	
46	Red blood cell	H	234	213.5
46	Macrophage	H	161	
46	Macrophage	H	113	
46	Macrophage	H	124	132.7
46	Red blood cell precursor	L	174	174
46	Late red blood cell precursor	L	226	226
46	Reticulocyte	L	161	
46	Reticulocyte	L	245	
46	Reticulocyte	L	204	203.3
46	Reticulocyte/Red blood cell	L	189	189
46	Red blood cell	L	162	
46	Red blood cell	L	188	
46	Red blood cell	L	170	173.3
46	Macrophage	L	73	
46	Macrophage	L	91	
46	Macrophage	L	123	95.7
47	Red blood cell precursor	H	138	
47	Red blood cell precursor	H	137	137.5
47	Late red blood cell precursor	H	238	
47	Late red blood cell precursor	H	202	220
47	Reticulocyte/Red blood cell	H	114	
47	Reticulocyte/Red blood cell	H	160	137
47	Red blood cell	H	225	225
47	Macrophage	H	177	
47	Macrophage	H	191	
47	Macrophage	H	93	153.7
47	Red blood cell precursor	L	239	
47	Red blood cell precursor	L	208	223.5

47	Latish red blood cell precursor	L	262	262
47	Late red blood cell precursor	L	283	
47	Late red blood cell precursor	L	254	268.5
47	Reticulocyte	L	302	
47	Reticulocyte	L	217	259.5
47	Reticulocyte/Red blood cell	L	165	165
47	Macrophage	L	79	
47	Macrophage	L	104	91.5
48	Red blood cell precursor	H	119	
48	Red blood cell precursor	H	137	128
48	Late red blood cell precursor/Reticulocyte	H	129	129
48	Reticulocyte/Red blood cell	H	121	
48	Reticulocyte/Red blood cell	H	114	117.5
48	Red blood cell	H	180	
48	Red blood cell	H	90	
48	Red blood cell	H	99	123
48	Macrophage	H	85	
48	Macrophage	H	66	75.5
48	Red blood cell precursor	L	232	
48	Red blood cell precursor	L	162	
48	Red blood cell precursor	L	184	192.7
48	Latish red blood cell precursor	L	256	256
48	Reticulocyte	L	255	255
48	Reticulocyte/Red blood cell	L	230	
48	Reticulocyte/Red blood cell	L	275	252.5
48	Red blood cell	L	190	
48	Red blood cell	L	240	215
48	Macrophage	L	86	
48	Macrophage	L	53	
48	Macrophage	L	124	87.7
1001	Red blood cell precursor	H	77	
1001	Red blood cell precursor	H	102	89.5
1001	Latish red blood cell precursor	H	77	77
1001	Late red blood cell precursor	H	127	127
1001	Reticulocyte	H	89	
1001	Reticulocyte	H	93	
1001	Reticulocyte	H	76	
1001	Reticulocyte	H	72	82.5
1001	Reticulocyte/Red blood cell	H	92	92
1001	Red blood cell	H	70	
1001	Red blood cell	H	90	
1001	Red blood cell	H	80	80
1001	Macrophage	H	40	
1001	Macrophage	H	72	
1001	Macrophage	H	50	54
1001	Red blood cell precursor	L	118	
1001	Red blood cell precursor	L	98	108
1001	Latish red blood cell precursor	L	132	
1001	Latish red blood cell precursor	L	141	136.5
1001	Late red blood cell precursor	L	103	103
1001	Late red blood cell precursor/Reticulocyte	L	110	110
1001	Reticulocyte	L	85	85
1001	Reticulocyte/Red blood cell	L	197	197
1001	Red blood cell	L	152	
1001	Red blood cell	L	113	132.5

1001	Macrophage	L	95	
1001	Macrophage	L	88	
1001	Macrophage	L	140	107.7
1003	Red blood cell precursor	H	167	
1003	Red blood cell precursor	H	148	157.5
1003	Late red blood cell precursor	H	147	
1003	Late red blood cell precursor	H	141	144
1003	Reticulocyte	H	175	
1003	Reticulocyte	H	169	
1003	Reticulocyte	H	167	170.3
1003	Red blood cell	H	179	
1003	Red blood cell	H	193	186
1003	Macrophage	H	144	
1003	Macrophage	H	140	
1003	Macrophage	H	161	148.3
1003	Red blood cell precursor	L	120	
1003	Red blood cell precursor	L	154	137
1003	Latish red blood cell precursor	L	124	124
1003	Late red blood cell precursor	L	135	135
1003	Reticulocyte	L	189	
1003	Reticulocyte	L	179	184
1003	Red blood cell	L	172	
1003	Red blood cell	L	191	181.5
1003	Macrophage	L	152	
1003	Macrophage	L	190	
1003	Macrophage	L	201	
1003	Macrophage	L	160	175.8
1005	Red blood cell precursor	H	171	
1005	Red blood cell precursor	H	225	
1005	Red blood cell precursor	H	154	
1005	Red blood cell precursor	H	235	196.3
1005	Late red blood cell precursor	H	176	176
1005	Reticulocyte	H	197	
1005	Reticulocyte	H	200	198.5
1005	Reticulocyte/Red blood cell	H	212	212
1005	Red blood cell	H	192	
1005	Red blood cell	H	192	192
1005	Macrophage	H	133	
1005	Macrophage	H	105	
1005	Macrophage	H	91	
1005	Macrophage	H	124	113.3
1005	Red blood cell precursor	L	160	
1005	Red blood cell precursor	L	94	127
1005	Late red blood cell precursor	L	148	
1005	Late red blood cell precursor	L	163	155.5
1005	Reticulocyte	L	163	
1005	Reticulocyte	L	102	
1005	Reticulocyte	L	214	159.7
1005	Reticulocyte/Red blood cell	L	185	185
1005	Red blood cell	L	121	
1005	Red blood cell	L	124	
1005	Red blood cell	L	137	127.3
1005	Macrophage	L	149	
1005	Macrophage	L	83	
1005	Macrophage	L	128	120

1006	Red blood cell precursor	H	136	
1006	Red blood cell precursor	H	81	
1006	Red blood cell precursor	H	76	97.7
1006	Latish red blood cell precursor	H	129	
1006	Latish red blood cell precursor	H	61	95
1006	Late red blood cell precursor	H	264	
1006	Late red blood cell precursor	H	86	175
1006	Reticulocyte	H	253	
1006	Reticulocyte	H	81	167
1006	Red blood cell	H	122	
1006	Red blood cell	H	141	131.5
1006	Macrophage	H	74	
1006	Macrophage	H	70	
1006	Macrophage	H	122	88.7
1006	Red blood cell precursor	L	267	
1006	Red blood cell precursor	L	218	
1006	Red blood cell precursor	L	259	248
1006	Latish red blood cell precursor	L	308	308
1006	Late red blood cell precursor	L	233	233
1006	Late red blood cell precursor/Reticulocyte	L	318	318
1006	Reticulocyte	L	258	258
1006	Reticulocyte/Red blood cell	L	277	
1006	Reticulocyte/Red blood cell	L	350	313.5
1006	Red blood cell	L	355	355
1006	Macrophage	L	101	
1006	Macrophage	L	110	
1006	Macrophage	L	193	
1006	Macrophage	L	121	131.3
1007	Red blood cell	H	129	
1007	Red blood cell	H	121	
1007	Red blood cell	H	110	120
1007	Macrophage	H	125	
1007	Macrophage	H	137	
1007	Macrophage	H	152	138
1008	Red blood cell precursor	H	147	
1008	Red blood cell precursor	H	161	154
1008	Late red blood cell precursor	H	157	
1008	Late red blood cell precursor	H	119	138
1008	Reticulocyte	H	136	
1008	Reticulocyte	H	157	146.5
1008	Reticulocyte/Red blood cell	H	147	147
1008	Red blood cell	H	132	
1008	Red blood cell	H	132	132
1008	Macrophage	H	30	
1008	Macrophage	H	68	
1008	Macrophage	H	111	69.7
1008	Red blood cell precursor	L	223	
1008	Red blood cell precursor	L	145	
1008	Red blood cell precursor	L	249	
1008	Red blood cell precursor	L	239	
1008	Red blood cell precursor	L	156	
1008	Red blood cell precursor	L	198	
1008	Red blood cell precursor	L	227	205.3
1008	Late red blood cell precursor	L	163	163
1008	Reticulocyte	L	340	

1008	Reticulocyte	L	140	
1008	Reticulocyte	L	182	220.7
1008	Red blood cell	L	212	
1008	Red blood cell	L	247	229.5
1008	Macrophage	L	134	
1008	Macrophage	L	107	
1008	Macrophage	L	73	104.7
1010	Red blood cell precursor	H	207	
1010	Red blood cell precursor	H	195	
1010	Red blood cell precursor	H	157	
1010	Red blood cell precursor	H	188	186.8
1010	Late red blood cell precursor	H	321	
1010	Late red blood cell precursor	H	235	278
1010	Reticulocyte	H	180	180
1010	Reticulocyte/Red blood cell	H	258	258
1010	Red blood cell	H	142	
1010	Red blood cell	H	127	134.5
1010	Macrophage	H	240	
1010	Macrophage	H	267	
1010	Macrophage	H	151	219.3
1010	Red blood cell precursor	L	270	
1010	Red blood cell precursor	L	162	216
1010	Late red blood cell precursor	L	247	
1010	Late red blood cell precursor	L	237	242
1010	Reticulocyte	L	310	
1010	Reticulocyte	L	332	
1010	Reticulocyte	L	309	317
1010	Red blood cell	L	288	
1010	Red blood cell	L	272	280
1010	Macrophage	L	224	
1010	Macrophage	L	151	
1010	Macrophage	L	158	177.7

References

1) Brittenham GM, Danish EH, Harris JW. Assessment of bone marrow and body iron stores: old techniques and new technologies. Seminars in Hematology 1981; 18(3): 194-221.

2) Krause JR, Brubaker D, Kaplan S. Comparison of stainable iron in aspirated and needle-biopsy specimens of bone marrow. American Journal of Clinical Pathologists 1979; 72(1): 68-70.

3) Fong TP, Okafor LA, Thomas W Jr., Westerman MP. Stainable iron in aspirated and needle-biopsy specimens of marrow: a source of error. American Journal of Hematology 1977; 2: 47-51.

4) DePalma L. The effect of decalcification and choice of fixative on histiocytic iron in bone marrow core biopsies. Biotechnic and Histochemistry 1996; 71(2): 57-60.

5) Stuart-Smith SE, Hughes DA, Bain BJ. Are routine iron stains on bone marrow trephine biopsy specimens necessary? Journal of Clinical Pathology 2005; 58: 269-272.

CHAPTER 7

THEORETICAL BACKGROUND AND EXPERIMENTAL EVALUATION OF THE TECHNIQUE FOR ULTRASTRUCTURAL IMMUNOLOCALISATION OF THE H-SUBUNIT AND L-SUBUNIT OF FERRITIN

1) Introduction

Ferritin, the major intracellular protein responsible for the storage of iron in all cell types consists of 24 subunits of various combinations of two types, the H-subunit and the L-subunit (Chapter 1). The combination of these two subunits in the ferritin protein shell plays an important role in ferritin's iron handling capabilities. In the bone marrow, iron is differently metabolised by the cells of the erythron including erythroblasts, reticulocytes and red blood cells on the one hand, and the macrophage on the other. Furthermore, iron is shuttled between the cells of the erythron and the macrophage to support erythropoiesis. In order to investigate the role of the H-subunit and the L-subunit of ferritin in the handling of iron by cells of the bone marrow it is necessary to investigate the expression of the two subunits of ferritin at the single cell level.

Ultrastructural electron microscopy can be employed to distinguish the different cells of the bone marrow from one another and, more importantly, to localise signals generated

from the different subunits to a specific cell. In this study, ultrastructural immunolocalisation was employed to investigate the expression of the H-subunit and L-subunit of ferritin in different cell types in the bone marrow.

2) Theoretical background of the technique for the immunolocalisation of the H-subunit and L-subunit of ferritin

The technique for the immunolocalisation of the H-subunit and L-subunit of ferritin had to be developed, since this technique was not available at the University of Pretoria. A thorough background study was undertaken to assist in the development and evaluation of this technique. This chapter presents an overview of the relevant background followed by the experimental evaluation.

2.1) Preservation of bone marrow tissue and protein for immunolocalisation

Ultrastructural immunolocalisation depends on well-preserved structural detail together with intact and recognisable antigens for proper binding of the antibody. The preservation of structural detail of tissue for transmission electron microscopy involves different steps each with its own purpose. These steps include fixation, dehydration and embedding. The aim of the fixation step is to stabilise cellular organisation to such an extent that ultrastructural relations are preserved despite the subsequent rather drastic treatments of dehydration, embedding and exposure to the electron beam (1). During the process of fixation the various side-groups of proteins are linked together, either intra-molecularly or inter-molecularly, to form a meshwork of proteins, other cellular molecules and organelles. After fixation the tissue is dehydrated, since most electron microscopy resins are not miscible in water. Dehydration of the fixed tissue will result in the removal of all water molecules whereupon the tissue is infiltrated with the resin. Once complete infiltration of the resin has occurred the resin is polymerised. The tissue

is embedded in a resin suitable for cutting thin sections of no more than a 100 nm for viewing by an electron microscope. All these procedures necessary for the preparation of the tissue for ultrastructural microscopy can have deleterious effects on the antigen resulting in the loss of antibody binding. Therefore, in order to successfully immunolocalise an antigen, a compromise has to be reached between the preservation of ultrastructural detail and the retaining of antigenicity.

2.2) Ultrastructural immunolocalisation of antigens

Various factors should be taken into consideration with the immunolocalisation of an antigen. These factors include an intact antigen at the end of the preparation procedure with minimal change in antigenicity, negligible translocation of the antigen and the accessibility of the antigen to the antibody. Furthermore, should the ultrastructural detail be preserved as close to the natural situation as possible (2). For ultrastructural immunolocalisation of antigens three well characterised methods have been developed. However, each of these procedures has their own advantages and limitations. These procedures include pre-embedding immunolabelling, post-embedding immunolabelling and cryo-immunolabelling. With pre-embedding immunolabelling the tissue is fixed followed by the immunolabelling procedure before dehydration, embedding and sectioning. Limiting factors include low antibody penetration necessitating the need for permeabilising procedures with detergents. This can result in irregular labelling, since the permeabilisation step does not always bring about homogenous antibody penetration of the tissue. The permeabilisation step can also result in loss of ultrastructural detail. The advantage of pre-embedding immunolabelling is that the antigen has not been exposed to the organic solvents used in dehydration and embedding procedures before immunolabelling takes place. For post-embedding immunolabelling the immunolabelling takes place only after fixation, dehydration, embedding and sectioning. The limiting

factor with post-embedding immunolabelling is that significant changes can be caused to the antigen's structure that can result in a decrease in binding of the antibody to the antigen. The advantage of post-embedding immunolabelling is that no tissue permeabilisation step is necessary to bring about the penetration of the antibody into the tissue. The third of these methods, cryo-immunolabelling, is considered to be the method giving superior results when compared to the first two methods. Firstly, the antigen is preserved the best during cryo-treatment of the tissue since the antigen is not exposed to any of the harsh treatments before the immunolabelling step takes place. Secondly, the cryo-sections are fully penetrable to antibodies. Nevertheless, a disadvantage with cryo-immunolabelling is that the antigen may be extracted during the immunolabelling step as a result of the weak fixation and absence of embedding (3, 4).

2.3) Steps in preservation of the tissue and antigen for post-embedding immunolabelling

For the present study post-embedding immunolabelling was chosen, since pre-embedding immunolabelling is more disadvantageous for quantifying the immunolabelling due to possible in-homogenous antibody penetration and the facilities for cryo-immonolabelling were not available at the time of the study. However, any manipulation of the tissue during its processing for post-embedding immunolabelling including the fixation, dehydration and embedding procedures can result in modifications of tissue components. Proteins are extremely prone to these modifications and as a consequence the binding of antibody to antigens can be changed or even completely lost. Furthermore, these procedures can affect different antigens to different extents. Therefore, conditions for optimal immunolabelling must be evaluated, which usually is a compromise between ultrastructural preservation and retention of antigenicity (3, 5). However, there are a number of theoretical guidelines.

2.3.1) Fixation

One of the purposes of fixation is to secure the antigen where it naturally occurs. However, one of the consequences of vigorous fixation may be that the antigen is damaged or altered so that it is unrecognisable or inaccessible to antibodies (6). For optimal preservation of ultrastructure the method of choice is generally primary fixation in a glutaraldehyde (GA) solution of more than one percent followed by post-fixation with osmium tetroxide (5). However, both of these substances can have a deleterious effect on immunolabelling efficiency. Glutaraldehyde, a di-aldehyde containing two free aldehyde groups, can bind to cellular components with both of these aldehyde groups. It is by binding to cellular components, such as amino acid side-chains, with both of these aldehyde groups, that extreme cross-linking occurs bringing about good preservation of the ultrastructure, but possible loss of immunolabelling efficiency. Nevertheless, not all antigens are affected by GA, but some antigens are extremely sensitive to cross-linking by GA so that the concentration of GA has to be reduced or, in the most extreme cases, omitted entirely. A fixative containing 0.5% GA is generally suitable for a wide variety of antigens (7). It has been shown that even lower concentrations of GA (< 0.2%) allow the labelling of not only the primary or high concentration antigenic sites, but also the secondary or low concentration antigenic sites, while higher concentrations of GA (> 1%) only allow labelling of the primary sites (8). When these low concentrations of GA are used, formaldehyde (FA) is added. Formalin is not added since it contains methanol, another substance deleterious to antigens (7). FA alone preserves the ultrastructure poorly, which is most probably due to the reversibility of the majority of formaldehyde-induced cross-links (2). For optimal ultrastructure preservation this primary fixation step is followed by fixation in osmium tetroxide. Osmium tetroxide fixes cellular lipids, especially those forming part of the cell membrane. All of these lipid-rich structures are poorly preserved by GA and FA therefore osmium post-fixation compensates for this

disadvantage. However, the use of osmium tetroxide is not advised for immunolabelling techniques.

In addition to composition, exposure time and temperature of fixation can also affect the ability to immunolabel a particular antigen. It is therefore preferable to fix tissues by perfusion, but if that is not possible, fixation at cold temperatures seem to reduce tissue degradation before proper stabilisation of the tissue has occurred. By keeping the time between removal of the tissue and fixation as short as possible, further tissue decomposition can be prevented before proper fixation (7).

2.3.2) Dehydration

Dehydration by an organic solvent follows the fixation of the tissue. This is necessary since the embedding solutions are not miscible in water. The tissue is therefore dehydrated by an appropriate organic solvent before the embedding procedure. The extent of this dehydration process is important when proteins are minimally cross-linked for the subsequent immunolabelling procedures. The advantages of minimally cross-linked proteins for subsequent immunolabelling procedures are lost if room temperature, complete dehydration protocols are used. Room temperature, complete dehydration can result in extraction of the minimally cross-linked antigens. This can be prevented if either, room temperature, partial dehydration or progressively lower temperature (PLT) protocols are followed. Both these methods are probably able to reduce extraction of soluble tissue components. In addition partial dehydration could also be performed at cold temperatures. This would result in further reducing the extraction of minimally cross-linked material. Lipid retention is said to be higher with partial dehydration. It has been shown that the worst effects of ethanol dehydration occur (shrinkage and other dimensional changes) when it is in excess of 70% and that it is important to avoid the

extreme concentrations of ethanol in order to best preserve the reactivity of the tissues to antibodies (9). Disruption of protein conformation is minimised by performing dehydration at low temperatures. At the low temperatures used for PLT protocols the hydration shells around proteins may be better preserved in an organic solvent than in the corresponding solvent concentration at room temperature. The fall in the dielectric constant at progressively lower temperatures is not as marked as the corresponding fall at room temperature with the use of 100% organic solvents (8).

2.3.3) Embedding

The choice of embedding agent is important for optimal immunolabelling. For post-embedding immunolabelling procedures the hydrophilic resins such as LR White, LR Gold and Lowicryl generally give better results than the epoxy-based hydrophobic resins such as the Epon substitutes or Spurr (6, 7, 10). There are a number of factors responsible for the attainment of better immunolabelling with the hydrophilic resins. LR White is compatible with about 12% by volume of water so that partial dehydration with an organic solvent is possible. The ability of some resins to tolerate water to a lesser or greater extent may create conditions for complementing a region of polarity (or water) around molecular structures. It is these properties of the acrylic resins that could be responsible for allowing a degree of hydration to be retained within the tissues, thus increasing the chances for improvements in ultrastructure and immunoreactivity (8). Furthermore, LR White is less lipophilic than epoxides and therefore less likely to disrupt ultrastructure by extraction of especially lipids when post-fixation with osmium tetroxide is omitted (2, 6). In addition LR White does not form covalent bonds with biological material during the polymerisation procedure. This is in contrast with epoxies that form covalent bonds with biological material. The epoxies particularly form covalent bonds with proteins, resulting in co-polymerisation instead of a polymerised mixture. The

reactive epoxy groups have a great tendency to react with hydroxyl and amino groups, which are chemical side-groups present in biological macromolecules such as proteins and nucleic acids. Therefore, the bio-molecules will be part of the polymer network when embedded in epoxy resin. LR White polymerises by free radical chain polymerisation, these free radicals react with double bonds of the acrylic monomer and have no affinity for proteins and nucleic acids. Thus, bio-molecules are not incorporated into the polymer network (11).

2.3.4) Curing of the resin (polymer cross-linking)

In the present study the embedding medium of choice was LR White. Different procedures are possible for curing of LR White. Firstly, LR White can be heat cured at 50°C with complete polymerisation within 24 hours. Secondly, due to the presence of benzoyl peroxide in the LR White solution, LR White can be chemically polymerised by the addition of an accelerator. When accelerator is added to pre-cooled LR White monomer (-20°C) the mixture begins to gel after about 30 minutes and the polymerisation procedure is complete after 24 hours at -20°C (LR White remains liquid to about -20°C). However, the end of the capsules distal to the tissue always retains a small amount of un-polymerised resin. This catalytic reaction is exothermic. Therefore, to ensure dissipation of heat the capsule should be placed in a cold aluminium block with drilled holes (8). Thirdly, polymerisation of LR White is possible with exposure to UV-light. Performance of this procedure can be accomplished at different temperatures and, depending on the temperature, the time of polymerisation of the resin can be manipulated. At -20°C polymerisation is completed in seven days whereas at 4°C and 20°C polymerisation is completed in four days and eight hours, respectively (12). For all three these curing procedures there exists different advantages and drawbacks. For both

the heat and UV-light curing procedures a decrease in immunolabelling efficiency is shown for certain antigens, which may be explained by a damaging influence of the monomer on antigenic sites. It is thought that prolonged exposure to the plastic monomer may cause considerable extraction of cellular material from the tissue (9, 12). This is not the case for the rapid chemical curing procedure. However, care must be taken because this is an exothermic reaction and will give of heat – sometimes damaging antigenicity. Furthermore, the use of excessive accelerator can result in over cross-linking (9). However, it has been shown that once the tissue is fixed and dehydrated, high temperatures do not damage the tissue any more. Significant denaturation is shown to occur only at temperatures above 70°C in unfixed purified proteins compared to virtually no effect on formalin-fixed proteins (13). For the low temperature curing procedures improved preservation of fine structural details of mildly aldehyde-fixed tissues is shown, together with superior preservation of sensitive antigens (14, 15). The degree of LR White cross-linking attained with curing can be changed by the polymerisation conditions (9). In theory the lower the cross-link density of the resin, the more penetrable it will be to aqueous solutions and therefore to immunoreagents. For example, slow curing at 50°C for 24 hours prevents LR White from becoming completely cross-linked and also induces linearity in its molecular arrangement, which favours penetration by aqueous solutions (9). Due to different methods of polymerisation the extent of polymer cross-linking can be changed so as to increase the sensitivity and ease of post-embedding immunolabelling (6). Hydrophilic plastics swell in aqueous solutions and the extent to which they swell depends on the extent to which they are cross-linked. Swelling may be the means by which immunoreagents gain access to antigens in the interior of LR White sections. Re-sectioning immunolabelled sections of rapidly embedded tissue has shown that the freely diffusible reagents of the immunoperoxidase method do penetrate into LR White. This could be the reason for

the greater sensitivity of this method compared to methods making use of colloidal gold and could also account for the high electron density that the diamino benzidine (DAB) deposited in ultra-thin sections can achieve (6). Therefore, no difference in immunolabelling efficiency is seen for different curing procedures with immunogold labelling since the gold particle is too large to penetrate the sections – no matter the extent of cross-linking achieved during the curing of the resin. However, with immunoperoxidase immunolabelling, slow-heat polymerisation will generally produce greater sensitivity to antibodies (9).

2.4) Surface relief upon sectioning and exposure of the antigen

With sectioning of the embedded tissue the surface of cleavage tends to follow the areas of least resistance, e.g., the interfaces between the resin and proteins (10). This tends to release the antigens from the embedding media resulting in the antigen being available for binding to an antibody – the stronger the surface relief the better the immunolabelling. The amount of corrugation – the depth of relief – is determined by the strength of co-polymerisation between the resin and proteins. With the strength of co-polymerisation determined by the chemical nature of the resin, the temperature at which curing takes place and the characteristics of the biological material that can be influenced by the process of fixation (16). For epoxy resins, with a large amount of co-polymerisation, sectioning results in little corrugation and surface relief. This results in hiding of antigens by thin layers of resin. For LR White, sectioning can result in a surface relief of 2-6 nm, which could be as much as three times more than that for epoxies. With this increase in the surface relief depth, antigens are more exposed for recognition by an antibody (8). Curing at low temperatures possibly causes a decrease in co-polymerisation followed by an increase in the depth of corrugation and an increase in immunolabelling. With low temperatures it is possible that the hydration shells that

surround all biological macromolecules suspended in aqueous cytosol, is not completely removed. This persisting shell of organised "ice-like" water could produce a sort of insulation against co-polymerisation at low temperatures. During cleavage of the resin this interspace between the antigen and the cured resin will favour the exposure of antigenic sites (16). Furthermore, the characteristics of the biological material determine the magnitude of co-polymerisation. Changing these biological characteristics by altering the surface of an antigen through fixatives such as aldehydes could alter its reactivity towards the resin, most probably increasing the ability to co-polymerise (16).

2.5) Antibody penetration of sections

Relative rapid penetration of antibodies into LR White sections is claimed in some reports, while no or only little penetration was observed in other studies (10). Due to the hydrophilic nature of LR White, it is suggested that the penetration of aqueous solutions could occur into thin sections of LR White embedded tissue (2). An indication of this penetrability of LR White is the swelling that occurs upon exposure to aqueous solutions. Furthermore, the formation of diamino benzidine (DAB) reaction product arising from horseradish peroxidise oxidation has been shown to not only cover the surface of the sections, but also to form within the resin (17). This penetrability of LR White to aqueous solutions makes it possible for antibodies to gain access into the plastic sections (10). This is important, as it has been suggested that the immunolabelling efficiency depends on how well immunoreagents are able to penetrate the section (17). However, the question remains as to whether LR White sections allow the penetration of gold-conjugated antibodies to the interior of the section. By comparing immunogold immunolabelling with immunoperoxidase immunolabelling, the immunoperoxidase reaction continues to be positive with primary antibody dilutions well beyond the detection sensitivity of the immunogold immunolabelling system (9). This can be

explained by the fact that, due to the size of the gold particulate, the immunogold immunolabelling reaction is confined to the exposed surface of the section. The immunoperoxidase label is not bigger than the size of an antibody and therefore it would be expected to be able to penetrate the sections. This would result in the labelling of antigenic sites not only on the surface of the section but also in the interior of the section (9). Therefore, if immunocolloidal gold is used the immunoreaction is immediately confined to the surface, in which case little difference will be made to the intensity of labelling by altering the polymerisation schedule (3, 9, 18).

2.6) Post-embedding procedures for increasing antigen availability

The ideal is to employ the most appropriate fixation, dehydration and embedding procedure in order to ensure optimal immunolabelling of the antigen in question. However, there are a few procedures available for increasing antigen availability for immunolabelling procedures when the fixation of the tissue is not optimal or a hydrophobic embedding medium has been used.

2.6.1) Etching of epoxy sections and removal of osmium tetroxide

Although the use of epoxy as an embedding medium for post-embedding immunolabelling procedures is theoretically not desirable, various antigens have been successfully immunolabelled with epoxy sections. However, immunolabelling is frequently only achieved once the bonds between the tissue and embedding media are broken – which is accomplished by etching (partial corrosion) of the section (6, 19). Etching pre-treatments involves a procedure whereby the resin (plastic) is removed upon breaking of the ester bonds, thereby decreasing the cross-linking density and increasing the hydrophilicity of the section (2, 5). Increased hydrophilicity of the section surface increases the accessibility of the antibody to the antigen. Partial corrosion of the epoxy

resin of the section can be achieved by exposing the section for ten seconds to saturated sodium ethoxide diluted to 50% with absolute ethanol (4), or by oxidising agents such as sodium metaperiodate, hydrogen peroxide or periodic acid. Treatment with a saturated aqueous solution of sodium metaperiodate for 30 to 60 minutes or with 1% aqueous periodic acid for 4 minutes results in successful immunolabelling (15). Deplastisising of epoxy sections with sodium ethoxide is possible because of the sensitivity of the ester bonds in polymerised epoxy resin to strong alkaline solutions. However, the rough treatment with sodium ethoxide may be harmful to sensitive antigens (20). By moderately increasing the amount of accelerator used during polymerisation, the amount of co-polymerisation of epoxy with the tissue can be decreased, resulting in superior immunolabelling with less need for harsh etching procedures with immunolabelling of sensitive antigens (21). In addition to the treatment with sodium ethoxide, it has been shown that the intensity of immunolabelling of epoxy sections can also be enhanced by heating of the sections in citrate solution. It is suggested that the mechanism for increasing the immunolabelling intensity on epoxy sections by heating is similar to the other etching procedures, i.e., by breaking the chemical bonds between the epoxy resin and the antigens (22). The following etching procedures were compared for superiority of immunolabelling of 2% glutaraldehyde fixed, 1% osmium tetroxide post-fixed and epoxy resin embedded tissue. The etching procedures included sodium metaperiodate, microwave irradiation in citrate buffer pH 6, microwave irradiation in EDTA solution pH 8 and microwave irradiation in an alkaline solution pH 10. Only heating of the sections in the alkaline solution pH 10 was shown to result in improvement and adequately labelled sections (23). In order to accomplish maximal immunolabelling with etching it is necessary to determine the right balance between the concentration of the etching agent and the etching time. This in order to provide sufficient permeability of the surface of thin sections for antibody access while avoiding structural damage, and to

retrieve antigens hidden by covalent bonds formed between the epoxy resin and biological material during polymerisation (4).

Not only are the epoxies heavily cross-linked, very hydrophobic and of a high tendency to form cross-links with tissue antigens, they are also strongly lipophilic. Due to this strong lipophilic nature of the epoxies, the tissue is also almost always post-fixed with osmium tetroxide to prevent the extraction of lipid cellular structures (6). However, post-fixation with osmium tetroxide results in complete loss of antigenicity. Nevertheless, oxidation of the reduced osmium could result in the restoration of the antigenicity. Oxidising agents oxidise the reduced osmium, which then becomes soluble and is then rinsed from the section (5, 24). By comparing osmicated and un-osmicated tissues embedded in epoxy resin it is shown that in addition to etching with 1% sodium ethoxide the osmicated sections also had to be oxidised with sodium metaperiodate for 60 minutes plus 5 minutes on 3% hydrogen peroxide at room temperature (25). Bendayan and Zollinger compared the following oxidising agents/procedures for their ability to retrieve antigens from glutaraldehyde-fixed post-osmicated tissues a) incubation for 10, 30, 60 and 120 minutes on a saturated aqueous solution of sodium metaperiodate, b) incubation for 10 minutes on a 10% solution of hydrogen peroxide, c) incubation for 2 minutes on a saturated alcoholic solution of sodium hydroxide diluted 1:10 with 100% ethanol, followed by successive incubations of 2 minutes in 100%, 95%, 75% and 50% ethanol, rinsed in distilled water and finally incubated for 5 minutes on 10% hydrogen peroxide and d) incubation for 10 minutes on a 5% solution of periodic acid. Treatment with the saturated aqueous solution of sodium metaperiodate for 30, 60 or 120 minutes restored the labelling without altering the structural information, with the restoration of labelling being time-dependent: after 10 minutes of treatment, the intensity of labelling was about half of that obtained after 30 minutes and maximal labelling intensity was

reached after 60 minutes. The other strong oxidising agents tested including the hydrogen peroxide and periodic acid and the combination of alcoholic solution of sodium hydroxide followed by hydrogen peroxide were also found to restore the labelling. However, in contrast to the results obtained with sodium metaperiodate these agents gave unsatisfactory results (24). Osmium fixation can be reversed with sodium metaperiodate and antibody access is improved in epoxy resin sections by etching with hydrogen peroxide or sodium ethoxide. However, incubation with sodium metaperiodate is generally preferred for both etching and removal of osmium tetroxide thereby avoiding treatment with sodium ethoxide. This method gives higher immunolabelling densities, causes less damage to the sections and retains the best ultrastructural details (26).

2.6.2) Etching of LR White sections

For LR White sections etching is not absolutely necessary since LR White is hydrophilic. Therefore, unlike the heavily cross-linked hydrophobic epoxy plastics, water will pass into LR White sections as demonstrated by the swelling of the sections (9). Furthermore, retention of antigenicity in LR White sections is demonstrated by the short antibody incubation times necessary for successful immunolabelling (19) and immunolabelling patterns closely resembling those obtained on cryo-sections (18). Nevertheless, etching procedures have been shown to enhance the labelling of material embedded in LR White resins (2). Of the etching agents used with LR White embedded tissue, a combination of an alcohol solution of sodium hydroxide followed by sodium metaperiodate, gave optimal labelling with minimal background (2). Hydrogen peroxide treatment gave comparable labelling. However, the resulting background was often significantly higher. This increased background was probably due to the production of aldehydes by oxidation of the resin components. Free aldehyde groups can non-

specifically bind to antibodies. Pre-treatment with saturated, aqueous sodium metaperiodate and 0.1 M HCl, while showing increased labelling compared to that obtained with untreated sections, appeared to dissolve the section and render it unstable in the electron beam (2). Etching pre-treatments of LR White embedded tissue improves the accessibility for immunolabelling and thus is essential if maximal labelling of antigens is to be achieved. However, it is essential to examine each combination of antigen/antibody individually as different fixation and etching regimes may need to be tested for optimal results (2). It was suggested that by pre-treating of LR White sections by sodium ethoxide the antigen damaging effect of sodium ethoxide could be evaluated. This applies when it is assumed that sodium ethoxide treatment makes no difference to the immunolabelling efficiency on LR White sections. However, it was shown that for some antigens better immunolabelling was achieved with sodium ethoxide treatment of LR White sections (20). It is presumed that in such cases the fixation bonds are released by the action of sodium ethoxide. Therefore, when the same intensity of immunolabelling are observed for both sodium ethoxide-treated and untreated LR White sections it cannot be excluded that the reason is a combination of damage to the antigens and release of the fixation bonds (20).

2.6.3) Non-specific labelling on etched sections

One of the drawbacks of etching is the possible occurrence of non-specific immunolabelling. More than one aspect may be responsible for this unwanted labelling on etched sections including the type of etching solution and the antibodies. In addition, etching of the section may result in the retrieval of not all of the antigens present in the cell. This might be due to the different localisations and interactions of the antigen in the cell. Immunolabelling of eosinophil lysozyme in unetched LR White sections demonstrated the presence of lysozyme in pale cytoplasmic granules and specific granule

matrices with no labelling in the crystalloid of the specific granules. However, lysozyme may also be present in the crystalloid but in a masked form – bound to major basic protein or sulfated glycosaminoglycans. Etching with sodium metaperiodate produced a distinct alteration in labelling pattern, with matrix label decreasing and crystalloids becoming positive. This change could be interpreted as destruction of accessible matrix antigen with concomitant release of more resistant masked antigen in the crystalloid. However, this treatment also produced labelling of crystalloids by normal rabbit IgG suggesting non-specific binding (27).

2.6.4) Antigen retrieval from formaldehyde-fixed tissue

Interaction of fixative with amino acid side-groups causes certain antigens to be unavailable for binding to the antibody with immunolabelling techniques. However, it has been shown that these cross-linkages can be reversed by high temperature heating (120°C) or strong alkaline treatment. This observation formed the basis for the development of antigen retrieval techniques (28, 29). Furthermore, as a result of the breakage of formaldehyde-induced cross-links between antigens, the extraction of diffusible blocking proteins could also play a role in the achievement of better immunolabelling (30). Other treatments employed for the successful retrieval of antigens include "chemical antigen retrieval procedures" such as exposure to 0.1% Triton X-100 (31) and 0.5% SDS (32). Heat-induced antigen retrieval produces a large increase of immunolabelling only when the tissue is fixed in formaldehyde. When the tissue is fixed in glutaraldehyde or ethanol, insignificant or only weakly increased immunolabelling is shown upon heat-mediated antigen retrieval. With ethanol fixation, a decrease in immunolabelling could even be shown, which may be explained by the possible extraction of antigens from the poorly ethanol-fixed tissue during the heating process, or by heat-induced destruction of the poorly fixed antigens (33). Although the precise

mechanism responsible for the retrieval of antigens during high temperature heating is not known, it has been shown that the extreme temperatures achieved during heat-mediated retrieval of antigens is an important factor for the successful retrieval of antigens (34). Other factors that could play a role in heat-mediated antigen retrieval procedures include the exposure time and the type and pH of the buffer. There are indications that the chelation or precipitation of tissue-bound calcium ions (and other divalent metal ions) could be a critical step in salt-mediated antigen retrieval (26). The acidity/alkalinity of different types of buffers is shown to result in differences in the success of the retrieval of the antigen. In a study by Boon it was shown that when the pH of the microwave-retrieval solution was between pH 3.5 and 5, little immunolabelling was demonstrated. However, upon an increase in the pH of the buffer to between 5 and 6.5 an increase in immunolabelling occurred (13). Although various studies indicated a difference in the success of immunolabelling with a change in the pH, it seems as though the critical factor for the successful retrieval of the antigen is the achievement of specific minimal temperatures. With heating at 100°C and above, better immunolabelling results are achieved than heating at 90°C. Furthermore, prolonging the exposure time at lower temperatures does not necessarily compensate for the lower temperatures, with heating at 90°C for 10 minutes being more effective than heating at 60°C for 120 minutes (28, 29). Nevertheless, when the time of heating at 65°C was increased to 24 hours and compared to heating at 121°C for 15 minutes and 99°C for 40 minutes, the immunolabelling achieved was similar and even better to heating at the higher temperatures for shorter times (35). In a study by Shi *et al.* various different solutions at different temperatures were compared for their antigen retrieval efficiency. The order of efficiency of the antigen retrieval methods were as follows; Tris (65°C and 99°C) and EDTA (65°C) > EDTA (99°C) and commercial solution (99°C) > distilled water (65°C and 121°C), commercial solution (65°C and 121°C), citric acid (65°C, 99°C and 121°C),

urea (65°C and 121°C), EDTA (121°C) and Tris (121°C) > phosphate buffer (65°C, 99°C and 121°C) at 5% significance level. The difference among antigen retrieval in Tris (65°C), EDTA (65°C) and Tris (99°C) could not be statistically determined. It can be seen that irrespective of the temperature certain solutions can bring about better retrieval of antigens followed by increased immunolabelling. Comparing the efficiency of antigen retrieval in different buffer solutions at similar temperatures (microwave heating), 0.1 M Tris-HCl buffer, pH 9.5 containing 5% urea, 0.1 M Tris-HCl buffer, pH 9.5 without urea, and citrate buffer pH 6, for a panel of 34 antibodies, the Tris-HCl buffer containing urea was superior to the citrate buffer for 22 antibodies, in 12 cases the Tris-HCl buffer with urea was also superior to the Tris-HCl buffer without urea, in 12 cases the intensity was similar for all three antigen retrieval solutions, the staining obtained with Tris-HCl with urea was equal to or better than with pH 6 citrate buffer in all cases. This demonstrates that with antigen retrieval in solutions with a higher pH (8-10) better results are obtained for many antibodies (35). Also in routine sections of normal and pathological samples fixed in 10% buffered formalin, including EDTA-decalcified bone marrow biopsies, the higher pH solutions are superior to lower pH solutions. Immunolabelling were evaluated for 61 antibodies following heating in three different fluids including 0.01 M citrate buffer pH 6, 0.1 M Tris-HCl buffer pH 8, and 1 mM EDTA-NaOH solution pH 8. The sections underwent either three cycles of microwave treatment (5 minutes each) or pressurised cooking for 1-2 minutes. In comparison with the other fluids the EDTA-NaOH solution appeared to be superior in terms of both staining intensity and the number of marked cells (36). In a study employing a citrate buffer 10-50 mM, pH 8.5-9 equally good immunolabelling was obtained at all temperatures between 80°C and 100°C for only a short period of heating (30 minutes) (37), again demonstrating the superiority of the high pH citrate buffer that compensates for the lower heating temperatures.

A mechanism that could contribute to the retrieval of antigens and increase in immunolabelling efficiency upon heat-induced antigen retrieval is the restoration of electrostatic (coulombic) forces. It has also been suggested that prolonging the antibody incubation time from 10 minutes to 60 minutes represented an effective alternative to heat-induced antigen retrieval. Formaldehyde is an electrophilic substance that reacts with various functional groups of biologic macromolecules in a cross-linking fashion. When reacting with proteins the reactive hydrogen atoms are replaced by formaldehyde, which may be loosely (as Schiff's bases) or tightly bound (to form methylene bridges). Formaldehyde also disrupts hydrogen bonding and electrostatic interaction between amino acids and peptides, thus leading to changes in the secondary and tertiary structures within the target proteins and between the same and other proteins or tissue. All of these reactions are known to diminish the hydrophilic nature and thereby very likely reduce the net electrostatic charges of tissue antigens (38).

Microwave heating is the conventional heating method employed during heat-mediated antigen retrieval, however it is difficult to produce a controlled and uniform heating temperature with a microwave. By comparing the following heating methods a) microwave heating at 100°C for three periods of 5 minutes, b) autoclaving at 120°C for 10 minutes, c) pressurised boiling in a domestic pressure cooker at 120°C for 1 minute, 2 minutes or 5 minutes and d) boiling in an open glass jar for 15 minutes, no difference in immunolabelling was found among the four methods of heat treatment. There was, however considerable ultrastructural damage shown with the pressure cooker (39).

2.6.5) Antigen retrieval with proteolytic enzymes

Not only can antigens be retrieved by high temperature heating, but tissue digestion with proteolytic enzymes can also result in the retrieval of masked antigens for

immunolabelling procedures. Treatment with proteolytic enzymes is said to act by cleaving peptide bonds, thus uncovering antigenic sites from the proteinaceous web into which they have become woven during fixation (5, 40). Proteolytic digestion with 0.25% trypsin in PBS, pH 7.4 for 15 minutes to 60 minutes at 37°C was shown to successfully retrieve masked loricrin antigens (41). However, uncontrolled treatment with proteolytic enzymes can cause damage to the antigen and microwave antigen retrieval is therefore superior to enzyme digestion for various antigens. Microwave antigen retrieval methods (in a jar containing 250 ml of buffer irradiated for 8 minutes, i.e., 2 x 4 minutes) compared to enzymatic antigen retrieval methods including 0.1% trypsin for 20 minutes at 37°C and 0.5% protease VIII for 10 minutes at room temperature has shown superior immunolabelling for a panel of antibodies on formalin-fixed, paraffin-embedded sections. Furthermore, the microwave method seems to produce uniform immunostaining over large surface areas with no loss of morphological detail (40). For a panel of 60 antibodies it was shown that for only five of the antibodies proteolytic digestion with 0.05% protease XIV at 37°C for 5 minutes was superior to the conventional heat-based antigen retrieval procedure (36).

Not only are there differences in the antigen retrieval for different antigens but, there can also be differences for the same antigen in different subcellular pools. Suboptimal heat-mediated antigen retrieval, due to an inadequate heating period, can be a pitfall in immunolabelling because it may fail to reveal yet undiscovered sub-cellular pools of a particular antigen. Bcl-2 is one such antigen for which the retrieval of the antigen varies for the different sub-cellular Bcl-2 pools. Treatment for 10 minutes at 80-100°C in sodium-citrate buffer compared to 10 minutes of microwave heating, prolonged microwave heating (30 minutes at 100°C) or high pressure cooking (60 minutes at 130°C) improves cytoplasmic but not nuclear/chromosomal immunolabelling of human bcl-2 in

formaldehyde-fixed tissue sections. In contrast, these procedures restore the nuclear and mitotic chromosome-associated rat 68-86 bcl-2 antigen (42).

Not all antigens can be retrieved by using conventional antigen retrieval techniques. For these antigens the high temperatures (boiling) employed during these techniques may induce a negative result due to the destruction of the antigen. In these cases a lower-temperature heating treatment or a combination retrieval protocol (heat and enzyme digestion) may provide better results. In order to investigate the sensitivity of the antigens it is necessary to include control sections. A tissue section not treated by antigen retrieval is required to rule out any false-positive results or altered immunolabelling patterns (34).

2.6.6) Combination of etching and formaldehyde-fixed antigen retrieval

The following combinations of treatments have been compared for post-embedding immunolabelling a) no treatment, b) etching in H_2O_2 for 10 minutes, c) treatment with saturated aqueous sodium metaperiodate for 60 minutes, d) heating in H_2O at 91°C, e) heating in sodium citrate buffer at 91°C, f) heating in EDTA at 91°C, g) etching in H_2O_2 for 10 minutes followed by heating in sodium citrate buffer at 91°C, i) etching in H_2O_2 for 10 minutes followed by heating in EDTA at 91°C, j) treatment with sodium metaperiodate for 60 minutes followed by heating in H_2O at 91°C, k) treatment with sodium metaperiodate for 60 minutes followed by heating in sodium citrate buffer at 91°C and l) treatment with sodium metaperiodate for 60 minutes followed by heating in EDTA at 91°C. Only for heating in EDTA, no other technique, pre-treatment, or antigen retrieval procedure significantly improved immunolabeling with anti-AA amyloid. Furthermore, different types of fixatives appear to have little effect on EDTA retrieval. When immunolabelling with anti-transthyretin was investigated, only the combined pre-

treatment with H_2O_2 and EDTA and sodium metaperiodate and EDTA, was shown to significantly improve the immunolabelling (43).

2.7) Immunolabelling of the H-subunit and L-subunit of ferritin

2.7.1) Characteristics of the H-subunit and L-subunit monoclonal antibodies

Ferritin is structurally and immunologically very complex and the antigenic determinants are highly repetitive on the outer surface of the ferritin protein shell (44). The ferritin protein shell consists of 24 subunits of two different types, the H-subunit and the L-subunit. These two subunits, although they share only 55% amino acid sequence homology, fold into similar three-dimensional structures. However, the H-subunit has a more relaxed secondary structure than the L-subunit (45). On the outer surface of each of the 24 subunits a limited number of antigenic determinants at a short distance from one another are available for antibody binding. However, due to the large size and overlapping nature of the antigenic sites and the compact structure of the subunit, only one antigenic site can be occupied by an antibody at a time (46, 47). It seems also that these antigenic determinants are rather topographical than sequential since antibody binding is highly reduced and in some cases disappears after denaturation of ferritin (46). This is due to the complex quaternary structure of the ferritin protein shell, which results in the formation of antigenic determinants by sequences belonging to different subunits. Furthermore, can amino acid changes at a site distant from the antibody-binding site influence antibody binding (46). Nevertheless, certain antigenic determinants are insensitive to denaturation or renature easily indicating that certain antigenic determinants are mostly constituted of sequential amino acids (48).

Although the antigenic determinants of the ferritin subunits are similar resulting in the highly repetitive immunogenicity of ferritin, differences are shown to occur with certain

combinations of subunits in the ferritin protein shell. For some isoferritins, with only slightly different subunit compositions, major conformational differences are displayed. Conformational changes can result in masking or internalisation of antigenic determinants from one subunit and may also result in exposing new antigenic determinants or formation of new antigenic determinants by certain subunit interactions. In individual isoferritins with known H-subunit and L-subunit contents the measured immunoreactivities for H-subunit and L-subunit specific monoclonal antibodies reflected the relative contents of the two subunits. However, for certain isoferritins such as L-subunit rich isoferritins the H-subunit content is underestimated and in H-subunit rich isoferritins the H-subunit content is overestimated (47). This demonstrates that the H- and L-subunits are probably not randomly distributed in the protein shell (48).

The H-subunit and L-subunit contain common antigenic determinants that are non-specific for the subunits, as well as specific antigenic determinants – resulting in the elicitation of monoclonal antibodies that can discriminate between the H-subunit and the L-subunit. The non-specific antibodies can either bind to the different subunits with similar affinity or to the different subunits, but not with equal affinity. As a result of these differences in the antigenic determinants of the H-subunit and L-subunit, large immunological differences are seen in some tissue ferritins (47). Not all ferritins are immunologically the same. It has been shown that heart ferritin (rich in H-subunits) is immunologically more heterogenous than liver ferritin (rich in L-subunits) resulting in the elicitation of populations of antibodies with different specificities (48).

Murine monoclonal antibodies specific for the human H-subunit and L-subunit of ferritin is produced by Dr Paolo Arosio from the Department of Science and Biomedical Technology, University of Milan, Italy, and commercially available through Ramco

Laboratories, Inc., Stafford, Texas, United States of America. The monoclonal antibody specific for the H-subunit, RH02 an IgG1, is elicited in mice by recombinant H-subunit ferritin and does not cross-react with the L-subunit (Ramco Laboratories, Inc., Stafford, Texas, United States of America). The H-subunit monoclonal antibody RH02 has specificity analogous, but a higher affinity, than the previously generated 2A4 (44). The monoclonal antibody 2A4 was elicited by human heart ferritin consisting of 95% H-subunits and 5% L-subunits. Human heart ferritin contains at least one antigenic site, which is not present in human liver ferritin (44). The monoclonal antibody specific for the L-subunit, LF03 an IgG2B, is elicited by human liver ferritin and does not cross-react with the H-subunit (Ramco Laboratories, Inc., Stafford, Texas, United States of America).

In the present study, with ultrastructural visualisation of the immunolabelled sections, ferritin was seen as free ferritin molecules, clusters of ferritin molecules and as haemosiderin (denatured form of ferritin). Ferritin (containing a substantial amount of iron) is visible with the transmission electron microscope since iron is electron dense. Depending on the amount of iron contained by ferritin the ferritin particle will appear more or less electron dense. In most clusters the particles appeared larger and more electron dense than the free ferritin molecules and were thus of the iron-rich variety.

In this study it was found that the monoclonal antibodies only bind to the relatively iron-poor ferritin molecules and not to the more iron-rich electron dense ferritin particles. These findings might be explained by a change in the immunoreactivity of the H-subunit and L-subunit upon iron loading of the ferritin molecule. This is supported by a previous study which has shown that upon iron loading of cells, changes in the antigenicity of the surface of the protein shell occur which may be unrelated to subunit

composition (49). It has furthermore been suggested that these surface changes of the ferritin protein shell are associated with the formation of clusters of ferritin and subsequently haemosiderin (50).

It has been published that ferritin present in the nucleus of cells are H-subunit rich (51) and a specific pathway has been shown for the translocation of cytoplasmic H-subunit rich ferritins, but not cytoplasmic L-subunit rich ferritins, into the nucleus (52). In the present study immunolabelling was seen for both the H-subunit and the L-subunit monoclonal antibodies in the nucleus of macrophages and the cells of the erythron. It is therefore suggested that the ferritins which are found in the nucleus do contain a substantial amount of L-subunits. The presence and ratio of these subunits in the nucleus have not been quantified in the present study.

2.7.2) Secondary antibody gold-conjugate

Localisation of antigens with the electron microscope is achieved by a secondary antibody conjugated to a gold particle. This technique was used for the first time in 1971 by WP Faulk and GM Taylor – "An immunocolloid method for the electron microscope". They reported the adsorption of various primary antisera to particles of colloidal gold and the use of such antibody-gold complexes for direct electron microscopic localisation of surface antigens of Salmonella (53). Particles of colloidal gold can adsorb various proteins such as antibodies. Conjugation of antibodies to the gold particles occurs without any significant loss or alteration of the biological activity of the antibodies (54). Furthermore, colloidal gold does not display spontaneous affinity for ultrathin sections of resin-embedded tissues minimizing background labelling (54). Due to the high atomic number of gold, these gold-conjugates are of very high electron density providing improved spatial resolution and facilitating multiple labelling and

quantification of immunolabelling (53). Quantification of immunolabelling is made possible by the particulate nature of the gold-conjugate, which facilitates the counting of these markers. These colloidal gold particles are spherical in shape and can be prepared in sizes from 1 to 25 nm. Particles of 5-15 nm in size are excellent for post-embedding immunolabelling, particles of smaller size, such as 1 nm, must, however, be silver enhanced to be visible by the electron microscope (54). Antibodies bind to gold particles through the interaction of charges at the surface of the particle with those of the antibody through electrostatic Van der Waals forces, as well as more complex interactions (54). Colloidal gold is a hydrophobic sol formed by electron dense negatively charged particles with the stability of the colloidal gold in water maintained by electrostatic repulsion. However, when the particles reach a critical distance from one another it can result in flocculation leading to cohesion and precipitation of the colloid. This occurs in the presence of electrolytes that lead to reduction of the electrostatic repulsion. Binding of antibodies prevent flocculation by their association with the sol to form a shell around each particle (54).

With conjugation of the secondary antibody to colloidal gold the indirect technique of immunolabelling can be employed. In the first step the primary antibody is used in its native form to generate a specific antigen-antibody complex. In the second step this primary antibody complex becomes the target of the secondary antibody that is tagged with gold particles. With the use of this indirect technique of immunolabelling amplification of the signal can be achieved (54).

2.7.3) Non-specific binding of antibodies to the section

With post-embedding immunolabelling on resin sections, non-specific binding of the antibodies can occur to either the resin itself, non-specific reactive sites on the tissue or

to bio-molecules resembling the antigen. Non-specific binding to the resin and the embedded tissue may be due to the presence of chemical groups that react with the antibodies such as the presence of oppositely charged groups between the antibody and the embedded tissue (55). To reduce this non-specific labelling, blocking agents are used to prevent the reactive sites on the resin or tissue from binding to the antibodies. These blocking agents can include bovine serum albumin (BSA), ovalbumin, foetal calf serum, a mixture of Tween-20 and 0.5 M NaCl and a gelatine-containing buffer. Blocking agents are added to the antibody diluting and rinsing buffers (55, 56). However, the type of non-specific labelling caused by bio-molecular structures resembling the antigen is not blocked by BSA, but non-specificity caused by reactive groups in the resin or by electrostatic attraction between the tissue and the antibodies may be blocked. BSA molecules bind to reactive sites on the sections and occupy them, when the section is blocked before the introduction of the antibodies binding of BSA is non-competitive, by diluting the antibodies in a BSA-solution the BSA molecules will compete with the antibodies for binding with the reactive sites on the section, the use of a considerable excess of BSA compared to antibodies will make the antibodies loose the competition, and the non-specific labelling can be significantly reduced. Furthermore, with fixation in FA or GA, free aldehyde groups may remain after fixation. These free aldehyde groups may react with the antibody resulting in non-specific immunolabelling. This applies especially to GA. Due to the presence of two aldehyde groups, one end can be bound to cellular constituents with the other end free to react with the antibody. Blocking of these free aldehyde groups can be achieved with any small molecular-weight compound containing an amino group such as glycine, but other quenching agents can also be used such as ammonium chloride and sodium borohydride (7).

LR White is a hydrophilic resin and therefore displays a low attraction for other hydrophilic substances such as antibodies. This results in the reduction of non-specific binding of antibodies to the resin of the LR White section (9). However, for each antigen/antibody combination the possible non-specific binding to the resin should be investigated. By comparing non-specific labelling between epoxy sections and LR White sections, the epoxy sections normally give higher background labelling than LR White sections. The monomers producing polymerised epoxy resin are chemically reactive and may react with proteins. Antibodies can be covalently linked to the surface of the epoxy section, to un-polymerised epoxy resin and to end groups of polymer chains in the section. The chemical qualities of the monomers of LR White resin are different, the monomers are polymerised because their carbon-carbon double bonds have reactivity towards the radicals originally created by the initiator. The radicals produced through the polymerisation are usually terminated and even if they had reactivity against proteins they would not be capable of linking antibodies to the LR White section. Un-polymerised LR White monomers do not have special reactivity for proteins. Nevertheless, blocking procedures with at least 5% BSA are recommended for both epoxy and LR White sections. Both epoxy sections and LR White sections display non-specific binding but to a different degree and blocking of this non-specific binding under similar conditions are different for these two resins. With different BSA concentrations and lengths of the pre-incubation step varying between 0 and 4 hours, results show that the non-specific labelling on the resin decreases significantly when the concentration of BSA or the length of the pre-incubation step is increased. The non-specific labelling is usually higher on the epoxy resin than on the LR White resin when using the same conditions with respect to BSA, but when the pre-incubation step lasts 4 hours the non-specific labelling is somewhat lower on the epoxy resin than on the LR White resin. The specific labelling for the antibodies decreases slightly when the concentration of BSA and incubation time

increase. This is probably due to steric hindrance performed by BSA molecules on the section (55).

A major source of non-specific binding is a property of the colloidal gold itself. Adsorption of proteins to colloidal gold involves a combination of electrostatic and hydrophobic interactions and the degree to which a particle is coated is likely to be a function of the protein used. This explains why, for example, only small additions of antibodies are required for a gold preparation to reach saturation in the flocculation test, yet it is necessary to store the probe in a buffer containing an excess of unrelated protein (such as bovine serum albumin). However, even in the presence of excess BSA, it was demonstrated that such probes are capable of interacting with cell components and of generating non-specific background in immunolabelling experiments. Nevertheless, a substantial reduction in non-specific binding was shown when fish gelatine was substituted for bovine serum albumin as a stabilising agent or simply when fish gelatine was added to the probe buffer. This probably indicates that fish gelatine acts to coat a greater portion of the colloidal gold particle than either the antibody or bovine serum albumin. Furthermore, can the method used to prepare the colloidal gold particles also affect the non-specific binding properties of the resulting gold probes. White phosphorus and borohydride gold probes gave significantly lower levels of background staining than did the citrate-tannic acid gold probe. These differences may be due to different groups retained on the surface of the gold particles. The effectiveness of fish gelatine as a stabiliser for citrate-tannic acid probes is probably due to a greater affinity of tannic acid for gelatine than bovine serum albumin, preventing further interaction with other cell components (56).

3) Experimental evaluation of the ultrastructural immunolocalisation technique for the H-subunit and L-subunit of ferritin

The following aspects of the immunolocalisation technique for the H-subunit and L-subunit of ferritin were evaluated:

- The affinity of the H-subunit and L-subunit monoclonal antibodies for their respective recombinant H-ferritin and L-ferritin proteins.
- The cross-reactivity of the H-subunit monoclonal antibody toward the recombinant L-ferritin protein and the cross-reactivity of the L-subunit monoclonal antibody toward the recombinant H-ferritin protein.
- The effect of fixation and dehydration on the binding of the monoclonal antibodies to their respective recombinant ferritin proteins.
- The non-specific binding of the gold-conjugate secondary antibody to the sections.
- The non-specific binding of the monoclonal antibodies to the resin and different blocking procedures in order to reduce the non-specific binding.
- The effects of different preparations on immunolabelling:
    - Investigation of the effect of different antigen retrieval procedures on immunolabelling.
    - Investigation of the effect of different polymerisation procedures on immunolabelling.

3.1) The affinity of the H-subunit and L-subunit monoclonal antibodies for their respective recombinant H-ferritin and L-ferritin proteins

The affinities of the H-subunit and L-subunit monoclonal antibodies to their respective recombinant H-ferritin and L-ferritin proteins and the cross-reactivity of the H-subunit

monoclonal antibody toward the recombinant L-ferritin protein and the cross-reactivity of the L-subunit monoclonal antibody toward the recombinant H-ferritin protein were investigated with an ELISA.

Materials

1) Multiwell Immuno plate, NUNC™, Maxisorp, cat. no. M9410 – 1CS, Sigma-Aldrich, Aston Manor, South Africa.

2) 0.05 M sodium bicarbonate ($NaHCO_3$) buffer, pH 9.6, Sodium Bicarbonate, cat. no. 6329, Merck Chemicals (Pty) LTD., Germiston, South Africa.

3) Recombinant H-ferritin protein (RHF) and recombinant L-ferritin protein (RLF), Ramco Laboratories, Inc., Stafford, Texas, United States of America.

4) Phosphate buffered saline – 20 mmol/l sodium phosphate buffer, 0.15 mol/l sodium chloride. Two stock solutions were prepared – 20 mmol/l Na_2HPO_4, 0.15 mol/l NaCl and 20 mmol/l $NaH_2PO_4 \cdot H_2O$, 0.15 mol/l NaCl. The $NaH_2PO_4 \cdot H_2O$ stock solution was added to the Na_2HPO_4 stock solution to pH 7.4. Sodium chloride, SigmaUltra, cat. no. S7653, Sigma-Aldrich, Aston Manor, South Africa. di-Natriumhydrogenphosphate, cat. no. 6586, Merck Chemicals (Pty) LTD., Germiston, South Africa, Natriumdihydrogenphosphate-1-hydrate, cat. no. 6346, Merck Chemicals (Pty) LTD., Germiston, South Africa.

5) BSA, Bovine Serum Albumin, Amersham Biosciences, cat. no. RPN 412 V, Separations Scientific, Randburg, South Africa.

6) Primary monoclonal antibodies, monoclonal antibody specific for the H-subunit of ferritin, RH02 at a concentration of 0.2 mg/ml, and the monoclonal antibody specific for the L-subunit of ferritin, LF03 at a concentration of 0.2 mg/ml, Ramco Laboratories, Inc., Stafford, Texas, United States of America.

7) Secondary antibody a – peroxidase-goat anti-mouse IgG + A + M (H + L), cat. no. 62-6420, Zymed Laboratories, Inc., Scientific Group, Midrand, South Africa.

8) Secondary antibody b – anti-mouse IgG (whole molecule) peroxidase conjugate, cat. no. A 9044, Sigma-Aldrich, Aston Manor, South Africa.

9) Substrate solution – 30 mM citrate acid ($C_6H_8O_7$), cat. no. C0759, Sigma-Aldrich, Aston Manor, South Africa, 70 mM phosphate ($Na_2HPO_4 \cdot 2H_2O$), di-Natriumhydrogenphosphat-2-hydrat, cat. no. 6580, Merck Chemicals (Pty) LTD., Germiston, South Africa, pH 5 with concentrated NaOH, 1.5 mg/ml OPD (o-phenylenediamine), cat. no. P-1526, Sigma-Aldrich, Aston Manor, South Africa, 0.2 mg/ml H_2O_2, urea hydrogen peroxide tablets, U-8879, Sigma-Aldrich, Aston Manor, South Africa.

Method

1) The ELISA plate was coated with 10 µg/ml of either the recombinant H-ferritin protein (RHF) or the recombinant L-ferritin (RLF) protein in a 0.05 M sodium bicarbonate ($NaHCO_3$) buffer, pH 9.6 for 18 hours at 8°C.

2) The plate was rinsed 3 times with 280 µl of a 1% BSA (bovine serum albumin), phosphate buffered saline.

3) The plate was blocked with 280 µl of a 1% BSA, phosphate buffered saline for 1 hour at 37°C.

4) The plate was rinsed 3 times with 280 µl of a 1% BSA, phosphate buffered saline.

5) The plate was incubated with the primary antibody (1°), either rH02 (monoclonal H-ferritin antibody) or LF03 (monoclonal L-ferritin antibody), at different

concentrations, in 100 µl of 1% BSA, phosphate buffered saline for 2 hours at 37°C.

6) The plate was rinsed 6 times with 280 µl of a 1% BSA, phosphate buffered saline.

7) The plate was incubated with either one of the secondary antibodies (2°), horse radish peroxidase labelled anti-mouse IgG (1:200), in 100 µl of 1% BSA, phosphate buffered saline for 1 hour at 37°C.

8) The plate was rinsed 6 times with 280 µl of a 1% BSA, phosphate buffered saline.

9) The substrate solution (100 µl) was added to the plate.

10) The absorbances were measured at wavelengths of 450 nm and 630 nm. The absorbance values obtained at 630 nm were deducted from the absorbance values obtained at 450 nm.

Results

Table 1 and figure 1 show the results obtained for the affinity ELISA for the H-subunit and L-subunit monoclonal antibodies, at different concentrations, for their respective recombinant proteins.

Table 1. The absorbances obtained for the affinity ELISA for the H-subunit and L-subunit monoclonal antibodies at different concentrations for their respective recombinant proteins

Concentration mg/ml	Absorbance H-monoclonal	Absorbance L-monoclonal
0.002	1.056	0.417
0.001	0.869	0.379
0.0005	0.756	0.268
0.0004	0.755	0.232
0.0002	0.682	
0.0001	0.571	
0.00004	0.42	
0.00002	0.331	

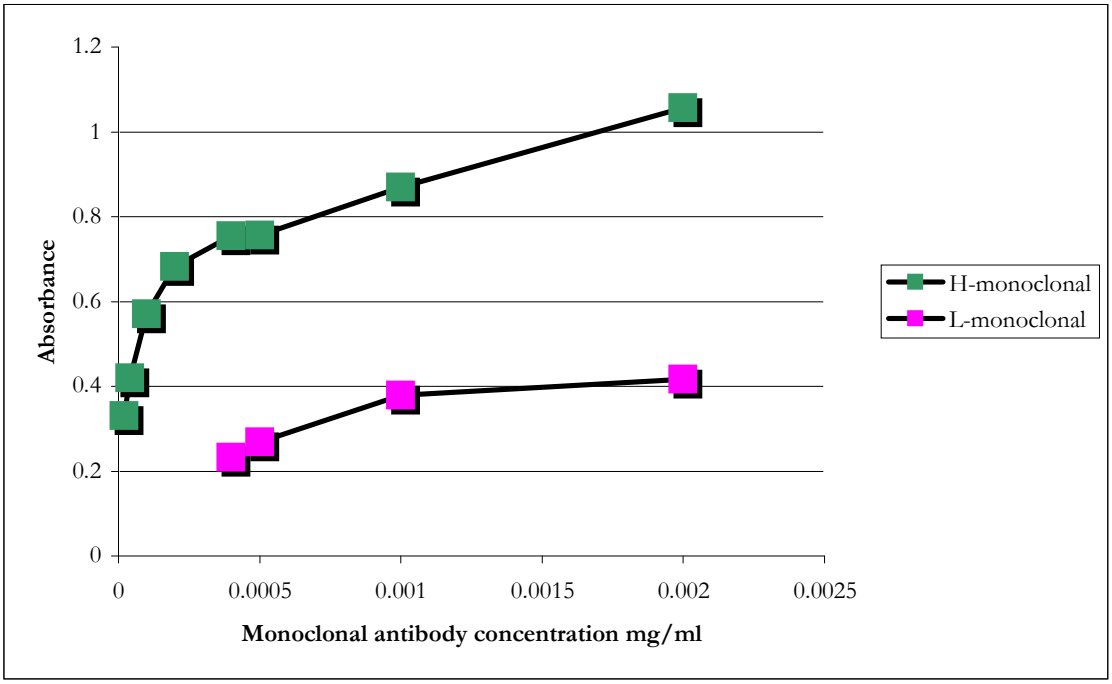

Figure 1. The absorbances obtained for the H-subunit monoclonal antibody (green) and the L-subunit monoclonal antibody (pink) at different concentrations for their respective recombinant proteins

The affinity of the H-subunit monoclonal antibody toward the recombinant H-ferritin protein was higher than the affinity of the L-subunit monoclonal antibody toward the L-ferritin recombinant protein. The affinity of the H-monoclonal antibody to the recombinant H-ferritin protein was shown to be about 2.5 times higher than the affinity of the L-monoclonal antibody to the recombinant L-ferritin protein.

3.2) The cross-reactivity of the H-subunit monoclonal antibody toward the recombinant L-ferritin protein and the cross-reactivity of the L-subunit monoclonal antibody toward the recombinant H-ferritin protein

Table 2 and figure 2 show the results obtained for the cross-reactivity ELISA for the H-subunit and L-subunit monoclonal antibodies for the recombinant proteins.

Table 2. The absorbances obtained for the affinity of the H-subunit and L-subunit monoclonal antibodies to their respective recombinant proteins and the cross-reactivities of the H-subunit and L-subunit monoclonal antibodies

	Absorbances
Coat RHF, 1° monoclonal H 1:100, 2°a 1:200	1.012
Coat RHF, 1° monoclonal H 1:100, 2°b 1:200	0.625
Coat RLF, 1° monoclonal H 1:100, 2°a 1:200	0.196
Coat RLF, 1° monoclonal H 1:100, 2°b 1:200	0.072
Coat RLF, 1° monoclonal L 1:100, 2°a 1:200	0.526
Coat RLF, 1° monoclonal L 1:100, 2°b 1:200	0.396
Coat RHF, 1° monoclonal L 1:100, 2°a 1:200	0.045
Coat RHF, 1° monoclonal L 1:100, 2°b 1:200	0.041

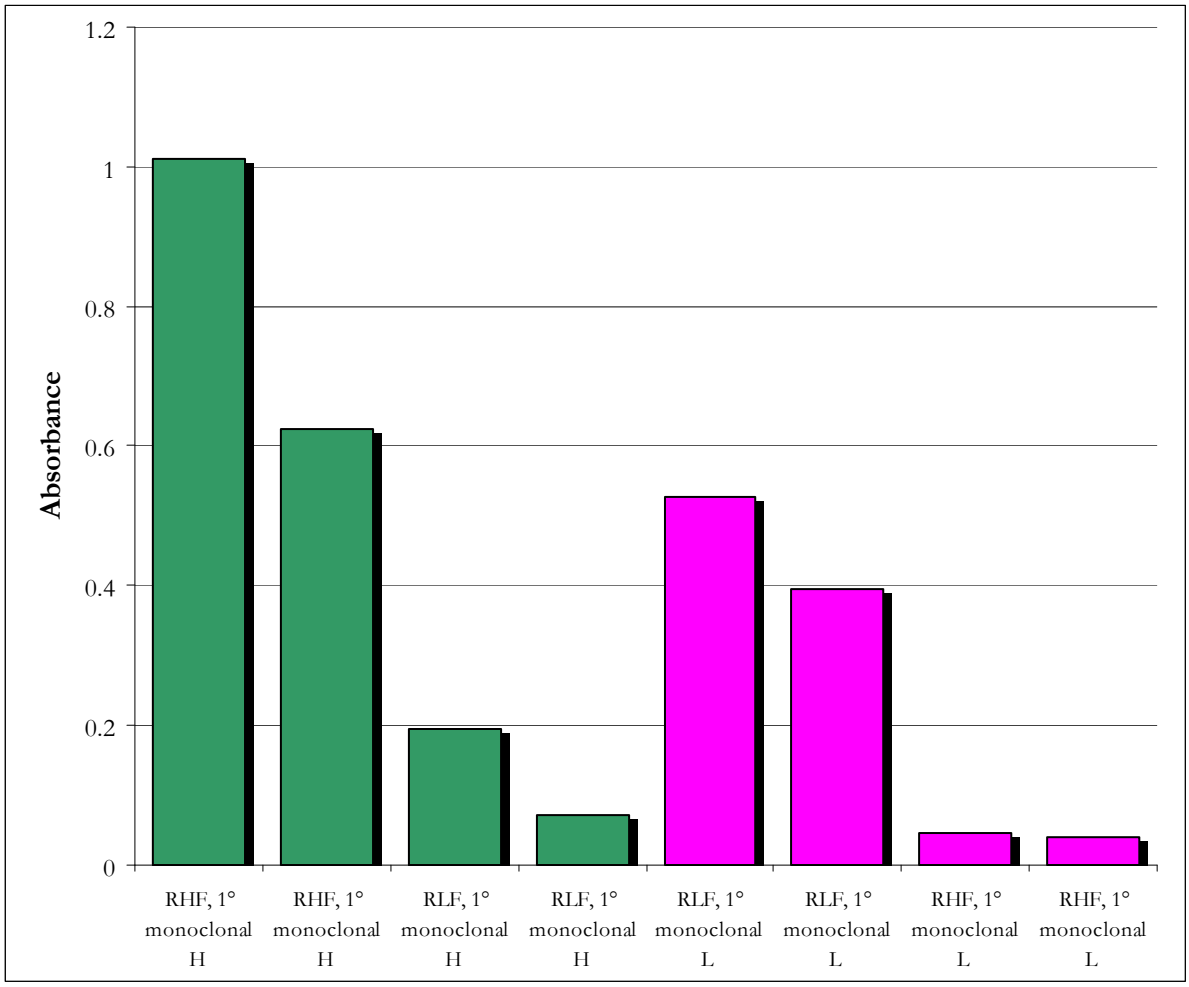

Figure 2. The absorbances obtained for the affinity of the H-subunit and L-subunit monoclonal antibodies to their respective recombinant proteins and the cross-reactivities of the H-subunit and L-subunit monoclonal antibodies

In figure 2 the first four columns (green) represents the binding of the H-subunit monoclonal antibody to the recombinant H-ferritin protein (first and second column) and recombinant L-ferritin protein (third and fourth column). Two different secondary antibodies were evaluated, secondary antibody a and secondary antibody b. Since different secondary antibodies will bind with different affinities to the primary antibodies. In the first column to the left and the third column, secondary antibody a was employed whereas in the second and fourth columns secondary antibody b was employed. The

absorbance of the first column (1.012) was the specific binding that the H-subunit monoclonal antibody had for the recombinant H-ferritin protein. The absorbance of the third column (0.196) was the cross-reactivity obtained for this combination of the H-subunit monoclonal antibody and secondary antibody to the recombinant L-ferritin protein. Thus, the H-subunit monoclonal antibody showed affinity for the recombinant L-ferritin protein, but 5 times less than that for the recombinant H-ferritin protein. For secondary antibody b, the absorbance of the second column (0.625) was the specific binding that the H-subunit monoclonal antibody had for the recombinant H-ferritin protein. The absorbance of the fourth column (0.072) was the cross-reactivity obtained for this combination of the H-subunit monoclonal antibody and secondary antibody to the recombinant L-ferritin protein. For this combination the H-subunit monoclonal antibody showed affinity for the recombinant L-ferritin protein, but 9 times less than that for the recombinant H-ferritin protein.

The last four columns (pink) of figure 2 represents the binding of the L-subunit monoclonal antibody to the recombinant L-ferritin protein and the recombinant H-ferritin protein. In the fifth column and seventh column secondary antibody a was employed whereas in the sixth column and eighth column secondary antibody b was employed. The absorbance of the fifth column (0.526) was the specific binding that the L-subunit monoclonal antibody had for the recombinant L-ferritin protein. The absorbance of the seventh column (0.045) was the cross-reactivity obtained for this combination of the L-subunit monoclonal antibody and secondary antibody to the recombinant H-ferritin protein. For this combination the L-subunit monoclonal antibody showed affinity for the recombinant H-ferritin protein, but 12 times less than that for the recombinant L-ferritin protein. For secondary antibody b, the absorbance of the sixth column (0.396) was the specific binding that the L-subunit monoclonal

antibody had for the recombinant L-ferritin protein. The absorbance of the eighth column (0.041) was the cross-reactivity obtained for this combination of the L-subunit monoclonal antibody and secondary antibody to the recombinant H-ferritin protein. For this combination the L-subunit monoclonal antibody showed affinity for the recombinant H-ferritin protein, but 10 times less than that for the recombinant L-ferritin protein. Therefore, the L-subunit monoclonal antibody showed negligible cross-reactivity towards the recombinant H-ferritin protein. Whereas, the H-subunit monoclonal antibody showed some cross-reactivity towards the recombinant L-ferritin protein but it was not critical.

3.3) The effect of fixation and dehydration on H-subunit and L-subunit monoclonal antibody binding to their respective recombinant H-ferritin and L-ferritin proteins

By coating an ELISA plate with the recombinant H-ferritin and L-ferritin proteins, followed by fixation and dehydration procedures similar to that as what will be used for tissue preparation, the effects of these processing steps on the binding of the monoclonal antibodies to their respective recombinant ferritin proteins can be investigated. Although, the effect of the prolonged exposure to 50°C is not investigated, it has been shown that this could have no effect. It is presumed that the fixative stabilises the antigen and prevents its destruction by exposure to such temperatures during polymerisation of the resin (57).

Additional materials

1) The fixative was prepared fresh immediately prior to the fixation step of the procedure. A 10% paraformaldehyde (Paraformaldehyde (Trioxymethylene), SPI Supplies, cat. no. 2615, Rick Loveland & Associates, Halfway House, South

Africa) solution in deionised H_2O was prepared fresh in a fume hood. The solution was heated to 60-70°C with constant stirring. Once the solution had reached the proper temperature stirring was continued for 15 minutes. At this point the solution was milky. One to two drops of 1 N NaOH was added, with stirring, until the solution cleared (7). The 0.15 M sodium phosphate buffer was prepared from two stock solutions. A 0.3 M Na_2HPO_4 stock solution (di-Sodium hydrogen phosphate Dihydrate, Fluka, BioChemika, Ultra, cat. no. 71643, Sigma-Aldrich, Aston Manor, South Africa) and a 0.3 M NaH_2PO_4 stock solution (Sodium dihydrogen phosphate Dihydrate, Fluka, Biochemika, MicroSelect, cat. no. 71505, Sigma-Aldrich, Aston Manor, South Africa). The 0.3 M NaH_2PO_4 stock solution was added to the 0.3 M Na_2HPO_4 stock solution to pH 7.25 immediately prior to the fixation step. This 0.3 M sodium phosphate buffer was then diluted 1:1 with the 10% freshly prepared formaldehyde stock solution and deionised H_2O. This was then followed by the addition of GA if necessary (Pure Glutaraldehyde 25% solution, E.M. grade, SPI Supplies, cat. no. 2607, Rick Loveland & Associates, Halfway House, South Africa).

2) Ethanol 99.9% Absolute A.R., Minema, Rick Loveland & Associates, Halfway House, South Africa.

3) Tween-20, Polyoxyethylenesorbitan monolaurate, Sigma for Molecular Biology, cat. no. P-9416, Sigma-Aldrich, Aston Manor, South Africa.

Method

1) The ELISA plate was coated with 10 µg/ml of either the recombinant H-ferritin protein (RHF) or the recombinant L-ferritin protein (RLF) in a 0.05 M sodium bicarbonate ($NaHCO_3$) buffer, pH 9.6 for 18 hours at 8°C.

2) The coating buffer containing either the recombinant H-ferritin protein or recombinant L-ferritin protein was removed from the plate.

3) The recombinant proteins were fixed with 100 µl of each of the following combinations; 4% formaldehyde; 4% formaldehyde, 0.05% glutaraldehyde; 4% formaldehyde, 0.1% glutaraldehyde; 4% formaldehyde, 0.5% glutaraldehyde in a sodium phosphate buffer for 1 hour at 8°C.

4) The plate was rinsed 1 time with 100 µl sodium phosphate buffer.

5) The plate was dehydrated as follows; 100 µl, 50% EtOH, 15 minutes at 8°C; 100 µl, 70% EtOH, 15 minutes at 8°C; 100 µl, 85% EtOH, 15 minutes at 8°C.

6) The plate was rinsed 3 times with 280 µl of a 1% BSA (bovine serum albumin), 0.05% Tween-20, phosphate buffered saline.

7) The plate was blocked with 280 µl of a 1% BSA, 0.05% Tween-20, phosphate buffered saline for 1 hour at 30°C.

8) The plate was incubated with the primary antibody (1°) either rH02 (monoclonal H-ferritin antibody) or LF03 (monoclonal L-ferritin antibody) in 100 µl of 1% BSA, phosphate buffered saline for 2 hours at 37°C, 1:100 dilution.

9) The plate was rinsed 6 times with 280 µl of a 1% BSA, 0.05% Tween-20, phosphate buffered saline.

10) The plate was incubated with the secondary antibody (2°), horse radish peroxidase labelled anti-mouse IgG (1:200) in 100 µl of 1% BSA, 0.05% Tween-20, phosphate buffered saline for 1 hour at 37°C.

11) The plate was rinsed 6 times with 280 µl of a 1% BSA, 0.05% Tween-20, phosphate buffered saline.

12) The substrate solution (100 µl) was added to the plate.

13) The absorbances were measured at wavelengths of 450 nm and 630 nm. The absorbance values obtained at 630 nm were deducted from the absorbance values obtained at 450 nm.

Results

Table 3 and figure 3 show the percentage of the optimal signal obtained for the binding of the H-subunit and L-subunit monoclonal antibodies to their respective recombinant proteins after different treatments.

Table 3. The percentage of the optimal signal obtained for the binding of the H-subunit and L-subunit monoclonal antibodies to their respective recombinant proteins after different treatments

Treatment number	Treatment	Percentage of optimal signal	
		RHF	RLF
1	4% FA	85%	118%
2	4% FA	85%	118%
3	4% FA, 0.05% GA	80%	79%
4	4% FA, 0.1% GA	71%	73%
5	4% FA, 0.5% GA	46%	60%
6	Dehydrate	93%	100%
7	4% FA, dehydrate	101%	146%
8	4% FA, 0.05% GA, dehydrate	87%	105%
9	4% FA, 0.1% GA, dehydrate	73%	118%
10	4% FA, 0.5% GA, dehydrate	54%	82%

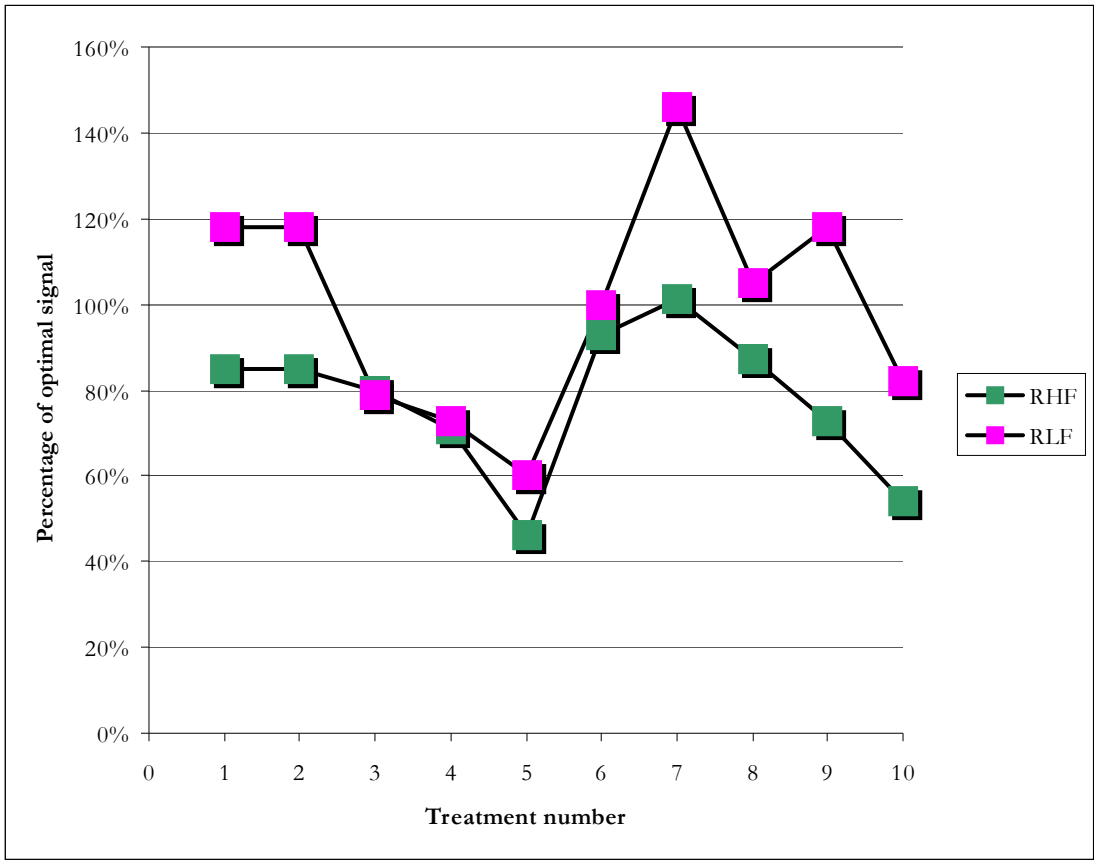

Figure 3. The percentage of the optimal signal obtained for the binding of the H-subunit and L-subunit monoclonal antibodies to their respective recombinant proteins after different treatments

In figure 3 for treatment 1 and 2 (fixation in 4% formaldehyde without dehydration) the affinity of the antibodies was shown to be influenced differently. For the H-subunit monoclonal antibody (green) there was a decrease in affinity to 85% whereas there was an increase in affinity to 118% for the L-subunit monoclonal antibody (pink). Treatment of the recombinant proteins with 4% formaldehyde and 0.05% glutaraldehyde (treatment 3), similar to what was used in the fixation of the bone marrow tissue, but still without dehydration, the affinity of the monoclonal antibodies were shown to be similarly decreased. A decrease to 80% was shown for the H-subunit monoclonal antibody (green) and a decrease to 79% was shown for the L-subunit monoclonal antibody (pink).

When the glutaraldehyde concentration was increased (treatment 4 and 5), both of the monoclonal antibodies were shown to have a decrease in affinity towards their respective recombinant ferritin proteins. However, the decrease for the H-subunit monoclonal antibody (treatment 5, green) was more than that of the L-subunit monoclonal antibody (treatment 5, pink) with a glutaraldehyde concentration of 0.5%. When the recombinant proteins were not fixed but only dehydrated (treatment 6) the affinity of the H-subunit monoclonal antibody (green) was shown to decrease (93%) whereas there was no difference shown for the affinity of the L-subunit monoclonal antibody (pink) from the optimal signal. Dehydration with ethanol could either have fixed the recombinant proteins, with or without changing the antigen, or extracted the recombinant proteins. With treatment 7 the recombinant proteins were fixed with 4% formaldehyde followed by dehydration with ethanol. No difference was shown for the affinity of the H-subunit monoclonal antibody (green), but a more pronounced increase was shown for the affinity of the L-subunit monoclonal antibody (pink) compared to when the recombinant L-ferritin was only fixed in 4% formaldehyde. With the addition of glutaraldehyde to the fixation solution (treatment 8, 9 and 10) followed by dehydration, a decrease was shown in the affinities for both the monoclonal antibodies to their respective ferritin proteins. However, it is different from that shown when the recombinant proteins were only fixed. The inclusion of dehydration could possibly have resulted in an additional fixation step and therefore an increase in the affinities of the monoclonal antibodies to their respective recombinant proteins.

3.4) Fixation of the core bone marrow tissue

With the suggestions found in the literature and the previous results the following method was used for the fixation, dehydration and embedding of the core bone marrow tissue.

Materials

1) Fixative consisting of 4% formaldehyde (FA), 0.05% glutaraldehyde (GA) in a 0.15 M sodium phosphate buffer. The fixative was prepared fresh immediately prior to the obtainment of bone marrow tissue. A 10% paraformaldehyde (Paraformaldehyde (Trioxymethylene), SPI Supplies, cat. no. 2615, Rick Loveland & Associates, Halfway House, South Africa) solution in deionised H_2O was prepared fresh in a fume hood. The solution was heated to 60-70°C with constant stirring. Once the solution had reached the proper temperature stirring was continued for 15 minutes. At this point the solution was milky. One to two drops of 1 N NaOH was added, with stirring, until the solution cleared (7). The 0.15 M sodium phosphate buffer was prepared from two stock solutions. A 0.3 M Na_2HPO_4 stock solution (di-Sodium hydrogen phosphate Dihydrate, Fluka, BioChemika, Ultra, cat. no. 71643, Sigma-Aldrich, Aston Manor, South Africa) and a 0.3 M NaH_2PO_4 stock solution (Sodium dihydrogen phosphate Dihydrate, Fluka, Biochemika, MicroSelect, cat. no. 71505, Sigma-Aldrich, Aston Manor, South Africa). The 0.3 M NaH_2PO_4 stock solution was added to the 0.3 M Na_2HPO_4 stock solution to pH 7.25 immediately prior to the obtainment of bone marrow tissue. This 0.3 M sodium phosphate buffer was then diluted 1:1 with the 10% freshly prepared formaldehyde stock solution and deionised H_2O. This was then followed by the addition of the GA (Pure Glutaraldehyde 25% solution, E.M. grade, SPI Supplies, cat. no. 2607, Rick Loveland & Associates, Halfway House, South Africa).

2) Ethanol 99.9% Absolute A.R., Minema, Rick Loveland & Associates, Halfway House, South Africa.

3) LR White Resin, medium grade acrylic resin, London Resin Company LTD., Rick Loveland & Associates, Halfway House, South Africa.

4) Gelatine capsules, SPI Supplies, cat. no. 2302, Rick Loveland & Associates, Halfway House, South Africa.

5) Nickel grids, 200 MESH Hexagonal grids, SPI Supplies, cat. no. 2480N, Rick Loveland & Associates, Halfway House, South Africa.

Method

1) A piece of core bone marrow was obtained during the biopsy procedure at the bedside of the patient and placed immediately in the fixative on ice.

2) The bone marrow tissue was fixed for 24 hours at 6°C whilst being rotated (TAAB rotator, Wirsam Scientific, Richmond, South Africa).

3) The bone marrow tissue was rinsed 3 times for 20 minutes with the sodium phosphate buffer at 6°C whilst being rotated.

4) The bone marrow tissue was dehydrated as follows 50% EtOH, 70% EtOH, 30 minutes each at 6°C whilst rotating followed by 85% EtOH, 2 times 15 minutes at 6°C whilst being rotated.

5) The bone marrow tissue was infiltrated with 1:1 85% EtOH:LR White mixture for 30 minutes at 6°C whilst being rotated. LR White dissolved in 85% EtOH but not in 80% EtOH.

6) The bone marrow tissue was infiltrated with LR White, 2 times 30 minutes at 6°C whilst being rotated.

7) The bone marrow tissue was placed in gelatine capsules in fresh LR White and was then polymerised, without any air bubbles, for 24 hours at 50°C.

8) The block of bone marrow tissue was sectioned and the sections were placed on nickel grids since copper grids can be oxidised during the immunolabelling procedures (54).

3.5) Outline of the method for the ultrastructural immunolocalisation of the H-subunit and the L-subunit of ferritin

An outline of the method for the immunolocalisation of the H-subunit and L-subunit of ferritin is presented here. The investigations that were done in order to determine the steps of the final method are presented in subsequent sections.

Materials

1) 8% $NaJO_4$, Sodium (meta) periodate, Fluka, Biochemika, Ultra, cat. no. 71859, Sigma-Aldrich, Aston Manor, South Africa.

2) Phosphate buffered saline – 20 mmol/l sodium phosphate buffer, 0.15 mol/l sodium chloride. Two stock solutions were prepared – 20 mmol/l Na_2HPO_4, 0.15 mol/l NaCl and 20 mmol/l $NaH_2PO_4 \cdot H_2O$, 0.15 mol/l NaCl. The $NaH_2PO_4 \cdot H_2O$ stock solution was added to the Na_2HPO_4 stock solution to pH 7.4. Sodium chloride, SigmaUltra, cat. no. S7653, Sigma-Aldrich, Aston Manor, South Africa, di-Natriumhydrogenphosphate, cat. no. 6586, Merck Chemicals (Pty) LTD., Germiston, South Africa, Natriumdihydrogenphosphate-1-hydrate, cat. no. 6346, Merck Chemicals (Pty) LTD., Germiston, South Africa.

3) 0.5% Glycine, Pharmacia Biotech, cat. no. 17-1323-01, AEC Amersham (PTY) LTD, Sandton, South Africa.

4) BSA, Bovine Serum Albumin, cat. no. RPN 412 V, Amersham Biosciences, Separations Scientific, Randburg, South Africa.

5) FBS, Fetal Bovine Serum, filtered and gamma irradiated, cat. no. 306, Highveld Biologicals (Pty) Ltd, Halfway House, South Africa.

6) Fish Gelatine (IGSS quality), cat. no. RPN 4160L/AB, Amersham Biosciences, Separations Scientific, Randburg, South Africa.

7) Tween-20, Polyoxyethylenesorbitan monolaurate, Sigma for Molecular Biology, cat. no. P-9416, Sigma-Aldrich, Aston Manor, South Africa.

8) Primary monoclonal antibodies, monoclonal antibody specific for the H-subunit of ferritin, RH02 and the monoclonal antibody specific for the L-subunit of ferritin, LF03 were obtained from Ramco Laboratories, Inc., Stafford, Texas, United States of America.

9) Secondary antibody, Anti-mouse IgG (whole molecule), gold conjugate, 10 nm, cat. no. G-7777, Sigma-Aldrich, Aston Manor, South Africa.

10) Glutaraldehyde, Pure Glutaraldehyde 25% solution, E.M. grade, SPI Supplies, cat. no. 2607, Rick Loveland & Associates, Halfway House, South Africa.

11) Uranyl acetate, SPI Supplies, cat. no. 2624, Rick Loveland & Associates, Halfway House, South Africa.

Method

1) Antigen retrieval step. All procedures were performed by placing the sections on a drop of the specific solution.

2) The sections were rinsed 3 times 5 minutes with phosphate buffered saline at room temperature.

3) First blocking step – the sections were blocked with 0.05% glycine in H_2O for 20 minutes at room temperature.

4) Second blocking step.

5) Incubation with the primary monoclonal antibodies in the second blocking solution.

6) The sections were rinsed 3 times 5 minutes with the second blocking solution at room temperature.

7) Incubation with the secondary antibody in the second blocking solution.

8) The sections were rinsed for 3 times 5 minutes with the second blocking solution at room temperature.

9) The sections were rinsed 5 minutes with phosphate buffered saline at room temperature.

10) The sections were fixed with 2% GA in phosphate buffered saline at room temperature.

11) The sections were rinsed 3 times 5 minutes with deionised H_2O at room temperature. A rinsing step in H_2O after the use of solutions containing phosphates is important to avoid the formation of artefactual electron dense deposits. The essential factors in the formation of electron dense deposits in tissues appear to be phosphate buffer, ethanol and uranyl acetate. The nature and intensity of the deposits seem to vary with the sequence of combination of these factors. Precipitation of phosphates has been observed in ethanol concentrations of 50% and more. Phosphates bind to uranyl ions due to a mordant action of the phosphate precipitates. Several different precipitate-forming processes may be involved: an interaction of phosphate and ethanol, of uranyl acetate and buffer and possibly an excess of unreacted aldehyde and uranyl acetate with or without phosphate (58).

12) To enhance the contrast of the sections, the sections were stained for 10 minutes with 0.3% uranyl acetate at room temperature.

13) The sections were dipped 15 times in 3 separate beakers with deionised H_2O.

14) The sections were then viewed with a Philips 301 transmission electron microscope.

3.6) Non-specific binding of the gold-conjugate secondary antibody

The possible non-specific binding of the gold-conjugate secondary antibody to the tissue section was investigated by incubating the tissue section with only the gold-conjugate secondary antibody – omitting the primary antibody from the incubation step (54).

Method

Steps were followed as for the outline of the immunolocalisation method with the specific solutions as follows:

1) The phosphate buffered saline was supplemented with 1% BSA.
2) The sections were incubated without the primary antibody for 2 hours in 1% BSA, phosphate buffered saline at room temperature.
3) The sections were incubated with the secondary antibody in the following dilutions 1:50, 1:150, 1:300 and 1:400 in 1% BSA, phosphate buffered saline for 1 hour at room temperature.

Results

No non-specific binding of the secondary antibody at any of the dilutions was shown. A dilution of 1:50 for the secondary antibody was used throughout.

3.7) Non-specific binding of the primary monoclonal antibodies to the resin

The investigation of the non-specific binding of the primary monoclonal antibodies was cumbersome. The primary monoclonal antibodies can bind non-specifically to the resin and to the tissue. The non-specific binding of the monoclonal antibody to the resin can be investigated more easily.

Method

Sections were made from clear polymerised resin without any embedded tissue. Steps were followed as for the outline of the immunolocalisation method with the specific solutions as follows. For the relevant rinsing steps, the blocking solution used for the section was also used for the rinsing steps.

1) One section was blocked with only phosphate buffered saline and 4 sections were blocked with 0.05% glycine in deionised H_2O for 1 hour at 30°C.
2) This was then followed by blocking with one of the following, phosphate buffered saline; 1% BSA in phosphate buffered saline; 1% FBS in phosphate buffered saline or 1% fish gelatine in phosphate buffered saline for 1 hour at 30°C.
3) The sections were incubated with the L-subunit monoclonal antibody at a final concentration of 1 µg/ml in each of the previous blocking solutions for 2 hours at 30°C.
4) The sections were incubated with the secondary antibody 1:50 in each of the previous blocking solutions for 1 hour at 30°C.
5) The sections were not stained with 0.3% uranyl acetate.

Results

The following number of gold particles was counted in a field of view at 22k magnification for each of the blocking procedures:

Only phosphate buffered saline	70 gold particles
Glycine and phosphate buffered saline	80 gold particles
Glycine and 1% BSA in phosphate buffered saline	25 gold particles
Glycine and 1% FBS in phosphate buffered saline	20 gold particles
Glycine and 1% fish gelatine in phosphate buffered saline	30 gold particles

With all these blocking procedures a substantial amount of non-specific binding was shown for the L-subunit monoclonal antibody. However, blocking with glycine followed by 1% FBS in phosphate buffered saline showed the least non-specific binding. In a second attempt the FBS was increased to 10%. The primary antibody solutions that were employed included the following final concentrations, 1 µg/ml, 0.4 µg/ml and 0.2 µg/ml.

Results

1 µg/ml L-subunit monoclonal antibody	3 gold particles
0.4 µg/ml L-subunit monoclonal antibody	0 gold particles in the field of view with a few on the whole section
0.2 µg/ml L-subunit monoclonal antibody	0 gold particles in the field of view with a few on the whole section

The non-specific binding obtained with the inclusion of 10% FBS resulted in negligible binding. Similar results were obtained for the H-subunit monoclonal antibody.

3.8) Investigation of the effect of the antigen retrieval procedures on non-specific binding to the resin of the monoclonal antibodies

Method

1) Sections of clear polymerised resin without any embedded tissue were used.
2) Sections were incubated with each of the following antigen retrieval solutions 0.01 M sodium citrate buffer pH 6, 0.01 M sodium citrate buffer pH 7.88, 0.05 M Tris-HCl buffer pH 10, 0.05 M Tris-HCl buffer pH 3 and 0.01 M EDTA-NaOH solution pH 8 for 30 minutes at 85°C or autoclaved at 121°C.

3) The sections were cooled down for 10 minutes.

4) The sections were rinsed 3 times 5 minutes with phosphate buffered saline at room temperature.

5) The sections were blocked with 0.05% glycine for 15 minutes at room temperature.

6) The sections were blocked with 10% FBS in phosphate buffered saline for 1 hour at 30°C.

7) The sections were incubated with the primary L-subunit monoclonal antibody at a concentration of 0.4 µg/ml in 10% FBS in phosphate buffered saline for 2 hours at 30°C.

8) The sections were rinsed 3 times 5 minutes with 10% FBS in phosphate buffered saline at room temperature.

9) The sections were incubated with the secondary antibody 1:50 in 10% FBS in phosphate buffered saline for 1 hour at 30°C.

10) The sections were rinsed 3 times 5 minutes in 10% FBS in phosphate buffered saline at room temperature.

11) The sections were not stained for contrast.

Results

For all the antigen retrieval solutions the amount of non-specific binding was negligible.

3.9) Investigation of the effect of different antigen retrieval procedures on immunolabelling

No specific immunolabelling was shown for the L-subunit and H-subunit monoclonal antibodies at a final concentration of 0.4 µg/ml or 4 µg/ml. Various antigen retrieval

procedures were tried to enhance the specific immunolabelling of the H-subunit and L-subunit monoclonal antibodies.

Materials

1) 0.01 M sodium citrate buffer, pH 6. The following two solutions were prepared, 0.01 M sodium citrate, analytical reagent, Protea Laboratory Services (PTY.) LTD., Johannesburg, South Africa and 0.01 M citric acid, analytical reagent, Hopkin & Williams LTD, Chadwell Heath, Essex, England. The 0.1 M citric acid solution was added to the 0.1 M sodium citrate solution to a pH of 6.
2) 0.05 M Tris-HCl buffer, pH 10, TRIS-HCl, Tris(hydroxymethyl)aminomethane hydrochloride, cat. no. 1.08219.0100, Merck Chemicals (Pty) LTD., Germiston, South Africa.
3) 0.01 M EDTA-NaOH solution, pH 8, Ethylene Diamine Tetra-acetic Acid, UNIVAR®, Saarchem, Krugersdorp, South Africa.
4) 0.1% TritonX-100 in deionised H_2O, Triton®X-100 Solution, cat. no. 93443, Fluka, BioChemika, MicroSelect, Sigma-Aldrich, Aston Manor, South Africa.
5) 0.5% SDS in deionised H_2O, Sodium dodecyl sulphate, cat. no. 17-1313-01, Pharmacia Biotech, Separations Scientific, Randburg, South Africa.
6) 3% H_2O_2 in deionised H_2O, Perdrogen 30% by weight H_2O_2, Riedel-de-Haën, cat. no. 31642, Sigma-Aldrich, Aston Manor, South Africa.
7) 0.1% and 0.25% trypsin, Trypsin / Versene in phosphate buffered saline, cat. no. 205, Highveld Biologicals (Pty) Ltd, Halfway House, South Africa.
8) 8% $NaJO_4$, Sodium (meta) periodate, Fluka, Biochemika, Ultra, cat. no. 71859, Sigma-Aldrich, Aston Manor, South Africa.

Method

1) Different antigen retrieval procedures were tried including heat-mediated antigen retrieval and chemical antigen retrieval. The procedures for the heat-mediated antigen retrieval were as follows; 0.01 M sodium citrate buffer pH 6, 0.05 M Tris-HCl buffer pH 10 and 0.01 M EDTA-NaOH solution pH 8. The sections were placed in 500 µl of the antigen retrieval solutions in an eppendorff and autoclaved at 121°C. The procedures for the chemical antigen retrieval procedures were as follows; 8% $NaJO_4$ in deionised H_2O for 1 hour at room temperature, 0.1% Triton X-100 in deionised H_2O for ten minutes at room temperature, 0.5% SDS in deionised H_2O for 10 minutes at room temperature and 3% H_2O_2 in deionised H_2O for 10 minutes at room temperature. All procedures were performed by placing the sections on a drop of the specific solution.
2) The autoclaved sections were cooled down for 10 minutes before the next step.
3) The sections were rinsed 3 times 5 minutes with phosphate buffered saline at room temperature.
4) The sections were blocked with 0.05% glycine in deionised H_2O for 20 minutes at room temperature.
5) The sections were blocked with 1% BSA, 5% FBS, 0.05% Tween-20 in phosphate buffered saline for 1 hour at 30°C.
6) The sections were incubated with the primary H-subunit monoclonal antibody at a concentration of 4 µg/ml in 1% BSA, 5% FBS, 0.05% Tween-20 in phosphate buffered saline for 2 hours at 30°C.
7) The sections were rinsed 3 times 5 minutes with 1% BSA, 5% FBS, 0.05% Tween-20 in phosphate buffered saline at room temperature.

8) The sections were incubated with the secondary antibody 1:50 in 1% BSA, 5% FBS, 0.05% Tween-20 in phosphate buffered saline for 1 hour at 30°C.

9) The sections were rinsed 3 times 5 minutes in 1% BSA, 5% FBS, 0.05% Tween-20 in phosphate buffered saline at room temperature.

10) The sections were rinsed 5 minutes with phosphate buffered saline at room temperature.

11) The sections were fixed with 2% GA in phosphate buffered saline at room temperature.

12) The sections were rinsed 3 times 5 minutes with deionised H_2O at room temperature.

13) The sections were stained for 10 minutes with 0.3% uranyl acetate at room temperature.

14) The sections were dipped 15 times in 3 separate beakers with deionised H_2O.

Results

No sufficient specific immunolabelling was achieved for the H-subunit monoclonal antibody at a concentration of 4 µg/ml with any of the antigen retrieval procedures.

3.10) Specific immunolabelling of the monoclonal antibodies

Specific immunolabelling was achieved (but low) only when the concentration of the primary antibodies was increased to 20 µg/ml and the incubation period prolonged to 4 hours at 30°C for both the H-subunit and the L-subunit. No antigen retrieval procedures. Figures 4a and 4b.

In an attempt to further increase the specific immunolabelling various antigen retrieval procedures were tried again. An increase in specific immunolabelling was achieved with antigen retrieval in 8% $NaJO_4$ for one hour at room temperature. Figures 4c and 4d.

An additional antigen retrieval step was included after antigen retrieval in 8% $NaJO_4$ for one hour at room temperature to possibly increase the specific immunolabelling. The following combined antigen retrieval procedures were tried; 8% $NaJO_4$ for 1 hour at room temperature and autoclaving in 0.01 M sodium citrate buffer pH 6, 8% $NaJO_4$ for 1 hour at room temperature and autoclaving in 0.01 M EDTA-NaOH solution pH 8 and 8% $NaJO_4$ for 1 hour at room temperature and autoclaving in 0.05 M Tris-HCl buffer pH 10. For all these combined antigen retrieval procedures an increase in specific immunolabelling was achieved over and above that for the 8% $NaJO_4$ for 1 hour at room temperature antigen retrieval step. Figures 4e and 4f, figures 5a and 5b and figures 5c and 5d.

Various chemical antigen retrieval procedures and enzymatic antigen retrieval procedures were also tried. The chemical antigen retrieval procedures included treatment with 0.1% Triton X-100 and 0.5% SDS. The enzymatic antigen retrieval procedures included digestion with 0.1% trypsin and 0.25% trypsin. Figures 5e and 5f, figures 6a and 6b and figures 6c and 6d.

3.11) Antigen retrieval with sodium ethoxide

Treatment with different antigen retrieval methods resulted in an increase in the specific labelling of the H-subunit and L-subunit of ferritin. However, it was not satisfactory. Antigen retrieval in sodium ethoxide was tried in order to possibly increase the specific immunolabelling.

Materials

1) An 11% solution of sodium ethoxide was prepared as follows; add 11% NaOH in absolute anhydric ethanol. Anhydric ethanol was prepared by using molecular sieves (Molecular sieves, 3 Å, powder, undried, cat. no. 23,364-1, Sigma-Aldrich, Aston Manor, South Africa). The molecular sieves were activated at 250°C for at least 3 hours. Absolute ethanol was incubated with the molecular sieves at a concentration of 5% (w/v) at room temperature for 12 hours on a magnetic stirrer. This was repeated with a new batch of molecular sieves. The container was closed with parafilm and the final anhydric solution was decanted into dried (250° celcius) glassware (25).

Method

1) The sections were incubated in a 1:10 or 1:100 dilution (1% and 0.1% sodium ethoxide) of 11% NaOH in absolute anhydric ethanol at room temperature for 60 seconds.
2) The sections were rinsed for 5 minutes in 100% ethanol at room temperature.
3) The sections were rinsed for 5 minutes in 70% ethanol at room temperature.
4) The sections were rinsed for 5 minutes in 50% ethanol at room temperature.
5) The sections were rinsed 3 times 5 minutes with phosphate buffered saline at room temperature.

Results

No increase in the specific immunolabelling was shown for antigen retrieval in sodium ethoxide. The sodium ethoxide resulted in damage to the plastic sections.

3.12) Investigation of the effect of different polymerisation procedures on immunolabelling

In a final attempt to increase the specific immunolabelling of the H-subunit and L-subunit of ferritin, different polymerisation procedures were tried. These included heat polymerisation, catalytic polymerisation and UV-light polymerisation.

Methods

Heat polymerisation

1) After the final change of pure LR White the bone marrow was placed in pure LR White in a gelatine capsule and polymerised at 50°C for 24 hours.

Catalytic polymerisation

1) The polymerisation mixture was prepared as follows. 15 µl of accelerator was added to 10 ml of pre-cooled (4°C) LR White monomer. This mixture was stirred gently, careful not to introduce any air bubbles.
2) After the final change of pure LR White the bone marrow was placed in this mixture in a gelatine capsule.
3) Catalytic polymerisation is an exothermal reaction, therefore in order to ensure dissipation of the generated heat the capsules were placed in a pre-cooled solid aluminium block with drilled holes.
4) The gelatine capsules were left at 4°C for 24 hours for completion of the polymerisation process.

UV-light polymerisation

1) After the final change of pure LR White the bone marrow was placed in pure LR White in a gelatine capsule.

2) The gelatine capsules were placed in a wire rack inside a polystyrene box coated with aluminium foil in a freezer (-20°C).

3) The UV light source (360 nm) was placed on top of the box with a distance of 17 cm from the gelatine capsules.

4) The gelatine capsules were left in the freezer for 36 hours for completion of the polymerisation process. The temperature in the freezer increased to -10°C as a result of the heat generated by the lamp.

Results

No increase in specific immunolabelling was shown for any of the polymerisation procedures. Heat polymerisation was used throughout. Figures 6e and 6f.

3.13) The achievement of satisfactory immunolabelling

It was only with the use of new antibodies at a higher concentration that sufficient immunolabelling was achieved. These antibodies were received from Prof Paolo Arosio. The concentration of these antibodies was 1 mg/ml and was employed at a final concentration of 50 µg/ml. However, a concentration of 25 µg/ml also resulted in sufficient immunolabelling. Figures 7a and 7b. In order to investigate the possible non-specific binding of these antibodies to the resin immunolabelling was performed with an increase in the Tween-20 concentration. No difference in non-specific binding was shown for Tween-20 concentrations of 0.05%, 0.1%, 0.5% and 1%. Figures 7c-7f.

3.14) Discussion

In order to determine the differential expression of the H-subunit and L-subunit of ferritin, monoclonal antibodies specific to only the subunit of interest is of paramount importance. Ideally these two monoclonal antibodies should have similar affinities to their respective subunits and show no cross-reactivity to the other subunit. By using an ELISA-based method and recombinant H-ferritin and L-ferritin proteins these characteristics of the H-subunit and L-subunit monoclonal antibodies were investigated. It was shown that the H-subunit monoclonal antibody had an affinity towards the recombinant H-ferritin protein about 2.5 times more when compared to the affinity of the L-subunit monoclonal antibody towards the recombinant L-ferritin protein. Furthermore, it was shown that the H-subunit monoclonal antibody has a low affinity for the recombinant L-ferritin protein – 5 times less than that shown for the recombinant H-ferritin protein. Whereas, the L-subunit monoclonal antibody showed a very low affinity for the recombinant H-ferritin protein – 10 times less than that shown for the recombinant L-ferritin protein. The question remains as to whether these results can be applied to ultrastructural immunolocalisation. Since it was shown in the present study that only at concentrations of 20 µg/ml did specific immunolabelling occur for both the antibodies, but with the specific immunolabelling of the H-subunit much more problematic. It should be noted that with the ELISA method the affinity of these monoclonal antibodies was evaluated for their respective recombinant proteins. These recombinant proteins contain 100% H-subunits and 100% L-subunits respectively. Ferritin molecules containing 100% of either the H-subunit or the L-subunit are not likely to be encountered *in vivo* (59). Furthermore, it was shown that different combinations of the specific subunits in a ferritin molecule could influence the binding of the monoclonal antibodies to their respective subunits (47).

Not only do the H-subunit and L-subunit monoclonal antibodies display different affinities toward their respective recombinant ferritin proteins, but these affinities are influenced differently by fixation and dehydration. The effects of fixation and dehydration were investigated by an ELISA-based method. The binding of the monoclonal antibodies was influenced differently by the solutions that were used for fixation and dehydration of the bone marrow tissue. The H-subunit monoclonal antibody showed a decrease in affinity to 87% of the optimal signal whereas the L-subunit monoclonal antibody showed a small increase in affinity to 105% of the optimal signal. Therefore, the H-subunit monoclonal antibody epitope was more sensitive to the fixation and dehydration solutions. This could possibly be part of the reason why immunolabelling of the H-subunit was more difficult than immunolabelling of the L-subunit.

In the present study, the changes in the expression of the H-subunit, the changes in the expression of the L-subunit and the changes in the H-subunit/L-subunit ratio were investigated in subgroups of patients and not the absolute amount of the H-subunit relative to the absolute amount of the L-subunit. The obtainment of proper specific immunolabelling for both the H-subunit and the L-subunit of ferritin on the LR White sections was therefore the main objective.

No specific immunolabelling for either the H-subunit monoclonal antibody or the L-subunit monoclonal antibody at a final concentration of 4 µg/ml was obtained on the LR White sections. Different antigen retrieval procedures were tried in order to achieve specific immunolabelling. The procedures for the heat-mediated antigen retrieval were as follows; 0.01 M sodium citrate buffer pH 6, 0.05 M Tris-HCl buffer pH 10 and 0.01 M EDTA-NaOH solution pH 8. The sections were placed in 500 µl of the antigen retrieval

solutions in an eppendorff and autoclaved at 121°C. The procedures for the chemical antigen retrieval procedures were as follows; 8% $NaJO_4$ in deionised H_2O for 1 hour at room temperature, 0.1% Triton X-100 in deionised H_2O for ten minutes at room temperature, 0.5% SDS in deionised H_2O for 10 minutes at room temperature and 3% H_2O_2 in deionised H_2O for 10 minutes at room temperature. No specific immunolabelling of either the H-subunit monoclonal antibody or the L-subunit monoclonal antibody at a final concentration of 4 µg/ml was achieved with any of these antigen retrieval procedures.

The achievement of specific immunolabelling for the H-subunit and L-subunit of ferritin was problematic. The highest concentration (20 µg/ml) was used that was possible with the first batch of antibodies at a dilution of 1:10. With this concentration specific immunolabelling of the L-subunit monoclonal antibody was shown which could also be increased by various antigen retrieval solutions. Little specific immunolabelling was achieved for the H-subunit monoclonal antibody at a final concentration of 20 µg/ml with only a little increase in specific immunolabelling with different antigen retrieval solutions. One of the major obstacles with post-embedding immunolabelling is that immunolabelling arises from antigen only exposed on the surface of the section (included within an essentially two-dimensional space), therefore, a relatively large improvement in the volumetric retention of the antigen is required to show even a modest increase in surface restricted immunogold immunolabelling. Such an improvement is seen with cryo-immunolabelling where extraction due to dehydration and plastic embedding is completely eliminated (9). Nevertheless, an increase in the final monoclonal antibody concentration to 50 µg/ml resulted in specific immunolabelling for both the H-subunit and L-subunit of ferritin.

3.15) Final method for the ultrastructural immunolabelling of the H-subunit and L-subunit of ferritin

The final method for the immunolocalisation of the H-subunit and L-subunit of ferritin is presented here.

Method

1) The sections were incubated with 8% $NaJO_4$ in H_2O for 1 hour at room temperature. All procedures were performed by placing the sections on a drop of the specific solution.
2) The sections were rinsed 3 times 5 minutes with phosphate buffered saline at room temperature.
3) The sections were blocked with 0.05% glycine in H_2O for 20 minutes at room temperature.
4) The sections were blocked with 1% BSA, 5% FBS, 0.05% Tween-20 in phosphate buffered saline for 1 hour at 30°C.
5) The sections were incubated with the primary monoclonal antibodies 1:20 diluted in 1% BSA, 5% FBS, 0.05% Tween-20 in phosphate buffered saline for 4 hours at 30°C.
6) The sections were rinsed 3 times 5 minutes with 1% BSA, 5% FBS, 0.05% Tween-20 in phosphate buffered saline at room temperature.
7) The sections were incubated with the secondary antibody 1:50 in 1% BSA, 5% FBS, 0.05% Tween-20 in phosphate buffered saline for 1 hour at 30°C.
8) The sections were rinsed 3 times 5 minutes with 1% BSA, 5% FBS, 0.05% Tween-20 in phosphate buffered saline at room temperature.
9) The sections were rinsed 5 minutes with phosphate buffered saline at room temperature.

10) The sections were fixed with 2% GA in phosphate buffered saline at room temperature.

11) The sections were rinsed 3 times 5 minutes with deionised H_2O at room temperature.

12) To enhance the contrast of the sections, the sections were stained for 10 minutes with 0.3% uranyl acetate at room temperature.

13) The sections were dipped 15 times in 3 separate beakers with deionised H_2O.

14) The sections were then viewed with a Philips 301 transmission electron microscope.

Figure 4 a and b

Specific immunolabelling was achieved when the concentration of the primary antibody was increased to 20 µg/ml and the incubation period prolonged to four hours for the H-subunit and the L-subunit, respectively. No antigen retrieval procedures.

Figure 4 c and d

An increase in specific immunolabelling was achieved with antigen retrieval in 8% $NaJO_4$ for the H-subunit and the L-subunit, respectively.

Figure 4 e and f

An additional increase in specific immunolabelling was achieved when the 8% $NaJO_4$ treatment was followed by an additional antigen retrieval step with 0.01 M sodium citrate buffer, pH 6 (autoclave) for the H-subunit and the L-subunit, respectively. Scale bar 1 µm.

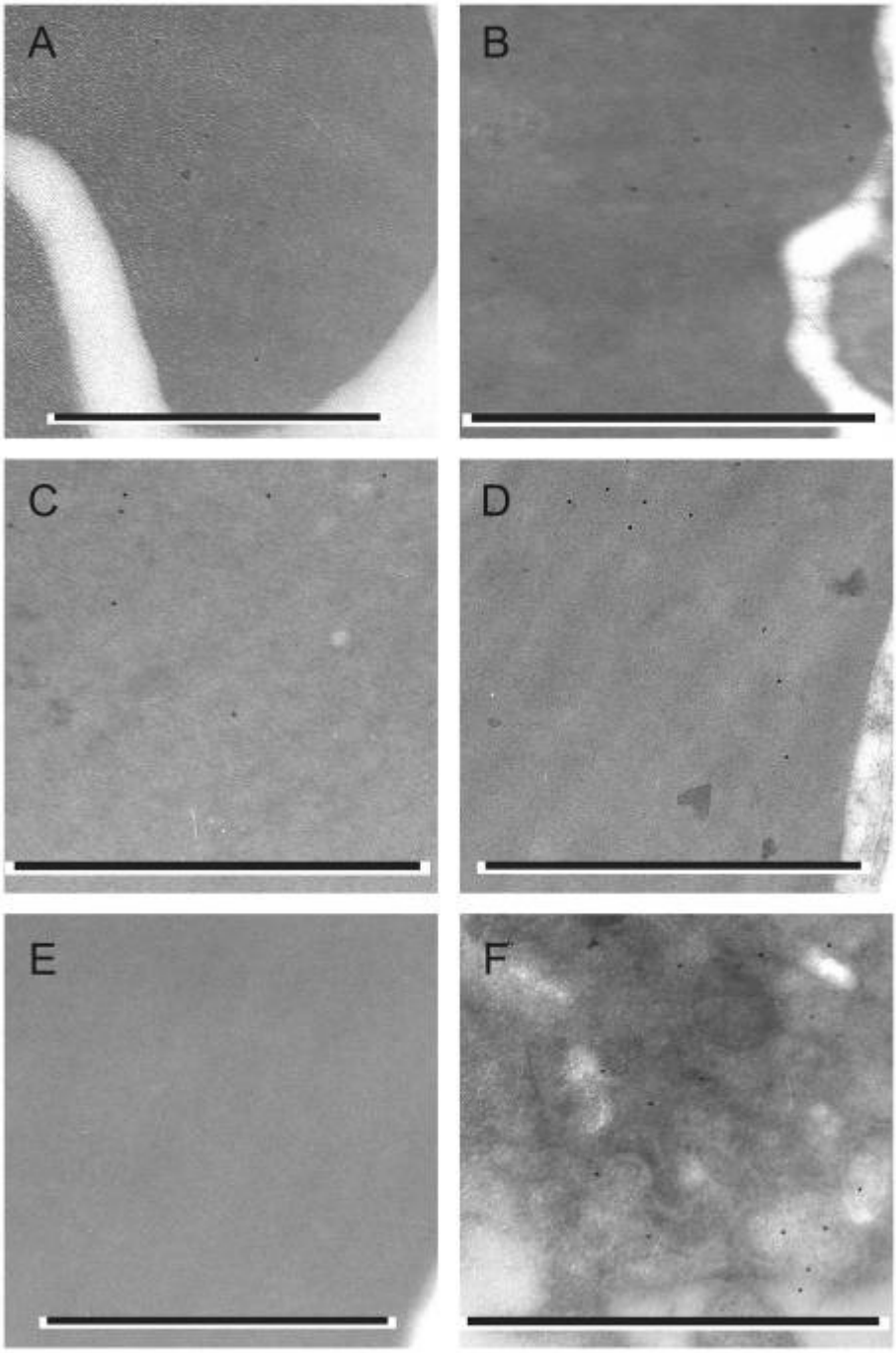
A
B
C
D
E
F

Figure 5 a and b

A further increase in specific immunolabelling was achieved when the 8% $NaJO_4$ was followed by an additional antigen retrieval step with 0.01 M EDTA-NaOH solution, pH 8 (autoclave) for the H-subunit and the L-subunit, respectively.

Figure 5 c and d

A further increase in specific immunolabelling was achieved when the 8% $NaJO_4$ treatment was followed by an additional antigen retrieval step with 0.05 M Tris-HCl buffer, pH 10 (autoclave) for the H-subunit and the L-subunit, respectively.

Figure 5 e and f

Antigen retrieval with 0.1% Triton X-100 for the H-subunit and the L-subunit, respectively. Scale bar 1 µm.

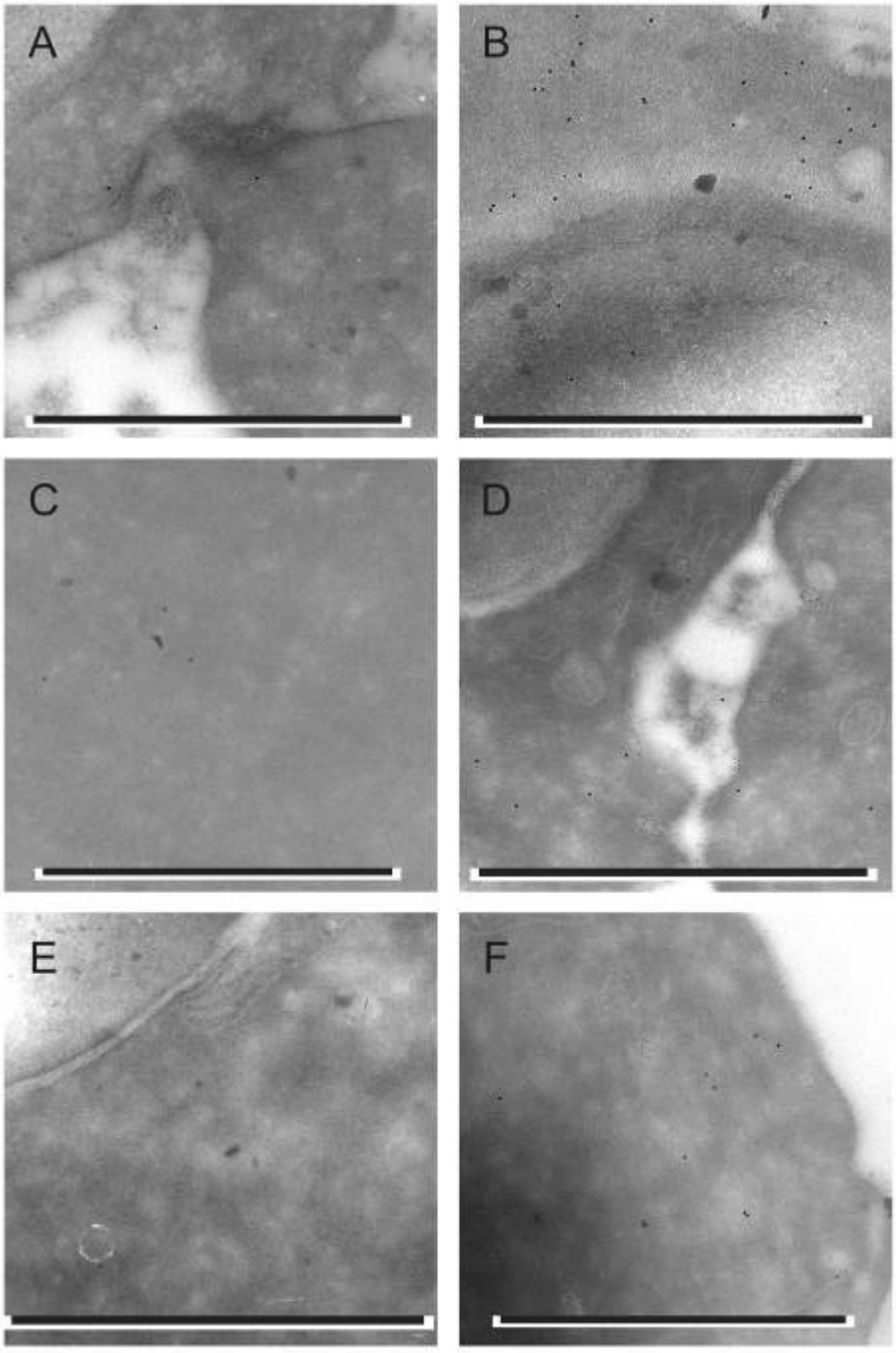
A
B
C
D
E
F

Figure 6 a and b

Antigen retrieval with 0.5% SDS for the H-subunit and the L-subunit, respectively.

Figure 6 c and d

Antigen retrieval with 0.1% trypsin for the H-subunit and the L-subunit, respectively.

Figure 6 e

Polymerisation of LR White at 50°C for 24 hours.

Figure 6 f

Polymerisation of LR White with UV light at 10°C for 36 hours. Scale bar 1 µm.

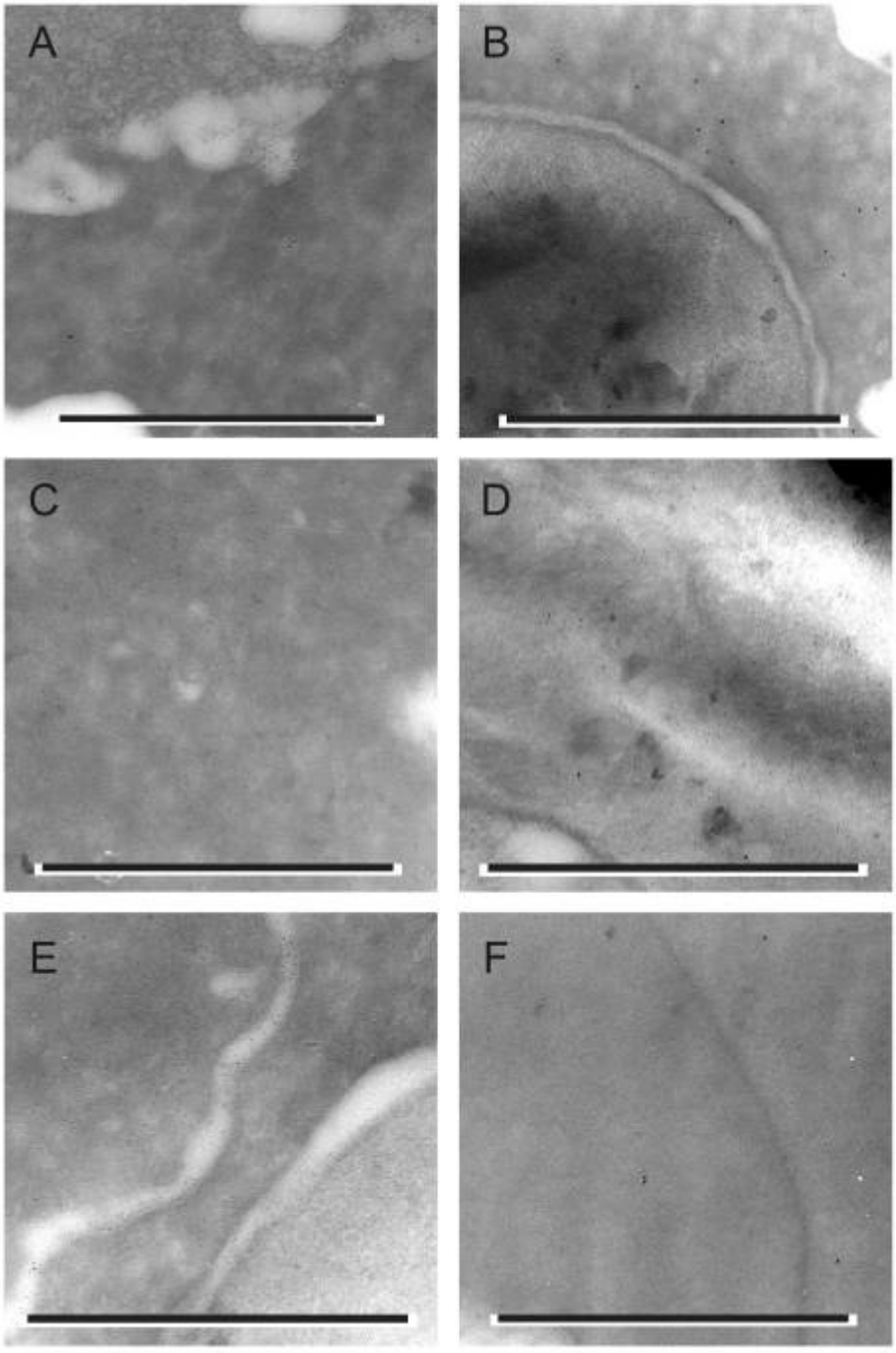
A
B
C
D
E
F

Figure 7 a and b

Immunolocalisation of the H-subunit and L-subunit with monoclonal antibodies at a concentration of 25 µg/ml, respectively.

Figure 7 c-f

The Tween-20 concentration was increased from 0.05%, to 0.1%, to 0.5% and finally to 1%. Scale bar 400 nm.

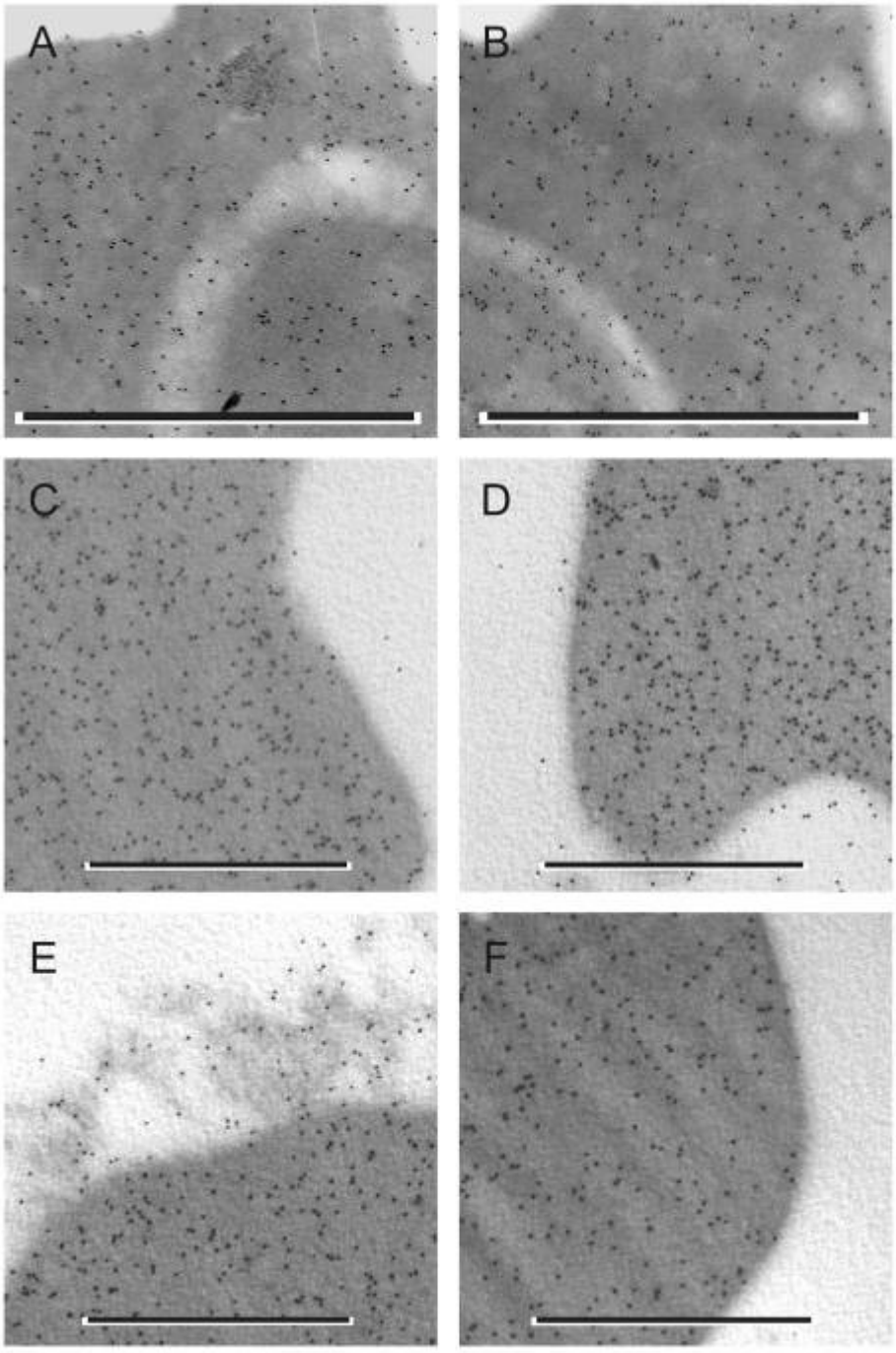
A
B
C
D
E
F

4) References

1) Glauert AM. Fixation, dehydration and embedding of biological specimens. In: Glauert AM editor. Practical methods in electron microscopy, vol. 3. Amsterdam: North-Holland Publishing Company; 1974. p. 1-207.

2) Ingram LT, Stenzel DJ, Kara UAK, Bushell GR. Localisation of internal antigens of *Plasmodium falciparum* using monoclonal antibodies and colloidal gold. Parasitology Research 1988; 74: 208-215.

3) Bendayan M, Nanci A, Kan FWK. Effect of tissue processing on colloidal gold cytochemistry. Journal of Histochemistry and Cytochemistry 1987; 35(9): 983-996.

4) Groos S, Reale E, Luciano L. Re-evaluation of epoxy resin sections for light and electron microscopic immunostaining. Journal of Histochemistry and Cytochemistry 2001; 49(3): 397-406.

5) Ring PKM, Johanson V. Immunoelectron microscopic demonstration of thyroglobulin and thyroid hormones in rat thyroid gland. Journal of Histochemistry and Cytochemistry 1987; 35(1): 1095-1104.

6) Newman GR, Hobot JA. Modern acrylics for post-embedding immunostaining techniques. Journal of Histochemistry and Cytochemistry 1987; 35(9): 971-981.

7) Oliver C. Fixation and embedding. In: Javois LC editor. Methods in Molecular Biology, vol. 34, Immunocytochemical Methods and Protocols. Totowa, New Jersey: Humana Press; 1994. p. 291-298.

8) Hobot JA, Newman GR. Strategies for improving the cytochemical and immunocytochemical sensitivity of ultrastructurally well-preserved, resin embedded biological tissue for light and electron microscopy. Scanning Microscopy Supplement 1991; 5: S27-S41.

9) Newman GR. Use and abuse of LR White. Histochemical Journal 1987; 19: 118-120.

10) Brorson S-H, Roos N, Skjorten F. Antibody penetration into LR-White sections. Micron 1994; 25(5): 453-460.

11) Brorson S-H. Antigen detection on resin sections and methods for improving the immunogold labelling by manipulating the resin. Histology Histopathology 1998; 13(1): 275-281.

12) Goght A. Use of LR White resin for post-embedding immunolabelling of brain tissue. Acta Anatomica 1992; 145: 327-339.

13) Boon ME. Microwave-antigen retrieval: the importance of pH of the retrieval solution for MiB-1 staining. European Journal of Morphology 1996; 34(5): 375-379.

14) Osamura RY, Itoh Y, Matsuno A. Applications of plastic embedding to electron microscopic immunocytochemistry and in situ hybridization in observations of production and secretion of peptide hormones. Journal of Histochemistry and Cytochemistry 2000; 48(7): 885-891.

15) Roth J. Post-embedding cytochemistry with gold-labelled reagents: a review. Journal of Microscopy 1986; 143(Pt 2): 125-137.

16) Kellenberger E. Learning about truth and biases through experience: section surface corrugation, protein denaturation, and staining. Microscopy Research and Technique 1998; 42: 33-42.

17) Ellinger A, Pavelka M. Post-embedding localization of glycoconjugates by means of lectins on thin sections of tissues embedded in LR White. Histochemical Journal 1985; 17: 1321-1336.

18) Timms BG. Postembedding immunogold labelling for electron microscopy using "LR White" resin. American Journal of Anatomy 1986; 175: 267-275.

19) Newman GR, Jasani B, Williams D. A simple post-embedding system for the rapid demonstration of tissue antigens under the electron microscope. Histochemical Journal 1983; 15: 543-555.

20) Brorson S-H. How to examine the antigen-damaging effect of sodium ethoxide on deplasticized epoxy sections. Journal of Histochemistry and Cytochemistry 1997; 45(1): 143-146.

21) Brorson S-H, Strøm EH. A new immunoelectron microscopy approach for the detection of immunoglobulin and complement deposits in epoxy-embedded renal biopsies. Ultrastructural Pathology 1998; 22: 449-457.

22) Brorson S-H. pH-dependent effect of heat-induced antigen retrieval of epoxy sections for electron microscopy. Micron 2002; 33: 481-482.

23) Tano S, Kashima K, Daa T, Urabe S, Tsuji K, Nakayama I *et al.* An antigen retrieval method using an alkaline solution allows immunoelectron microscopic identification of secretory granules in conventional epoxy-embedded tissue sections. Journal of Histochemistry and Cytochemistry 2003; 51(2): 199-204.

24) Bendayan M, Zollinger M. Ultrastructural localization of antigenic sites on osmium-fixed tissues applying the protein A-gold technique. Journal of Histochemistry and Cytochemistry 1983; 31(1): 101-109.

25) Bettica A, Johnson AB. Ultrastructural immunogold labelling of glial filaments in osmicated and unosmicated epoxy-embedded tissue. Journal of Histochemistry and Cytochemistry 1990; 38(1): 103-109.

26) Stirling JW, Graff PS. Antigen unmasking for immunoelectron microscopy: labelling is improved by treating with sodium ethoxide or sodium metaperiodate, then heating on retrieval medium. Journal of Histochemistry and Cytochemistry 1995; 43(2): 115-123.

27) Stirling JW. Ultrastructural localization of lysozyme in human colon eosinophils using the protein A-gold technique: effects of processing on probe distribution. Journal of Histochemistry and Cytochermistry 1989; 37(5): 709-714.

28) Evers P, Uylings HBM, Suurmeijer AJH. Antigen retrieval in formaldehyde-fixed human brain tissue. Methods: A Companion to Methods in Enzymology 1998; 15: 133-140.

29) Shi S-R, Cote RJ, Taylor CR. Antigen retrieval immunohistochemistry: past, present, and future. Journal of Histochemistry and Cytochemistry 1997; 45(3): 327-343.

30) Saito N, Konishi K, Takeda H, Kato M, Sugiyama T, Asaka M. Antigen retrieval trial for post-embedding immunoelectron microscopy by heating with several unmasking solutions. Journal of Histochemistry and Cytochemistry 2003; 51(8): 989-994.

31) Qu-Hong, Dvorak AM. Ultrastructural localization of osteopontin immunoreactivity in phagolysosomes and secretory granules of cells in human intestine. Histochemical Journal 1997; 29: 801-812.

32) Robinson JM, Vandré DD. Antigen retrieval in cells and tissues: enhancement with sodium dodecyl sulphate. Histochemistry and Cell Biology 2001; 116: 119-130.

33) Brorson S-H. Fixative-dependent increase in immunogold labeling following antigen retrieval on acrylic and epoxy sections. Biotechnic and Histochemistry 1999; 74(5): 248-260.

34) Shi S-R, Cote RJ, Taylor CR. Antigen retrieval techniques: current perspectives. Journal of Histochemistry and Cytochemistry 2001; 49(8): 931-937.

35) Shi S-R, Cote RJ, Young L, Imam A, Taylor CR. Use of pH 9.5 Tris-HCl buffer containing 5% urea for antigen retrieval immunohistochemistry. Biotechnic and Histochemistry 1996; 71(4): 190-196.

36) Pileri SA, Roncador G, Ceccarelli C, Piccioli M, Briskomatis A, Sabattini E *et al.* Antigen retrieval techniques in immunohistochemistry: comparison of different methods. Journal of Pathology 1997; 183: 116-123.

37) Jiao Y, Sun Z, Lee T, Fusco FR, Kimble TD, Meade CA *et al.* A simple and sensitive antigen retrieval method for free-floating and slide-mounted tissue sections. Journal of Neuroscience Methods 1999; 93: 149-162.

38) Boenisch T. Heat-induced antigen retrieval restores electrostatic forces: prolonging the antibody incubation as an alternative. Applied Immunohistochemistry and Molecular Morphology 2002; 10(4): 363-367.

39) Xiao J-C, Adam A, Ruck P, Kaiserling E. A comparison of methods for heat-mediated antigen retrieval for immunoelectron microscopy: demonstration of cytokeratin no.18 in normal and neoplastic hepatocytes. Biotechnic and Histochemistry 1996; 71(6): 278-285.

40) McQauid S, McConnell R, McMahon J, Herron B. Microwave antigen retrieval for immunocytochemistry on formalin-fixed, paraffin-embedded post-mortem CNS tissue. Journal of Pathology 1995; 176: 207-216.

41) Ishida-Yamamoto A, Tanaka H, Nakane H, Takahashi H, Iizuka H. Antigen retrieval of loricrin epitopes at desmosomal areas of cornified cell envelopes: an immunoelectron microscopic analysis. Experimental Dermatology 1999; 8: 402-406.

42) Hoetelmans RWM, van Slooten H-J, Keijzer R, van de Velde CJH, van Dierendonck JH. Comparison of the effects of microwave heating and high pressure cooking for antigen retrieval of human and rat Bcl-2 protein in formaldehyde-fixed, paraffin-embedded sections. Biotechnic and Histochemistry 2002; 77(3): 137-144.

43) Röcken C, Roessner A. An evaluation of antigen retrieval procedures for immunoelectron microscopic classification of amyloid deposits. Journal of Histochemistry and Cytochemistry 1999; 47(11): 1385-1394.

44) Cavanna F, Ruggeri G, Iacobello C, Chieregatti G, Murador E, Albertini A *et al.* Development of a monoclonal antibody against human heart ferritin and its application in an immunoradiometric assay. Clinica Chimica Acta 1983; 134: 347-356.

45) Arosio P, Albertini A. Structure and immunochemistry of isoferritins. Italian Journal of Biochemistry 1984; 33(4): 275A-277A.

46) Arosio P, Cozzi A, Ingrassia R, Levi S, Luzzago A, Ruggeri G *et al.* A mutational analysis of the epitopes of recombinant human H-ferritin. Biochimica *et* Biophysica Acta 1990; 1039: 197-203.

47) Roberts DD, Drysdale JW. Immunoreactivities of human isoferritins. Clinica Chimica Acta 1985; 150: 41-51.

48) Luzzago A, Arosio P, Iacobello C, Ruggeri G, Capucci L, Brocchi E *et al.* Immunochemical characterization of human liver and heart ferritins with monoclonal antibodies. Biochimica *et* Biophysica Acta 1986; 872: 61-71.

49) Hoy TG, Jacobs A. Changes in the characteristics and distribution of ferritin in iron-loaded cell cultures. Biochemical Journal 1981; 193(1): 87-92.

50) Hoy TG, Jacobs A. Ferritin polymers and the formation of haemosiderin. British Journal of Haematology 1981; 49(4): 593-602.

51) Thompson KJ, Fried MG, Ye Z, Boyer P, Connor JR. Regulation, mechanisms and proposed function of ferritin translocation to cell nuclei. Journal of Cell Science 2002; 115: 2165-2177.

52) Surguladze N, Patton S, Cozzi A, Fried MG, Connor JR. Characterization of nuclear ferritin and mechanism of translocation. Biochemical Journal 2005; 388: 731-740.

53) Roth J. The silver anniversary of gold: 25 years of the colloidal gold marker system for immunocytochemistry and histochemistry. Histochemistry and Cell Biology 1996; 106: 1-8.

54) Bendayan M. A review of the potential and versatility of colloidal gold cytochemical labeling for molecular morphology. Biotechnic and Histochemistry 2000; 75(5): 203-242.

55) Brorson S-H. Bovine serum albumin (BSA) as a reagent against non-specific immunogold labelling on LR White and epoxy resin. Micron 1997; 28(3): 189-195.

56) Birrell GB, Hedberg KK, Griffith OH. Pitfalls of immunogold labelling: analysis by light microscopy, transmission electron microscopy, and photoelectron microscopy. Journal of Histochemistry and Cytochemistry 1987; 35(8): 843-853.

57) Kaur R, Dikshit KL, Raje M. Optimization of immunogold labelling TEM: an ELISA-based method for rapid and convenient simulation of processing conditions for quantitative detection of antigen. Journal of Histochemistry and Cytochemistry 2001; 49(3): 355-367.

58) Louw J, Williams K, Harper IS, Walfe-Coote SA. Electron dense artefactual deposits in tissue sections: the role of ethanol, uranyl acetate and phosphate buffer. Stain Technology 1990; 65(5): 243-250.

59) Santambrogio P, Levi S, Cozzi A, Rovida E, Albertini A, Arosio P. Production and characterization of recombinant heteropolymers of human ferritin H and L chains. Journal of Biological Chemistry 1993; 268(7): 12744-12748.